MARINE SCIENCES INSTRUMENTATION

Volume 1

MARINE SCIENCES INSTRUMENTATION

Volume 1

▶ In order that the scientific information herein might be disseminated to the public as rapidly as possible this publication has been produced by offset reproduction of material furnished by the authors.

A publication of
INSTRUMENT SOCIETY OF AMERICA

MARINE SCIENCES INSTRUMENTATION

Volume 1

A Collection of Instrumentation Papers
Presented at the Marine Sciences Conference
Held September 11-15, 1961, at Woods Hole, Mass.,
Sponsored by the Instrument Society of America
and the American Society of Limnology and Oceanography

and

Papers from the Marine Sciences Sessions of the 1961
Instrument Society of America Symposia Held at
Toronto and Los Angeles

EDITORS

Roy D. Gaul
Agricultural and Mechanical College of Texas
David D. Ketchum
Woods Hole Oceanographic Institution
Jack T. Shaw
Minneapolis-Honeywell Regulator Company
James M. Snodgrass
Scripps Institution of Oceanography

Distributed by
PLENUM PRESS
NEW YORK

$14.00

INSTRUMENT SOCIETY of AMERICA
Penn-Sheraton Hotel
530 William Penn Place
Pittsburgh 19, Pa.

CONTENTS

THE DESIGN AND INSTALLATION OF THE FIXED ACOUSTIC BUOY

by RICHARD P. OBERLIN
Project Engineer, Fixed Acoustic Buoy
The Martin Company, Baltimore, Maryland

ABSTRACT

The Fixed Acoustic Buoy is a deep sea instrumentation device which measures acoustic data at a depth of 14,000 feet. It is controlled and powered from shore via a cable and has numerous modes of operation. Signal processing is accomplished in the deep sea unit to allow use of a single coaxial cable. The paper describes the electronic system design and the techniques used to protect the components from the high ambient pressure while still allowing electrical interconnections. The installation technique and problems encountered are also discussed.

INTRODUCTION

System design of deep ocean acoustic equipment is impaired by lack of data at the desired depths. The Fixed Acoustic Buoy (FAB) is a system which was designed for the Navy to obtain some of this missing data. The data itself and the types of tests involved are classified and will therefore not be discussed in this paper.

The great significance of FAB, as far as oceanographic instrumentation is concerned, is that it is a radical design departure from normal practice. In FAB almost all of the signal processing is accomplished electronically in the deep sea portion. This results in a considerable cost saving because it allows use of a single coaxial cable with medium bandwidth requirements instead of 21 pair medium bandwidth cable or one high bandwidth coaxial cable with 21 channel multiplexing. The suitability of this approach has been considerably strengthened with the successful implantment of the system during December 1960 in 14,000 feet of water south of Bermuda. System operation and data collection has continued since that time in a satisfactory manner.

SYSTEM DESCRIPTION

The system consists of a bottom unit, a coaxial cable and shore equipment. The bottom unit is shown in Figure 1. It consists of a 21 element vertically steerable acoustic array, a buoyancy tank to hold the array vertical, a pressure tight sphere housing the electronics and beamforming networks, a battery, a tilt indicator and an anchor.

The cable consists of about 27 miles of coaxial cable which is similar in construction and characteristics to the A. T. & T. Trans-Atlantic telephone cable linking the United States and Europe. Slightly over one mile of this cable is double armored and magnetically shielded. The remainder is single armored with no magnetic shielding.

The shore equipment consists of the control circuitry, data recording equipment and power supplies required to manually operate the system. The shore equipment is located on a Texas Tower type structure called "Argus Island".

Five normal control functions are available to the shore operator, as shown in Figure 1. These are steer forward (a command for the deep unit to acoustically look at the next higher angle), reset (a command to return to the lowest angle), steer feedback instrumentation on and off, tilt-pitch instrumentation on and off, and tilt-roll instrumentation on and off. The commands are initiated by sending the appropriate frequency (in the range of 10 to 12 KC) down the cable to the sea unit. An additional function ("fail safe") is commanded by a reversal of the power supply voltage to the deep unit. This causes a large portion of the circuitry to be bypassed in case of a failure.

Fifteen different modes of acoustic data collection can be commanded via the steer channel. Thirteen of these are narrow listening beams at various vertical angles from 0° to 90°. The last two are omnidirectional listening modes. In "fail safe" operation, only the 0° beam is available. The acoustic data is acquired in the range of 400 cps to 5 KC.

The instrumentation functions answer back with FM signals in the range of 6 to 8 KC. Steer feedback tells which particular step the beam is on and the tilt channels give the tilt of the array from vertical in two mutually perpendicular axes.

The block diagram of the system is shown in Figure 2. As can be seen, the DC power and

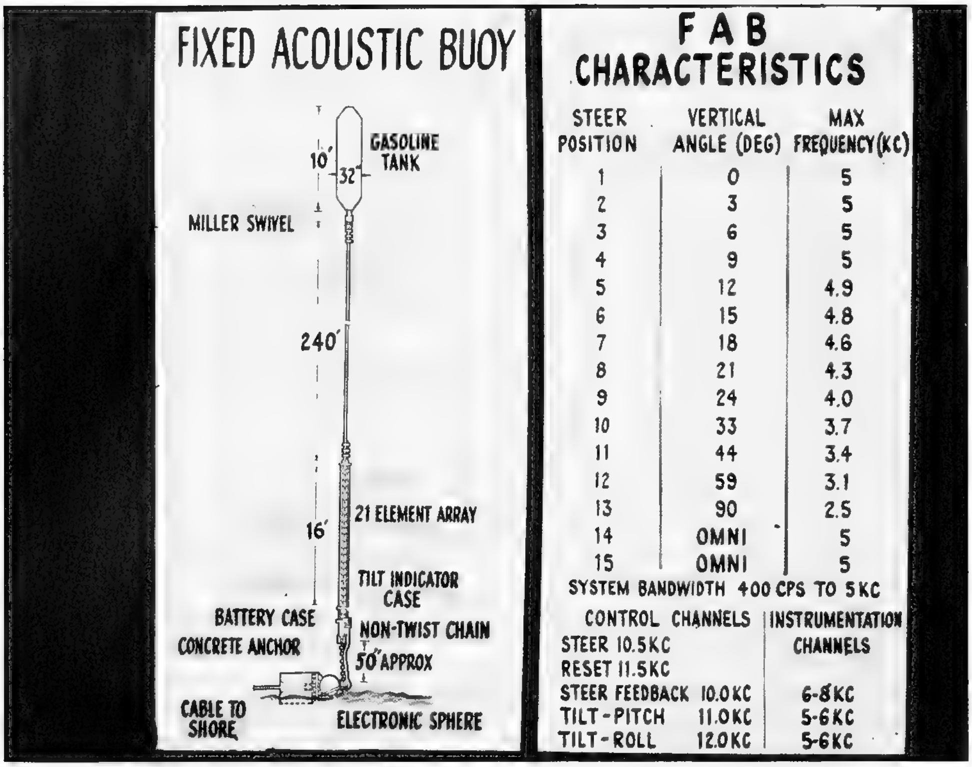

Figure 1

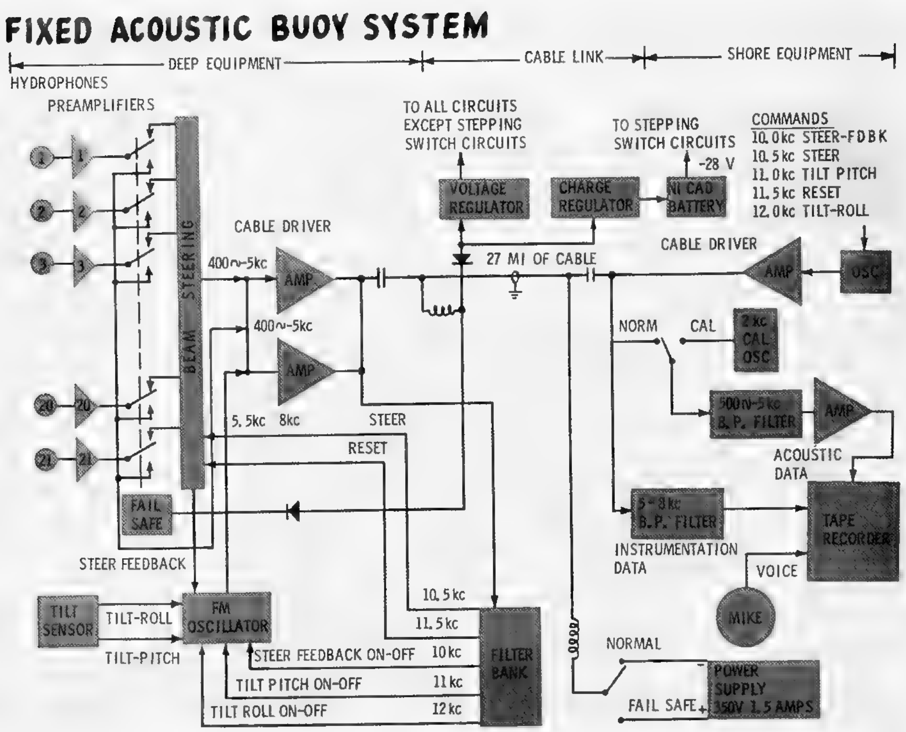

Figure 2

command functions are put in from the shore end. These pass through the necessary cable driving circuits and then the cable itself. At the deep end, the various commands are sorted out according to frequency and polarity. These cause the deep unit to go to the desired configuration. Instrumentation and acoustic data are mixed together and amplified by a pair of cable driver amplifiers (for redundancy). These signals are separated at the shore end of the cable by the appropriate filters and then recorded in analog form on magnetic tape. The data is then sent back and reduced using existing reduction facilities at Martin-Baltimore. The deep electronics are entirely powered from shore except for the stepping switches themselves. These operate from a ni-cad battery which is charged from the shore supply.

The deep sea electronics circuitry contains over 200 transistors most of which are protected from the 6000 psi ambient pressure by a large steel sphere. The hydrophone preamplifiers are protected by being placed in a small steel chamber located inside each hydrophone. The tilt indicators and the battery are similarly protected by individual steel cylindrical chambers.

The various components are thus protected but necessarily must be electrically connected together. This means reliable electrical feedthroughs are required which must be able to withstand a pressure differential of at least 6000 psi. The design used is shown in Figure 3. This design is an adaptation of that used on Piccard's Bathyscaphe and in fact was suggested by Mr. Jacques Piccard who was used as a consultant on the mechanical problems.

The operation of the feedthrough is as follows: The high pressure differential forces the araldite (an epoxy) into the tapered hole thus effectively sealing the hole. The Bathyceri (a wax like substance) is forced into the voids between the araldite and the polyethylene wires and prevents water from causing electrical faults between adjacent wires. The PR701 (a sticky putty like substance) is used to prevent water from getting into the feedthrough when the pressure level is too low to ensure sealing due to the above actions. Feedthroughs throughout the FAB equipment are of this design.

The hydrophone, of necessity, must withstand direct exposure to the 6000 psi pressure and this involves some tricky problems also. These problems are dealt with in more detail in the subsequent paper by Mr. Delaney.

INSTALLATION

The installation procedure is shown in Figure 4. A two ship operation was necessary utilizing a cable laying ship and a smaller auxiliary ship.

The first step of the installation was to bring one end of the shore end cable to Argus Island. This was accomplished by use of a work boat in conjunction with the cable layer. The cable was firmly attached to one of the tower legs by the work boat and personnel on the tower. The cable ship then laid the 1+ miles of shore cable and attached a marker buoy to the end of the cable. At this point, the cable ship went to the desired implantment location but due to a failure of the polyethylene covered array harness in the FAB array the operation was postponed while the harness was reworked at the factory.

The array harness had failed at the molded splice joint due to improper annealing of the molded polyethylene. A second harness was constructed and properly annealed. This was used to replace the original harness.

Prior to the second implantment attempt, the completed deep sea unit was lowered into the water over the cable layer bow while dockside in Bermuda. Final checkout was completed and the deep sea unit was attached to the front of the bow sheaves.

The cable layer took it's position as shown in Figure 2 and three miles of nylon line were paid out to the auxiliary ship. The nylon line was attached to the top of the buoyancy tank through a corrosive link and the tank was attached to the array by 240 feet of grapnel rope. The gasoline filled tank was allowed to slide in the water from a skid attached to the side of the cable layer.

The corrosive link was not designed to take any lateral force but inadvertently was subjected to considerable lateral forces during the release of the buoyancy tank. Due to this, two links were broken during the installation. A three foot piece of steel rope was inserted between the top of the tank and the link and proved to be a satisfactory universal joint preventing any further link failures.

The tank was towed away from the cable ship by ship No. 2 and the deep unit was lowered by it's coaxial cable to the bottom of the sea, 14,000 feet down. At this point, the cable layer laid the rest of the cable toward Argus Island, picked up the marker buoy and the end of the shore cable and spliced the two ends of the cable together.

The shore equipment had been installed on the cable ship to operate and monitor the deep equipment during checkout and installation. The installation was completed, except for the removal of the nylon line, with the transfer of the shore equipment to Argus Island and subsequent connection with the cable.

The nylon line was used during the operation to prevent fouling of the gasoline tank and the coaxial cable. It was also to be used to retrieve the deep unit in case of failure during the three

HIGH PRESSURE ELECTRICAL FEEDTHROUGH

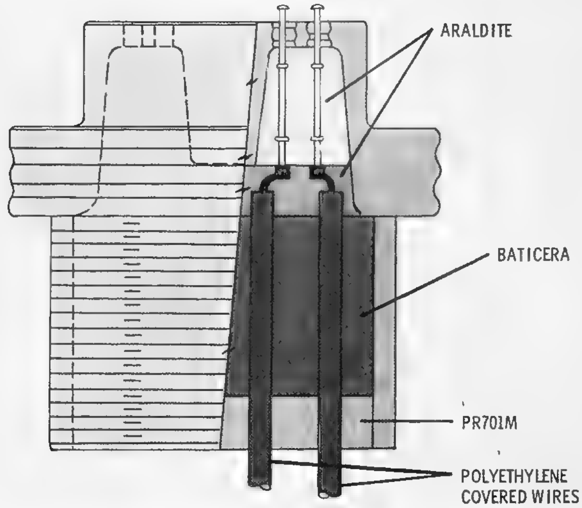

Figure 3

FAB IMPLANTMENT

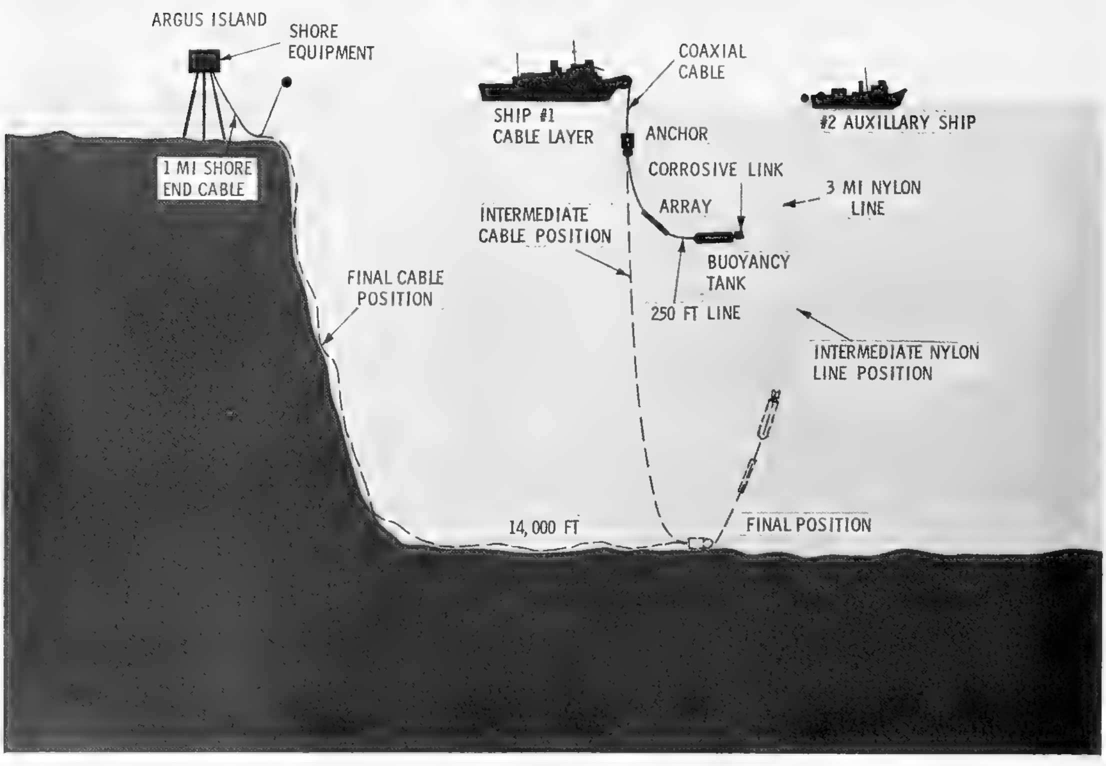

Figure 4

days following implantment. The corrosive link was supposed to release the nylon after four days but either never completely released or the line became entangled. The nylon line was then weighted and allowed to sink. The array went from 20° tilt to less than three degrees during this operation as the line sank and the hydrodynamic drag forces were reduced.

The unit was accepted with a demonstration of it's performance and data collection was started.

CONCLUSIONS

A fairly complex electronic-acoustic device can be successfully designed and installed in a deep ocean environment.

THE QUIET PLATFORM, KEY TO SUCCESSFUL OCEANOGRAPHIC ACOUSTIC RESEARCH

by A. DONN COBB, Electronic Engineer
U.S. Navy Underwater Sound Laboratory
Fort Trumbull, New London, Connecticut

ABSTRACT

This paper discusses the surface vessel as a platform from which to conduct acoustic research. It points out the main problems attendant to such a platform and discusses techniques for control and for elimination of many types of acoustic self-noise. An attempt is made in this paper to bring cause and effect together in the light of available corrective measures to provide a foundation for valid measurements of acoustic data.

* * * * * * * * * *

In any electroacoustic investigation which is predicated on the detection of low-level signals especially when they have a broad spectral distribution, the signal-to-noise ratio is of great importance. This is particularly true in acoustic survey work such as the mapping of a muddy bottom or the recording of sounds of biological origin. A quiet platform is essential to this type of work; when a ship is used for the surveys, every effort should be made to keep interfering noise at a minimum.

NOISE SOURCES

It is the intent of this paper to describe a method of determining the principal noise sources of a vessel and to suggest remedial action. Let us first consider the types of noise that may be encountered. Assuming the presence of a signal of some finite level, the interfering noise may be divided into three broad types. These are:

1. Electrical noise.
2. Sea state noise.
3. Self-noise of the carrying vessel.

For the purpose of this article it will be assumed (1) that electrical noise can be controlled, and (2) that sea-state noise can be kept at a predetermined level by the selection of the time and place for the conduct of the experiment. We are then left with the self-noise of the vessel, which will be the subject of this article.

The acoustic self-noise of a vessel dead in the water is usually composed of noises generated by main propulsion machinery, auxiliary machinery, ventilating system, etc. , and when under way, by all these plus the hydrodynamic flow noise of water.

To determine the charateristics of the machinery noises, a comprehensive machinery noise survey should be conducted. To this end a calibrated broad-band, omni-directional hydrophone should be installed at, or as near as is feasible to, the location of the research transducer. A word of caution seems in order here: inasmuch as the machinery noise to be measured is generated to a large extent as structural vibration and then transferred to the water surrounding the ship's hull, a suitable vibration isolation mounting for the hydrophone must be provided in order to prevent direct vibrational excitation. The simple expedient of suspending the hydrophone with shock cord is often very effective; where more permanence is desired, a mounting consisting of several flanges alternately of brass and rubber can be used.

EQUIPMENT

Since accurate analysis equipment is generally too large to take to sea, it is usually necessary to record data on magnetic tape for later analysis in the laboratory. An idealized system for such recording would include all battery-operated equipment, with a preamplifier between the hydrophone and the tape recorder.

A word here about the preamplifier will help anyone interested in conducting this type of survey. Typical acoustic noise, when plotted as a curve of amplitude versus frequency, displays about a 6-db-per-octave negative slope. If we consider the 10 octaves of frequency between 20 cycles and 20 kilocycles as the observational band, we find that our tape recorder must be able to accept a dynamic range of amplitude of 60 db. Even the most ambitious sellers of tape recording equipment do not claim this capability. If, however, 6-db-per-octave pre-emphasis is added to the preamplifier, it becomes apparent that theoretically all portions of the spectrum from 20 cycles to 20 kc will have the same amplitude; consequently, very unsophisticated recording equipment will suffice. In practice, the noise to be observed is not precisely random, and the deviation from the mean noise level may cause as much as ±10 db of signal amplitude difference through this system. This 20-db dynamic range is well within the capabilities of most tape-recording equipment.

Some provision should also be made for a low-level calibrate signal at the input of the preamplifier. Before commencement of the noise survey, a suitable number of discrete calibration frequencies should be recorded on the tape to provide a means of determining the recording system gain throughout the spectrum of interest. These levels, along with the calibration of the hydrophone, will provide means for reducing the recorded noise data to equivalent plane-wave sound pressure in the water.

RECORDING

Once the equipment is set up and properly checked out, the vessel should proceed to deep water, i.e., more than 100 fathoms, where Sea State 2 or less prevails. On arrival, the vessel should stop and secure all machinery. A sample of this noise field should be recorded; this is the base line or quietest condition attainable. Then each item of machinery should be operated individually, insofar as possible, with samples recorded under each condition. If the basic acoustic research to be conducted will require the vessel to be under way, a noise-versus-speed observation should be made by recording data at one- or two-knot intervals throughout the speed range desired.

CORRECTIVE ACTION

If the analysis of the sea-test data indicates that the vessel is too noisy (as it probably will), there are several potential "fixes" available:

1. Quite often relocation of the research transducer away from known high-intensity noise sources can be effective.

2. Isolation mounting of machinery observed to be noisy may solve the problem. There are many fine isolation mountings available.

3. If the machinery to be isolated is too large or for some other reason cannot be isolated, a visco-elastic damping material applied to the machine and/or the hull in the vicinity of the acoustic research transducer may effectively dissipate this energy.

4. If the research to be conducted does not require the research transducer to see in all directions, baffles can be arranged in the desired blind spots as well as above the transducer.

In the preparation of the research transducer for the under-way portion of any research project, care should be exercised to provide a suitably vibration damped and isolated streamlined enclosure. Any smoothing of hull discontinuities ahead of the research transducer location should assist in hydrodynamic noise reduction especially at high speeds. Generally speaking, the achievement of a quiet platform requires some or all of the previously mentioned devices.

If a truly quiet platform is to be achieved, it may be necessary to repeat the sea test several times after various remedial measures have been taken.

CONCLUSION

In conclusion, it should again be emphasized that the end result of good interference-free data more than justifies the effort required to achieve a quiet working platform.

INSTRUMENTATION FOR THE MEASUREMENT OF HYDRODYNAMIC FLOW-NOISE

by CHESTER L. WAKAMO, Associate Research Engineer,
and ROBERT C. FITZPATRICK, Research Associate
Institute of Science and Technology, The University of Michigan,
Ann Arbor, Michigan

ABSTRACT

An experimental study of the generation of acoustic energy by fluid turbulence near an extended solid boundary was performed. For this study, a free-falling self-contained missile was conceived. Parameters affecting the design of the vehicle were stability, velocity, recovery of the vehicle, skin vibration or "Self noise" factor, and the effects of acceleration and deceleration on equipment performance. An inboard magnetic tape data recording system stores the acoustic signals for subsequent analysis. Detailed information on the depth-measurement circuitry, automatic recovery mechanism, calibration procedure and check-out for a typical launching and recovery are presented.

INTRODUCTION

The study of acoustics is primarily concerned with the generation, transmission, and reception of energy in the form of pressure and velocity fluctuations. One particular aspect of this study is the process of generation of acoustic energy by fluid turbulence near an extended solid boundary. Effects of boundary-layer turbulence are of special importance in high speed aircraft and missiles; torpedos, submarines, and surface ships.

To measure the acoustic noise generated by boundary-layer turbulence the use of a missile type vehicle moving through water was considered. It was decided that a free-falling finless body with a self-contained electronic system to record noise data was the best approach. Such a missile was designed, fabricated, and tested. The electronic system consisted of hydrophone transducers, a suitable magnetic-tape recorder, batteries for power, a pressure transducer to determine pressure and depth, and pressure-operated control switches. The vehicle was released from a launching rack suspended just below the surface of the water. It would fall freely, with no ropes or cables attached, to a depth of no more than 500 ft. At some controllable predetermined distance its descent was checked when the pressure-controlled switches caused the release of drag fins at the sides of the missile. As the deceleration produced by the drag fins occurred, switches shut off the recording system and released a bouyant tail section from the main body; this section rose to the surface, pulling with it a nylon recovery line which was unreeled from a spool secured to the main body. Figure 1 shows the missile in its launching frame.

Preliminary tests were conducted at Orchard Lake, Michigan, a semi-private lake 40 miles northeast from Ann Arbor, chosen for its depth and relatively low background noise. A launching platform was moored in 110 ft of water, permitting about 5 sec of flow-noise data from each drop of the missile. Provision was made to record the depth during the missile descent by utilizing a pressure transducer and associated electronics. The depth record was later used to calculate the velocity.

VEHICLE DESCRIPTION

Parameters affecting the design of the vehicle were stability, velocity, recovery of vehicle, skin vibration or "self-noise" factor, and the effects of acceleration and deceleration on equipment performance.

The vehicle consisted of 3 sections: a cast-aluminum nose, an extruded, tubular, aluminum midsection, and a cast-aluminum tail (Fig. 2 and 3).

The nose section was an ellipsoid of revolution with the radius ratio $a/b = 1.3$, and dimensions of 7 in. and 10-3/4 in. A 100-lb lead ballast plug was bolted into the nose dur-

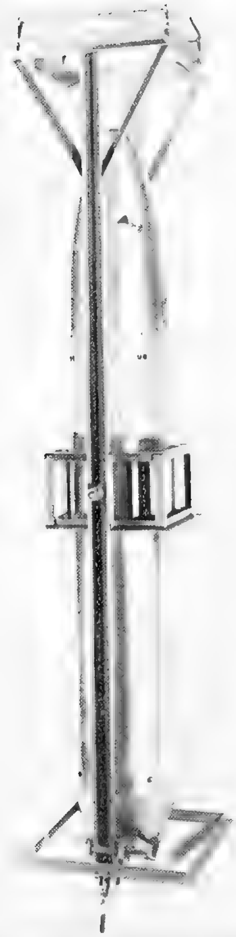

FIG. 1 MISSILE IN LAUNCHING FRAME

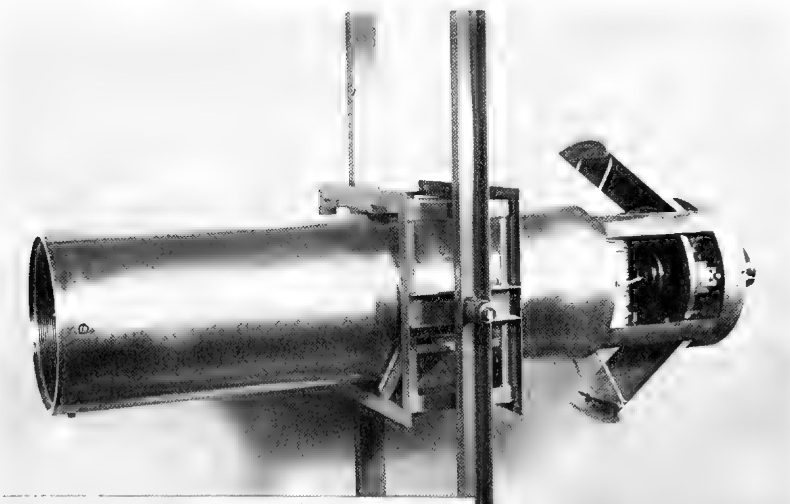

FIG. 2 MIDSECTION OF MISSILE, NOSE OFF. With access to electronics and drag fins open.

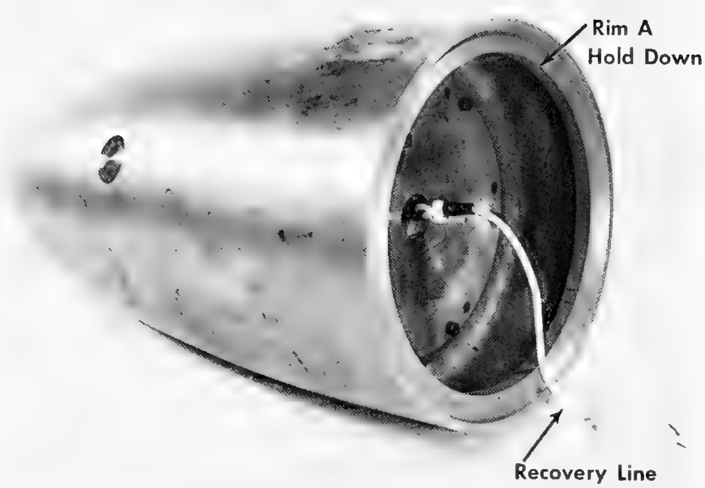

FIG. 3 TAIL SECTION OF MISSILE

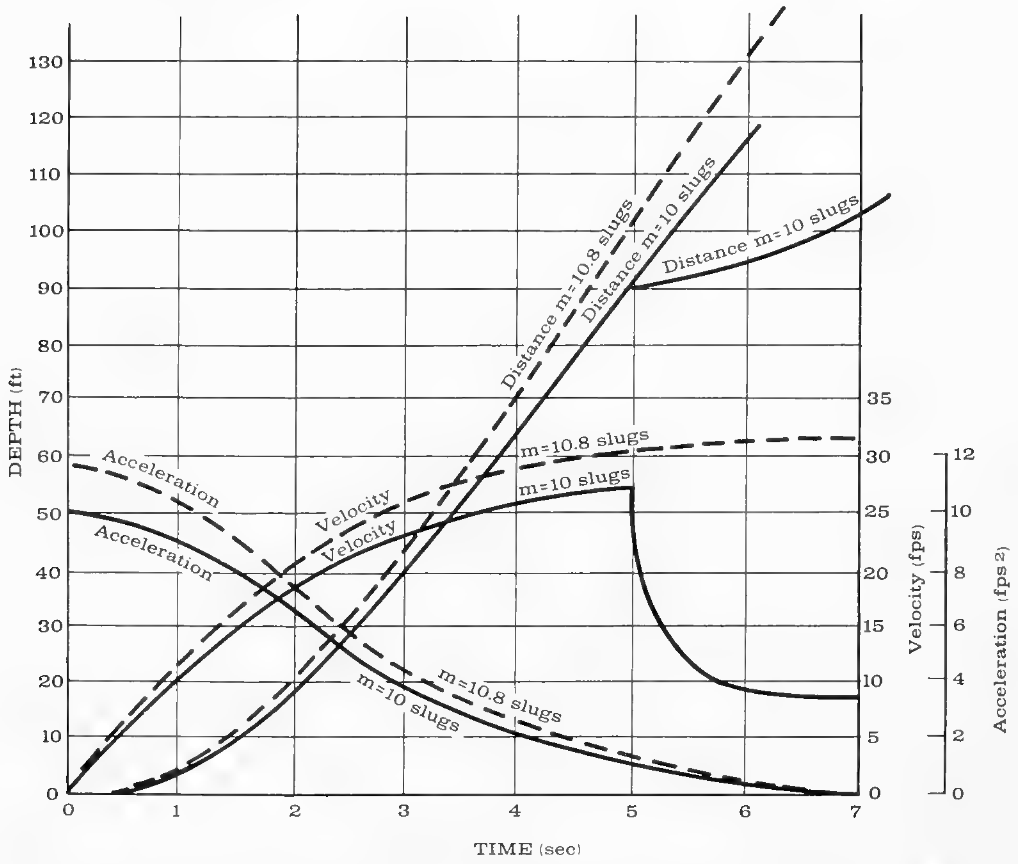

FIG. 4. DESIGN AND VELOCITY CHARACTERISTICS OF HYDRODYNAMIC-FLOW-NOISE MISSILE

ing the test drops. The nose was screwed into the midsection using an "O Ring" seal to make the connection watertight.

The midsection or main body of the vehicle (Fig. 2) was an extruded aluminum tube 10-3/4 in. in diameter, 48 in. long, with 3/8 in. walls. The forward two thirds of the midsection made up a watertight compartment containing the recorder and all the accessory electronics and components of the data system. Two flush-mounted hydrophones were located on opposite sides of the midsection at its midpoint. On the rear of the bulkhead terminating the watertight section was fixed the recovery mechanism and holddown clamps for securing the tail section. Four rectangular doors or "drag fins" were mounted flush with the outside surface in the afterend of the midsection. These were opened (to decelerate the missile) by the recovery and tail-locking assembly to be described.

The tail section of the missile (Fig. 3) was a cast-aluminum ellipsoid of revolution with the ratio $a/b = 4$. It was 10-3/4 in. in diameter and 21-1/2 in. long. This section was a sealed bouyant body which, when released from the forward bodies, rose to the surface trailing a nylon recovery line secured to the midsection. The tail was clamped tightly in place on the afterend of the midsection by means of four toggles which were locked and released by action of the release-recovery mechanism. Figure 2 shows the completed missile. Figure 4 shows the theoretically predicted performance characteristics of the missile.

Model studies indicated that the vehicle as designed, with a fineness ratio of 7.15 and with its mass distribution, would be stable through its maximum test velocity.

The data-recording system and accessory components were mounted on a shock- and vibration-isolated assembly in the midsection. The equipment was integrated into a rigid frame which in turn was slid into tracks on a structure secured to the watertight after bulkhead by Barrymount shock mounts. When the missile was in the vertical or drop attitude, the equipment was suspended on the Barrymounts and was held rigidly in the tracked structure by four wing nuts on threaded steel rods. The suspended structure was isolated from the shell of the missile by suitable rubber pads. The equipment rack was easily removable for access to the recorder and electronics for calibration and changing the tape supply prior to test drops. Figure 5 is a view of the electronics rack partially inserted into its tracked supporting frame in the missile.

PRINCIPLES OF OPERATION

Data Recording System

The recorder was a special modification of the Stancil-Hoffman standard Model M8 Minitape Recorder. This recorder used 1/4 in. tape and operated at 15 in./sec. The two record-track widths were 0.100 in., separated by 0.062 in. The recording heads were shielded to reduce crosstalk. The recorder motor was driven at 3600 rpm; speed control was obtained by using a centrifugal governor which varied the shunt-field current to keep the speed constant. A 12-volt Sonotone sintered-plate nickel-cadmium battery supplied power to both the motor system and the amplifier system of the recorder.

Each of the two channels of the recorder's electronic system consisted of a preamplifier, Model AC23, and a record amplifier, Model AR23. A jack was provided by which the output of a single full-track playback head could be monitored. This output provided a signal to an external playback amplifier during the checkout and calibration procedure described below.

The two transistorized AC23 amplifiers had gains of approximately 85 db and input impedances designed for 1000 ohms. Each had a push-pull stage, using four RCA 2N105 transistors, transformer coupled to a Texas Instrument 2N185 transistor. The automatic gain control employed in the AC23's of the original M8 model was disconnected for preliminary tests.

The two Model AR23 recording amplifiers fed audio signals mixed with a 60-kc bias from the AC23's to the recording heads. The input to the AR23 was approximately 0 dbm at less than 1000 ohms impedance. The output impedance of the amplifier fed a recording head of approximately 3.5 mh. The 60-kc bias appearing across the head was 7.5 volts.

Wow and flutter for the recorder was found to be 1% rms, using the standard test. The signal-to-noise ratio, measured at 400 cps, was determined to be 31 db. The signal level for this test was chosen to be the 3% distortion point (including nonlinear distortion, hum, tape noise). The cross-talk ratio between the record tracks was measured to be 55 db.

Channel 1 of the recorder was used to record the audio information from one of the hull-mounted hydrophones. The second hydrophone, mounted diametrically opposite the first on the cylindrical midsection, was connected to the input of channel 2 on the tape recorder. A frequency-modulated signal containing depth information and operating with a carrier frequency of 13.5 kc was also recorded on channel 2. This depth information originated in a pressure transducer and associated circuitry.

Depth Measurement Circuitry

Channel 2 was specially adapted by appropriate filtering to record flow-noise data in the region below 6 kc and to record depth and time information in the region above 10 kc, using a frequency-modulated 13.5-kc carrier. A functional diagram of the depth-measurement circuit is shown in Fig. 6.

From the recorded pressure and time information the depth and velocity of the missile was determined for any time during the missile's fall. The carrier frequency of 13.5 kc was modulated by a 200-cps voltage the amplitude of which was decreased linearly with water pressure by means of the pressure potentiometer (Fig. 6). The 200-cps frequency which modulated the 13.5-kc carrier was used as a time reference by demodulating the tape information and counting the number of cycles during any desired data period. The amplitude of the 200-cps voltage from the pressure potentiometer determined the frequency deviation of the FM carrier. Upon demodulation, the 200-cps amplitude was proportional to pressure and therefore to depth. Velocity and acceleration were calculated from depth and time data.

The 200-cps oscillator, the 20-db amplifier, the 14-db amplifier, and the varicap modulator were designed and built by this laboratory. Detailed schematics of each of these units are shown in Figs. 7-10.

The most critical unit in the depth-information system was the 200-cps oscillator. The frequency of this oscillator had to be an accurate 200-cps. The final design showed an accuracy of 1% in laboratory tests. For accurate depth information it was necessary that the amplitude of the oscillator remain stable from the time of the field calibration (described later in this section) to the end of the drop. Small changes in oscillator amplitude from day to day were of no concern.

The pressure potentiometer was a commercial transducer, Type 47152, produced by G. M. Giannini and Company. The modulator utilized varicap capacitors in parallel with the tuned circuit of the modulator oscillator. Voltage from the pressure potentiometer, amplified by 20 db to put it within the varicap's linear range, was inserted across the varicap capacitors. The varicap capacitance was proportional to the voltage across it, hence the tuning of the modulator was proportional to the 200-cps oscillator's input amplitude.

Deviations in linearity of the pressure transducer and the varicap characteristics were not sources of error because of the field calibration procedure used. During this calibration a separate potentiometer which accurately simulated the pressure potentiometer was inserted in its place. The potentiometer was hand set to simulate various pressure levels, and the corresponding 200-cps signal amplitudes were recorded on the tape. The simulating potentiometer accurately duplicated the pressure transducer in resistance variation. Precision resistor steps were used, and the duplication was accurate to ± 1%.

The high- and low-pass filters used in channel 2 recording were United Transformer Company Type HML 12000 and LML 6000. An attenuator pad was connected to the 600-ohm impedance level of the 14-db output amplifier. This amplifier raised the combined signal level up to the necessary 0 dbm record level.

Automatic Recovery Mechanism

The recovery-system mechanism consisted of the equipment shown in Fig. 11; this was mounted in the afterend of the cylindrical midsection of the vehicle (Fig. 12) and in the tail section (Fig. 3). When the tail section was mounted in place, the heads of four toggle clamps, one of which is A (Fig. 11), bore against the top inside of rim A (Fig. 3) of the bouyant tail section, thereby holding the tail tight against the midsection (Fig. 12). In the locked-down attitude the levers of the toggle clamps were then horizontal and held down, bearing against the bottom of disk C. Disk C is an integral part of locking unit O, which is moved downward against spring F during loading. The tail was thus held securely in place against the midsection by means of the four toggle clamps. The locking unit O (Fig. 11) was in turn held down by toggle clamp D, the head of which bore against the bottom of slot E of the locking unit O. This required that spring F, sliding with the locking

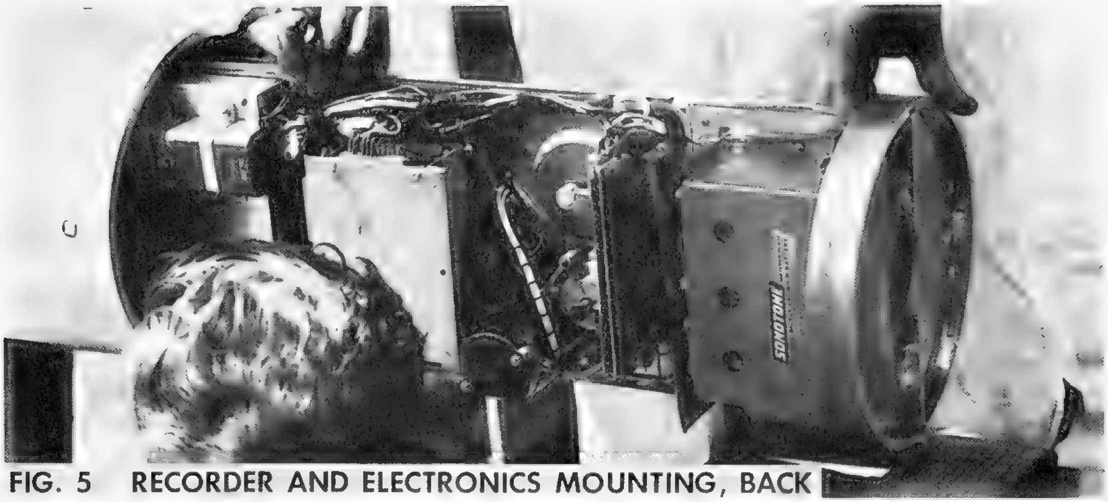

FIG. 5 RECORDER AND ELECTRONICS MOUNTING, BACK

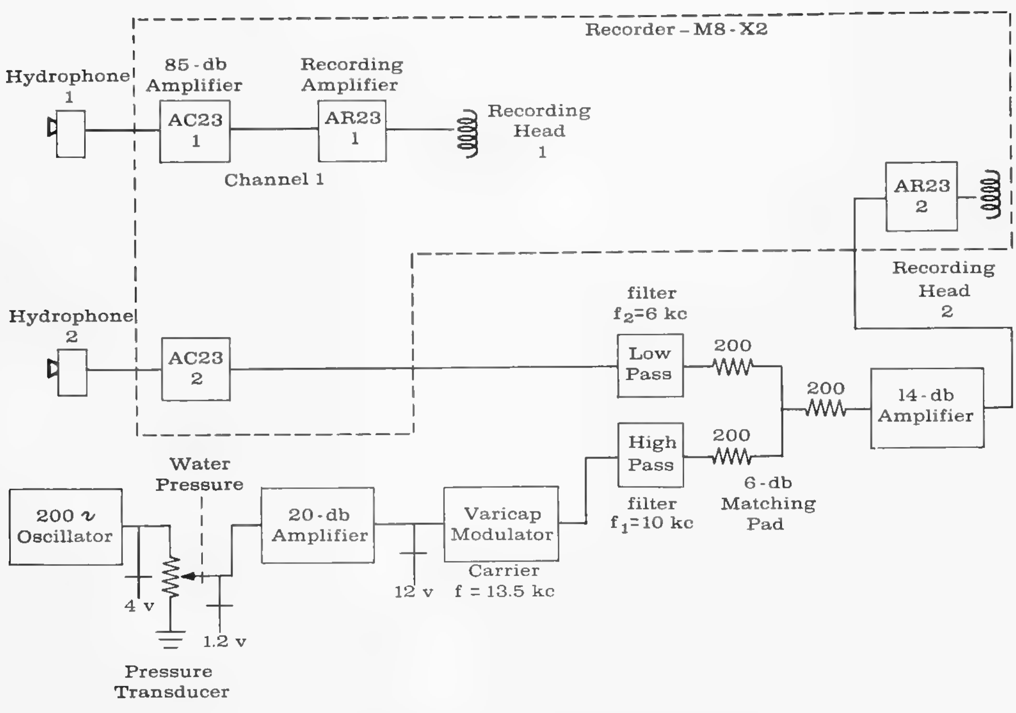

FIG. 6. DIAGRAM OF DEPTH-DATA CIRCUITRY

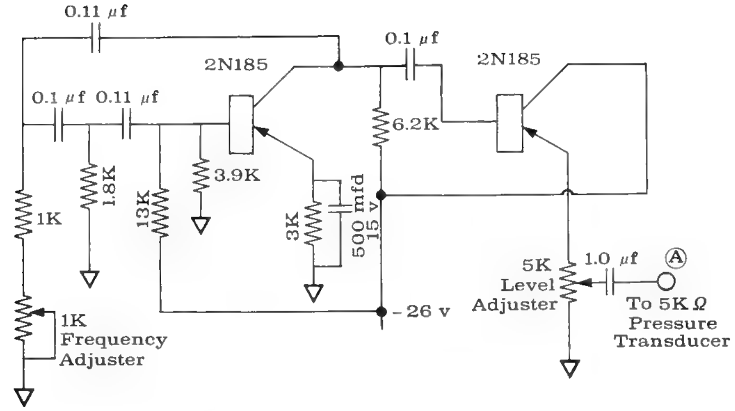

FIG. 7. 200-CPS OSCILLATOR AND GROUNDED COLLECTOR STAGE

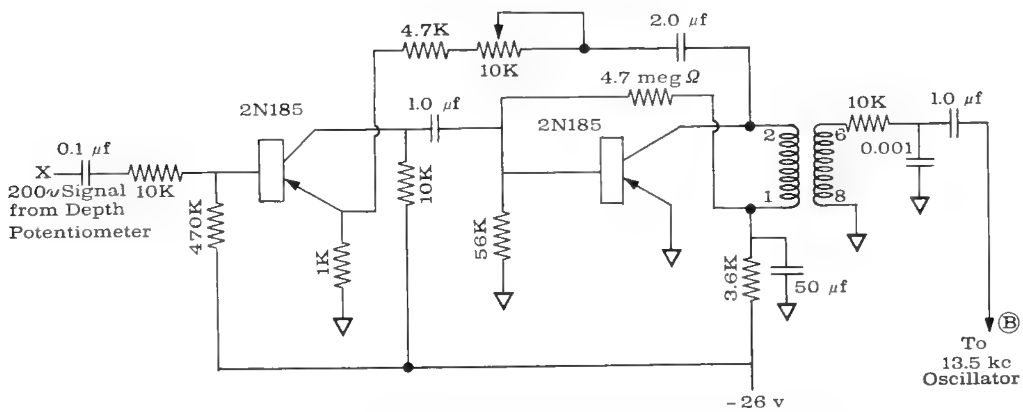

FIG. 8. 200-CPS FM MODULATOR AMPLIFIER, -20 DB

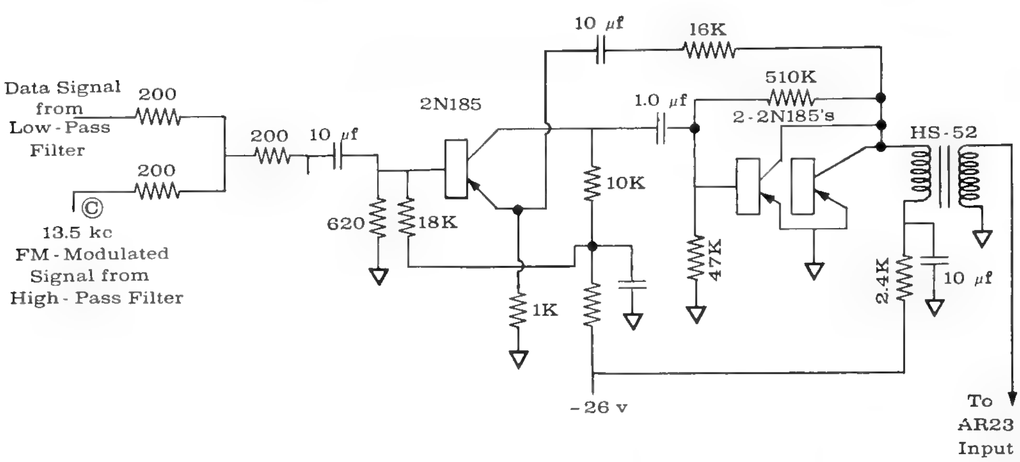

FIG. 9. DATA- AND DEPTH-SIGNAL AMPLIFIER, -14 DB

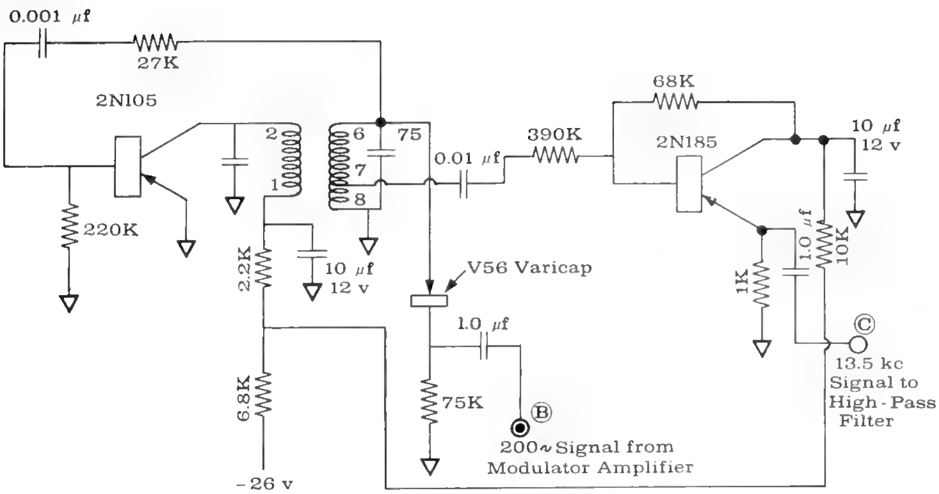

FIG. 10. 13.5-KC OSCILLATOR AND GROUNDED COLLECTOR STAGE

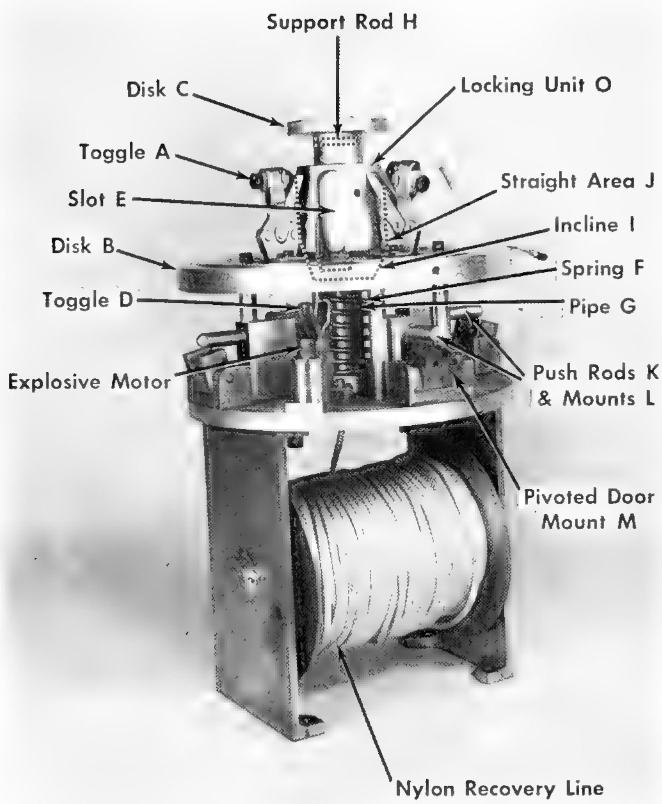

FIG. 11. RECOVERY MECHANISM

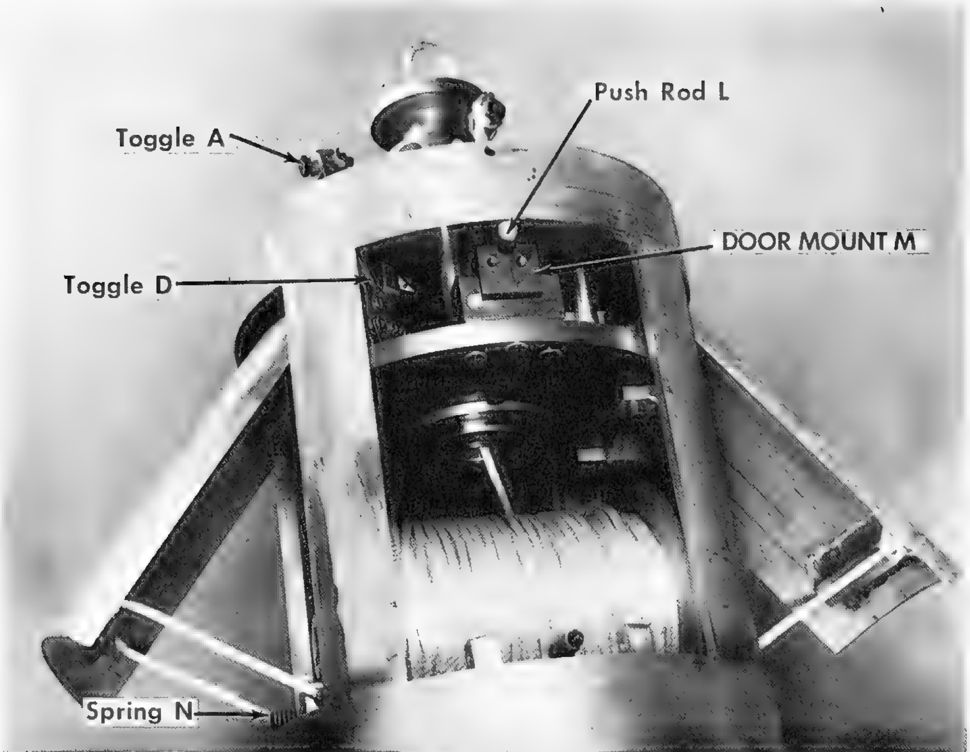

FIG. 12 RECOVERY MECHANISM IN PLACE. Drag fins open, one removed

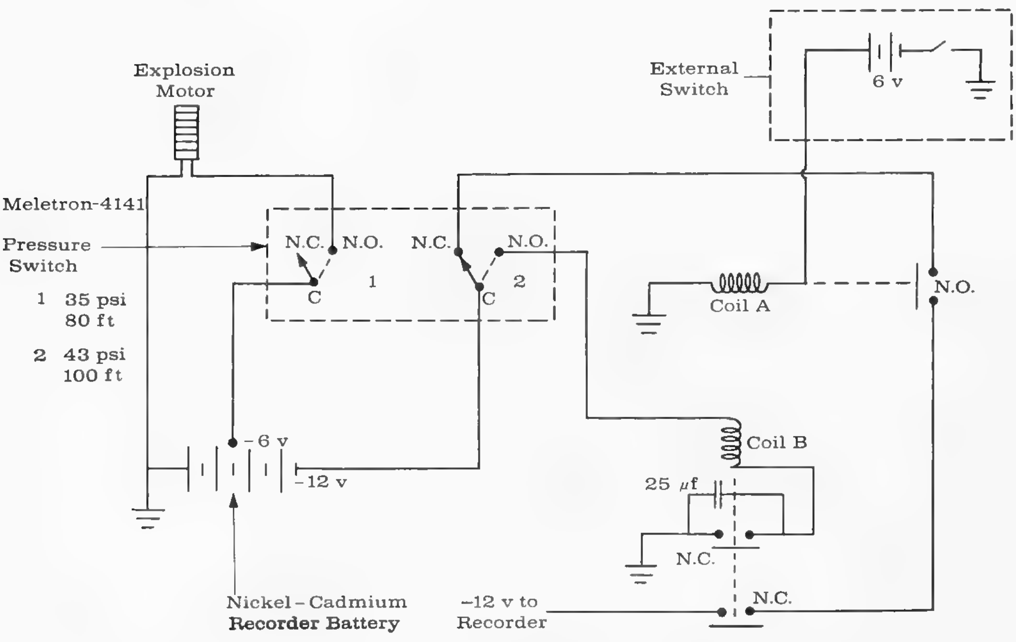

FIG. 13. RECOVERY CIRCUITRY

unit along steel pipe G, be compressed completely. Spring F was compressed by hydraulically loading a long, thin, slotted steel rod which fitted over support rod H in the locking unit and passed up through the center fluid pressure equalizing tube through the tail. When spring F was completely depressed, toggle D was closed manually through one of the door ports. "Loading" the tail was done in the launching frame with the missile in the launch attitude.

In Fig. 12, the drag fins are open and one is removed. Toggle clamp D, the key element in the tail-locking assembly, was released when the explosion motor, mounted as shown, received a d-c electrical impulse from a pressure switch. On release of toggle D the spring quickly expanded, pushing up the locking unit which released the four toggle clamps and imparting an initial thrust to the tail section.

The locking unit also controlled the doors or drag fins. At the time of "loading" three of the doors which were secured to their mounts were locked into place. The fourth was fixed in place after loading and locking toggle D. The doors were closed by push rods K, forced outward by the inclined surface I, acting against their inside upper edge. Each door was fastened by two bolts to a mount M which revolved vertically around a pin. The force exerted on the door by the push rods above the revolving mounts kept the bottom of the doors locked flush with the surface of the missile by simple lever action. The push rods were forced outward by incline I as the spring and locking unit were forced down under load. In the locked position the push rods were pressed between the straight area J and their contact points at the tops of their respective doors. Upon release of the spring F, push-rod force was released from the doors, or fins, and they were snapped open by the action of spring N (Fig. 12) against their bottom inside edge. The fin opening angle was restricted (Fig. 12). The position of the closed doors was kept to close tolerance and was critical because of the outside surface had to be flush, and the doors tightly held. Any door rattle or protrusion of the door edges above the missile surface during fall would distort the hydrodynamic-flow-noise data.

Recovery Circuitry

The recovery circuitry served two functions:

(a) It applied a 6-volt signal across the explosion motor when the missile reached a predetermined depth, thus initiating the tail-releasing sequence.

(b) It shut off the recorder at another predetermined depth to keep the recorder from loading the nickel-cadmium battery during the time of missile recovery.

Figure 13 is a complete schematic of the recovery circuitry. The main controlling circuit element was a Meletron Model 4141 pressure switch. Switch No. 1 of the pressure switch was set at 35 psi or 80 ft. When the missile reached a depth of 80 ft, the normally open contact closed and the explosion motor was set off. Water pressure reached the switch through a hydraulic hose from the water-filled afterend of the cylindrical midsection of the missile, which acted as an accumulator.

A few seconds prior to each drop of the missile, the recorder was turned on by the external switch (Fig. 13). This energized the normally open relay, and closed and mechanically latched it. Through this switch, 12 volts was fed to recorder. When the missile reached 100 ft the normally open contact of Switch No. 2 closed, shutting off the recorder. A second coil was used to keep the recorder off during the recovery of the missile as it was returned to lower pressure. Coil B is energized long enough to throw the normally closed contacts open and latch the relay mechanically in the open position. This terminated the 12-volt recorder supply. By cutting off the current to the coil, the drain of current from the 12-volt battery was stopped. The 25-μ f condenser prolonged the current pulse through self-cutting coil B.

Checkout and Calibration Procedures

A calibration and circuit test unit (Fig. 14) was designed and built for use in the field. This unit included a VU meter, the AP23 playback amplifier, a pressure-transducer simulator consisting of a potentiometer with precision resistor steps, two inputs to the recorder amplifiers bypassing the hydrophone inputs, control switches, and a 27-pin Jones plug connector. During the checkout the Jones plug from the checkout unit was inserted into the missile electronic system in place of a similar Jones-plug dummy connector through which the circuits were connected during normal operation.

The calibration-test unit provided means to determine:

Fig. 14 CHECKOUT AND CALIBRATION UNIT AND WAND

(1) The voltage of the 12-volt nickel-cadmium battery under load.

(2) The voltage of the 26-volt depth-circuit battery.

(3) The frequency and voltage level of the 200-cps oscillator in the depth circuit.

(4) The presence and level of the 13.5-kc carrier in the depth circuit.

(5) The operating condition of the recorder and its four amplifiers.

Test-unit information was obtained visually from the VU meter. A four-position selector switch and a visually monitored VU meter permitted reading the 12-volt, 200-cps and playback signal levels. The 12-volt, 26-volt, and 200-cps levels were put directly on the VU-meter terminals through an appropriate series resistance so that the meter read in decibels above or below the design level.

With the VU-input selection switch in the "playback" position, the AP23 playback-amplifier output was monitored. The VU meter which indicated the recorded signal of all the channel signals combined or of channel 1, channel 2 audio, or channel 2 FM alone was recorded. The desired signal was selected by properly setting a four-position "record monitoring" switch which controlled the B+ voltages to the amplifiers in channel 1, channel 2, and the depth circuit. This arrangement provided a separate visual indication of the recording of any signal on channel 1 or channel 2 audio inputs or of the recording of depth-circuit signals.

A "remove 200 cycles" button made it possible to record the unmodulated 13.5-kc carrier signal on "channel 2 FM" and obtain a visual indication of the "clear" carrier recorded level on the VU meter.

The hydrophone inputs were bypassed and had no connection to the electronic system during checkout. Prior to launching, the continuity of the complete system, from the hydrophones to the tape, was tested.

The calibration precedure performed two important functions. First, reference-signal levels at 1000 cps and 8000 cps were recorded on the tape by means of an oscillator wand and the proper attenuation pad. Second, a calibration of the depth-measuring circuit was made by feeding channel 2 FM of the tape a calibrating signal.

The insertion of the checkout unit into the electronic system replaced the pressure-transducer potentiometer by the checkout unit's pressure-transducer-simulator potentiometer made up of precision resistors accurate to ± 0.5 ohm. The simulator passed signal levels corresponding to actual pressures of 0, 15, 30, 37.5 and 45 psi used to modulate the 13.5-kc carrier. Each of the resulting FM signals was recorded during the checkout procedure by setting the record-monitor switch to "channel 2 FM," the VU-meter monitor switch to "playback," turning on the recorder, and setting the simulator to various pressure levels by hand.

The record-level calibration signals with which to compare hydrodynamic-flow-noise data were recorded during the checkout procedure by inserting the oscillator wand (a small battery-powered oscillator for field use) connected to an attenuation pad into the channel 1 and channel 2 checkout-unit inputs. The wand and pad fed to the recorder amplifiers reference signals of -75 db on a 1-volt reference at 1000 and 8000 cps. Only the 1000-cps signal was recorded for channel 2 audio because of the 6000-cps cut-off of the audio portion of this channel. By comparing the hydrodynamic-flow-noise level to these signal levels on the tape, an accurate value of the hydrodynamic-flow-noise level was obtained.

Launching and Recovery Procedure

Preceding the actual drop, the missile midsection was mounted horizontally in the launching frame (Fig. 2) and the electronics partially inserted by sliding the electronics rack along the tracks mounted inside the missile midsection. The checkout procedure and calibration already described were then performed, the installation of the electronics rack was completed, and the missile was rotated to a vertical attitude in the launching frame. The missile nose section was threaded onto the midsection and the tail mounted and locked by means of a hydraulic jack located at the top of the launch frame. The jack loaded the release spring by forcing down a long steel rod which slides down the middle of the tail and fits over the support rod mentioned previously. The missile completely assembled, was held in the launch frame as shown in Fig. 1. The launch frame and missile assembly were lowered through the center of the launching platform by means of a winch and steel cable until the upper end of the launch frame was just below the surface of the water.

The missile was released on opening the

doors by which it was held at the base of the launch frame.

After the drop, the tail section was recovered and the recovery line secured to a winch. The missile was then pulled back up into its launching frame. The doors holding the missile were then shut and made safe by the insertion of a pin in the toggle clamp. The entire launch frame and missile were then lifted to the deck level, secured, and readied for the next drop.

CONCLUSIONS

The results of tests conducted by the Acoustics and Seismics Laboratory indicated that the experimental approach using a free-falling vehicle was sound and that this type of instrument could be valuable in acquiring information to increase the present knowledge of the physics of hydrodynamic-flow noise.

This work was supported by the DTMB and a contract administered by the Office of Naval Research.

ACOUSTICAL NOISE MEASURING BUOY WITH DIGITAL DATA RECORDING

by DR. T. F. HUETER, D. M. BAKER, and J. T. SHAW
Minneapolis-Honeywell Regulator Company
Ordnance Division, Seattle Development Laboratory
Seattle, Washington

ABSTRACT

An ambient noise measuring system is being developed for use in a deep-water moored buoy. The acoustic spectrum between 50 and 400 cps is measured at four discrete frequencies and sampled at regular intervals. The analog signal is converted to a binary digital code and photographically recorded for later processing.

A qualitative measurement of sea state is made during each measurement cycle, permitting a correlation between wave height and ambient noise to be accomplished.

Auxiliary devices are provided which effect buoy recovery upon reception of a coded acoustic command signal. The buoy is designed for operation at depths to 1000 feet with a duration on station of three months. Solid-state devices are used where possible to keep power consumption to a relatively low value.

INTRODUCTION

Generally, the variations in the ambient noise spectra at frequencies above 500 cps can be identified with one of several sources which happen to predominate at a given time and location. Examples of these sources are marine life, precipitation, ship traffic and man-made noise, seismic sources, and the wind-generated agitation of the sea surface itself. The well-known Knudsen curves demonstrate the dependence of acoustic noise levels on sea state over the range of frequencies for which the curves have been calculated.

In the case of frequencies below 500 cps, however, investigations have shown that the dependency of noise levels upon surface conditions decreases as the frequency is lowered and that below 100 cps the variations may be independent of that source.

The development of a remotely operated buoy system for the measurement of ambient noise in the ocean could be expected to provide a useful tool in furthering the investigation of mechanisms involved in the low-frequency acoustic phenomena. The use of a submerged buoy system for such a purpose offers several important advantages as a "listening platform" from which to make low-level measurements. A submerged buoy can be an inherently quiet platform, free of unnatural disturbances and noise produced by extraneous sources. The mooring problem is simplified and the probability of buoy loss reduced due to the absence of strain on the anchoring system created by storms and high sea states. A degree of freedom from possible damage to the system from encounters with surface traffic is also realized.

Electrical power derived from storage batteries or other low voltage dc power sources results in an electrically quiet environment in which to operate low-level, high-gain amplifier circuitry. The absence of interfering electrostatic and magnetic fields associated with systems operating from high voltage ac power sources or with systems which employ long lengths of electrical cable is a distinct advantage in reducing extraneous electrical noise. This results in better signal-to-noise ratios and increased dynamic ranges in measurement circuitry.

The Office of Naval Research has sponsored the development of such a buoy by the Minneapolis-Honeywell Regulator Company. The buoy system to be described is intended for use in the open ocean for the measurement and recording of ambient noise levels at specific frequencies in the range between 50 and 400 cps.

ACOUSTIC MEASUREMENT BUOY SYSTEM

The acoustic measurement buoy is designed for continuous remote operation for periods up to three months. Simultaneous measurements of wave height and the acoustic spectrum level in discrete bands at center frequencies of 50, 100, 200, and 400 cps are made at predetermined intervals and photographically recorded on 35-mm film. The acoustic levels are recorded in digital form by use of a 6-bit binary coding system.

The acoustic measurement buoy is composed of seven basic subsystems: (1) buoy hull and mooring system, (2) timing and programming system, (3) acoustic measurement system, (4) wave-height measurement system, (5) data conversion and recording system, (6) recovery system, and (7) the electrical power system.

The basic buoy hull is a cylindrical aluminum tube (Alloy 6063-T5) approximately 16 inches in diameter by 7 feet long with a one-half inch wall thickness. The pressure capability of the hull design allows for a 1000-foot submergence. A net positive buoyance of approximately 150 pounds is obtained including all internal components. Calculations made for assumed conditions of buoy attitude, mooring line length, and wire diameters indicate reduced drag and, consequently, the least heeling angle is obtained with the buoy moored in a horizontal position. Minimum heeling angle is desired to obtain satisfactory operation of the wave-height sensor which in the existing design has a depth limitation of 80 feet. Provision is made for the attachment of buoyance adjustment tanks and fairings at nose and tail.

The noise hydrophone mount is attached to the underside of the main hull with provisions for suspending the hydrophone at desired depths below the hull as required. The wave-height measuring transducer is mounted on top of the hull with provisions for buoying the transducer above the main hull if desired.

A taut-wire mooring system is used which employs a concrete block anchor and anchor line attachment bridle at the buoy end. An explosive anchor release is incorporated in the anchor line at the buoy end which effects buoy release and return to the surface under control of the recovery system.

Access to the buoy interior is gained through an "O" ring sealed end cap held in place by a flanged coupling. Electrical connections from the buoy interior to the hydrophone and wave-height sensor are made by means of Marsh Marine bulkhead fittings in the end cap.

The measurement circuitry, data recording system, and electrical power supply are contained as a modular assembly which can be removed from the buoy hull in one piece. This arrangement permits simplified bench testing and servicing procedures. The equipment components are mounted on coaxially aligned stacked circular decks and the complete assembly is held in place within the hull by means of integral guide rails.

TIMING AND CONTROL SYSTEM

An electrically wound spring-driven clock (Massey Dickenson) provides the basic measurement sampling interval and control of buoy operation by means of the programmer. The accuracy of the clock is ±10 seconds per day. The programmer provides for the sequential application of voltages to the measuring systems and the operation of the photo-data recording system through a series of motor-driven cam-operated switches. Adjustable contacts on the main clock trigger the programmer into a measurement cycle once each sampling interval.

During a measurement cycle, power is first applied to a thermal delay relay by the clock which allows a 20-second warmup period for the noise-measuring amplifiers. In series and simultaneously with the end of the warmup period a 60-second solid-state delay relay is actuated. During the delay period, the acoustic integrations are performed. Closure of the 60-second solid-state delay relay at the end of its cycle actuates the programmer which performs all subsequent functions, including channel selection, comparison for each channel, sea-state sensing, and frame shift of the camera. At the end of the program, the system is returned to its initial standby state.

The programmer also controls a predetermining counter. The counter reading is recorded on each film frame along with the acoustic noise and wave-height data. When the predetermined timing interval has been reached, the counter contacts energize the acoustic command recovery system, thereby initiating the recovery cycle at the end of the buoy operational period.

ACOUSTIC MEASUREMENT SYSTEM

The acoustic measurement system consists essentially of the hydrophone and associated preamplifier, the bandpass filter and matching amplifiers, and the rectifier/integrator circuits. All amplifier and integrator circuits are transistorized with the exception of the input stage of the hydrophone preamplifier.

The measurement technique involves amplification and selective filtering of the acoustic signal. The output of each filter is rectified and integrated to produce one minute averages of the sound pressure in four, 1/3 octave bands at 50, 100, 200, and 400 cps.

The hydrophone signal is first amplified and shaped by a passive filter with bandpass from 30 to 600 cps. This filter serves to eliminate frequencies outside the band of interest and reduce the possibility of amplifier overloading. The bandpass filter output is then applied to four, 1/3 octave band filters connected in parallel through impedance matching amplifiers. The output of each 1/3 octave filter is matched to identical rectifier/integrator circuits through variable gain linear power amplifiers. The averaged spectrum level output of the integrator circuits is stored in low-loss tantalum capacitors (General Electric Type 29F1074).

The hydrophone is an omnidirectional barium-titanate unit with a sensitivity of -85 db reference to one volt per microbar. When terminated in a 20-megohm load, the response is essentially flat between 10 cps and 2 kc.

The hydrophone signal is amplified in a hybrid preamplifier stage which provides a voltage gain of 280. A vacuum tube is employed in the input stage in order to achieve the necessary high input impedance and low equivalent noise input. A Sylvania 5904 subminiature triode with a 24-volt filament and plate supply eliminates the need for a special vacuum tube plate supply. This tube is powered directly from the transistor amplifier supply. The equivalent noise input of the preamplifier referred to the input grid over a 600-cycle bandpass is less than one-half microvolt.

The voltage gain from the hydrophone preamplifier input to the rectifier/integrator circuit is approximately 100,000, and the dynamic range of the voltage amplifier and filter channels up to the rectifier/integrator input is 95 db. The rectifier/integrator circuit has a useable dynamic range of 40 db with corrections for nonlinear operation and is linear over a 30-db range.

WAVE-HEIGHT MEASUREMENT

A qualitative measurement of wave height is accomplished by means of a small transistorized depth sounder operating at 198 kc. The transducer is mounted in a small buoy which can be either fastened directly to or floated upward above the main buoy hull. The transducer beam is directed upward and uses the underside of the air-water interface as the reflecting surface. The rotating neon lamp wave-height indication is converted to a linear display providing a measurement of the wave-height in one-foot increments. The wave-height data is displayed in the data photo matrix along with the acoustic digital display and main counter reading. The wave-height recording extends for a period of 15 seconds during each measurement cycle.

DATA CONVERSION AND PHOTO-RECORDING SYSTEM

The analog-to-digital conversion of the acoustic level measurements is recorded on 35-mm film in digital form. The digital encoding is accomplished by a 12-bank, 52-point stepping switch and a matrix of neon lamps. The lamp matrix consists of four rows of eight lamps. Six lamps in each row are used in a six-bit gray code. The seventh lamp is used to provide a parity check, and the eighth lamp provides for channel identification.

Seven banks on the stepping switch are used to provide the grounding pattern for the binary code on the lamp matrix corresponding to the switch wiper arm position as it steps through the 52 levels. One bank contains a precision resistor divider network providing one db step changes in the voltage level picked off by the wiper. Therefore, the voltage picked off the divider network at any switch level is represented simultaneously by the binary digital code established in the neon lamp matrix through the grounding pattern.

The voltage picked off the precision resistor divider network in the stepping switch is compared to the voltage stored in the integrator capacitor. As the stepping switch operates, the divider voltage eventually equals or slightly exceeds the capacitor voltage at some particular switch level. At the balance or crossover point, the voltage comparator circuit discharges a capacitor through the neon lamp matrix. The binary code corresponding to the integrator capacitor voltage is exposed on the film by the flash of the appropriate lamps.

The programmer selects and applies each integrator output sequentially to the voltage comparator and the corresponding row in the digital matrix. Each film frame, therefore, contains the digitized spectrum level from each of the four bandpass filters.

RECOVERY SYSTEM

Buoy recovery will be effected in three phases. Assuming the general situation in which the buoy is moored in the open ocean, the first phase in recovery is essentially a navigation problem in which the recovery ship must return to the general area where the buoy is moored. The first stage is accomplished by use of ordinary navigational methods (LORAN, DF bearings, celestial navigation, radar fix, soundings, etc.), employing whichever methods are best suited to the particular conditions at hand. The second phase in recovery results in release of the buoy and its return to the surface in a free-floating condition accomplished by an acoustic interrogation from the recovery ship. The third recovery phase required localization of the buoy on the surface and subsequent retrieval by the ship.

Each phase in the recovery procedure requires the solution of particular interrelated problems in order to achieve reliable operation. The navigational accuracy requirements are determined primarily by the acoustic interrogation ranges which can be achieved and secondarily by the localization and visual sighting aids employed when the buoy is on the surface.

The buoy contains two separate and electrically independent anchor release circuits providing three modes of actuation. In normal operation, the main buoy clock/programmer actuates the acoustic command receiver circuits at the end of the timed measurement period. The acoustic command receiver circuit is energized for a period of approximately three days during which time reception of the correct acoustic code will fire the anchor release. The enable period is designed to be adjustable and can be set anywhere between 9 and 99 hours in increments of 10 hours. If the proper acoustic code has not been received at the end of the enable period, the main buoy programmer will fire the anchor release.

An additional separate timer powered from its own battery pack will also fire the release mechanism through completely independent circuits, providing backup to the acoustic command receiver circuit in the event of a failure in the main battery or electrical control system. The secondary timer will be set to fire after runout of the acoustic enable period has occurred.

The acoustic command receiver function provides two valuable features in the recovery system. In normal operation, the recovery ship is not required to be in a precise position at a precise time to insure that the buoy will surface relatively close at hand. Therefore, an allowance is made for the routing emergencies and delays which continually arise such as equipment breakdown or inclement weather conditions. Secondly, the relatively short acoustic command range provides a higher probability that the buoy will surface within visual sighting range. The backup circuit provides for eventual buoy release and return to the surface in case of a failure in another part of the recovery system.

The acoustic command receiver responds to a pair of accurately timed signals provided by small explosive charges (No. 6 blasting caps). This system was chosen because of the simplicity and inexpensiveness of the signal generator requirements. The recovery ship does not need a specialized transmitting transducer and associated electronics.

Provision is also made against actuation of the release mechanism by random background and/or ship noises. Decoder circuit, therefore, is incorporated in the receiver design to discriminate against background noise, reducing the probability of false triggering.

POWER SUPPLY

Electrical power is supplied by a Yardney silver-cadmium battery assembled from 22 YS-40 units in a series connection. This combination supplies 960 watt-hours of electrical energy which is sufficient to make 1600 measurement cycles leaving a 20-percent battery charge in reserve.

DEEP TRANSDUCER DESIGN

by R. P. DELANEY
The Martin Company
Baltimore, Maryland

ABSTRACT

The problem of design of deep sea (10,000 ft) transducers is a severe one particularly from the point of view of maintaining good efficiency without conventional pressure release materials.

The design of the MBP-1 Transducer met this problem by pressure equalization. This projector has been operated at 10,000 ft deep with 50% efficiency at 2700 cps. Similar transducers designed for lower frequencies have displayed similar performance. Design data and performance of these transducers are discussed.

INTRODUCTION

The title of my paper is somewhat misleading in that I intend to confine my remarks to a particular type of transducer, namely, configurations based on ceramic cylinders. Since 1958 The Martin Company has designed, built, and tested a number of projectors and hydrophones suitable for employment at great depth (below 5000 ft). I have selected 4 of the more successful configurations to describe today and I shall try to point out how and why they work in order to assist others in avoiding pitfalls attending this field.

When faced with a new environment and new design problem, it is a common approach to take a familiar design suitable for another environment and seek to adapt or modify it for the new environment. This tendency probably accounts for our use of ceramic cylinders when faced with the problem of designing hydrophones and projectors for deep use, because for near surface applied ceramic cylinders are a very common transducer type. Operated in the fundamental circumferential mode as projectors, the outside surface of the cylinder is commonly exposed to the medium by means of a rubber boot while the inside wall is pressure relieved with air or one of the common pressure release materials, celltite rubber or corprene. They are a simple design acoustically and mechanically and a very effective one. Hydrophones of this design exhibit desirable broad band characteristics below resonance and projectors when using the stave construction methods of Mr. Green of NEL show excellent efficiencies. However, this rather pleasant situation is upset when the static pressure of the deep ocean environment is introduced. On a theoretical basis the wall thickness of ceramic cylinders can be increased to the part where an air backed hydrophone becomes possible. We have never been able to build an air backed unit which survives long periods under pressure. We have had units last 6 weeks at 9000 psi only to implode. We therefore turned our attention toward the development of configurations which are pressure equalized using oil or water at ambient pressure on the back or inside of the cylinder to reduce the stress levels in the ceramic, and using one means or another to prevent the loss of sensitivity (about 15 db) which occurs when the inside is acoustically short circuited.

HYDROPHONE DESIGNS

I should now like to describe two hydrophone configurations which we have successfully tested and used. I would first like to acknowledge a debt of gratitude we owe to the Hudson Laboratories who first developed the equalization method described below and who were most generous in their advice and assistance. Mr. Oberlin has discussed the Fixed Acoustic Buoy installed and the first hydrophone I shall describe was designed for the FAB. The active element is a PZT-5 cylinder 2 in. tall by 1.5 in. OD and 0.25 in. wall thickness. The inside of the cylinder is pressure equalized with castor oil which is connected to a reservoir outside the cylinder via a small orifice in the rigid end caps. Mr. Ted Madison of General Electric gave a paper in the Fall of 1960 at the Under Water Acoustic Symposium on the theory of operation of such a device. It is based on Helmholtz Resonator theory where the orifice is transparent at frequencies below the resonance frequency of the orifice--chamber combination, so that the inside and outside are in static equilibrium; while at frequencies above resonance the orifice is opaque and the acoustic pressure will not be transmitted. In such a transducer the main design problems are to make the cylinder large enough for the desired sensitively, design the orifice and chamber to push the Helmholtz Resonance below the band of interest and yet have the cylinder small enough so that its lowest length resonance considering the mass loading of the end cap is above the upper end of the desired frequency band. I mention the length resonance because the mass loading effect of the end caps will often reduce the length resonance below the fundamental circumferential mode resonance. Slide 1 gives an idea of the FAB hydrophone configuration. Slide 2 is the receiving response of the FAB hydrophone.

FAB HYDROPHONE CONFIGURATION

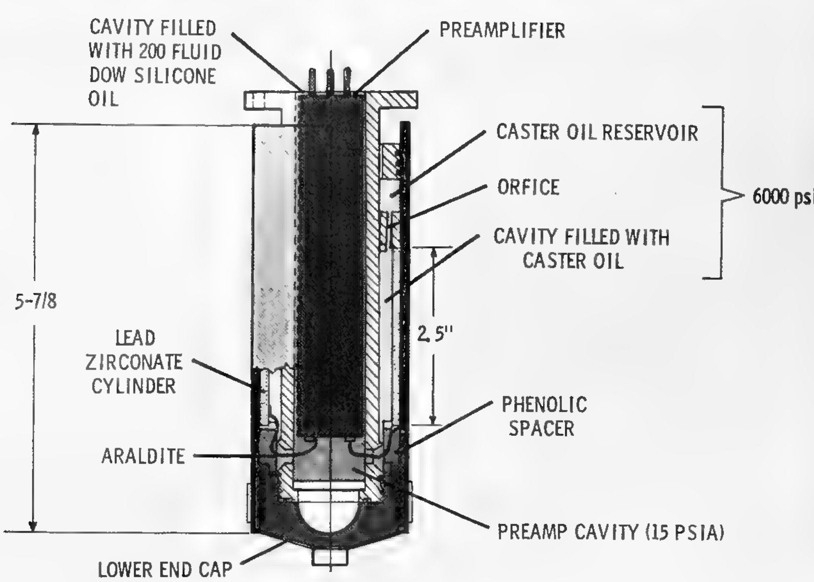

ASSEMBLY STAGES--FIXED ACOUSTIC BUOY HYDROPHONE

The FAB hydrophone is sufficient to its task and showed no change in sensitivity with pressure to 9000 psi and has since performed effectively over the last 9 months. However, its sensitivity was not all one would wish and its upper frequency limit was too low for many applications. We therefore embarked on a hydrophone development program utilizing the same basic equalization system but seeking ways to increase the sensitivity and to drive down the Helmholtz Resonance and to increase the basic cylinder resonances. The design of one of the resulting hydrophones is shown in slide 3 and whose response is shown in slide 4. As can be seen, this hydrophone is quite an improvement on the FAB unit. The use of a very small orifice and a smaller cavity reduced the frequency of the Helmholtz Resonance. The sensitivity of the unit was increased while the cylinder size was reduced by decreasing the wall thickness. The upper resonance was raised by use of a shorter cylinder and aluminum end caps. We also feel we get some increase in sensitivity by the end caps acoustically coupling to the cylinder ends.

PROJECTOR DESIGNS

The projectors I shall discuss are of the pressure equalized segmented cylinder type. The MBP-1 represents the first real experience with the design of an acoustic projector for a very high pressure ambient. Projector design is in general a more difficult problem than hydrophone design because of the necessity for good efficiency. This is especially true in the case of deep transducer design where the back radiation is a problem. In the case of the MBP-1 our approach was to take a transducer mechanism which is basically efficient (namely the large cylinder made up of staves polarized and energized in the circumferential direction) and accept the losses which the lack of pressure release on the inside of the cylinder causes. This was done because of the need for this transducer to series of experiments we carried out with the Naval Research Laboratory under the direction of Mr. Benhannan. The cylinder was 20 in. OD, 9 in. high with a 1 in. wall thickness; the inside was filled with castor oil, the top and bottom plates of the cavity were 1/4 in. steel. The unit is shown in slides 5 and 6. The response of this unit is shown in slide 7. The efficiency of this unit, about 60%, indicates that the back wave and the lack of pressure release causes us no significant problem. The calibration of this unit at 1000 psi shows no change from shallow water measurements and, at sea measurements at depths up to 12,000 ft showed no change in response within the accuracy of measurement. One of the MBP-1 units has been operated for more than 150 hours at depths exceeding 10,000 ft. At the end of this series of tests the unit was recalibrated and shows no sign of deterioration either acoustical or mechanical. We feel that the attainment of such high efficiency in a unit of such simple and reliable design whose performance is independent of depth is a significant step forward in transducer design.

The MBP-2 is an improved version of the proven techniques of the MBP-1 and is shown in slides 8 and 9. It was designed and built by The Martin Company under contract to the Bell Telephone Laboratories. As can be seen from the slide, it uses two rather short rings 4 in. high 0.4 in. thick and 20 in. in diameter. These rings are contained in separate watertight housings. The thinness of the rings has two main effects on the performance. It lowers the mechanical Q and decreases the resonance frequency since the mass loading effect of the medium is a more significant part of the vibrating system mass. These effects can be seen in slide 10. Even though the circumference is the same as that of the MBP-1 the frequency has dropped to 1900 cps and the mechanical Q is only two. The efficiency has dropped to 35% because of the power loading at the lower frequency. Stacking more than two rings should improve the loading and therefore, the efficiency appreciably. A single ring by itself has an efficiency of only 20%. Slide 11 shows the efficiency of the MBP-2 as a function of frequency. The smooth response and low Q shown in slide 10 lead to a transducer which has a useful efficiency over a broad frequency band making it of real value as a general purpose sound projector. This is especially true when one considers that they can be stacked in the vertical to get higher efficiency, better power handling and some directivity. The calibration of this unit has been checked at 1000 psi with no change in characteristics and it is expected that it will be as insensitive to depth as was the MBP-1.

CONCLUSIONS

We have reviewed the design of a number of transducers which are suitable for operation at great depth. Two of these have operated at depth for appreciable time. The design of transducers for this environment presents problems new to the transducer designer none of these problems, however, are insuperable. By the application of known transducer theory and by careful testing under pressure, we feel that the problem deep transducer design can be placed on as firm a foundation as present day shallow transducer design. We have confined our remarks to a cylindrical ceramic type but there are several other configurations under development which fit other needs and applications.

LOCATION OF UNDERWATER OR SURFACE SOUND SOURCES BY MEANS OF COMPUTER-LINKED CABLED-HYDROPHONE FIELDS

by JAMES H. MORRISSEY, Engineering Specialist
Philco Corporation
Philadelphia, Pennsylvania

ABSTRACT

A method is described whereby the position (xyz) of a sound source already detected by multi-static sonar field of hydrophones may be determined, from observed time delays, by means of a data processing algorithm involving pre-solution of two redundant systems of linear simultaneous equations. Geometrically this algorithm, now designated MULCAP (MUlti-station Linear CArtesian Positioning)[1], may be interpreted as sound-source location by means of intersecting planes. The direction cosines of these planes are determined only by the hydrophone-field configuration; they are independent of the position of the sound source and of its velocity.

INTRODUCTION

During pre-proposal effort on undersea surveillance systems, there was developed, early in 1960 by the Advanced Systems Group of the Communications and Weapon Systems Division of Philco Corporation, the new geometry-oriented data-processing technique since designated MULCAP. Although this new data-processing technique is believed to have potential applicability to many systems, radar and sonar, existing or proposed, involving acquisition or tracking of transmitting or reflecting vehicles, its first implementation with realistic input data has occurred in connection with a proposed precision underwater tracking system. An error analysis of MULCAP, with particular emphasis on errors attributable to refraction effects peculiar to the ocean medium, is now being carried out by Philco Corporation under contract with the Naval Underwater Ordnance Station, at Newport, Rhode Island.

The vehicle located by MULCAP methodology is assumed to be a source of sound in either of two senses: (1) it may carry a transmitter, by design or by necessity; (2) it may reflect a transmitted signal. In the former case the inputs are the differences in arrival time among the n fixed receiving stations(hydrophones). In the latter case, where the n stations are assumed to consist of p transmitters and q receivers, the inputs are the pq possible transmitter-to-vehicle-to-receiver propagation intervals. The first case is designated the "passive" mode; the second case, the "active" mode.

Before the advent of MULCAP, systems appropriate to its passive mode were known as "hyperbolic systems" because the mathematical routine whereby the transmitter was located involved the simultaneous solution of quadratic equations representing hyperbolas or hyperboloids, respectively, for plane or space applications. Systems appropriate to its active mode ("pinging", for example) were known, before its advent, as "elliptic systems" because the mathematical routine for determining position coordinates of the reflecting vehicle consisted of the simultaneous solution of quadratic equations representing ellipses or ellipsoids, respectively, for plane or space applications.

MULCAP makes it possible to eliminate completely from the multistation vehicle-location routine the simultaneous solution of quadratic equations. In situations where the hydrophone configuration effectively spans the surveillance space, MULCAP locates the vehicle by a completely linear process, i.e.,by a series of matrix-by-vector multiplications. On the other hand, in those situations where physical or economic factors prevent effective spanning of the surveillance space, MULCAP's linear

Superior numbers refer to similarly numbered references at the end of this paper.

process yields, by itself, the projection of the sound source's location on whatever sub-space is effectively spanned. For example, if the hydrophones constituting the "front end" of a sonar surveillance system must, for reasons of economy, be mounted on a flat portion of the ocean bottom, then MULCAP yields by itself merely the projection on that bottom of the sound source's location. In this case, however, a supplementary routine involving n square-root operations is employed to obtain the necessary depth (z) coordinate from the already-known (xy) coordinates; the supplementary routine does not involve the simultaneous solution of quadratic equations. MULCAP abolishes the latter process from all multi-static location systems; in so doing it opens the way to much more rapid computation of vehicle location. It also eliminates entirely the need for rejection of false roots of quadratic equations.

By virtue of the greater speed of a MULCAP system (resulting from its exclusive use of linear equations), and of the related convenience and ease with which such a system can be established, augmented, and calibrated, data from many hydrophones can be processed almost as easily as that from a minimum number. Precision of vehicle location is directly dependent on the number of hydrophones in the field. Thus any desired accuracy can, in principle, be obtained, provided the economics of the situation permit, merely by increasing the number of hydrophones to a suitable value. Five non-co-planar hydrophones constitute a useful minimum for three-space applications; four non-co-linear hydrophones constitute a useful minimum for planar applications. MULCAP is, however, a location system based in a fundamental sense on the exploitation of redundancy; minimal configurations are, therefore, not to be encouraged. Because of the importance of redundancy to optimum utilization of MULCAP, the principle of least squares plays a central role therein; ten or more linear equations (equations of planes) must be utilized in order to determine three Cartesian spatial coordinates; six or more linear equations (equations of lines) must be utilized in order to determine two Cartesian planar coordinates.

GEOMETRIC INTERPRETATION

The "families" of planes or lines (more generally, of linear loci) which are utilized in this method of sound-source location are, each of them, associated with a distinct transducer-hydrophone or hydrophone-hydrophone pair, depending on whether the active mode or the passive mode is under discussion. If a field of p transducers and q hydrophones is utilized to locate a reflecting vehicle, there are pq families of planes. Similarly if a field of n hydrophones only is used to locate a transmitting vehicle, there are $\frac{1}{2}n(n - 1)$ families of planes. Each member of a family of lines, or planes, is parallel to every other member of the same family; thus each member has the same set of direction cosines as every other member, that set determined by a line joining the two members of a pair of field elements. A vehicle, transmitting or reflecting, in the surveillance space, is located by the common intersection of a set of planes, a "locating cluster", consisting of one plane from each of the families.

Only in a completely noise-free situation will the intersection of the planes, or lines, in the locating cluster be "clean", i.e., only then will all these planes pass through a single point. A residual sum-of-squares measure of the departure of the planes in the cluster from a unique common intersection provides a measure of the precision of vehicle location. In a noise-free situation, this measure is zero.

A crucial step in the series of arithmetic operations which constitutes MULCAP, is the computation of the critical, or true, value of "mean range" (the sum, divided by n, of the n ranges from the vehicle to the n hydrophones). This quantity may be thought of as a variable parameter; its critical value is that value which minimizes the residual sum-of-squares value referred to above.

ALGEBRAIC FORMULATION

Since, in the development of a satisfactory precision underwater tracking system, toward which this presentation of MULCAP is oriented, vehicle acquisition is not a major problem, the presentation of the acquisition-loop portion of MULCAP will be omitted. Furthermore, for the sake of brevity, only MULCAP's passive mode will herein be presented in detail.

Let there be known an n x 1 vector d_o whose n elements are the n ranges to the vehicle from the n hydrophones each diminished by their common mean. Let the squares of these n elements constitute the n elements of b_o. Matrices b_o and d_o contain the information derivable from time-of-arrival data of the sort assumed for passive-mode MULCAP. The initial lack of knowledge of the vehicle's true n ranges is reflected in the initial, quite arbitrary, assumption that their mean value is zero.

Let N be an n x 3 matrix whose elements are the doubles, in (xyz) order, of the n hydrophone coordinates. Let the 3 x m matrix M denote the conditional inverse of ZN, where Z is a systematic differencing matrix of order m x n, where $m = \frac{1}{2}n(n - 1)$. Let the n elements of the n x 1 matrix r denote the n distances, squared, from the origin to each of the n hydrophones.

It is assumed that the field characteristic n x n matrix F defined as follows:

(1) $$F = Z^TZ - Z^TZN(N^TZ^TZN)^{-1}N^TZ^TZ,$$

is stored in the computer.

The mean range ρ_c to the vehicle is computed by means of the formula:

(2) $$\rho_c = \frac{d_o^TF(r - b_o)}{2d_o^TFd_o} .$$

Let the 3 x 1 matrix p_o be computed by means of the formula:

(3) $$p_o = MZ(r - b_o) .$$

p_c, a 3 x 1 matrix whose three elements are respectively the best estimates available of the Cartesian coordinates of the position of the sound source, is, finally, computed as follows:

(4) $$p_c = p_o - (2\rho_c)MZd_o .$$

CONCLUSION

When the locations of underwater sound sources near the surface are computed utilizing a MULCAP routine based upon equations (1), (2), (3), and (4) above, from simulated data obtained with a velocity profile representing the real-ocean medium at depths of 6000 feet and with bottom-mounted hydrophones with base lines up to 10,000 feet, in hexagonal configuration, the precisions attained are better than one part in 10^4 .

REFERENCE

1. Morrissey, J. H., MULCAP, Philco Tech Rep Division Bulletin, Vol. 11, No. 2, March-April, 1961.

EFFECTS OF THE SPECTRAL COMPOSITION OF RANDOM THERMAL VARIATIONS ON PHASE AND AMPLITUDE FLUCTUATIONS OF A SOUND WAVE PROPAGATING IN THE SEA

by AIMO SALENIUS
Sperry Gyroscope Company
Great Neck, New York

ABSTRACT.

Equations are derived for the spectral densities of the phase and amplitude fluctuations, as well as the mean square fluctuation of the wave front normal direction in terms of the spectral density of the index of refraction variations for the wave of a harmonic point source in a slightly random medium whose mean index of refraction is constant. Since in the sea the spectral density of the refractive index fluctuations is, for all practical purposes, determined as a multiple of the spectral density of the thermal variations, the equations permit the study of the effects of the spectral composition of the random thermal variations over various space wavelengths in order to determine the sampling distances required to obtain relevant statistics of the thermal variations.

I. INTRODUCTION.

The phase and amplitude fluctuations of a sound wave propagating in the sea have considerable effects on reducing the quality of performance of sonars. The phase fluctuations contribute to bearing errors while the amplitude fluctuations create difficulties in detection and signal processing. It is well known that a major portion of these fluctuations are caused by the random thermal structure of the sea which causes the speed of sound to vary randomly from point to point in the medium.

In the following analysis we shall assume that the mean temperature is known throughout the medium and that the fluctuations about the mean are stationary to the second order. Furthermore, in order to make the problem tractable we shall also assume the random field of the temperature variations to be homogeneous and isotropic. A better characterization of the temperature variations would be to consider them axisymmetric about the depth axis, however, the additional complexities would not significantly contribute to the qualitative aspects of the results.

One may consider the thermal variations as consisting of a continuous distribution of periodic variations of random amplitudes over various space wavelengths, or component sizes. The average power of the fluctuations can be represented by means of a continuous distribution of power density over the various size components. This is achieved mathematically by the Fourier transform of the autocorrelation function of the temperature variations. The resulting power density spectrum will be simply referred to as the spectrum of the thermal variations. For small variations of temperature, neglecting the effects of the extremely small variations in salinity, the power density spectrum of the index of refraction variations is determined as a multiple of the power density spectrum of the thermal variations. Thus, when we refer to the spectrum of the index of refraction variations we are also referring to the spectrum of the thermal variations.

We shall be concerned particularly with the effects on the phase and amplitude fluctuations of the manner in which the power of the thermal variations is distributed among its various size components. Knowing the effects of the thermal fluctuations of various size components, it will be possible to plan experiments for gathering the statistics of the temperature variations such that they will be useful in the study of sonar performance. In particular, it will be possible to determine the smallest sampling distances required to secure adequate statistics.

Since target bearings obtained by correlation sonars are determined by measuring the orientation of the wavefront, we shall also investigate the effects of the spectrum of the thermal variations on the mean square fluctuation of the direction of the normal to the wave front in order to get a measure of sonar bearing accuracies.

In most sonar applications the sound source is considered as a point source and the sound field is very nearly spherical. For this reason we shall study the case of a harmonic point source in a medium whose mean index of refraction is a constant. Furthermore, since correlation sonars are concerned primarily with the correlation of signals along a base line transverse to the direction of wave propagation, we shall concern ourselves with the spectra of the transverse phase and amplitude fluctuations.

Tatarski[1] has analyzed the problem of the mean square fluctuation of phase and amplitude at a point in the field of a point source in a random medium whose mean structure is constant. The results herein are obtained by a modification and extension of the approach used by Tatarski in order to determine as well the transverse phase and amplitude spectra, and the mean square fluctuation of the wave front normal direction.

II. PHASE AND AMPLITUDE FLUCTUATION SPECTRA.

We shall assume the wavelength of the sound to be very much less than the dimensions of the smallest size component of the thermal variations. We shall also assume that the source is located at the origin of the coordinate system. Following Tatarski we may express the fluctuations of the phase and the logarithmic amplitude (hereinafter simply termed the amplitude fluctuation) at the plane $x = L$ by means of the stochastic Fourier-Stieltjes integrals:

$$S_1(L,y,z) = S - S_o = \int\!\!\int_{-\infty}^{+\infty} e^{i(K_2y+K_3z)}\, ds(K_2,K_3,L) \qquad (1)$$

and

$$B(L,y,z) = \log(A/A_o) = \int\!\!\int_{-\infty}^{+\infty} e^{i(K_2y+K_3z)}\, da(K_2,K_3,L) \qquad (2)$$

with random complex amplitudes ds and da.

In particular, the correlations of the phase and amplitude fluctuations at the points $(L,r/2,0)$ and $(L,-r/2,0)$ using (1) and (2) are given by

$$R_S(r) = \overline{S_1(L,r/2,0)S_1^*(L,-r/2,0)} = \int\!\!\int_{-\infty}^{+\infty} e^{i(K_2+K_2')(r/2)}\,\overline{ds(K_2,K_3,L)ds^*(K_2',K_3',L)} \qquad (3)$$

and

$$R_A(r) = \overline{B(L,r/2,0)B^*(L,-r/2,0)} = \int\!\!\int_{-\infty}^{+\infty} e^{i(K_2+K_2')(r/2)}\,\overline{da(K_2,K_3,L)da^*(K_2',K_3',L)} \qquad (4)$$

where the star (*) denotes the complex conjugate.

Using equation (9.17) in Tatarski[1] and its analog for the correlation of the amplitudes of the random phases, we get

$$\begin{matrix} R_S(r) \\ R_A(r) \end{matrix} = k^2L^2 \int\!\!\int_{-\infty}^{+\infty} dK_2dK_3 \int_0^L\!\!\int_0^L \frac{dx_1dx_2}{x_1^2} \times F_N\left[\frac{K_2L}{x_1}, \frac{K_3L}{x_1}, |x_1-x_2|\right] \times \begin{matrix}\cos\\ \sin\end{matrix}\left[\frac{L(L-x_1)K^2}{2kx_1}\right] \begin{matrix}\cos\\ \sin\end{matrix}\left[\frac{Lx_2(L-x_2)K^2}{2kx_1^2}\right] \times \exp\left[\tfrac{1}{2}iK_2(1+x_2/x_1)\right] \qquad (5)$$

where F_N denotes the two dimensional spectral density of the index of refraction fluctuations and k denotes the wave number of the sound. We observe that the correlation functions are symmetric abount the origin in the plane $x = L$. Using polar coordinates and employing the simplifying approximations used by Tatarski, equation (5) may be reduced to

$$\begin{matrix} R_S(r) \\ R_A(r) \end{matrix} = 4\pi^2k^2 \int_0^{+\infty} dK\, K\, \phi_N(K) \times \int_0^L J_o\left[\frac{xrk}{L}\right] \begin{matrix}\cos^2\\ \sin^2\end{matrix}\left[\frac{x(L-x)K^2}{2Lk}\right] dx, \qquad (6)$$

where $\phi_N(K)$ is the three dimensional spectrum of the index of refraction variations.

If we let $x = (LK')/K$ in the inner integral of (6) and interchange the order of integrations we get

$$\begin{matrix} R_S(r) \\ R_A(r) \end{matrix} = 4\pi^2k^2L \int_0^{+\infty} K\, dK\, J_o(KL) \times \frac{1}{K}\int_K^{+\infty} \phi_N(K') \begin{matrix}\cos^2\\ \sin^2\end{matrix}\left[K(K'-K)\frac{L}{2k}\right] dK \qquad (7)$$

where K and K' have been interchanged.

Now, since

$$\begin{matrix} R_S(r) \\ R_A(r) \end{matrix} = 2\pi \int_0^{+\infty} J_o(Kr) \begin{matrix} F_S(K) \\ F_A(K) \end{matrix} KdK \qquad (8)$$

where $F_S(K)$ and $F_A(K)$ are the two dimensional spectra of the phase and amplitude fluctuations, then comparing (8) with (7) we have

$$\begin{matrix} F_S(K) \\ F_A(K) \end{matrix} = \frac{2\pi k^2L}{K} \int_K^{+\infty} \phi_N(K') \begin{matrix}\cos^2\\ \sin^2\end{matrix}\left[K(K'-K)\frac{L}{2k}\right] dK'. \qquad (9)$$

Defining

$$K_p = \sqrt{\frac{2\pi k}{L}} = \frac{2\pi}{\sqrt{\lambda L}}$$

as the <u>process wave number</u>, and writing

$$n = \frac{K}{K_p} \quad \text{and} \quad n' = \frac{K' - K}{K_p},$$

we may express (9) finally as

$$\begin{matrix} F_S(n) \\ F_A(n) \end{matrix} = \frac{2\pi k^2L}{n} \int_0^{+\infty} \phi_N(n'+n) \begin{matrix}\cos^2\\ \sin^2\end{matrix}\left[nn'\pi\right] dn' \qquad (10)$$

Given the three dimensional spectrum of the index of refraction variations, equation (10) may be used to determine the spectra of the transverse phase and amplitude fluctuations. If the results are inserted in equation (8) we may also obtain the correlation functions of the transverse phase and amplitude fluctuations.

III. MEAN SQUARE FLUCTUATION OF THE WAVE FRONT NORMAL DIRECTION (BEARING FLUCTUATION).

If we consider the phase at two points $(L,r/2,0)$ and $(L,-r/2,0)$ where $r \ll L$ then the angle θ_z made by the normal to the intersection of the wave front at $(L,0,0)$ and the plane $z = 0$ and the x axis is given approximately by

$$\theta_z \approx \frac{S_1(L,r/2,0) - S_1(L,-r/2,0)}{rk} \tag{11}$$

Similarly, the angle made in the plane $y = 0$ is given approximately by

$$\theta_y \approx \frac{S_1(L,0,r/2) - S_1(L,0,-r/2)}{rk} \tag{12}$$

If the angles θ_y and θ_z are small, then the angle θ between the normal to the wave front at $(L,0,0)$ and the x axis is given by the relationship

$$\theta^2 \approx \theta_y^2 + \theta_z^2 . \tag{13}$$

Squaring (11) and (12), substituting in (13), averaging the sum and noting that

$$\overline{[S_1(L,r/2,0)]^2} = \overline{[S_1(L,-r/2,0)]^2} = \overline{[S_1(L,0,r/2)]^2} = \overline{[S_1(L,0,-r/2)]^2}$$

and

$$\overline{S_1(L,r/2,0)S_1^*(L,-r/2,0)} = \overline{S_1(L,0,r/2)S_1^*(L,0,-r/2)}$$

(13) becomes

$$\overline{\theta^2} \approx \frac{4}{r^2k^2}\left[\overline{[S_1(L,r/2,0)]^2} - \overline{S_1(L,r/2,0)S_1^*(L,-r/2,0)}\right]. \tag{14}$$

If r is very small, then

$$\overline{[S_1(L,r/2,0)]^2} \approx \overline{[S_1(L,0,0)]^2} = R_S(0)$$

whence (14) becomes

$$\overline{\theta^2} \approx \frac{4}{r^2k^2}\left[R_S(0) - R_S(r)\right]. \tag{15}$$

As $r \to 0$ (15) becomes an equality or

$$\overline{\theta^2} = \lim_{r\to 0} \frac{4}{r^2k^2}\left[R_S(0) - R_S(r)\right]. \tag{16}$$

Using equation (6), we may write (16) as

$$\overline{\theta^2} = \lim_{r\to 0} 16\pi^2 \int_0^{+\infty} dK\, K\, \phi_N(K) \int_0^L \frac{1}{r^2}\left[1 - J_0\left(\frac{xrK}{L}\right)\right] \times \cos^2\left[\frac{x(L-x)K^2}{2Lk}\right] dx. \tag{17}$$

Carrying out the limiting operation we get

$$\overline{\theta^2} = \frac{4\pi^2}{L^2}\int_0^{+\infty} dK\, K^3\, \phi_N(K) \int_0^L x^2 \cos^2\left[\frac{x(L-x)K^2}{2Lk}\right] dx. \tag{18}$$

Evaluating the inner integral and making the substitution $n = K/K_p$ where K_p is defined above, (18) becomes

$$\overline{\theta^2} = \frac{\pi^2 LK_p^4}{2}\int_0^{+\infty}\left\{ \frac{4}{3} + \frac{1}{n}\left[\cos\left[\tfrac{1}{2}\pi n^2\right]C(n) + \sin\left[\tfrac{1}{2}\pi n^2\right]S(n)\right] - \frac{1}{\pi n^3}\left[\cos\left[\tfrac{1}{2}\pi n^2\right]S(n) - \sin\left[\tfrac{1}{2}\pi n^2\right]C(n)\right]\right\} \times n^2\, \phi_N(n)\, n\, dn \tag{19}$$

where $C(n)$ and $S(n)$ are the Fresnel integrals.

IV. EFFECTS OF THE COMPOSITION OF THE INDEX OF REFRACTION SPECTRUM (THERMAL SPECTRUM).

From the theory of isotropic-turbulent scalar fields[2] the thermal spectrum, or the index of refraction spectrum, can be represented approximately by a Von Kármán type interpolation formula, or

$$\phi_N(n) = \mu^2 \frac{5\Gamma(5/6)}{6\pi^{(3/2)}\Gamma(1/3)K_o^3\left[1+(nK_p)^2/K_o^2\right]^{(11/6)}} \quad ; n < n_i$$

$$= 0 \quad ; n > n_i , \tag{20}$$

where n_i is the wave number of the smallest size component of the refractive index fluctuations in terms of the process wave number and μ is the rms fluctuation of the index of refraction variations. Fig.1 shows the plot of the spectrum.

Although the spectrum of the thermal variations in the sea may not correspond exactly to that of an isotropic-turbulent scalar field, the use of the above approximation should result in reasonably good qualitative relationships between the thermal spectrum and the spectra of the phase and amplitude fluctuations, especially over the small size components. In any event, should the spectrum be considerably

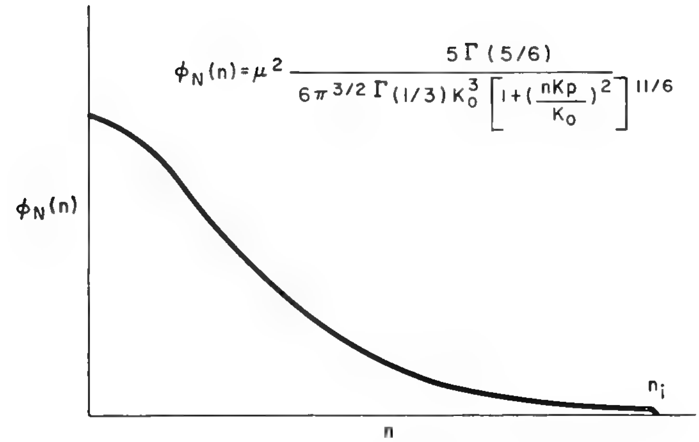

FIG. I - SPECTRUM OF THERMAL VARIATIONS APPROXIMATED BY VON KÁRMÁN INTERPOLATION FORMULA

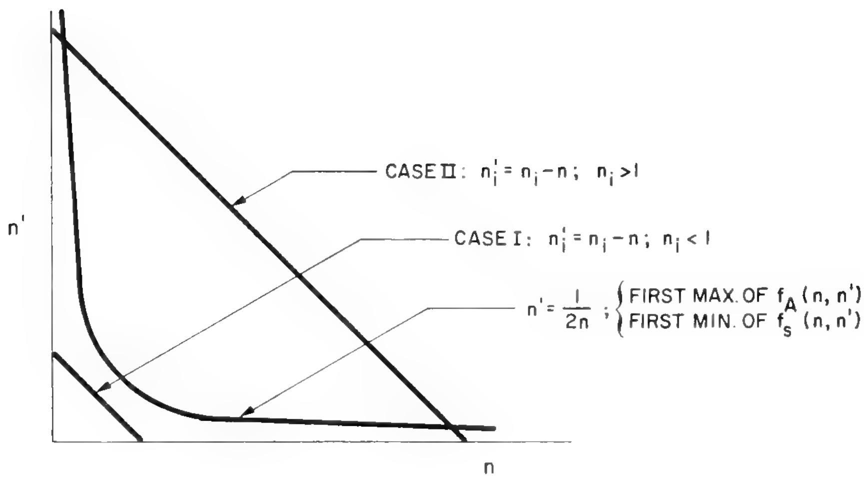

FIG. 2 – PLOT OF FIRST MAXIMUM OF $f_A(n, n')$, FIRST MINIMUM OF $f_s(n, n')$ AND TERMINAL POINT OF THE SPECTRUM FUNCTION $\phi N(n)$

different from the assumed approximation, the analysis herein presented can be similarly applied to any other spectrum.

We shall examine the two cases:

Case I : $K_i < K_p$ or $n_i < 1$, and

Case II: $K_p > K_i$ or $1 < n_i$.

Writing

$$\begin{matrix} f_S(n,n') \\ f_A(n,n') \end{matrix} = \frac{1}{n} \begin{matrix} \cos^2 \\ \sin^2 \end{matrix} \left[nn'\pi \right]$$

then from equation (10) the spectra of the phase and amplitude fluctuations may be written

$$\begin{matrix} F_S(n) \\ F_A(n) \end{matrix} = 2\pi k^2 L \int_0^{+\infty} \phi_N(n'+n) \begin{matrix} f_S(n,n') \\ f_A(n,n') \end{matrix} dn'. \quad (21)$$

For each value of n the integral in (21) determines the contribution to the power density spectra $F_S(n)$ and $F_A(n)$ of the power density from the various wave numbers of $\phi_N(n)$. It is observed that as n increases the function $\phi_N(n'+n)$ is shifted to the left on the n' axis. Also, as n increases the period of the functions $f_S(n,n')$ and $f_A(n,n')$ increase with respect to n'.

The first minimum of $f_S(n,n')$ and the first maximum of $f_A(n,n')$ for a given n occur when $n' = 1/(2n)$, while the spectral function $\phi_N(n'+n)$ will terminate at $n' = n_i - n$. If both of these points are plotted against n for case I and case II the results would appear as shown in Fig. 2.

From the figure we see that for case I the first minimum of $f_S(n,n')$ and the first maximum of $f_A(n,n')$ on the n' axis will occur at higher values of n' than at which the spectral function $\phi_N(n'+n)$ terminates. Fig.3 illustrates the relationships that exist between $\phi_N(n'+n)$ and the functions $f_S(n,n')$ and $f_A(n,n')$ for case I. For these relationships we note that

$$f_S(n,n') \approx \frac{2}{n}$$

and

$$f_A(n,n') \approx \frac{n\, n'^2 \pi^2}{8} .$$

For the integrand involving $f_S(n,n')$ the maximum will fall near the origin or at low values of n'. For small n the contributions will come from the large size components of ϕ_N. For large n the contributions will come from the smaller components of ϕ_N, however, their effects will be considerably less since $\phi_N(n'+n)$ is less in value and $f_S(n,n')$ falls off as n^{-1}.

Since $\phi_N(n'+n)$ is nearly constant at the origin and increasingly decays until the rate is proportional to the -11/3 power of n' over the larger values of $n' < n_i - n$, the integrand in (21) involving $f_A(n, n')$ will have a maximum on the n' axis between the middle to large values of $n' < n_i - n$ for small values of n and at small values of n' for large values of n. Thus, the chief contributions will occur from the middle to small size components of ϕ_N.

For case II we see from Fig.2 that the first minimum of $f_S(n,n')$ and the first maximum of $f_A(n,n')$ will generally occur at values of n' much smaller than the value $n_i - n$ at which the spectral function $\phi_N(n'+n)$ terminates as shown in Fig.4. For both integrands the maximum for most values of n will occur over the large size components of the spectrum ϕ_N, especially for the integrand in the formula for the phase spectrum which has its maximum at $n' = 0$. For the integrand involving the function $f_A(n,n')$ the maximum will tend to lie over the range of large to middle size components of ϕ_N. The effects of the small size components as n increases is reduced by the fact that the average values of $f_S(n,n')$ and $f_A(n,n')$ fall of as n^{-1}. It can be shown by examples that the maximum contributions to the amplitude fluctuation spectrum will come from components of ϕ_N whose dimensions are of order $\sqrt{\lambda L}$.

We shall now examine the effects of the spectrum $\phi_N(n)$ on the mean square fluctuation of the wave front normal direction. Defining the term in the curled brackets of the integrand of equation (19) as $f_\theta(n)$ we may write equation (19) as

$$\overline{\theta^2} = \tfrac{1}{2}\pi^2 L K_p^4 \int_0^{+\infty} f_\theta(n)\, n^2\, \phi_N(n)\, ndn. \quad (22)$$

Fig.5 shows the relationships between the spectral function $\phi_N(n)$ and the function $f_\theta(n)$ for case I. We observe that in this case $f_\theta(n) \approx 8/3$. Since $\phi_N(n)$ decays as n to the -11/3 power over the higher wave numbers, the integrand of (22) will be a maximum over the largest size components of the spectrum ϕ_N. However, comparing this with case I for the phase fluctuations we observe that the contributions from the smaller size components of ϕ_N are more significant for the wave front normal fluctuations because of the presence of the additional term n^2.

Fig. 6 shows the relationships between $f_\theta(n)$ and $\phi_N(n)$ for case II. Except in the vicinity of very low wave numbers, the function $f_\theta(n) \approx 4/3$. Thus, the maximum contribution to the mean square fluctuation of the wave front normal direction will come from the large size components of ϕ_N.

V. CONCLUSIONS.

1. The small components of the thermal variations principally affect the spectrum of the amplitude fluctuations when the smallest component of the thermal variations is greater than $\sqrt{\lambda L}$. The manner in which the small components affect the

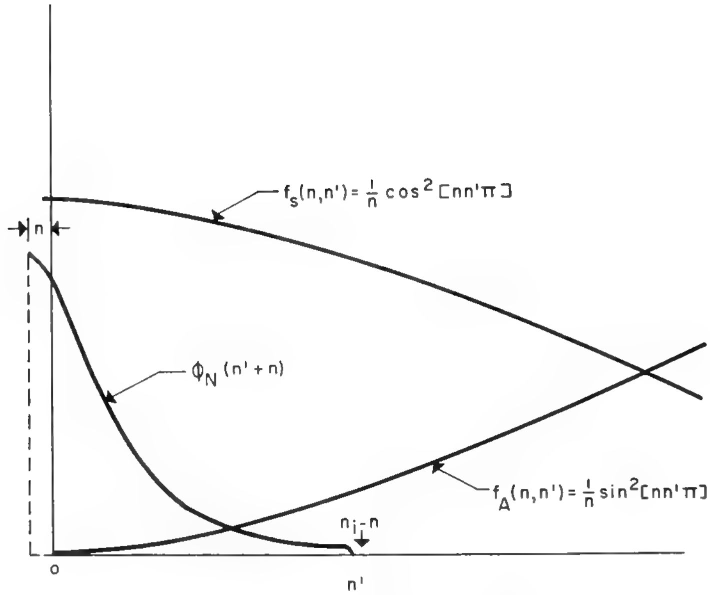

FIG. 3-CASE I: $n_i < l$; RELATIONSHIPS BETWEEN $\phi_N (n'+n)$ AND THE FUNCTIONS $f_A(n,n')$ AND $f_s(n,n')$.

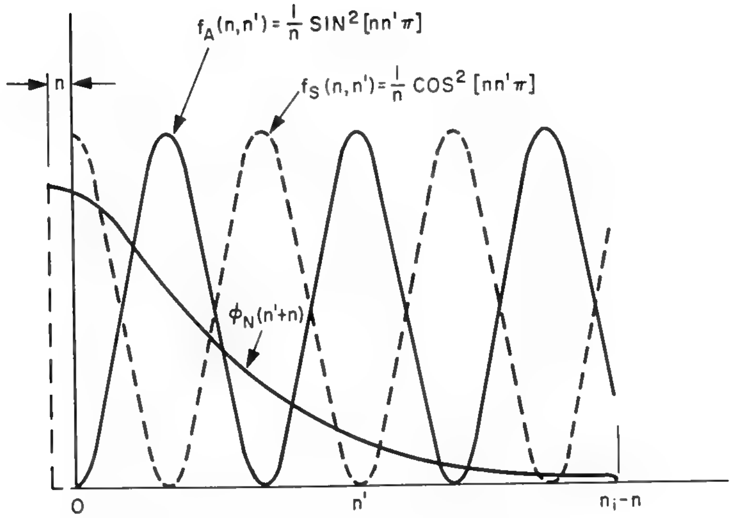

FIG. 4 - CASE II: $n_i > l$; RELATIONSHIPS BETWEEN $\phi_N (n'+n)$ AND THE FUNCTIONS $f_A (n,n')$ AND $f_S (n,n')$

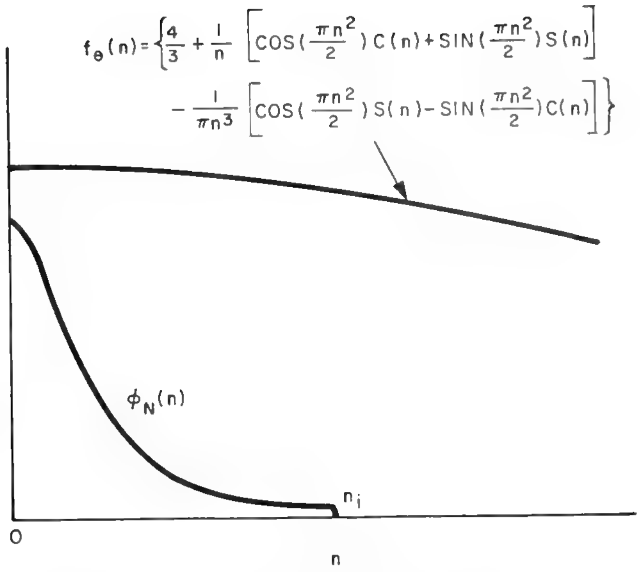

FIG. 5 - CASE I: $n_i < 1$; RELATIONSHIP BETWEEN $\phi_N(n)$ AND $f_\theta(n)$

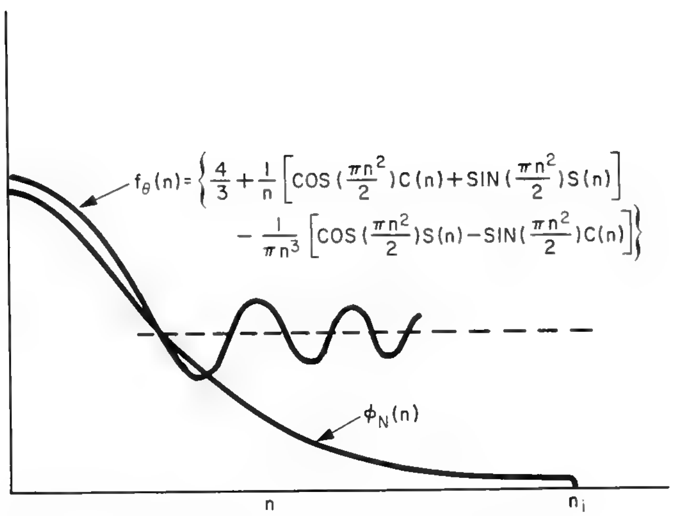

FIG. 6- CASE I: $n_i > 1$; RELATIONSHIP BETWEEN $\phi_N(n)$ AND $f_\theta(n)$

spectrum of the amplitude fluctuations depends strongly on the decay rate of the thermal variation spectrum over the small components, or high space wave numbers.

2. When the smallest component of the thermal variations is less than $\sqrt{\lambda L}$ (as is generally the case in sonar), then the components whose dimensions are of order $\sqrt{\lambda L}$ have the greatest effect on the spectrum of the amplitude fluctuations. As an example, at a range of 4000 yards at 20 kc. the thermal variations of dimensions of the order of 18 yards have the greatest effect on the amplitude fluctuations. This implies that in order to gather the statistics of the thermal variations which most affect the amplitude fluctuations the temperatures must be sampled over distances less than 18 yards.

3. The spectrum of the phase fluctuations is principally affected by the large size components of the thermal variations, while the mean square fluctuation of the wave front normal direction is principally affected by the large to middle size components.

4. Should the form of the spectrum of the thermal variations differ considerably from the one used in the analysis, represented by the Von Kármán interpolation formula, the conclusions reached above may differ considerably, especially for the amplitude fluctuations which are most sensitive to the form of the thermal variation spectrum. Thus, measurements are needed to establish the form of the thermal variation spectrum, which requires making measurements over small as well as large distances.

5. In order to overcome the effects of phase and amplitude fluctuations, statistical processing of sonar signals seems in order. If the random thermal structure changes rapidly in time then a good statistical sample of target bearings can be obtained which when processed will reduce the errors due to the fluctuations. This implies that all the component sizes in the thermal variations change rapidly in time. It is more likely, however, that the larger components will vary more slowly in time than the smaller components. Under this condition, it becomes necessary that the statistics of the thermal variations in time also be investigated in order to establish the effectiveness of statistically processing the fluctuating sonar data.

REFERENCES.

1. Tatarski, V.I., "Wave Propagation In A Turbulent Medium", McGraw-Hill Book Co.,Inc., New York, 1961.
2. Hinze, J.O., "Turbulence, An Introduction to Its Mechanism and Theory", McGraw-Hill Book Co., Inc., New York, 1959, Chapter 3.

A TELEMETERING THERMOMETER

by DR. ANGELO J. CAMPANELLA, Senior Physicist
HRB-Singer, Inc.
State College, Pennsylvania

ABSTRACT

A temperature transducer for temperature measurement at depth for a radio telemetering link from a drift buoy has been developed. The nominal design depth is 200 meters for the transducer. It has an accuracy of 0.1 °C or better depending on radio link quality. The system is operational and has been tested at shallow depths, approximately 4 meters, by the Woods Hole Oceanographic Institute.

INTRODUCTION

Radio drift buoys currently in use[1] provide a means for tracing the motion of surface waters in the open sea. No information concerning the identity of the water in which the buoy rests at the moment of observation is available other than that accumulated from past sampling. In drift experiments it is important to know whether the buoy has remained with the water mass in which it was deposited or conversely to know some parameter of the water immediately under it. Surface temperature is relatively meaningless due to environmental influences. The temperature at a depth of 200 meters is suitable for the purposes of identification since it lies below the daily, and most seasonal, influences. A length of multi-conductor cable that is suitable for suspension at this depth is well-logging cable. The temperature can be measured to 1 °C or better depending upon the radio link signal-to-noise ratio. The unit has been laboratory calibrated from 0° to 30°C and is repeatable to within .03°C. The response time for a temperature excursion from room temperature to 0°C is about one minute for 2% full scale accuracy and about one hour for the remainder, all within calibration accuracy. The longer lag is due to the temperature coefficient of the Mylar capacitors in the Wien Bridge. The response time can be reduced to a few seconds by simple design improvements.

COMPONENT DESCRIPTION

BUOY

The drift buoy developed by Franz, Walden, and Ketchem is shown in Figures 1 and 2. Figure 3 is a block diagram of this system. In its quiescent state the receiver is tuned to a radio frequency of 2398 KC. When a radio signal modulated by the proper audio tone is picked up by the antenna, one of two resonant reed relays is actuated, depending on the particular tone, and a sequence of events then occurs. If the first relay is actuated, the call sign of the buoy is transmitted in international morse code in A-1 emission(CW), followed by a long dash. If the second relay is actuated by the proper tone, either a long dash, or some special signal is transmitted.

For the telemetering thermometer application this buoy was used in a slightly modified form which included the attachment of a temperature transducer. The mode of transmission was changed to F-1 (frequency shift keying). The mark-space rate of shifting was made to depend on the temperature at the depth of the transducer. FSK modulation is used due to its FM-like noise rejection and good anti-fade qualities.

To effect F-1 modulation of the transmitted signal, several components were added to the crystal oscillator circuit. See Figure 4. A 300 picofarad capacitor was placed between the 2398 KC crystal and ground. The final R.F. stage is allowed to run continually, and the diode across the capacitor self biases itself to a high impedance. When the keying contacts close, the diode CR2 no longer can bias itself and consequently shorts the 300 picofarad capacitor. The carrier frequency is then shifted 140 cps lower in frequency. Crystal diode CR3 and the .001 capacitor isolate the circuits from the keying leads, and hence remote keying is possible. To produce conductance switching, a transistor can adequately replace the relay in this operation.

TRANSDUCER SUSPENSION

Short length of BT wire is used for suspension of the pressure case for shallow water so that no mechanical support is required from the conducting cables. See Figure 2. No difficulty is anticipated for the 200 meter suspension especially since it comprises not a mooring but merely a suspension for the pressure case plus whatever weight is needed to maintain a suitably vertical wire angle in the presence of current shear. Extra flotation may be required at the surface buoy to support this.

Electrical leads were brought through the heavy top plate by water-tight connection and a joint made with a Joy 3-prong connector. A 3-conductor cable ran down to the temperature transducer and terminated in a Joy single contact pressure connector. Although a sea return or suspension cable could have been used as one lead,

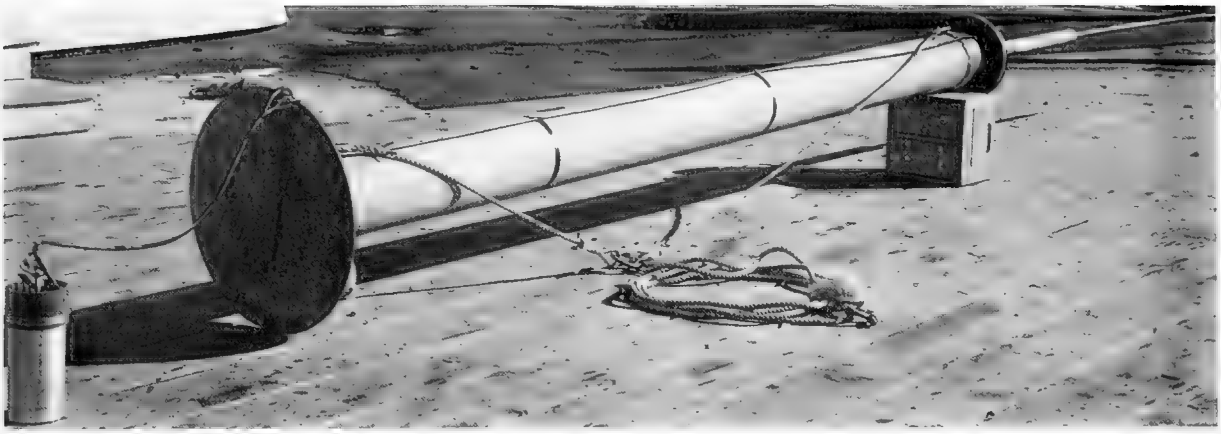

Fig. 1 - Buoy with Temperature Transducer

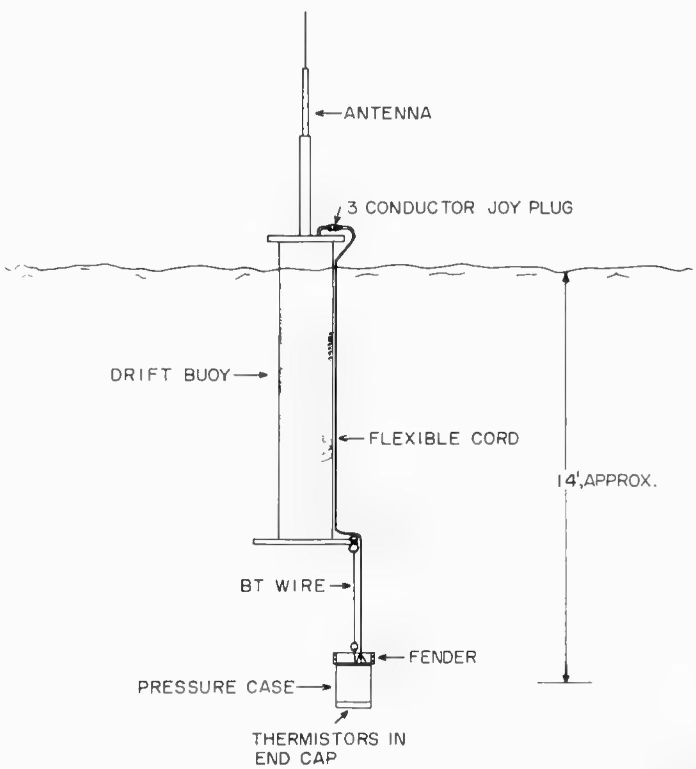

Fig. 2 - Buoy - Temperature Transducer System

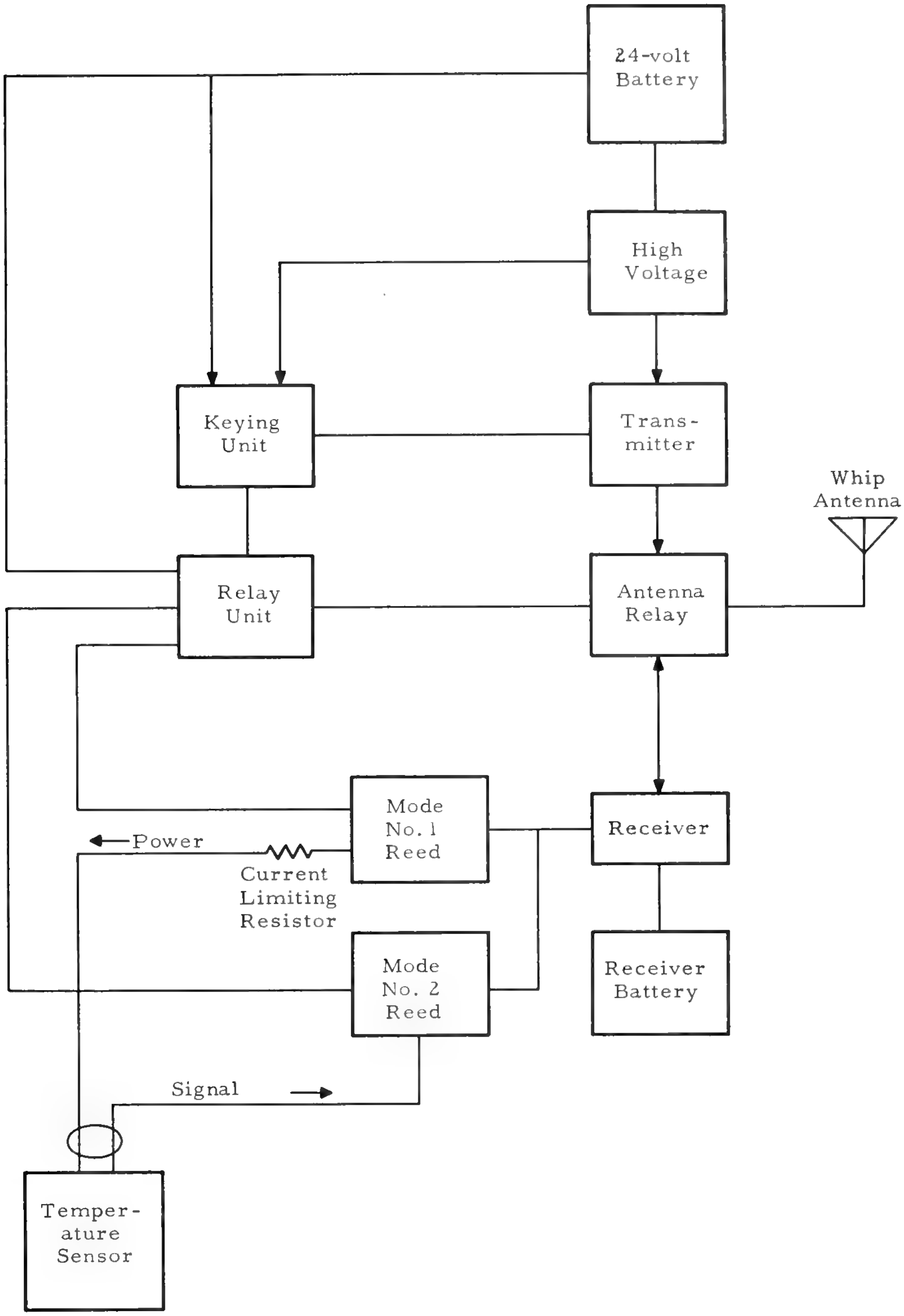

Fig. 3 - Buoy Block Diagram

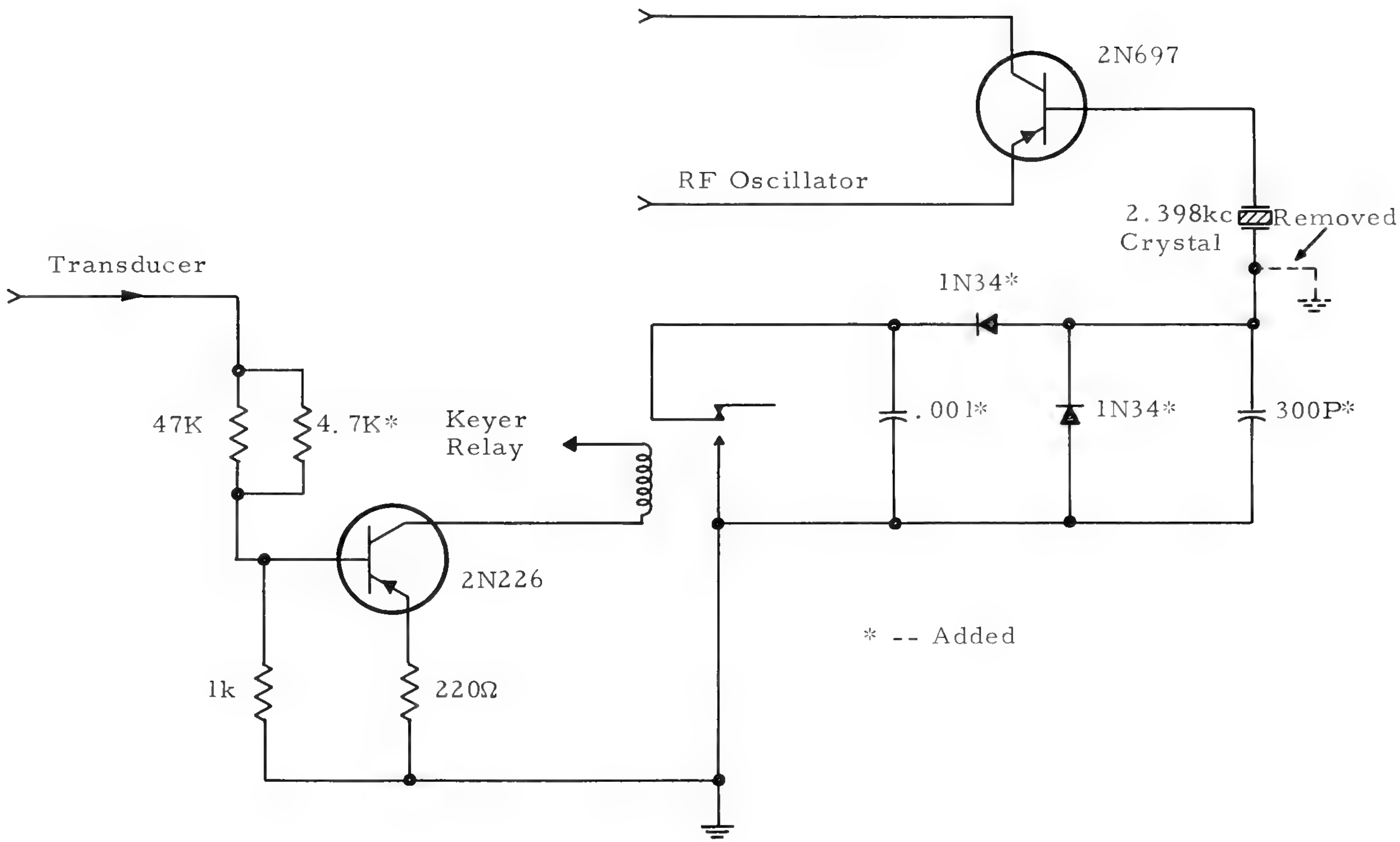

Fig. 4 - Drift Buoy Modifications

it was chosen not to do so to ensure good reliable contacts. The signal circuit impedance is about 500 ohms so that small conductance cable leaks will not adversely affect performance.

TEMPERATURE TRANSDUCER

The transducer pressure case contains thermistors imbedded in the lower end cap. See Figures 5, 6, and 7. The transistorized electronic oscillator and the Zener voltage regulator diode are attached to the upper end cap. The buoy's 24v batteries are used to power the temperature transducer through a dropping resistor. In the event that a short circuit occurs in the cable, only about 0.1 amps will flow through the resistor. This is small compared to the current consumed by the rest of the transmitter.

The transducer oscillator is a Wien Bridge type well known for its amplitude and frequency stability. This bridge is shown in Figure 8.

The active thermistors R1 and R2 in the right hand arms are the frequency determining resistors along with capacitors C1 and C2. The frequency of oscillation is determined by the relation

$$f = \frac{1}{2\pi\sqrt{R_1 R_2 C_1 C_2}} \qquad (1)$$

The thermistors R1 and R2 are located in the lower end cap. The capacitances C1 and C2 are the Mylar dielectric type chosen for a degree of temperature stability. They are attached to the back of the circuit board. Their temperature coefficient is such that their capacity at 0°C is 2% less than that at room temperature. This is better than paper capacitors but not as good as the polyethylene type which has a nearly zero temperature coefficient. With the latter units, the response time for good accuracy can be reduced to that time required for the thermistors to come to equilibrium with their surroundings. In the drift buoy application the transducer will remain continuously in its environment and hence it is acceptable to calibrate the entire unit in a constant temperature bath.

A square wave is generated by a squaring amplifier. It is fed by the divided outputs of the push-pull oscillator. The square wave is fed through an emitter follower for additional isolation and low impedance. The signal output is a square wave from 0 to +13 volts for a positive supply and 0 to -13 for a negative supply. The frequency of this square wave ranges from about 2 to 10 cps or from 100 to 500 milliseconds per cycle. The latter time period expression is commonly used in this report. The transmitter keying relay can run at the highest repetition rate encountered and is used unmodified. Conductance switching can be used if higher rates are ever required. The buoy transmitter keying is achieved by opening the internal keying circuit and allowing the temperature transducer output signal to do the keying. See Figure 4.

CALIBRATION DATA

Figure 9 is a reproduction of the calibration curve from which the integer temperature readings were made. A table was prepared which gave interpolation values to 0.1°C. Further interpolation to 0.01°C could be made with the listing of proportional parts. The raw data is good to ± .01°C, the manual curve fit to perhaps ± .03°C. For accurate calibration to within ±.03°C a least-square-curve fit should be made with the raw data.

RECEIVING STATION ASHORE

The buoy transmits on a frequency of 2398 KC with a power output of approximately 20 watts. The radiated power is on the order of 2 watts due to antenna inefficiency. A downward shift of the R.F. carrier frequency of 140 cps occurs when the keying contacts close.

The receiving station is shown schematically in Figure 10. The carrier is converted to an audio tone by operating the receiver in the BFO-ON position. The carrier shift of 140 cps downward produces an audio tone shift of 140 cps downward when the BFO frequency is below the carrier frequency and 140 cps upward when the BFO frequency is above the carrier frequency. See Figure 11.

In the case of temperature measurement it is inconsequential whether the BFO is set above or below the carrier since the datum comprises the total time period for one complete cycle of frequency shift. To convert the FSK audio signal into a signal suitable for triggering a timing circuit, the signal is fed through a standard IRIG subcarrier discriminator centered at 1700 cps. This discriminator as a linear output over a ± 7.5% range. The discriminator response limits the bandwidth to that frequency occupied by its "S" curve. A narrow pass frequency occurs for lower center frequency units. The 960 cps center frequency (IRIG Channel No. 4) has a pass band of slightly more than 144 cps. The reason for choosing a low oscillator frequency is so that a very narrow shift hence a narrow discriminator response can be used and still have a high modulation index. The narrow shift allows a narrow band pass, off the shelf, discriminator to be used to advantage. Keying of the transmitter is simplified to merely "pulling" the crystal R.F. oscillator with series capacitance. Also the FSK mode of transmission has good antifade qualities. This is not to say that a wider shift, or extremely wide shift, say 6 KC, couldn't be used to advantage, to allow frequency diversity reception techniques. This requires some special filters, keyers, etc. and comprises a new field of development effort.

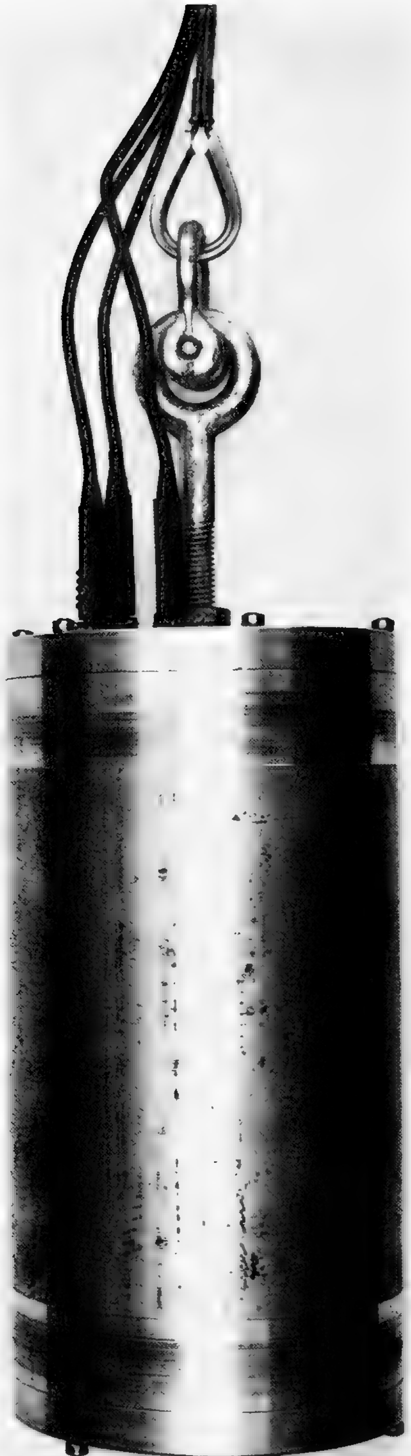

Fig. 5 - Pressure Case

Fig. 6 - Electronic Circuitry

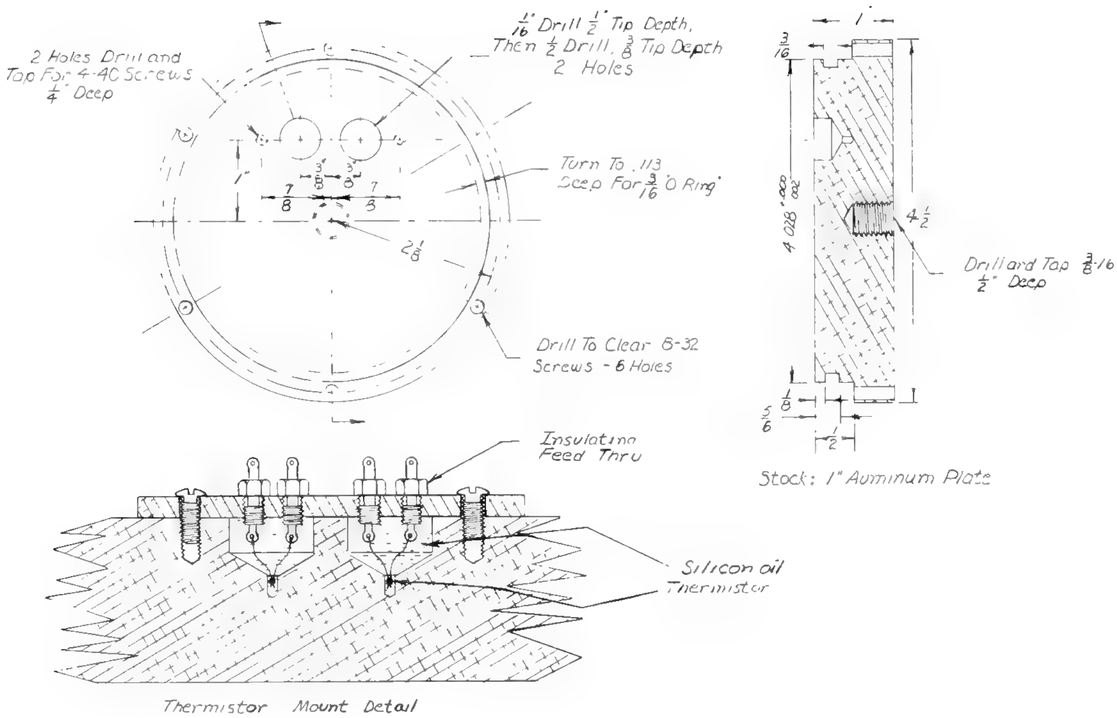

Fig. 7 - Lower End Cap

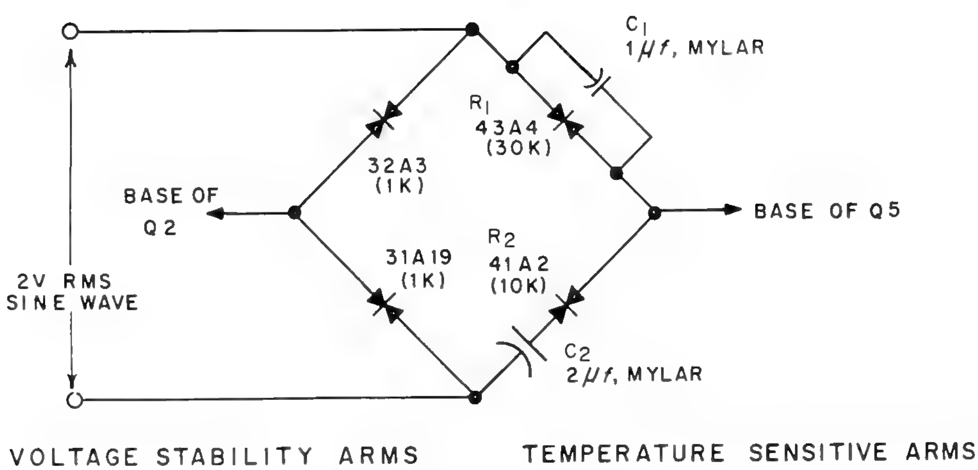

Fig. 8 - Wien Bridge

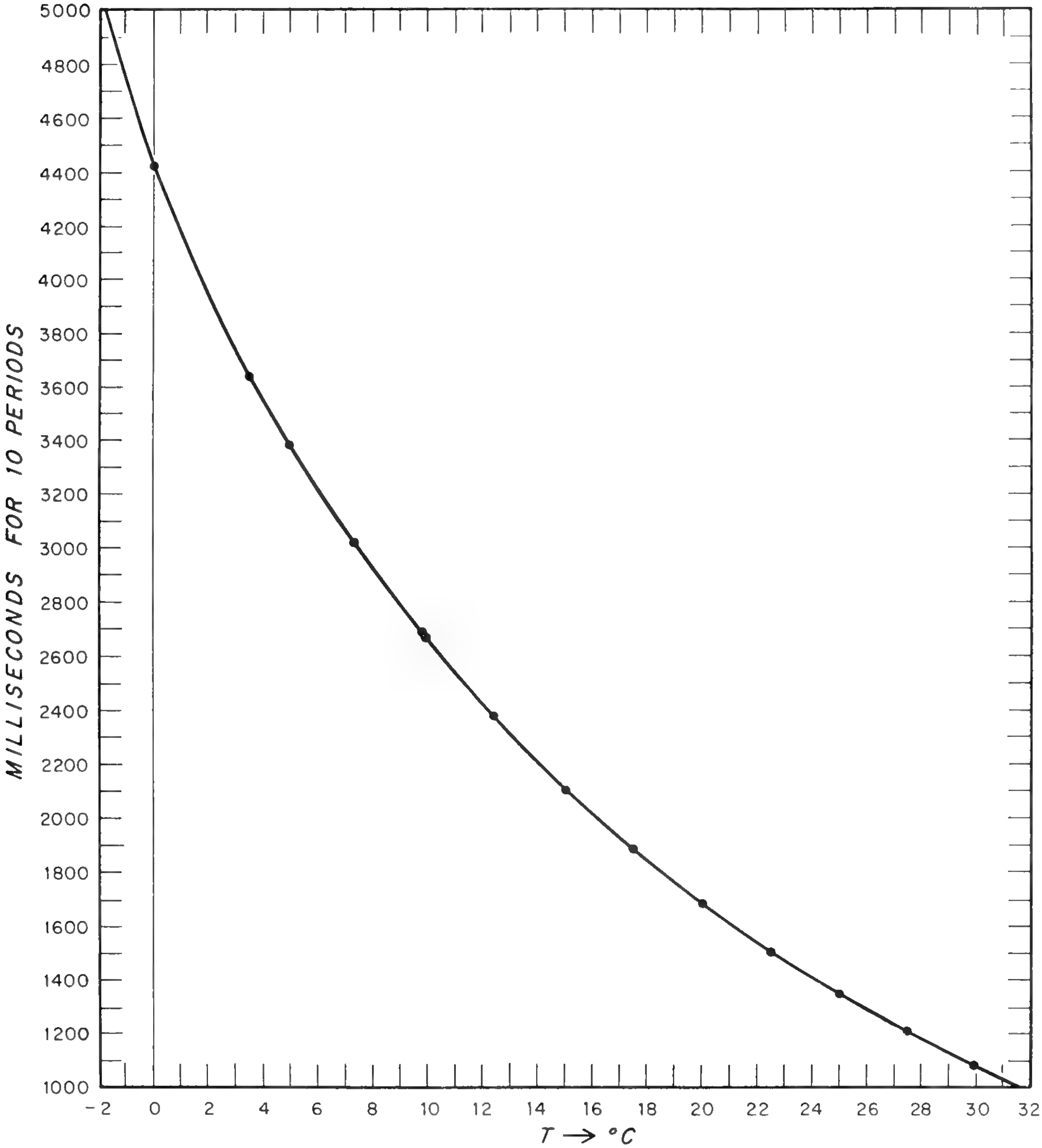

Fig. 9 - Calibration Curve

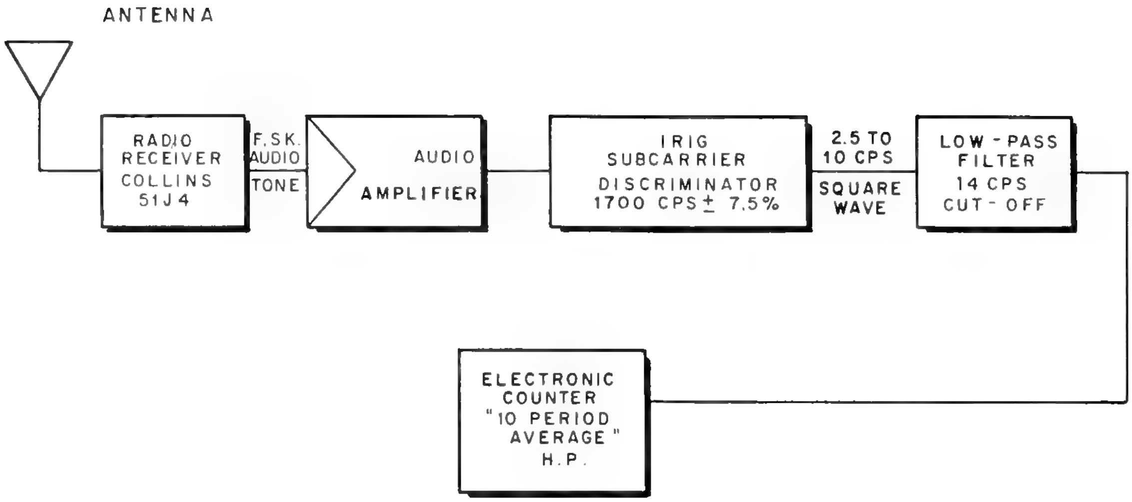

Fig. 10 - Receiver Station Block Diagram

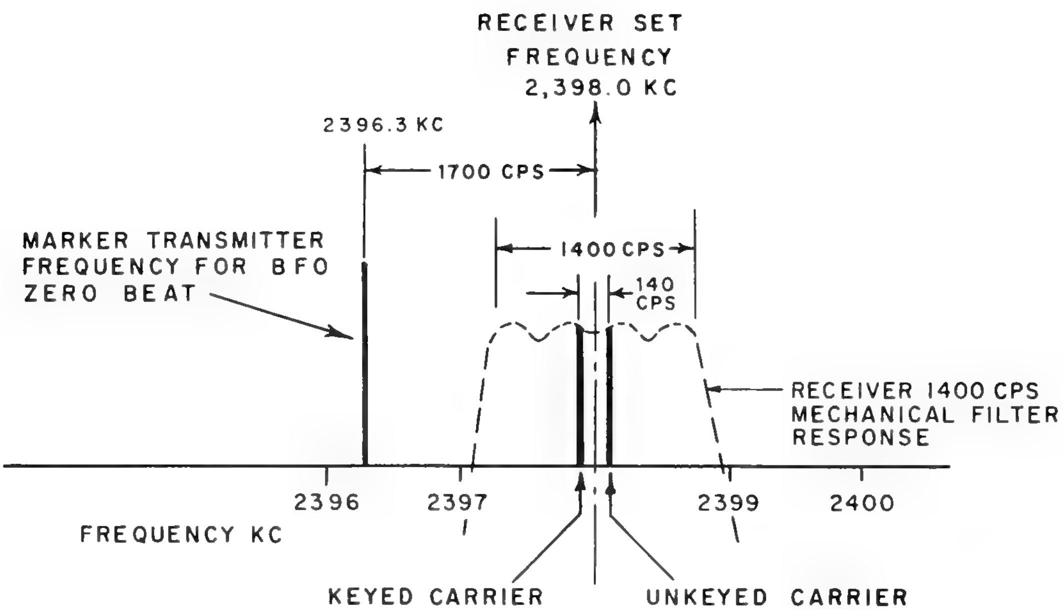

Fig. 11 - Spectral Presentation of Receiver Adjustment

The discriminator output is a square wave whose period is to be measured. It is first filtered by an output filter of high cutoff anywhere from 14 to 80 cps. It is suitable to trigger an electronic counter set in its period position or the 10-period average position. The latter was used in initial calibration measurements and may suit the data acquisition as well. The average over 10 periods could be adversely affected by static noise bursts under poor signal conditions when the buoy is a long distance away. In this case several 10-period measurements should be made and those widely different from a median are disregarded. Single period measurement between static crashes provides a second alternative.

CONCLUSION

The temperature transducer attachment to the buoy, elementary telemetering link, and calibration are completed. Tests at a depth of 14 feet have been carried out. A test at a depth of 100 meters is included in a paper by Walden and Franz[2] of this conference.

BIBLIOGRAPHY

1. "A Radio Telemetering System for Oceanography," Franz, Ketchum, and Walden, W.H.O. I#58-29. May 1958.
2. "Long Range Oceanographic Telemetering System," Walden, R. G., and Franz, D. H. Jr. ASLO and ISA Marine Sciences Conference, Woods Hole, Massachusetts. September 11-15, 1961.

ACKNOWLEDGMENT

The facilities of the Woods Hole Oceanographic Institution were used for the construction of the unit. Mr. Neil Brown is responsible for the basic stable oscillator circuit. The author's work represented by this report was accomplished during a stay at the Woods Hole Oceanographic Institution arranged by mutual agreement with HRB-Singer, Inc.

A LONG-RANGE, OCEANOGRAPHIC TELEMETERING SYSTEM

by ROBERT G. WALDEN
Woods Hole Oceanographic Institution
Woods Hole, Massachusetts
and DAVID H. FRANTZ, Jr., President
Ocean Research Equipment Company
Vineyard Haven, Massachusetts

ABSTRACT

A low cost transponding buoy for medium frequency, long-range ocean telemetry has been developed at the Woods Hole Oceanographic Institution, and further refined commercially. Its use as a drift buoy has been previously described; more recently a series of propagation tests at 2.4 mc. and 7 mc. has been conducted out to a 1400 mile range, and temperature measurements have been transmitted on a regular schedule. The buoy, and associated receiving and recording equipment are described, as well as the necessary buoy control circuitry for certain typical problems in physical oceanography.

INTRODUCTION

Almost ten years ago, Henry Stommel then of the Woods Hole Oceanographic Institution, designed an experiment to study the movement of water in the Sargasso Sea near the region of Bermuda, and more specifically to establish the effect of a given wind on the water column to a considerable depth as a function of time. The primary tool used in this study was a set of radio drift buoys designed and built by Hodgson, Parson, Walden and Stommel, primarily out of sheet steel, plywood, surplus stepping relays and a few vacuum tubes, automobile clocks, and, as I recall, a rattrap. The rattrap was a vital part of a scuttling device which was to sink the buoy after a month, to prevent its remaining a menace to navigation. We could never bring ourselves to arm the rattrap, even though the useful life was considerably less than a month. The buoy transmitted on schedule a series of tone modulated signals representing the output of a number of transducers, which included two current meters to measure current velocity relative to the buoy itself at the surface and at depth, the motion of the buoy being determined by daily fixes. We obtained the fixes by getting bearings with a portable radio direction finder mounted on a jeep. Since Bermuda is about one sixth the size of Martha's Vineyard, the accuracy of the fixes deteriorated rapidly with distance from the island. Additional transducers on the buoy were an anemometer, a compass, and later, thermistors.

The experiment was a success; enough of the buoys survived long enough to give a valuable insight into the behavior of the water mass influenced by wind and of the general drift around Bermuda. It also suggested a host of ways in which similar experiments could be conducted in the future, using radio telemetering buoys.

If this story were to be presented in the classic format, the description of this early, crude buoy design would be followed by one of more recent developments which have enabled us to perform much more sophisticated experiments working with greater quantities of data. We could describe the greater reliability of modern oceanographic telemetry systems, their greater range and longer life. Unfortunately, I am aware of no automatic oceanographic data gathering system involving more than one or two buoys which has produced any more real scientific, unclassified data via a radio telemetering link than the one operated by Stommel in the winter of 1953-4. Nor am I able to explain why this is so. It is certainly within the state of the art that there be such systems in successful operation since by now, most components of such a system have had considerable sea experience. Apparently it has been rare until now that the financing, the engineering talents, and the scientific interest have all occurred at the same time. The major program coming closest to it is Richardson's buoy line to Bermuda, and to date this has involved recording rather than telemetering techniques, and for very adequate reasons.

THEORY OF OPERATION

The vast extent of oceanic areas has required a re-evaluation of our past telemetry schemes. Frequencies in the two to three megacycles range are inadequate for distances of over a few hundred miles. Transmissions and coding systems such as FM/AM quickly become useless due to the signal to noise ratios involved.

We are presently using a completely transistorized buoy operating on 6970 kiloycles for our long range oceanographic telemetry. This buoy, manufactured by Concord Control, Inc. of Boston, is some thirteen feet long and eight inches in diameter. The bottom plate is two feet in diameter made of bronze, and acts both as a ground and as a vertical motion damper. The case is fiberglass or polyvinyl chloride. The electronics are built in modules which plug into a rack frame four feet long attached to the top plate. Figure 1 shows this rack. The top plate contains the antenna base insulator, tuning meter and necessary tuning and loading controls. The batteries, located in the bottom portion of the case, are LeClanche cells packaged in an eight inch cylinder three feet long. The receiver is a more or less standard crystal controlled super-heterodyne whose output drives two resonant reed relays. These relays, through special delay circuitry energize command function relays. Three interrogation command functions are thus possible, one or the other resonant reed relays or both simultaneously. Once interrogated, a timer is activated which causes the transmitter either to send out its call sign or a data transmission, depending upon the function chosen. The transmitter supplies 30 watts of power to a center-loaded marine type whip antenna. We have been using frequency-shift keying with a nominal shift of 240 cycles in our experiments.

I would like to discuss a recent experiment which was designed to determine the feasibility of 1) the modest power output 2) the 7 mc. frequency chosen, and 3) the FSK mode of operation. Accordingly a tract of land in Waquoit, Massachusetts (twelve miles from Woods Hole) was leased, and a beam antenna for 6970 kc. erected. A communication van housing receiving equipment, discriminators, and a tape recorder, was installed at the base of the antenna as shown in Figure 2. This receiving site proved excellent from a noise standpoint. The beam constructed was a three element array with parasitically excited reflector and director. Subsequent field pattern tests run with the aid of our Helio Courier aircraft acting as a signal source, established the major lobe at 140 degrees true, the direction desired for our tests. The front to back ratio was better than 15 db. and the horizontal beam width about 80 degrees. A Concord buoy, like the one just described, was taken to sea and put in the water at intervals. Measurements of signal strength and readability were then made at Waquoit. Because of the small number of transmissions, we are unable to present reliable statistics, but we can make certain generalizations of the results. The buoy was put overboard and allowed to drift away from the ship about a thousand feet and interrogated from the ship. A typical picture of the buoy in the water is shown. It was put over at different times of day and at ranges between 200 and 1400 miles from Waquoit. At least 50% of the transmissions were received at each range at Waquoit well enough to retrieve data regardless of time of day. Obviously this modest percentage is greatly weighted by the fact that some of the tests were run at the most adverse times of day, as far as propagation was concerned. At optimum time of day, the percentage was better, and by providing some sort of redundancy, we feel that we can have a reliable link. We believe that low power, high frequency FSK transmissions can be practically utilized for oceanographic telemetry, assuming that the optimum time of day be utilized, and that interrogation techniques be used. The interrogation technique allows repeat of transmissions to allow data redundancy during periods of high noise or interference. The data rate was 10 bits per second during these tests; however we anticipate rates of up to 100 bits per second.

CONCLUSIONS

The serial observation of oceanographical data from buoys located at certain remote sensitive areas of the ocean can in many instances supply the oceanographer with information not otherwise obtained. A monitor of this sort might provide a warning of some specific change, or it might indicate a trend whose correlation with other data ashore proves valuable.

What of the immediate future as far as telemetry systems are concerned? We feel that regardless of the admittedly higher data handling capabilities of the VHF bands, the line of sight limitation imposes too heavy a burden on auxiliary equipment to make it an immediate solution to the long range telemetry problem. If and when there are hundreds of buoys in the water, satellite relaying or data collection by high-flying aircraft may be worthwhile, and in fact necessary because of problems of frequency allocation, but if we were to start now to design a system of more modest extent for use in a given ocean area, there is no doubt in our minds that the high frequency bands will be utilized.

For example, Richardson's buoy line between here and Bermuda is presently recording at about ten buoy stations, and as far as we know, it is the only area now being monitored by a whole system of buoys for scientific purposes. Presumably it is well worthwhile to maintain this line more or less indefinitely, and as soon as the telemetry can be as reliable as the recording apparatus, and the platforms can maintain themselves reliably for six months or more, it will undoubtedly be more desirable

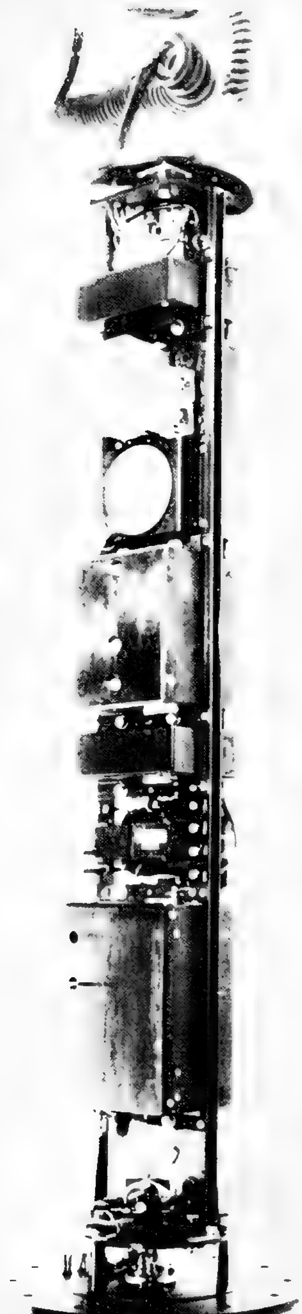

Figure 1

Figure 2

Figure 3

to transmit the data to a shore station than to collect it by ship. When we consider how best to convert this line to telemeter data either on schedule or on demand to Waquoit, there can be little doubt that it will be done using the high frequency bands rather than the VHF bands. The number of units is too small to justify air cover and a satellite is out of the question. Even at several times the present sampling rate and several times the present number of buoys, an HF link is quite feasible, and we can use existing equipment which has already proven at least its capability of functioning at sea.

At this point we must emphasize that we are attempting to describe a system which will be a tool useful and readily acceptable to the practicing oceanographer. I have made no mention of transducers, or of the transducer to surface link, or of the storage method. The design of the system must in no way dictate what the oceanographer should measure or how accurately he measures it, subject to the real technical limitations imposed by the state of the art. It is complicated enough and expensive enough to require a degree of standardization of components, but it must be adaptable to a wide variety of measurements by the choice of specific transducers.

ACKNOWLEDGMENT

The work discussed in this paper was made possible by support from the Office of Naval Research, Department of the Navy, under Contract Nonr 2196(00).

A DATA ACQUISITION AND REDUCTION SYSTEM FOR OCEANOGRAPHIC MEASUREMENTS

by DAVID D. KETCHUM and RAYMOND G. STEVENS
Woods Hole Oceanographic Institution
Woods Hole, Massachusetts

ABSTRACT

A system for recording and reducing oceanographic data in many time-dependent variables is described. The system permits recording up to twelve simultaneous data channels with a nominal frequency response from DC to 10 cycles. Transducer outputs are converted to FM-analog form using standard telemetry techniques and components. The data multiplex is recorded on magnetic tape with or without an intervening telemetering link.

The tape recorded data is played back into an analog to digital data reduction system, which samples the individual channels, converting the analog data into digital format suitable for entry into an electronic digital computer.

The use of a standardized tape format and modular components in field data acquisition units assures a highly flexible system applicable to a wide variety of oceanographic and marine meteorological problems.

INTRODUCTION

One unusual feature of oceanographic science is the fact that the basic phenomena which we strive to understand are characterized by variables which are both time and space dependent.

Most of the early work, and much of the present work, in oceanography consists of a spatial sampling of oceanographic parameters wherein observations are made from ships covering the wide expanse and depth of ocean. In many cases the time dependence of such data must be ignored since it cannot be observed. The so-called "classical" oceanography which has so carefully traced the spatial distribution of water masses and their chemical and thermal content falls into this category. However, since we know that the ocean is dynamic, always in motion, always influenced by spatial and time varying solar radiation, atmospheric winds and precipitation it would seem essential to observe the time variable characteristics of the ocean as well as its spatial variability if we are to gain an understanding of its dynamic processes.

Until very recently oceanographers have not had the technological or financial resources at their disposal to carry out extensive time dependent observations. However, some recent technological advances make possible the design of compact fast response transducers for the measurement of many physical and chemical variables. Another important technological advance is in the area of information transmission, storage and retrieval which provides the link between field observations and the digital computer, thus forming a unified system for observation and analysis of time varying data.

The remainder of this paper is devoted to a description of one system which performs the function of information transmission, storage and retrieval. It should be pointed out before entering into the technical discussion that there are many subtle but important differences between serial time dependent observations and the broad scale spatial observations in oceanography. For example, time serial observations tend to accumulate vast quantities of data which must be handled by rather elaborate statistical techniques - thus the requirement for a digital computer and automatic data reduction systems. Furthermore it is absolutely essential that the dynamic characteristics of the entire data acquisition and reduction system be considered in addition to the more usual consideration of accuracy of the measuring system. In fact accuracy and dynamic response are inextricably linked when measuring time dependent variables.

FUNCTIONAL DESCRIPTION

In recognition of the need for a system capable of recording several simultaneous channels of continuous time-dependent data with frequency components ranging

Woods Hole Oceanographic Institution
Contribution No. 1227

up to the order of 10 cps, a system has slowly been developed at Woods Hole. An early effort by Farmer[1] on this line was used for the measurement of ocean waves, where a record of heights and instantaneous slopes at fixed points on the sea surface was desired. Initial experiments where these variables were measured and directly recorded on a multichannel galvanometer recorder soon revealed the necessity for a more sophisticated approach.

First, the need for remote measurements beyond the reach of a conveniently handled cable link was recognized. Second, the task of manually reducing the data from a continuous strip-chart recording was soon found to be far too tedious to be practical or economical. Further, the requirements of the various analyses applied to the data were of such a nature that automatic digital computing techniques were mandatory. Thus at an early stage in the wave measurement program the need for a telemetry and data processing system, whose final output would be sampled data in a format suitable for entry into a digital computer, was recognized.

As the system evolved and it became evident that it could usefully be applied to a wide variety of problems in oceanography and meteorology, the following desirable characteristics were specified:

1) Flexibility: The input to the system should be compatible with a wide variety of transducers.

2) Analog storage: The data should be stored in analog form with minimum degradation, and the storage medium should be chosen to allow fast, automatic sampling and digitization for ultimate entry into a computer.

Functionally, the system may be represented by the block diagram shown in Figure 1[2]. It is divided into two major parts, which perform the functions first of data acquisition and storage, and second of playback and processing. The data acquisition and storage function is performed as follows.

The electrical outputs of the transducers (usually voltages which are analogs of the physical quantities being measured) are processed by signal conditioners to bring them to level and form suitable for operating the modulators. The modulators further operate on the transducer signals in such a way that they may be transmitted and stored with minimum degradation. A second function of the modulators is to multiplex the several signals for transmission over a single link. The data multiplex, after passing through the transmission link, is stored in analog form. Note that at this point the raw data is still in existence, degraded only by the distortion and noise inherent in the system. The analog storage medium is of a permanent nature so that the raw data can be stored indefinitely, if desired.

An inspect function is shown, which allows the investigator to observe the progress of his experiment and determine the proper operation of the system. The position of this function is shown at the input of the modulators, but it may actually be located anywhere between the transducer outputs and the output of the transmission link.

Processing begins with playing back the raw, multiplexed data. The individual channels are separated out by the demultiplexers and demodulated. The result of these operations is a set of voltages directly proportional to the transducer outputs.

At this point the data may be displayed for inspection, for example on a graphic recorder, to allow the experimenter to examine and edit his data for further analysis. It is now necessary to prepare the data for entry into the computer. The several channels are scanned in sequence by the commutator, and the sampled voltages are converted into binary coded numbers, which are entered into the computer.

TECHNICAL DESCRIPTION

In choosing the techniques and components to realize the various functions shown in Figure 1 every attempt was made to utilize standard hardware and well-developed methods wherever possible. At an early stage it became apparent that the needs of the aircraft and missile industry had fostered the development of standard telemetry systems which could be adapted to the needs of our science. Accordingly we were able to draw heavily upon the accumulated experience of specialists in this field and find "off the shelf" components produced by several companies specializing in the techniques of data transmission.

The method chosen was a well-proven technique of frequency-division multiplexing wherein the signal from each transducer frequency modulates an audio oscillator over a rather narrow range. A separate center frequency is assigned to each oscillator and sent over the transmission link. It is generally most convenient, where a radio link is necessary, to use FM transmission. In this case the technique is referred to as FM-FM telemetry, signifying that both the subcarriers

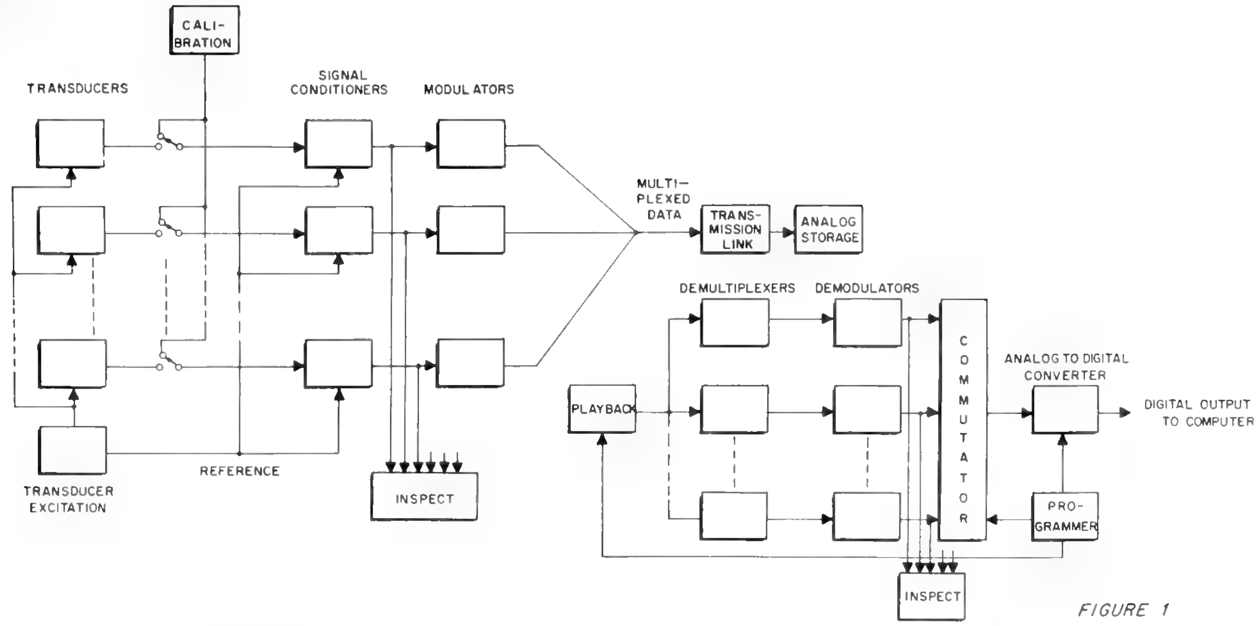

FIGURE 1

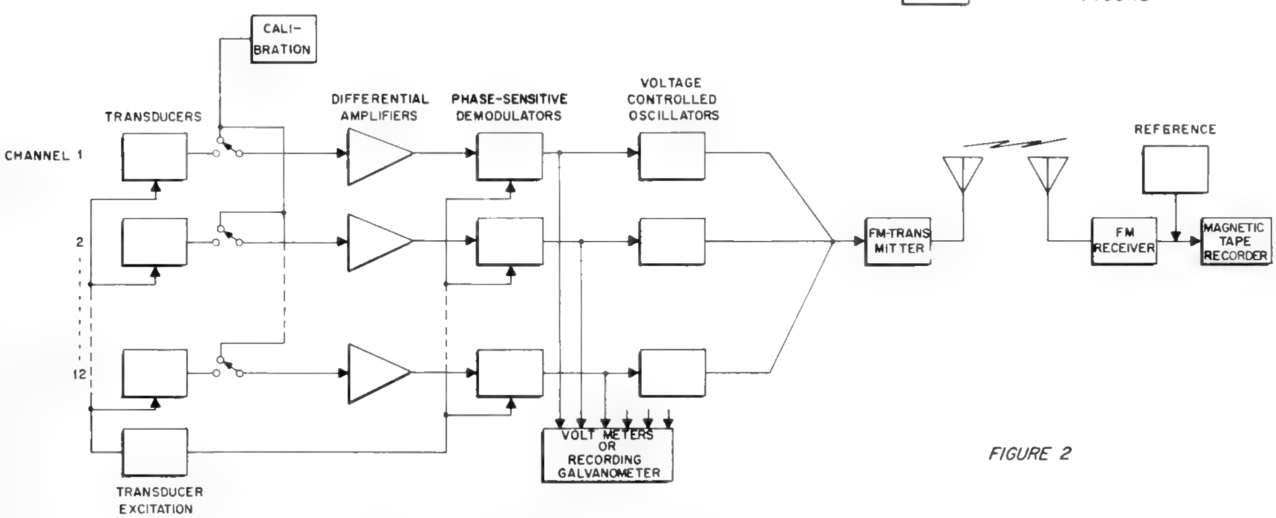

FIGURE 2

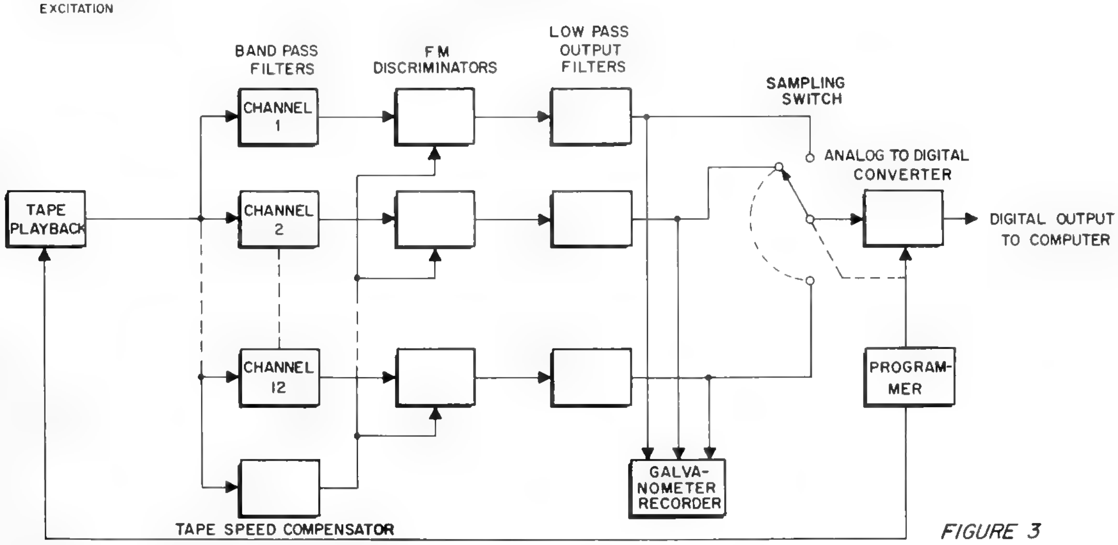

FIGURE 3

and the RF carrier are frequency modulated. At the receiving terminal the subcarrier multiplex is recovered from the RF carrier by means of a conventional FM receiver and directly recorded on magnetic tape.

The advantages of the FM-FM technique are several:

1) The use of frequency-division multiplexing makes possible the simultaneous recording of several continuous time-dependent variables without introducing the sampling errors encountered in time-division schemes.

2) Frequency modulation of the subcarriers not only carries with it the well-known advantages of signal to noise ratio improvement in the transmission link, but also overcomes the problem of intolerably large amplitude fluctuations caused by lack of uniformity in the magnetic tape.

3) FM subcarriers allow the recording of DC levels on magnetic tape.

A limitation of the FM-FM system is imposed by its large bandwidth, which requires the use of a very high frequency carrier. Although there is a valuable reduction in atmospheric noise in this part of the radio frequency spectrum, the transmission distance is limited by the line of sight. It is, however, possible to employ the FM-AM technique, where the frequency-modulated subcarriers amplitude modulate a carrier at a lower frequency suitable for trans-horizon communication. The bandwidth allowable at these frequencies severely limits the number of channels, and transmitter power must be increased to offset the increase in atmospheric noise.

Figure 2 shows the actual components of a typical data acquisition system, representing merely one of several variations which are compatible with the data reduction equipment. In this case the transducers are AC excited bridges, and it is required that the sense of the bridge unbalance be known. The bridge output voltages are therefore fed to differential amplifiers in order to bring them to a level suitable for operating phase-sensitive demodulators. The outputs of the demodulators are DC voltages proportional to the AC transducer outputs. Their polarity is determined by the phase of the amplified transducer signals with respect to the reference voltage, which is derived from the transducer excitation source. The DC output voltages from the demodulators vary the frequency of voltage-controlled subcarrier oscillators, and the frequency multiplex modulates an FM transmitter operating in the VHF telemetry band. An FM receiver at the receiving terminal recovers the frequency multiplex, which is recorded on a single track of magnetic tape.

There are many cases where the telemetry link is not necessary, and it is merely desired to record the data in a compact form at the site of the experiment. Here, of course, the mixed output from the subcarrier oscillators is directly recorded on the magnetic tape. The individual components shown in the data acquisition system are all either available commercially as standard transistorized plug-in units or as designs developed at WHOI. Thus data acquisition units for field use may easily be designed using the modular concept with a minimum of circuit development. Both voltage-controlled and resistance-controlled oscillators are available for a wide range of sensitivities. Where DC excited transducers are used, the amplifiers and demodulators are, in most cases, unnecessary. For AC systems a specially developed differential amplifier-demodulator combination is now available commercially. The inspect function would probably be omitted in remote, unattended installations, but a monitoring arrangement then becomes desirable at the output of the FM receiver or cable link. Calibration signals are inserted in the usual manner at the input to the system by substituting standardized signals for the transducer output.

In the recording process a certain amount of variation in the transport speed of the tape is always present. Tape speed variation frequency modulates the recorded signal, and in an FM system results in noise. A well-known method is used to overcome this difficulty. In addition to the data multiplex a signal from a frequency-stabilized oscillator operating at a different frequency from any of the subcarriers is recorded on the tape. During play-back the deviations in the frequency of this signal are detected and used to compensate for variations in the data signals caused by tape speed variation.

The playback and processing system known as ADDReSOR, (Analog to Digital Data Reduction System for Oceanographic Research) has recently been put into operation at the Woods Hole Oceanographic Institution, supplanting earlier apparatus of more limited scope. Figure 3 shows a much simplified block diagram of the device which was manufactured by Tele-Dynamics Division of American Bosch Arma to WHOI specifications. A total of twelve channels may be accommodated. Demultiplexing and demodulation are accomplished by standard subcarrier discriminators, each of which contains in one unit an appropriate band-pass filter for selecting the desired subcarrier, an FM discriminator, and a low-pass filter in the output for removing subcarrier ripple from the recovered data signal. One more discriminator is used to detect variations in the frequency of the reference signal. The output of this unit is applied to the other discriminators in such a way that it corrects the effects of tape speed variation. The inspect function may be provided by connecting a multi-channel recording galvanometer to the outputs of the discriminators.

The function of the Programmer-Digitizer is to sample analogue voltages and convert them into a binary digital format suitable for direct entry into the Recomp II computer. This may be done simultaneously with, or independently from the graphic presentation.

The Programmer-Digitizer has 12 input connections on a patch panel to receive up to 12 analog voltages. The number of input connections used in a given case is called the GROUP SIZE and may be any number from 1 to 12. A dial marked GROUP SIZE SELECTOR is set to correspond with the number of input connections in use.

An internal switching device scans all of the active input voltages in sequence and transmits the voltage to an analog-digital converter. The frequency with which the switching device scans the entire GROUP of voltages is called the GROUP SAMPLING RATE and is adjustable by dial settings from 1 to 100 times per second. Since the patch panel permits plugging the same voltage into any or all twelve inputs it is possible to sample a single voltage 1200 times per second, two voltages 600 times per second, 12 voltages 100 times per second and so on. It should be noted, however, that the sampling speed of the Programmer-Digitizer may exceed the ability of the computer to receive digitized information. If need arises, and as opportunity is presented, the computer capabilities will be suitably improved.

Since the computer memory has a finite capacity it is necessary to provide a means of limiting the number of samples which will be stored. A panel control marked TOTAL is set to the total number of samples per channel desired. The computer capacity is in excess of 12,000 DATA WORDS so that for a GROUP SIZE of 12 the maximum permissible TOTAL setting would be something over 1000. For a GROUP SIZE of 2 the TOTAL setting could be over 6000 and so on.

Manual controls are provided to allow the programmer to be advanced manually through the sampling sequence, during calibration and test procedures, and to permit sampling rates to be controlled by accessory apparatus.

A visual binary display of the buffer contents is provided on the panel.

The sampling sequence is as follows:

1) Upon receipt of a signal from the computer the analog tape playback is energized.

2) The channel selector switch steps to input number 1 and samples the voltage at that input. In order to achieve accuracy when sampling rapidly varying data the time duration of the sample, called the aperture time, is limited to 1 microsecond.

3) The sampled voltage is converted into a 10 bit binary number and read directly into the computer. The actual timing sequence of this operation depends upon the input capability of the computer.

4) The channel selector switch is then stepped to input number 2 and the above operation repeated. Stepping continues through successive inputs until the number of inputs specified by the GROUP SIZE selector have been sampled. The channel selector switch is then returned to its off position. At this point a timing device is actuated causing the channel selector to wait an interval of time before recycling through the various inputs. The time delay is determined by the setting of the GROUP SAMPLE RATE dials.

5) After completion of each group sampling the programmer advances the group counter by one count and compares the counter with the setting of the TOTAL dials. When the two numbers agree the programmer generates a termination sequence to the computer which stops data filling and may cause the computer to start executing an internal program.

The present computer used with the ADDReSOR is an Autonetics Recomp II which requires 7.5 ms to enter and store each DATA WORD. Thus a total of 90 ms is required to scan all 12 channels, or in other words a phase lag of nearly 180° would occur between 10 cps data on channel 1 and channel 12. Furthermore, this relatively slow input rate limits the system to 11 samples per second per channel when using all 12 channels, 22 samples per second per channel for 6 channels and so on. This restriction means that no more than 5 cps intelligence frequency can be recovered when using all twelve channels, 10 cps intelligence frequency can be recovered when using 6 channels, etc. Present plans call for incorporating a faster computer into the data processing system in the near future so that these restrictions will be removed.

The data entered into the computer from ADDReSOR consists of 10 binary bit words. This would imply an accuracy of 0.1% if taken at face value. However, FM subcarrier system accuracy is probably no better than ± 1% so that some of the binary bits are extraneous and should be ignored in the computations.

A few general purpose programs have been developed for use with the ADDReSOR. First, a control program is used to enter and evaluate the calibration signals and enter the data samples. This program reads into the computer 100 samples of the field calibration signals, computes the mean and variance of these signals and the calibration constants for each variable. The operator may inspect these results before proceeding with further computations. Up to 12,000 data samples may then be entered and the means and variances of each variable may then be computed if desired.

A second program consists of an unpack and punch routine which multiplies each variable by its appropriate calibration factor and punches the calibrated data in either 10 bit binary format or in teletype format. The punched tape may be used for reentry into RECOMP II or for entry into other computers.

Using a computer as a medium for temporary storage of the digitized data has certain advantages. First of all, it is not feasible to use either a tape punch or a magnetic tape transport directly on the output of ADDReSOR since the sampling rate may be too high for mechanical punches and too variable for magnetic tape transports without some means of temporary storage. Secondly, a small or medium size computer is probably the most economic means for temporary data storage, particularly since it may be used for a wide variety of other computing problems. Thirdly, elementary calculations such as means and variances, running means, calibration, etc. may be performed before punching the data onto tape.

CONCLUSIONS

We have described here a completely integrated data acquisition and reduction system which has the following general characteristics at the present time:

1. 12 channels of continuous data storage
2. Frequency response for 12 channels ~ 5 cps
   6 channels or less ~ 10 cps
3. Accuracy overall is presumed to be better than ± 2%
4. Total data samples 12,000 +

Restrictions on the frequency response can be improved by using a faster computer and by replacing the output low pass filters on certain subcarrier discriminators. It is possible also that the total number of data samples may be increased by using a high speed computer. For the moment, however, there is a vast area of oceanographic research which can be accomplished within these restrictions.

ACKNOWLEDGMENTS

The authors wish to acknowledge the invaluable assistance of Mr. Raymond A. Stahl of Tele-Dynamics Division of American Bosch Arma Corporation who designed and supervised construction of the ADDReSOR, the personnel of Geodyne Corporation who developed the special purpose amplifier, and Mr. Leonard Shodin of the WHOI staff who designed and constructed much of the data acquisition system. The developments reported in this paper were made possible by the Office of Naval Research Contracts Nonr 2196 (00) Nonr 3351 (00).

REFERENCES

1. Farmer, H. G. and Ketchum, D. D. (1960). An Instrumentation System for Wave Measurements, Recording and Analysis. Proc. 7th Conf. Coastal Eng. Council Wave Res., Univ. of Calif. Berkeley

2. Proceedings of the Conference on Automatic Data Handling for Oceanographic Observations (1959). Ref. No. 60-10. Woods Hole Oceanographic Institution, Woods Hole, Mass. (Unpublished manuscript).

THE PROBLEMS OF RELIABLE LONG-RANGE TRANSMISSION OF REMOTE OCEANOGRAPHIC MEASUREMENTS

by C. McLOON, Member Technical Staff
Hughes Aircraft Company
Los Angeles, California

PRECIS

Data telemetry transmission falls basically into two categories: line-of-sight and beyond-line-of-sight. When the transition to long range is made, entirely new telemetry techniques are required. This paper describes the problems involved with long range telemetry, together with some state-of-the-art solutions.

INTRODUCTION

With the advent of mass oceanographic measurements brought about by the emphasis the Government is placing on oceanography, techniques must change to handle the increased volume of data. One of the principal changes will be in the manner in which measurements are taken. The trend will be toward full automatic electronic systems wherever possible. This, then, will mean an expansion in the field of data telemetry.

Because of the "remote nature" of the oceans, remote measurements will be required. For year-round data collection automatic telemetry systems will be used. At the field location this will entail an automatic examination of the sensor, coding of the information, and transmission of this coded information. At the receiving station these data will be received, detected, decoded, and presented or stored in some manner. These techniques are not new to the telemetry and communication industries but, considering the ranges involved, the application to oceanography is unique. The problems involved in the long range transmission of these measurements are discussed below.

TELEMETRY SYSTEMS

Radio telemetry appears to have had its inception[1] about 1930 by telemetering data from weather balloons in Germany. Since that day, the word telemetry has become practically synonymous with aircraft data, missile data, and space data whereas, in reality, the word is synonymous with data transmission. In reading telemetry texts, published articles, and papers on the subject, it would seem reasonable to guess that about 99 percent of them make reference to radio telemetry application in one of the fields of science listed above.

The work in the above areas has advanced the field of telemetry using techniques such as AM-FM, PPM, PAM, and PDM, to name but a few. For reasons to be explained later, these systems are limited to use in line-of-sight VHF and UHF systems and certain scatter systems, but are not usable in HF systems. Beyond-line-of-sight telemetry has somewhat lost its association with the telemetry industry and is now termed data transmission systems. Unfortunately, this field has not received the attention given to line-of-sight telemetry and therefore is open for improvement. In general, there are presently three means of propagation that are used to one degree or another for beyond-line-of-sight radio telemetry: high frequency radio, ionospheric scatter, and tropospheric scatter. Each of these methods has certain disadvantages such as the extreme multipath problems[2] experienced in HF radio, a degree of multipath[3] in the scatter systems, and high power requirements of the scatter systems.

It will be assumed that for remote oceanographic measurements an unmanned buoy of small size is to be used. Therefore, large power sources are out of the question from a physical standpoint, thereby eliminating scatter systems. This paper will detail the HF radio technique which is judged to show the greatest promise.

HF TELEMETRY PROBLEMS

Long range operation in the HF spectrum depends wholly on the ionosphere. The ionosphere functions to reflect radio waves of certain frequencies. Characteristics affecting the use of the ionosphere are: time of day (or night), season, 11-year cycle sunspot activity, frequency, and geographical location. Unexplained anomalies

Superior numbers refer to similarly numbered references at the end of this paper.

exist which occasionally cause what are apparent holes or areas of absorption in the ionosphere where radio waves are not reflected. Ordinarily, during daylight hours, the ionosphere consists of three layers of ionization capable of reflecting radio waves. This is best illustrated in Figure 1. The signal from point A to point B traverses three different paths simultaneously but, due to the differences in path lengths, do not arrive at point B simultaneously. This is another characteristic of the ionosphere called multipath propagation.

When reliable signals are required that are not distorted in amplitude, frequency, or time, HF systems cannot be tolerated. It was stated earlier that the pulse modulation techniques used in VHF and UHF systems were not usable in HF systems and only to a degree in scatter systems. This limitation results from the effects of multipath.

HF TECHNIQUES

Perhaps the oldest use to which the HF spectrum has been applied for pulse propagation is radio-telegraph. Here data are transmitted in the form of short or long pulses called dots and dashes. The alternate signal paths caused by multipath ordinarily do not cause differential delays of more than 2 to 3 ms although, in some cases, delays of up to 14 ms have been measured. Three-ms delay is negligible at normal telegraph speeds and therefore causes no trouble. However, attempts to speed up a conventional radio-telegraph transmission beyond, say, 300 wpm, become unsuccessful because delayed, or multipath, components of one signal element start to overlap the first arriving components of the succeeding signal element. Preceding the arrival of those pulse components over longer transmission paths, the first arrived pulse will have an amplitude determined solely by ionospheric conditions, transmitted power, antennas, frequency, and like factors. The succeeding train of received pulses resulting from the one transmitted pulse and arriving via different propagation paths, will be of such phases and amplitudes as to increase or decrease the amplitude of the first arrived pulse and to distort its waveform. In the simple case of the two paths providing equal signal strengths, the resultant received signal may vary from zero to twice the amplitude of either in the overlapping area, depending upon the relative r-f phase. This point is best shown by using an illustration. Figure 2 shows a series of transmitted pulses with the assumed position of a single multipath component. If the r-f of the multipath pulse is in-phase with the first arrival or primary pulse, both amplitude and width distortion will occur. If out-of-phase distortion occurs for a nonsynchronous system, the number of pulses have been multiplied. Figure 3 shows actual photographs of a transmitted pulse and the corresponding received pulse train with the many multipath pulses.

Another old HF pulse system is FSK radio-teletype. This system uses two carrier frequencies separated conventionally by about 800 cps. When one carrier is on it is called a teletype mark, the other carrier being called a teletype space. The two channels are never keyed simultaneously. The pulses, at normal speeds of 60 or 100 wpm, are somewhat distorted by multipath components but usually do not cause garbling; however, greatly increased speeds are not reliably attainable.

Several other pulse systems exist which are used in the HF spectrum. For these the same argument holds that the pulse repetition frequency must be limited to retain intelligence. Any of these systems may be used quite successfully for slow speed data systems. They should be considered seriously if they will handle the data rate desired.

STATE-OF-THE-ART

The communications industry has been faced with this multipath problem for years in their digital systems for data, printed-message communications, and speech. The solution to the problem lies in keeping the pulse width sufficiently narrow to allow the primary pulse to completely arrive before its multipath components and to space these primary pulses out in time so as to allow all the multipath components of one pulse to arrive before the second pulse. If it is assumed that a 3-ms gap between pulses will allow for the arrival of all important strength multipath components and a 1-ms pulse is transmitted, the data rate becomes 250 pps.

The problems of multipath have been overcome successfully in several systems built for the U. S. Government. These systems utilize a modulation technique called Quantized Frequency Modulation. [4] Many tests have proved that these systems will continue to perform satisfactorily when the more conventional systems fail. This technique enables the data rate to be increased and, at the same time, provides multipath protection. Quantized Frequency Modulation (QFM) is a frequency shifting technique applicable to digital transmission systems in which the transmitter carrier frequency is caused to change cyclically with time in quantized increments. By means of discrete frequency changes in the receiving system, in synchronism with those in the transmitter, the receiving system is made responsive to the QFM channels in use at any instant in time, and ignores the other channels. Alternatively, the receiver may have a bank of filters, one for each QFM channel and, by means of sampling techniques, achieve the same results. In both cases, signals propagated to the receiver over paths that have transmission time delays that differ from that of the prime path, arrive at the receiver at a time such that they are not normally effective in the receiver's digital decision process. In this manner, the deleterious effects of multipath are greatly diminished. A similar technique, termed Quantized Phase Modulation (QPM), contains the intelligence in the r-f phase as opposed to the dual symbol type intelligence of QFM. (A dual symbol system is one where the binary intelligence is contained in a pulse on either of two channels, such as FSK teletype.)

Table I shows the modulation modes of the Air Force AN/URC-23 equipment.

TABLE I

AN/URC-23 Modulation Modes

Data Rates (bits/second)	Modulation	Number of QFM/QPM Channels	Band-width (kc)
1000	QFM-DCAM	8	7
2000	QFM-DCAM	16	14
1000	QPM-PM-2ϕ	4	4
2000	QPM-PM-2ϕ	8	7
4000	QPM-PM-2ϕ	16	14
4000	QPM-PM-4ϕ	8	7
8000	QPM-PM-4ϕ	16	14

The above table illustrates several of the modulation schemes possible with QFM and QPM but does not include any of the redundant modes of operation. (A redundant system is one where the same binary bit of intelligence is represented on two or more channels, thus giving repetition.) To illustrate the modulation technique in more detail, a dual channel system with a redundancy factor of four will be described.

Figure 4 shows a typical transmitter output as viewed at the antenna. The signal consists of a series of cosine-squared shaped pulses but not all at the same radio frequency and each group of four representing one binary digit. The separate received waveforms are shown with a small amount of multipath which exists in the receiver system through detection and integration, but has no effect on the converted digital output. This form of redundancy serves to improve reliability in the presence of interference.

There are many possible configurations of QFM and QPM. Categorically, a particular system cannot be recommended for oceanographic use until such parameters as data rate, reliability, bandwidth allocation, and geographical locations are determined. In addition, several other problems enter into the system. If continuous 24-hour data are required and interim storage at the source is impossible, operating frequency becomes a problem. Usually, the optimum frequency for daytime use will not even be usable at nighttime and vice versa, therefore, multiple frequencies will be required for continuous duty. Power, of course, will be a never-ceasing problem for an unmanned buoy but will not be treated here.

The final problem, but not in the technical area, is one of getting a frequency allocation in the HF band. A recent letter from the FCC to the author indicates that there are presently no allocations for oceanographic data use, nor is the Commission anticipating the allocation of any for such work. This will not interfere with data collection by Government organizations because their current allocations may be used as they see fit in most cases; but the private institution will suffer unless their sponsoring agency grants an allocation. However, experimental licenses and allocations may be obtained and, although good only for a limited period of time, may be adequate to complete a specific program.

FUTURE TECHNIQUES

It has been suggested that in the future data may be collected in remote locations and telemetered to shore via a satellite system.[5] This is probably very practical and feasible, but is still many years in the future considering the other more pressing requirements of communication satellites.

A possible new field of communications exists where the earth strata found just under the deep ocean floor may propagate transmitted energy to a receiver site. If so, oceanographic equipment may be placed on or near the ocean floor, thus eliminating the need for surface equipment, except for a subsurface buoy for maintenance purposes. This would eliminate the surface equipment which is always subject to pilferage and ship damage. Investigation of these techniques is now in progress.

REFERENCES

1) Nichols and Ranch, Radio Telemetry, 2nd edition.

2) J. D. Lambert, "High Frequency Multipath Analysis by the Short Pulse—Long Pulse Method," IRE Convention Record, Part 1, pp 294 to 299, 1957 Wescon.

3) J. H. Chisholm, et al, "Investigation of Angular Scattering and Multipath Properties of Tropospheric Propagation of Short Radio Waves Beyond the Horizon," Proc. IRE, Vol. 43, pp 1317 to 1335, October 1955.

4) George A. Scheer, "New System Defeats Multipath Effect," Electronic Industries, May 1960.

5) J. M. Snodgrass, "Problems of the Oceanographer in the Space Age," Proc. of the National Telemetering Conference, p 12-9, 1961.

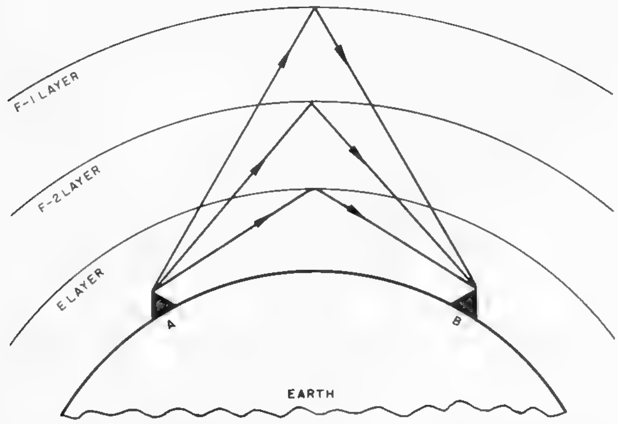

FIGURE 1. MULTIPLE SIGNAL PATHS VIA THE IONOSPHERE.

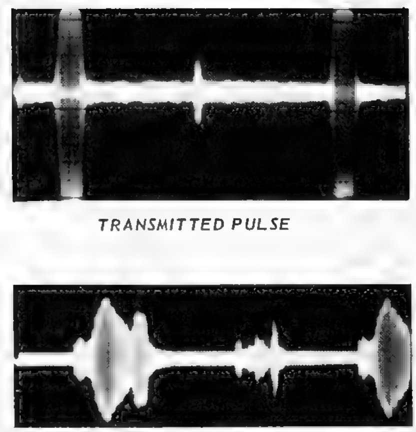

FIGURE 3. PHOTOGRAPH OF MULTIPATH COMPONENTS.

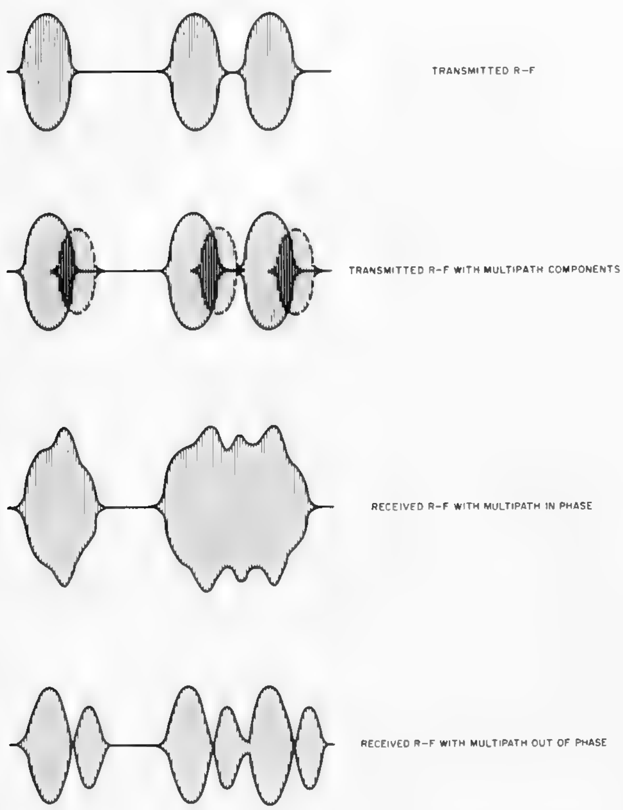

FIGURE 2. EFFECTS OF MULTIPATH.

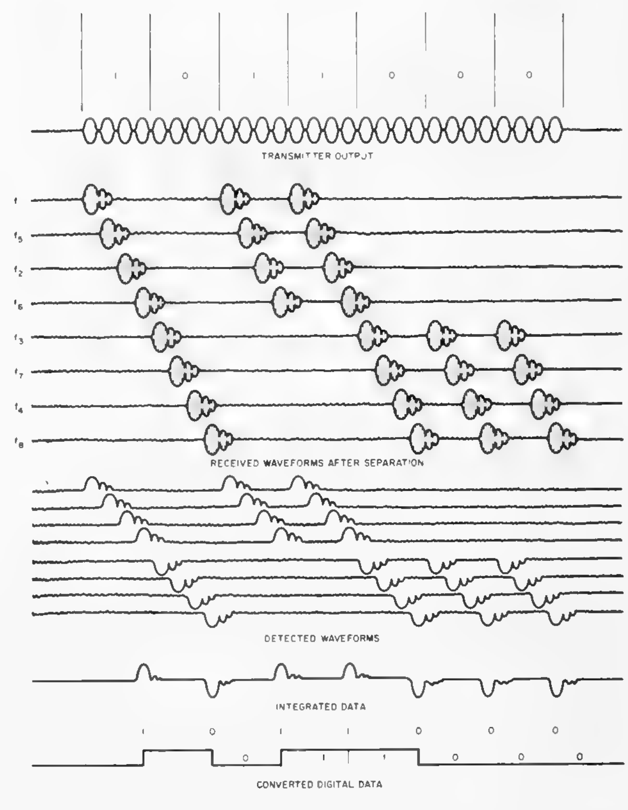

FIGURE 4. DUAL SYMBOL REDUNDANT SYSTEM WAVEFORMS.

A DATA PROCESSING AND DISPLAY INSTRUMENT FOR OCEANOGRAPHIC RESEARCH

by JOSEPH T. LAING, Section Manager, Ocean Survey Systems
Westinghouse Electric Corporation, Ordnance Department
Baltimore, Maryland

ABSTRACT

A data processing and display instrument consisting of a high-speed digital computer and precision X-Y plotter is described. Originally developed by Westinghouse for navigational purposes, the instrument is suitable for similar use in oceanographic survey work as well as real-time processing and plotting of such oceanographic research data as temperature, depth, sound velocity, water currents, and similar parameters. By means of a universal input-output system and the capacity for general purpose programming, the instrument can be easily adapted to a wide range of oceanographic problems at sea and in the laboratory. Pictures are shown depicting the type of equipment currently available, and modifications for several specific applications are discussed.

INTRODUCTION

The expanding effort on the national scene of oceanographic research and world-wide surveys is presenting the scientific community with greater challenges than ever before in the collection and analysis of oceanic data. No less challenge is presented to industry in supporting the scientific community through mechanization of instrumentation systems which are truly responsive to the oceanographic problems at hand. There is perhaps no greater challenge in this area than the processing and reduction of the vast quantities of data emanating from oceanographic research and survey programs. In this paper I will describe one general-purpose instrument designed for shipboard processing and recording of certain types of data, and I will attempt to show its application to a wide range of oceanographic data processing problems.

GENERAL DESCRIPTION OF OPERATION

The instrument is essentially a digital computer and X-Y plotter integrated into one package. It was originally designed and built for the U.S.Navy Bureau of Ships as part of a military defense system. The nature of its mission here required that it be versatile in its adaptability to various modesof operation related to the original problem. The same versatility also permits the solution of problems of a somewhat different nature.

In its principal mode of operation the instrument accepts analog data in the form of ranges or bearings from navigational control stations, computes the precise geographical position of the ship, and plots this position on a nautical chart. In addition, the position data are transmitted digitally to other output devices. Fig. 1 is a block diagram of the instrument. In the main computer-plotter console, a bank of analog-to-digital converters converts the voltages from various sensors into binary form for entry into the computer. Sensor voltages are, in the case shown, cabled to the console from the navigational control system (such as Shoran, Loran C, or OMEGA) and entered into the computer by this route. The computer, having been previously instructed by insertion of an appropriate program, performs the computations necessary to determine the geographic position of the ship. Upon command from the computer, this position is plotted on the chart and simultaneously transmitted to remote output devices which include a Friden Flexowriter and remote digital displays. Note that in the case of the plotter the position data must be converted to analog voltages for driving the plotter servo system. Full digital accuracy is, of course, preserved in the data printed out on the Flexowriter and displayed elsewhere.

The steering aid shown is actually a by-product of the position computation, in that it permits the comparison of the computed position with a desired position based on some preselected course of the ship. An appropriate error signal, proportional to distance off course or preferably distance plus angle, may be displayed at the helm as an aid in following survey lines.

Other sensor data may be brought in as desired. The plotting of some position other than ship position, as, for example, that of a remote sensor in communication with the ship, may require a correction for ship's heading. In another case, on-station plots of temperature versus depth for synoptic surveys may be desired and may be cabled in along with other parametric data. In yet another case, ship's course and speed may be brought in to operate the instrument as a dead-reckoning tracer.

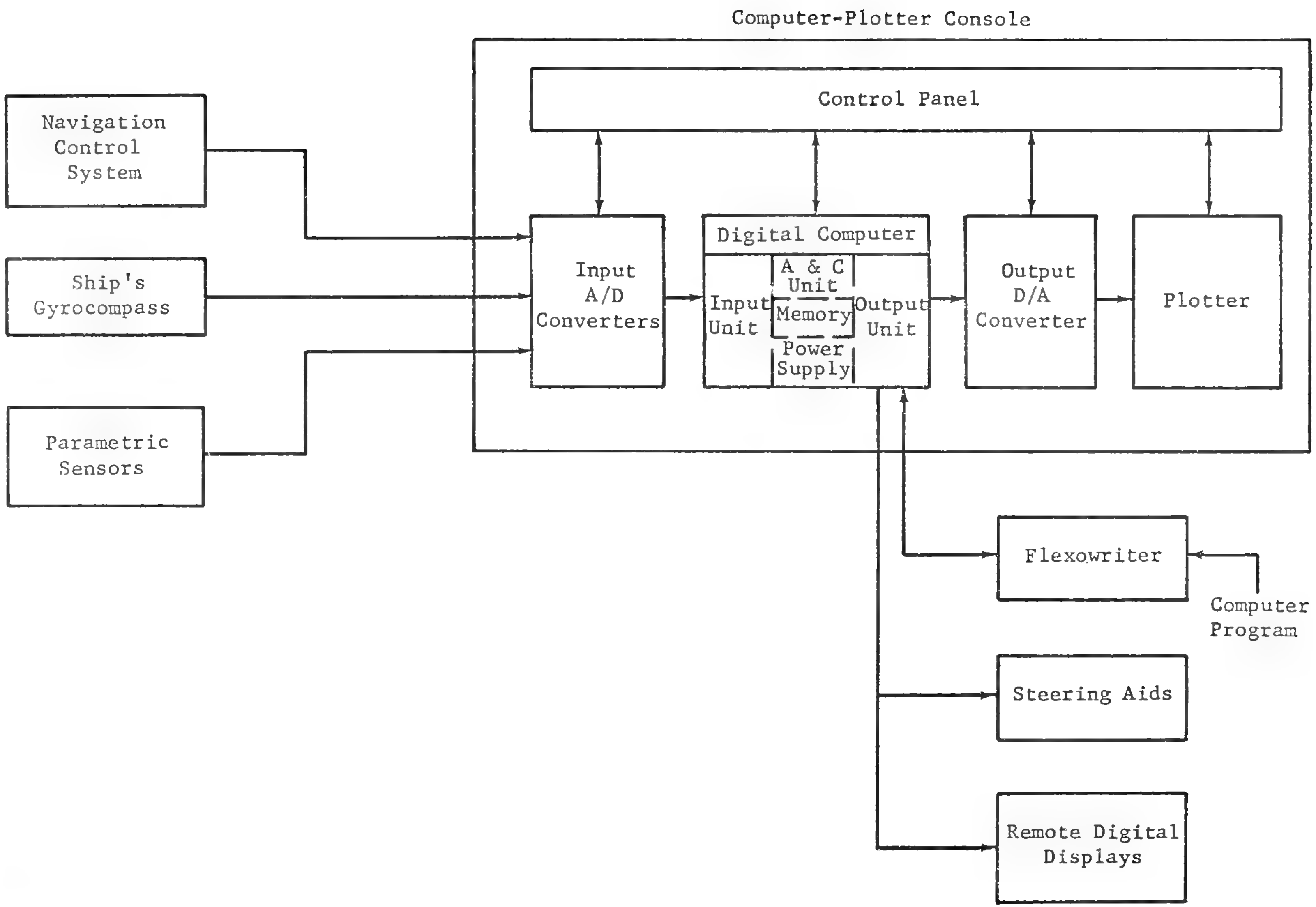

FIGURE 1 DATA PROCESSING AND DISPLAY SYSTEM BLOCK DIAGRAM

In all cases the computer program is the key to the use of the instrument. The computer may by considered a general purpose machine to the extent that the desired functions fall within its storage and arithmetic capacities, which I will discuss later on. Programs which have been previously written, coded, and prepared on punched paper tape are loaded through the tape reader on the Flexowriter. In this way a change from one mode of operation to another may be achieved with convenience and minimum down time.

DESCRIPTION OF EQUIPMENT

Fig. 2 shows the main computer-plotter console with the plotter cover in the raised position. Thisunit is 51 inches long, 46 inches wide, and 44 inches high. It weighs approximately 1600 pounds. The X-Y plotter was built by Electronic Associates, Inc., to our specifications and, for installation, is separable from the base cabinet containing the digital computer and input-output units. The base cabinet is modular and can be further subdivided to facilitate installation or removal of the equipment. The master control panel shown governs operational mode selection, insertion of operational constants germane to the task being performed, and various other control functions affecting the computer and plotter. One of the operational constants mentioned would be,in a typical case, the geographical coordinates of the navigational control stations. Another would be the chart scale factor, etc.

Fig. 3 shows the Friden Flexowriter used with the instrument. In a typical case the machine prints out positional and other parametric data required by the program and simultaneously punches the same data on coded paper tape. The punched tape data may be used for further data processing at a central facility as well as for recreating the plotted data on the same or similar instrument at another time.

INPUT ANALOG-TO-DIGITAL CONVERTERS

As mentioned previously, data enters the console as analog voltages which are converted internally to binary form. 400 cps.synchros have been standardized on for transmission of shaft positional data to the console. A bank of several shaft position-to-digital converters is provided to accept this information and convert it into 10-bit binary numbers. Relays are used to switch the limited number of converters among the many data sources necessitated by the various operating modes, thus attaining a measure of input flexibility while maintaining economy of equipment.

Fig. 4 is a schematic diagram of one analog-to-digital converter presently used. It is a simple servo follower in which the voltage from the 400 cps. synchro transmitter at the data source feeds the stator of the control transformer in the converter unit. The amplitude of the voltage across the rotor will be proportional to its angular displacement from the null position and the phase of the voltage will indicate the direction of the displacement. The error voltage is amplified by the transistor servo amplifier,which then drives a servo motor coupled through a gear train to a 10-bit code wheel and to the control transformer rotor. With the servo nulled, the digital number generated by the code wheel corresponds to the angular position of the remote synchro transmitter. A photograph of one of the servo follower units is shown in Fig. 5. These units are manufactured by the Datex Corporation.

Other means of data entry can be provided in those cases where digital data are already available or where voltage-to-digital conversion is required.

DIGITAL COMPUTER

The digital computer contained in this instrument is a general purpose transistor computer designed for shipboard applications. The program is stored in a magnetic drum memory. Physically, the computer is subdivided into printed card chassis, as shown in Fig. 6, which are mounted on the cabinet doors and hinged on one side to provide access to the chassis wiring at the back. Each chassis contains approximately one hundred printed solid-state logic cards of standard Westinghouse design. They contain accessible test points for trouble shooting and are easily removed and replaced. The computer contains five such chassis, including input-output units, in addition to other subassemblies containing power supplies and memory circuits in the interior of the cabinet.

Although the design of the computer is an interesting subject in itself, a detailed discussion of it would not be appropriate or possible here. Needless to say, it is, in terms of physical and technological complexity, the principal item in the instrument. The philosophy of its design was founded on the requirement for a computing facility combining rapid arithmetic computation in real time, precision, reasonable storage capacity, and physical compactness. A summary of the important computer characteristics should be of interest and will be listed.

Summary of Computer Characteristics

Input-Output Unit:

Up to 32 programmed inputs of 23 bits each (parallel transfer)

Up to 512 outputs of 23 bits each (parallel transfer)

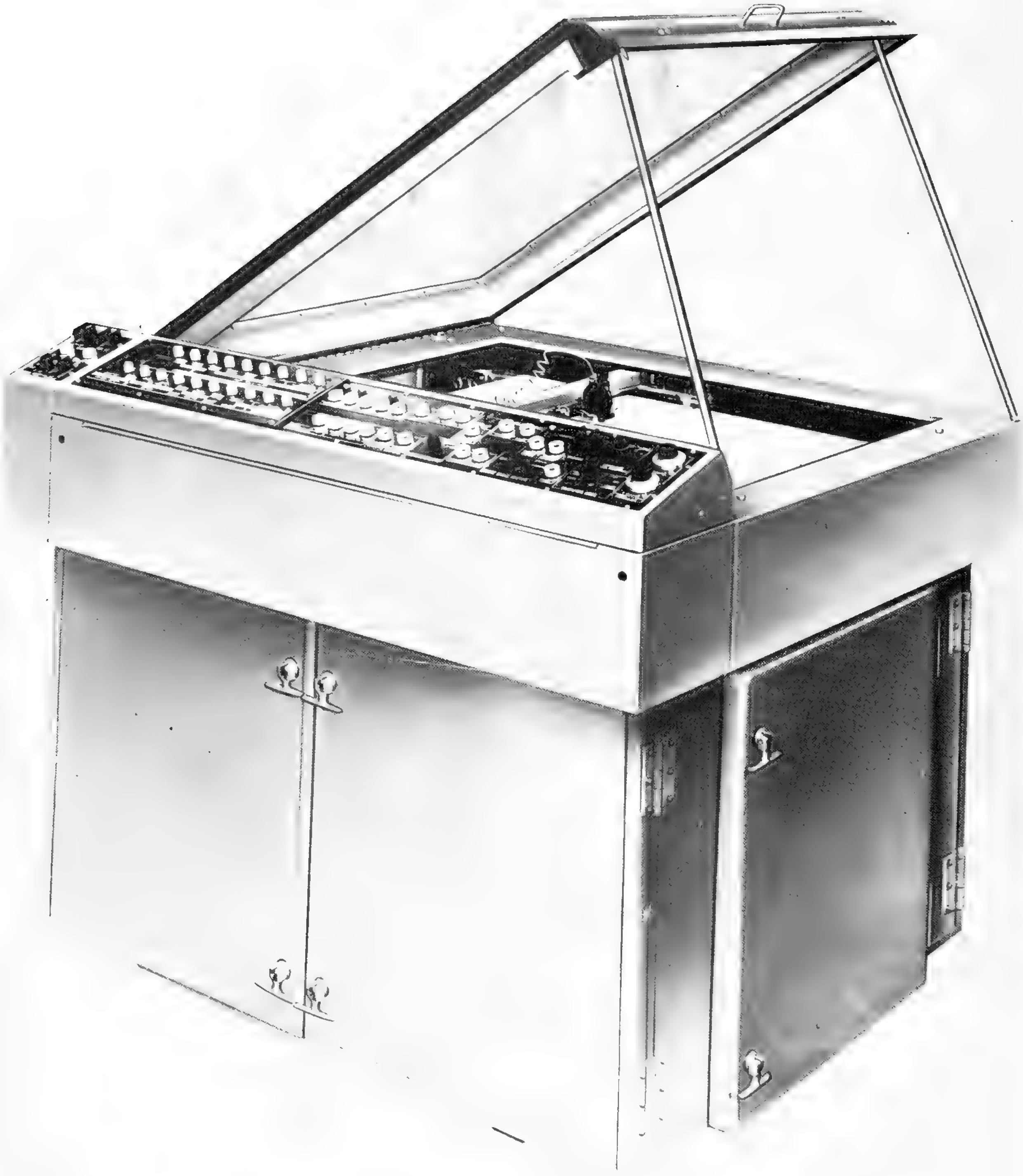

FIGURE 2 COMPUTER-PLOTTER CONSOLE

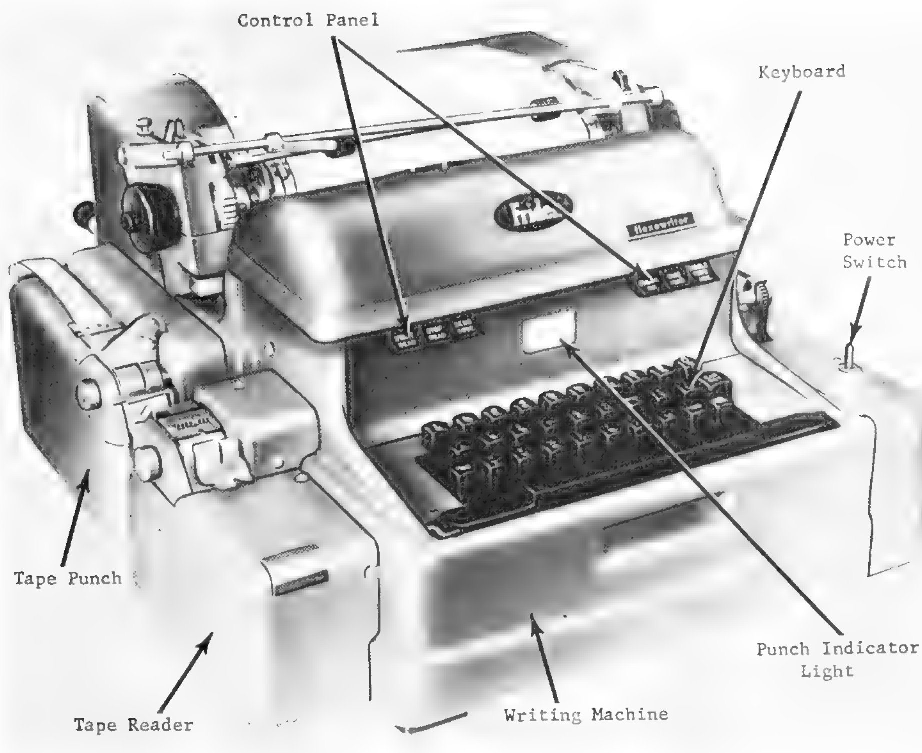

FIGURE 3 FRIDEN FLEXOWRITER

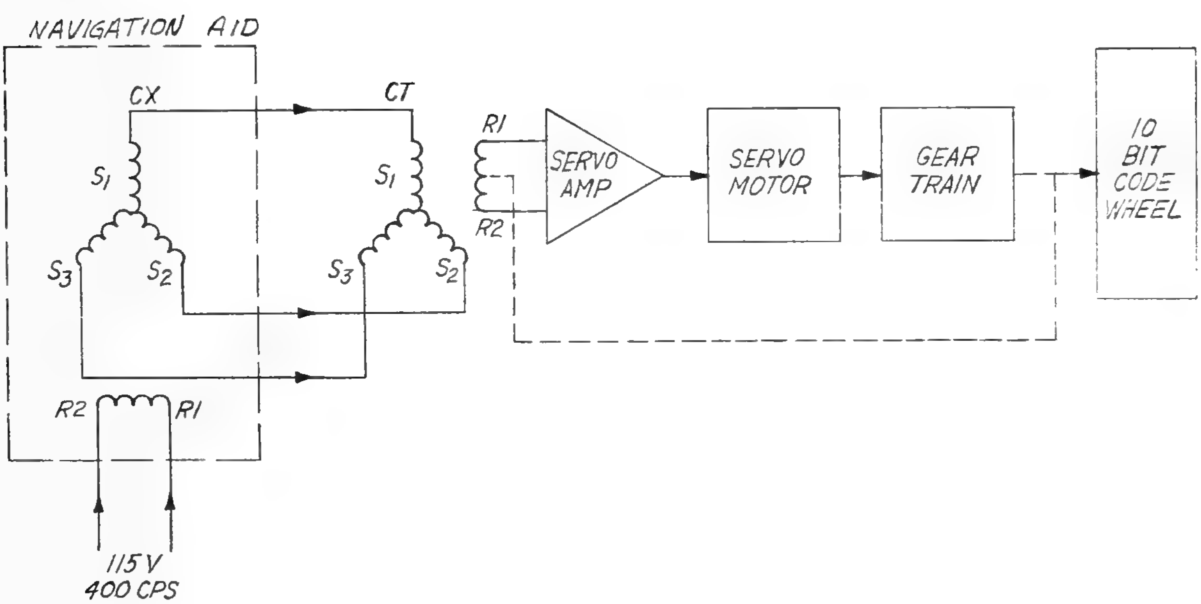

FIGURE 4 INPUT SERVO SYSTEM SCHEMATIC DIAGRAM

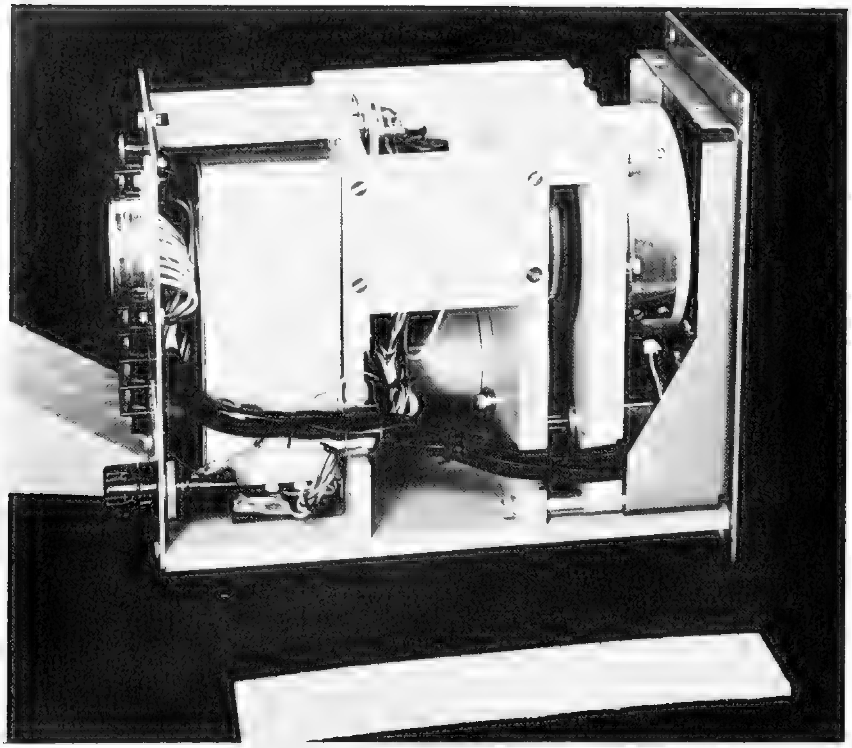

FIGURE 5 INPUT SERVO FOLLOWER UNIT

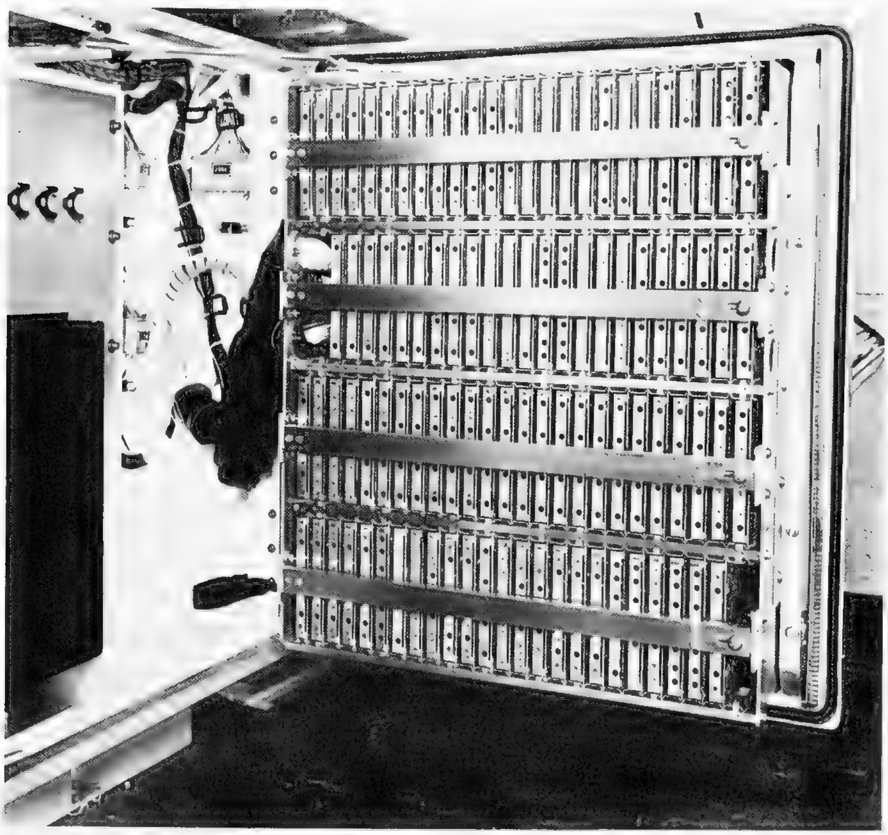

FIGURE 6 DIGITAL COMPUTER SUBASSEMBLY

Memory Unit:
- 4032 words of command storage
- 1008 words of constant storage
- 404 words of data storage
- 5 fast access registers of 2, 3, 5, 7, and 9 words

Arithmetic and Control Unit:
- Modified 5-address command structure
- 6 arithmetic commands:
  - Add - 165 microseconds
  - Subtract - 165 microseconds
  - Multiply - 165 microseconds
  - Divide - 2000 microseconds
  - Square root - 2000 microseconds
- 3 transmit commands
- 5 conditional transfer commands
- Number representation: binary, fixed point, fractional
- Instruction and data word length: 23 bits + sign
- Clock rate: 300 KC

The above characteristics of the computer, combined with suitable programming, endow the instrument with the capacity to compute geographic positions to a net accuracy of about one part in 18,000, which is considerably better than the accuracy of any navigational control system in existence today. However, the basic computer itself is about ten times more accurate than this, allowing some margin for future accommodation of more accurate navigation systems through reprogramming and reorganization of input circuits. Similar considerations apply for other types of data to be processed.

DIGITAL-TO-ANALOG CONVERTER AND PLOTTER

The digital-to-analog converter converts binary-coded-decimal data from the computer to highly accurate D.C. voltages to drive the plotter. This conversion process takes place with an accuracy of about one part in 10,000. The servo drives in the plotter and the plotting mechanism itself reduce the overall plotting accuracy to about one part in 1,000, which on the 30-inch plotting surface is 0.03 inch. The plotting accuracy is thus far less than the inherent digital accuracy of the instrument, but this is of little consequence since the digital data are printed and punched in code on the Flexowriter for whatever use one wishes to make of them.

A simplified schematic diagram of the plotter servo system is shown in Fig. 7. The analog voltage from the operational amplifier in the digital-to-analog converter is added in series with the voltage across a feedback potentiometer which is energized from a constant voltage source. The resultant error voltage is chopped and amplified to drive a servo motor coupled to the feedback potentiometer and to the printer carriage in a conventional servo loop. The servo is nulled and the printer carriage correctly positioned when the feedback voltage equals the input voltage. A similar servo is used to position the plotter arm on which the printer carriage moves. All converter and plotter circuits are solid-state.

The symbol printer, shown in Fig. 8, contains a stamping mechanism, ribbon supply, a cross-hair for visual alignment, and symbol selector logic governing the selection of any of twelve different symbols. In normally automatic operation, plotting is performed upon command of the computer when plotter arm and printer carriage are sensed to be correctly positioned. Symbol selection is also normally governed by programmed instructions in the computer, which transmits the commands in accordance with the binary coding arrangement shown in Fig. 9. The symbols shown are located around the periphery of a small disc which also contains the conductive coding pattern. The symbols are selected by matching the 4-bit word associated with each symbol with the corresponding word sent by the computer.

In automatic operation, data points relatively close together may be plotted as fast as once per second. Points separated by distances up to the maximum dimension of the plotting area may require two or three seconds. Points may also be plotted manually from the master control panel through appropriate controls for setting in data and energizing the symbol printer.

OCEANOGRAPHIC USES

With this brief description of the instrument itself in mind, I would like to direct your attention to two possible uses of this instrument in oceanographic work. They are both elementary examples and both make use of the position computation mode I have described.

In the first case, assuming the availability of an adequate fathometer, one has the means at hand to generate a bottom contour map in real time during a survey. As shown in Fig. 10, the computer can be instructed by its internal program to recognize preselected contour intervals and to plot them accordingly with chosen symbols. It is assumed here that corrections in either positional or bathymetric data can be made either at the source or transmitted separately to the computer for inclusion in the data processing. As fathometers and navigation systems improve, the resulting increase in the volume of meaningful data collected will furnish great incentive for this type of instrumentation.

In the second case, shown in Fig. 11, the printer is modified to select numbers instead of abstract symbols. The result is simply a depth plot similar to a hydrographic smooth sheet and

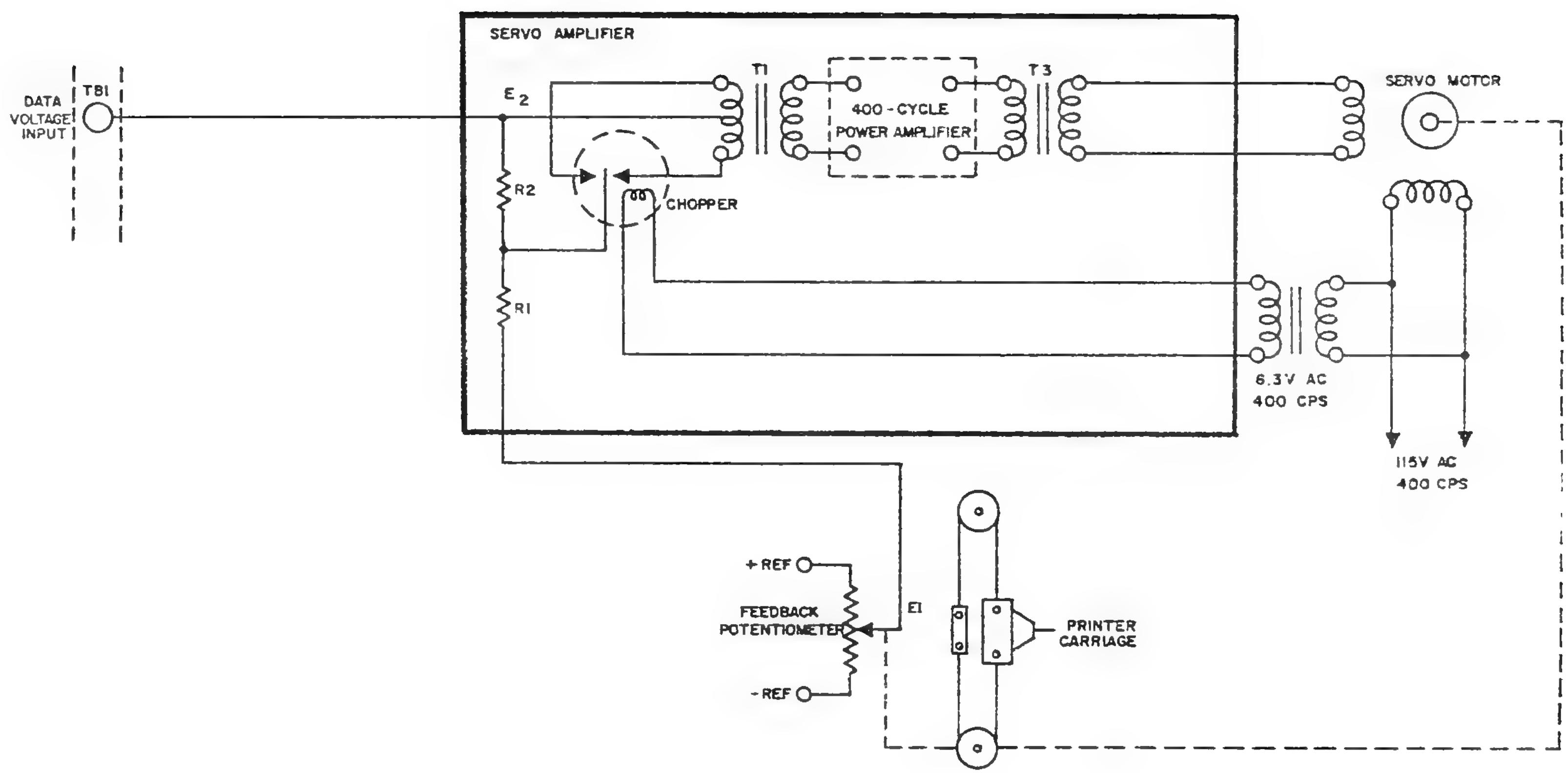

FIGURE 7 PLOTTER SERVO SYSTEM SCHEMATIC DIAGRAM

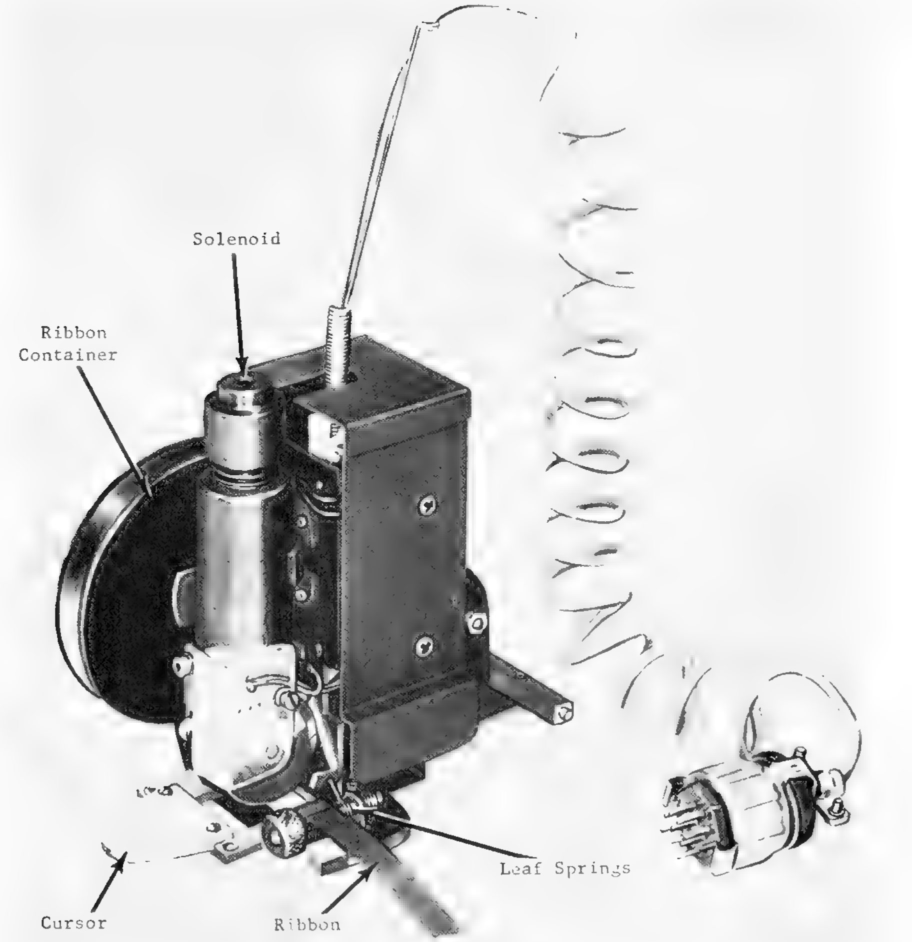

FIGURE 8 SYMBOL PRINTER

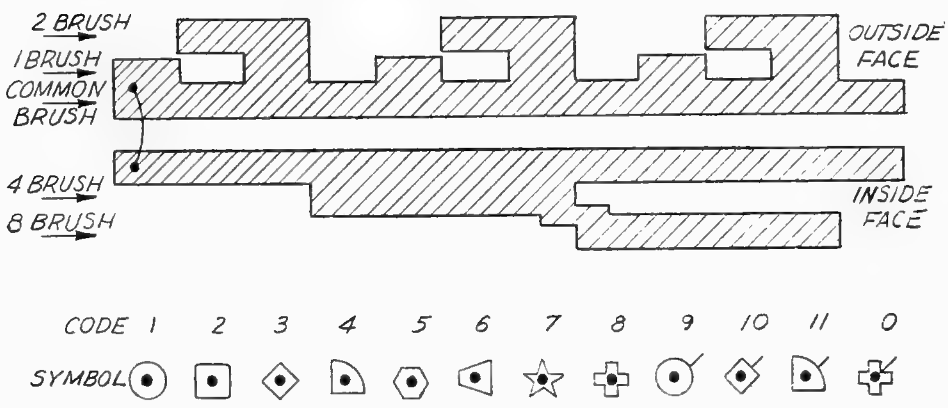

FIGURE 9 SYMBOL PRINTER CODE

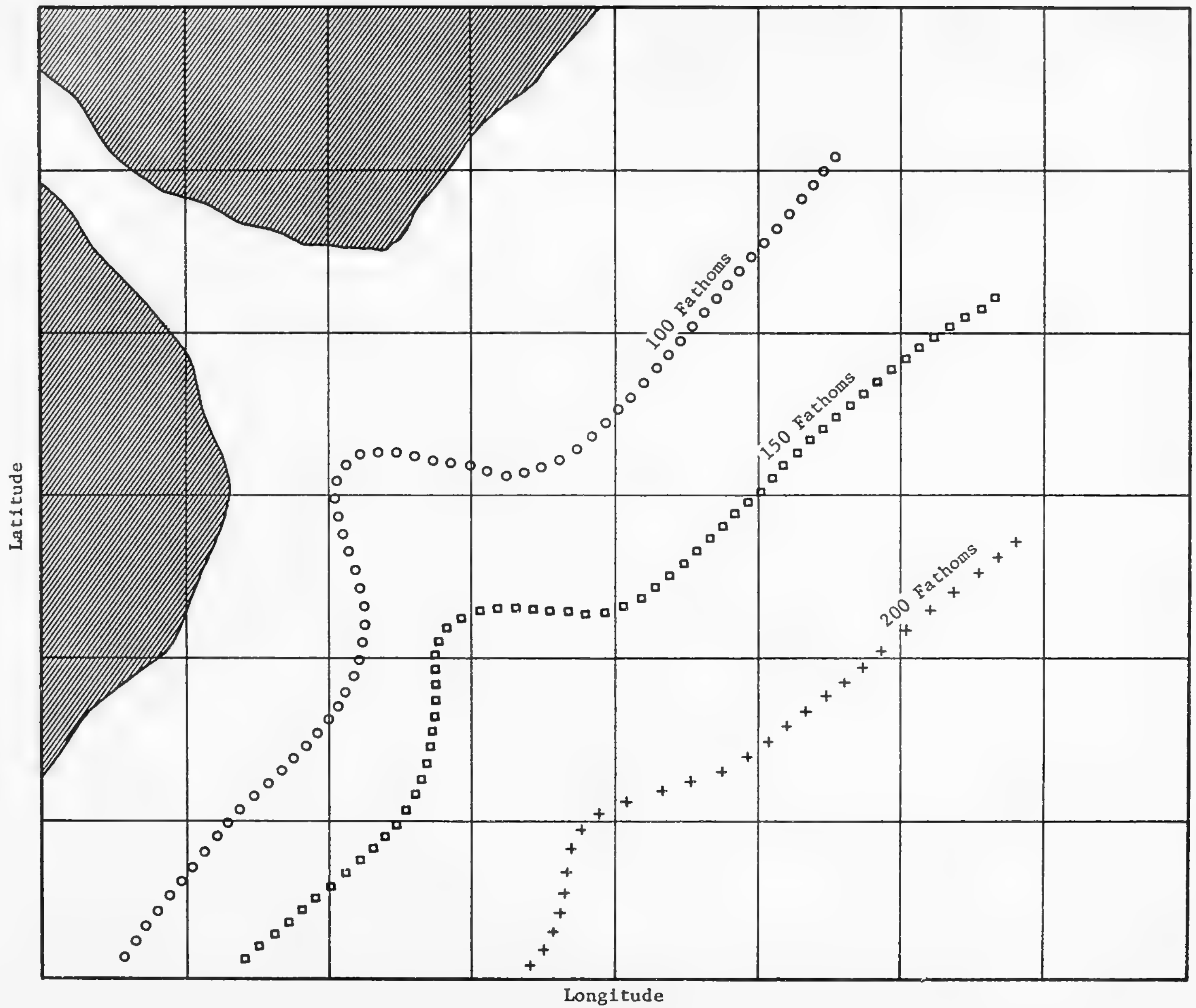

FIGURE 10 HYPOTHETICAL DEPTH CONTOUR PLOT

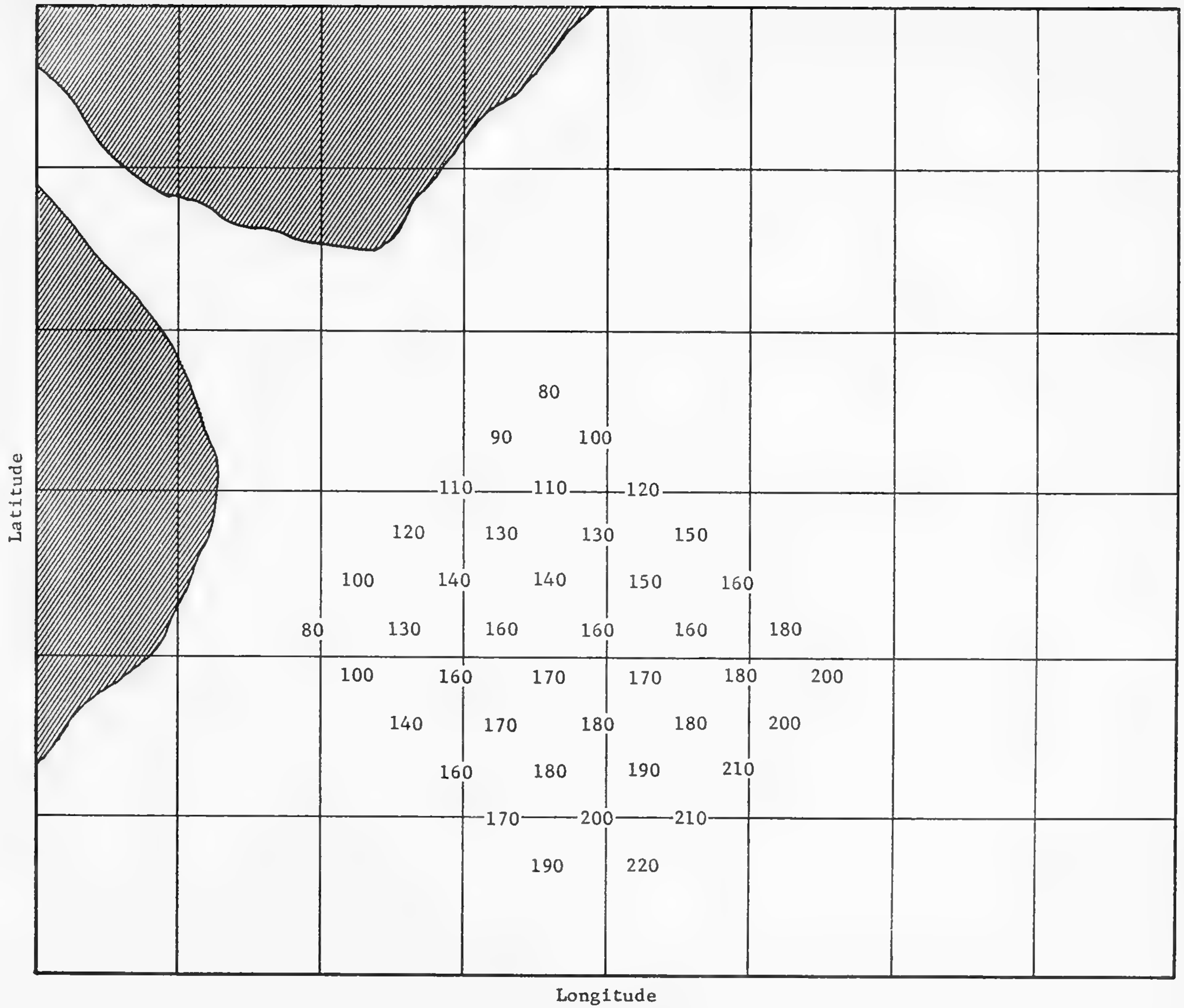

FIGURE 11 HYPOTHETICAL HYDROGRAPHIC PLOT

any contouring would be performed manually. Parameters other than depth could be similarly plotted in this mode.

CONCLUSION

In conclusion, I have described a digital data processing and display instrument of rather broad capabilities as an example, if you will, of the tools which modern-day technology is making available to scientists working in oceanography. I have attempted to relate certain characteristics of the instrument, such as precision, real-time reduction, flexibility, and functional completeness, to similar requirements which seem to me to be pertinent to the oceanographer's task. And finally, I have shown two elementary examples, and there are many more, of how such an instrument could be put to work in a very practical sense, relieving the scientist of much of the burden of his own data reduction.

ACKNOWLEDGMENT

I would like to acknowledge the efforts of the many people whose individual skills and hard work are represented collectively by this instrument; in particular, the contribution of D. M. Scott of the Westinghouse Electronics Division, under whose supervision the digital computer was designed and built.

TIMING CONTROL METHODS AVAILABLE FOR SELF-CONTAINED RECORDING SYSTEMS

by ALEXANDER L. M. DINGEE, Jr., and A. FRED FEYLING
Geodyne Corporation
Waltham, Massachusetts

ABSTRACT

Timing methods are important in data collection. There are a large variety of direct current powered timing devices which might be used in self-contained data recording or transmitting devices. This paper discusses accuracy, price and some of the significant aspects of various timing devices which can be used in oceanographic and limnological equipment.

INTRODUCTION

In recording oceanographic and limnological data, the time axis is often as important as the variables being recorded. Recording or controlling with respect to time can be difficult without 60 cycle A.C. power available. For example, in self-contained recording or telemetry buoys, using lapse-time techniques to store or transmit information, the simple closure of a switch on cycle presents significant problems which can easily be solved in the laboratory with a \$1.98 clock motor.

Oceanographers are not the only group faced with this problem. Lincoln Laboratories, at M.I.T., received an ionospheric sounder to measure the time it takes a radar pulse to travel to the ionosphere and return. These units were used throughout the world for the International Geophysical Year. The equipment also required a switch closure once every fifteen minutes to control a film advance mechanism. Two large crates were delivered to Lincoln Laboratory. The first contained a six-foot rack of sophisticated space-age electronics for measuring the radar reflectance time. This was the ionospheric sounder unit. The second crate, larger than the first, contained the time standard for the film recorder, complete with proper cams and micro switches. It stood over 6' tall in the original beautiful mahogony case. This timing unit, supplied by a well-known space-age company, was a good, reliable grandfather's clock.

In this study of small, self-contained D.C. powered timing sources capable of low frequency switching, cycles of one minute to twelve hours were covered. Other considerations were: temperature range, dependability, size, weight, power consumption and ease of maintenance and adjustment. Repeatability, accuracy ran from 1 part in 10^8 to 1 part in 5. For practical purposes we eliminated atomic resonance for we felt that most oceanographers would not want to pay between \$10,000 and \$100,000 for accuracies of one-ten millionth of a second per day.

DISCUSSION OF TIMERS

Points to be considered with electronic timers are the effect of voltage variation, temperature variation, moisture and aging of parts. Generally electronic timers operate at high frequencies and require preset counting circuits to trigger switches. The contact closure is usually controlled magnetically or by solid-state relay. Types of timers are as follows:

Crystal Controlled Oscillator. A crystal which can operate at frequencies as low as 1 kilocycle can easily obtain accuracy of ±1/10 of a second per day. The use of counting circuits is necessary to count down to the desired number of pulses per hour. Due to this counting the price of such a unit will run from approximately \$500 to \$2,000.

Tuning Fork Oscillator. This is much the same as a crystal oscillator except that a tuning fork is used for the frequency source. Such a unit may operate as low as 50 cycles per second. The accuracy is ±10 seconds per day. The counting circuit is simplified because the base frequency is lower. Cost of such a unit would be \$350 to \$1,600.

L.C. Resonant Circuit. Proper combination of inductance and capacitance will give a circuit which will oscillate at a given frequency. Accuracy can be better than ±1 minute per day. An L. C. circuit can be made to operate as low as 5 or 10 cycles per second. A counting circuit for switch closure is still required. The approximate price would be \$200 to \$500.

Relaxation Oscillator using resistive and capacitive or inductive circuitry. An example is the charging of a capacitor with a battery to a given voltage level at which point a neon bulb, or other detector, triggers and discharges the capacitor. The cycle time is limited by the size and leakage from the capacitor. It is fairly easy to make such circuits with cycle times of several minutes. These can be extended with care to 1 hour. Accuracy of ±14 minutes per day can be obtained. Such a unit might draw anywhere from 2 to 5 watts maximum power. The price would run between $100 and $200.

Reed Controlled Count Down. A more inexpensive version of the tuning fork method is to use a vibrating reed which directly makes an electrical contact. This circuit closure then would be counted down the same as the tuning fork frequency. Estimated accuracy on such a unit is ±7 minutes per day. Life would be dependent upon contacts and might be as much as 2,000 hours. The estimated price would run $100 to $200.

MECHANICAL TIMERS

Possible trouble points in mechanical timers are: position sensitivity, temperature compensation, variation of rate with battery voltage, life of brushes, life of the rate controlling mechanism, power consumption, resistance to shock, low torque, generation of electrical interference and lubrication, bearing quality and lubrication.

D.C. motors are used widely as timers. Ungoverned D.C. motors as a rule cannot be counted on for accuracies of better than ±2 hours per day because of battery life. Also, if the temperature in the winding increases, the resistance drop increases and, therefore, speed will drop. Prices on D.C. motors can range anywhere from thirty cents to many hundreds of dollars.

Governed D.C. Motors. (a) Centrifical Speed Control. Centrifically operated contacts mounted on the motor shaft will break motor power contacts or switch in dropping resistors as the desired speed is exceeded. Approximate accuracy is ±14 minutes per day. This motor would draw .03 to .06 watts and give 4 ounce inches torque at 1 R.P.M. The life will be around 1,000 hours. The price can be as low as $17. To construct a timing device from a D.C. motor, one must add cost for cam, switch, bracket and housing; (b) Reed Contact Control. The motor receives part of its power through contacts mounted on a reed which vibrate at a given frequency. The reed passes current to the motor shaft in pulses. If pickup on the shaft is not in phase with the reed pulse, pulse duration to the motor is shortened or lengthened, depending on whether the motor is lagging or leading the control speed; thus, the length of time that power is applied to the motor per pulse is varied as a speed control. This method can hold accuracies of ±7 minutes per day. If it is adjusted closely and voltage fluctuations are not too great, accuracies approaching ±3 minutes per day may be obtained. The unit is position sensitive, however. Life figures on this unit are incomplete. Life may approximate 3,000 hours, but there is some question of contact failure. Power input is 1/2 to 2 watts. The price of the motor itself is $45. The switching assembly would be extra; (c) Chronometric Contact Control. This unit functions approximately the same as the reed contact control except that the frequency standard is chronometric rather than reed. It is capable of holding ±8 minutes per day in a temperature range -10° to 100°F. Speed can be held to ±2 minutes per day in narrow temperature ranges. The current required by this unit is 250 micro amperes at 1.5 volts. Points to check in this unit are: ability to withstand shock, contact life and position sensitivity. Life is estimated to be in the order of years. The approximate price is $100 for the motor without the cam-switch assembly. There is another unit available which has higher current drains but has better resistance to shock and more torque output. Price of this unit is $75. Life is guaranteed for 1,200 hours.

Clock Movements. These are used the same as the D.C. motor, i.e., to rotate a cam against a micro switch at uniform rate. (a) Impulse Type. The balance wheel is given an impulse every cycle. This type of movement generally has few or no jewelled bearings. The estimated price is $10 to $12, not including timing assembly; (b) Solenoid or Motor-Winding Type. In this unit a spring is wound by a solenoid or motor once every few minutes. The average power input of this type is approximately 1 milliwatt. Torque output of such units covers a wide range--a representative figure might be 4 grams centimeters torque at 1 revolution per hour. As the movements operate from spring power, voltage fluctuations do not affect them. The units should be checked for jewelled bearings, shock mounting of pivot shaft and proper temperature compensation. Accuracies can be expected of ±10 seconds per day with a life of 1 to 5 years. This type of movement will cost from $12 to $30 with no provision for timing assembly; (c) Spring-Wound Movement. In these units a heavy-duty clock movement is driven by a hand-wound spring. The torque output is sufficient to be used as a circular chart drive. Thirty-one day movements can be obtained. Accuracy is estimated at ±10 minutes per day. Price of such a unit without the timing assembly--$12.50.

Thermal Timers. A bi-metallic strip is deflected by an electric heater, making or breaking a contact. Reset time is determined by how quickly the unit cools off. The cycle depends upon voltage and ambient temperature. Accuracy of about ±2 hours per day. Price--$.50.

Restricted Flow of Mass. A series of timers depend upon an orifice restricting mass flow at a given rate. An example would be air compressed by a solenoid-driven piston and released slowly through an orifice. These units provide reliable operation with an accuracy of ±2 to 3 hours per day but are limited to maximum intervals of

20 minutes. Average power consumption is 6 watts. The price will range from $.50 to $150. The price of the above air device is $30.

CONCLUSION

To solve our switching problems, we used the grandfather clock technique. We selected a solenoid-wound chronometric movement for our base timing source because it offered acceptable accuracy of ±10 seconds per day at a reasonable cost. Also involved in our consideration were low power consumption, independence from voltage fluctuations, long life, small size, simplicity, dependability and flexibility in selection of cycles ranging from 1 minute to 12 hours by changing cams. We adjust these sequence timers on a crystal oscillator time standard recorder and ship the recording slip with the unit. The timers have been produced for over a year and have proven their ability to retain reliability and accuracy after the rough handling and droppage involved in placing an instrument package in the ocean.

Grandfather's old clock is still good.

A CONCEPT FOR A REMOTELY INTERROGATED SYNOPTIC OCEANOGRAPHIC DATA SAMPLING BUOY

by RICHARD A. ZLOTKY, Project Engineer
Chance Vought Corporation
Dallas, Texas

ABSTRACT

A concept is proposed for a remotely interrogated synoptic oceanographic data sampling buoy system. It is an anchored system capable of sampling oceanographic data from the ocean surface to a depth of approximately 4,000 feet. An electro-mechanical system that converts ocean wave energy into electrical power is discussed. It is this power generator that makes the proposed long life buoy concept feasible.

INTRODUCTION

Chance Vought Corporation, in its effort to develop more effective ASW systems, realizes the necessity for more knowledge about the ocean environment than is presently available. Synoptic conditions in the sea must be known before ASW prediction systems become successful, and before ASW acoustic techniques become reliable. As a result of this need, Chance Vought Corporation has examined the feasibility of providing a long life buoy to be deployed in large areas of the ocean. The proposed concept can sample and store data, and can be interrogated by an airplane, ship or shore station.

GENERAL ARRANGEMENT

The general arrangement of the buoy system is shown in Figure 1. The Company name for the buoy is TELME which stands for TELemetered Medium Environment. The buoy consists of a power generator system called MECH-CON-SEA which stands for MECHanical CONversion of SEA power, an equipment buoy, a bobbing buoy and a taut line anchoring system. The equipment buoy houses the main batteries, power generator, recording equipment, transmitter and receiver. The bobbing buoy houses a small battery supply, buoyancy cycle control system sensors, and tape recorder. The equipment buoy is located approximately 50 ft. below the sea surface and the bobbing buoy rides the anchor cable from a depth of 50 ft. to approximately 4,000 ft.

CYCLE DESCRIPTION

The cycle description is shown in Figure 2. The first phase consists of a three hour period for charging the batteries in both the equipment buoy and bobbing buoy. The main batteries are charged by the MECH-CON-SEA power generator and the bobbing buoy batteries are charged by the main batteries. In the second phase, the buoyancy of the bobbing buoy is changed from plus 5 lb. to minus 5 lb. During this 6 minute period the electronic equipment is given sufficient time to warm-up. During the third phase the bobbing buoy descends to a depth of 4,000 ft. while data is being sampled and recorded. The descent velocity is approximately 4 ft. per second which precludes instrument sensing lag time if data is sampled approximately once per second. The buoyancy change from minus 5 lb. to plus 5 lb. takes place during the 6 minute fourth phase and the buoy makes the 16 minute ascent back to the equipment buoy. The data recorded during the bobbing buoy descent and ascent is transferred to the equipment buoy whereby the bobbing buoy tape recorder is erased. All data is stored by the equipment buoy tape recorder until it is interrogated. Upon a successful data transmission, the equipment buoy tape recorder is given an erase command.

MECH-CON-SEA POWER GENERATOR

The MECH-CON-SEA power generator operates on the principle of obtaining maximum relative motion between the float and cable reel shown in Figure 3. Maximum relative motion is obtained by utilizing the taut wire plus a large trapped water mass in the lower compartment of the equipment buoy. The trapped water mass minimizes the tendency of the equipment buoy to rise along with the float. Energy is put into the power accumulator spring on the float upstroke only. The cable is rewound by the reel rewind spring as the float falls. The stored energy in the power accumulator spring is released through a gear box, A.C. generator, and a rectifier and regulator.

TELME BUOY

GENERAL ARRANGEMENT

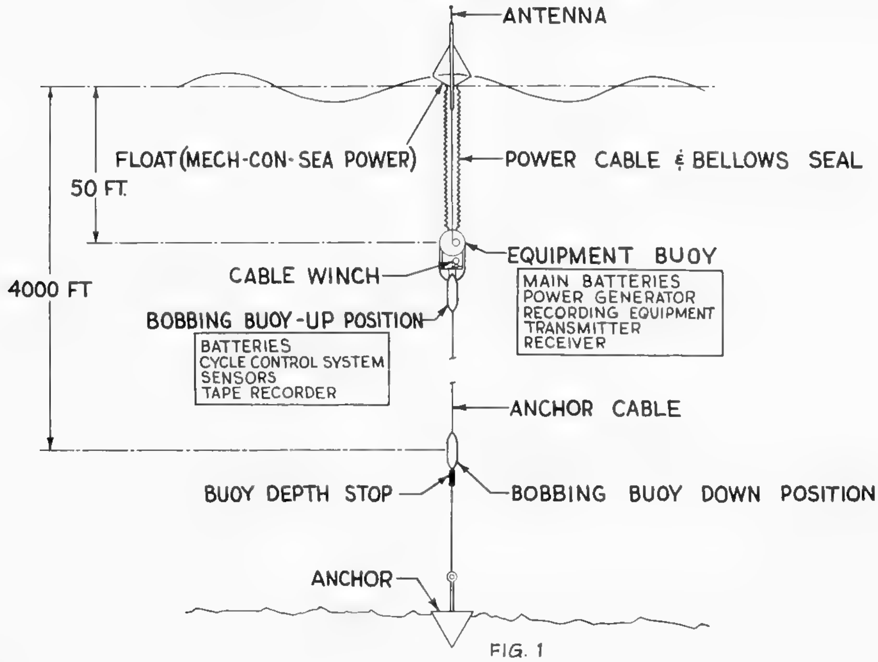

FIG. 1

CYCLE DESCRIPTION

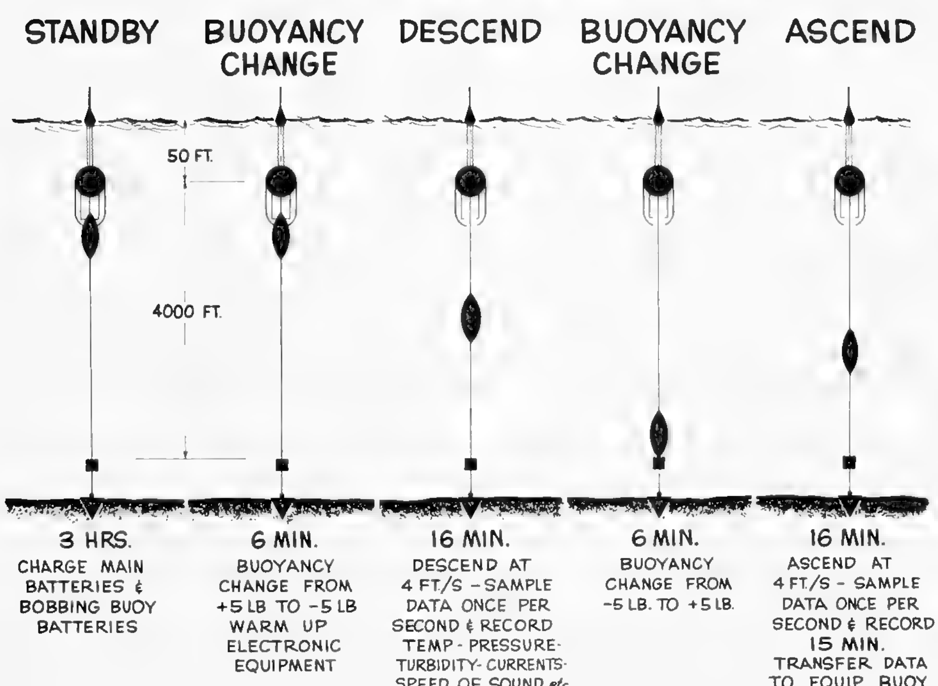

FIG. 2

MECH-CON-SEA POWER GENERATOR

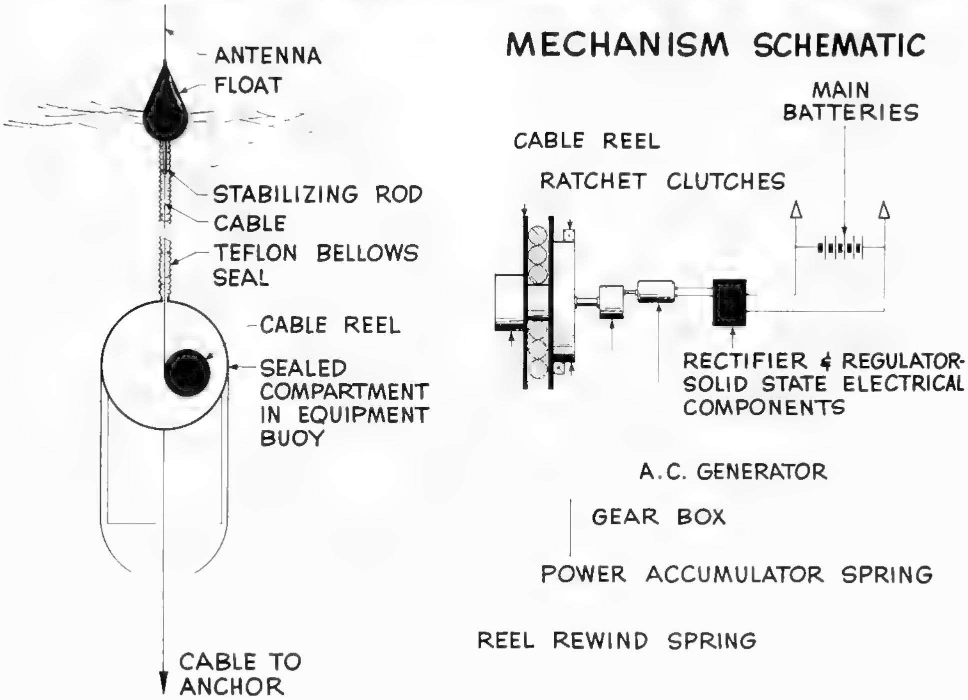

FIG. 3

EQUIPMENT BUOY

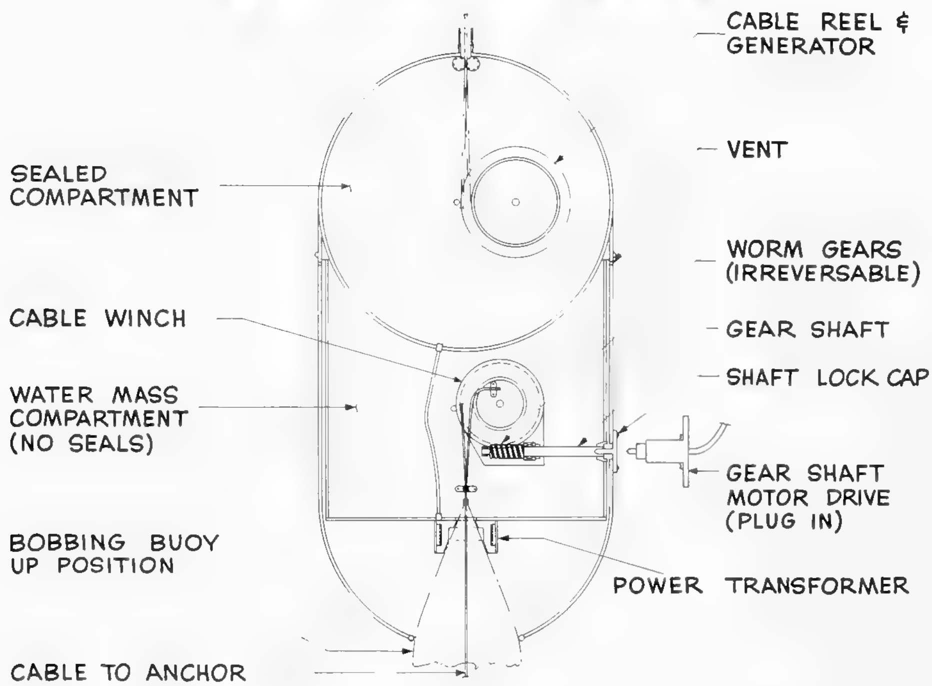

FIG. 4

EQUIPMENT BUOY

A sketch of the equipment buoy is shown in Figure 4. It consists of a sealed compartment for electronic equipment, MECH-CON-SEA mechanism, and a trapped water compartment. The bobbing buoy is shown in its up position as it is nested in the power transformer receptical. An inductance connection is used to transfer power from the equipment buoy to the bobbing buoy. The small winch shown in the sketch is used to winch the buoy down to the 50 ft. level.

BOBBING BUOY

The bobbing buoy cycling system is shown in Figure 5. The principle used is to take in water for negative buoyancy and to expel it for positive buoyancy. This is done with hydraulic accumulators. The timer provides a signal to the cycle control which starts the motor and hydraulic pump. In going from positive to negative buoyancy, hydraulic oil is pumped from the accumulators into the air bottles until the liquid level sensor shuts off the motor. The average air pressure in the bottles is 1,000 psi so that the pump operates against a delta pressure of 1,000 psi both at the ocean surface and at the 4,000 ft. level. Pressure cut-off switches are provided in case the liquid level sensor fails to operate properly. The bobbing buoy configuration is shown in Figure 6. The buoy length is 72 in. and the maximum diameter is 20 in. A hollow tube used to guide the bobbing buoy down the cable extends lengthwise through the buoy. A rough and fine ballast adjustment is provided so that the buoy can be adjusted to neutral buoyancy in the water. A bilge pump is also provided to take care of any seepage of sea water into the buoy.

ELECTRONIC EQUIPMENT

A block diagram of the TELME buoy system electronic equipment is shown in Figure 7. The operation of the equipment is as follows. Timer #1 completes timing the period between cycles and opens the relay through which power is supplied from the battery to the static inverter. Power across the transformer is momentarily interrupted. Timer #2 is started by the power interruption and it provides a signal to energize switch unit #2. Switch unit #2 completes the circuit to start the electronic equipment in the bobbing buoy and it also sends a down signal to the buoyancy system. After the momentary interruption of power across the transformer, the relay is deenergized and power flows normally to the bobbing buoy. Its battery is therefore fully charged as it starts the dive. At the end of the buoyancy change period, power to the transformer is again interrupted. The bobbing buoy, now negatively buoyant but held in place by magnetic clutch action between the two transformer cores, is released to dive. Timer #2 times out the period necessary for the dive to 4,000 ft. at which time it energizes the buoyancy system to go positive. Timer #2 times a 30 minute period after the up signal is given. Normally the bobbing buoy will return to the equipment buoy within approximately 23 minutes. However, if something on the line prevents the return of the bobbing buoy, timer #2 will reverse the buoyancy in 30 minutes. This procedure is repeated until the bobbing buoy battery is depleted or until it returns to the equipment buoy. The battery has sufficient capacity for three complete up and down cycles. When the bobbing buoy returns and the power transformer is activated timer #1 starts timing a new cycle. Timer #1 energizes the recording system in the equipment buoy and timer #2 energizes the playback system in the bobbing buoy. Data is then transferred from the bobbing buoy to the equipment buoy. The receiver in the equipment buoy operates continuously. When an interrogation signal is received, switch unit #1 is energized from the receiver. The switch unit interrupts power to the timer and data acquisition system and energizes the data transmission system. An operator monitors the data received and after a satisfactory data reception he signals the buoy to erase the tape.

SYSTEM POWER REQUIREMENTS

The system power requirements are shown in Figure 8. Power requirements are broken down into the various parts of the 4 hour cycle. The total power required is 236 watt-hours. The power available from the MECH-CON-SEA power generator is shown in Figure 9. Wave data, height and period, are taken from statistical sea state information from the Pacific Ocean. The average long time continuous power output of MECH-CON-SEA is 105 watts for a 40% efficient system. Therefore on a long term basis, the power input to the system is 420 watts for a 4 hour period whereby the power consumed is 236 watts. Size optimization of the MECH-CON-SEA power generator for the TELME buoy system has not yet been completed. Since ocean conditions are highly variable with reference to location, the main battery supply capacity is approximately 4,000 watt-hours. This is based on the assumption that three consecutive days of calm periods may occur and 4,000 watt-hours will permit 6 bobbing buoy cycles per day for the three days before the batteries are depleted.

BOBBING BUOY CYCLING SYSTEM

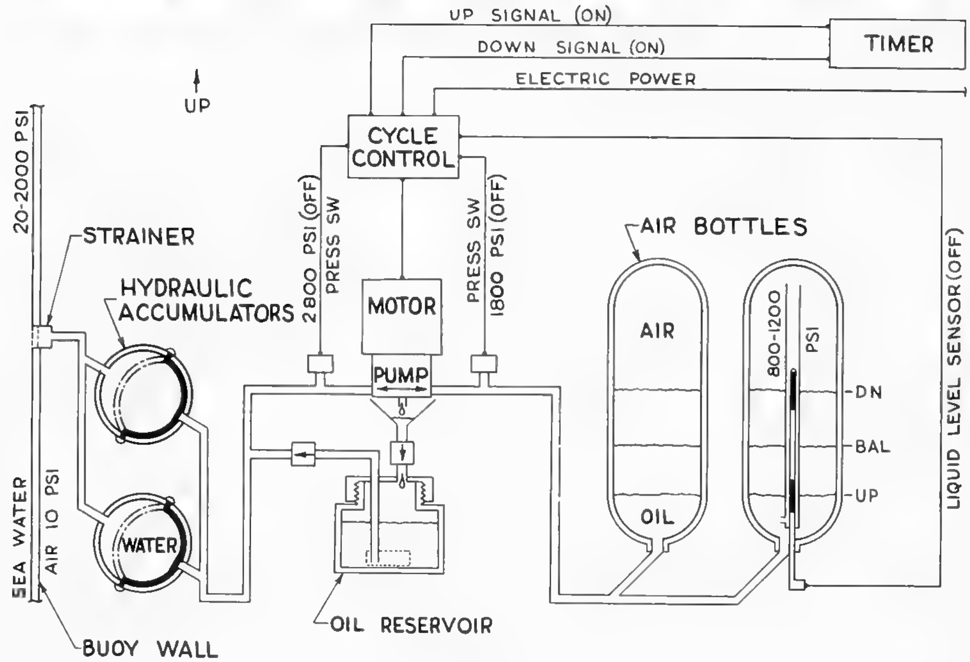

FIG. 5

BOBBING BUOY

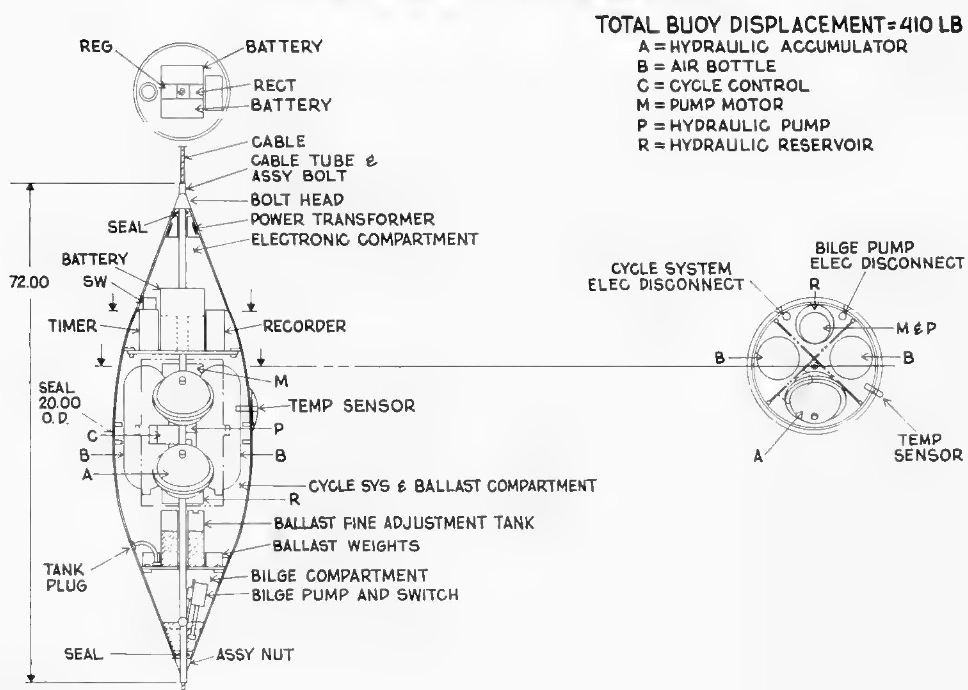

FIG. 6

ELECTRONIC EQUIPMENT

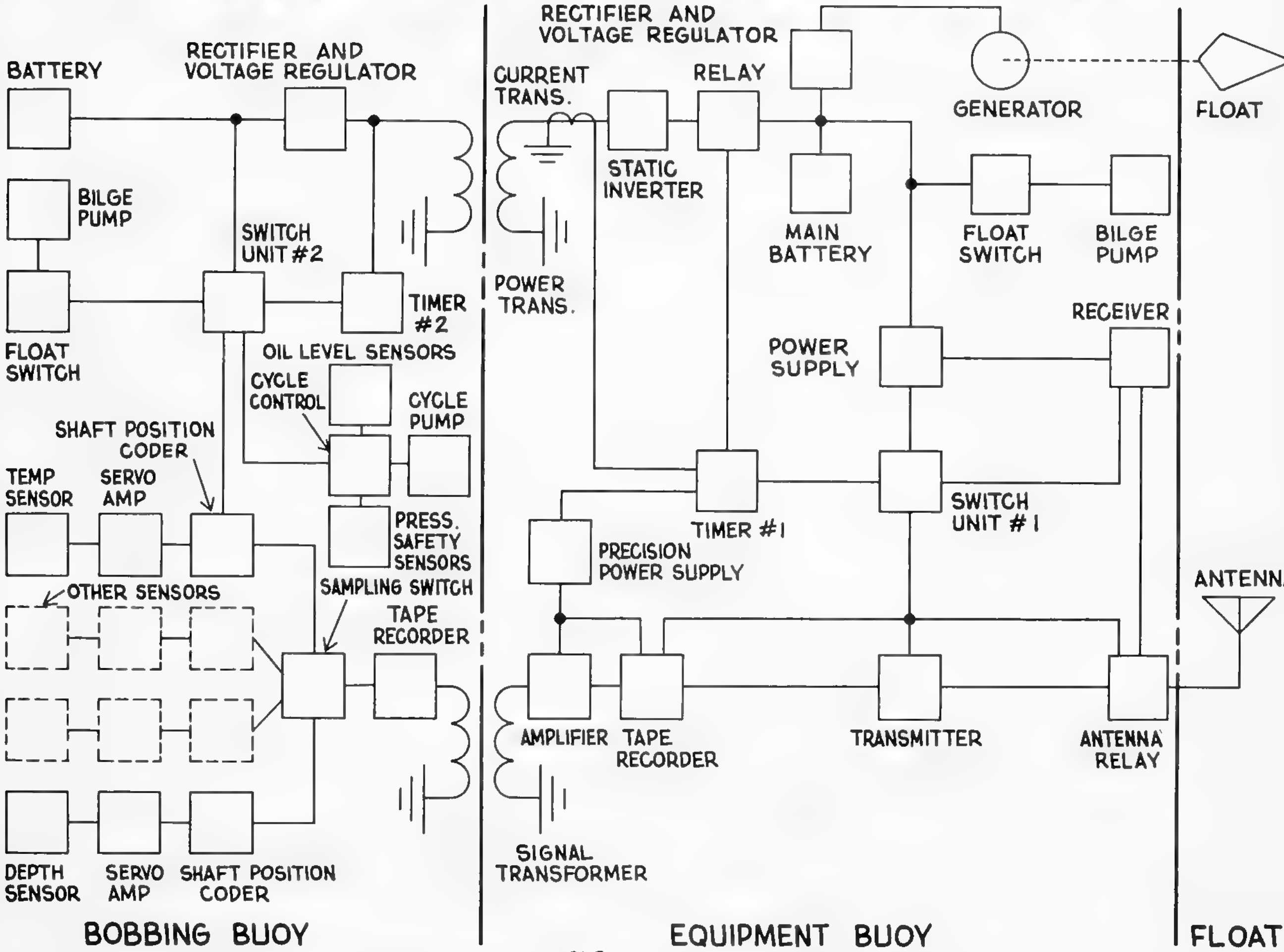

FIG. 7

SYSTEM POWER REQUIREMENTS

OPERATION		BUOYANCY CHANGE	DESCENT	BUOYANCE CHANGE	ASCENT	DATA TRANSFER	STAND-BY
TIME	MIN.	6	16	6	16	16	
	HRS.	.10	.27	.10	.27	.27	3.0
EQUIPMENT BUOY	WATTS	59	11	8	11	105	46
	WATT-HRS	5.9	2.9	.8	2.9	28	138
BOBBING BUOY	WATTS	216	30	203	30	0	0
	WATT-HRS	21.6	8.1	20.3	8.1	0	0

TOTAL EQUIPMENT BUOY POWER REQUIRED = 178.5 WATT-HOURS
TOTAL BOBBING BUOY POWER REQUIRED = 58.1 WATT-HOURS
TOTAL POWER REQUIRED FOR A 4 HR. CYCLE 236.6 WATT-HOURS

FIG. 8

MECH-CON-SEA POWER AVAILABLE

SURFACE WAVE HEIGHT (H_s) FT.	WAVE PERIOD SECONDS *	AVERAGE WATT OUTPUT **	% TIME FOR H_s & ABOVE	% TIME AT H_s	WATT OUTPUT TIMES % TIME AT H_s
CALM	0.0	0.0	100	27	0.0
1 1	4.2 1.8	82	73	27	22.3
2 2	5.6 2.4	146	46	22	32.0
3 3	6.4 2.8	194	24	12	23.3
4 4	7.2 3.2	222	12	10	22.2
6 6	8.7 3.7	275	2	2	5.6

AVG. LONG TERM CONTINUOUS POWER OUTPUT = 105.4 WATTS

* STATISTICAL DATA FROM OBSERVED SEA STATES IN THE PACIFIC OCEAN

** MECH-CON-SEA OPERATES AT 40% EFFICIENCY

FIG. 9

SYSTEM LIFE AND RELIABILITY

Preliminary studies on the system life and reliability of the TELME buoy system indicate that a 6 month life, unattended, can be expected with a probability of 70% - 80% for completing the 6 month period satisfactorily. Components are off-the-shelf items with the exception of sensors. Total operating time of components are kept to a minimum by on-off utilization. Derated components can be used where weak links in the reliability chain exist.

CONCLUSIONS

More knowledge about the ocean environment is not only a pressing task before the military, but a necessary requirement for understanding and exploiting the sea. Synoptic surveillance of large areas of ocean necessitates the use of long life remote buoys. The economics of collecting oceanographic data over these large ocean areas suggests the use of aircraft as data collecting sources. The airplane, with its speed, altitude, and range capability coupled with long life buoys is an approach that seems worthy of development. Chance Vought Corporation has studied the feasibility of providing a long life buoy system. The results of the study are favorable and hardware development is a logical next step.

ACKNOWLEDGMENT

The information presented in this paper resulted from the cooperative efforts of Mr. C. E. Lankford, Avionics Engineer, and Mr. R. A. Nelson, Electro Mechanical Engineer, both of Chance Vought Corporation.

DATA RECORDING DEVICE FOR UNDERWATER INSTRUMENTATION

by JAY W. HARFORD, Engineer
and EARL D. VAN REENAN, Senior Geophysicist
Edgerton, Germeshausen&Grier, Inc.
Boston, Massachusetts

ABSTRACT

Modified versions of a standard EG&G underwater camera are described with necessary circuitry to use as lapse-time data cameras. The standard camera can be modified to have one or two data chambers. The dual chamber data camera will take 4,000 data pictures sequentially in six pairs to handle up to 12 sensing instruments. The data camera can act as a versatile nucleus of an underwater instrument package for the recording of various oceanographic variables.

I INTRODUCTION

Recording of oceanographic variables in situ requires a reliable recording device which can record sequentially over extended periods of time while in an oceanographic environment. This paper describes a simple and compatible data recording system which can serve as a nucleus instrument package for the read out of several measuring instruments. The basic recorder consists of a data camera which is readily adaptable for many uses. This data camera can take data pictures from one end or both ends depending on the number of sensing elements used and type of meters required.

II DESCRIPTION

A. Single Ended Data Camera

The basic single ended data camera is a special modification of the EG&G Model 200 Underwater Camera. The camera is contained in a high strength stainless steel housing designed to withstand 20,000 psi. The read out meters are placed on the end cap. The data camera film capacity is 100 feet of 35 mm film on a daylight loading spool. This gives 2,000 frames per roll with 15 millimeters per frame. The data lens is a Wollensak Cine-Raptar 13 millimeter focal length, f2.5. The light source consists of an internal tungsten bulb. Automatic timing control can be provided by a 6 volt d-c cam type timer which is available in various time intervals.

B. Dual Ended Data Camera

The dual ended data camera is an extension of the single ended data camera with data pictures taken at both ends. This provides greater meter area and more efficient utilization of film space. The dual ended data camera will take 4,000 data pictures per 100 foot roll. The camera lenses on either end of this camera are staggered to give a double row of data pictures. A maximum of 12 separate instruments can be sequentially recorded by this data camera. It is possible to use 2 or more meters with different ranges to reduce the problem of having the measuring instruments compatible with the read out. A clock, pressure gauge, and data card can be provided on one end of the camera if desired. The dual ended camera with a single meter is shown in Figure 1.

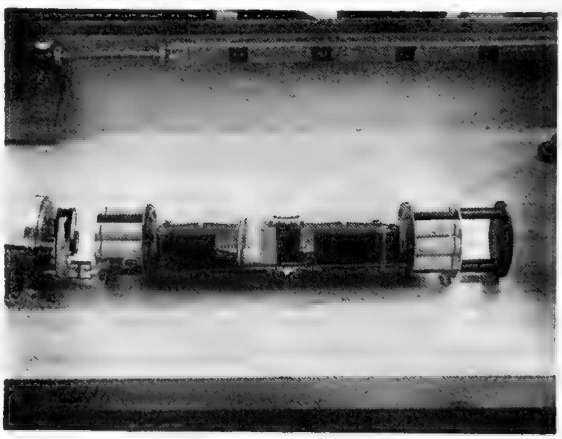

Fig. 1 Data Camera Mechanism

III OPERATION

The basic single ended or dual ended data cameras are highly versatile and can be applied with various electronic systems for sequential read out. This section describes a particular type of circuitry which allows up to 12 separate sensors to be sequentially read out on meters.

A. Circuitry

The camera is driven by a d-c motor which serves two purposes: it advances the film and drives a 6-position selector switch which sequentially reads out the various instruments.

For a 12-instrument sequential read out, a meter is placed at each end. The two ends of the data camera take pictures of the meters at either end simultaneously. At the same time, a small indicator light at one end of the camera will indicate in the picture which instruments are being read out. For example, instruments No. 1 and 7 are read out with the No. 1 indicator light on, and instruments 2 and 8 correspond to the No. 2 indicator light, etc. Each time the film is advanced one frame, the selector switch is moved to a new position to read the next two instruments in sequence. The selector switch is mounted on top of the film advance socket mechanism as shown in Figure 1. A sample of the data picture is shown in Figure 2.

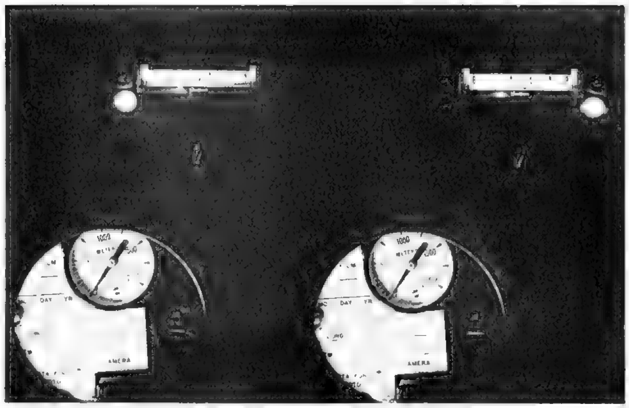

Figure 2. Sample film strip from dual ended data camera.

The camera is activated by momentarily grounding the power lead to the 6 volts d-c supply. Each time this occurs, three separate circuits operate on the camera: (See Figure 3)

1) the data lamp capacitors (C_6) discharge through the incandescent bulb (B_2) exposing the data chamber frame,

2) the indicator light capacitors (C_5) discharge through the indicator bulbs in the end cap to show which instrument is being read out.

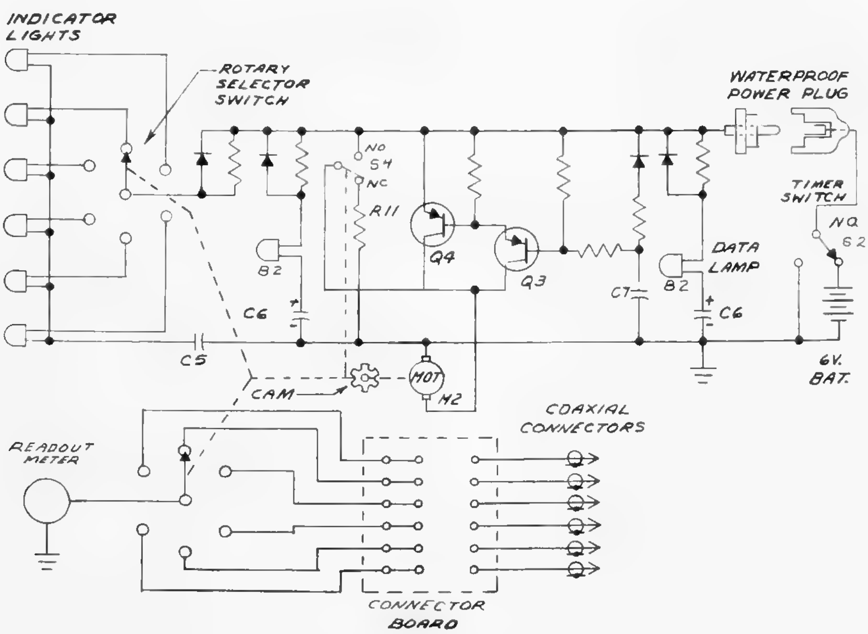

Fig. 3 Data Camera Circuit Diagram

3) the motor starting capacitor (C_7) discharges.

When the timing motor cam returns S_2 to position NO current is again fed to the indicator data lamp and motor starting capacitors. As capacitor C_7 starts to charge up again, transistor Q_3 conducts, and current flows into the base of Q_4. Operating current is supplied to the film driven motor M_2 when transistor Q_4 starts conducting. This current is transitory (lasting about 1 sec) and lasts until the voltage C_7 rises to 6 volts. The film drive motor simultaneously drives cam switch S_4 during this period into position NO which connects the film drive motor directly to the 6 volt current line. The film motor advances the film one frame. When cam S_4 moves back into position NC, power is removed from the motor. The film stops advancing, and the operating cycle is complete. Resistor R_{11} limits overtravel when current is removed from the motor by a dynamic braking action on the motor.

B. Adaptability

A terminal board at one end of the data camera facilitates wiring changes of the selector switch. The instrument outputs and selector switch leads are terminated at this board. The sensor instrument inputs are wired up patch panel fashion. The terminal board also allows placement of any meter shunts necessary to make each sensing instrument compatible with the read out meter.

IV APPLICATIONS

The data camera can be used for a wide variety of oceanographic data collecting applications. It is very useful for lapse time data recording over extended periods of time up to several months. The data camera with associated sensing elements can be lowered to the sea floor and left for extended periods. For example, such things as temperature probes for heat flow measurements can be recorded from a number of thermistors and bottom water temperatures can also be measured along with variables such as the current velocity and direction from current meters, salinity variation, and acoustical variables. Continuous hourly and daily variations of oceanic factors can be clearly and concisely recorded in this manner and analyzed when the entire unit is recovered and the film processed.

PROGRESS REPORT ON TRANSIT

by R. B. KERSHNER
The Johns Hopkins University
Applied Physics Laboratory
Silver Spring, Maryland

"TRANSIT" is the code name for a program to develop and establish in being a system of near-earth satellites to provide a means for establishing locations (navigating) anywhere on the surface of the earth. The development phase is being carried out for the Bureau of Naval Weapons primarily by the Applied Physics Laboratory of The Johns Hopkins University with cooperative efforts by the Naval Weapons Laboratory at Dahlgren, Virginia, the Naval Ordnance Test Station at China Lake, and the Pacific Missile Range. The launching of the satellites is conducted by the Air Force Ballistic Missile Division.

As a navigation system, TRANSIT will have the virtue of true global coverage, all weather operation, relative immunity to interference (either natural or man-made), unlimited traffic handling, frequent availability of fixes (every 100 minutes or oftener), and very high accuracy. On the other hand, since position is available only intermittently and not continuously, for some purposes TRANSIT may not replace the various radio aids that do provide continuous position fixing in the areas where such aids are available. However, it should be noted that a relatively modest quality inertial system would suffice to provide continuous interpolation between TRANSIT fixes.

The principle on which the design of the TRANSIT system is based is quite simple. Briefly stated, the entire system is based on the fact that a constant frequency radio transmission from an earth satellite is received by a ground station at the surface of the earth with an apparent variation of frequency. This variation in received frequency, the result of the well known Doppler effect, is an accurate measure of the rate of change of the slant range between the transmitter and the receiver and hence is influenced both by the motion of the satellite in inertial space and by the motion of the receiving station as a point on a rotating earth. Because of the severe constraints imposed on the path of an earth satellite by Newton's laws and our reasonably complete knowledge of the forces acting, it is possible, simply from an accurate measurement of the Doppler shift at a ground station during the passage of a satellite within line-of-sight to do either of two things: (1) determine the orbit of the satellite if the position of the ground station is known, or (2) determine the location of the ground station if the orbit of the satellite is known.

These two calculations are the basis of the TRANSIT system; the second calculation is performed by the navigator using a description of the orbit provided to him and a measurement of the Doppler shift which is made by his (navigating) equipment, the first calculation (or an elaboration of it) is used by the organization operating the system to determine the orbits for distribution to the users using Doppler measurements made at special ground stations at known locations. Of course the second calculation is vastly simpler than the first and can be done with much more accuracy since only two variables (latitude and longitude) are required to specify the location of a ground station while the specification of a satellite orbit requires that at least six parameters be determined. Fortunately, the first calculation usually need not be done since it is generally possible, for tracking the satellite, to acquire more information than the Doppler data for a single pass at a single ground station. In fact, the tracking of TRANSIT satellites is accomplished by the use of the Doppler data measured at a multiplicity of ground stations and extending over a period of time (say 12 hours) that includes a number of passes at each ground station. However, it is technically of interest that the multiplicity of

Doppler curves simply provides redundancy and a consequent increase in accuracy and that each Doppler curve, in principle, provides enough data to determine the orbit.

To complete a description of the operation of the TRANSIT system, it is only necessary to add that the formidable communication problem of disseminating a description of the orbit to all potential users is solved by using the TRANSIT satellites as a special communication link for this purpose. Specifically, after the orbit is determined on the ground a parametric description of this orbit is transmitted to the satellite, recorded in a memory system contained in the satellite and subsequently broadcast at regular (2 minute) intervals. Thus the user receives a description of the orbit of the satellite simultaneously with his measurement of the Doppler shift. By this means it is possible to improve the description of the orbit frequently; in fact, it is intended to insert a current or updated description every twelve hours.

While the above description of the TRANSIT system sounds relatively simple, it can perhaps be imagined that there were a number of rather formidable technical difficulties to be overcome before a practical operating system could be designed in detail. It is the purpose of this article to indicate some of these problems and the progress that has been made toward their solution by the TRANSIT launchings to date.

To the time of this writing there have been three TRANSIT satellites placed in orbit out of a total of five attempts. A few of the significant parameters of these three satellites are displayed in Fig. 1. It will be noticed that, although we have been moderately fortunate in getting satellites placed into orbit, we have been less fortunate in the orbits achieved. None of the three orbits has very closely approached the circularity that was desired and two of the three have had perigee at so low an altitude that atmospheric drag very seriously affected the calculation of the orbit. The last

Project TRANSIT

	Nav 1B	Nav 2A	Nav 3B

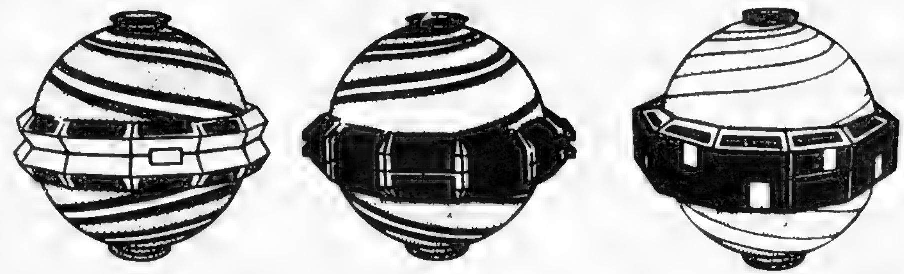

		Nav 1B	Nav 2A	Nav 3B
LAUNCH DATE:		APRIL 13, 1960*	JUNE 21, 1960	FEB 21, 1961**
FREQUENCIES (100 MW EACH):	"B" SYSTEM: "C" SYSTEM:	162–216mc 54–324mc	162–216mc 54–324mc	162–216mc 54–324mc
RMS FREQUENCY NOISE AS MEASURED AT TRACKING STATIONS:	"B" SYSTEM: 162–216mc "C" SYSTEM: 54–324mc	5 PARTS IN 10^9 5 PARTS IN 10^{10}	1 PART IN 10^9 7 PARTS IN 10^{10}	5 PARTS IN 10^{10} 5 PARTS IN 10^{10}
FREQUENCY STABILITY: (Changes with mean satellite temperature)	"B" SYSTEM: 162–216mc "C" SYSTEM: 54–324mc	1 PART IN 10^9/HR 1 PART IN 10^9/HR	3 PARTS IN 10^9/HR 5 PARTS IN 10^{10}/HR	5 PARTS IN 10^{10}/HR 5 PARTS IN 10^{10}/HR
AREA/MASS RATIO:		5.98×10^{-2} cm^2/gm	8.12×10^{-2} cm^2/gm	3.0×10^{-2} cm^2/gm
INITIAL PERIGEE ALTITUDE:		378 km	621 km	178 km
INITIAL APOGEE ALTITUDE:		754 km	1070 km	978 km
INCLINATION:		51.3 deg.	66.7 deg.	28.4 deg.

* NOTE: Nav 1B ceased radiating on July 11, 1960.

** Nav 3B entered the atmosphere on March 30, 1961

Figure 1

REV. MAY 1961

satellite, TRANSIT 3-B, had perigee so low that it had a life of only 36 days and it reentered the atmosphere and was consumed on March 30. There have also been a few equipment failures in the satellites themselves. A temperature sensitive switch, included in TRANSIT 1-B to protect the storage battery from overcharge, opened improperly and permanently on or about July 11, 1960, and the satellite ceased radiating due to loss of power. Thus TRANSIT 1-B had a useful radiating life of 89 days. The same switch malfunctioned in TRANSIT 2-A. In this case a command by-pass of the switch had been incorporated and was actuated to prolong the life of the satellite. However, bypassing this switch removed the overcharge protection which was the reason for incorporating the switch and the storage battery was destroyed by overcharge during the period October 28 to November 14, 1960, while the satellite was in the sunlight at all times and correspondingly receiving maximum power from its solar cells. Since the loss of the storage battery the TRANSIT 2-A radiates only when it is in sunlight, receiving power directly from the solar cells. With this intermittent operation the stability of the oscillators is, of course, not up to the level that obtained during the period of proper, full-time operation. TRANSIT 3-B operated fully throughout its short life.

In spite of these various limitations, it has been possible, with the three satellites placed in orbit to date, to demonstrate rather remarkable progress toward overcoming the major technical obstacles that lay in the path of establishing an operational system. In particular, there are no longer any questions about the feasibility of the operational concept and it is now possible to specify a detailed design with confidence that it will meet the requirements.

In what follows, the various areas that were expected to provide technical difficulties will be discussed and the state of progress toward their solution will be described.

1. Stability of the Satellite Oscillator

This was initially expected to be one of the difficult problems. The fact is that while the Doppler shift does determine the relative geometry of the satellite orbit and receiving station it requires a very accurate measure of the Doppler shift to obtain a good measure of this relative geometry. Although there is no simple relationship between an error in Doppler measurement and the corresponding position error, a crude rule-of-thumb relationship, usually valid within an order of magnitude, is given by the statement that an error of 1 cps in Doppler gives an error of 1 mile in position if the transmitter frequency is 100 mcps. Since, in the TRANSIT system, any variation in transmitted frequency during the time of a pass will be erroneously ascribed to the Doppler effect, it is clear that a frequency drift of only 1 part in 10^8 during the time of a pass can result in a serious error in position determination. It is true that many oscillators with stability better by orders of magnitude than 1 part in 10^8 had been built before the start of the TRANSIT program, but these were generally rather elaborate devices including proportional heating ovens to control the crystal frequency and were not suitable for use in small and simple satellites. Actually, as can be seen from Fig. 1, the oscillator stability has not proved a very difficult problem. A rather elaborate temperature isolation of the crystal from external heat sources, taking advantage of the superb vacuum available in the operating environment, has kept the rate of change of frequency due to temperature change at the crystal within acceptable limits, and careful circuit design has minimized other sources of frequency change. Other techniques used include long burn-in of all crystals and selection of crystals on the basis of stability after this burn-in period. While techniques for still further improvement are under investigation, the presently achieved stabilities are good enough to meet the program objectives.

2. Refraction by the Ionosphere

The Doppler shift exhibited in the reception of a transmission from an earth satellite is not strictly proportional to the rate of change of the true slant range but rather is proportional to the rate of change of the transmission path length. If, as is normally the case, the satellite is above the ionosphere, then the transmission path is not the straight line joining the transmitter and receiver but instead is some longer curved (or bent) path due to the refraction effect of the ionosphere. Hence, for a precision analysis of the Doppler shift, account must be taken of the effect of this ionospheric refraction on the Doppler. A rough model of the ionosphere indicates that the effect of ionospheric refraction on the Doppler shift should be inversely proportional to the square of the transmitter frequency. This suggests that refraction can be made negligible by going to a sufficiently high frequency. And, indeed, at microwave frequencies (and above) the ionosphere has a negligible effect on the received Doppler shift. Unfortunately the use of microwave frequencies would require either the use of large directional antennas for reception or of very high transmitter powers. The first solution would be undesirable for many potential users of TRANSIT (e.g., submarines or aircraft) and the second is unavailable with small, easily launched satellites. Accordingly, it has been considered wise to restrict the TRANSIT frequencies to the range (hundreds of megacycles) where solid state amplifiers were usable. In this range, ionospheric refraction cannot be neglected with high accuracy. The technique used in TRANSIT is to transmit a pair of harmonically related (coherent) frequencies rather than a single frequency. From the Doppler shift obtained on each of these frequencies it is possible to obtain a measure of the integrated electron density between the transmitter and the receiver, and then to develop a good estimate of the Doppler shift that would have been measured in the absence of the ionosphere. It is this so-called refraction corrected Doppler or vacuum Doppler that is actually used in the TRANSIT program for orbit determinations and precision navigation fixes. Actually, the generation of the vacuum Doppler from the individual Doppler shift at the two harmonically related frequencies is accomplished by a relatively simple analog computer[1/] which would yield a precisely correct answer if the $1/(\text{freq.})^2$ refraction law were precisely correct.

Results to date in the TRANSIT program indicate that at mid-latitudes or lower the refraction correction based on the $1/(\text{freq.})^2$ assumption is sufficiently accurate to meet the TRANSIT program goals even in times of magnetic storm activity. However, there is need to explore further the refraction effect at high latitudes during heavy auroral activity to determine if this correction remains sufficiently accurate in these most severe conditions. Considerable effort in this area is planned for the next year.

3. Transmission of the Orbit Parameters

In principle the transmission of the orbit parameters from the satellite poses a relatively easy communication problem and can be accomplished straightforwardly in a number of ways. Practically it is desirable to develop a means which poses the least increase in complexity or power on the part of the satellite equipment and the least special equipment for reception on the part of the navigator. To this end a system has been developed in which the orbit parameters are transmitted in binary notation (zeros and ones) coded as a phase modulation of the basic transmission which are used to generate the Doppler shift. A specific modulation (60° phase advance followed by a 60° phase retard) is used which does not interfere with the ability to measure the Doppler shift with precision. The use of this approach avoids the need for an extra transmitter in the satellite or an extra receiver in the ground equipment.

1/ Weiffenbach, G.C., "Measurement of the Doppler Shift of Radio Transmissions from Satellites," Proceedings of the Institute of Radio Engineers, Vol. 48, No. 4, pp 750-754, April 1960

This system for the distribution of data by means of a satellite link was incorporated, for the first time, in the short-lived TRANSIT 3-B and operated perfectly throughout its life.

4. Time Synchronization

Since the time at which orbit parameters are transmitted is controlled by a satellite clock based on the same stable oscillator that controls the two basic frequencies, it is clear that the time of reception of orbit parameters can be used as a time signal by the ground equipment. This makes the TRANSIT system completely self contained and independent of any other time source such as WWV. Actually, because of the short, well defined transmission path for the TRANSIT line-of-sight frequencies and the excellent knowledge of satellite position, the time signals available from TRANSIT will be more accurate than those available from WWV in most areas of the world. In fact, a precision of 100 microseconds should be readily available. A system has been developed for including along with the orbit parameter transmission a special word ("Barker" word) which serves the purposes of a start of message and time synchronization signal. This system also was successfully tested in TRANSIT 3-B.

5. Thermal and Power Balances

One technical problem that proved quite serious in the design of early satellites was to achieve the proper control of satellite temperature and input power under the varying conditions that occur in orbit. If one considers polar satellites, it is clear that when the orbital plane is roughly at right angles to the earth-sun line then the satellite will be exposed to sunlight throughout its orbit. At the other extreme, if the sun lies in the orbital plane the satellite will be in the earth's shadow for a considerable portion (about 40% for the satellites at altitudes intended for TRANSIT) of each orbit. Since for a polar satellite the orbital plane remains fixed in inertial space while the earth-sun line rotates in inertial space once a year, it is clear that each of these conditions is reached at different times in the life of the satellite. Thus, there is considerable variation of the total amount of input thermal radiation and of the total power input from solar cells. Since the maximum electrical power and maximum thermal input occurs simultaneously, a serious battery temperature and overcharge condition is likely to occur in 100% sunlight orbits. This problem was responsible for the failures that eventually occurred in both TRANSIT 1-B and TRANSIT 2-A. Recently a very simple solution to this problem has been found by the proper choice of satellite configuration and limited attitude stabilization.

Imagine a satellite in the shape of a drum with a magnet aligned with the symmetry axis of the drum. If proper damping is provided and competing torques are kept low, such a satellite will be constrained by the magnetic torques to have its symmetry axis in the same plane as the earth's magnetic axis. Since the magnetic axis of the earth is approximately the rotation axis, the symmetry axis of the satellite will lie approximately in the orbital plane. It is then seen that during the 100% sunlight axis, when the orbital plane is at right angles to the earth-sun line, then the satellite's symmetry axis will also be approximately orthogonal to earth-sun line; in other words, the sun will illuminate the edge of the drum at all times and not the top and bottom.

In the other extreme case, when the sun lies in the plane of the orbit, it is clear that the sun will illuminate the top and bottom of the drum-shaped satellite a reasonable percent of the time. It is clear that by making the top and bottom of the satellite large in area compared to the edge, it is possible to arrange that the effective received solar radiation at the satellite is just as great in the 60% sunlight case as it is in the 100% sunlight case.

By the use of the design principle outlined above, a configuration has been developed for the operational TRANSIT satellite in which the total temperature extremes will vary by no more than 10° and the total power input will remain constant within a few percent throughout the life of the satellite.

6. Tracking Accuracy

When the TRANSIT program was first proposed, the most serious technical questions raised concerned the feasibility of tracking the satellites with sufficient accuracy. Obviously, to determine your position on earth by reference to the position of a satellite, it is necessary that the position of the satellite, at a given time, be known to higher accuracy than the accuracy with which your own position is to be determined. At the time the initial TRANSIT program proposal was being considered, typical satellite tracking or prediction errors ranged from 5 miles to as much as 50 miles. There was a wide spread belief among even well informed people that there were mysterious or at least unpredictable forces of large magnitude acting on satellites which would for years prevent orbit prediction with an accuracy of better than a number of miles. Fortunately, most of the difficulties of that period were a result of poor measurement rather than of a reflection of basic unknowns. It is true that there were and still are, areas of ignorance concerning the precise formulation of the forces acting on a near earth satellite (for example, the proper description of the earth's gravitational field is not too well known) but the effect of these uncertainties on the trajectory is one or two tenths of a mile rather than a number of miles. The fact that present knowledge of the forces acting on a satellite is sufficiently accurate to enable tracking and short term (12 hour) prediction of satellite position to an accuracy of a few tenths of a mile has been shown conclusively by our tracking experience with TRANSIT 1-B and TRANSIT 2-A.

One way to judge the accuracy with which orbit determinations are made is simply by observing the consistency of the determination from one day to the next. In the TRANSIT program an orbit is determined for each day based solely on the data obtained on that day so that each determination is totally independent of all preceding data. Hence, the day-to-day consistency of orbit parameters is a very good indication of the precision of the system. The determination of orbit parameters through most of the radiating life of TRANSIT 1-B is given in Figs. 2 through 9. It will be seen that the first four or five points show a much larger scatter than the subsequent points (particularly in Figs. 7 and 9). This results from the fact that for this initial period the satellite was still spinning and the spin caused a modulation on reception that was interpreted by the ground equipment as a change in the Doppler frequency. After this initial period the satellite was despun[2/] and the data became much cleaner. It can be seen, particularly from Figs. 2 and 3 that, after the spinning period, the scatter of the day-to-day determinations of orbit parameters is generally well within one half of a kilometer or one quarter of a mile.

The nature of the long term variation of the orbit parameters, particularly Figs. 2, 3, 4, and 5, is quite interesting. It is seen that both apogee and perigee exhibit a linear decrease with a sine wave oscillation superimposed. This oscillation has an amplitude of about 6 km and its period is the period of the precession of perigee. Thus the sine wave terms in the formulae given for apogee and perigee are zero when perigee occurs at the equator and reaches its extreme values when perigee reaches the extremes of latitude. The linear decrease of apogee and perigee is due, of course, to drag. The effect of drag on apogee is five times as great as the effect on perigee. This is reasonable since most of the drag occurs as the satellites goes through perigee. This results in a velocity decrease at perigee so that the satellite does not swing out quite as far at apogee the next time around.

2/ Using the yo-yo technique. See "The TRANSIT Program", June 1960 Astronautics

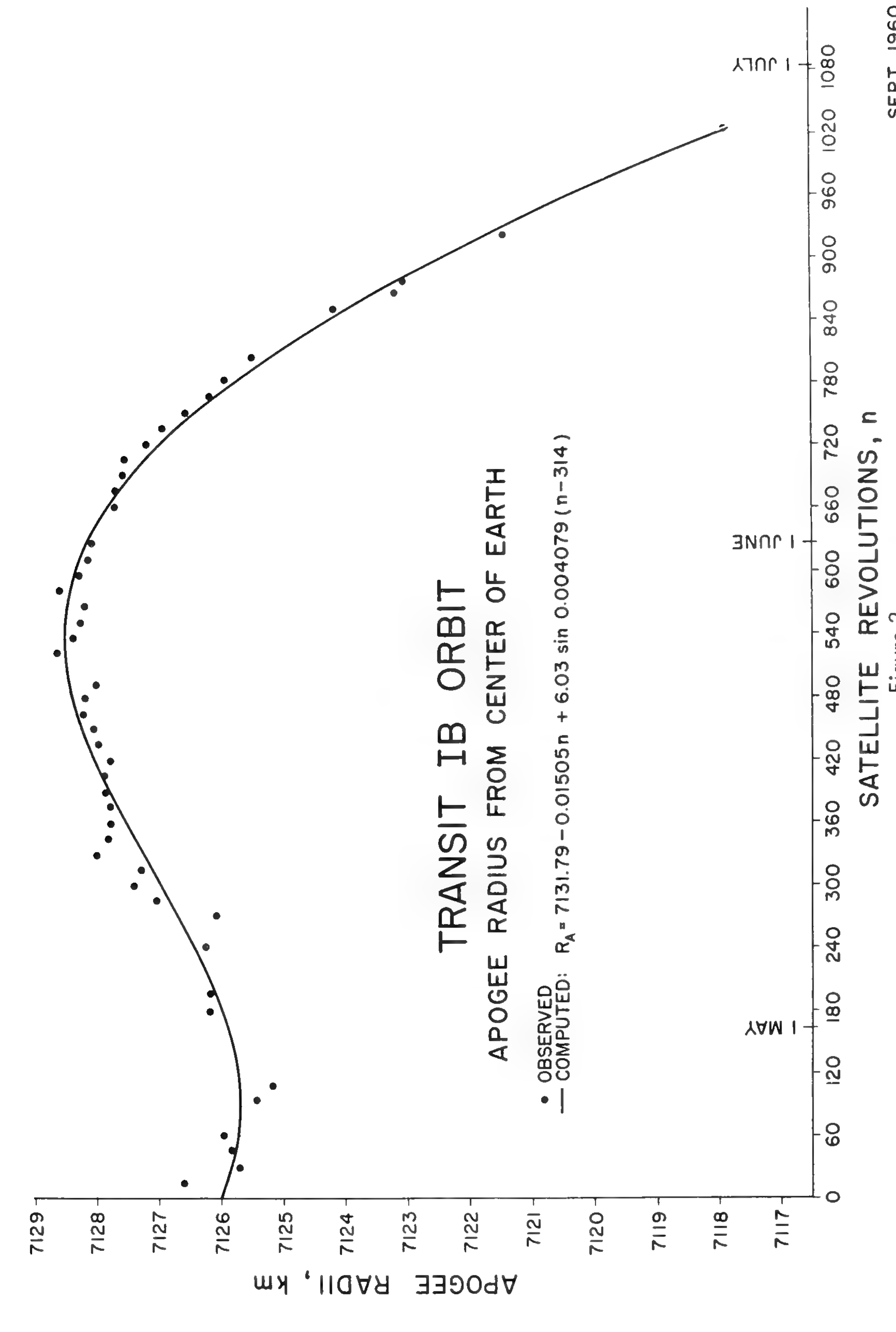
TRANSIT IB ORBIT
APOGEE RADIUS FROM CENTER OF EARTH
• OBSERVED
— COMPUTED: R_A = 7131.79 - 0.01505n + 6.03 sin 0.004079 (n-314)
APOGEE RADII, KM
7129
7128
7127
7126
7125
7124
7123
7122
7121
7120
7119
7118
7117
0
60
120
180
240
300
360
420
480
540
600
660
720
780
840
900
960
1020
1080
1 MAY
1 JUNE
1 JULY
SATELLITE REVOLUTIONS, n
SEPT 1960

Figure 2

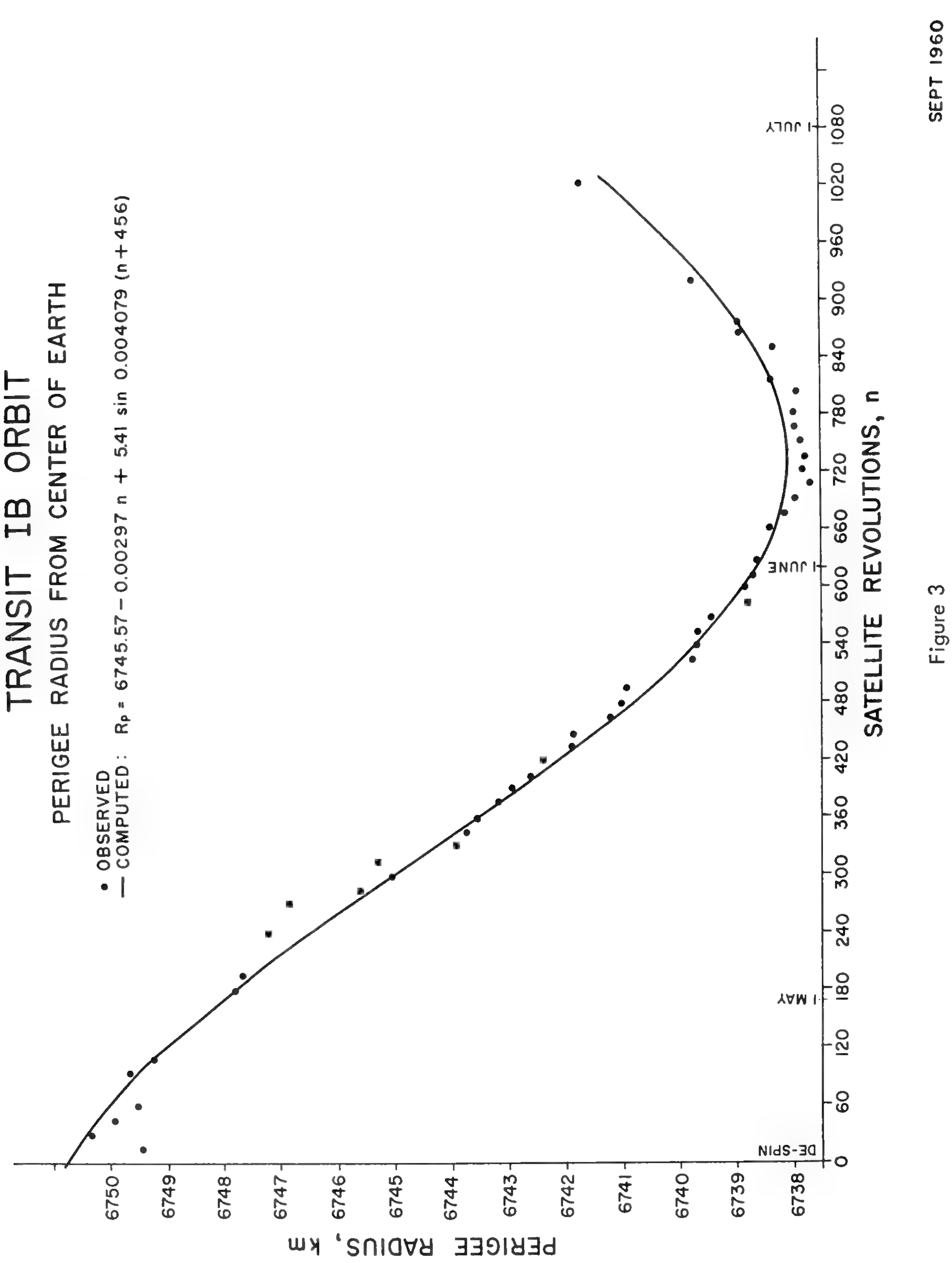

TRANSIT IB ORBIT
PERIGEE RADIUS FROM CENTER OF EARTH
• OBSERVED
— COMPUTED: $R_p = 6745.57 - 0.00297\,n + 5.41 \sin 0.004079\,(n+456)$
PERIGEE RADIUS, km
6750
6749
6748
6747
6746
6745
6744
6743
6742
6741
6740
6739
6738
SATELLITE REVOLUTIONS, n
0
60
120
180
240
300
360
420
480
540
600
660
720
780
840
900
960
1020
1080
DE-SPIN
1 MAY
1 JUNE
1 JULY
SEPT 1960

Figure 3

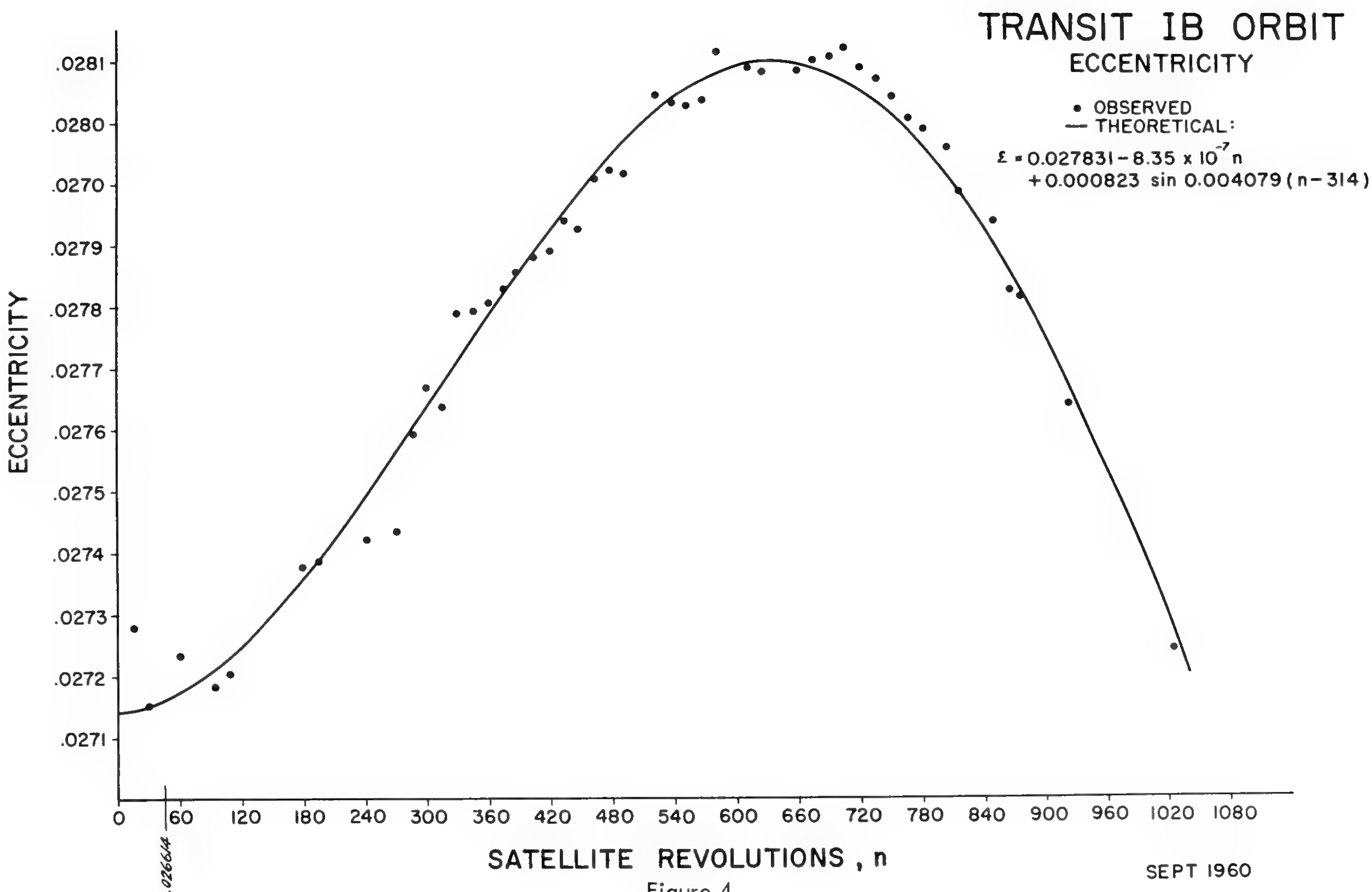
TRANSIT IB ORBIT
ECCENTRICITY
• OBSERVED
— THEORETICAL:
£ = 0.027831 − 8.35 x 10^-7 n
+ 0.000823 sin 0.004079 (n − 314)
ECCENTRICITY
.0281
.0280
.0270
.0279
.0278
.0277
.0276
.0275
.0274
.0273
.0272
.0271
0
60
120
180
240
300
360
420
480
540
600
660
720
780
840
900
960
1020
1080
.026614
SATELLITE REVOLUTIONS, n
SEPT 1960

Figure 4

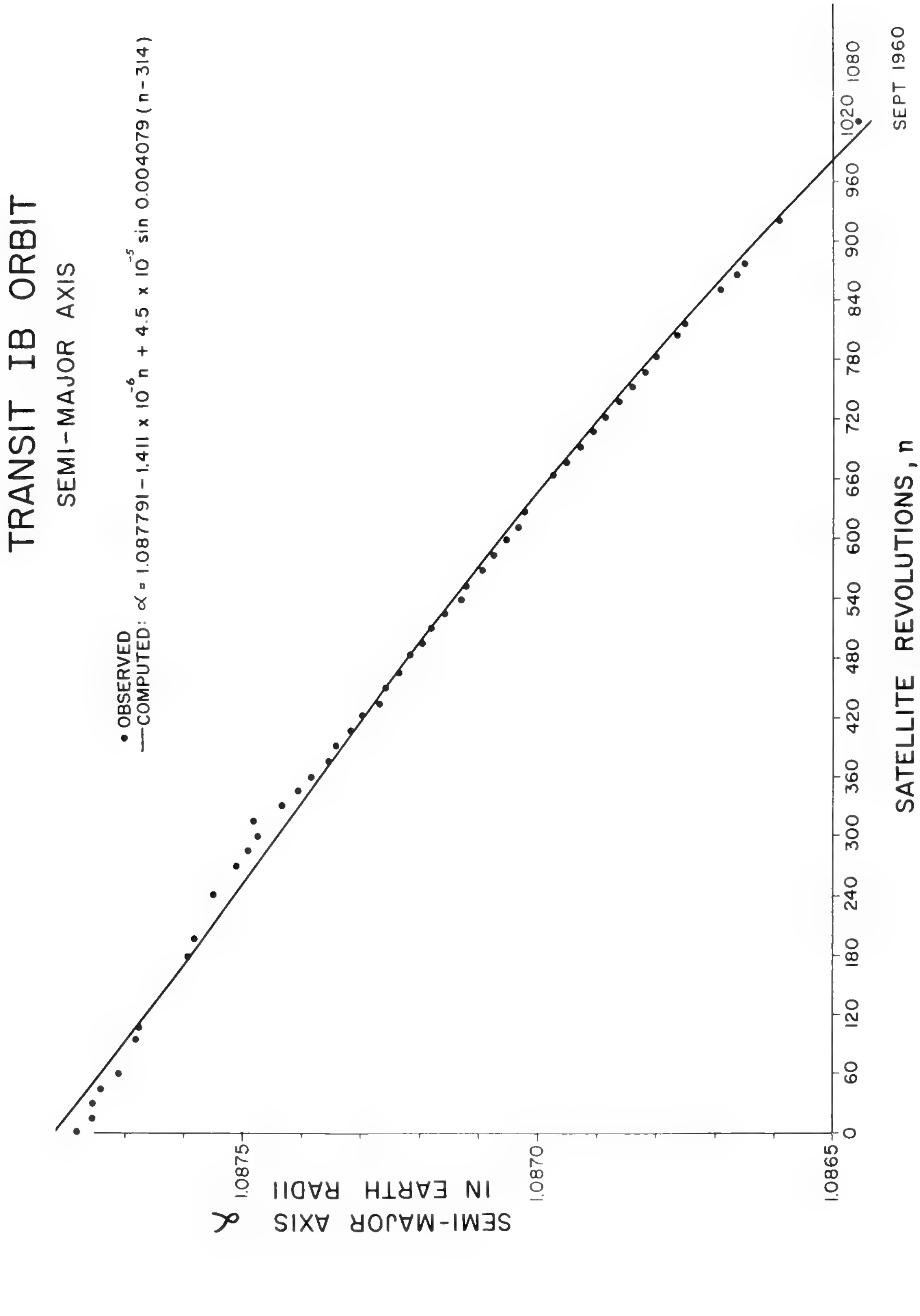
TRANSIT IB ORBIT
SEMI-MAJOR AXIS
• OBSERVED
—COMPUTED: α = 1.087791 − 1.411 x 10⁻⁶ n + 4.5 x 10⁻⁵ sin 0.004079 (n − 314)
SEMI-MAJOR AXIS α
IN EARTH RADII
1.0875
1.0870
1.0865
0
60
120
180
240
300
360
420
480
540
600
660
720
780
840
900
960
1020
1080
SEPT 1960
SATELLITE REVOLUTIONS, n

Figure 5

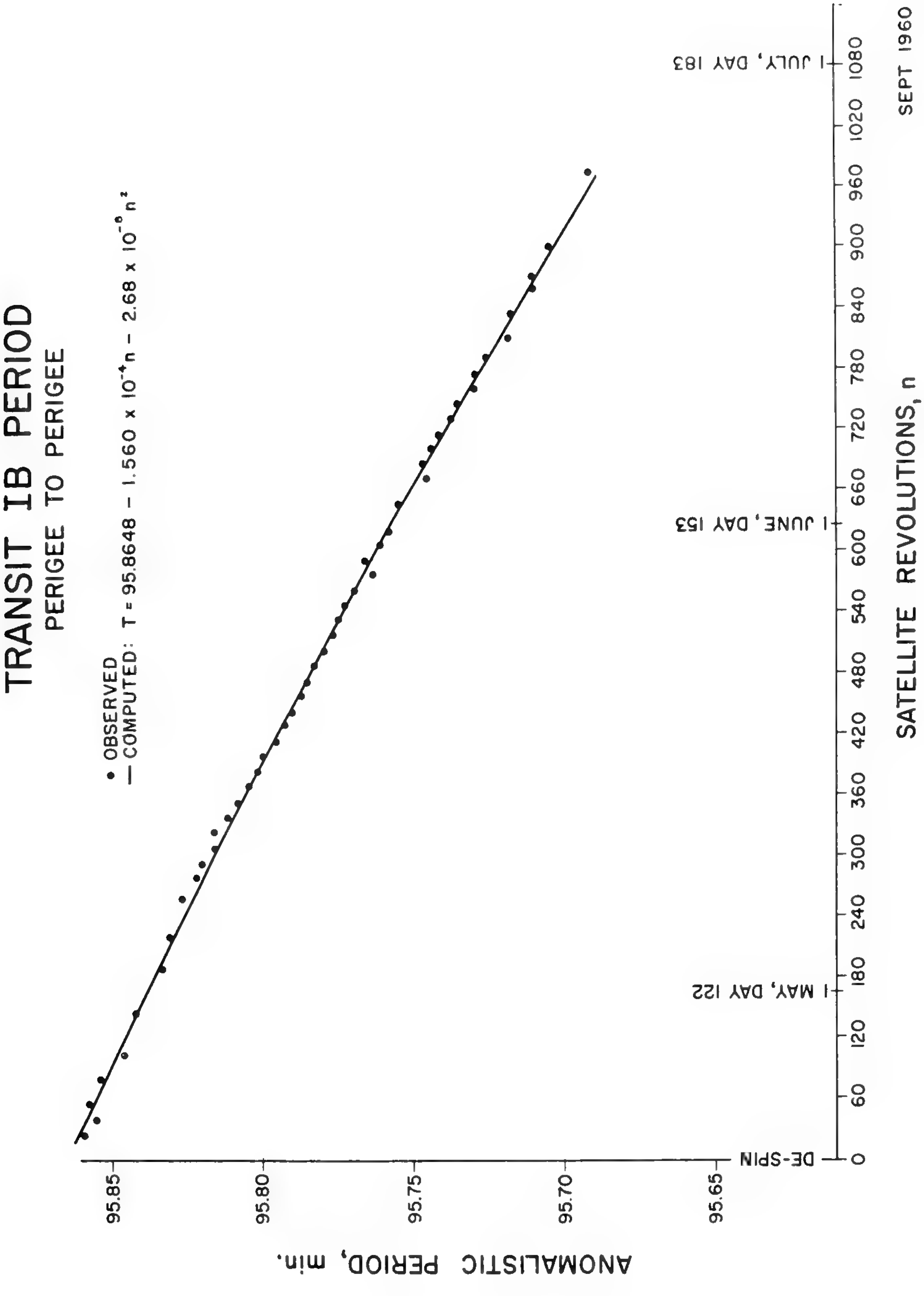

TRANSIT IB PERIOD
PERIGEE TO PERIGEE
• OBSERVED
— COMPUTED: T = 95.8648 − 1.560 x 10⁻⁴n − 2.68 x 10⁻⁸n²
ANOMALISTIC PERIOD, min.
95.85
95.80
95.75
95.70
95.65
DE-SPIN
0
60
120
180
240
300
360
420
480
540
600
660
720
780
840
900
960
1020
1080
1 MAY, DAY 122
1 JUNE, DAY 153
1 JULY, DAY 183
SEPT 1960
SATELLITE REVOLUTIONS, n

Figure 6

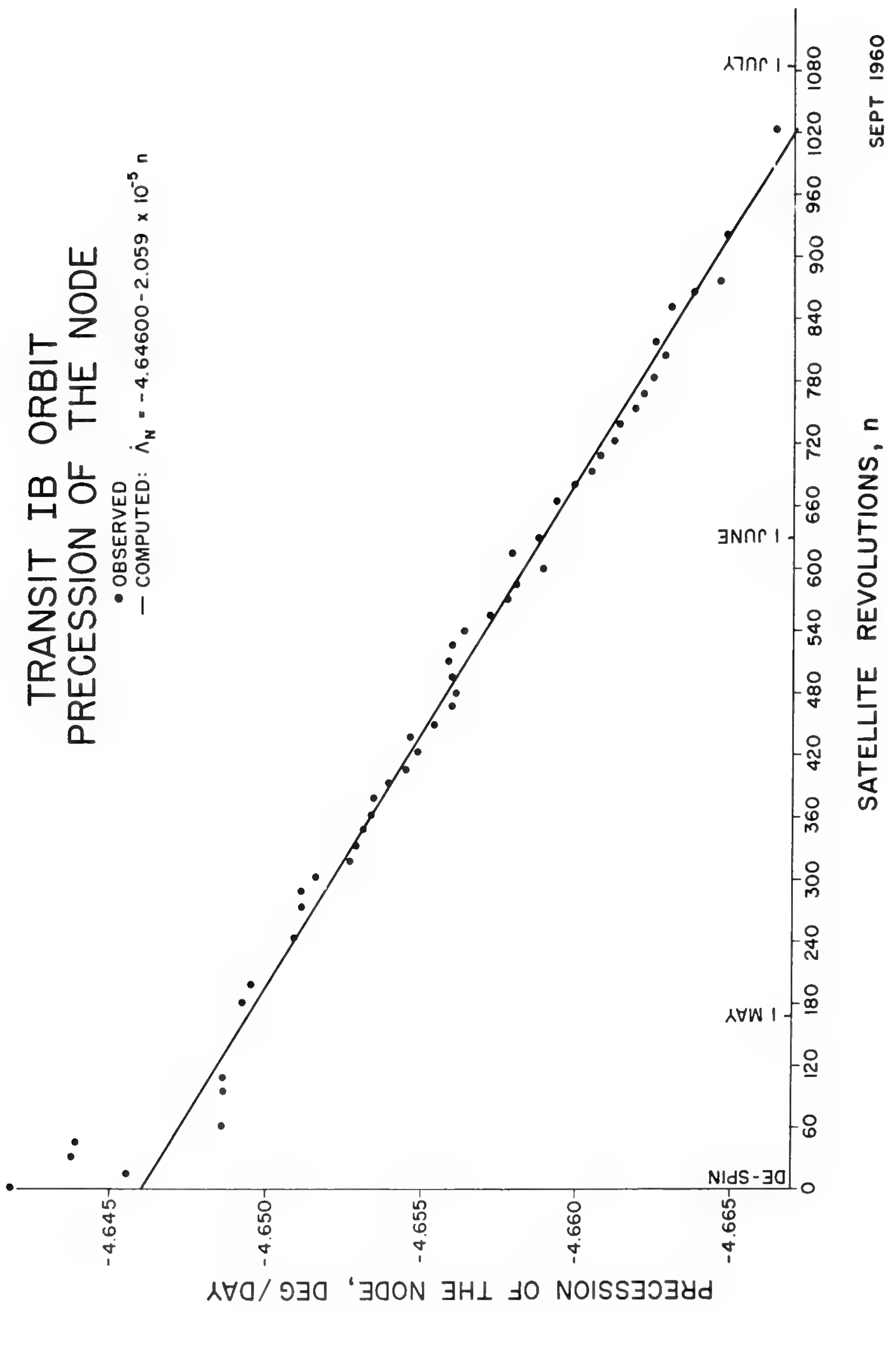

TRANSIT IB ORBIT
PRECESSION OF THE NODE
• OBSERVED
— COMPUTED: $\dot{\Lambda}_N = -4.64600 - 2.059 \times 10^{-5}\, n$
PRECESSION OF THE NODE, DEG/DAY
-4.645
-4.650
-4.655
-4.660
-4.665
DE-SPIN
1 MAY
1 JUNE
1 JULY
0
60
120
180
240
300
360
420
480
540
600
660
720
780
840
900
960
1020
1080
SEPT 1960
SATELLITE REVOLUTIONS, n

Figure 7

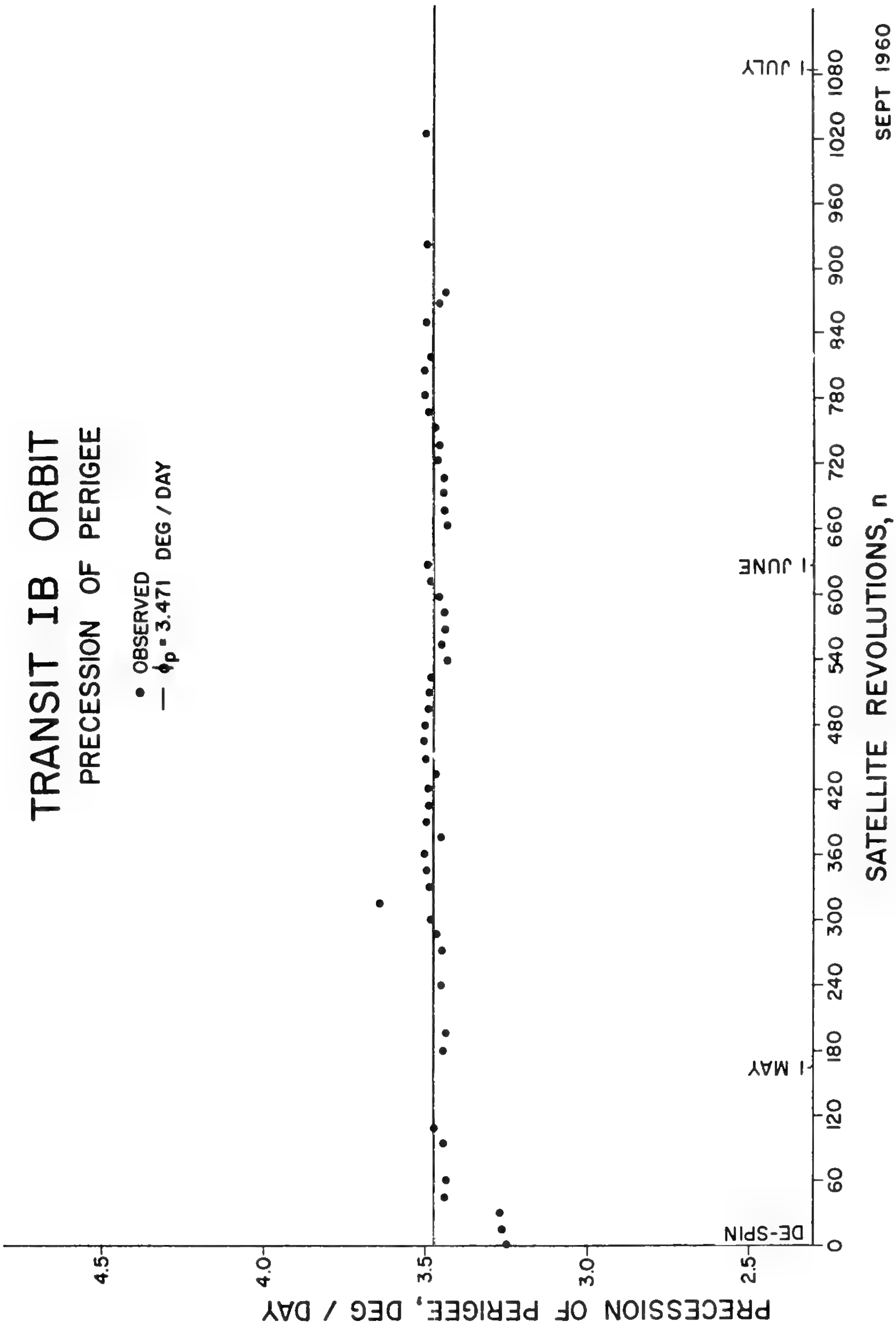
TRANSIT IB ORBIT
PRECESSION OF PERIGEE
• OBSERVED
— $\dot{\phi}_p$ = 3.471 DEG / DAY
PRECESSION OF PERIGEE, DEG / DAY
4.5
4.0
3.5
3.0
2.5
SATELLITE REVOLUTIONS, n
0 60 120 180 240 300 360 420 480 540 600 660 720 780 840 900 960 1020 1080
DE-SPIN
1 MAY
1 JUNE
1 JULY
SEPT 1960

Figure 8

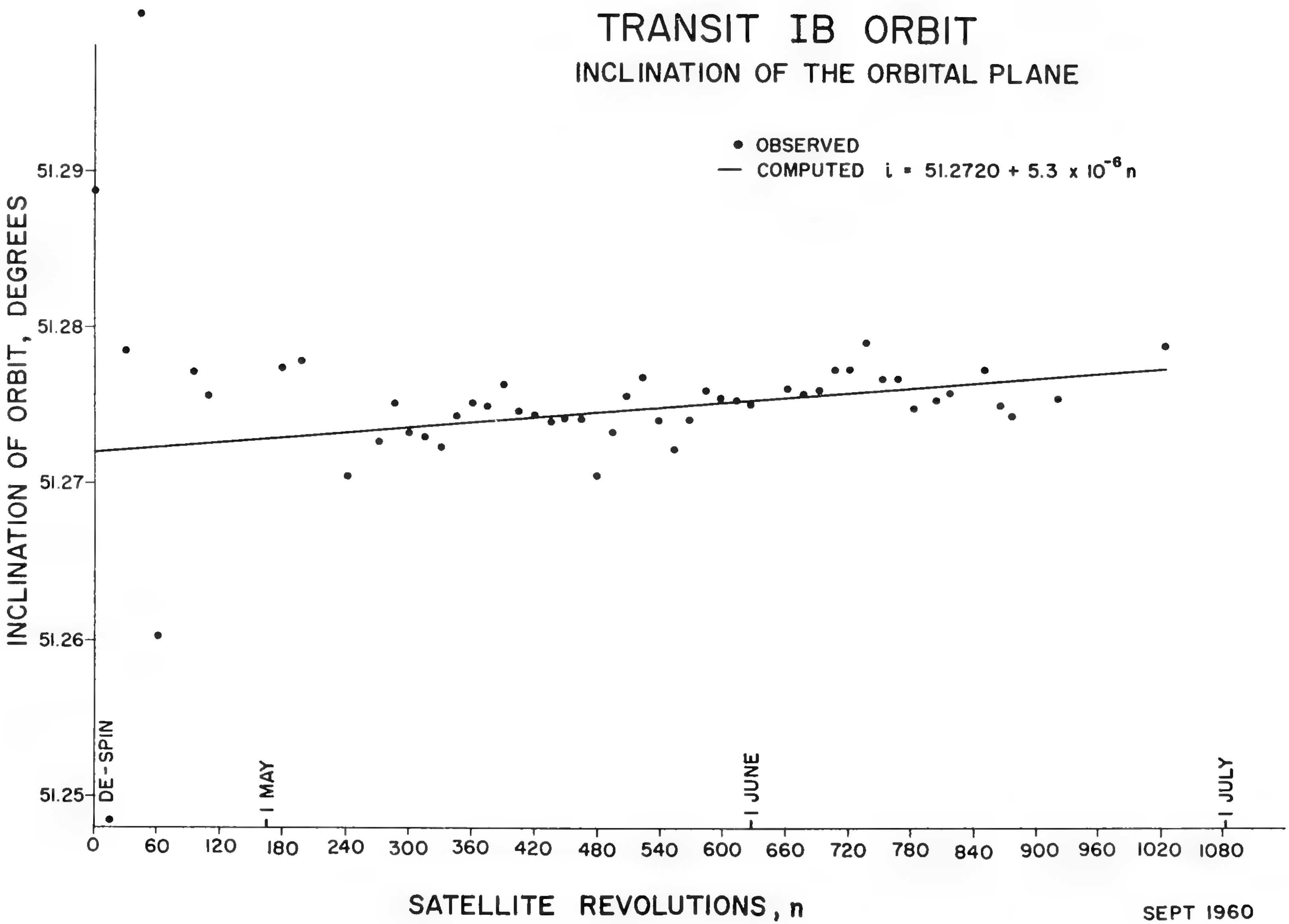
TRANSIT IB ORBIT
INCLINATION OF THE ORBITAL PLANE
OBSERVED
COMPUTED $i = 51.2720 + 5.3 \times 10^{-6} n$
INCLINATION OF ORBIT, DEGREES
51.29
51.28
51.27
51.26
51.25
DE-SPIN
1 MAY
1 JUNE
1 JULY
0
60
120
180
240
300
360
420
480
540
600
660
720
780
840
900
960
1020
1080
SATELLITE REVOLUTIONS, n
SEPT 1960
Figure 9

The sine wave oscillation in the amplitude of apogee and perigee, in phase with the precession of perigee, clearly shows that the orbit behaves differently depending on whether perigee occurs in the northern or the southern hemisphere. This is a striking illustration of the existence of a north-south dissymmetry in the earth - the famous "pear-shaped" term in the expansion of the earth's gravitational field, first deduced by O'Keefe from Vanguard data. It is, of course, possible to confirm, quantitatively the value of J_3, the "pear-shaped" coefficient in the expansion of the gravitational field of the earth in spherical harmonics. In fact, from this data for TRANSIT 1-B together with similar data for TRANSIT 2-A, R. R. Newton[3/] has improved on the value for J_3 and also obtained values for J_5 and J_7, the next two odd-order coefficients beyond J_3.

Not all of the long term effects shown in Figs. 2 through 9 are understood. For example, the very small but clearly significant increase in the inclination of the orbit through May and June has not been explained to date.

The day-to-day consistency of the Kepler orbit elements is not the best way of judging the accuracy of the tracking and could indeed be misleading since there has been perforce some smoothing of data involved in the very act of describing the orbit by means of Kepler elements. Actually the true orbit, obtained by a numerical integration of the full equations of motion, departs from a Kepler ellipse (even with allowance for precession of perigee and the line of nodes) by one or two tenths of a mile. Obviously the "smoothness" of parameters which, at best, can only approximately describe the orbit, cannot accurately indicate the precision of the system.

[3/] R.R.Newton, "Odd Harmonics of the Earth's Gravitational Field" (to appear)

A somewhat better indication of the accuracy of TRANSIT tracking is obtained by a sort of closed-loop consistency calculation. To accomplish this consistency check, the data for one particular pass at one station are held in reserve and the orbit is determined by the remaining passes during a particular time period. Then, using this orbit and the reserved single-pass data the location of the ground station is computed - just as would be done in a typical navigation fix. The result of this position determination is compared with the known ground station location and the assumption is made that the error in satellite position is no greater than this resulting error in station location (actually it should be appreciably less, on the average, since there would be some error in station location even with a perfectly known orbit). Large numbers of these "closed-loop" calculations have been performed[4/] based on data from TRANSIT 2-A, and the resulting sigma is well under one-quarter mile.

It might be thought that the calculations described in the preceding paragraph are a direct test of the ability to perform navigation fixes by TRANSIT. Unfortunately this is not quite the case. For, in order to use TRANSIT for navigation in the practical operating system, it is necessary to base the calculation on an orbit determined previous to the time of the navigation fix (based on prior data). In other words, the practical use of TRANSIT for navigation always involves orbit extrapolation. This extrapolation process introduces a further error which obviously depends on the state of knowledge of the forces acting on the satellite and in particular on the knowledge of the gravitational field. Calculations similar to those of the previous paragraph but where the data used for the position determination were obtained a day later than those used for the orbit determination (thus requiring a full day orbit extrapolation) indicate that the resulting error in position determination is now about one-half mile. Extending the orbit

----

[4/] R.B.Kershner, "The TRANSIT System" Proceedings of the Institute of Radio Engineers, Sept. 1960 extrapolation further, for example to four days, increases the error to about three miles, with the error occurring mostly along the satellite track.

All the above methods for estimating the error of tracking by TRANSIT techniques still leave a small uncertainty about the absolute precision since they are only self-consistency checks and it is possible to imagine some form of consistent bias that cancels out when you "close the loop." For example, all the consistency checks above could remain valid for a system that consistently tracks a phantom point five miles ahead of the real satellite on the same orbit. This would not matter for navigation but would introduce real trouble when one attempted to use the results to deduce geodetic consequences. Fortunately a completely independent check has been made possible by the availability of optical sighting data of reasonable precision reduced by Smithsonian. The data for sightings of TRANSIT 1-B from optical stations in the United States agree with TRANSIT determination of the satellite position to about one-quarter mile[5/]. Optical sightings elsewhere in the world disagree somewhat more (sometimes 1 to 1-1/2 mile) because of uncertainties in the absolute location of these overseas sites relative to the center of the earth.

It is seen that the precision of measurement now possible with TRANSIT techniques is quite good. However, both the determination of orbit during a one day period and the ability to extrapolate the orbit for a day are presently limited (to a few tenths of a mile in each case) by inaccuracies in the present model of the force field (gravitational field, drag, etc.). On a world-wide basis there are further difficulties introduced by the unavailability of sufficiently accurate datum ties. To meet the ultimate program goals for TRANSIT thus requires considerable improvement in the present knowledge of these factors (roughly the shape and mass distribution of the earth).

[5/] W.H.Guier, "The Doppler Tracking of Project TRANSIT Satellites" Proceedings of the Institute of Radio Engineers, Sept. 1960.

This is the primary remaining development challenge of the TRANSIT program. Fortunately, the TRANSIT system itself provides one of the most powerful tools available for accomplishing these goals. Furthermore, considerable effort using both TRANSIT and other techniques is planned, or already under way, not only in the TRANSIT program, but by many other programs in the Army, Navy, Air Force and NASA. It is clear that the next year or two will see tremendous advances in these basic problems of geodesy.

7. Other Problems

While the discussion above covers the major technical aspects of the TRANSIT program, there have been, of course, a host of detailed technical or practical operational problems that required solution. Some of these solutions are sufficiently novel to merit comment. The problem of de-spinning satellites, alluded to above, is one such example. TRANSIT 1-B used the so-called yo-yo, devised independently by APL and JPL. Subsequently, it was found the same objective could be accomplished even more simply, without moving parts, by using magnetic damping in the earth's magnetic field. A combination of two phenomena, hysteresis loss and induced current loss, provides very effective despin.[6/]

A practical problem that has been solved quite effectively is that of making full use of the launch capabilities of the launch vehicles when these exceed the requirements of a specific payload. The solution adopted is to fire a multiplicity of payloads in a pick-a-back configuration (see Figs. 10 and 11). This technique has worked quite well. It is true there has been one failure to separate (TRANSIT 3-B) but this was caused by a simple programmer malfunction during the launch phase and not by any difficulties inherent in the multi-payload technique.

[6/] R.E.Fischell, "Magnetic Damping of the Angular Motions of Earth Satellites" American Rocket Society, 15th Annual Mtg., Dec. 1960.

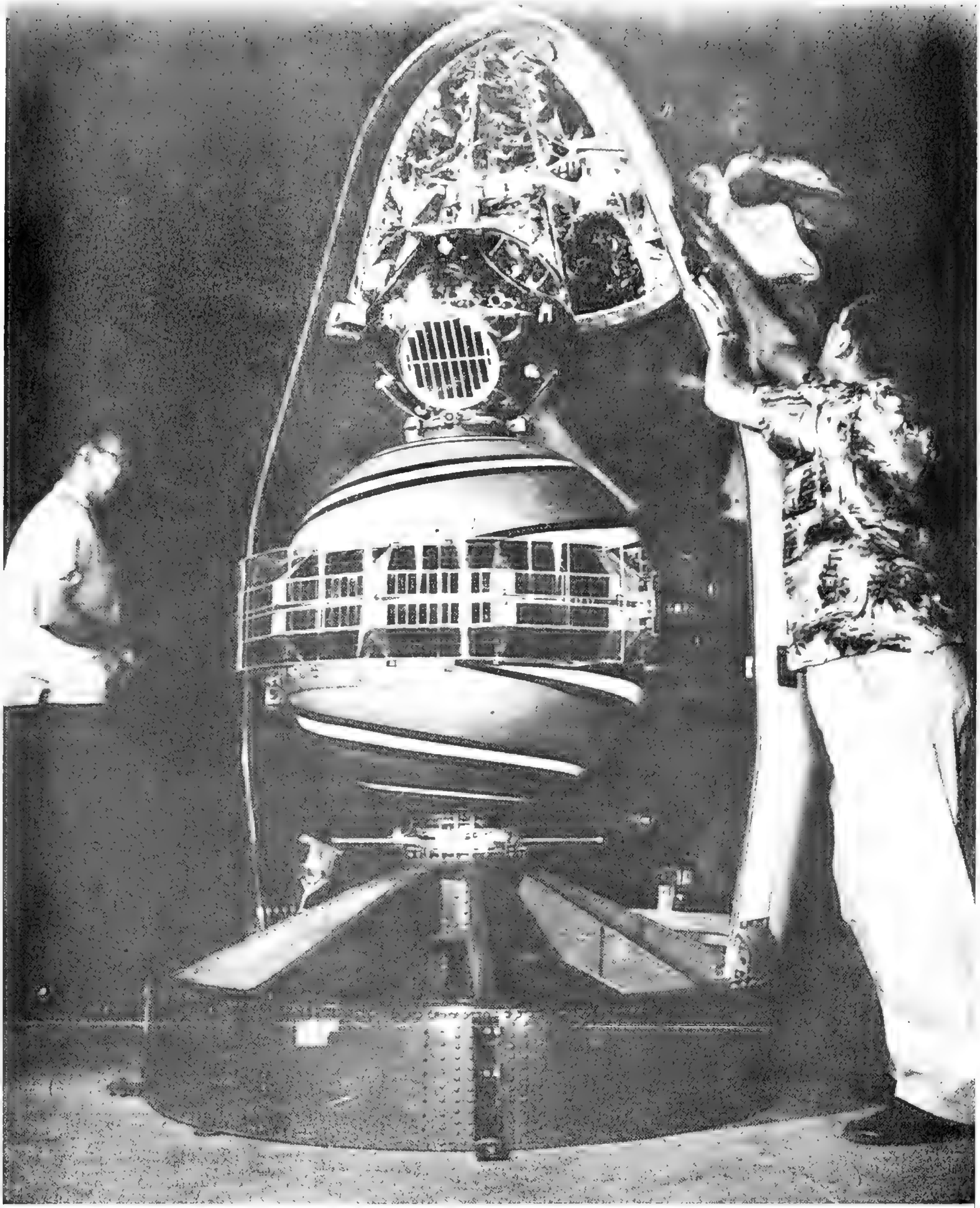

Figure 10

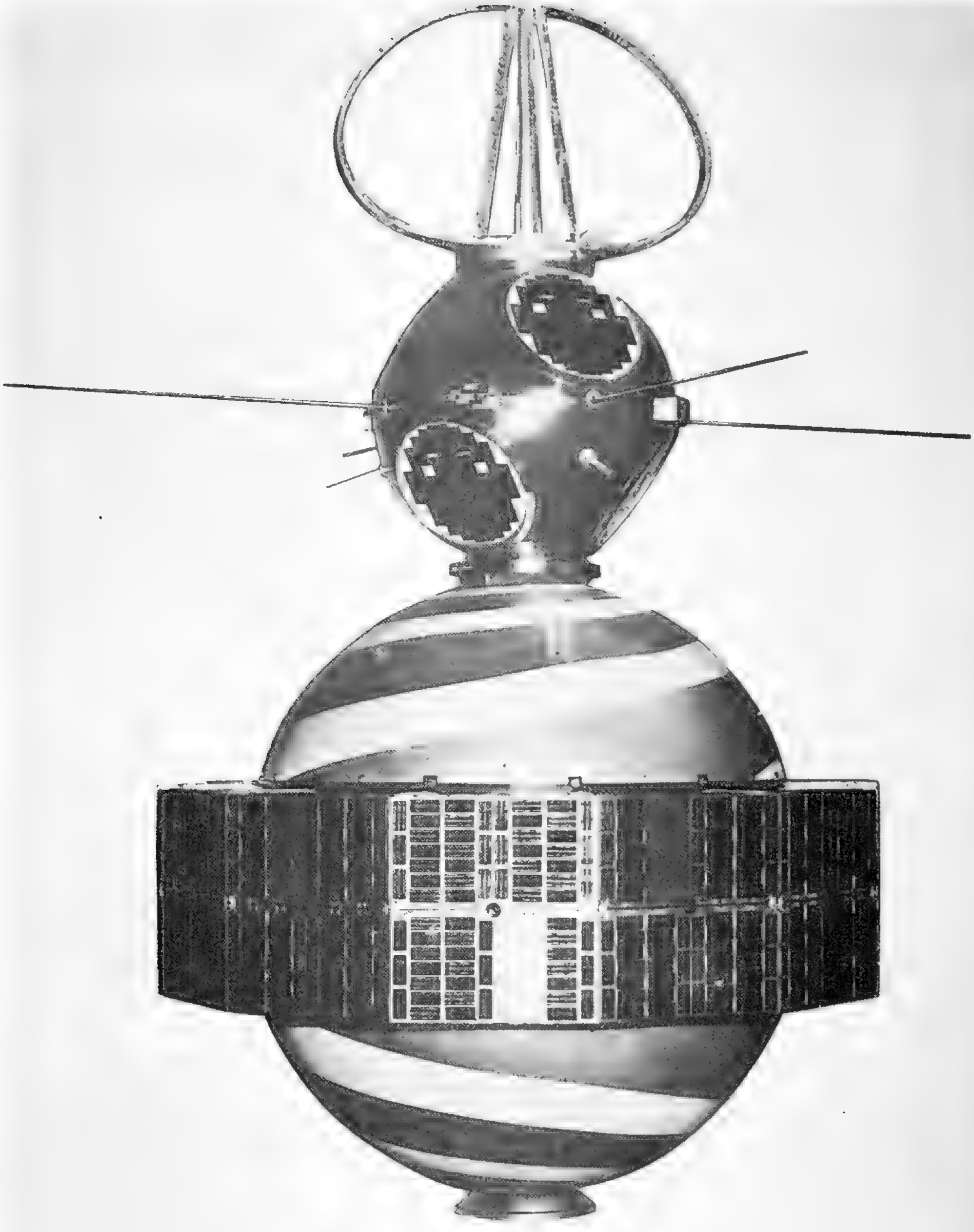

TRANSIT 3B SATELLITE
WITH LOFTI

FEB. 1961

Figure 11

Project TRANSIT

OPERATIONAL TRANSIT SATELLITE NAVIGATION SYSTEM (HIGH ACCURACY)

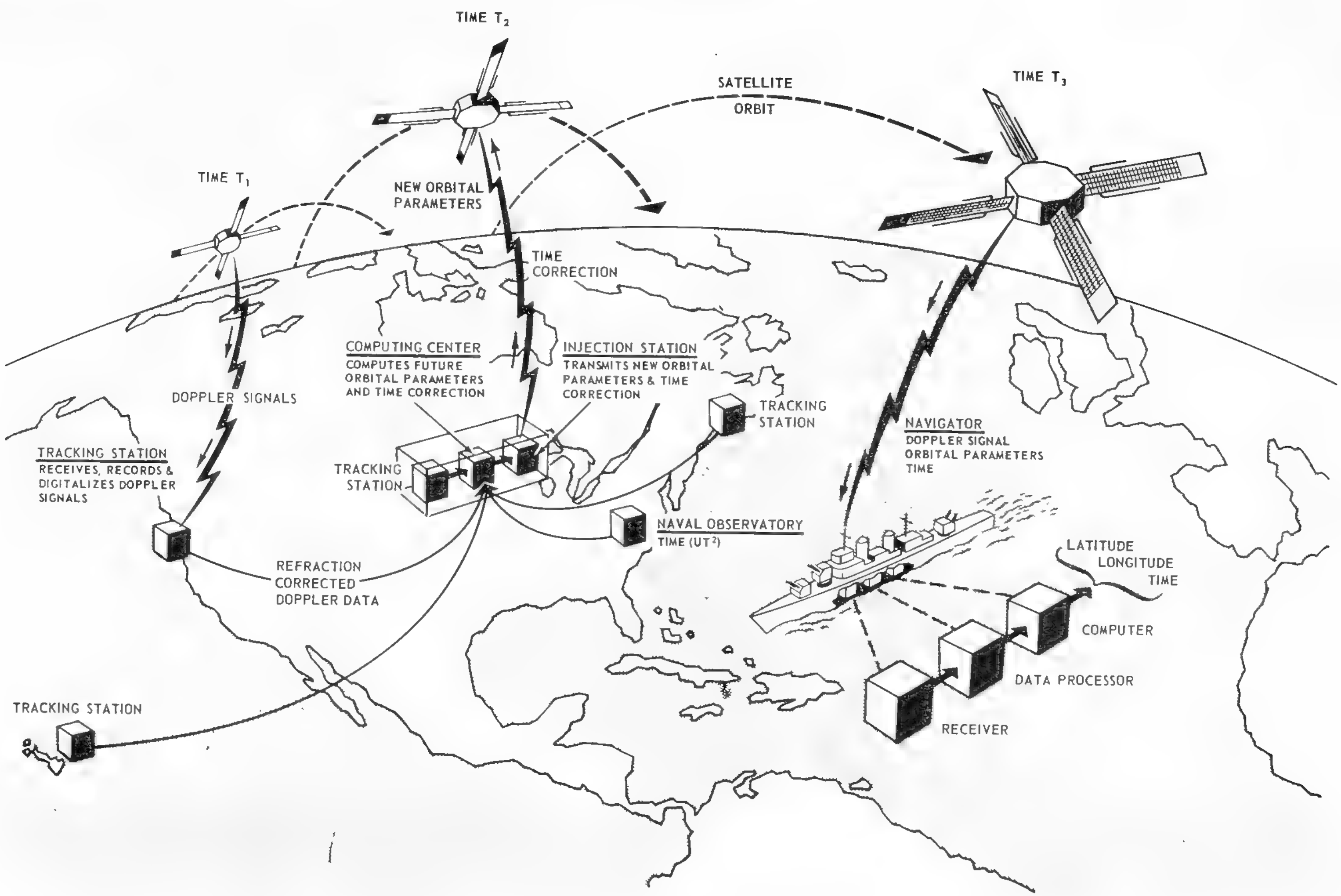

Figure 12

8. Conclusion

In conclusion, it may be stated that the TRANSIT program not only will provide a very useful practical application of earth satellites to the solution of a serious terrestrial problem (navigation) but in the course of its development is making many important contributions to space technology and earth sciences.

INFLUENCE OF A HIGH HYDROSTATIC PRESSURE ENVIRONMENT ON ELECTRONIC COMPONENTS

by CHESTER L. BUCHANAN, Branch Head
and MATTHEW FLATO, Electronics Section Head
Sonar Systems Branch, Sound Division
U.S. Naval Research Laboratory
Washington, D.C.

ABSTRACT

The rapidly expanding field of Oceanographic Instrumentation portends a large increase in the use of electronic instrumentation in various forms of deep ocean probes. One part of the oceanology program at USNRL is directed toward the development of such instruments.

Two approaches toward this development are available: The equipment can be sealed in rigid pressure-proof capsules with pressure-proof seals, or the equipment can be made of components which are inherently capable of operating satisfactorily under the environmental pressure. The latter approach is attractive because of the probable savings in weight and cost. To this end, a series of commonly used electronic components have been tested in an oil bath under hydrostatic pressures up to 10,000 psig. Components of each type tested have been found which will operate satisfactorily at all pressures up to 10,000 psig. Diodes, transistors and even vacuum tubes have been found which operate at this high pressure. Entire circuits capable of operation under 10,000 psig have been built from readily available components.

INTRODUCTION

It is a certainty that the rising tempo in Oceanographic Research will require an increase in the use of electronic instrumentation with various forms of deep sea probes. Instruments designed for deep submergence must be constructed to withstand the pressure experienced at great depths. One part of the oceanographic instrumentation program at the U. S. Naval Research Laboratory is directed toward the development of packages for instruments whose electronic components are exposed to hydrostatic environments equivalent to more than four miles submergence in the ocean. The initial phase of this study was exploratory; the objective was two-fold, to gain familiarity with techniques for testing components under high hydrostatic pressure and to determine the magnitude of the difficulties to be expected while operating equipment under such conditions. Initially several approaches are available: the equipment can be constructed of components which are inherently capable of operating satisfactorily under the environmental pressure, or the equipment can be encapsulated in plastic which fully protects the components. As an example of the results to be expected from the first mentioned approach, the "velocimeter", in which electronic circuit components weigh less than four ounces, requires a housing that weighs 25 pounds to protect the components at a pressure of 10,000 psi. This high package to circuit weight ratio is typical of that to be expected from this practice. The probable saving in weight and cost, which can be expected from the latter two approaches, makes the further study of these techniques attractive.

Several classes of electronic components have been tested in laboratory tanks (Figures 1 and 2) which were designed to apply high hydrostatic pressure.

RESISTORS

The first class of components tested was resistors. How the various types reacted under hydrostatic pressure may be compared in Figure 2. The resistance of those manufactured by depositing either carbon film or tin oxide on glass rods was not changed by the application of pressure; the behavior of these two types of resistors strongly suggests their use in critical circuits.

The standard carbon composition resistors were found to change very radically with the application of pressure. Figure 3 summarizes the behavior of 100 to 10,000,000-ohm resistors under the same hydrostatic pressure environments (10,000 psig). Because of their marked sensitivity to pressure change, composition carbon resistors appeared attractive for use as pressure transducers.

CAPACITORS

A number of capacitors (molded mica, ceramic disk, glass, and paper) have undergone tests to 10,000 psig. All of these capacitors worked satisfactorily under the high pressure and suffered no damage. The molded mica and glass types showed no appreciable change in capacitance with varying pressure. Some ceramic types showed changes in capacitance of as much as two per cent but no effort was made to test all the types now available. Paper capacitors selected were mainly of the miniature types, in which size reduction had been accomplished by such methods as depositing the conductor directly on the dielectric. These miniature capacitors also are usually impregnated with wax and carefully treated to exclude all air bubbles. Surprisingly enough, these miniature types withstood the pressure and showed very little change in capacitance. Changes in the range of 1% were common with this type of capacitor.

Capacitors sealed with air entrapped were not satisfactory for use under hydrostatic pressure; an example of such a capacitor is shown in Figure 5. Electrolytic capacitors frequently contain a considerable amount of void space and consequently collapse at a relatively low pressure. These units usually are operable at reduced voltages even after collapse. Some types of paper capacitors are inserted into a paper tube and sealed by pouring wax or plastic compound into the end of the tube. Such capacitors usually contain entrapped air and collapse at a relatively low pressure.

There appears to be no problem at this time in selecting capacitors to meet the common electronic circuit requirements and to operate under hydrostatic pressures up to 10,000 psig.

MAGNETIC MATERIALS

Measurements of various magnetic materials were conducted by subjecting coils wound on various types of magnetic cores to hydrostatic pressures as high as 10,000 psig and measuring the inductance as the pressure was varied. The magnetic materials tested were some of those commonly used in electronic circuits for instruments of various types. The materials tested were:

1. Grain oriented silicon steel
2. 75% nickel-iron
3. 50% nickel-iron
4. Powdered iron (high-frequency formulation)
5. Powdered iron (low-frequency formulation)
6. Powdered iron (medium frequency formulation)
7. Molybdenum-nickel-iron dust core
8. Ferrite core.

The grain-oriented silicon core was of the split-rectangle type, while all other cores were torodial and approximately 1 inch in outside diameter. In all measurements the frequency was 1000 cps.

The most dramatic change observed was in the 50% nickel-iron core of the grain-oriented square-loop type. This core nearly doubled in inductance at a very low pressure as shown in Figure 4. It is interesting to note that after the change occurred, further changes in pressure had very little effect on the inductance. Changes observed in the other types were less dramatic, but the grain-oriented silicon core was interesting in that it was the only type tested which exhibited a large decrease in inductance as the pressure increased. The total change observed was about 14% (negative), but the residual effect was a slight positive inductance change. The molybdenum-nickel-iron cores exhibited a change of about the same amount but in the opposite direction.

Inductors using the powdered iron and the 75% nickel-iron cores were found to exhibit inductance changes of less than 5% as the hydrostatic pressure was cycled between atmospheric pressure and 10,000 psig, as shown in Figure 5. The inductors wound on the powdered iron cores showed an increase in inductance with increased pressure. The percentage increase was proportional to the amount of iron in the core and inversely proportional to the frequency range in which the core was designed to be operated. The inductance of the coil wound on the 75 per cent nickel-iron core did not change significantly as the pressure was increased to 8000 psig. This coil also showed some permanent effects and a very small change in inductance as the pressure was increased from 8000 psig to 10, 000 psig.

A "flux-gate" type magnetometer was tested under pressure with some rather peculiar results. It should be noted that whereas the toroidal cores for the previous test were essentially free from external magnetic effects, the "flux-gate" element was readily susceptible to external magnetic field changes. Tests with the "flux-gate" element in the tank showed that a considerable change occurred as the pressure was increased. Similar changes were noted with the "flux-gate" element taped to the outside of the tank wall as the pressure was increased inside the tank. These results appear to indicate that considerable changes in the magnetic condition of the tank occur as the pressure in the tank is varied.

GLASS TUBES AND ENVELOPES

Various types of glass tubes and envelopes were subjected to high hydrostatic pressures. A type 6AL5 miniature tube (Figure 8) was tested and observed to fail by catastrophic implosion at about 2000 psig. Some subminiature types (Figure 9), however, were found to withstand the full 10,000 psig without mechanical or electrical failure.

Penlight bulbs, instrument bulbs, and small commercial neon bulbs were tested and a high percentage of these were found capable of withstanding the full 10, 000 psig without mechanical or electrical failure. Several dozens of the penlight bulbs were tested, and there were a few failures in each test group. Failure sometimes occurred by implosion and sometimes by oil leaks through the seal. Penlight bulbs which did not fail were set aside for use in illuminating samples under test.

The pressure vessel (Figure 1) used in these experiments has been fitted with an optical viewing port (Figure 10), a and b. Illumination from a number of penlight bulbs is directed on the object to be viewed within the tank, permitting observation of mechanical deformation of samples under pressure. A picture taken through the pressure window with illumination from these penlight bulbs is shown in Figure 11. Power to operate the bulbs is derived from a nickel-cadmium cell (Figure 12). The vent of the cell was removed, and a rubber tube partially filled with electrolyte was installed for pressure equalization purposes. This cell was tested under a heavy-duty charge-discharge cycle both at 0 psig and 10, 000 psig with no significant difference in performance noted. While discussing the pressure tank, it should be mentioned that all the measurements are made with the tank filled with paraffin oil. Electrical leads are brought out the cover through pressure glands. Glass tubing of various diameters was tested by sealing both ends of short lengths of tubing and then subjecting the samples to high pressure. The seals consisted of surgical rubber tubing fitted over the glass tubing. The opposite ends of the rubber tubes were blocked with small solid cylinders of the same diameter as the glass tubes (see Figure 4). When the hydrostatic pressure increases, the rubber seals are squeezed tighter around the glass tube and the solid cylinder. Glass tubes with a wall thickness of 0. 039 in. and an outside diameter of as great as 0. 355 in. successfully withstood 10,000 psig. It should be observed that glass has a compressive strength comparable to that of some steels.

These results indicate that where the need arises some components in glass envelopes may be used in a high-pressure environment.

SEMICONDUCTORS

Many semiconductor devices (diodes, tunnel diodes, rectifiers, and transistors) were tested under hydrostatic pressures to 10, 000 psig. It is common practice to seal the active transistor element in a metal case filled with some inert material to prevent contamination of the transistor and subsequent change in characteristics, if not complete failure. Transistor cases are not constructed to withstand the high pressure involved in this study, so most of the transistors failed the test. A few of the very small elements did withstand 10,000 psig successfully, but most of the cases collapsed (Figure 14). Also, some early transistor types which were potted in an epoxy resin were able to operate satisfactorily under hydrostatic pressures of 10,000 psig. Most types of small transistors can be potted in plastic resins (either with their circuit, or separately) and made to withstand the high pressure. Several transistors of the type which failed because the case crushed were further tested after piercing the case with a sharp pointed tool and allowing it to fill with the paraffin oil in which it was submerged. In general, these transistors were able to perform normally while under pressure, and for the short duration of the tests no contamination effects could have been expected.

Several manufacturers are beginning to construct semiconductors with passivated surfaces, so they can be immersed in fluids or potted in resins without fear of contamination. In addition, since they are very small, no case is needed. Several transistors and diodes of this type were tested and found to operate well under great hydrostatic pressure. One interesting type consisted of a silicon rectifier only 0.04 in. in diameter and 0.019 in. thick. Its conduction characteristics are shown in Figure 7. As can be seen, performance under high pressure was slightly improved over that under normal pressure.

The results of these tests indicate that the semiconducting materials themselves are immune to the effects of pressure, at least for the short test periods used in this study. The passivated transistors now becoming available will serve very well under pressure. Where cased types must be used, it appears that standard potting compounds can provide sufficient protection to permit operation up to 10,000 psig for at least short time periods.

POTTING AND PACKAGING

Several tests were devised to measure the amount of protection afforded by potting methods and materials. One such test measured the degree in which the pressure was transmitted to the component under test. Since the resistance of composition carbon type resistors is nearly linear with pressure, resistors were used as sensors for these measurements. Comparison of resistance of resistors, before and after encapsulation, resulted in a relative measure of the pressure transmitted. It was found that with most plastics the pressure is transmitted directly to the resistor without any appreciable loss. To overcome this problem, epoxies of different types were molded over resistors, previously coated with a spongy type of silicone rubber. Figure 8 shows that the two types of epoxies used over the silicone rubber had widely different capabilities in resisting transmission of pressure to the component.

Components, such as transistors and capacitors which have internal cavities or voids, were found to be damaged when placed under pressure. A test was devised to determine the thickness of potting material necessary to protect such components. Figure 9 shows four very thin-walled, 1/2-inch diameter, sealed aluminum tubes cast into a block. The four specimens were separated from the surface of the plastic block in increments of 1/32 of an inch, starting with 1/32-inch. The two closest to the surface imploded at about 2500 psig, while the other two successfully withstood the full 10,000 psig. This result illustrates the ability of the plastic casting to lend rigidity to embedded components and to prevent crushing. The end of the test block containing the two tubes which were not crushed in the original pressure test were placed in the small pressure tank illustrated in Figure 18 and were maintained continuously under high pressure to determine whether "cold flow" of the plastic material will eventually permit collapse of the tubes.

Several types of transistors and capacitors which, when unprotected, had failed under pressure have been potted and used successfully in electronic circuits which were directly under the influence of hydrostatic pressure. Figure 19 is the electronic circuitry for a velocity meter which was operated satisfactorily in an oil bath for a period of forty hours at 10,000 psig without failure.

Another approach to this problem is the encapsulation of the entire circuit as a single unit. A complete three-stage transistor amplifier, Figure 20, was encapsulated in an epoxy-type resin and subjected to a hydrostatic pressure of 10,000 psig for several days. The thickness of the plastic over the components was less than 1/16-inch at some points. The circuit operated normally in spite of the fact that it contained many components which, in their original casing, would not have been capable of operating under hydrostatic pressure.

The use of fillers, such as small glass spheres, may permit construction of complete electronic circuits which will float. Figure 21 shows a 25-gram test block, containing a "payload" of resistors weighing 5-grams, floating in fresh water. Illustrated in Figure 22 is an encapsulated circuit of the velocimeter, similar to that used in Figure 19. The entire unit can be constructed so that its specific gravity is at least 1. 1. The actual weight of the electronic circuit components in this instrument is only four ounces. By using the standard technique of enclosing the electronic circuits in a pressure-proof metal housing, the total instrument weight is increased by about 25 pounds. The saving in weight and size which may be achieved by the development of instruments which can operate without pressure cases is obvious.

To date, the results indicate that it is feasible to operate virtually every type of component required in electronic circuits under hydrostatic pressures up to 10, 000 psig, at least for short periods of time. It appears further that circuits can be constructed of lightweight materials and encapsulated in filled resins to obtain operating units which are lighter than water. Such techniques may well become mandatory in construction of complicated oceanographic or acoustic instrumentation systems.

FIGURE CAPTIONS

Fig. 1 Small pressure tank with electrical feed-through and optical viewing port closures

Fig. 2 Large pressure tank (4 ft diameter, 8000 psi) showing screw plug and inner plug

Fig. 3 Resistance as a function of pressure

Fig. 4 Pressure sensitivity of carbon composition resistors

Fig. 5 Typical failure of capacitor containing void spaces

Fig. 6 Inductance changes in three types of cores under pressure

Fig. 7 Inductance changes in five types of cores under pressure

Fig. 8 Response of a type 6AL5 vacuum tube to hydrostatic pressure (about 2000 psig)

Fig. 9 Subminiature vacuum tubes subjected to 10,000 psig without mechanical or electrical failure

Fig. 10 a. and b. Inside (a) and outside (b) views of optical port for observing objects under test in hydrostatic pressure tank

Fig. 11 Transistor under test at 10,000 psig as seen through optical viewing port

Fig. 12 Nickel cadmium battery with pressure equalization

Fig. 13 Glass tubing of various diameter was sealed as illustrated, then subjected to high hydrostatic pressures

Fig. 14 Semiconductors subjected to hydrostatic pressure tests (10,000 psig, paraffin oil bath)

Fig. 15 Conduction characteristics of a "passivated" diode under 0 psig and 10,000 psig

Fig. 16 Resistance of transmission of pressure to a component for two types of epoxies

Fig. 17 Aluminum tube test block

Fig. 18 Pressure tank for long-term test of electronic components

Figure Captions continued

Fig. 19 Velocimeter circuit which operated in oil bath at 10,000 psig

Fig. 20 Encapsulated amplifier

Fig. 21 Floating test block with a total weight of 25 grams and with a "payload" (resistors) of 5 grams

Fig. 22 Encapsulated velocimeter circuit

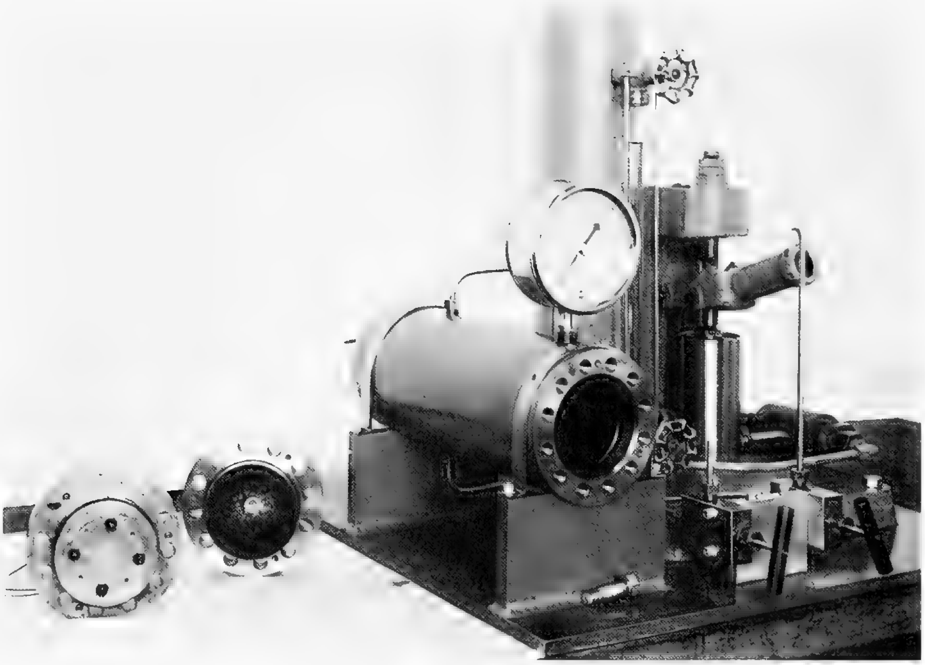

Figure 1

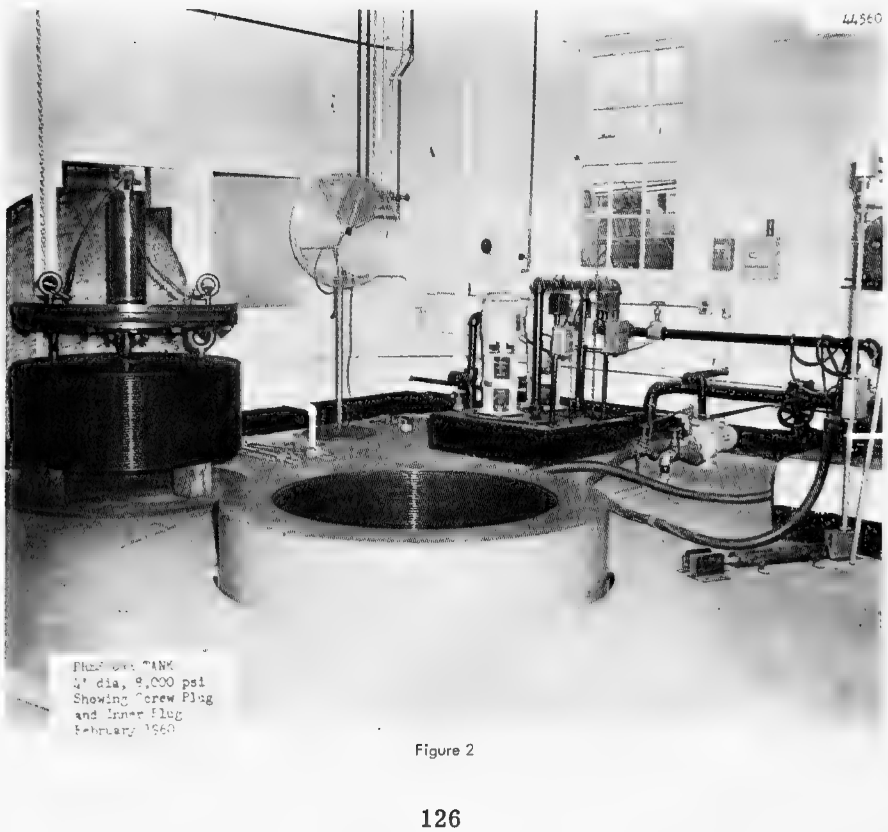

Figure 2

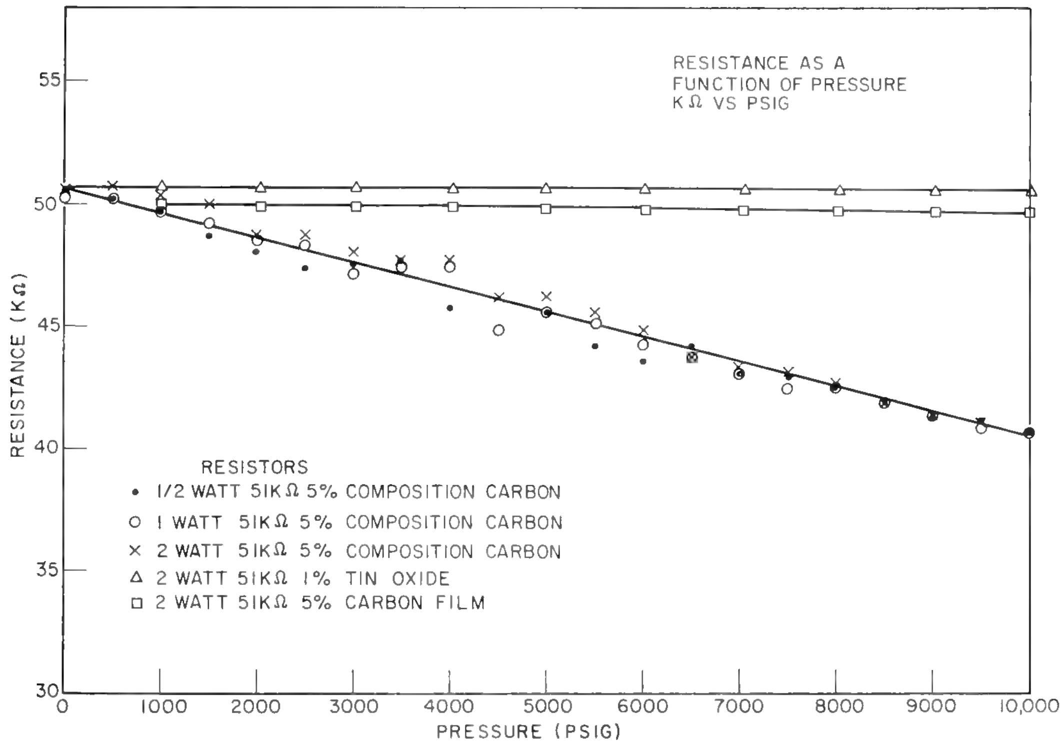

Figure 3

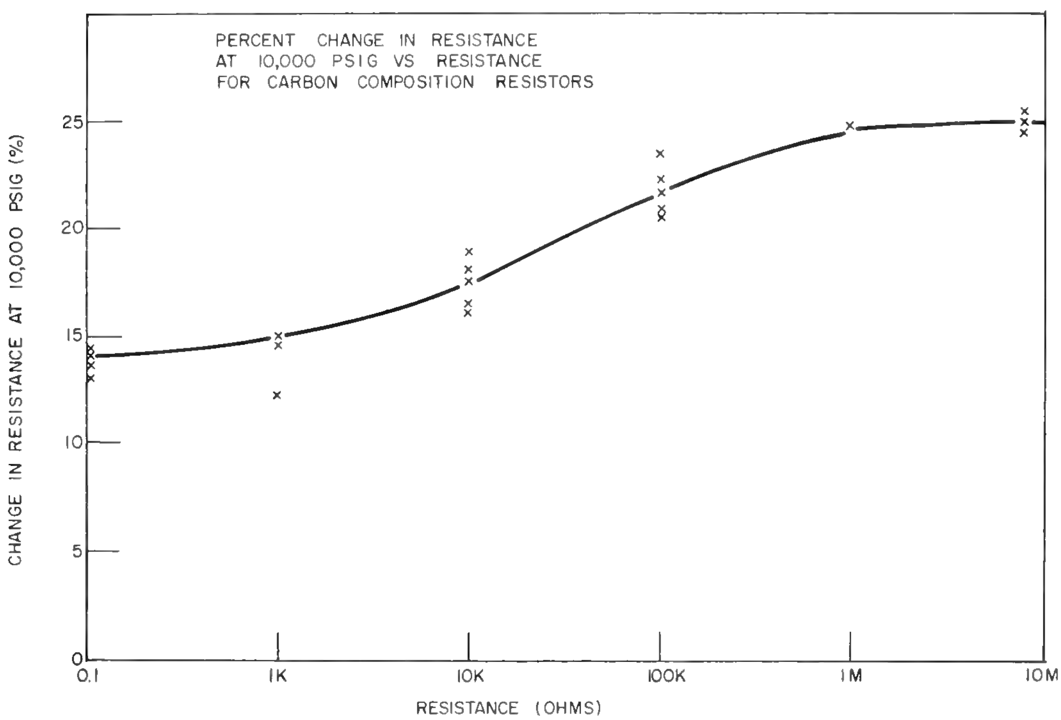

Figure 4

Figure 5

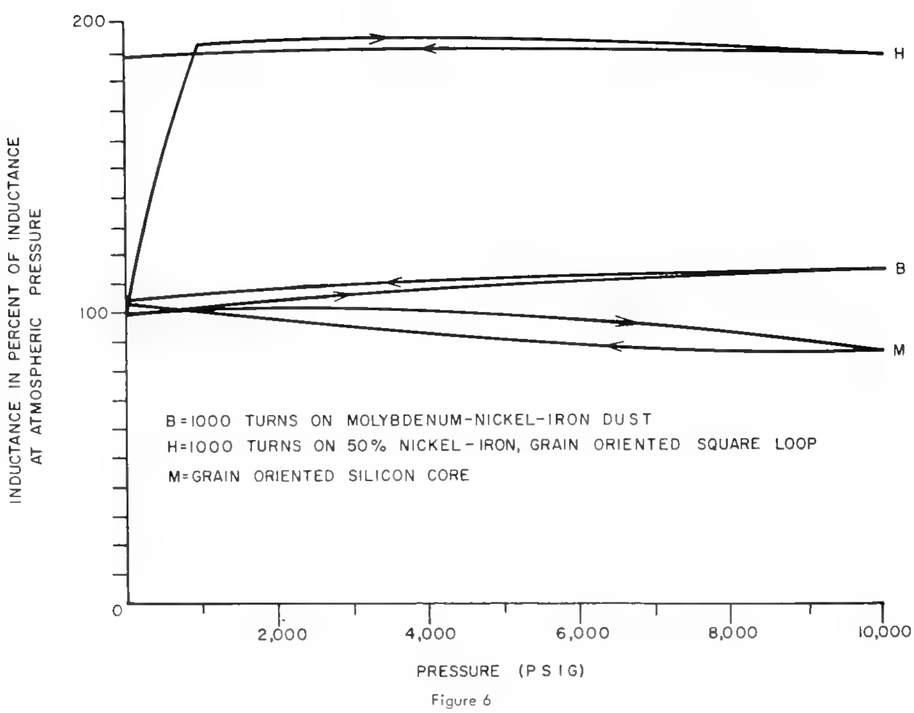

Figure 6

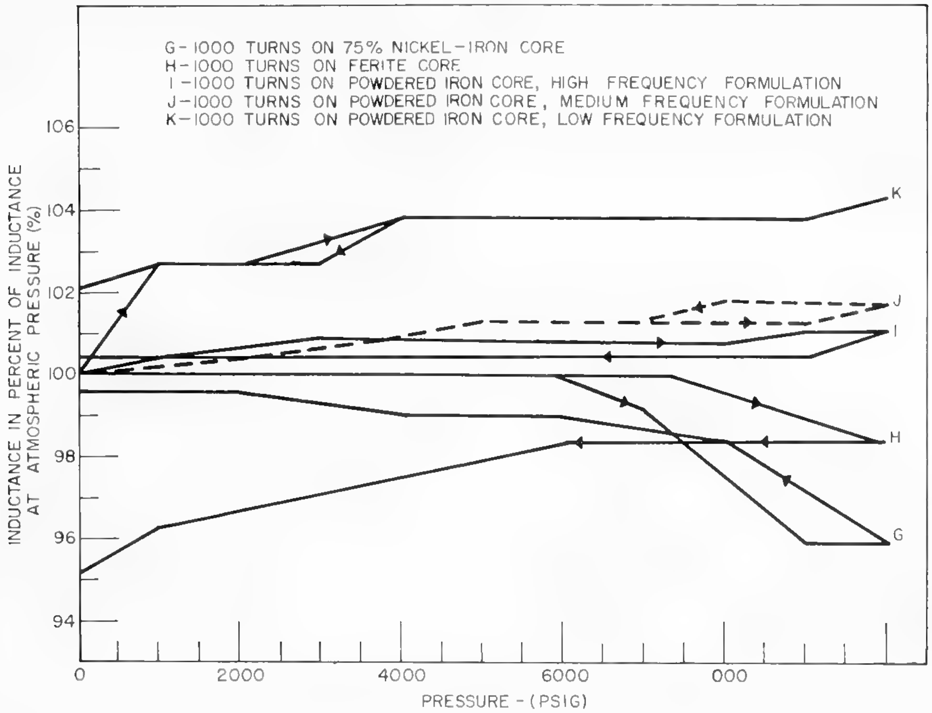

Figure 7

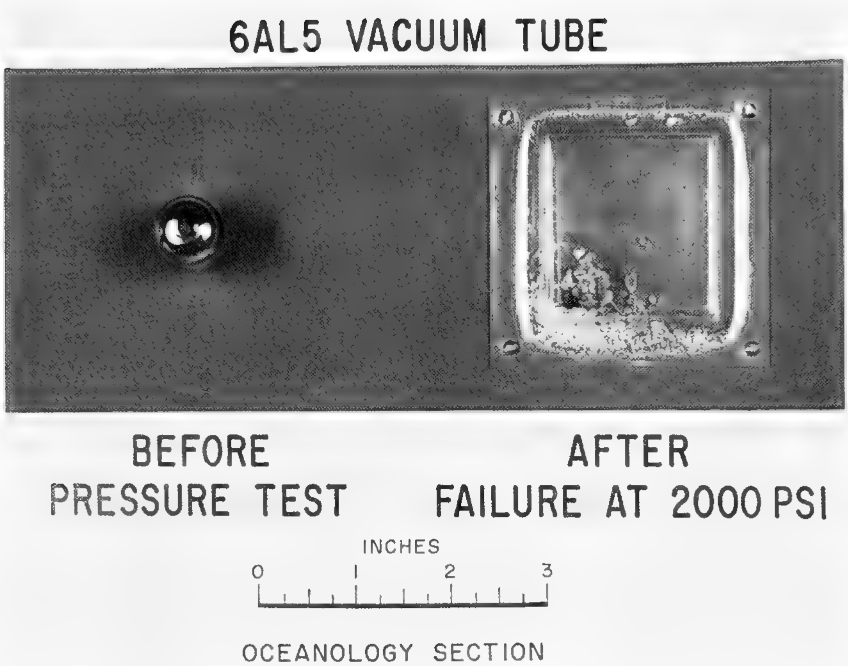

Figure 8

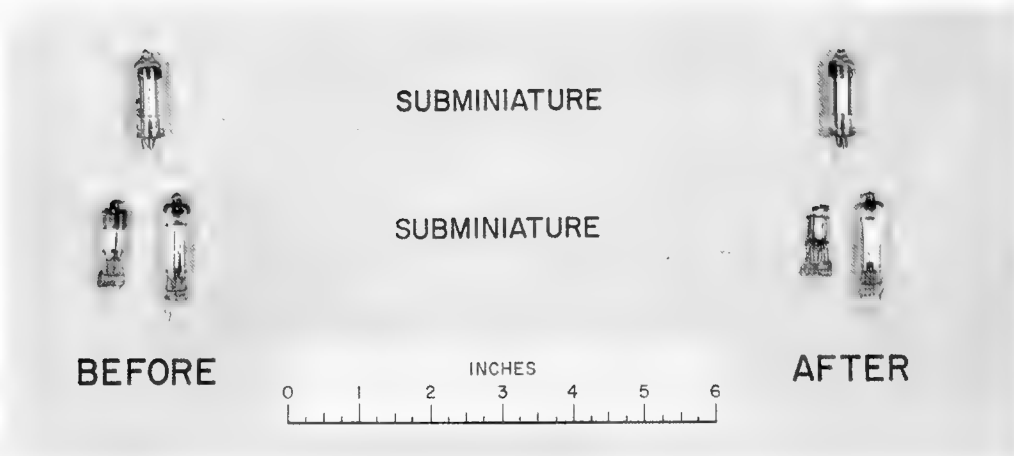

Figure 9

Figure 10 (a)

Figure 10 (b)

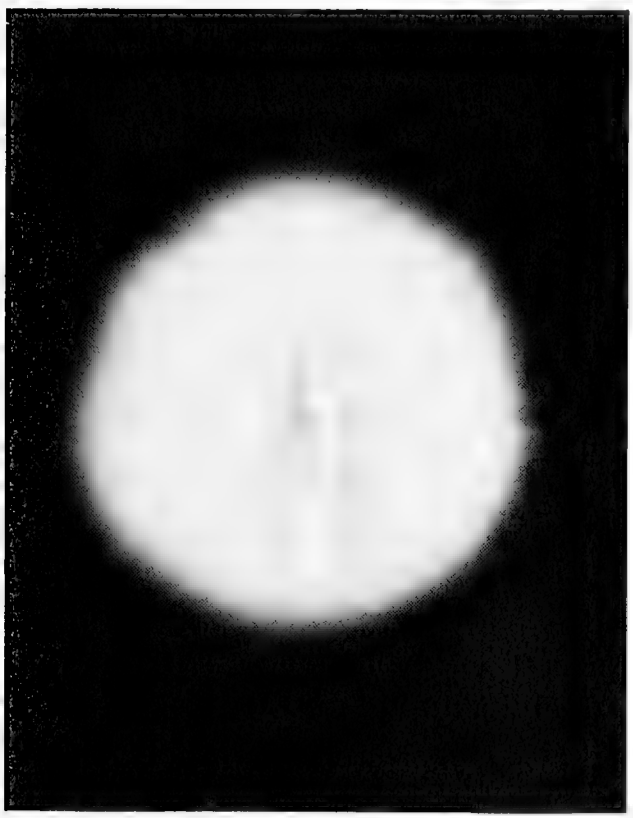

Figure 11

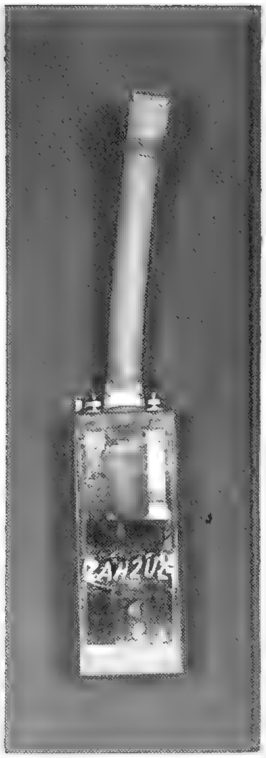

ADMIUM BATTER
ESSURE EQUALIZATIO
CHARGE AND DISCHARGE
OPERATIONS NORMA'

Figure 12

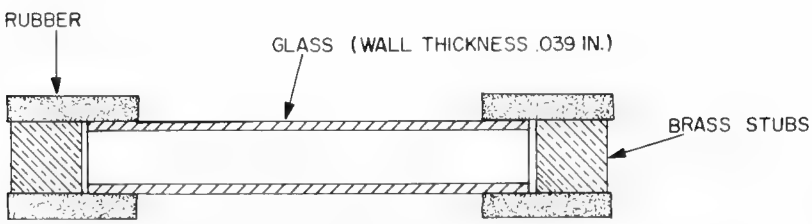

GLASS TUBES WHICH WITHSTOOD HYDROSTATIC PRESSURE OF 10,000 PSIG

O.D	LENGTH
.23 IN.	2.13 IN.
.27 IN.	2.43 IN.
.35 IN.	2.50 IN.

Figure 13

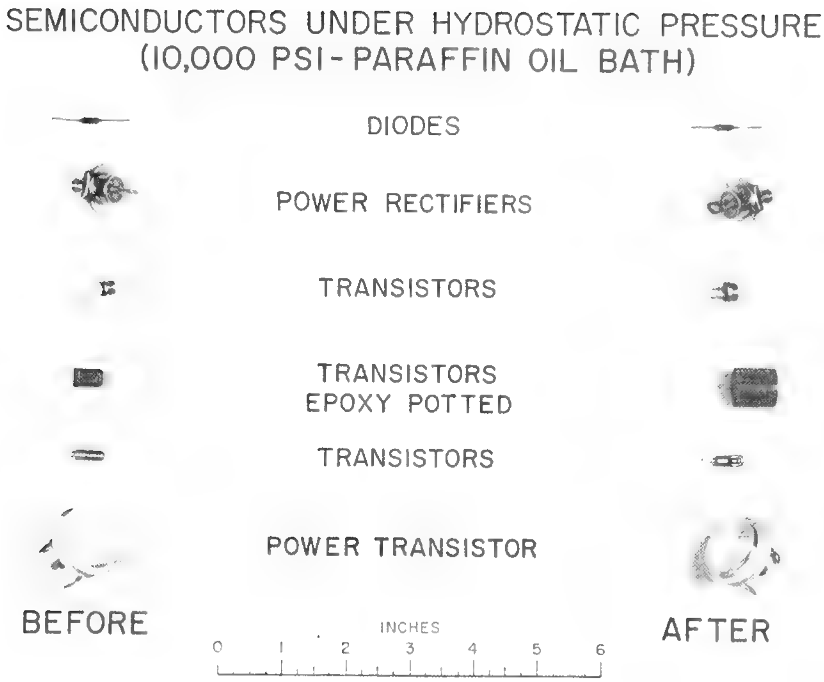

Figure 14

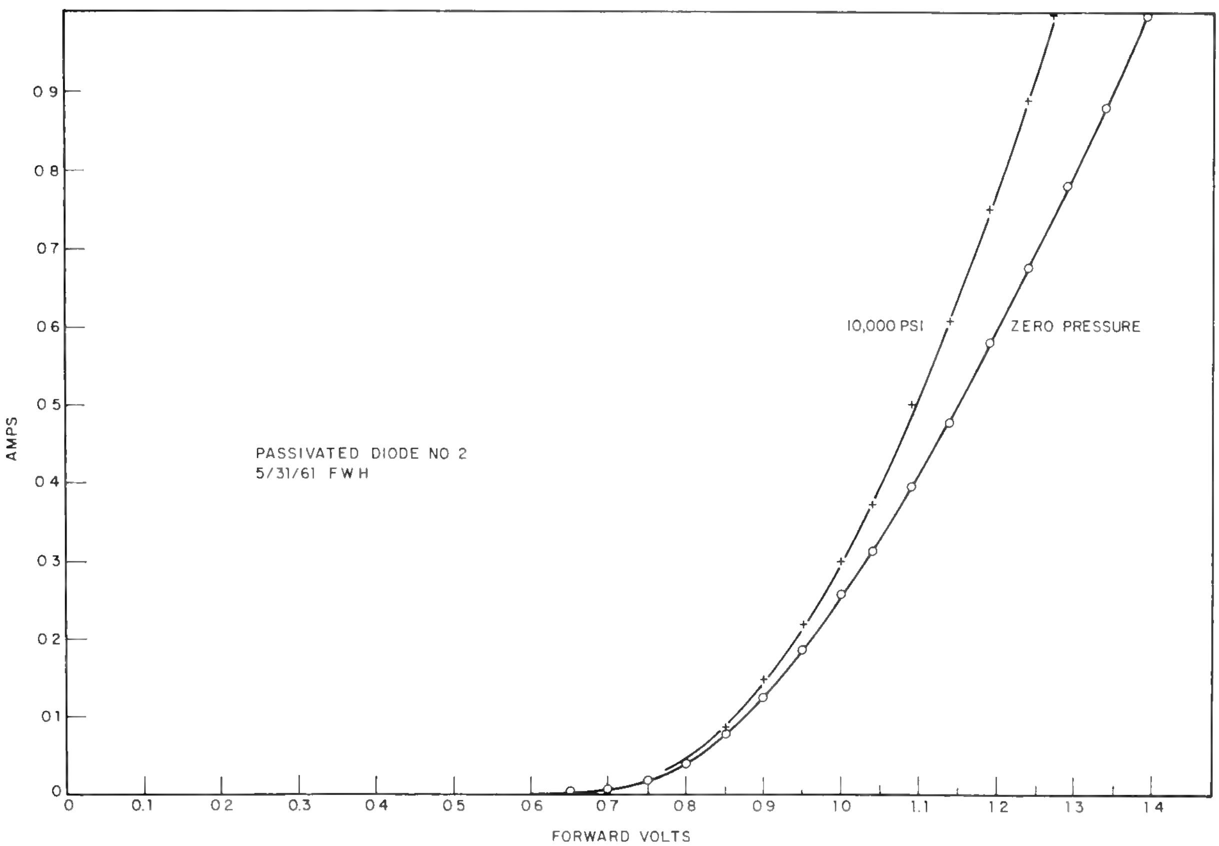

Figure 15

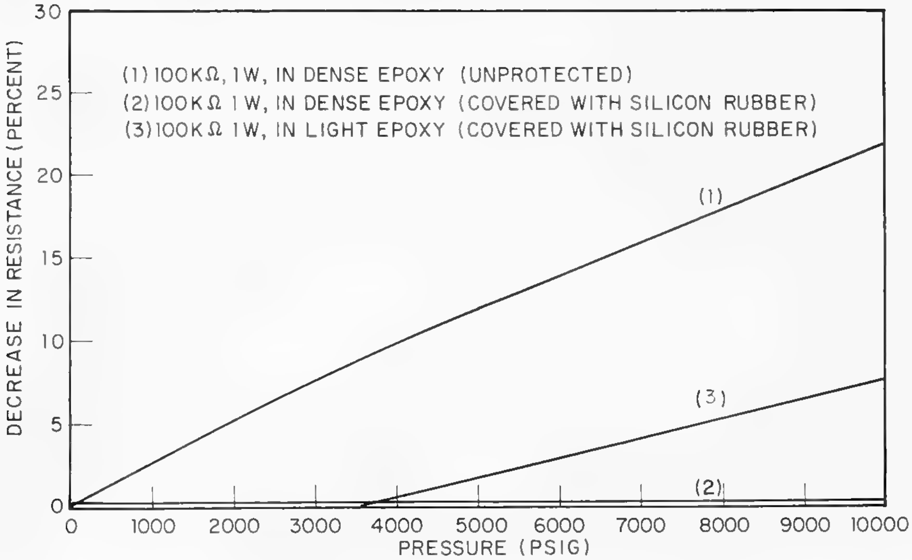

Figure 16

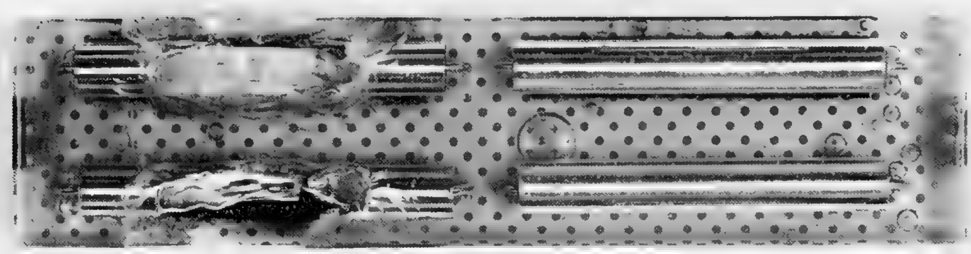

Figure 17

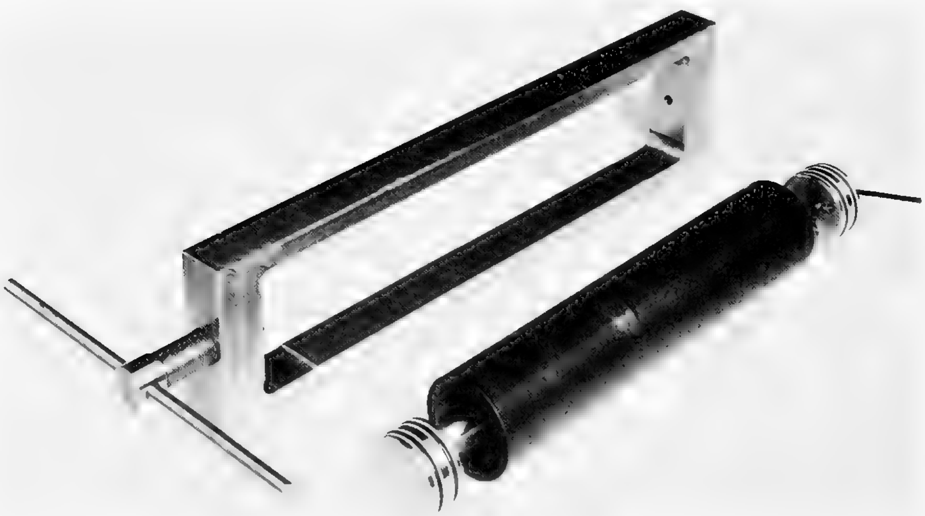

Figure 18

Figure 19

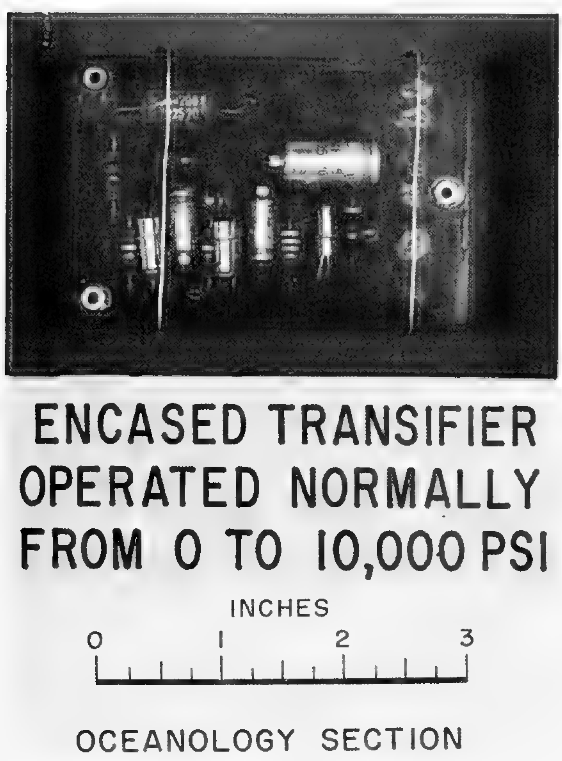

Figure 20

Figure 21

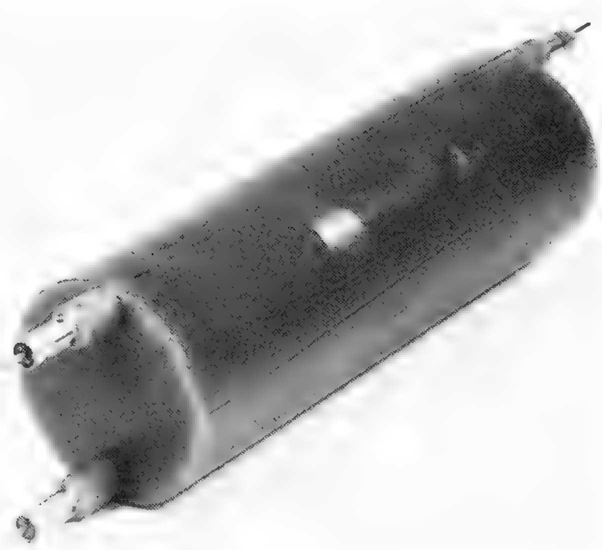

Figure 22

INTERNAL WAVES AND THEIR MEASUREMENT

by E. C. LaFOND, Head, Marine Environment Studies Branch
U.S. Navy Electronics Center
San Diego, California

INTRODUCTION

Internal waves are undulating swells occurring between subsurface water layers of varying density, even though the density change be slight. By contrast, in a homogeneous fluid only surfaces waves are possible, and the amplitude of their motion decreases with depth. In the ocean, vertical density gradients are virtually always present. Thus internal waves are found in all oceans and probably most bays and lakes, and vary widely in amplitude, period, and depth. Although their amplitudes may exceed those of surface waves, internal waves are usually slower in speed.

In a simple, two-layer density system, maximum amplitude exists at the boundary of the two layers and decreases linearly with distance above and below.[1] In a multiple-layer or continuous-density gradient system, as in the sea, the wave motions become much more complex. Under these conditions multiple wave patterns, having different characteristics, have been observed at different levels.

CAUSE OF INTERNAL WAVES

The exact causes of specific internal waves have not yet been firmly established, but they are probably of varied origins. Experiments in the Norwegian fjords[2] showed that a slow-moving sailboat initiated internal waves at the shallow-layer boundary of nearly fresh water and higher-density sea water. The internal waves, produced by the keel of the slow-moving ship, reduced its speed and created the phenomenon known as "dead water".

Since internal waves are commonly found at water mass boundaries or "fronts," they are probably produced through direct displacement of one water mass by another. The front is characterized by a group of relatively large internal waves followed by a change in the depth of the thermocline (fig. 1). Visual evidence of internal waves forming at water mass boundaries has been shown in high-altitude photography[3] of slick-type surface phenomena in Georgia Strait,* where such occurrences were attributed to large-scale discharge of water of varying density (fig. 2). Masses of fresh water created a tidal front, or zone of convergence and divergence, in which internal waves developed. Internal waves, coincident with tidal periods whether semidiurnal or diurnal, were commonly observed; thus, it was concluded, tidal forces must be instrumental in generating them.[4,5]

Certain internal waves may be created by two adjacent flows or by a flow impinging on a continental shelf or other obstruction. Experiments[6] that showed internal waves to occur when a tidal stream flowed against a coastal bank have been conducted. It was further proven that obstacles in the path of an advancing wave give rise to internal waves.[7] The significant fact is that vertical oscillations in the thermal and density structure of sea, which are termed internal waves, are apparently present in all oceans and at all depths. This indicates that their cause is likewise universal.

MEASUREMENT EQUIPMENT AND TECHNIQUES

Internal waves can be present only in water where a vertical density gradient exists. The vertical gradient may be caused either by temperature or salinity, or both. In fresh-water lakes, measurements of temperature alone are sufficient to establish the existence of density gradients. In the sea, measurements are commonly of temperature since they are easily accomplished, and the temperature and salinity gradients usually coincide. In addition, the salinity gradients are normally small.

On one occasion, however, internal waves were directly measured by their vertical oscillations of density. A large, buoyant container[8] was floated on a given density boundary and its depth recorded. A drum, filled with glass balls, was guided vertically by a cable. A recording manometer on the drum successfully furnished a 7-day record of the depth when it was weighted sufficiently to float on the maximum density gradient found in the southern Kattegat** in summer.

Various instruments have been employed to measure vertical oscillation of temperature

*The channel between Vancouver Island and southwest British Columbia.

**An arm of the North Sea, between Sweden and Denmark.

"Superior numbers refer to similarly numbered references at the end of this paper.

(sometimes simultaneously with salinity). For long-period waves, reversing thermometers and water bottles were used. Repeated bathythermograph lowerings were made, and more recently the fast-responding thermistor beads have been utilized.

THERMISTOR BEADS

The most common method of measuring sea temperatures at the present time is with fast-responding thermistor beads. These come in various types; the most common is a small, glass-encapsulated, high-thermal-resistant material with connecting leads. A current passing through the beads is greatly influenced by temperature. Thus the temperature of the sea water is proportional to the electrical current.

Since the beads are not precisely matched, resistance-wise, to each other, and temperature-resistance relations are not exactly linear, several schemes have been devised to increase accuracy by using compensating resistors in with the bead or by amplifying short stretches of the most linear part of the resistance-temperature curve. Another problem is their fragility and the watertight integrity between the glass beads and electrical connections (fig. 3).

One effective thermistor device to determine sea temperatures and identify internal waves is the 16-channel temperature-sensing unit developed by the U. S. Navy Electronics Laboratory (NEL).[9] It includes 16 thermistor beads cast in plastic and attached to electric leads. The leads and beads are part of a bridge circuit that feeds a recording-type potentiometer. The recorder prints numbered points consecutively from 1 to 16 on a power-driven strip chart, the location of each number indicating a particular temperature. In normal operation, a full cycle of 16 recordings requires approximately half a minute (fig. 4). The temperature at each depth is indicated on the chart to an accuracy of better than 0.02°F.

The beads are suspended in one or more vertical series from a ship, anchored buoy, or fixed platform (fig. 5). Temperature can thus be recorded at up to 16 depths for any desired period of time. However, to determine the character of internal waves, the depth of the isotherms must be scaled from the measured temperatures at fixed depths.

THERMISTOR CHAIN

Strings of thermistor beads may be towed from a ship and their sensing elements scanned electronically. This procedure allows the isotherms to be identified and printed directly[10] with reference to time or distance.

NEL thermistor chain, from which are suspended the strings of thermistor beads, makes it possible to sense vertical sections of temperature structure from the surface down to 800 feet when the ocean-going NEL research vessel USS MARYSVILLE cruises in waters of greater depth (fig. 6).

The thermistor chain, together with the drum on which it is wound, is large and rugged, weighing 37,500 pounds. The chain is composed of large, flat links about a foot long, 9 inches wide, and an inch thick. At its end is a 2300-pound, streamlined torpedo-shaped weight to hold it down. The weight and its connected chain are lowered from the stern as the oceanographic vessel proceeds through the water.

About 80 pairs of insulated wires fit through grooves inside the flat links. Every 27 feet the wires connect with the thermistor beads, which sense the sea temperature.

The upper ends of the electrical leads connect to a recorder located in the vessel's laboratory. Signals from the beads are scanned electronically every 10 seconds, and lines showing the depths of constant temperatures are printed on 19-inch-wide tape. This is equivalent to taking a bathythermograph lowering every 100 feet if the ship proceeds at 6 knots. Recorded on the same tape are the depth of the weight (or maximum depth of observation) at the end of the chain and, in addition, the sea surface temperature (the uppermost bead in the chain). This instrument thus gives essentially a two-dimensional picture of oceanic thermal structure and internal waves from the surface to 800 feet.

ISOTHERM FOLLOWER

Another device for directly measuring the temperature of internal waves is the isotherm follower[11], which automatically traces isothermal vertical oscillations with reference to time. This instrument is comprised of (1) a sea sensing unit; (2) an electric winch containing a cable to which the sea sensing unit is attached; (3) electronic components (servomechanism, amplifiers, power supply, controls, etc.); and (4) two recorders (depths and temperature) (fig. 7).

The sea sensing unit contains a thermistor bead balanced in a bridge circuit with a resistance corresponding to the desired isothermal temperature. If the bridge becomes unbalanced, a thyratron tube is fired. This activates a winch and causes it either to wind in or let out the sea unit, "locking it" onto the desired isotherm. The isotherm depth is continuously recorded on the ship by means of a pressure sensor in the sea unit. The net result is a trace of the given isotherm depth, effective to 600 feet, with reference to time.

The isotherm followers have been employed singly, or in triangular arrangements of three, to acquire the speed and direction of internal waves[12] by time of arrival and phase shifts[13]. Virtually continuous operations throughout the summer months up to periods of one week have been successfully conducted from the NEL Oceanographic Research Tower. Here they are suspended from the structure by 40-foot booms (fig. 8).

TOWED ISOTHERM FOLLOWER

A modification of the isotherm follower is a recently developed towed version. The principle is the same -- the follower seeks out a selected isotherm and traces it as the sea unit is towed from a ship.

The sea unit is a torpedo-shaped device with fins (fig. 9) that are moved up or down by its small motor which, like the winch, is directed by a signal from a thermistor bead in the nose of the sea unit. The instrument thus follows the isotherm up and down as its depth by pressure is recorded on the towing ship.

The towed isotherm follower is generally used in shallow water (where the thermistor chain cannot be towed) to determine the nature of internal waves as they cross the continental shelf and eventually impinge on the bottom.

NATURE OF INTERNAL WAVES

CHARACTERISTICS

Internal waves have been measured in all oceans and in several lakes throughout the world. Off southern California in summer, the vertical oscillations of the temperature structure were measured by use of thermistor beads suspended vertically at a depth of 50 feet,[9] later by isotherm followers at a depth of 60 feet,[13] by the NEL thermistor chain in the San Diego Trough,[14] and in the deep, open sea. In the next sections are described the characteristics of internal waves that were determined in these experiments.

WAVE HEIGHT

The depth of a single isotherm in the thermocline was observed to fluctuate widely during one day in water only 60 feet deep. A day's record of smaller internal waves in the thermocline, as recorded by the isotherm follower, is shown in figure 10. The short-period vertical oscillations are superimposed on the longer period tidal oscillations in the thermocline. Generally, the magnitude of the small vertical fluctuations was inversely proportional to the gradients through which they protruded. Small fluctuations were nearly always present.

Long periods of continuous isotherm or thermocline depth measurements have been recorded. It was found that a frequency plot of thermocline depth for one 7-day series, recorded in summer off Mission Beach, California, had a trimodal distribution. The central primary mode (1) around 32 feet was interpreted to be the depth of the seasonal thermocline. The others, (2) and (3), around 18 and 44 feet, were caused by internal tide and amounted to 26 feet at this time and place (fig. 11).

During the periods of investigation, the maximum daily vertical migration of an isotherm in the middle of the thermocline was 31 feet.

The frequency distribution of shallow internal wave heights at this location for part of 12 days throughout the summer of 1958, and 7 consecutive days in 1959, is shown in figure 12. Only waves higher than 2 feet were considered since the lower ones were probably only random fluctuations. It was found that 50 per cent of the internal waves were higher than 5.6 feet.

In the San Diego Trough 20 miles from shore in 600 fathoms of water, the upper thermocline during a June period contained vertical oscillations that were no higher than those observed from the nearby NEL Oceanographic Research Tower. The median vertical change for changes greater than 1 foot was only 4.6. This and other characteristics of the thermocline are shown in figure 13.

During the same season, 200 miles from shore, the upper thermocline contained waves a little higher than those near shore. However, the vertical oscillations of constant temperature were much higher at depths from 300-800 feet, their height being inversely related to the vertical temperature gradients. Here they were from 50 to 200 feet (fig. 14). This inverse relationship probably holds at greater depth where the vertical thermal and density gradients are even weaker.

The tidal circulation described above also influences long-period wave heights and wave periods (fig. 15). In the deep sea areas as well as on the continental shelf, internal waves of tidal period are commonly found[15]. However, the relative phase of surface and internal tide is not consistent.

WAVE PERIOD

The frequency distribution for the duration of 1061 shallow-water internal waves is shown in figure 15. Waves with periods of less than 2 minutes were excluded. Fifty per cent of all waves longer than 2 minutes had periods greater than 7.3 minutes.

In deep water the internal-wave period is difficult to measure because of lack of suitable platforms and adequate knowledge of the currents at different levels. An easier procedure is to measure the wave length or distance between crests with the towed chain. In the San Diego Trough, the upper thermocline oscillations greater than one foot occurred on the average of 0.4 mile apart, whereas in the deeper and more open areas, they occurred about 1 per mile at depths of about 500 feet.

SPEED

In shallow water, the speed of internal waves was determined by measuring vertical oscillations simultaneously in three locations[16,12] and deduced from the movement of their associated sea-surface slicks.

Time-lapse films of surface slicks off southern California* showed that internal waves

*Mission Beach, La Jolla, and San Diego Bay moved toward shore at speeds of 0.11 to 0.6 knot. Other measurements from anchored ships with range markers indicated an average speed of 0.31 knot. More recent measurements averaged with three isotherm followers were 0.29 knot in 60-foot-deep water (fig. 16).

The observed speed (c) agrees well with prior theoretical considerations[2] when dealing with long internal waves as compared to their depth.

$$c = \left(\frac{g\,h\,h'}{h + h'} \; \frac{\rho - \rho'}{\rho} \right)^{\frac{1}{2}}$$

where h' and h are the depth of a two-layer system having densities ρ' and ρ, respectively.

In 180 feet of water in the Atlantic Ocean, internal wave speed still agreed with established equations and gave speeds of about 1.0 knot[17], thus it must be supposed that internal waves in deep water, especially deeper ones, must travel at considerably greater speeds.

DIRECTION

The shape of internal waves varied with shoreward movement and refraction as they moved into shallower areas. Their shape was also influenced by their proximity to the surface sea floor[18]. Nearly all internal waves proceeded from a west-to-southwest (mode 72.4°T) direction at the Mission Beach location (fig. 17). Efforts to obtain information on internal wave direction were ineffective in deep water. One such action involved towing of the NEL thermistor chain in different directions, but no clear-cut doppler effect could be established. It appeared from this experiment that deep-water internal waves are not in long parallel lines as they frequently are in shallow water.

OTHER RELATED MOTIONS

One approach to the study of internal wave motion in the sea is the assumption that they are progressive waves. In lakes and partially closed bodies of water, standing waves are found. The nature of progressive waves between two liquids of different densities has already been analyzed.[19,20] The nature of this circulation as applied to the sea has been investigated by direct and indirect means. For example, sea surface slicks, which often represent visible evidence of internal waves below, are seen as streaks or patches of relatively calm surface water surrounded by rippled water. The absence of wavelets in a slick gives it a glassy appearance in contrast to the adjacent rippled water (fig. 18). These slicks have been studied in oceans, bays, and lakes.[21,22,23,9]

The occurrence of visible slicks is contingent upon proper wind, lighting, sufficient organic matter on the water, and the nature of internal waves. The concentration of surface film depends on the interrelation of internal wave height and period. The average depth of the internal wave and its relation to water depth also influence the type of circulation and thus have a bearing on the formation of slicks. In 85 out of 105 cases, the slick was on the descending thermocline somewhere between the crest and the following trough (fig. 19). This relationship is undoubtedly the result of convergent water circulation created by internal waves. The significant motion is therefore a surface convergence over the trailing slope of the internal wave.

Direct measurements of current associated with internal waves were made at the NEL Oceanographic Research Tower. By means of a closed-circuit television, observing dye and motion streamers, and a current meter that dampens surface wave motion, the existence of convergence-type circulation associated with a slick was confirmed. The reverse circulation over shallow crests and over troughs was also established, thus substantially confirming in part the above circulation theory of a two-layer internal wave system in shallow water.

SUMMARY AND CONCLUSIONS

Internal waves are now being measured by a number of instruments, including vertical strings of temperature sensors, which are suspended in one location, as with isotherm followers, or towed, as with the NEL thermistor chain. The vertical oscillations observed in the thermal structure, commonly termed internal waves, are present in the sea virtually all the time. Their height, speed, direction, period, and other characteristics are found to vary widely with time, area, and depth. The larger waves are associated with weaker gradients and thus have larger amplitudes in the deeper layers where temperature changes are small. Studies of their motion, spatial distribution, and cause are continuing.

REFERENCES

1. Fjeldstad, J. E., 1933, INTERNE WALLEN GEOFYSISKE Publikasjoner, Vol. 10, No. 6, 53 pp., 1933 Oslo.
2. Ekman, V. W., 1904, ON DEAD WATER, Sci. Results, Norwegian North Polar Exp. 1893-96, Vol. 5, No. 15, pp. 1-152.
3. Shand, J. A., INTERNAL WAVES IN GEORGIA STRAIT, Trans. Amer. Geophys. Union, Vol. 34, pp. 849-856, 1953
4. LaFond, E. C. and Poornachandra Rao, VERTICAL OSCILLATIONS OF TIDAL PERIODS IN THE TEMPERATURE STRUCTURE OF THE SEA, Andhra University Memoirs in Oceanography, Vol. 1, pp. 109-116, 1954.
5. Munk, W. H., 1941, INTERNAL WAVES IN THE GULF OF CALIFORNIA, Jour. of Mar. Res., Vol. 4, pp. 81-91.
6. Zeilon, N., 1934, EXPERIMENTS ON BOUNDARY TIDES, Goteborg Vetensksamh. Handl. Folj. 5, Ser. B, Bd. 3, No. 10.
7. Zeilon, N., 1913, ON THE SEICHES OF THE GULLMAR FJORD, Svenska Hydrogr-Biolog. Komm. skrifter 5.

8. Kullenberg, B., 1935, INTERNAL WAVES IN THE KATTEGAT, Svenska Hydro. Biolog. Komm. Skrifter, Ny Serie Hydrografi, XII (A.C.S.I.L. Translation #561).
9. LaFond, E. C., SLICKS AND TEMPERATURE STRUCTURE IN THE SEA, U.S. Navy Electronics Laboratory Report 937, 2 November 1959.
10. Richardson, William S., 1958, MEASUREMENT OF THERMAL MICROSTRUCTURE, W.H.O.I. Reference No. 58-11.
11. LaFond, E.C., 1961, THE ISOTHERM FOLLOWER Jour. of Mar. Research, Vol. 19, No. 1, pp. 33-39, March, 1961.
12. Lee, Owen S., 1961, OBSERVATIONS ON INTERNAL WAVES IN SHALLOW WATER, Limnology and Oceanography, Vol. 6, No. 3, July 1961.
13. Lee, O. S. and E. C. LaFond, 1961, ON SHORT-PERIOD CHANGES IN ISOTHERM DEPTHS IN SHALLOW WATER OFF SAN DIEGO (In press).
14. LaFond, E. C., 1961, TWO-DIMENSIONAL OCEANOGRAPHY, BUSHIPS Journal (In press).
15. LaFond, E. C., THE USE OF BATHYTHERMOGRAMS TO MEASURE OCEAN CURRENTS, Amer. Geoph. Union, Vol. 30, No. 2, pp. 231-237, April 1949.
16. Ufford, C. W., 1947, INTERNAL WAVES MEASURED AT THREE STATIONS, Trans. Amer. Geophys. Union 28, (1), pp. 87-95.
17. Gaul, Roy D., 1961, INTERNAL WAVE OBSERVATIONS NEAR HUDSON CANYON, Jour. of Geoph. Research (In press).
18. LaFond, E. C., BOUNDARY EFFECTS ON THE SHAPE OF INTERNAL WAVES, Indian Jour. of Meteorology and Geophysics, 12 April 1961.
19. Lamb, H., HYDRODYNAMICS, 6th Edition, p. 372, Dover Pub. Co., New York, 1945.
20. LaFond, E. C., 1961, THE TEMPERATURE STRUCTURE OF THE UPPER LAYERS OF THE SEA AND ITS VARIATION WITH TIME, Proc. of the 3rd Symposium — Temperature, Its Measure and Control in Science and Industry Instrument Society of America (In press).
21. Dietz, R. S. and E. C. LaFond, NATURAL SLICKS ON THE OCEAN, Jour. of Mar. Res., Vol. IX, No. 2, pp. 69-76, October 1950.
22. Woodcock, A. H. and T. Wyman, 1946, CONVECTIVE MOTION IN AIR OVER THE SEA, Ann. N.Y. Acad. Sci. 48, 749-776.
23. Forbes, A., 1945, PHOTOGRAMMETRY APPLIED TO AEROLOGY, Photogrammetric Eng. 2, 181-192.

FIGURES

Figure 1 - Internal waves associated with a change in depth of a thermocline. (Waves are moving from right to left)

Figure 2 - Sea surface appearance showing the probable formation of internal waves by tidal action between low-density discharge water and the Georgia Strait water (British Columbia Government Air Photo).

Figure 3 - Thermistor beads and resistors mounted in plastic used for temperature sensors.

Figure 4 - Sixteen-channel temperature recording unit.

Figure 5 - Internal wave measurements from an anchored ship.

Figure 6 - U.S. Navy Electronics Laboratory's thermistor chain on USS MARYSVILLE (EPCER 857).

Figure 7 - Isotherm follower assembly

Figure 8 - Three isotherm followers in operation from booms suspended out from the U. S. Navy Electronics Laboratory oceanographic research tower.

Figure 9 - Sea unit of towed isotherm follower.

Figure 10 - Depth of isotherm measured with isotherm follower off Mission Beach, California (summer, 1961).

Figure 11 - Distribution of minute readings, over 7 consecutive days, of the depth of an isotherm in the thermocline.

Figure 12 - Frequency distribution of internal wave heights over 2 feet (1958 and 1959 data).

Figure 13A - Operation area in San Diego Trough off Southern California.

Figure 13B - Thermal structure of the sea as measured with the thermistor chain.

Figure 13C - Depth to the top of the thermocline.

Figure 13D - Maximum vertical temperature gradients in °C per fifty feet.

Figure 13E - Roughness of the thermocline.

Figure 14 - The nature of internal waves in deep ocean water.

Figure 15 - Frequency distribution of internal wave periods over 2 minutes (for 1958 and 1959 data).

Figure 16 - Internal wave speed in 60-foot water from 674 observations using isotherm followers during the 1960 summer.

Figure 17 - Internal wave direction in 60-foot water from 674 observations using three isotherm follower during the 1960 summer.

Figure 18 - Sea surface slicks near the USNEL Oceanographic Research Tower. Slicks are surface evidence of internal waves below.

Figure 19 - Relation between internal waves and sea surface slicks. Heavy bar at surface and vertical dashed lines represent the observed position of sea surface slicks with reference to thermal structure.

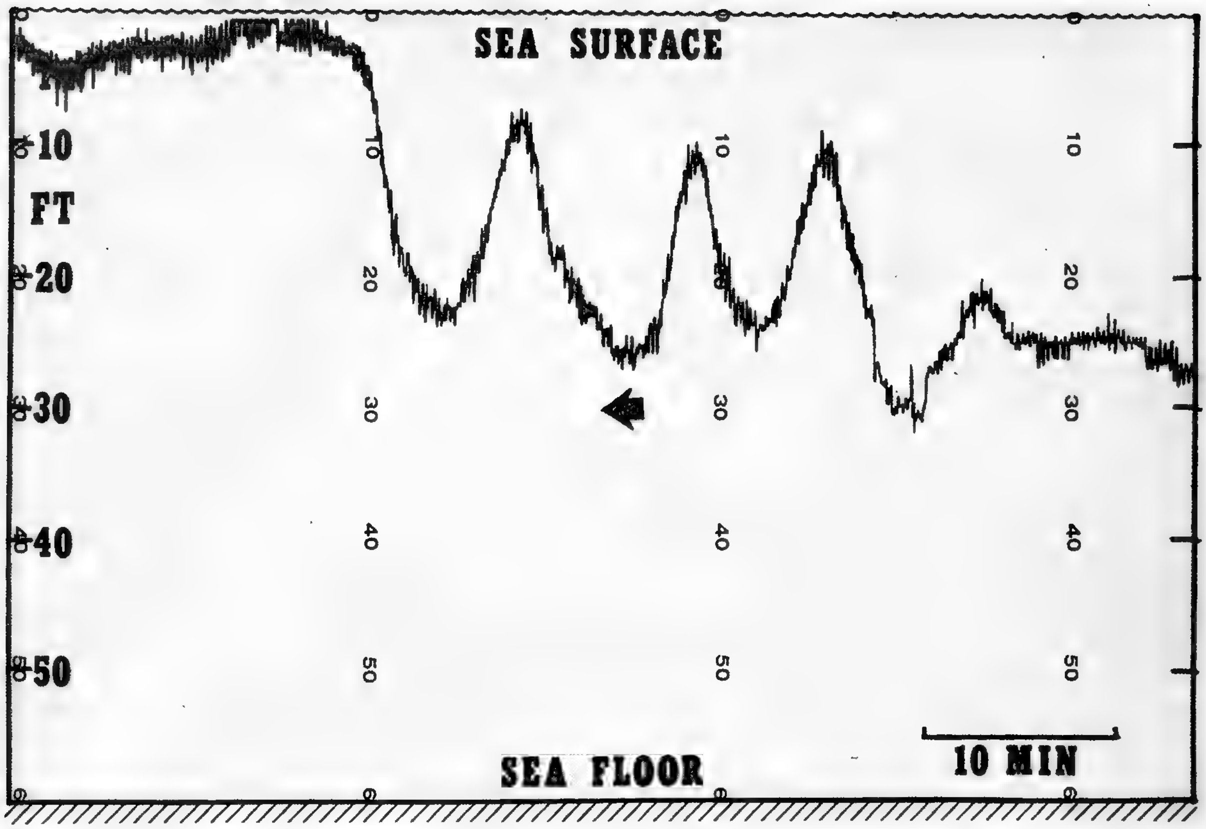

Figure 1

Figure 2

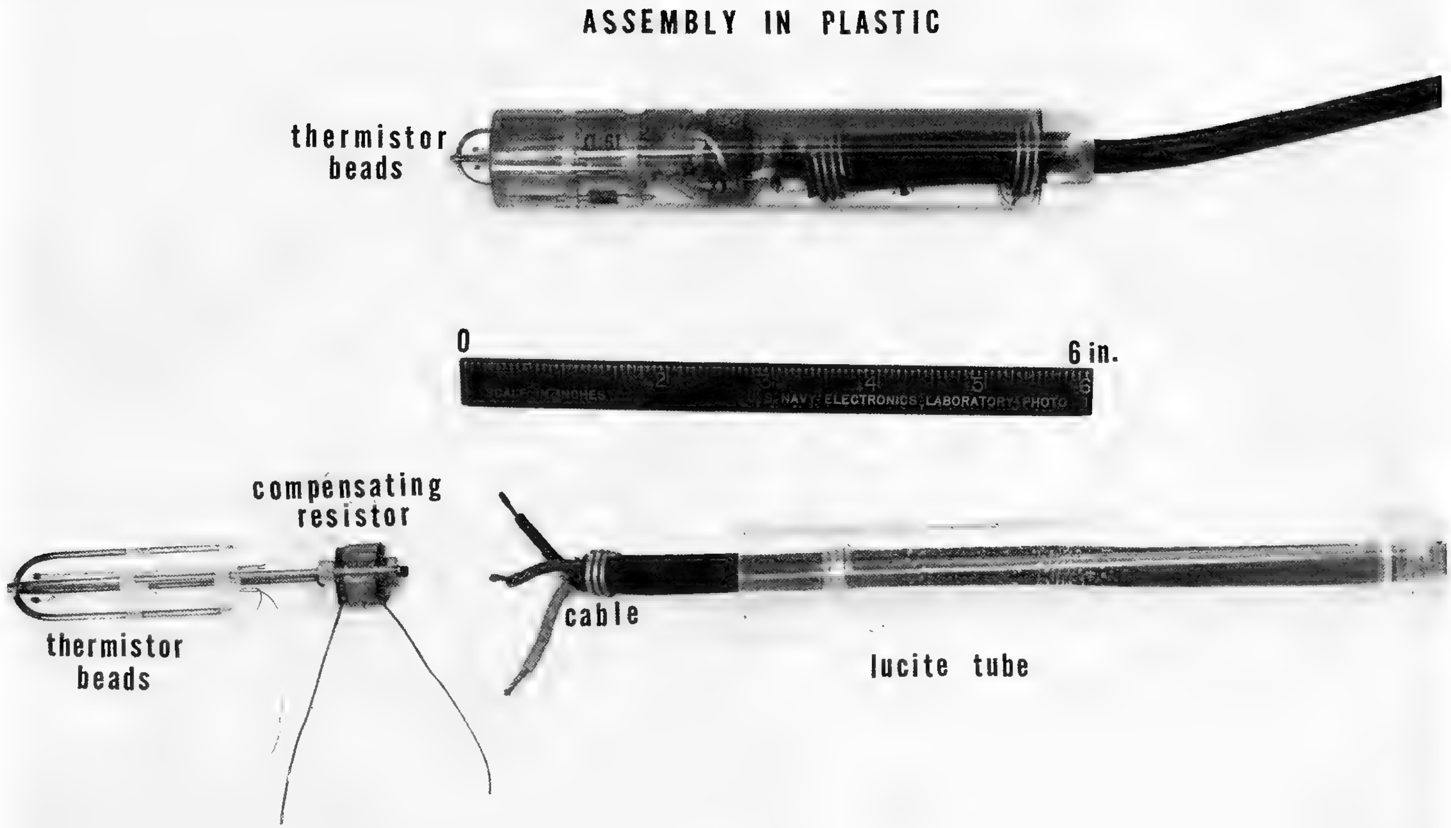
ASSEMBLY IN PLASTIC
thermistor beads
0
6 in.
SCALE IN INCHES
U.S. NAVY ELECTRONICS LABORATORY PHOTO
compensating resistor
thermistor beads
cable
lucite tube

Figure 3

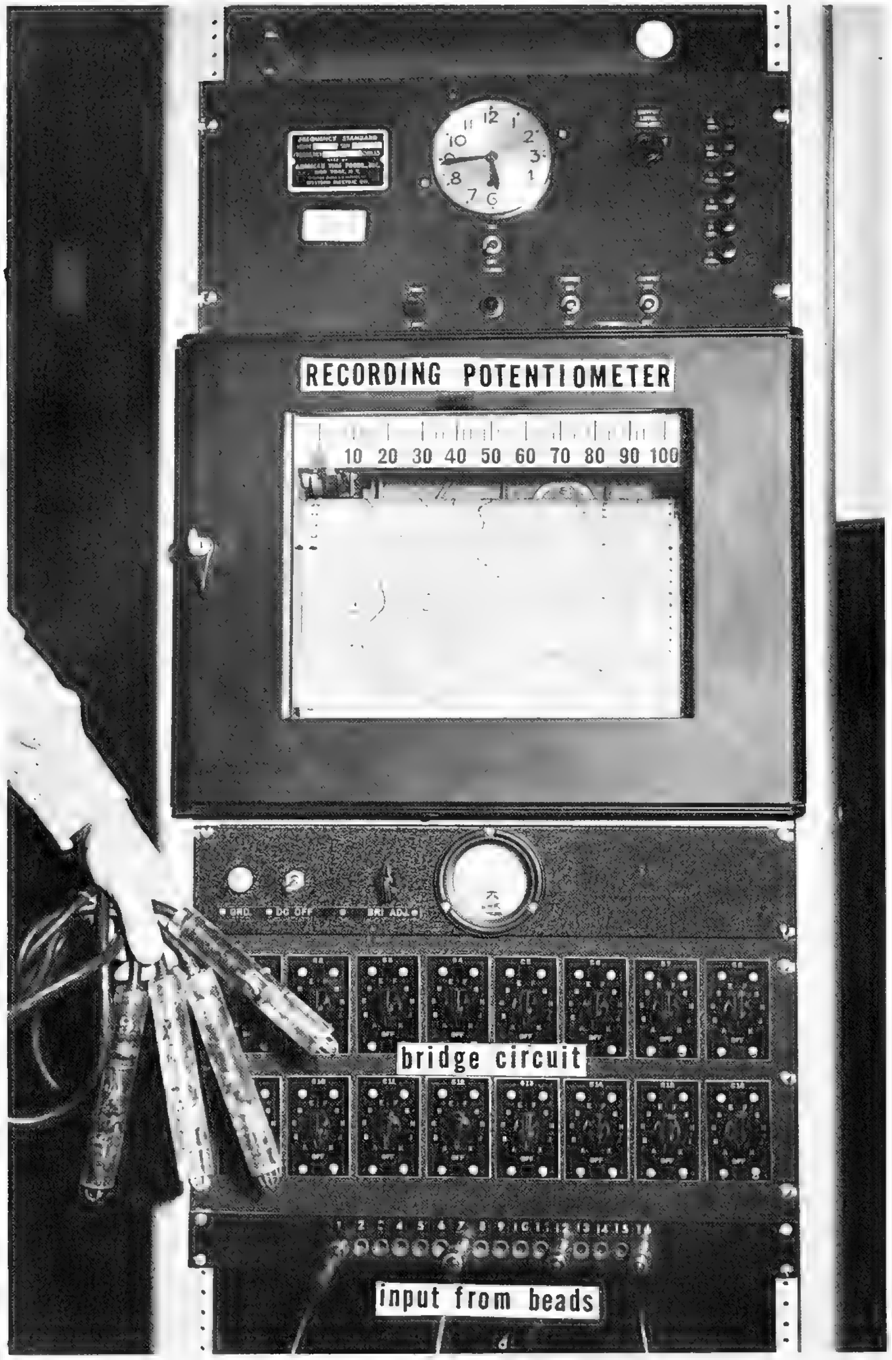
RECORDING POTENTIOMETER
10 20 30 40 50 60 70 80 90 100
bridge circuit
input from beads

Figure 4

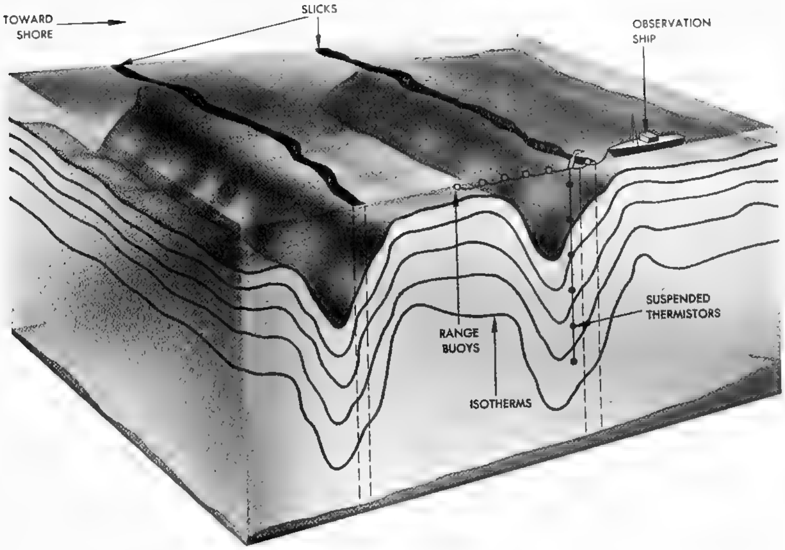

Figure 5

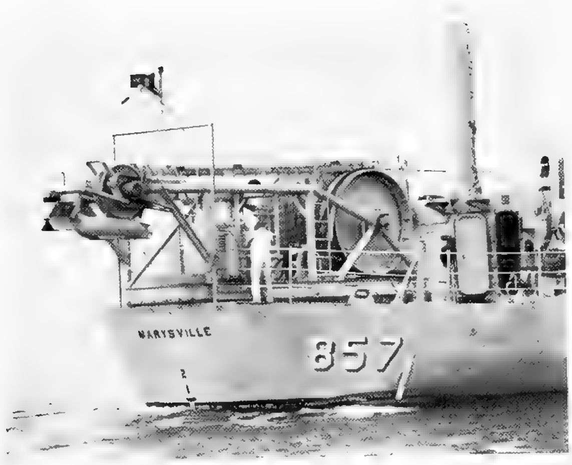

Figure 6

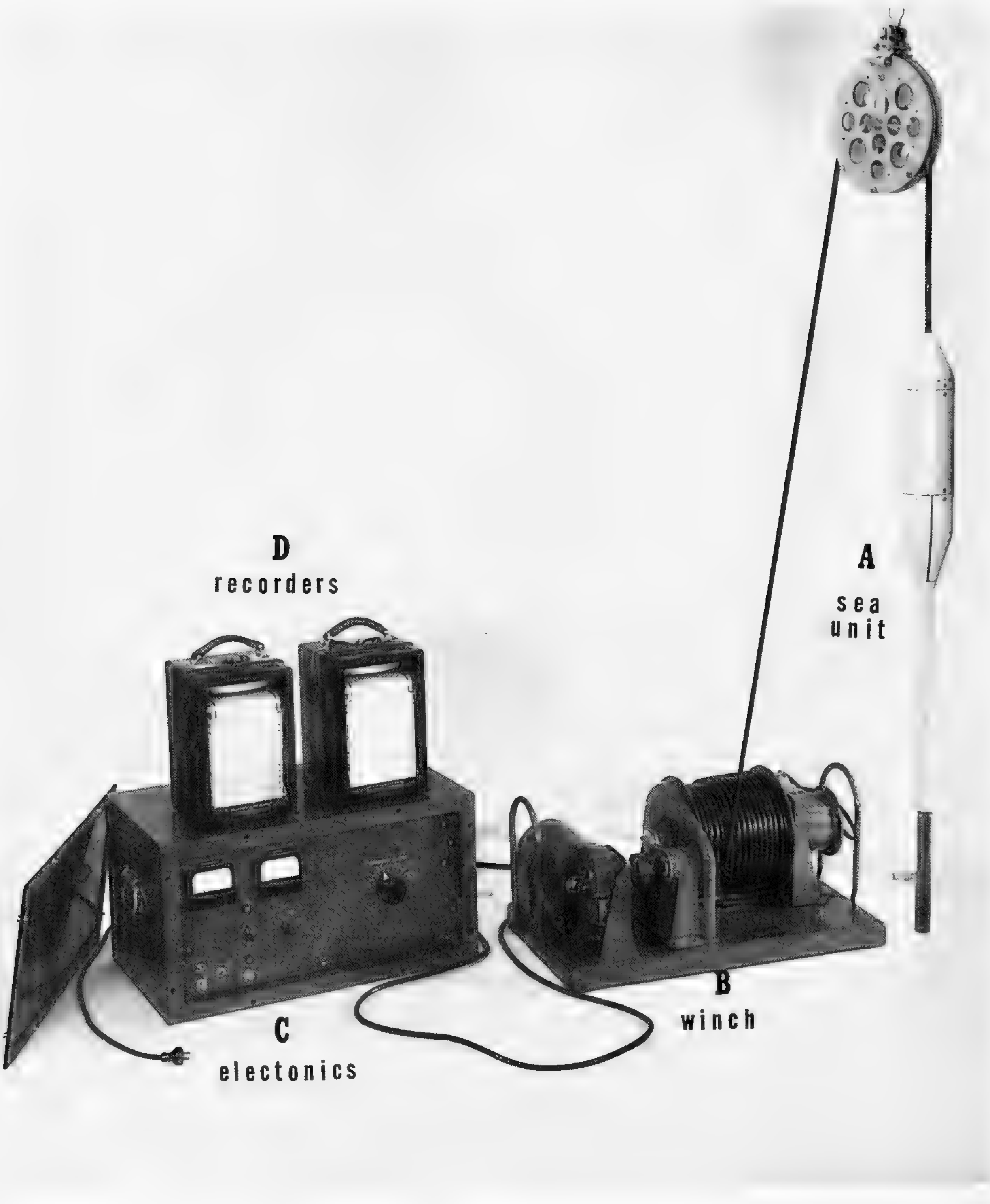

Figure 7


U S NAVY ELECTRONICS LABORATORY
OCEANOGRAPHIC RESEARCH TOWER

Figure 8

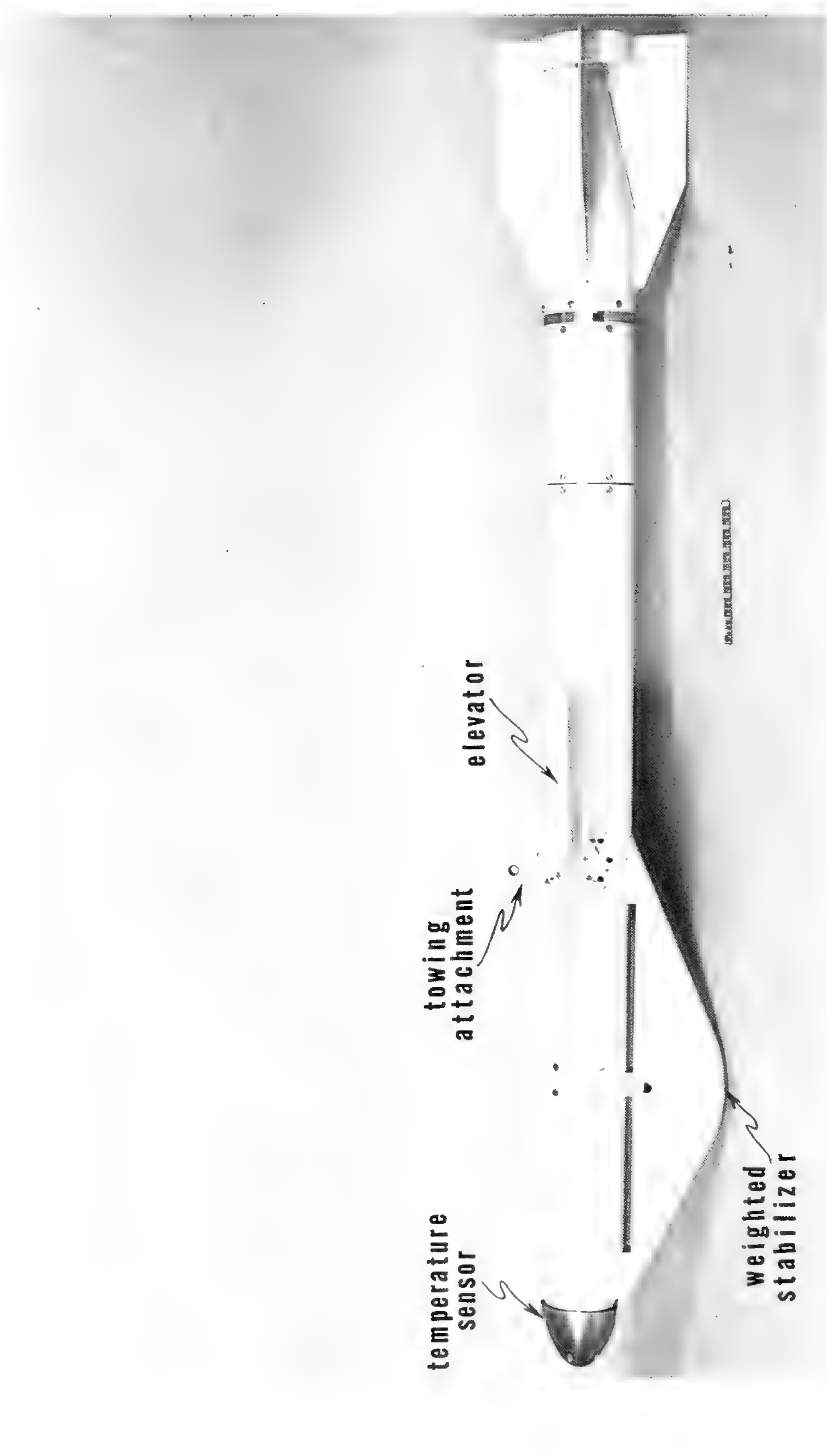
temperature sensor
towing attachment
elevator
weighted stabilizer

Figure 9

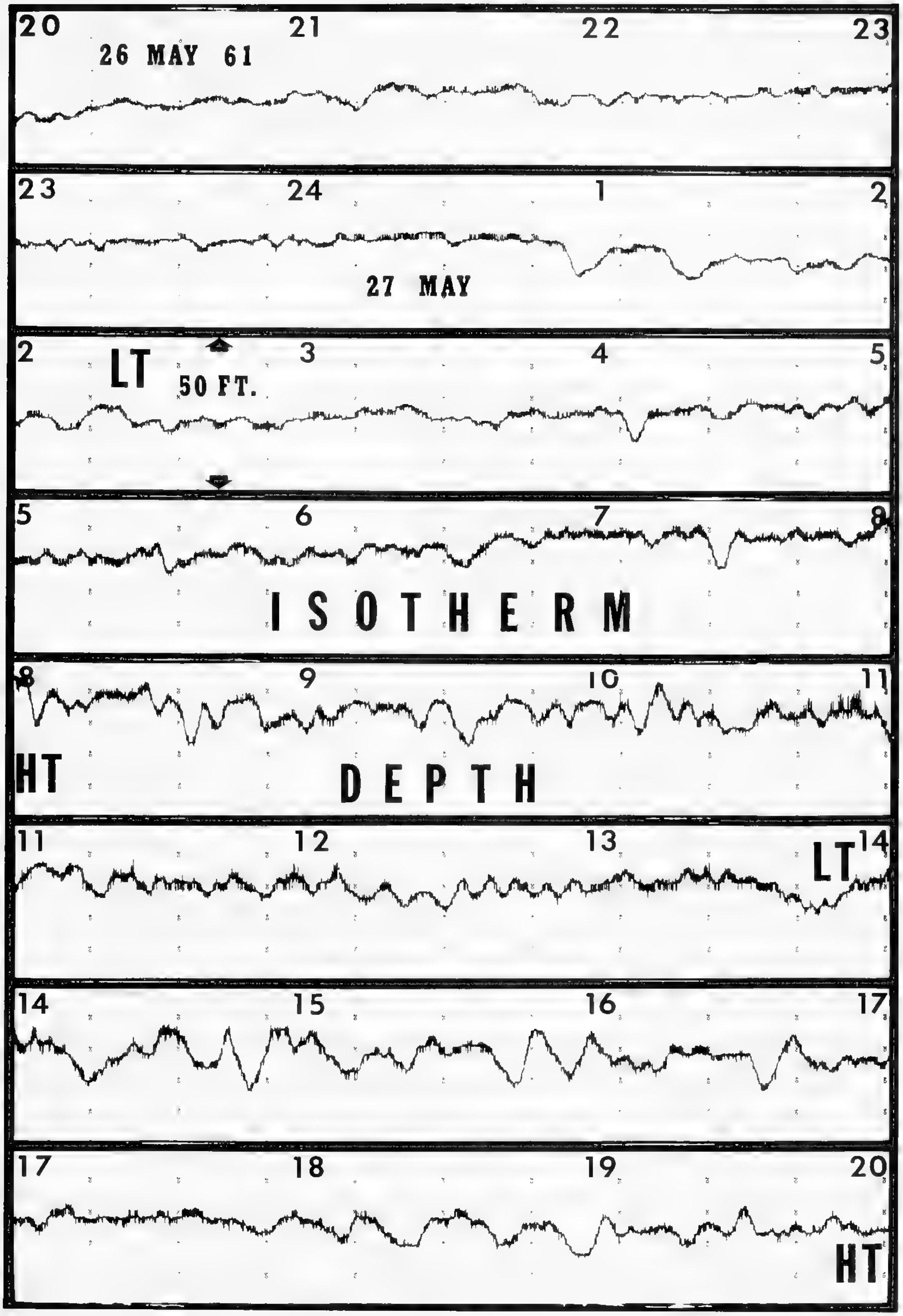
20
21
22
23
26 MAY 61
23
24
1
2
27 MAY
2
LT
50 FT.
3
4
5
5
6
7
8
ISOTHERM
8
9
10
11
HT
DEPTH
11
12
13
LT
14
14
15
16
17
17
18
19
20
HT

Figure 10

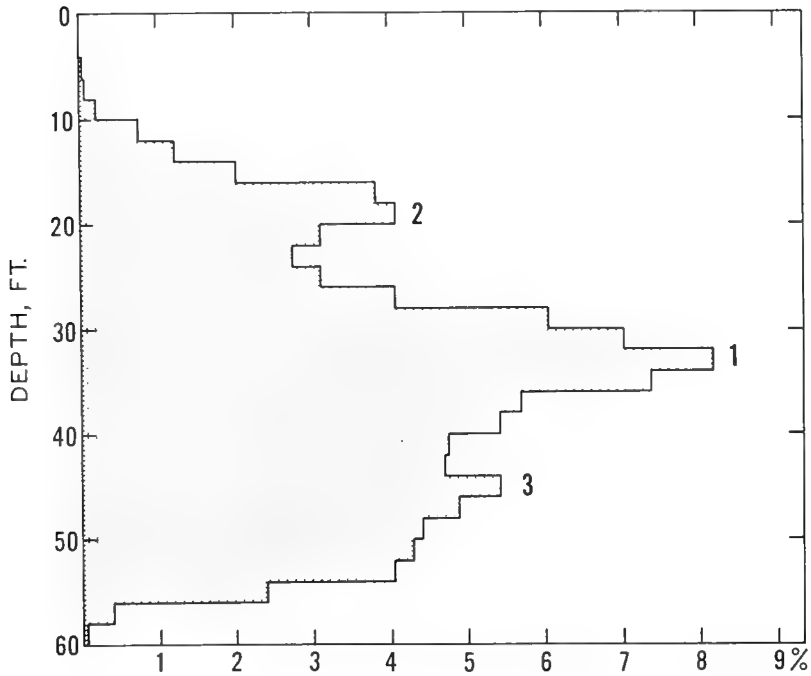

Figure 11

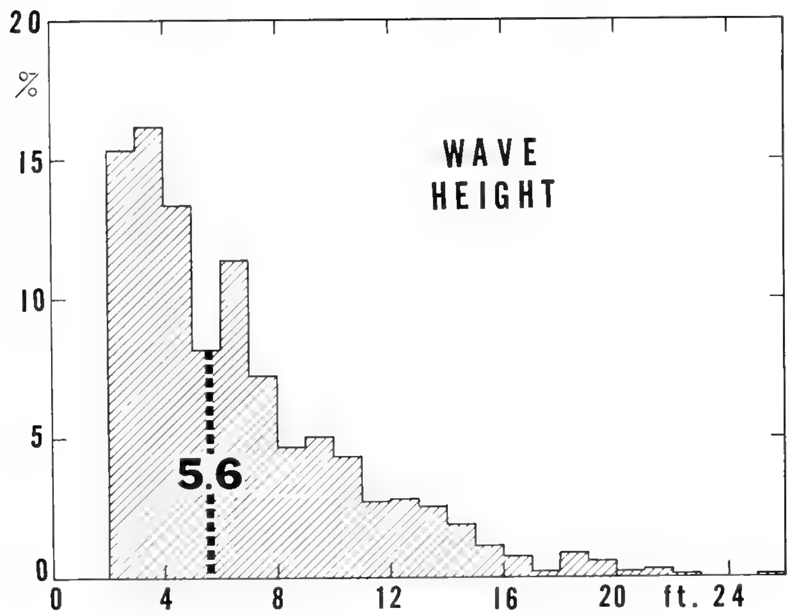

Figure 12

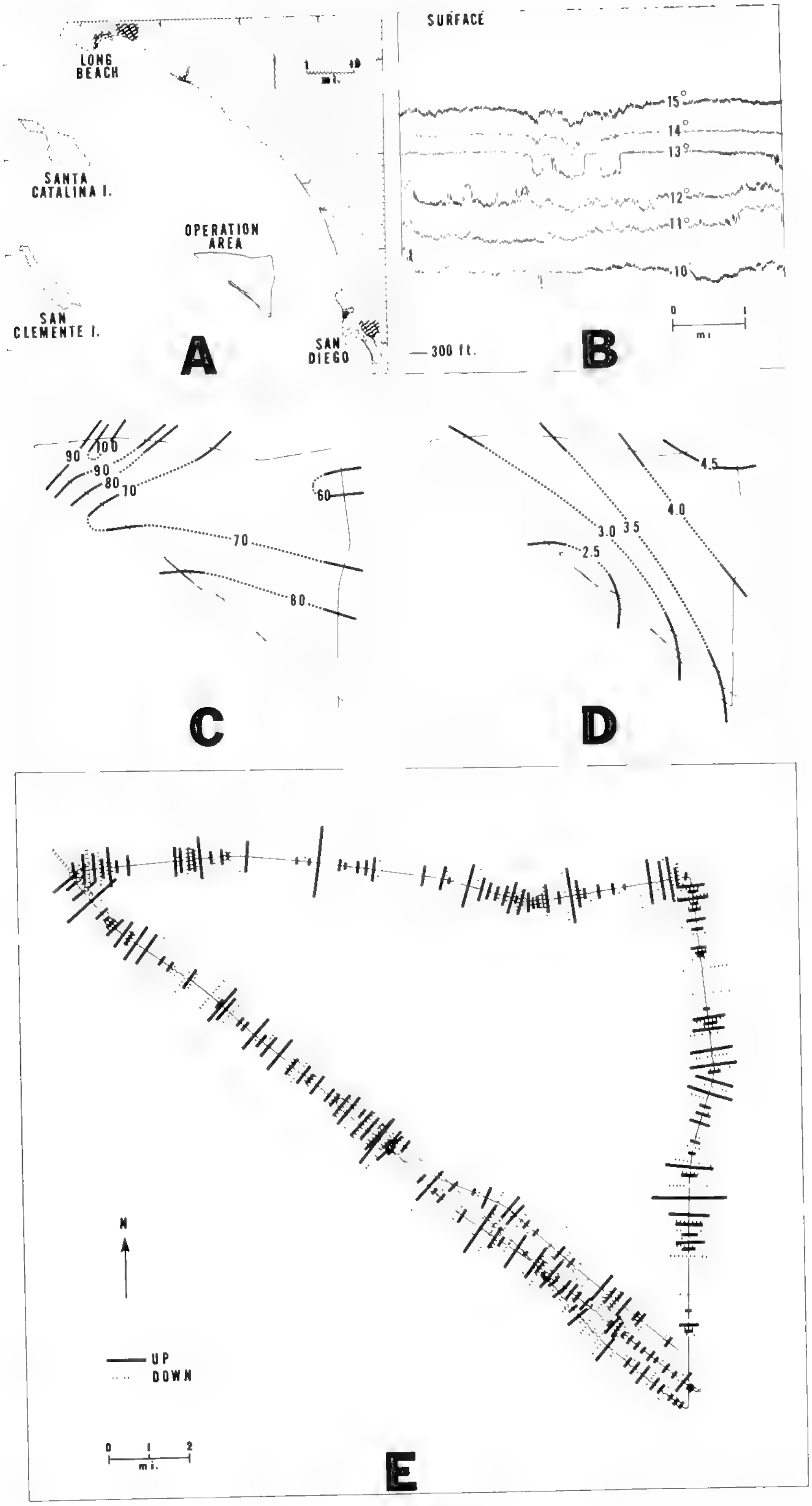
LONG BEACH
SANTA CATALINA I.
OPERATION AREA
SAN CLEMENTE I.
SAN DIEGO
A
SURFACE
15°
14°
13°
12°
11°
10°
300 ft.
mi
B
90
100
90
80
70
60
70
80
C
4.5
4.0
3.0
3.5
2.5
D
N
UP
DOWN
0 1 2
mi.
E

Figure 13

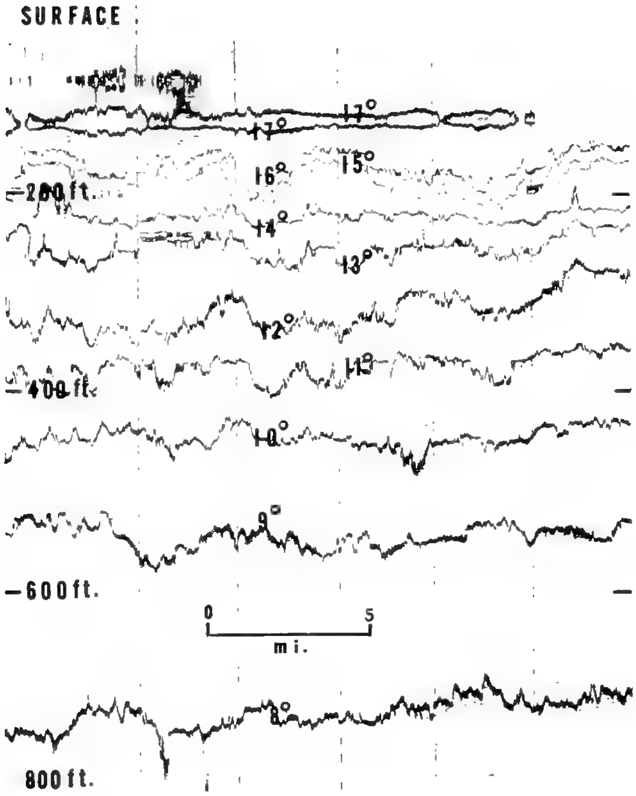

Figure 14

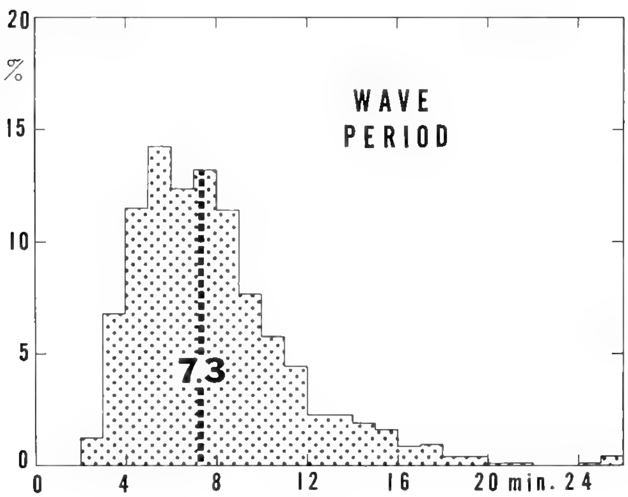

Figure 15

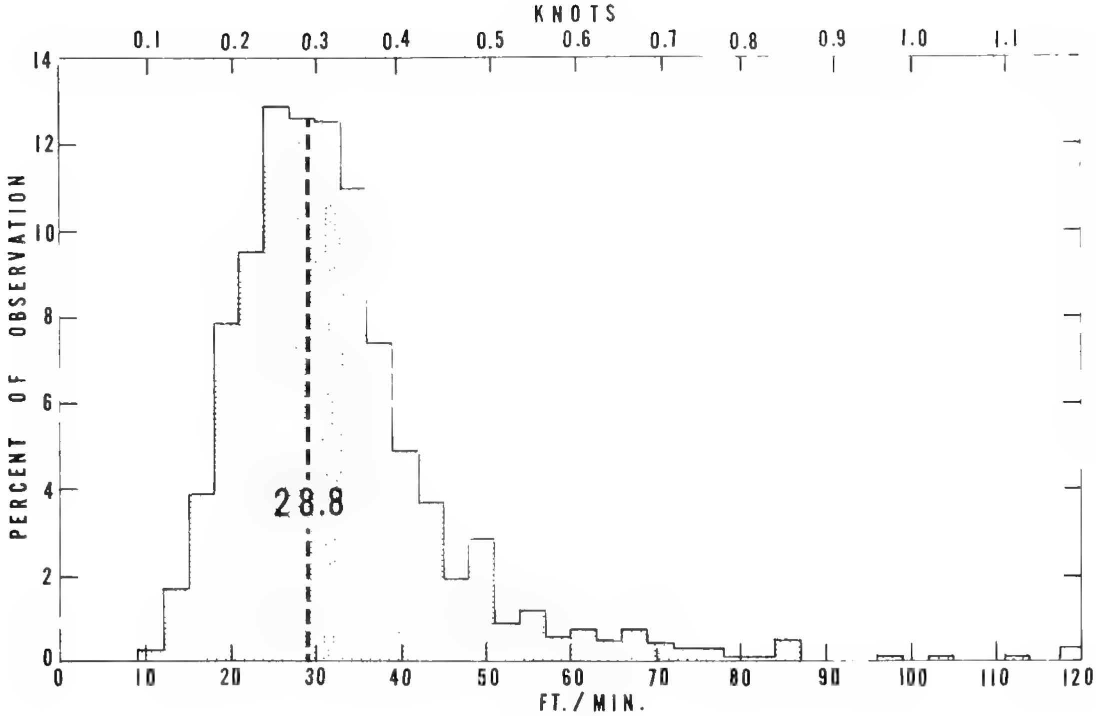

Figure 16

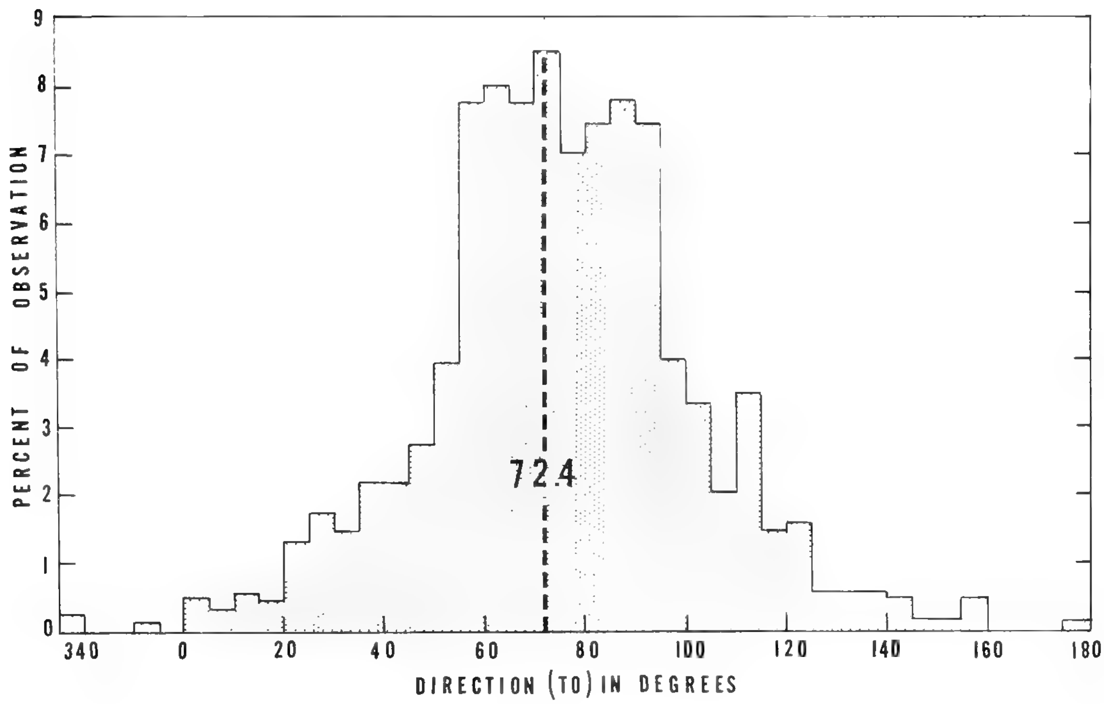

Figure 17

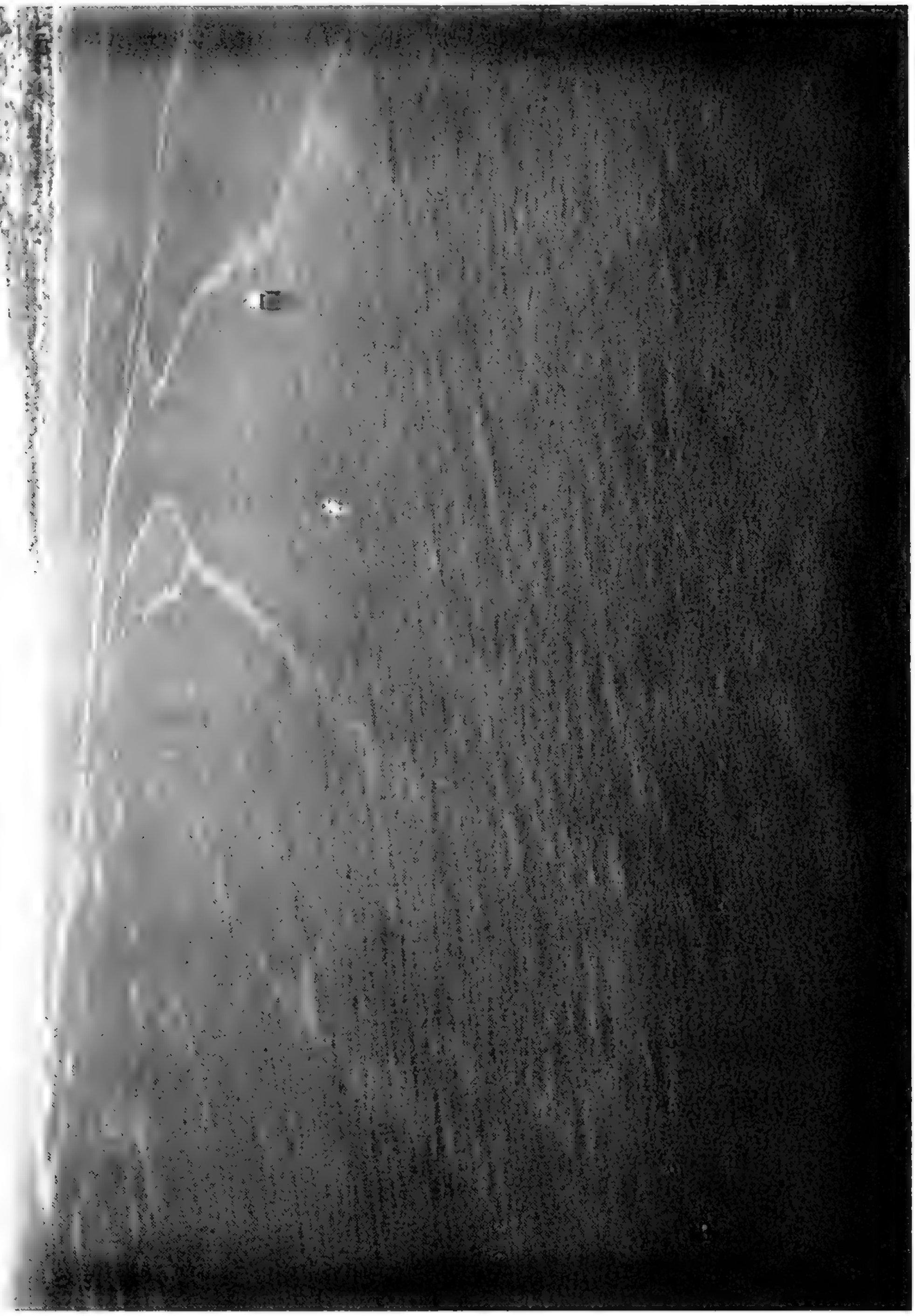

Figure 18

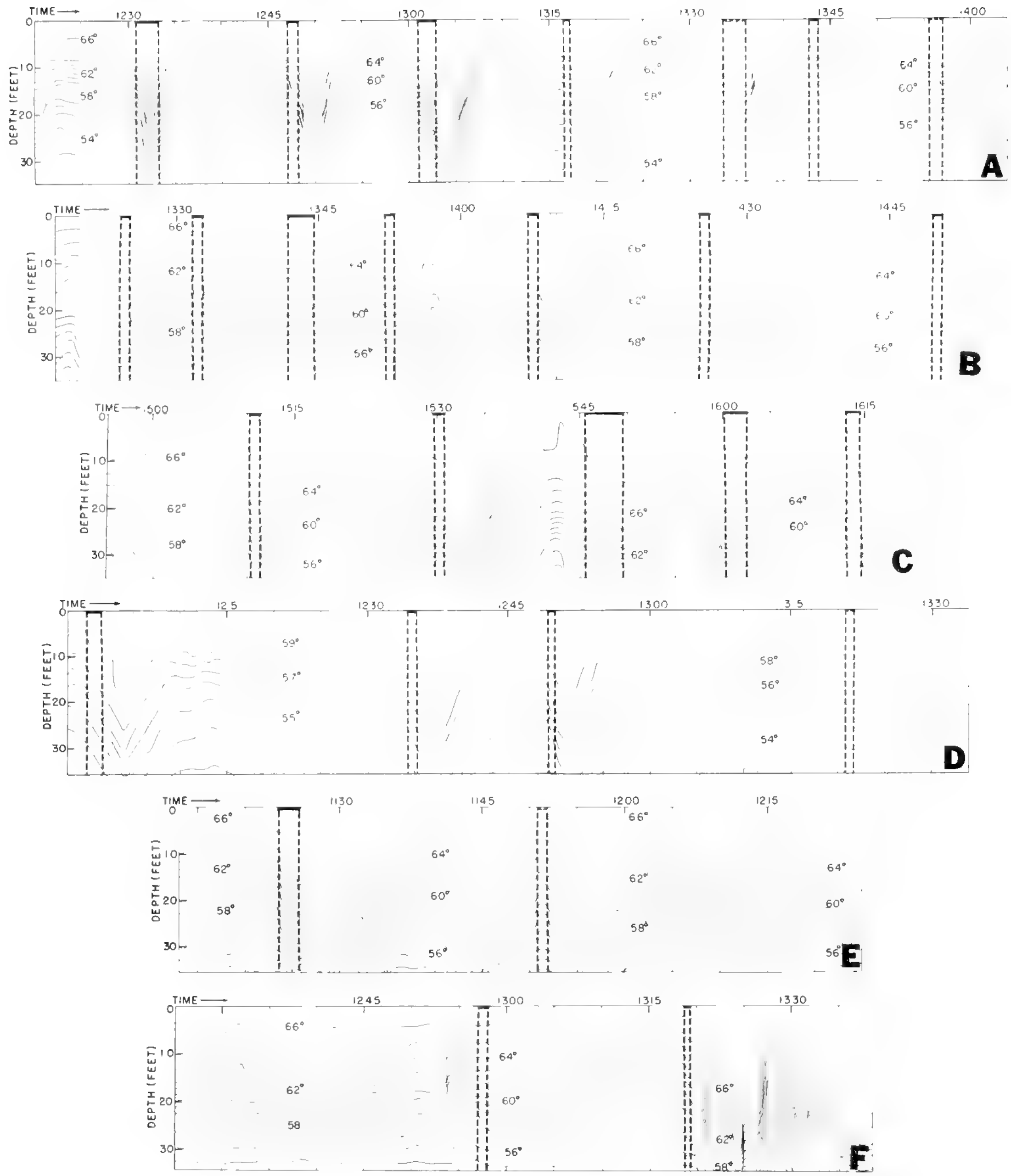

Figure 19

QUANTITATIVE MULTIPLE OPENING-AND-CLOSING PLANKTON SAMPLERS

by DR. ALLAN W. H. BÉ
Lamont Geological Observatory
(Columbia University)
Palisades, New York

ABSTRACT

Two quantitative opening-and-closing plankton samplers are described for serial sampling of zooplankton in the upper 1000 meters of water. The Multiple Plankton Sampler (MPS) is designed for towing at three depth ranges (0-100 m; 100-250 m; and 250-500 m) in the upper 500 meters, and the Bathypelagic Sampler (BPS) is intended for simultaneous towing in the more sparsely populated 500-1000 m depths.

THEORY OF OPERATION

The two samplers were specifically designed for:

a. filtering large volumes of water (10 m^3/min. or more) through horizontal and oblique towing;
b. reliable opening-and-closing actions at the mouths of the nets, without fear of catch loss or contamination;
c. obtaining a bathymetric series of plankton samples at accurately predetermined depth levels by means of a fool-proof release mechanism; and
d. reducing ship's time operation by the use of multiple nets in single lowerings.

It should be emphasized that the present samplers require towing at 2 to 4 knots with wire angles of 30° to 50°. Thus, they are primarily intended for deep bathymetric studies of zooplankton and are in a different category from the high-speed plankton samplers[1,2,3,4], which are towed mainly in the 0-100 m, near-surface zone. The ability of horizontal and oblique towing of the present samplers is considered an important improvement over the other multiple plankton samplers requiring vertical hauls.[5,6,7]

Multiple Plankton Sampler

The MPS is designed to take three samples and allows opening-and-closing actions of three separate plankton nets. Its operation depends upon the following components:

a. $\frac{1}{2}$ m x $\frac{1}{2}$ m square fiberglass frame containing three pivoting rods with a common axis of rotation in one corner. Three one-half meter nets are attached to the rods and to the corner opposite the common axis in such a manner that each net may be folded (closed) and/or opened by 90°-rotation of its corresponding pivoting rod (the rotational force upon the rods is provided by three elastic cords, attached to the frame's exterior and the outwardly extending ends of each pivoting rod);
b. pressure-actuated, piston-type release mechanism with three release levers; and
c. three flowmeters.

At the start of the tow all three rods are fastened by thin cables to each of the release levers, which in turn are held in cocked position by the piston stem of the release mechanism. The "shallow" net is open when lowered and ready to fish on the way down, while the other two nets are folded.

At the first selected depth level (e.g. 100 m), the piston stem will have travelled past and released the upper lever -- thus triggering a 90°-rotation of the first rod and closing the first or "shallow" net while simultaniously opening the second net. At the end of the second depth interval (e.g. 250 m), the second net is closed and the third net is opened simultaniously. The closing of the third net at 500 m depth concludes the MPS operation.

"Superior numbers refer to similarly numbered references at the end of this paper."

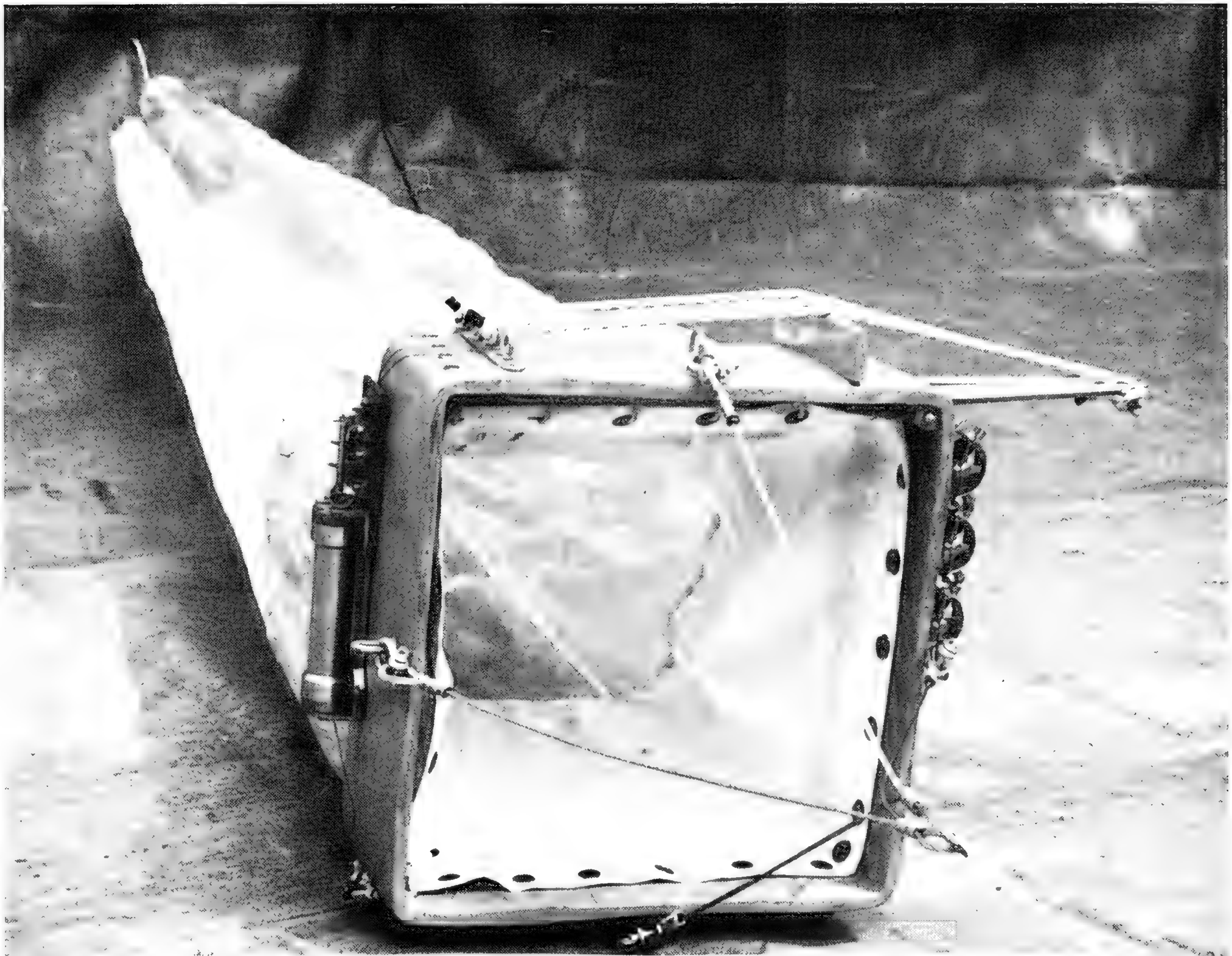

Fig. 1 Multiple Plankton Sampler with $\frac{1}{2}$ m x $\frac{1}{2}$ m frame. Step 1. First net open (0-100 m tow). Note all three pivoting rods are horizontal in cocked positions.

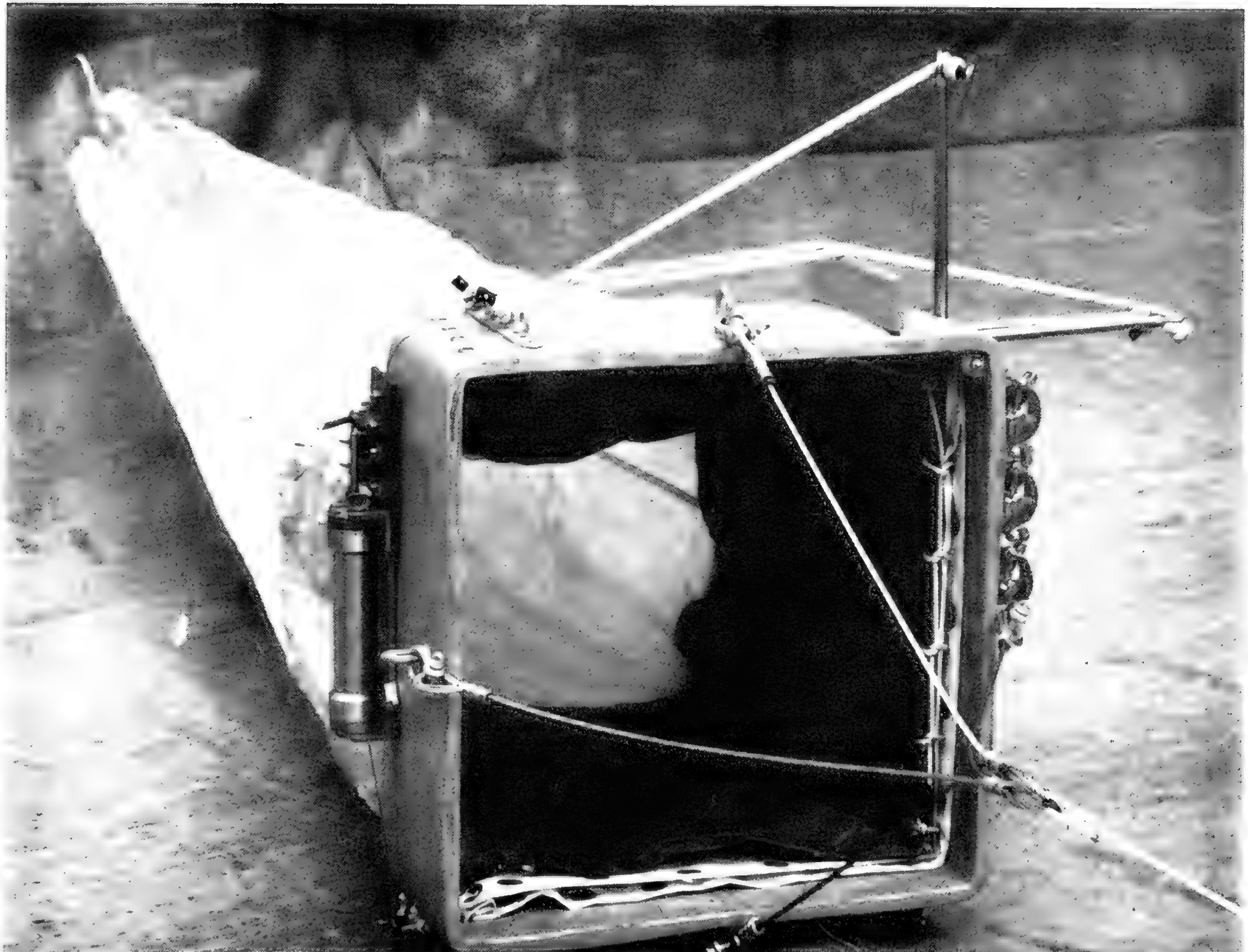

Fig. 2 Multiple Plankton Sampler. Step 2. Second net open; first net closed (100-250 m tow). Note the vertical position of the first pivoting rod and the release of the small, upper lever.

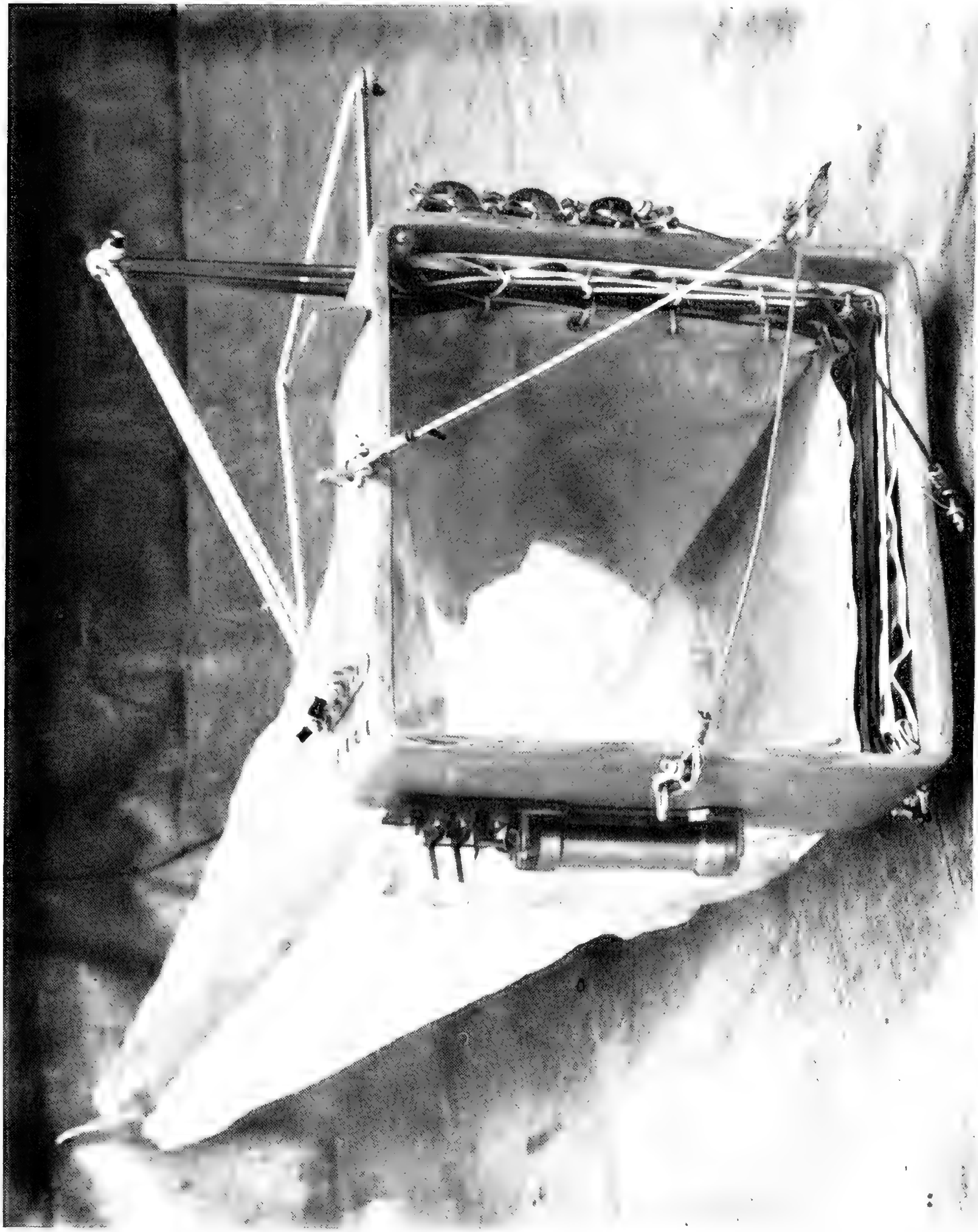

Fig. 3 Multiple Plankton Sampler. Step 3. Third net open; second net closed (250-500 m tow).

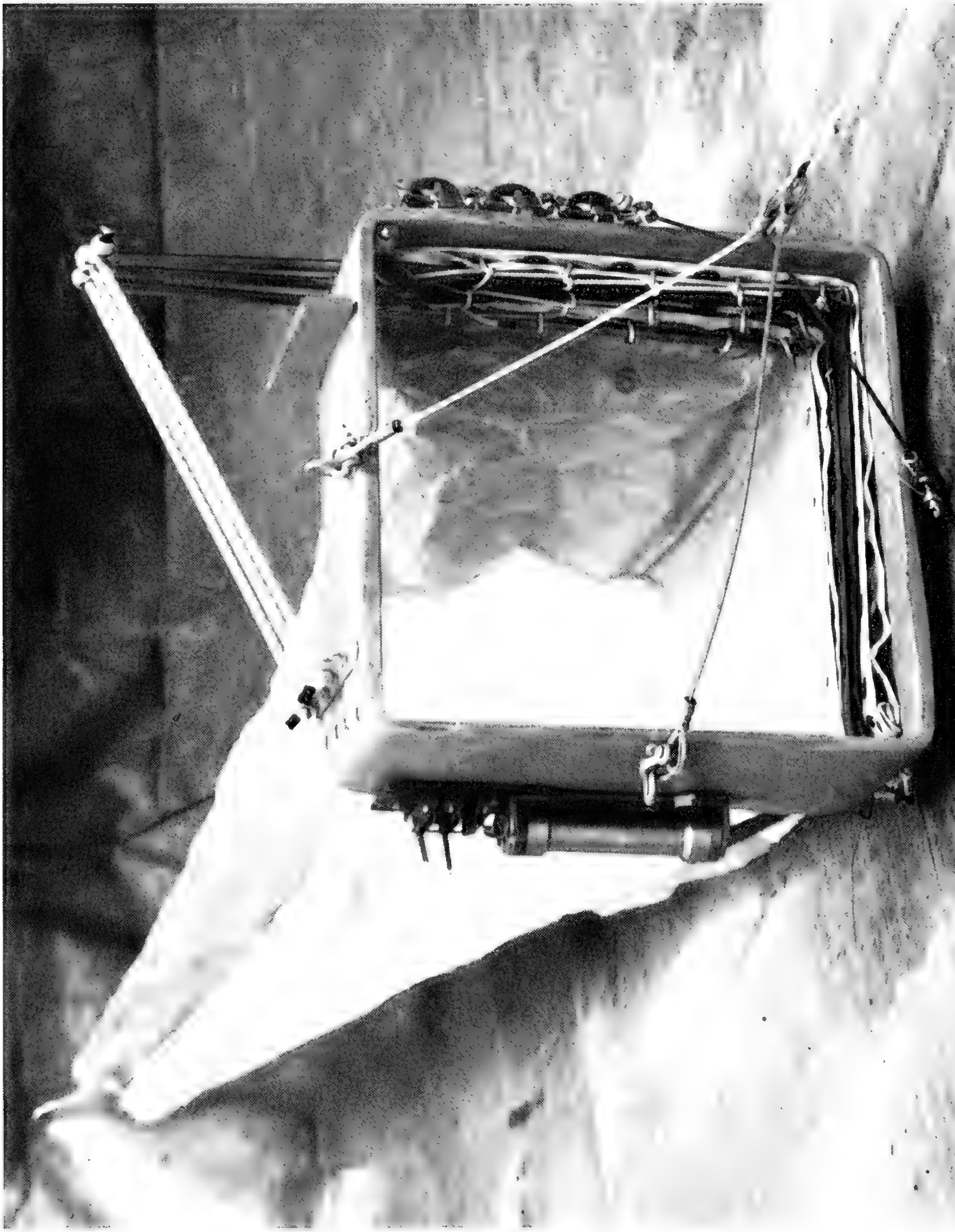

Fig. 4 Third net closed (at 500 m depth).

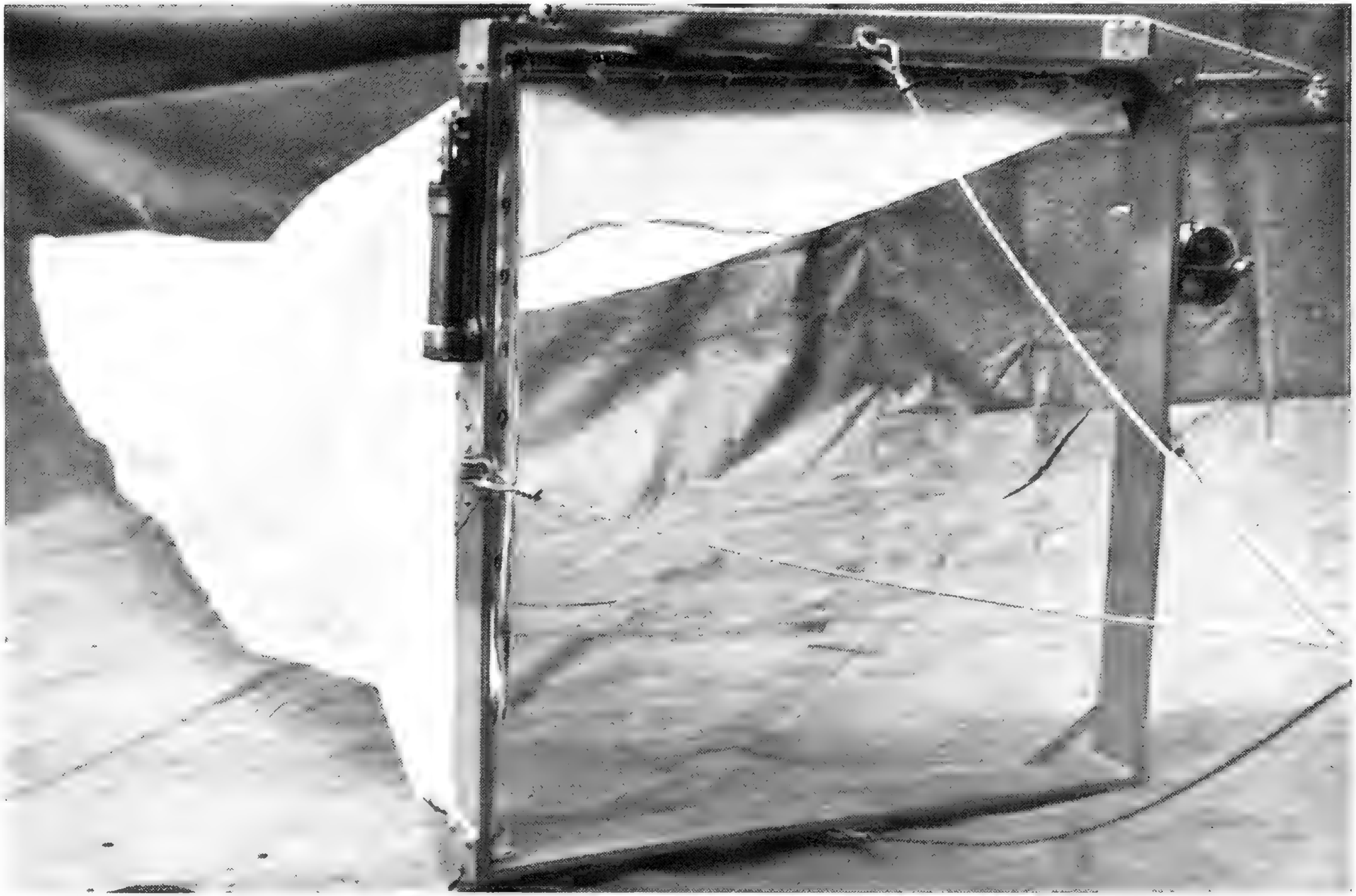

Fig. 5 Bathypelagic Sampler, having a 1 m x 1 m frame with a single, one-meter net. Initial, closed position.

Bathypelagic Sampler

The Bathypelagic Sampler (BPS) is essentially a larger version of the MPS. It has a 1 m x 1 m square frame with a single, one-meter net and is made to sample the 500-1000 m depth zone. Both the MPS and BPS have flow-meters that can record the amount of water filtered by each net tow.

The principle of the present samplers may be modified to suit the specific needs of other investigators, particularly with respect to size of frame opening, number of nets and depth ranges to be sampled. Larger frames and more nets, for instance, are recommended for sampling the abyssopelagic realm.

REFERENCES

1. Hardy, A.C. (1926), "The herring in relation to its animate environment. Part II: Report on trials with the plankton indicator". MAFF, Fish. Invest., Ser. 2, 8(7): 1-13.
2. Gehringer, J.W. (1952), "An all-metal plankton sampler (Model Gulf III)". U.S. Fish and Wildl. Serv., Spec. Sci. Rep. Fish., No. 88: 7-12,
3. Glover, R.S. (1953), "The Hardy plankton indicator and sampler: a description of the various models in use". Bull. Mar. Ecol., 4(26): 7-20.
4. Ahlstrom, E.H. (1958), "High-speed plankton sampler". U.S. Fish and Wildl. Serv., Fish. Bull., 58 (132): 187-214.
5. Motoda, S. (1953), "New plankton samplers". Bull. Fac. Fish., Hokkaido Univ., 3 (3): 181-86.
6. Motoda, S. (1959), "Devices of simple plankton apparatus". Mem. Fac. Fish., Hokkaido Univ. 7 (1/2): 73-94.
7. Bé, A.W.H., & Ewing, M., & Linton, L.W., (1959), "A quantitative multiple opening and closing plankton sampler for vertical towing". J. du Cons. int. Explor. Mer, 25: 36-46.

ACKNOWLEDGMENT

The present samplers were constructed by S.M. Harrison at the Lamont Geological Observatory and were successfully field tested on board the Observatory's research vessel VEMA during July and August 1961. Financial support was given by the National Science Foundation (NSF G-9557 and G-11593) and the Office of Naval Research (Nonr 266 (48)).

LONG-RANGE OUTLOOK FOR OCEANOGRAPHIC TELEMETERING

by JAMES M. SNODGRASS, Head, Special Developments
Scripps Institution of Oceanography
University of California, San Diego
La Jolla, California

ABSTRACT

With expanding oceanographic research programs, communications promise tc be a troublesome problem. Existing frequencies in the radio communications spectrum are almost completely absorbed by military, commercial and amateur interests. New means must be devised to communicate with research and survey ships. Circuits which will permit large amounts of data to be transmitted with high accuracy are needed.

Data telemetering over vast ocean areas will require many new techniques since present practice in the missile and flight test field is limited to line of sight. Conflicts with ocean missile ranges will need to be resolved, as well as devising suitable international agreements to permit long-range telemetering and the establishment of unattended deep-sea buoys and instrument stations.

Telemetering over ranges of several thousands of miles is necessary from unmanned floating instrument stations. Proposed communications types of satellites offer promising possibilities.

Communications, in one form or another, is inextricably linked with oceanographic research and oceanographically-oriented research projects. Unfortunately, it is only within comparatively recent time that the oceanographers have begun to become aware of their needs. The oceanographers' needs involve truly world-wide requirements.

Expanding oceanographic programs are planned which will require the use of instrumented buoys and the transmission of information by means of radio telemetering both to ship and shore based stations. It appears to be almost impossible to plan anything like a serious

*Contribution from the Scripps Institution of Oceanography, New Series, No.000. This work was supported in part by funds from the Office of Naval Research, U.S. Navy. Reproduction in part or entirety is permitted for any purposes of the United States Government.

program involving the use of remote buoys or ocean stations, if we must count on presently available frequencies in the electromagnetic communications spectrum. The difficulties are complicated by the fact that available frequencies are already largely allocated and are used almost completely by the military, commercial and amateur interests. There do not appear to be any suitable frequencies for extensive reliable communications available to the oceanographically-oriented research program.

Anticipating the general problems of the oceanographer, the Office of Naval Research sponsored a study contract on oceanographic telemetry (Contract Nonr-3062(00)) with the Convair Division of the General Dynamics Corporation. The first phase of the study has been completed, and an excellent report has been submitted to ONR. One of the purposes behind the study contract was to investigate various factors involved in telemetering data from remote oceanographic instrument buoys to shore based facilities. The factors which must be considered in this operation are tremendously involved and complicated. Some of the factors involve the behavior of specific radio frequencies in regard to radio propagation characteristics, such as skip distances, seasonal variations of noise with respect to latitude, solar induced radio propagation anomalies, power requirements, frequency bandwidths, etc. All of these variables have now been organized and collected together in the report submitted to ONR by Convair.

It appears that long-range communication may not be considered reliable using whatever frequencies may be available between a shore based receiving station and remote buoy or ocean station. This is assuming that dependable communication is required and that data be transmitted without objectionable error. It is quite true that one may obtain occasionally, and even for a limited period, transmission which might be considered acceptable. The difficulty is, however, that such conditions cannot be counted upon if reliable transmission is required. It is therefore necessary to seek modifications of the system whereby reliable communications may be established.

For somewhat over a decade Mr. E.F. Corwin, Mr. L.J. Allison and Mr. J.C. Appleby of the Meteorological Branch, Bureau of Naval Weapons,[1] and Mr. Hakkarinen of the Electronics Branch, National Bureau of Standards, have been carrying out highly significant work in the development of radio telemetering ocean buoys and instrument stations. It is interesting to note that, as time went on, each succeeding buoy design involved the use of larger amounts of radiated RF power. Later designs tended to evolve around the "squirt" techniques and used radiated power levels as high as 5kw.

The "squirt" system combined with knowledge gained in ionospheric research by the Canadian Defence Research Establishment may well prove to be valuable. The substance of the method developed involves the use of an interrogation technique between the shore based station and the remote buoy. In this technique the buoy would be equipped with a transponder system which would be interrogated by means of short pulses on a short duty cycle transmitted repetitively by the shore based station. When the radio propagation conditions are suitable, and the interrogation pulse is able to reach the buoy, the buoy transponder would send out a pulse to the shore station. The received pulse signifies that the communications path is for the time being open between the two stations. The shore based station then would send a coded request to the buoy to transmit its stored information. When this cycle is completed, the shore based station then seeks to interrogate another buoy, etc. This particular system is based upon the fact that when a given transmission channel becomes open between two stations it may be expected to remain open for a period of from four to five minutes. If suitable recording and memory systems are on board the buoy, it is quite practical to count on interrogating the buoy at some time during a given 24-hour period. However, it is quite apparent that one cannot establish over a long period of time precisely when it will be possible to interrogate the buoy, and the memory system must take such variables into account.

There is an additional alternative to the above-outlined system, which is recommended by the Canadian Defence Research group, and that is to have available a selection of a wide range of radio frequencies for such a communication system and that the shore based interrogation system transmit an interrogation pulse in sequence through the different assigned frequency bands. This means, of course, that the remote buoy must have a somewhat more sophisticated receiving system, i.e., one which can listen simultaneously on all of the expected frequency bands. However, if such a system is used, the assurance of being able to effect communication with the remote station when desired is tremendously improved. This latter method is the method which apparently receives the most favorable recommendation by the Canadian group.

It is quite possible if such a system as proposed were used that it would involve substantial modifications in methods of licensing. This is considered to be beyond the scope of this discussion and will not be further considered.

Whether we like it or not, the research institutions find themselves involved in the problem of obtaining space in the electromagnetic communications spectrum. Since we have not been notably successful in the past in obtaining suitable radio frequency assignments for research programs, it appears that we should turn our attention to methods of operation which will not be conflicting with existing operations.

The problem of non-interference with existing services is an extremely sticky one. An installation for the collection of oceanographic information now beinginstalled in the Gulf of Mexico by Mr. Roy D. Gaul of the Department of Oceanography and Meteorology, A. & M. College of Texas, has encountered an entirely new series of headaches from the standpoint of the oceanographer. It so happened that the area in which it was planned to locate the telemetering system was physically in an overlap area between Patrick Air Force Base Missile Range and Eglin Air Force Base Missile Range, and it appeared to be almost impossible to find a suitable means of using any radio frequencies which would be considered acceptable by the Air Force.

After considerable difficulty, Mr. Gaul has worked out a temporary arrangement for operation which meets with approval of the Air Force representatives concerned. A significant point which his operations raise, however, is the problem faced in major buoy programs in both the Atlantic and the Pacific Oceans which undoubtedly will run afoul the Atlantic Missile Range and the far more extensive Pacific Missile Range. We are already having problems in the San Diego area with respect to interference by transmitters in the San Diego area with the Pacific Missile Range operations. These are considered serious and they are by no means resolved at the present time.

Looking first at techniques which would permit buoy operation, we have considered the possibility of systems which would permit the use of relatively low-power transmitting systems in the buoys. Perhaps the most available method at present to begin to solve the buoy-shore communication problem, and evolve a method which could be put into effect with existing technical facilities, is the use of high flying aircraft to serve as an interrogation platform for communicating with floating buoys, etc. This would permit the use of relatively low-power radio transmitters in the buoys and a relatively simple information storage system. The high flying plane would transmit a suitable coded interrogation pulse which would insure the response of the desired buoy. Since the airplane would be carrying a suitable recording system, such as magnetic tape, the information transmitted by the buoy could be recorded as desired. In this system it would be planned to have the data processed at the conclusion of the flight. Difficulties with this system are not to be minimized since it requires the availability of suitable high flying long-range aircraft, as well as the necessary operating bases. However, it would be possible to carry out some fairly extensive programs with existing bases and aircraft. It should also be pointed out that suitable radio frequency assignments must be made if communications of this type are to be carried out. Unquestionably, a suitable long-range aircraft for our purposes would be the U-2, which satisfies many of our basic requirements. Whether the plane would actually prove adequate for such operations, remains to be seen.

Another and most promising system for long-term operation is to be found in the various types of communication satellites. For practical purposes we may discard the passive satellites of the ECHO type, since this involves very large high power and highly directive antenna systems which are quite impractical on buoys, and, for that matter, even on ships the size of oceanographic research vessels. The active satellites, however, would appear to be useful. The satellites which are planned on being programmed for orbits between 5,000 and 6,000 miles will undoubtedly require powers that are not readily available to small floating buoys and instrument stations. However, these satellites can be counted upon for communicating between ships and shore bases using stabilized dish-type antennas. It would thus be possible to transmit a very large amount of data with high reliability from ship-to-shore and vice versa using the satellite system. This would mean that it would be possible to send data directly ashore for data analysis as desired. The active satellites which are referred to for this type of data relaying operate in real time. Another type of satellite known as the COURIER type is perhaps the most adaptable under the present basis of operation. The COURIER type of satellite does not retransmit radio signals in real time, but involves a memory system. The COURIER satellite is planned on being programmed to a much lower orbit, namely, the range from 300 to 400 miles. Since it is much lower, it will require a great deal less power to effect reliable communication between buoy and satellite. At present the COURIER type of satellite is designed to record information received via radio and play it back on proper interrogation from the ground based station. It is considered practical to program the COURIER type of satellite to interrogate buoys as it passes over various portions of the ocean and then to playback the data obtained from the buoy when it passes over a suitable land based station. The land based station would be able to keep a longer contact with the satellite, since it would have a much superior antenna system than that possessed by the floating station.

In view of the many difficulties which are found in the use of the conventional portions of the electromagnetic communications spectrum, perhaps we should search out other regions.

A most significant problem presently exists with the proposed use of any of the satellites and this is the fact that there are now tremendous demands upon the electromagnetic communications spectrum that is expected to be available to the satellite systems, and unless the research groups interested in obtaining ocean data make a very strenuous effort to obtain proper frequency allocations, or time allocations, on the communications types of satellites, it is quite probable that none will be available when needed at some future date. It is almost impossible to overemphasize the amount of pressure being brought to bear to obtain communications frequencies in the satellite programs. Since groups interested in collecting data from the ocean are not in any way represented on the committees and boards making such studies, it is imperative that remedial steps be taken along this line as soon as possible.

Since the oceanographers' communication problems extend well beyond the continental limits of the United States, it is apparent that international relationships are involved. This would be true whether high flying aircraft or satellites are used in the solution of the communication problems.

Unfortunately, the groups interested in various aspects of marine research in this country are not organized from the standpoint of representation to the FCC for frequency assignments. Also, there is no voice from the oceanographers in the ICSU (International Council of Scientific Unions), which through the CCIR (International Radio Consultative Committee), reports directly to the ITU, or International Telecommunications Union, for ultimate international frequency allocations.

So much for the background. We have seen something of the problems confronting the oceanographer. We will now concern ourselves with the current status and what is being done. As of June 29, the National Academy of Sciences Committee on Oceanography, acting for the oceanographic and meteorological community, voted to initiate a formal study of the problem. The direct responsibility is placed with the Panel on New Devices which serves as a sub-committee.

An engineering firm has been retained to assist in delimiting the engineering requirements from the inputs supplied by oceanographers and meteorologists. After the preliminary study is complete, the report will be studied by the Panel on New Devices and plans developed to carry out the major program, which is the development of engineering requirements for the justification of a new type of service in the field of radio communication. It will be necessary to work up a complete case which may then be ultimately presented to the FCC.

The major engineering study will be worked up with the advice and assistance of the National Academy of Sciences Committee on Radio Frequency Assignments for Science. This committee was formed initially to justify the radio frequency requirements of the radio astronomers, and will now be fulfilling a somewhat broader purpose.

The National Academy of Sciences Committee on Oceanography will undertake to check the input requirements from the standpoint of oceanographers and meteorologists, and the National Academy of Sciences Committee on Radio Frequency Assignments for Science will check and evaluate the engineering considerations.

It should be apparent that the entire problem is one of a rather complex sort and that its ultimate, satisfactory solution is of direct interest to industry. Since industry has a definite stake in the field of oceanography and meteorology, it is hoped that representatives of industry will be interested in assisting directly in formulating and recommending possible systems which may assist in the solution of our communications problem.

The areas to be covered are essentially those of the oceans, so that in effect we require world-wide coverage. As an example of the numbers of unattended ocean instrument stations or buoys which may be required the figure of 100 buoys for the northeast Pacific, i.e., the area east of 180° and north of the Equator may be used. It is felt that this is a somewhat conservative figure. This does not, however, include special buoys and instrument stations for studying short-time projects, but rather represents the number which would be necessary for routine, relatively long-time programs. Integrated into this are also the requirements of the ship-to-shore communications, ship-to-ship, ship-to-buoy, buoy-to-ship, etc. It is quite probable that multiple solutions to the problem exist but major efforts will be centered toward determining what system, or systems, appear to be most suitable for the purpose. We earnestly solicit assistance from industry and research laboratories and will welcome serious recommendations and suggestions.

REFERENCES

1. "The Floating Automatic Weather Stations of the United States Navy," Weatherwise, Vol. 12, No. 5, October 1959.

THE SVTP INSTRUMENT AND SOME APPLICATIONS TO OCEANOGRAPHY

by J. R. LOVETT
Oceanic Research Division
Research Department
U.S. Naval Ordnance Test Station
China Lake, California

ABSTRACT

In the SVTP instrument, sound velocity is measured by a modified NBS "sing-around" velocimeter, temperature by a Wien-bridge oscillator, and pressure by a Vibrotron.

The sound-velocity section may exhibit shifts in calibration of about 2.25 m/sec unless adjusted correctly and then calibrations are stable within 0.15 m/sec. The temperature oscillator is accurate to ±0.01°C for periods of several months. The Vibrotron has a short-term repeatability of 0.25% of bandwidth.

Data processing systems consist of counters, discriminators driving X-Y plotters, and tape recorders with data later digitized or displayed on X-Y plots.

Some applications in oceanography are in fathometry and internal wave studies.

DESCRIPTION OF THE INSTRUMENT

A sound-velocity, temperature, and pressure (SVTP) instrument was built at the U. S. Naval Ordnance Test Station (NOTS) to give continuous, concurrent measurement and data transmission of these three oceanic parameters at any depth (Fig. 1).

This completely transistorized instrument uses potted plug-in modules. The modules use the new welded-cordwood stacking construction for greatest reliability in the smallest space (Fig. 2).

The sound-velocity section of the instrument is the velocimeter developed by Greenspan and Tschiegg of the National Bureau of Standards and modified to operate in IRIG telemetry band 8 (3,000 cps center frequency). This is achieved by decreasing the free-running frequency and increasing the path length to 24.7 cm. Care must be taken in setting the reflective path length, or the instrument may exhibit shifts in calibration of about 2.25 m/sec due to the input triggering on a precursor of the 3-megacycle pulse (Fig. 3). The connection between the amplifier and the triggering circuit is broken thus disabling the sing-around circuit. Leads are brought out to adjacent pins on the plug. Then the output of the amplifier is observed while the reflectors are adjusted so that the pulse has a good clean rise and there are no multiple reflections. When the desired waveform is obtained, the two pins are connected in order to trigger the blocking oscillator. There is a provision made to add negative feedback if the amplifier stages are oversensitive. The sound-velocity section is accurate to 0.30 m/sec and has a repeatability of 0.15 m/sec.

Temperature is measured by a thermistor-controlled Wien-bridge oscillator developed at NOTS. This oscillator works in the temperature range 0-30°C and in the frequency band 5,000-8,000 cps, thus giving a sensitivity of 0.01°C per cycle per second. By using aged thermistors, capacitors stable to less than 10 ppm/°C, and other techniques, the accuracy is ±0.01°C. Maximum variation from a best straight line 5-20°C of ±0.02°C is achieved by a 3-point match of the oscillator and thermistor curves.

The Vibrotron is used for pressure measurements in the SVTP instrument; however, there is some uncertainty as to the future availability of this transducer. Pressure is sensed by deformation of a diaphragm that in turn produces a change in tension, and, hence, in frequency (IRIG band 12) of a vibrating wire. A simple oscillator is used to sustain the forced vibrations. Repeatability, short term, is ±0.25% linearity is within ±3% of a straight line between end points; and temperature sensitivity is less than ±0.1% of bandwidth per °C change of zero frequency.

A summing cable-driving amplifier combines the sound-velocity, temperature, and pressure signals so that they may be transmitted as a mixed frequency signal over a single-conductor cable. Six thousand feet of semi-buoyant polyethelene covered cable with a breaking strength of 900 pounds has been used. When in sea water it acts like a 50-ohm coaxial cable, and if driven with a matched amplifier, the voltage loss at 10 kilocycles is 2 db/1,000 ft. When on the winch, capacitance of the cable is negligible while the inductance is about 310 millihenries. At 10,000 cps, this inductance gives an impedance of about 20,000 ohms. Therefore, to avoid an intolerable voltage loss, a high input impedance amplifier must be used to drive the filters which separate the signals.

Nickel-cadmium batteries are internally

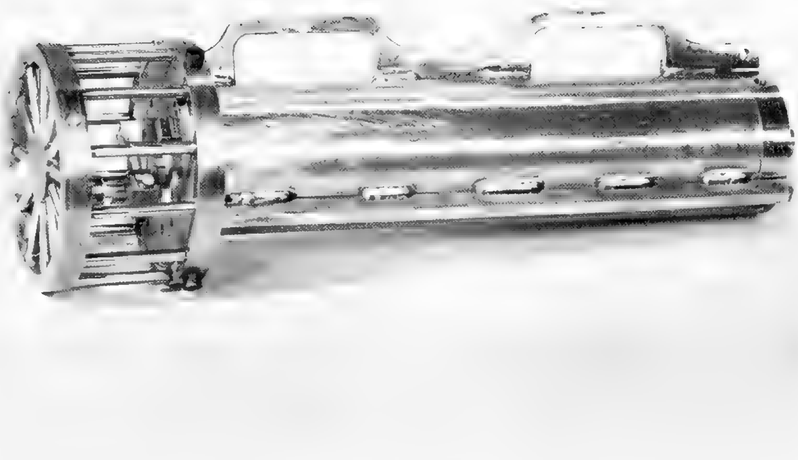

FIG. 1. [illegible]

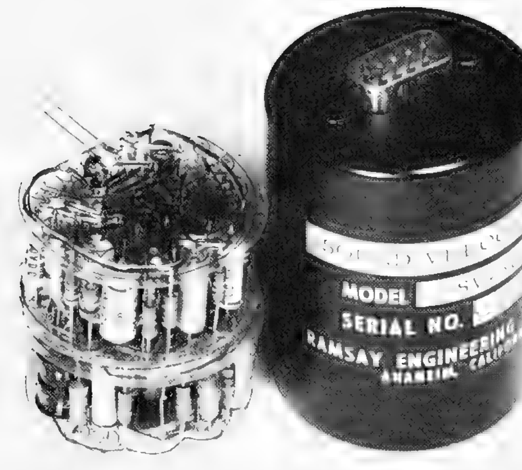

FIG. 2. Sound Velocity Oscillator Showing Welded-Cordwood Construction.

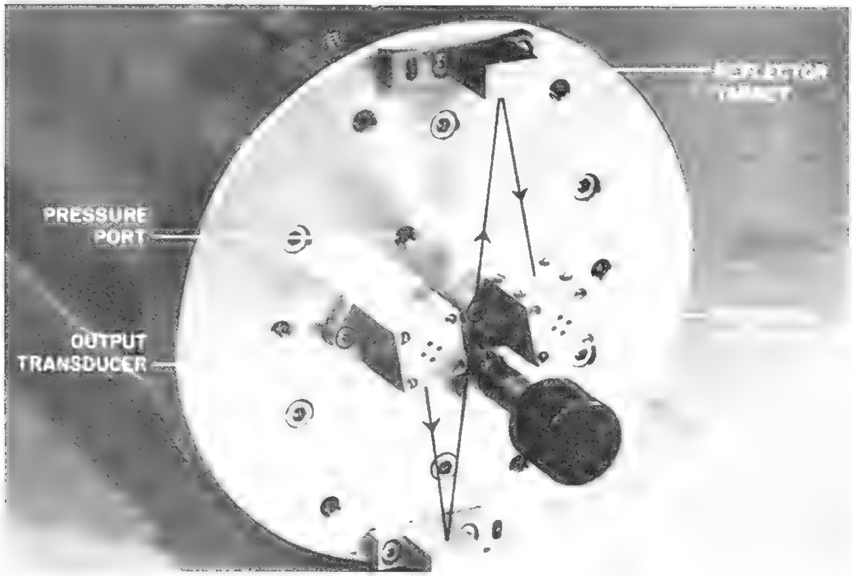

FIG. 3. End Plate With Reflected Sound

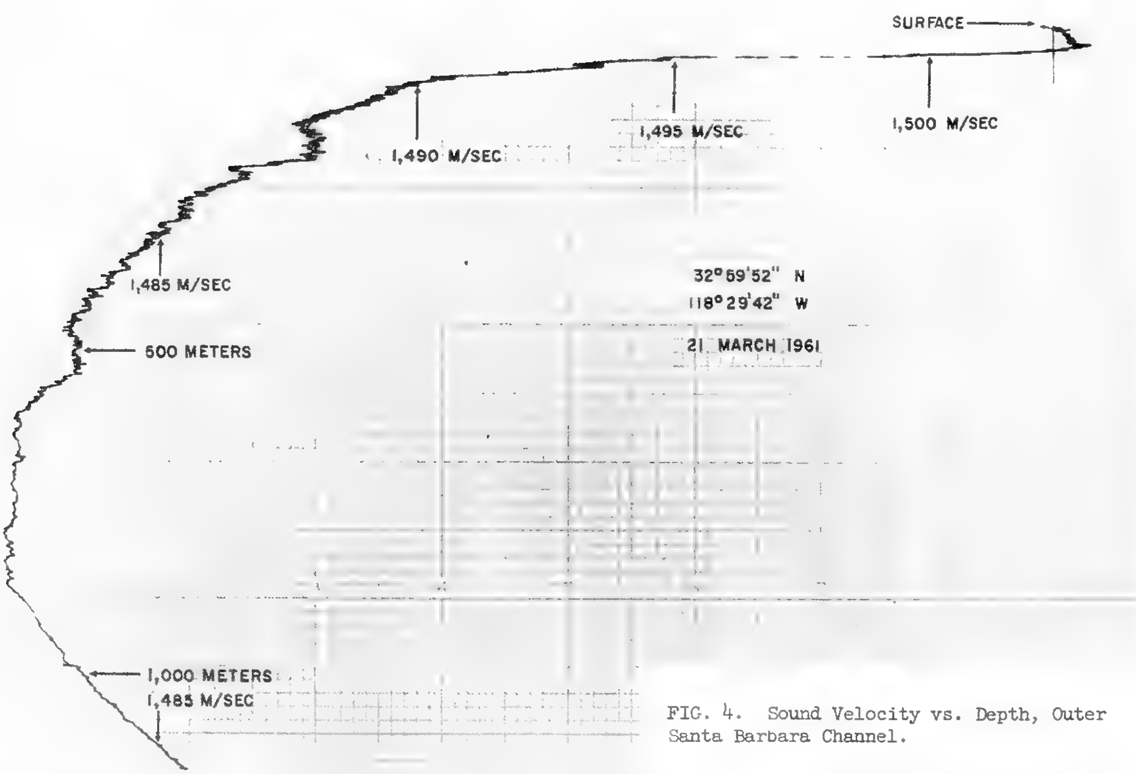

FIG. 4. Sound Velocity vs. Depth, Outer Santa Barbara Channel.

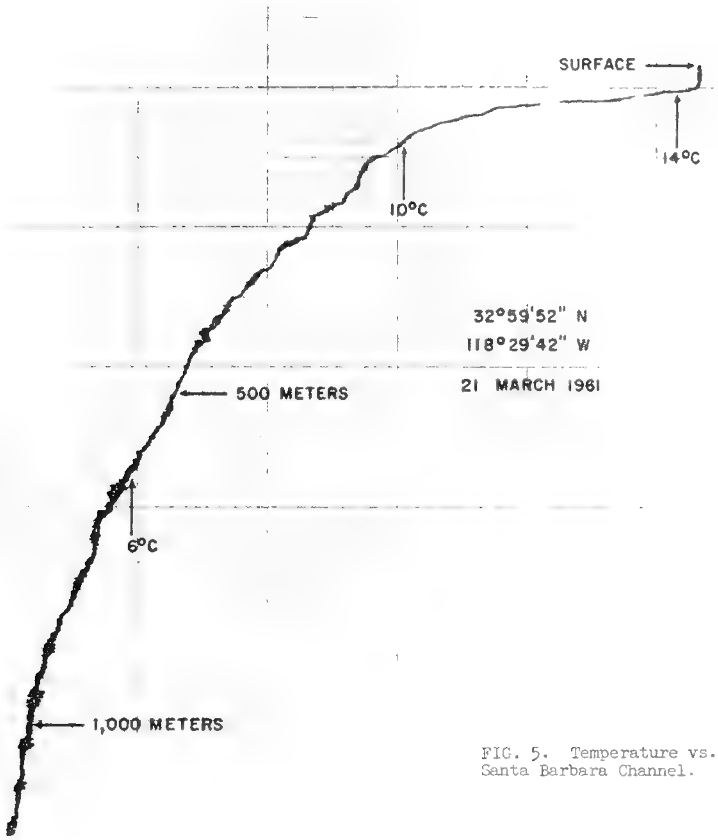

FIG. 5. Temperature vs. Depth, Outer Santa Barbara Channel.

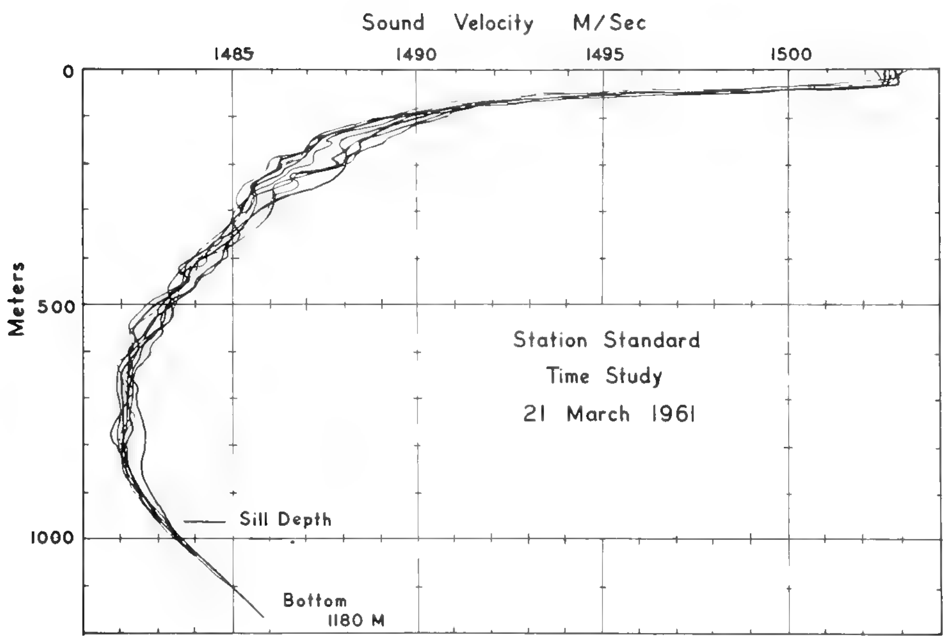

FIG. 6. Sound Velocity vs. Depth, Outer Santa Barbara Channel. Time Study, 21 March 1961.

mounted, and are recharged through use of gravity-actuated mercury switches.

DATA RECORDING AND PROCESSING SYSTEMS

Counters are always used for a visual check of the frequencies and for precise end-point measurements.

Three FM discriminators driving two X-Y plotters have been used for immediate visual display of the data (Fig. 4 and 5). Four-track tape recordings are also made with a precise 25-kc reference frequency recorded on one track. (Voice data may also be recorded on the same track.) The tapes are recorded at 15 ips and played back at 60 ips into the NODAC analog-to-digital converter. The IBM 7090 computer can linearize the Vibrotron output and utilize the temperature data to compensate the sound-velocity data for path-length changes due to temperature. The data may be printed digitally with time information, or digital X-Y plots may be made.

APPLICATIONS OF THE SVTP INSTRUMENT

Two of the uses to which the SVTP instrument has been put by NOTS are given below.

In fathometry, sound-velocity measurements to the bottom have yielded information for correcting a precision fathometer that assumes a sound speed of 4,800 fps.

A study of the time variation in the distribution of sound velocity with depth at fixed stations has been made in the Outer Santa Barbara Channel. X-Y plots were made every 2 hours for 36 hours down to the bottom of the basin, 1,180 meters. Sound profiles obtained showed considerable activity in the water above the sill depth of 970 meters (Fig. 6). The observations obtained suggest a tidal influence with a semi-diurnal periodicity. Previous observations in the Southern California waters indicate a high degree of variability due to internal waves. Present measurements made with the SVTP instrument are too widely spaced to detect the shorter periods of such internal waves. More rapid sampling is planned in future studies.

BIBLIOGRAPHY

a. Greenspan, Martin, and Carroll E. Tschiegg. "Sing-Around Ultrasonic Velocimeter for Liquids," REV SCI INSTRUMENT, Vol. 28, No. 11 (Nov. 1957), pp. 891-901.

b. Tschiegg, C. E., and E. E. Hays. "Transistorized Velocimeter for Measuring the Speed of Sound in the Sea," ACOUS SOC AM, J, Vol. 31, No. 7 (July 1959), pp. 1038-1039.

c. U. S. Naval Ordnance Test Station. An Instrument for Continuous Deep-Sea Measurement of Velocity of Sound, Temperature, and Pressure, by J. R. Lovett and S. H. Sessions. China Lake, California, NOTS, 9 May 1961. (NAVWEPS Report 7650, NOTS TP 2673.)

THE WORLD'S LONGEST SALT BRIDGE

by DR. PAUL C. MANGELSDORF, Jr.
Woods Hole Oceanographic Institution
Woods Hole, Massachusetts

ABSTRACT

A variation of the Geomagnetic Electrokinetograph has been developed in which the electrodes remain aboard ship immersed in sea water at constant composition and temperature. The electrical connection to the sea is made with lengths of polyethylene tubing filled with sea water. This arrangement greatly reduces the sensitivity of the system to gradients of salinity and temperature in the sea. It also permits a direct electrode zero by means of a sea water shunt between the two electrodes.

INTRODUCTION

It was Faraday, in 1832, who first pointed out that the motions of flowing water masses in the earth's magnetic field might be detected by the measurable EMFs which such motions ought to induce.[1] Although Faraday was himself unable to verify the effect, his predictions were amply confirmed by later observers. Ultimately, in 1950, Von Arx reported the successful development of a practical instrument, which he named "Geomagnetic Electrokinetograph", for measuring the motionally induced potentials in the ocean.[2] The theoretical interpretation of these potentials was also developed by Von Arx in the same paper; by Malkus and Stern[3]; and by Longuet-Higgins, Stern, and Stommel[4].

The biggest problem in measuring electromagnetic potentials in the ocean arises from the fact that most measuring circuits are metallic and conduct electricity by means of free electrons. Sea water is an electrolyte solution which conducts by means of assorted ions, both positive and negative. Any metallic electrode inserted into the ocean as a probe can only function with the occurrence of one or more electrode reactions involving both ions and electrons. Such electrode reactions will be sensitive to temperature, to pressure, to ionic concentrations (i.e. salinity), to contamination (z.b. oxygen tension). Moreover, if any of the participating reactions are at all irreversible, the electrode will be polarizable and its contact potential will change as current is passed.

To overcome these difficulties, Von Arx used massive silver/silver chloride electrodes which are reasonably reversible to chloride ion in sea water (though they are probably poisoned somewhat by sulfate and bromide ions which are also present[5]). By taking great care to match each pair of electrodes as exactly as possible, Von Arx was able to minimize the differential responses to temperature, salinity, and oxygen tension which would cause spurious signals. But even the best electrode pairs displayed small, slow, residual drifts in contact potential, which could only be evaluated by interchanging the positions of the electrodes in the water. With towed electrodes, the simplest way to do this, though time-consuming, has been to reverse the ship's course.

This system of towed silver/silver chloride electrodes has proven quite successful and has been widely used during the past decade for determining the horizontal potential gradients at the surface of the ocean. However, it is quite unsuitable for measuring vertical potential gradients. Two electrodes at different depths will automatically sense the corresponding differences in pressure, salinity, temperature, and oxygen tension, and will report these as large spurious potential differences. But, according to Malkus and Stern, the vertical potential distribution in the ocean would also be extremely valuable, if it could be measured, since it would yield directly the total east-west transport at the point of measurement.

THE SALT BRIDGE PRINCIPLE

After these difficulties had been drawn to our attention by Dr. Malkus, it occurred to us that there ought to be some advantage in moving the electrodes with their very sensitive metal/electrolyte junctions up out of the ocean entirely, and keeping them in a controlled environment on shipboard. The electrical contacts with the ocean could then be made with columns of salt solution contained in insulating tubing of some sort. This is exactly the principle of the salt bridge - a familiar device frequently used by electrochemists to avoid dipping an electrode directly into a solution, if either the electrode or the solution would suffer thereby.

Superior numbers refer to similarly numbered references at the end of this paper.

Any kind of electrolyte solution could, in principle, be used in such a salt bridge. However, the boundary between two different electrolyte solutions has a contact potential, called a liquid junction potential, somewhat analogous to that between an electrode and a solution, though much less sensitive. While the traditional use of concentrated potassium chloride in laboratory salt bridges is supposed to minimize such liquid junction potentials, we preferred to eliminate them entirely, if we could, using sea water throughout.

CHOICE OF TUBING

The conductance of standard sea water is only .03-.05 $(\text{ohm-cm.})^{-1}$. The resistance of a long, thin column of sea water is large and increases with length. The electrical leakage path from such a column through the walls of an insulating tubing to sea water outside should be slight, but will increase with length. The net result, barring pronounced local leakages, will be that a sea-grounded DC signal fed into an infinite length of tubing filled with, and surrounded by, sea water - or any other conductor, for that matter - will damp out exponentially according to the formula

$$V = V_0 e^{-\sqrt{SR}\, x} \qquad (1)$$

where S is the leakage conductance per unit length through the walls of the tubing, R is the resistance per unit length of the sea water column, x is the linear distance along the tubing.

The damping length $(SR)^{-\frac{1}{2}}$, thus defined, depends on the specific bulk resistivity ρ, the thickness τ, and the internal diameter d of the tubing, as well as on the specific conductivity σ of the sea water column according to the following approximate relation:

$$(SR)^{-\frac{1}{2}} \simeq \left(\frac{\sigma \rho d \tau}{4}\right)^{\frac{1}{2}} \qquad (2)$$

We have determined the damping lengths with sea water of a number of assorted samples of readily available tubing, with the results given in Table I. It is evident from the Table that polyethylene tubing is the most suitable for long distances. Since the polyethylene, at 2.7 cents/ft., was also the cheapest of the tubings we tested, and since it is quite inert chemically and very tough physically, the choice was not difficult. The polyethylene tubing as supplied by the manufacturer (Crystal-X Corporation, Lenni Mills, Pa.), came in assorted lengths, some 500, 1000, and 2000 lengths, but mostly 100 ft. lengths. We found that new and unused lengths of this tubing could be easily welded together by heating the ends over a gentle flame until they became transparent and sticky; and then joining them together with a little pressure causing them to flare out slightly. Quenching with cold water speeds the hardening. A well-formed joint of this kind does not appear to weaken the tubing either physically or electrically.

Once the tubing has been exposed to sea water, however, these welds do not take very well, even when the two ends have been well cleaned in all the different ways we could think of. Some improvement can be had by sloshing the two ends in mineral oil before heating, but the joints are still likely to be bad and should be tested carefully before they are used.

The 5/16" o.d. polyethylene tubing which we have used proved to be very well suited for towing. It is buoyant, even when filled with water, and snakes along very freely on the sea surface. The small diameter and smooth surface help keep the towing resistance very low. At 10 knots in a moderate sea, a 200 meter length of tubing can be held with one hand without too much difficulty.

The breaking strength of this tubing is about 200 lbs.

To connect the polyethylene tubing to glass tubing, or to make temporary connections between two lengths of the polyethylene, we have used short lengths of snug-fitting (¼" i.d.) tygon tubing as couplings. Because polyethylene, like most insulators, develops a markedly conducting surface film after sea water has dried on it, such connections tend to be very leaky electrically unless made with clean tubing. A liberal application of mineral oil to all surfaces prior to making the connection seems to help a little. In any case, electrical leakage can be expected if the connection has borne the 20 lbs. pumping pressure for any length of time: some seepage evidently occurs. For this reason, the welded connections are decidedly preferable for connecting polyethylene pieces to one another. Glass-to-polyethylene connections should be kept well insulated in dry surroundings.

CIRCUITRY REQUIREMENTS

Sea water is not a very good conductor. A 3/16" i.d. tubing filled with sea water offers about a megohm of resistance for every 100 meters of length. This high impedance of a long salt bridge is the biggest single drawback to the salt bridge technique at sea. While high impedance measurements and shipboard working conditions are not totally incompatible, neither are they very congenial. Most insulating surfaces seem to develop leakage resistances of the order of 10^{11} ohms or less when exposed to damp sea air. Such leakage paths are electrolytic; when they connect two different metals, they form electrolytic cells with EMFs of the order of several tenths of a volt. If one of these leakage cells happens to discharge across a circuit element, such as a salt bridge, with a resistance of the order of 10^8 ohms, a spurious signal of the order of several tenths of a millivolt may be developed in the circuit. If by some mischance, such a leakage path makes connections with the shipboard DC power supply, the situation can be many times worse. Clearly extraordinary precautions are called for.

Fortunately the greater part of our circuitry problems have been solved for us in recent years by the electronics industry with the development of reliable high-impedance electrometers. We have found that the Keithly 603 Electrometer Amplifier is very satisfactory in taking a few DC millivolts from a pair of high impedance salt bridges and converting this signal to a low impedance output of several volts. The Keithly performance seems to be quite immune to the damp salt air and power supply fluctuations of shipboard operation.

THE ELECTRODE SYSTEM

As the whole advantage of the salt bridge system arises from the thermal and chemical isolation of the electrodes, it follows that the actual electrode arrangement is very important. The system we have employed is shown in Figure I.

The electrodes are sealed into pyrex electrode chambers immersed in an oil-filled thermos flask. Each electrode chamber connects to a 3-way stopcock, permitting it to connect down to the sea or up to an inverted-Y shunt, or to be cut off from the circuit entirely. The inverted Y leads up to a third 3-way stopcock by means of which the sea water in the system may be admitted and manipulated. The temperature in the thermos flask is not regulated, but is allowed to drift in a gradual pursuit of the ambient room temperature. The fishhook shape of the electrode chambers is intended to protect the electrodes from sudden exposure to colder or saltier (i.e. denser) water that may make its way down from the stopcocks by convection. As long as no sudden changes occur at the electrodes, the long term drifts can be followed easily by means of the inverted-Y shunt.

THE SEA WATER SHUNT

This inverted-Y arrangement provides the one unique feature of the salt bridge system which promises to give it greatest usefulness. By raising the water levels on both sides until they join at the Y, a low impedance sea water shunt can be established between the electrode compartments, permitting the electrode zero to be determined quickly and directly. By lowering the water level the shunt is broken and the measurements of sea voltages may be resumed. In this manner the unknown, and slowly drifting, contact potentials of the electrodes can be determined as often as may be needed during any set of measurements. In towing experiments, the burdensome procedure of reversing the ship's course can be dispensed with, although right-angle legs will still be necessary if both components of the surface potential gradient are to be determined.

DETAILS OF CONSTRUCTION

We have used the conventional G.E.K. silver/silver chloride electrodes developed by Dr. von Arx, several of which were kindly provided for us by his assistant Mrs. Nellie Anderson. These are sealed into the pyrex electrode chambers with epoxy cement.

The 1-liter thermos flask filled with mineral oil is closed with a wooden lid saturated with oil and coated outside with paraffin. The flask is mounted in a wooden carrier which is also liberally smeared with paraffin.

The 4 mm. standard taper pyrex stopcocks are used only as hydraulic switches; they do not provide effective electrical switching because their leakage resistance between branches is usually less than a megohm. They do protect the electrodes from the hydraulic pressure variations which occur when the lines are drained or filled. These stopcocks are wired to a sheet of paraffin-coated masonite mounted on the frame of the wooden carrier.

All the glass-to-glass connections, as well as the glass-to-polyethylene connections are made with tygon couplings for flexibility and shock resistance.

The tygon leaders in the branches of the Y are especially important, since they provide the necessary high impedance when the Y is drained and the shunt broken. Most materials, including glass and polyethylene, tend to form moist, juicy, highly conducting surface films when repeatedly exposed to sea water. Fortunately, tygon seems to be entirely immune to this. We have found that a tygon Y will drain quickly to something like 10^{11} ohms after having been filled with sea water for 60 hours.

Our high pressure sea water supply is provided by a little centrifugal pump, Eastern

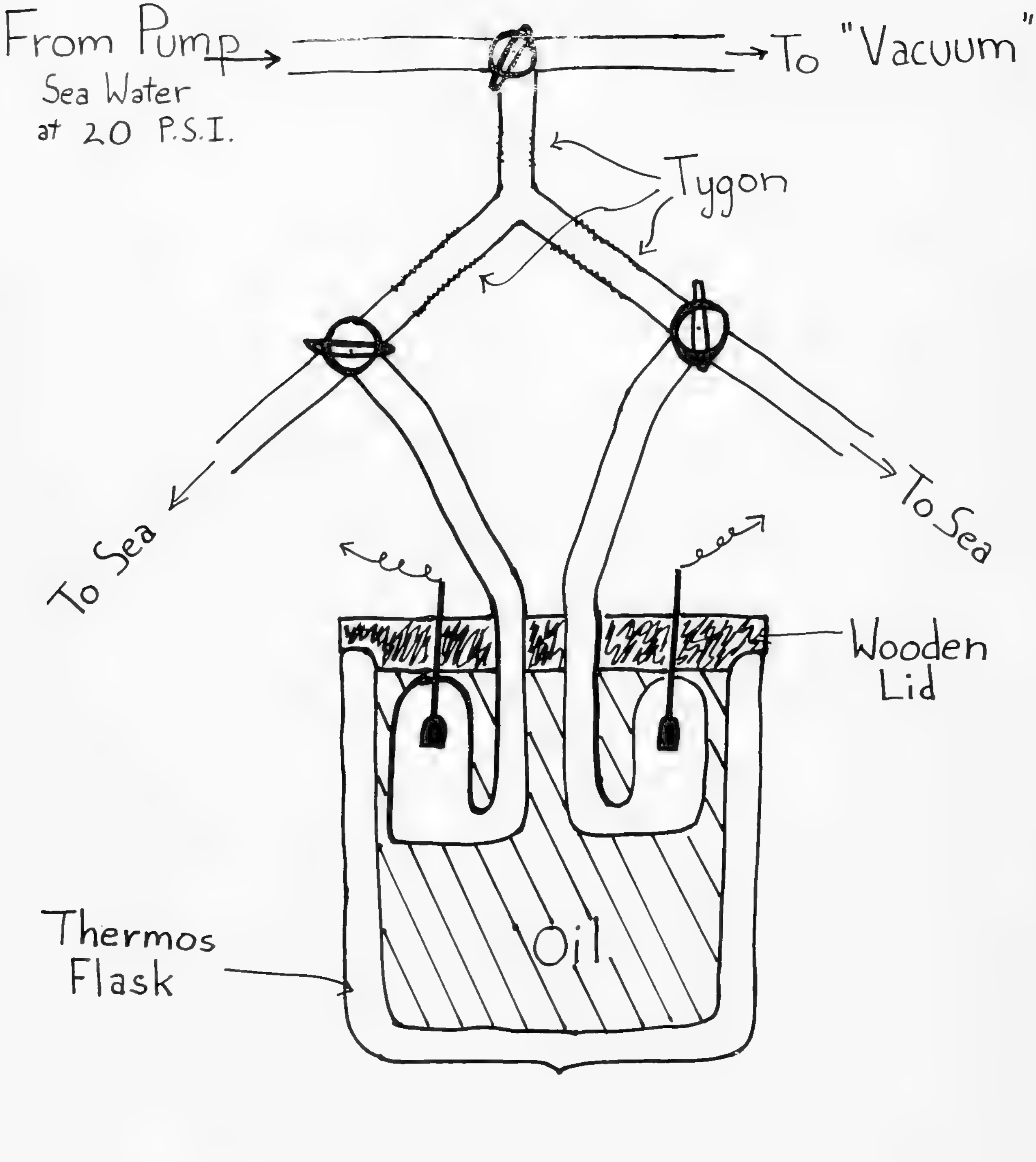
From Pump
Sea Water
at 20 P.S.I.
To "Vacuum"
Tygon
To Sea
To Sea
Wooden
Lid
Thermos
Flask
Oil

FIGURE I

Industries, Inc., Model E-1 with Monel fittings, which is mounted on the side of the carrier. This pump gives a no-flow pressure of about 20 psi, which is adequate for moderate lengths of tubing. However, the filling time of a piece of tubing goes up as the square of the length; it took us an hour and forty minutes to pump through 1 kilometer of our polyethylene tubing.

In our apparatus the "vacuum" indicated in Figure I is provided by the experimentalist. With a 12 or 15 foot drop to water level, the necessary suction may be too much for anyone who is not an experienced pipe smoker. Mechanical alternatives are available.

BUBBLE TRAPS

Bubbles in the line can be a serious problem. Even when they do not break the electrical continuity entirely, they can raise the impedance to a point where leakage voltages dominate the signal. Fortunately, no bubbles can arise or persist in tubing that is well submerged. Even quite long bubbles in a line filled on deck will disappear completely if the line is dropped 20 or 30 meters below the surface. Nor do bubbles seem to form or collect in floating lines being towed at the surface of the water. Most of the bubble trouble occurs in the lines on deck (or on shore) which carry a negative hydraulic head because of their height above sea level, and which may be exposed to the heat of the sun. The high permeability of polyethylene to atmospheric gases may also contribute to bubble formation.

We have found it convenient to introduce glass bubble traps into the lines at points of greatest elevation. These permit quantities of gas to collect without breaking the circuit. A valve in each trap allows the gas to be withdrawn periodically. These traps also prevent accidental bubbles from being pumped into lines during the initial filling. Because these bubble traps require breaking into the polyethylene line, they are potential sources of leakage voltages and should be carefully insulated from accidental electrical contacts.

It is useful to have an auxiliary electrode in each line so that one can test for continuity to the sea with an ohm-meter, without passing current through the operating electrodes. A platinum wire electrode sealed directly into a pyrex bubble trap, and plated with silver/silver chloride serves this purpose very nicely.

With towed lines one has to worry about bubbles which may enter the open end of the line which is dragging at the surface. A narrow piece of torn bed-sheet, wrapped several times around the end of the line so as to form a sort of tubular wick two or three feet long dragging behind the line, is apparently enough to solve this problem.

GROUNDING

With the Keithly 603, the ground connection serves as a common input for both high impedance leads. Between the ship and the sea there may be large fluctuating potential differences due to corrosion, or electrical leakages. Even with the large in-phase rejection of the Keithly instrument, such a ground signal is unacceptable. To get around this, we isolate all of our electronics from the ship, except for AC power, and use a towed G.E.K. electrode for a single common ground directly to the sea.

This arrangement produces considerable AC pickup, but the AC can easily be kept out of the electrometer by connecting the inputs to ground with by-pass capacitors.

OPERATING PROCEDURE

The salt bridges must first be filled with sea water. It is safer to start with a completely empty line; otherwise a small amount of water will tend to collect in the low spots in a line and one may discover that one has inadvertently created enough U-tube manometers connected in series to defeat the pump's best efforts. If the line is on a reel, the reel can be turned on its end; if the line is weighted to the bottom of a channel, and is looping gently from weight to weight, one has a nasty problem.

After the lines are full the pump is turned off and disconnected, and air is admitted into the Y to drain the shunt. The lines are separately tested for continuity. The line resistances ought to be perfectly steady and proportional to the line lengths. Otherwise one looks for a bubble or a leak.

If the lines are all right, the water levels are drawn back up in the Y to form the shunt, and the electrode zero is determined. The adjustable zero on the Keithly 603 permits one to make this initial electrode zero coincide with the zero on a chart recorder. Since the electrometer zero will drift slowly with time, even more than the electrode zero, it is also desirable to record the signal produced by shorting the electrometer inputs together. The difference between this signal and the electrode zero is due to the mismatch between the two electrodes. It will be small and will change slowly and steadily with time, unless the electrodes have been mistreated in some way.

When the zero has been determined the Y is drained, the electrode chambers are connected directly to the sea, and the recorder output should give true sea-voltages without correction.

Excessive wave signal can be eliminated by crossing the inputs with a capacitor. One of the few advantages of the high impedance of the salt bridge circuit is the small amount of capacitance required to give a long time constant.

If a salt bridge line is relatively dry and clean, it will pick up an external electrostatic charge when brushed or touched, which will show up as a sharp pip on the chart record. This is not usually objectionable.

THE PROOF OF THE PUDDING

Our first successful measurements using the salt bridge technique were made on a stationary line strung across the bottom of Woods Hole harbor from the home of Allyn Vine on Juniper Point to the dock on Mink Point, Nonamesset Island; a distance of 875 yards. The line itself was about 1000 yards in length, weighted with 10 lb. sash weights every 16 ft. (When we later took up the line we decided that one such weight every 100 feet would have been ample, except in shallow water.) We made a continuous recording, with several interruptions, from July 21 to August 9.

On several occasions the signal was blocked by bubbles, which probably could have been prevented if we had used bubble traps. On another occasion the pump was inadvertently and disastrously connected to an electrode chamber instead of to the short line which was to be pumped free of bubbles. We had to close down for two days while we repaired the damage and modified the design to withstand future mistakes of this sort. Twice the chart recorder ran out of ink. Otherwise the operation was nearly trouble-free.

We were distressed, at first, by the large noise level in our signal. There were large fluctuations a millivolt or more in magnitude, which often continued for many minutes or even hours with no visible physical cause. Sometimes, especially in the early hours of the morning, the fluctuations were beautifully periodic with two or three minute cycles for a half an hour at a time. Sometimes there were no fluctuations at all.

When we showed our records to Dr. von Arx, he immediately identified these disturbances as being due to earth currents associated with magnetic storms. In fact, his original paper on the G.E.K. warns of the possibility of such interference "in shoal waters near the land". When our noise level was compared with the magnetic noise level reported for each three-hour period by the Fredericksburg Magnetic Observatory of the U. S. Coast & Geodetic Survey, the agreement was overwhelming.

The record reproduced in Figure II was chosen as being the quietest 12-hour tidal cycle which we obtained. It also happens to be the quietest such period in the magnetic records. While it is atypical in this respect, we believe it to be a fair reflection of the intrinsic precision of the instrument and the method.

The pronounced disturbances occurring between 1715 hrs. and 1830 hrs. on July 30 are recurrent with a 24-hour period, as can be seen by a comparison with the juxtaposed record of the corresponding period on the preceding day. They are caused by the ferryboats which operate out of Woods Hole to Nantucket and Martha's Vineyard. Like most large vessels, these steamers produce strong electrical fields in surrounding water due to bottom corrosion or electrical leaks. The sharp pulses correspond to ship passages across our line. The half-hour long prolonged 2-millivolt downward shift is due to the steamer Nantucket, as she stands at the wharf 250 yards away with her stern facing us, waiting for the Islander to leave the ferry slip. When the Islander leaves (sharp downward peak), the Nantucket is warped around into the slip and her signal vanishes. The later downward peak is the Nantucket crossing our lines going out.

The R.V. Chain creates a similar electrical signal when she is in port, which is why we did not run our line from the Institution dock in the first place. The electrode zero which our instrument permits, is of small value when an unknown stationary signal of such origin exists in the water.

To test our zero, we examined our measured voltages at the times of slack water in Woods Hole channel as predicted in Eldridge's tables. During our first week, while the Chain was at sea, these averaged to zero within a tenth of a millivolt. After the Chain returned, the average was off zero by a steady 2 millivolts. In order to get the true zero for the tidally-produced voltages, we were obliged to use these averages to correct for the non-tidal potential drop across the harbor. The true zero, thus estimated, has been drawn in as a heavy horizontal line in Figure II.

In Figure II the full vertical scale is 20 millivolts. Positive signals are due to water flowing westward through Woods Hole into

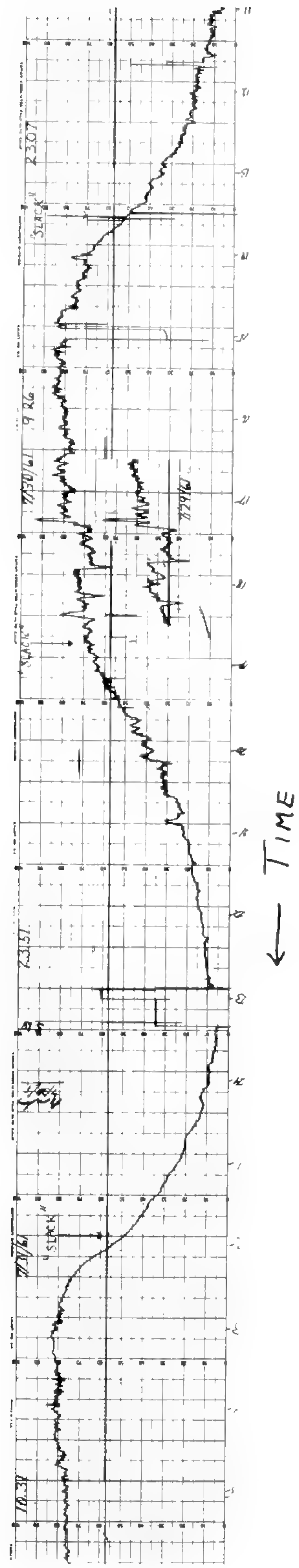

FIGURE II

Buzzards Bay; negative signals are due to water flowing eastward into Vineyard Sound.

There is a pronounced disparity between the amounts of water flowing in the two directions. In this cycle, over two and a half times as much water passed through Woods Hole when the current was running eastward, as had passed through the other way during the preceding westward flow. The inequality is frequently much worse than this, sometimes amounting to four times greater eastward flow than westward. Woods Hole passage acts as a half-wave rectifier!

We were worried that this might be an artifact produced by a change in the flow geometry with the current direction. The G.E.K. output represents an integrated velocity average across the cross section, rather than an integrated flow. A shift in the current from a deep part of the channel will increase the G.E.K. signal. However, there seemed to be no reason to expect such an effect across the harbor where our measurements were made. Moreover, the same asymmetry shows up quite distinctly on the U. S. Coast & Geodetic Survey hourly tidal current charts for all stations in the passage between Buzzards Bay and Vineyard Sound, except the one in the most constricted part of the Hole.

From the U. S. Coast & Geodetic Survey chart of Woods Hole, we estimate the average depth of the channel across our section to be 26 feet at mean low water. From this we reckon that 1 millivolt on our chart is equivalent to a water flow of about 160 cubic meters a second, or 5.7×10^3 cubic feet per second. Accordingly, the maximum westward flow in Figure II is about 860 m^3/sec.; the maximum eastward flow is about 1600 m^3/sec. The total westward flow is about 11×10^6 m^3; the total eastward flow is about 27×10^6 m^3.

Part of this discrepancy arises from the greater duration of the eastward flow; this phenomenon has been nicely explained by Redfield[6]. The remainder of the difference is probably due to the rectifying action of a shallow sill on tidal oscillations. The tidal range in Buzzards Bay is about twice as great as in Vineyard Sound at Woods Hole, so that more water is pumped over the sill to the eastward.

VERTICAL SOUNDINGS

We took the apparatus to sea aboard R. V. *Atlantis* and attempted vertical soundings in the Gulf Stream southeast of Nantucket.

The first lowering was made north of the Stream at *Atlantis* Station 6156, in the vicinity of Richardson Buoy "E". We started with a 6000 foot length of tubing wound on a reel, but could not get an acceptable signal through this. A reel of tubing on deck with a negative internal hydrostatic head presents a standing invitation to bubble formation. We also found it quite cumbersome to have to disconnect the line each time we needed to turn the reel.

We next tried working with a free 250 meter length of tubing with much better results, as shown in Figure III. For this lowering the shorter reference line was weighted and dropped to a depth of 30 meters. The long sounding line was taped to the hydrographic wire, with the weighted end of the line dangling about 10 meters below the lead weight on the wire, so as to avoid electrical pickup from the wire. On this occasion the line was taped to the wire every 20 meters, but we later found that 50 meter intervals were not too long. As the line was brought in again, these tapes were cut. Instead of reeling the line in, we just let it float freely away from the ship in a big loop.

The absence of any voltage gradient below 100 meters in Figure III implies that the water there had no east-west motion relative to the ship: the ship and the water were moving together, if at all. Since the loran log covering this period shows the ship to have moved eastward only about one-fifth of a mile in 4 hours, there would appear to have been very little east-west current.

The very pronounced signal near the surface in Figure III is, of course, due to the ship.

A second lowering was made at *Atlantis* Station 6157 (38°15'N, 68°15'W) well inside the Gulf Stream. The results of this lowering are shown in Figure IV. The reference line in this case went to 15 meters, while the long line extended an equal amount below the hydro wire.

At this station we were greatly troubled by a signal fluctuation amounting to several millivolts with a period of five to ten minutes. It was very difficult to see what changes, if any, were produced as we raised and lowered the line to measure at different depths. Not until we had returned to Woods Hole did we discover that the gyrocompass record of the ship's heading showed similar fluctuations. These were reportedly due to a practice of putting the rudder hard over when the ship was hove to on station: the ship headed up into the wind as she drifted forward and then fell away from the wind drifting backwards. These heading changes could probably have been avoided without too much difficulty, if they were indeed the source of the trouble. However, fluctuations in the wind force and in the resulting wind drift of the

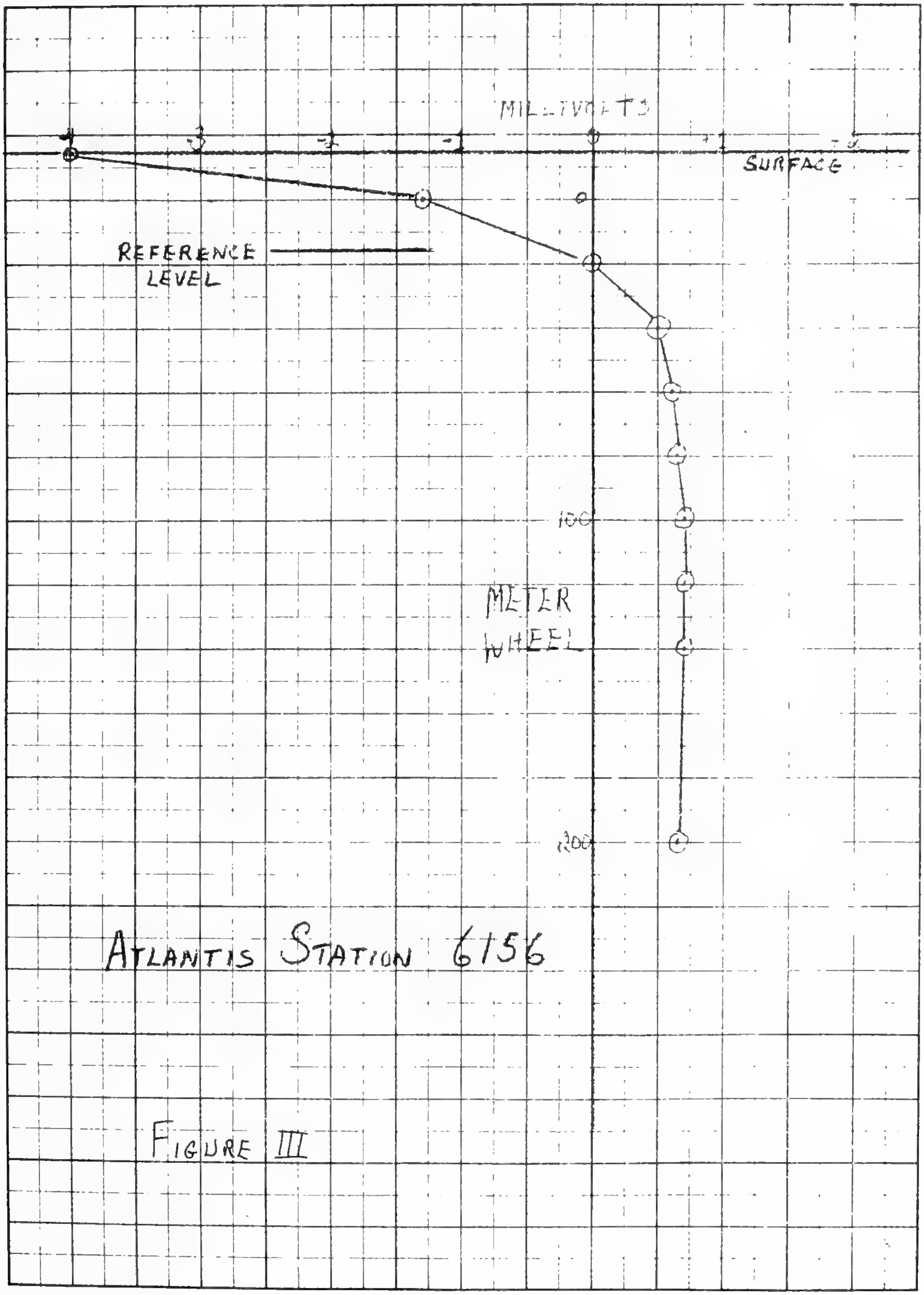
MILLIVOLTS
SURFACE
REFERENCE LEVEL
100
METER WHEEL
200
ATLANTIS STATION 6156

FIGURE III

ship would have had the same effect and could only have been overcome with some kind of sea anchor.

Despite the scatter due to these fluctuations, the points in Figure IV show a distinct over-all trend, especially after the observation nearest the surface has been corrected for the ship's bottom signal by reference to the curve in Figure III. If the profile is taken to be a straight line with a slope of about 1.5 millivolts per 100 meters, one obtains a uniform flow velocity relative to the ship of about 1.5 knots to eastward. There is some suggestion of a steeper voltage gradient at the lower depths, corresponding to an eastward flow of 2 knots or more. These velocities will be somewhat low because meter wheel readings were used instead of the true depths.

It should be emphasized that it is only the east-west component of the flow velocity relative to the ship which is determined directly by vertical measurements of this sort. To obtain the true east-west flow velocity, one must add the eastward set of the ship as determined by loran, by horizontal G.E.K. measurements, or by carrying the vertical measurements to still water at great depths, as suggested by Malkus and Stern.

At this station, the loran determinations gave a set to eastward of 1.7 knots corresponding to a true eastward flow velocity of about 3.2 knots. Horizontal G.E.K. measurements made in the same vicinity several hours after the vertical measurements, indicated a set to eastward of 1.4 knots.

The vertically measured 1.5 knot flow velocity relative to the ship is due, of course, to the wind drift of the ship. Had there been no wind, so that the ship coasted with the Gulf Stream, no vertical potential gradient would have been observed on this shallow lowering. Approximately this situation arose the following day when the next lowering was attempted in the same general area. The estimated loran set was about 3.2 knots to eastward; the vertical voltage gradient, if any, was less than 0.1 millivolt per 100 meters.

Because the results of these three lowerings were grossly misinterpreted at the time, due to the adverse effect of the sea state on the Chief Scientist, the vertical measurements were prematurely discontinued. No really deep soundings were attempted. It now appears that deep soundings could be carried out using the same procedures without difficulty.

TOWING TESTS

For towing experiments of the type customarily made with the G.E.K., we used a pair of lines taped together, one 200 meters long, the other 100 meters long. This gave a 100 meter probe interval towed at 100 meters behind the ship.

Though the polyethylene tubing is nowhere near as strong as the conventional G.E.K. line, it bore up quite well under sustained towing at 10 knots. But it could not, we discovered, take the sudden strain of being brought up short after 100 meters or so had been let out all at once. This treatment snapped 100 meters off the long line of the towing pair during the first tests. As the failure occurred at a welded joint, it is possible that a single continuous line would not have failed.

We had some difficulty in repairing this tubing successfully, since the repair weld was made perforce with tubing which had been exposed to sea water. These joints gave way or sprang leaks with great rapidity. We finally got a weld to hold together permanently by taping the line into a loop, so that the strain by-passed the joint.

With this repaired line, we were able to make a continuous G.E.K. record from the Continental Shelf to Woods Hole harbor. The record was satisfactory in every respect.

Figure V is an excerpt from that record showing the signals obtained on running a square. The pattern shows the expected symmetry around the electrode zero.

SEA WATER THERMOCOUPLE

The sea water salt bridge is theoretically free of first order errors due to variations in pressure, temperature, or salinity. These are all supposed to be the same in both electrode chambers regardless of what may be happening in the sea. There is, however, a possibility of second order errors if the changes in one variable in going around the circuit do not coincide with the changes in another variable.

If one constructs a sea water thermocouple with high salinity water as one element and low salinity water as the other, one can produce an EMF by heating one junction between the two while cooling the other junction. Part of this EMF will be due to the temperature coefficient of the liquid junction potential between the two; part will be due to a concentration dependence of the Thomson EMFs in the arms.

We have constructed such sea water thermocouples, and find that the EMF is about 0.2 microvolts per degree per part-per-thousand salinity difference.

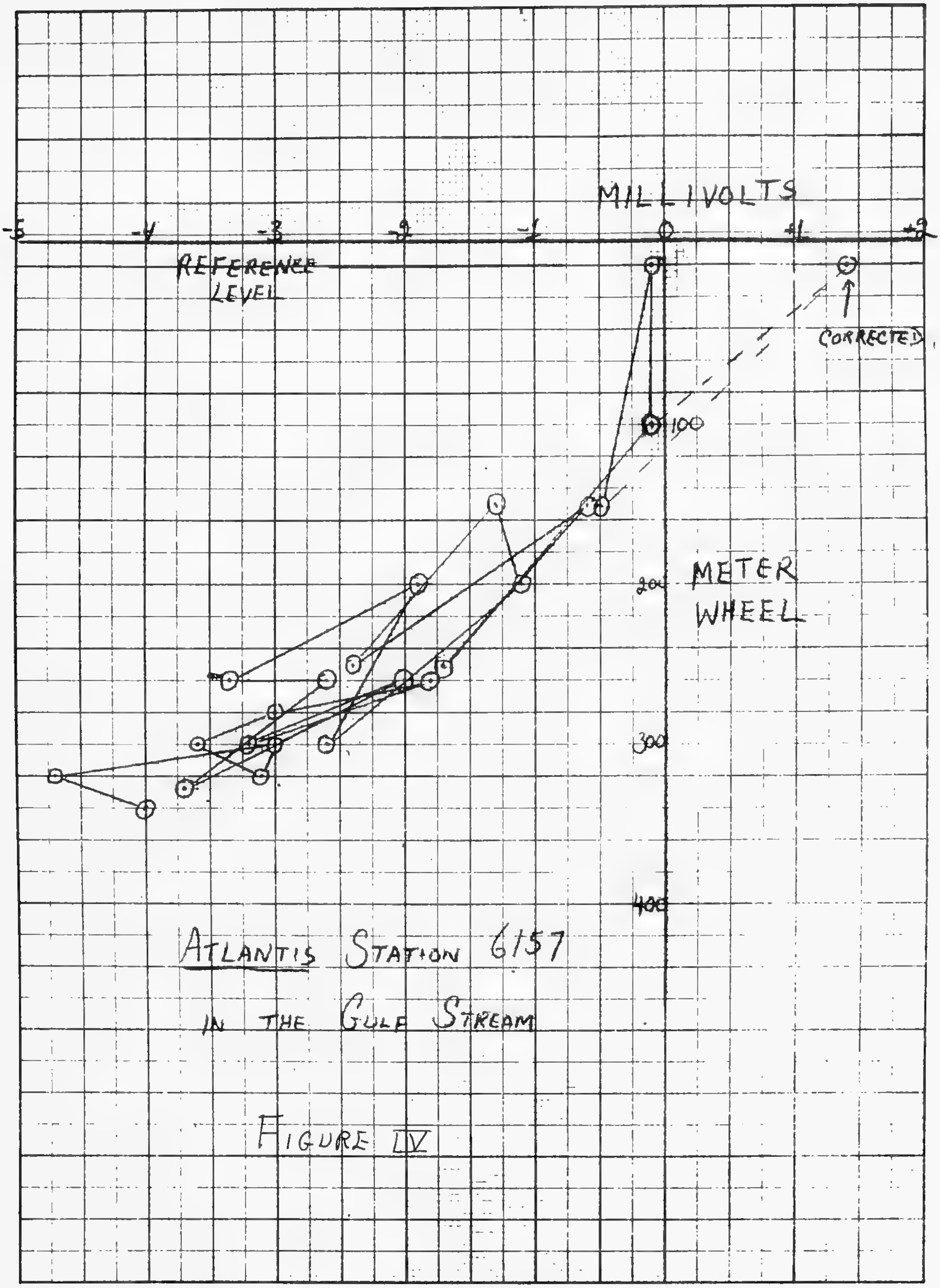
MILLIVOLTS
-5
-4
-3
-2
-1
0
+1
+2
REFERENCE LEVEL
CORRECTED
100
METER WHEEL
200
300
400
ATLANTIS STATION 6157
IN THE GULF STREAM
FIGURE IV

On a conventional T/S diagram, such a thermocouple would appear as a rectangle parallel to the axes. The EMF is proportional to the area of the rectangle. The corresponding EMF in our sea water salt bridge circuit will be proportional to the net area, if any, enclosed by the T/S diagram of the circuit.

From this it appears that the largest error to be expected in the open ocean would occur on a deep vertical measurement, if the long line carried water of surface salinity to great depths. This error would be about 10 microvolts, which would be negligible.

Strangely enough, the other two possible second order errors will be identically zero. The pressure and temperature will be the same inside a submerged tube as outside, so all cross effects between these two variables will cancel out. The pressure and salinity would seem a more likely pair. However, it is clear that if the salt consisted of a single thermodynamic component, say sodium chloride, the influence of both variables would be exercised through changes in the one thermodynamic chemical potential, and no cross effects would be possible. Any cross effects arising from the presence of several components in the sea salt, would have to be considered as third order errors.

OTHER CONSIDERATIONS

We have received several suggestions that we avoid our bubble problems by continuous pumping of sea water through our lines. Even if this could be done without electrical leakages through a pump, we would expect undesirable electrokinetic potentials to be set up in the line by the water flow.

Because of the traditional use of concentrated KCl in laboratory salt bridges, we have also considered its use in our system. While it would greatly enhance the thermocouple effect, KCl solution might be desirable for horizontal measurements in rivers and estuaries where the local water is not suitable anyhow. It would be most undesirable for deep vertical measurements at sea: the added weight of the salt in a kilometer of tubing would create a prohibitive hydrostatic pressure difference on a vertical sounding.

Similar, though less severe, hydrostatic pressure problems will arise if tubing filled with high salinity surface water is lowered to great depths. This can be prevented by an appropriate initial dilution of the water used to fill the tubing.

OTHER USES

Another potential use of the salt bridge technique at sea may be of interest to biologists. If two salt bridges are lowered together, and one of them is closed at the end by a membrane permeable to only one kind of ion, the signal produced will be a direct measure of the ratio of chemical "activities" of the ion inside and outside the membrane on the two sides of the membrane. Since the temperatures and pressures will be the same on both sides, and the salinities nearly the same, this ratio will vary essentially only as the concentration of the ion varies with depth.

Suitable glass membranes for H^+, Na^+, K^+ and Ca^+ now exist. Moreover, any simple coated metallic electrode, such as the Ag/AgCl electrode, can be made thin with two identical faces to serve the same purpose. Thus the possibility exists of making simple, direct, _in situ_ measurements of individual ionic concentrations at depth.

REFERENCES

1. Michael Faraday, Phil. Trans. Roy. Soc. 1832: Part I, 163.

2. W. S. von Arx, Pap. Phys. Oceanogr. Meteor. 11(3) (1950).

3. W.V.R. Malkus and M. E. Stern, J. Mar. Res. 11(2), 97 (1952).

4. M. S. Longuet-Higgins, M. E. Stern and H. Stommel, Pap. Phys. Oceangr. Meteor. 13(1) (1954).

5. G. J. Janz, "Reference Electrodes", Academic Press, New York, 1950. Chapter 4, 220-222.

6. A. C. Redfield, J. Mar. Res. 12(1), 121 (1953).

ACKNOWLEDGMENT

The author is especially indebted to Dr. Willem Malkus for first suggesting this investigation, to Dr. W. S. von Arx for indispensable advice, and to Dr. Vaughan T. Bowen for generous encouragement. He is also most grateful to the Allyn Vines for the use of their basement during the current measurements in Woods Hole. Finally, special mention must be made of Phil Ballard and Ellen Langenheim, the other two-thirds of the "we" so often mentioned.

This work was supported through a grant from the National Science Foundation.

Contribution No. 1225 from the Woods Hole Oceanographic Institution.

TABLE I

Tubing	Damping Length
Green Vinyl Garden Hose	0.38 kilometers
Ortac (Goodyear), two layer, rubber. ½" i.d., 3/16" wall	0.41 "
Nalgon Lab Hose ½" i.d., 3/32" wall	1.0 "
Gum Rubber Surgical Tubing 3/16" i.d., 1/16" wall	4.7 "
Car Heater Hose (Gates), three layer, rubber. 5/8" i.d., 5/32" wall	8.7 "
Black Rubber Lab Hose 3/8" i.d., 1/8" wall	12.5 "
White Rubber Lab Hose (A. H. Thomas) ½" i.d., 1/8" wall	12.6 "
Polyethylene Tubing 3/16" i.d., 1/16" wall	64 "

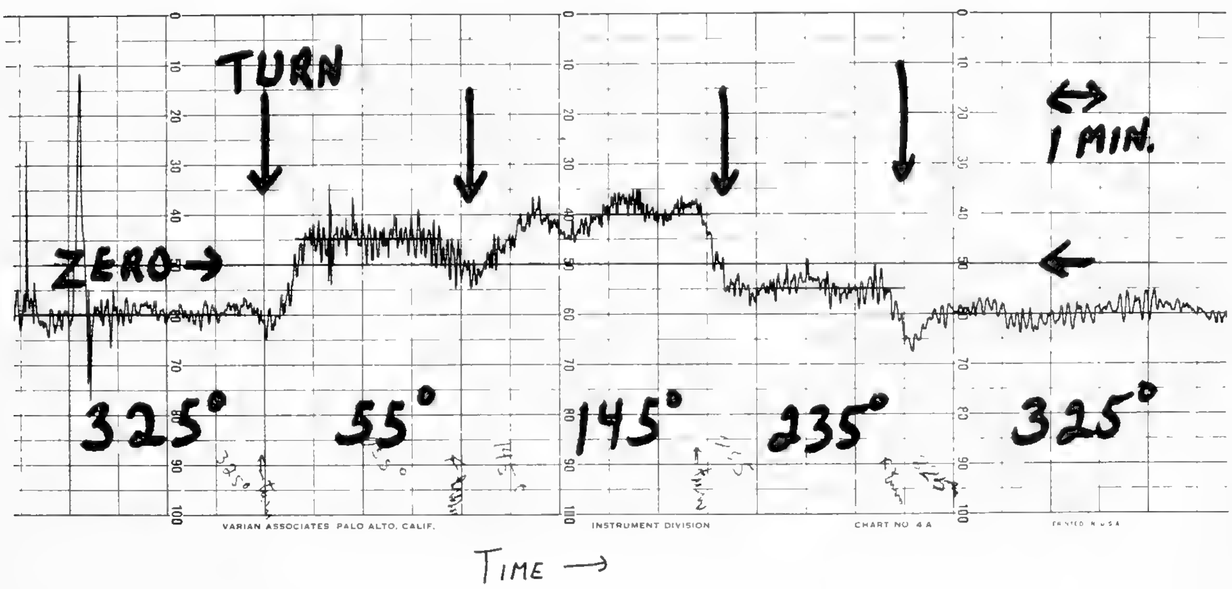

FIGURE V

AN INSTRUMENT FOR THE DIRECT MEASUREMENT OF THE SPEED OF SOUND IN THE OCEAN

by F. J. SUELLENTROP, A. E. BROWN, and ERIC RULE
Lockheed Missiles and Space Company
Palo Alto, California

ABSTRACT

An instrument has been developed which operates on the same principle as the National Bureau of Standards velocimeter, but in which a considerable reduction in size and circuit complexity has been achieved. This reduction in size has been made possible by selecting electronic components which are insensitive to extreme pressures (up to 20,000 psi), so that the pressure housings of previous instruments have been eliminated. Results of calibration and stability tests on the instrument are given.

INTRODUCTION

The need for a simple and direct method of measuring the speed of sound in the ocean has recently been stressed in the literature.[1] At present, the speed of sound is usually derived indirectly by considering the speed to be a function of the temperature, pressure and salinity in the ocean. Knowing or measuring the values of these parameters, the speed of sound is obtained using any one of a number[2,3,4] of empirically-derived formulae which contain up to six terms. This process involves considerable computation, and controversy exists as to which formula is most suitable.[5]

Where the need exists to establish speed-of-sound profiles rapidly or to monitor continuously the speed of sound, the advantages of a direct-measuring instrument are obvious. It should also be noted that direct measurement is to be preferred because the computational methods referred to above may not take account of all factors influencing the speed of sound.

An instrument capable of measuring the speed of sound in fluids has been developed at the National Bureau of Standards[6] and has recently been adapted for use in the ocean.[7] These devices use the well-known "sing-around" principle in which the frequency of an oscillator is governed by the transit time of a pulse of ultrasonic energy between two transducers separated by a fixed distance in the liquid in which the speed-of-sound propagation is to be measured.

The instrument described in the present paper, developed by Lockheed Missiles and Space Company, also makes use of the "sing-around" principle but uses different circuitry (many fewer components) and a completely different packaging philosophy (which results in a great reduction in size) than earlier instruments. The improvement in packaging was made possible by a systematic study of the effect of extreme pressure on the characteristics of electronic circuit components such as transistors, resistors, inductors and capacitors. This study made possible the selection for use in the velocimeter of components known to be stable over the pressure range 0 - 20,000 psi. The electronic circuitry of the velocimeter can then be encapsulated in standard epoxy potting compound, when it is effectively exposed to the ambient pressure, instead of being contained in the bulky pressure housings which have been an undesirable feature of earlier instruments.

PRINCIPLE OF OPERATION

The principle of operation of the instrument and the functions of the major electronic circuits are shown in Fig. 1. The pulse generator sends out a pulse to the piezoelectric transmitter, causing it to emit a 3-megacycle

Superior numbers refer to similarly numbered references at the end of this paper.

acoustic pulse into the liquid. After traversing the distance L at the speed of sound C, the pulse is received at the piezoelectric receiver and converted into an electrical pulse. This pulse is then amplified and used to trigger the pulse generator, causing the pulses to sing around with a pulse repetition frequency being a function of the speed of sound.

The relation between speed of sound in the liquid and output frequency of the instrument is not quite linear because of the finite time delay introduced by the electronic circuitry and piezoelectric transducers. Referring to Fig. 1, we have --

$$\text{Period of pulses} = T + t$$

where T is the transit time in the liquid and t is the delay time in the electronics. The expression for the pulse repetition frequency is then --

$$f = \frac{1}{T + t}$$

Since $T = \frac{L}{C}$, where L is the path length and C is the speed of sound, we have --

$$f = \frac{1}{\frac{L}{C} + t} \quad \text{or}$$

$$f = \frac{C}{L}\left[\frac{1}{1 + \frac{tC}{L}}\right] \qquad (1)$$

The term $\frac{tC}{L}$ in equation (1) leads to nonlinearity in the relation between f and C and becomes less important as t becomes smaller with respect to T. Typical values for velocimeters constructed so far are C = 1500 m/sec, L = 0.1 meters, and t = 0.6 microseconds so that the nonlinearity over small ranges in the speed of sound is small enough that the errors introduced by assuming a linear relation are within allowable limits. For example, if the speed of sound were to be measured over a range of 1490 to 1550 m/sec, the error introduced by assuming the linear relation is only ±0.5 meters per second. If, however, a larger range in the speed of sound is to be measured or the accuracy is to be improved, there are at least two methods of reducing the data.

The first method is to construct a calibration curve giving the relation between f and C, which is derived by measuring the output frequency of the instrument when immersed in distilled water at different temperatures in which the speed of sound is known.[6] Such a calibration curve is shown in Fig. 2.

The second method is to determine the values of L and t for each instrument such that the data can be reduced using the relation --

$$C = \frac{Lf}{1 - tf}$$

For either of these methods to be valid under all oceanographic conditions it is necessary that the quantity t should not vary over the complete range of temperature and pressure encountered in the ocean, and quite elaborate test procedures are necessary to determine that this condition is fulfilled. The tests involve maintaining the transducers in a water bath in which temperature and pressure are constant while the electronic circuitry is subject to temperature and pressure changes over the range -5°C to 40°C and 0 - 20,000 psi, respectively. Any change in output frequency is then undesirable and must be attributed to changes in the electronic circuitry.

These tests have been carried out on the Lockheed velocimeter. It was found that the change in time delay in the electronic circuitry over the temperature range of -5°C to 40°C affected the speed-of-sound readings by less than ±0.2 m/sec. The change in time delay in the circuitry over the pressure range 0 to 20,000 psi affected the speed-of-sound readings by less than ±0.1 m/sec.

Another factor which may cause the time delay in the electronics to vary is variations in the voltage from the power supply. Tests on several of these instruments have shown that a change in voltage of +0.1 volt causes the speed-of-sound reading to change by less than +0.2 m/sec.

INSTRUMENT DESIGN

The general form of the instrument is shown in Fig. 3. The transducers are located in the square end plates, which are made of Invar, as are the three rods which establish the transducer separation and which serve to protect the transducers from accidental damage. Use of Invar ensures that changes in path length due to temperature differences in the ocean are negligible (less than one part in 25,000). The transmit-and-receive transducers are

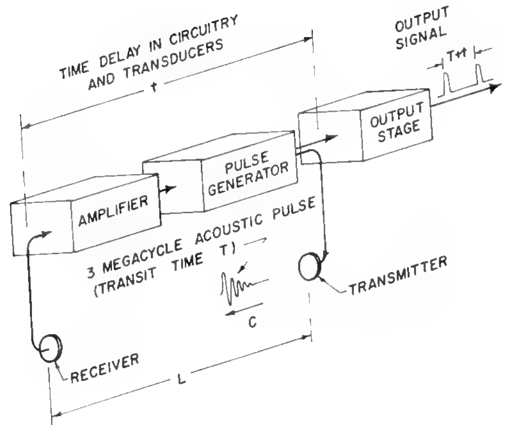
TIME DELAY IN CIRCUITRY
AND TRANSDUCERS
t
OUTPUT
SIGNAL
T+t
OUTPUT
STAGE
PULSE
GENERATOR
AMPLIFIER
3 MEGACYCLE ACOUSTIC PULSE
(TRANSIT TIME T)
TRANSMITTER
C
RECEIVER
L

FIG I

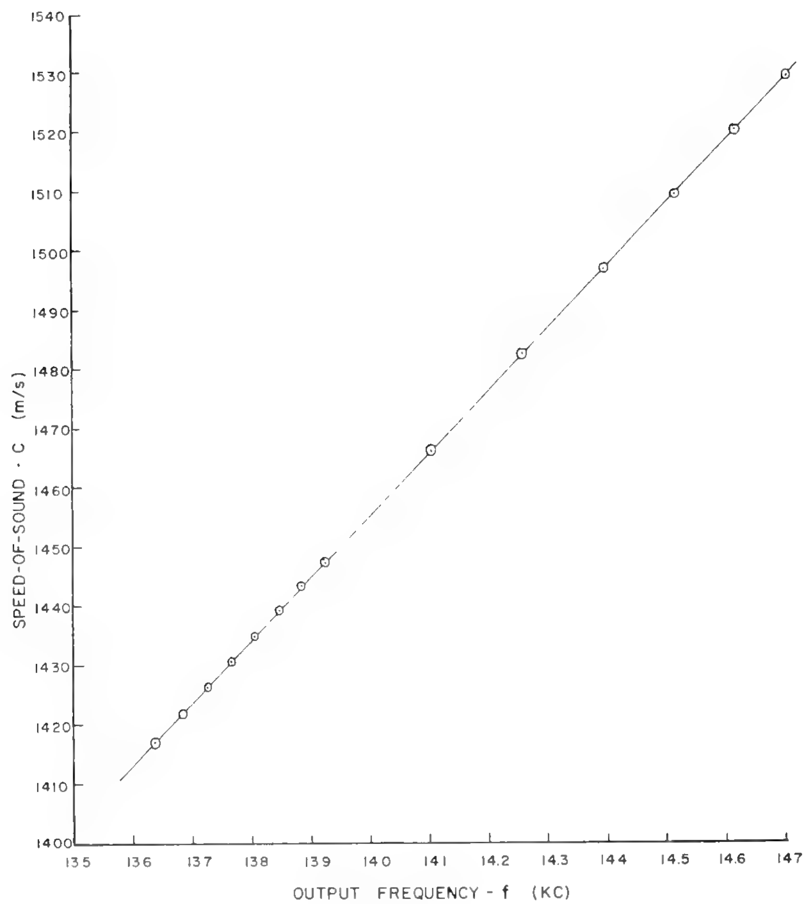
SPEED-OF-SOUND - C (m/s)
1540
1530
1520
1510
1500
1490
1480
1470
1460
1450
1440
1430
1420
1410
1400
13.5
13.6
13.7
13.8
13.9
14.0
14.1
14.2
14.3
14.4
14.5
14.6
14.7
OUTPUT FREQUENCY - f (KC)

FIG. 2

polarized discs of piezoelectric ceramic backed with potting compound and operating in the thickness-resonant mode at about 3 megacycles per second. The electronic circuitry has only five transistors (all type 2N393) and requires a $1\frac{1}{2}$-volt power supply from which it draws less than 5 milliamps. A regulated power supply employing a rechargeable battery, which can be submerged with the velocimeter, has also been developed at LMSC.

NOMENCLATURE

C = speed of sound, meters per second
f = pulse repetition frequency, pulses per second
L = path length, meters
t = time delay in electronic circuitry and transducers, seconds
T = transit time in liquid, seconds

REFERENCES

1. Thomas D. McGrath, Capt., USN - UNDERWATER ENGINEERING, 1, 3, p. 38 (1960).
2. V. M. Albers, UNDERWATER ACOUSTICS HANDBOOK (The Pennsylvania State University Press, University Park, Pennsylvania, 1960).
3. K. V. Mackenzie, J. ACOUST. SOC. AM. 32, 100 (1960).
4. Wayne D. Wilson, J. ACOUST. SOC. AM. 32, 641-644 (1960).
5. F. E. Bellas, J. ACOUST. SOC. AM. 33, 249 (1961).
6. M. Greenspan and C. E. Tschiegg, REV. SCI. INST. 28, 11, 897-901 (1957).
7. C. E. Tschiegg and E. E. Hays, J. ACOUST. SOC. AM. 31, 7, 1038-1039 (1959).
8. M. Greenspan and C. E. Tschiegg, J. RESEARCH OF NATIONAL BUREAU OF STANDARDS 59, 4, 249-254 (1957).

FIG. 3

AN ACOUSTIC OCEAN-CURRENT METER

by F. J. SUELLENTROP, A. E. BROWN, and ERIC RULE
Lockheed Missiles and Space Company
Palo Alto, California

ABSTRACT

An ocean-current meter has been developed which is essentially two sing-around velocity-of-sound meters in which the directions of pulse transmission are opposite in sense. The instrument is oriented so that the direction of acoustic pulse transmission is parallel to that of the flow to be measured, so that the time of pulse translation is greater in one velocimeter than in the other. The difference in sing-around frequencies is then proportional to ocean-current velocity. Electronic circuitry is described by means of which a signal with frequency proportional to flow velocity is extracted. It is shown that the current flow measurement is independent of variations in the velocity of sound.

INTRODUCTION

The mechanical-impeller type of instrument most commonly used to measure ocean-current speeds is generally unsatisfactory because of bearing-friction problems and because inherent high-inertia leads to slow response to changing rates of flow. Acoustic flowmeters which effectively measure the results of the velocity of propagation of sound in a fluid and the velocity of the fluid with respect to a transmitting and receiving transducer have been described in the literature.[1] These instruments are subject to error when used in a fluid in which the velocity of propagation can vary. In the case of a single-path instrument the error in flow-velocity measurement is equal to the deviation in the velocity of sound from the value pertaining when the instrument was calibrated. Refinement of the instrument to a two-path type reduces this error to the extent that a given percentage variation in the velocity of sound from calibration conditions will result in the same percentage error in flow measurement. The possible variation in the velocity of sound over the complete range of oceanographic conditions is about 12 per cent so that an unacceptable error in flowmeter readings can be introduced in this way. A further objection to the type of acoustic flowmeter usually described is that the technique involves a measurement of phase difference; therefore, the requirement of providing sufficient sensitivity, on the one hand, and the need to avoid ambiguity, on the other, become contradictory in a wide-range instrument.

The instrument described in the present paper, being developed by Lockheed Missiles and Space Company, avoids the difficulties of the acoustic-type instruments described above. The instrument is basically simple and consists of two sing-around velocimeters arranged so that the transmission paths in the liquid are side-by-side and of equal length. The directions of pulse travel are opposite in the two velocimeters. One velocimeter measures the sum of the speed of sound and the speed of current flow while the other velocimeter measures the difference between the two speeds. Therefore, by taking the difference of the sing-around frequencies of the velocimeters, we achieve a signal having a frequency proportional to current flow.

THEORY OF OPERATION

In the case of the ideal velocimeter, the output frequency (f) is given by

$$f = \frac{C}{L}$$

where C is the velocity of propagation and L is the separation between transmitter and receiver. If one uses two velocimeters sending pulses in opposite directions and introduces a current flow (v), the two sing-around frequencies are

$$f_1 = \frac{C + v}{L}$$

and

$$f_2 = \frac{C - v}{L}$$

Then, by taking the difference of the sing-around frequencies, we obtain the frequency

$$f_v = f_1 - f_2 = \frac{2v}{L}$$

which is proportional to current flow. In this ideal case, variations in the speed of sound do not affect the flow measurement.

There is, however, a small but finite time delay in the electronic circuitry of each velocimeter which complicates the expression for f_v. The individual velocimeter output frequencies taking the time delay (t) into account are --

$$f_1 = \frac{\frac{C+v}{L}}{1+\frac{t(C+v)}{L}} = \frac{C+v}{L}\left[1-\frac{t(C+v)}{L}+\cdots\right]$$

$$f_2 = \frac{\frac{C-v}{L}}{1+\frac{t(C-v)}{L}} = \frac{C-v}{L}\left[1-\frac{t(C-v)}{L}+\cdots\right]$$

Typical values for the velocimeters used are $(C \pm v) \simeq 1500$ meters per second, L = 0.15 meter and t = 0.6 microseconds. The value of $t(C \pm v)/L \simeq .006$ is small enough that the higher order terms in the expansions can be ignored. The expression for f_v is now --

$$f_v = \frac{2v}{L}\left[1 - \frac{2tC}{L}\right]$$

and the percentage error in f_v caused by a change in C can be shown to be 0.012 times the percentage change in C (see Appendix A). This makes the error so small that it can be ignored.

The foregoing discussion does not take into account differences in path length and delay times in the circuitry between the two velocimeters. The effect of having these differences is to limit the resolution of the instrument. These problems have been investigated at LMSC and it has been found in laboratory models that they limit the resolution to ±0.1 foot per second.

DESIGN

In order to achieve the necessary sensitivity for a flowmeter of practical dimensions, some multiplication of the individual sing-around frequencies, before subtraction, is necessary. A flowmeter with the desired characteristics is shown in the block diagram of Fig. 1. The function of the balanced modulator is to take the sum and the difference of the frequencies of the two signals being injected into it. By using the low-pass and high-pass filters it is then possible to obtain signals proportional to current speed and velocity of sound, respectively. Such an instrument, in the form of an initial laboratory prototype, has been built at LMSC and has been shown to function in the laboratory. The general form of this prototype is shown in Fig. 2.

APPENDIX A

Taking the expression for the output frequency --

$$f_v = \frac{2v}{L}\left[1 - \frac{2tC}{L}\right]$$

it is possible to find the change in this frequency caused by a change in the speed of sound C --

$$\Delta f_v = \frac{4vt}{L^2}\,\Delta C$$

The percentage error in f_v caused by a change Δ C in the speed of sound is then shown to be -

$$\frac{\Delta f_v}{f_v} \times 100 = \frac{\frac{2t\Delta C}{L}}{\left[1-\frac{2tC}{L}\right]} \times 100$$

$$= \frac{2t\Delta C}{L}\left[1+\frac{2tC}{L} - \cdots\right] \times 100$$

$$= \frac{\Delta C}{C}\left[\frac{2tC}{L} + \left(\frac{2tC}{L}\right)^2 - \cdots\right] \times 100$$

For the values of C = 1500 m/sec, L = 0.15 meter and t = 0.6 microseconds, the value of 2tC/L is found to be 0.012. Therefore, the percentage error in f_v caused by a percentage change in the speed of sound $\Delta C/C \times 100$ is shown to be 0.012 times the percentage change in the speed of sound.

NOMENCLATURE

C = speed of sound, meters per second
f = frequency, cycles per second
f_C = output frequency proportional to C, cycle per second

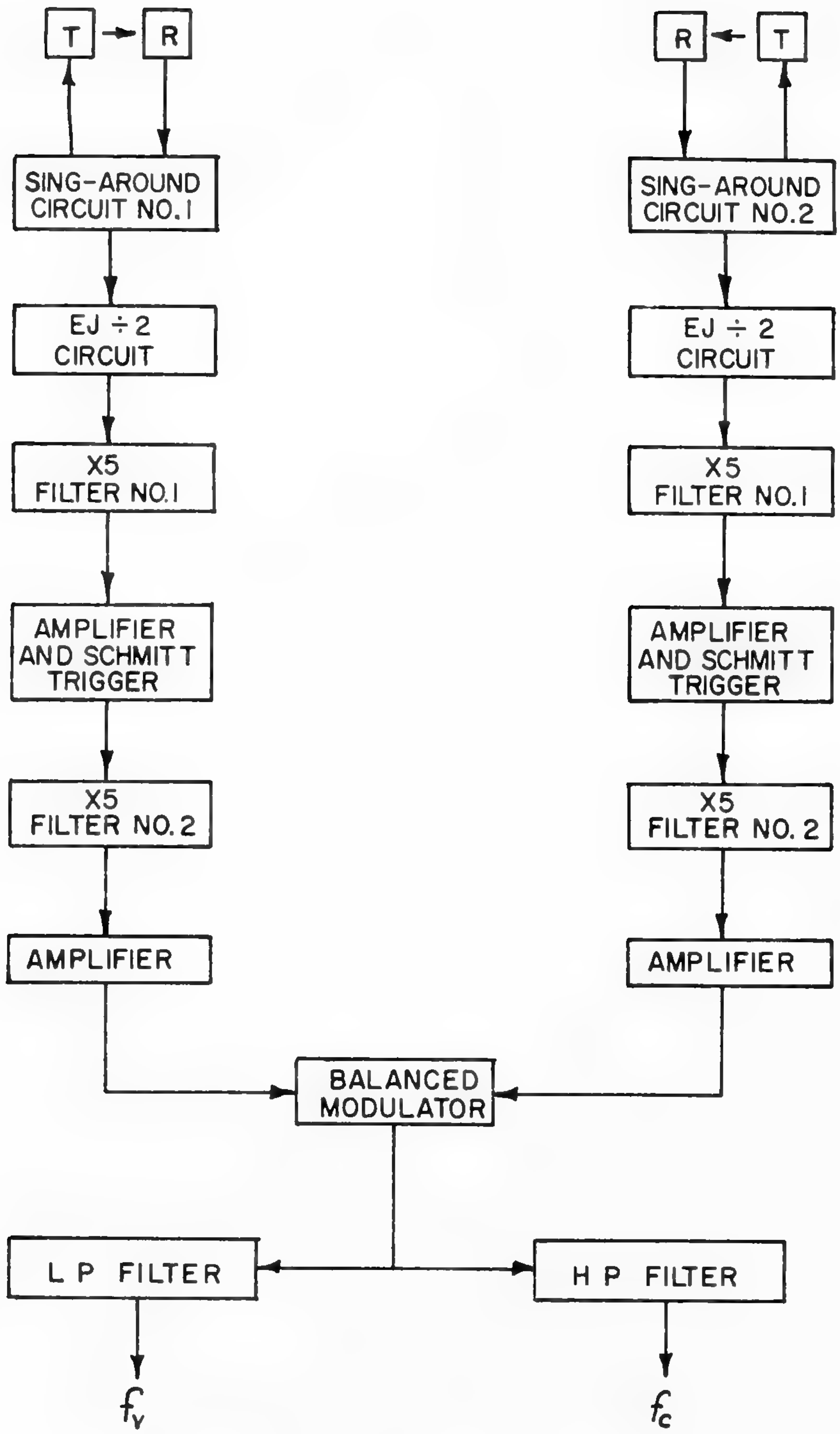

T
R
R
T
SING-AROUND CIRCUIT NO. 1
SING-AROUND CIRCUIT NO. 2
EJ ÷ 2 CIRCUIT
EJ ÷ 2 CIRCUIT
X5 FILTER NO. 1
X5 FILTER NO. 1
AMPLIFIER AND SCHMITT TRIGGER
AMPLIFIER AND SCHMITT TRIGGER
X5 FILTER NO. 2
X5 FILTER NO. 2
AMPLIFIER
AMPLIFIER
BALANCED MODULATOR
L P FILTER
H P FILTER
f_v
f_c

FIG. 1

f_v = output frequency proportional to v, cycle per second
L = path length in liquid, meters
t = time delay in electronic circuitry, seconds
v = speed of current flow, meters per second

REFERENCES

1. H. P. Kalmus, "Electronic Flowmeter System", REV. SCI. INST., Vol. 25, No. 3, pp. 201-206, March 1954.

FIG. 2

A DOPPLER-SHIFT OCEAN-CURRENT METER

by J.D. CHALUPNIK and P.S. GREEN
Lockheed Missiles and Space Company
Palo Alto, California

ABSTRACT

An ocean-current meter utilizing the Doppler effect has been developed and tested. With this device a collimated beam of ultrasonic energy is projected into the water and a volume reverberation signal received. The meter detects the difference between the transmitted and received frequencies, this difference being proportional to the speed of the water past the meter. The device can be made to indicate sense as well as flow rate.

INTRODUCTION

Ocean-current meters commonly in use are mechanical devices using impellers turned by the dynamic pressure of the current, although other instruments which measure (1) dynamic pressure on static members, (2) electromotive force generated by the conducting liquid flowing in a magnetic field, (3) cooling effect of the current on hot wires, and (4) time required for a sound pulse to travel a specified distance have been tried. [1*]

The impeller devices respond slowly to changing flows and operate over limited ranges of flow rates. They are large and do not give continuous readings. The instruments which measure dynamic pressures on static members are limited in operating range. Electromagnetic current meters are limited in operating range and are expensive. Hot-wire anemometer-type devices are difficult to use and require frequent cleaning due to films forming on the wires. Ultrasonic current meters which have been reported prior to this meeting have been electronically complicated and expensive. A paper being presented at this meeting by F. J. Suellentrop describes an improved version of this instrument which gives speed-of-sound information as well as flow rate.

This paper describes a new instrument which makes use of the Doppler frequency shift to measure flow rates in ocean water and other liquids containing inhomogeneities.

THEORY OF OPERATION

When a beam of ultrasonic energy is projected into an inhomogeneous liquid, it is scattered by irregularities in the liquid and some of the energy is returned in the direction of the transmitter. This returned signal is called volume reverberation. The volume reverberation signal is found to shift in frequency due to the Doppler effect, provided there is net movement of the inhomogeneities along the axis of the beam.[2] If the scatterers are stationary with respect to the liquid, then the observed Doppler shift is proportional to the speed of the liquid relative to the meter. The Doppler-shift ocean-current meter is a continuous-tone sonar device which detects the volume reverberation signal with a receiving transducer located adjacent to a transmitting transducer, then detects any shift in frequency between the transmitted and received signals. It is assumed that the vast majority of the contributing scatterers are nearly neutrally buoyant and move with the water.

The application of the Doppler-shift principle to measuring currents in the ocean appeared to be feasible, provided enough scatterers were present in the water. Since Rayleigh scattering increases with the fourth power of frequency, only high frequencies were investigated, 2.5 and 10 megacycles being chosen as favorable operating frequencies. Most considerations indicated that the higher frequency should be used, the principal objection being the inherent difficulties encountered in high-frequency transistor circuitry. At 10 mc the number of scatterers one wavelength or greater (λ = .15mm) in size is quite large, with small marine organisms, particulate matter, and minute bubbles abounding.

For a stationary transducer-pair and moving target (scatterers), the frequency of the re-

* Superior numbers refer to similarly numbered references at the end of this paper.

turned signal is

$$f_{v_x} = \left(\frac{c - v_x}{c + v_x}\right) f, \qquad (1)$$

where f_{v_x} is the frequency of the volume reverberation signal at the receiver, v_x is the velocity of flow along the axis of the transducer-pair, c is the speed of sound in the medium, and f is the transmitting frequency. The velocity v_x is considered positive in the direction the transmitted wave is projected. The received signal beats with the transmitted tone, the beat frequency being the Doppler frequency. The Doppler frequency is given by

$$\Delta f = f - f_{v_x} = f - \left(\frac{c - v_x}{c + v_x}\right) f$$

$$= \frac{2v_x}{c + v_x} f. \qquad (2)$$

Since the speed of flow is small compared to c, the Doppler shift may be approximated by

$$\Delta f = \frac{2v_x}{c} f. \qquad (3)$$

It is convenient to use the quantity

$$\varphi = \frac{2}{c} \times 10^6, \qquad (4)$$

the normalized sensitivity for Doppler-shift devices, which has the units cps/mc/m/sec. The normalized sensitivity for sea water is about 1300 cps/mc/m/sec. Rewriting (3), we have

$$\Delta f = \varphi v_x f', \qquad (5)$$

where f' is the transmitting frequency in megacycles. It is desirable to have f' as large as possible for good resolution. The normalized sensitivity, $\varphi = \varphi(c)$, is dependent on the speed of sound in the water; therefore, if very accurate measurements of flow rates (less than ±5% error) are to be made, it would be necessary to determine or estimate the speed of sound at the point of measurement. Although the speed of sound varies widely in the ocean, it is possible to estimate the speed of sound at a point of measurement closely enough to ensure satisfactory flow-rate determinations.

The sensitivity at 10 mc is about 13,000 cps/m/sec, making practical an instrument with a working range of 1 mm/sec to 10 m/sec. If it is desired, the range can be extended to higher and lower flow rates with little additional effort.

The transmitting frequency must be held constant for accurate measurements to be made. Errors can be caused by short- or long-term instability in the transmitting frequency. Errors due to short-term instability occur when changes in frequency occur during the time it takes a transmitted wave to return to the receiver. This round-trip time is on the order of one millisecond; hence, the frequency drift rate would have to be extremely high to introduce any appreciable error. Long-term drift of the oscillator frequency produces an error in the Doppler signal that is proportional to the error in the transmitting frequency.

A change in the sense of v_x results only in a 180° phase change in Δf; therefore, if the instrument is to determine sense as well as speed, it is necessary to beat the returning signal with a reference signal differing in frequency from the transmitted wave by more than the maximum Doppler frequency to be measured.

$$\delta f = (f^* - f) + \frac{2v_x}{c} f \qquad (6)$$

Here f* is the reference frequency (assumed greater than f for this discussion) and δf is the new difference frequency. For zero flow, the difference frequency is not zero, but is the offset frequency f* - f. When δf is less than the offset frequency, this corresponds to a negative v_x, or flow toward the transducer-pair. If f* is assumed to be less than f, similar results are obtained. If the current meter is oriented facing the current by a vane arrangement, the sense information would not be required.

One further advantage was gained by using a transmitting frequency of 10 mc, that being the control over the region in which the current is to be measured. Attenuation at 10 mc is about 20 db/m, which effectively limits the distance the instrument "sees". There is an area immediately in front of the transducer-pair which gives no return, because the transducers are spaced a small distance apart. The beam width of the transducers is narrow, so the lateral area covered is small. Because of these conditions, the region of observation is limited to a narrow volume extending from about 40 to

Fig. 1 The Doppler shift ocean current meter.

Fig. 2 Photo of the meter showing the construction.

70 cm in front of the transducer-pair, in the clear water where the flow pattern is unaffected by the presence of the meter.

Since the current meter has no moving parts it can respond almost instantaneously to flow changes, being limited by the transit time of an acoustic wave from the point of measurement to the receiver (less than 1 ms). Spectrum broadening and rapid shifts of frequency of the returned signal can be expected in turbulent flows and should provide a reliable index of turbulence in the measured current.

DESCRIPTION OF THE CURRENT METER

The current meter consists of an oscillator driving the transmitting crystal, an amplifier tuned to the oscillator frequency (10 mc) and driven by the receiving crystal, a detector, and an audio frequency stage with emitter follower output. These elements are enclosed in a pressure-tight case. The instrument operates on 1.5 v and, except for the battery, is completely enclosed in a cylindrical package about 12 cm long and 3.2 cm in diameter. The crystal transducers are mounted on one end of the cylinder, while the electrical connectors exit from the other. The complete current meter is shown in Fig. 1.

Complete isolation of the oscillator and amplifier stages is provided by the internal shields shown in Figs. 2 and 3. The outer case provides structural strength to withstand the water pressure and is sealed at both ends with O-rings. The two electrical conductors, one for -1.5 v and the other for the audio signal output, pass through small O-ring stuffing boxes to prevent leakage around them.

The transmitting and receiving crystals are standard stock barium titanate discs 6.5 mm in diameter and about .25 mm thick. The thickness-resonant frequency is about 10 mc. The theoretical half-beamwidth of these crystals at 10 mc is 1.7° and the actual measured half-beamwidth is about 2.5°, as shown in Fig. 4. The crystals are mounted 8 mm on centers and backed with .8 mm of epoxy circuit board.

The oscillator is of unique design, employing a single tunnel diode as the active element. The tunnel diode is superior to conventional transistors in this application because of its small size and excellent current-handling ability at high frequencies. Although the impedance of the crystal is low at 10 mc, it is possible to apply 2.0 v peak-to-peak across the crystal with the tunnel diode.

The tuned amplifier stages employ MADT, high-frequency transistors operating well below their rated voltage. There are three stages with a gain of about 20 per stage. There is enough acoustic coupling between the transmitting and receiving crystals to provide the reference frequency; hence, no electronic mixing is required. The Doppler frequency appears as amplitude modulation on the 10-mc carrier.

The Doppler frequency is extracted from the 10-mc carrier with a highly sensitive backward diode detector, then amplified. The Doppler frequency shift for a flow range of 1 mm/sec to 10 m/sec is 13 to 130,000 cps. In this form the data can be processed for recording on tape recorders or for telemetering to data-gathering stations.

The Doppler-shift flowmeter requires very little power and operates on 1.5 v, drawing only 50 ma. It could be operated continuously on a single rechargeable flashlight cell for about 48 hours.

RESULTS

The Doppler-shift ocean-current meter has been tested in the laboratory in a flow tube. Results indicated that, if sufficient scatterers are present, the instrument will function well, although it was necessary to add scatterers to Palo Alto tap water to get satisfactory returns. The observed Doppler frequency checked closely with the measured velocity in the tube. In order to try the meter in "ocean" water, it was taken to Palo Alto Yacht Harbor on San Francisco Bay for additional tests. Sufficient scatterers were present in the yacht harbor water to get return, and the meter performed as anticipated. The signal-to-noise ratio was low, but work is underway to decrease the noise level.

CONCLUSIONS

This paper describes an ocean-current meter which uses the Doppler shift in continuous-tone volume reverberation to measure flow rates. Operation of the instrument depends on sufficient scatterers being present in the water that is to be measured. It is assumed that, at an operating frequency of 10 mc, there are

Fig. 3 Photo showing the electronics.

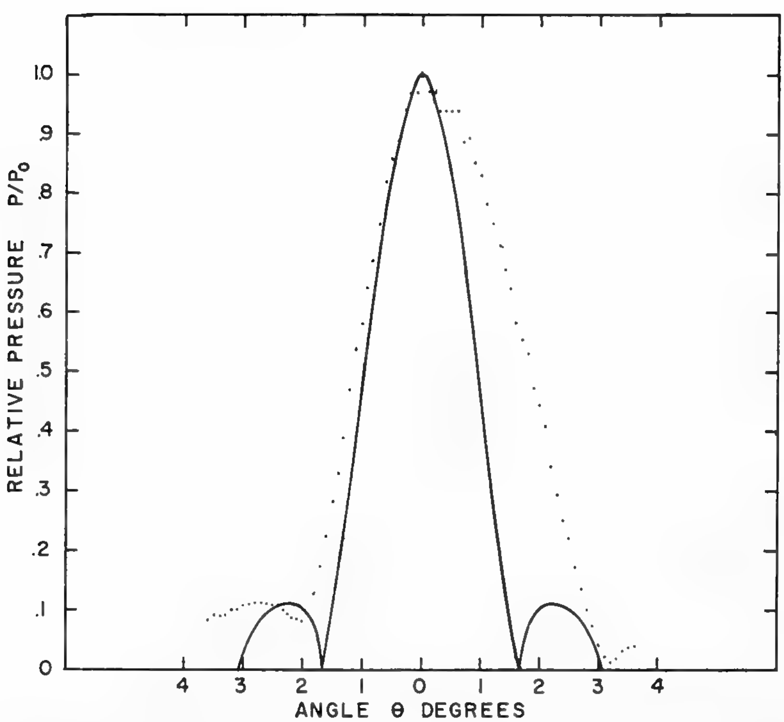

Fig. 4 Transducer pressure pattern at 10 mc. Solid curve is the theoretical pattern.

enough of the necessary scatterers present to operate the instrument satisfactorily in ocean water. Although the device described was designed to operate over a range of 1 mm/sec to 10 m/sec, it is reasonable to assume that, with minor modifications, it would operate over a much wider range. This instrument should provide a reliable index of turbulence in ocean currents because of its excellent response to rapidly changing flows.

NOMENCLATURE

c = speed of sound, m/sec
f, f^* = transmitting frequency, cps
f' = transmitting frequency, mc
Δf = Doppler frequency, cps
δf = difference frequency, cps
f_{v_x} = returned frequency, cps
P/P_0 = relative pressure, dimensionless
v_x = velocity of flow along the axis of the transducer-pair, m/sec
θ = an angle, deg.
γ = normalized sensitivity, cps/mc/m/sec

REFERENCES

1. J. W. Johnson and R. L. Wiegel, "Investigation of Current Measurement in Estuarine and Coastal Water", September 1958, California State Water Pollution Control Board Publication #19, Sacramento, California.

2. G. A. Klotzbaugh, "Theory of Continuous-Tone Reverberation", J. ACOUST. SOC. AM. 27, No. 5, September 1955.

HIGH-ACCURACY, SELF-CALIBRATING ACOUSTIC FLOW METERS

by R. A. LESTER, Research Engineer
Westinghouse Research Laboratories
Pittsburgh, Pennsylvania

ABSTRACT

A number of acoustic flow meters have been developed and tested for a variety of uses. All of the units transmit in opposition and compare the received phases; the phase difference is a function of the water velocity. The first unit was one which used an amplitude-modulated continuous wave signal and measured speeds from 0.15 ft/sec to 15 ft/sec to an accuracy of 1%. A second type compares the carrier frequency and measures speeds from approximately 0.005 ft/sec to 0.5 ft/sec with an accuracy of 1%. A third pulse-type system is being developed; it is simpler than the original unit and eliminates a number of the inherent inaccuracies of the above-mentioned units. One of the desirable features of all of these units is the ability to be calibrated or checked for zero reference in the field.

INTRODUCTION

For monitoring ocean currents, wave particle velocities, flows about ships and models, and flows in pipes, flow meters which are both accurate and dependable are required. Acoustic flow meters show great promise of fulfilling this need. Acoustic meters have several salient features: one, they are nonfouling since there are no moving parts; two, they are linear devices with good accuracy; three, they are directive; last, but no means least, they may be calibrated in the field. Several acoustic flow meters have been built and tested to measure flows in the ocean. The construction and limitations of these meters will be discussed.

OPERATING PRINCIPLE

These flow meters, like most acoustic flow meters, measure the difference in travel time of sound in the upstream and downstream directions of the flow. The fluid velocity is then:

$$V = \frac{\Delta t \ C^2}{2L} \qquad \text{if } V \ll C$$

where V = velocity of the fluid,
L = distance the sound travels,
C = speed of sound in the medium, and
Δt = difference in time delays.

To get an order of magnitude of the numbers involved, consider a flow of 1 ft/sec in water. If L is 10 feet, then $\Delta t = 2\ LV/C^2 = 0.8\ \mu$sec.

To obtain accuracies of .1 ft/sec this system must be capable of resolving time delays of less than 1 μsec. This is most conveniently done by measuring the relative phases of two sinusoidal signals. Since the measurements of the upstream and downstream travel times are to be made simultaneously, there must be two sets of receiving equipment with their associated time delays. Therefore, an error in the measurement of Δt will be introduced unless the two receivers have equal time delays. In the meters described here, provision is made to balance the receiving equipment and thus "zero calibrate" the meter from time to time to insure accuracy. In the first two of these meters, this "zero calibration" may be made in the presence of a flow. The third meter must be "zero calibrated" under zero flow conditions; thereafter, its calibration is a function of the stability of quartz crystal oscillators.

THE EQUIPMENT

The first meter built was a CW dual frequency system which was designed to measure flow up to 15 ft/sec. For the particular application, it was desirable that the flow be averaged over a ten-foot distance. This system represents perhaps the most straightforward electronic circuitry which will make the measurement (see Fig. 1). Four transducers are used in this flow meter, two on each probe. The pairs of transducers are separated by about an inch. In order to get a narrow acoustic beam width, high frequency carriers of 1.1 and 1.6 mcps are used. These are modulated at 20 kc. The received signals are amplified, detected, and applied to the phase meter. The relative phase of the 20 kc signals is then proportional to the flow. Zero calibration is accomplished by reversing the direction of the acoustic path of one of the frequencies. With the signals in the same direction the water path time delays of both signals are identical; hence the electrical delays of the system may be adjusted to "zero".

This system, although quite simple electronically, has a number of potential weaknesses. To begin with, it requires 2 cables to each post, 2 transducers in each post, 2 transmitters operating at

2 widely separated frequencies and, because of the physical separation necessary due to transducer size, two acoustic paths are required. Errors may occur because of electrical leak-through or due to acoustic path separation in a highly inhomogeneous medium; it is also possible that errors of a secondary nature may occur due to the large frequency separation of the transmitted signals.

The following system, shown in Fig. 2, was constructed to circumvent these two weaknesses. In this flow meter, the high frequency carrier with a 20 kc modulation is again used. Two transducers are driven from the same pulsed 1.1 mcps transmitter. The transmitter is turned off when the space between the transducers is filled with acoustical energy. The signals are detected and again the phase difference of the 20 kc signal is proportional to the flow. A sampling circuit after the phase meter remembers this phase difference until the phase is altered by the next received signal. In this way, 250 samples of the fluid velocity are taken each second. The resistors shown are included to insure that the transducers will see the same impedance when transmitting as when receiving, thus insuring their reciprocity. This system uses a single cable to each post, one transducer in each post, a single acoustic path and a single frequency. Crosstalk problems and acoustic path problems are minimized and equipment problems due to water exposure are halved.

The third system, shown in Fig. 3, is a pulse system which uses free running crystal oscillators to store the phase information. It was built to measure flows of less than two knots maximum velocity. In this meter the transducers are spaced at a two foot interval. A pulsed 1 mcps signal is applied to the two transducers for 400 μsec. This signal is received and used to lock two slave oscillators. These slave oscillators are then heterodyned with a local oscillator and the resulting audio signals are applied to the phase detector. The output of the phase detector then indicates the flow. During the time no energy is received, the slave oscillators free-run, thus providing continuous information to the phase meter. The range of the velocities to be measured or the post spacing may be varied by changing the carrier frequency.

SOURCES OF ERROR

The error of these systems due to the electrical circuits is quite small. The phase meter has been the limiting component and its error is approximately 0.3%.

In homogeneous water the accuracy of the instantaneous readings is limited by the vortices created by the leading transducer when the acoustic beam is in the wake of this probe. This vortex shedding causes a fluctuation in the output which increases in magnitude and frequency with increasing speed. For the 2-3/8" probes used, the measured velocity fluctuated about 0.2 knots at a speed of 8 knots, and the fluctuation had a frequency of about 17 cps. If the flow meter is run at an angle to the flow, such that the acoustic beam is not in the wake of the leading transducer, there is no error due to vortex shedding.

In inhomogeneous water, the errors introduced are a function of the velocity of the fluid, the magnitude of the velocity anomalies, the patch size and the distance between transducers. These inhomogeneities can introduce errors in several ways.

One mechanism which can cause errors is the phenomenon of multiple path transmission which results in signal amplitude fluctuations. This occurs when parts of the acoustic beam are refracted in a nonuniform manner so that they arrive at the receiving element out of phase. This effect varies as the distance between the transducer elements; however, the exact manner in which it varies is, at present, not completely understood. The effect of this secondary path is to add to the direct signal another signal of slightly different phase. The sum of these two signals results in a fluctuating received amplitude. Tests were conducted at sea, at Scripps Institute, and in the Laboratory to determine the magnitude of this effect. It was determined that the signal level fluctuated approximately 12 db under fairly severe thermal conditions. Using this as a figure for the kind of fluctuation one might expect at sea, the velocity error due to the multiple path transmission may be calculated. If it is assumed that the second path signal is equal in magnitude to the direct signal, a delay of 166 electrical degrees of the carrier frequency would be required in order for the resulting amplitude to change to one-fourth of its original value. The resultant phase of the received signal would then be 83° different from the phase of the direct path. This condition would lead to an apparent time delay of about 0.25 μsec or an instantaneous error of about 0.3 ft/sec in the measured velocity. This error does indeed occur occasionally under severe thermal gradients in the order of 1° to 2° F per foot. A secondary effect of the multiple path is the effect of the amplitude change on the time delay of the receivers. The receivers may be designed so that error due to amplitude fluctuations are negligible.

Inhomogeneities can also cause errors due to the fact that the acoustic signals traveling in opposite directions are not in the same water at the same time. If the water velocity is large enough and the thermal patches sufficiently small, the sound traveling in one direction will travel through different water than the sound traveling in the opposite direction. This effect is quite difficult to separate from the effect of

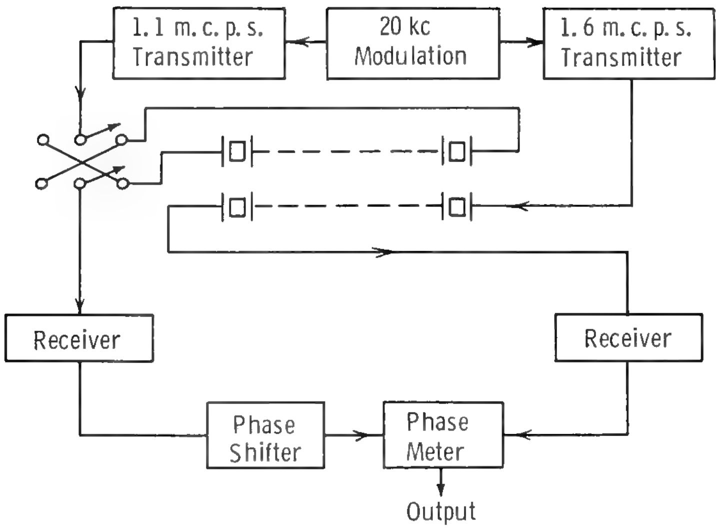

Block Diagram of 0-15 ft./sec. Acoustic Flow Meter Using Four Transducers

Fig. 1

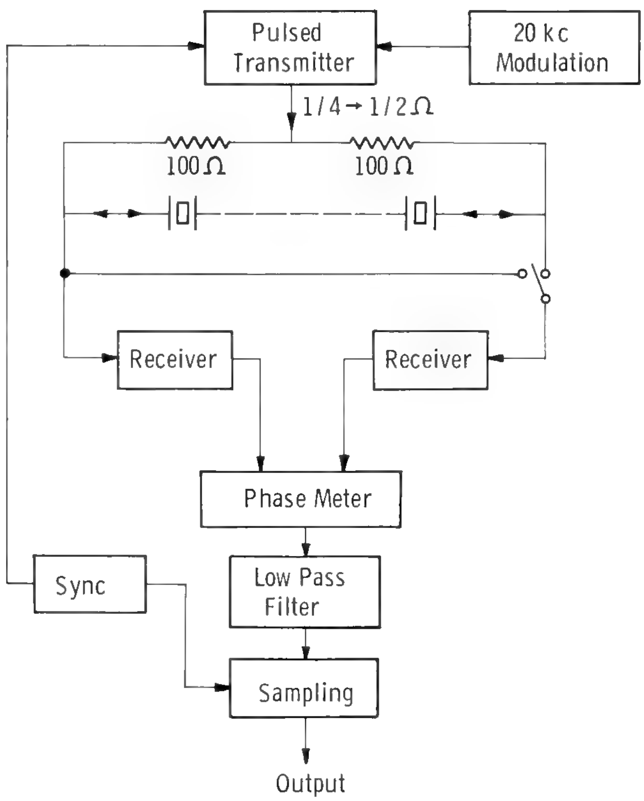

Block Diagram of 0-15 ft./sec. Acoustic Flow Meter

Fig. 2

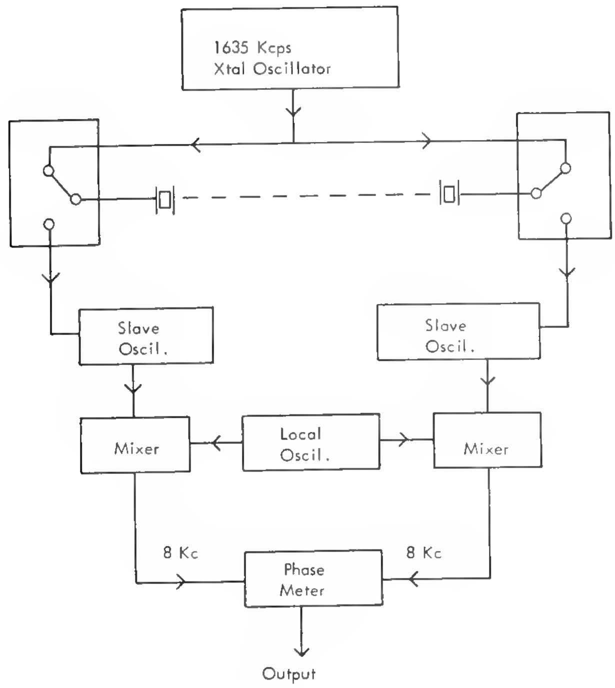

Fig. 3 Block Diagram of O-2 Knot Flow Meter. Switches are Electronic.

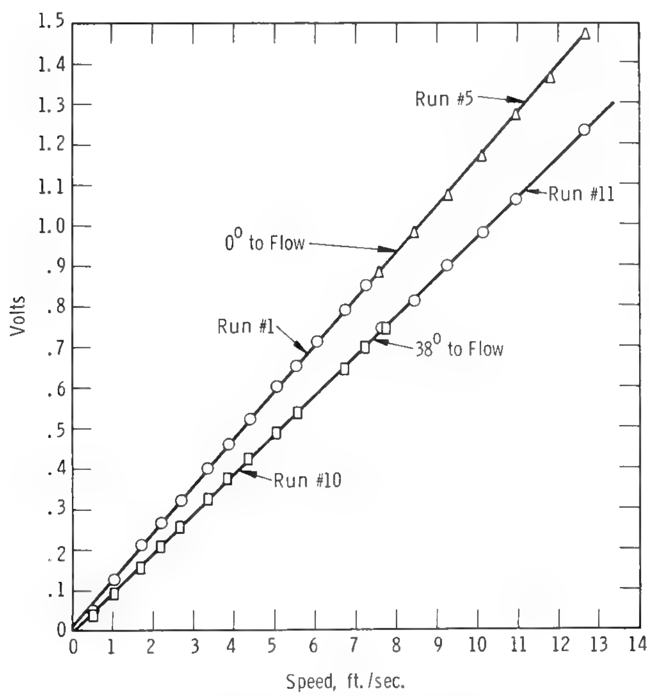

Flow Meter Output vs. Carriage Speed

multiple path transmission and since the errors which were measured can be accounted for by the multiple path effect, the errors due to very turbulent water are assumed to be small or at least rare.

Water tank tests have been conducted which indicate that selective fading of the carrier or side bands does not occur, or at least does not detract significantly from the accuracy of the system. Also, there does not seem to be a sufficient density of scatterers in the ocean at these frequencies to seriously affect these systems.

RESULTS

The meters were tested at David Taylor Model Basin. Fig. 4 shows a graph of the output of the two frequency 10-foot model of the flow meter vs carriage speed for two different alignments to the flow. The graph shows that the meter is accurate to better than 1% and is linear to its maximum velocity. Similar results were obtained for the other two meters.

The two-frequency meter has also been tested at Scripps Institute and at sea aboard the USS Redfin. Under operating conditions at sea the error in the readings can be measured by putting the flow meter in the "zero calibrate" mode. Any indicated velocity is then a noise signal or error of the system. Here it was found that the accuracy varied with thermal conditions from 0.5 ft/sec or 3% of full scale for severe thermal conditions, to better than .08 ft/sec in isothermal water. The average meter reading under all sea conditions approaches the accuracy of the electronic equipment or about 0.3%. Indications are that the 2-foot meter will perform better under nonisothermal conditions, but it has not yet been tested.

The accuracy obtained by these meters is sufficient for many applications, especially at depths where isothermal water is found. The "zero calibration" and the nonfouling feature makes them ideally suited to long-term installations. Their directivity indicates the flow direction. Work is proceeding to improve operation under inhomogeneous conditions.

ACKNOWLEDGMENT

The contributions of O. J. Allen to the development of the two-foot flow meter are gratefully acknowledged.

(A part of this work was done under Contract NOrd 18783)

CURRENT MEASUREMENTS FROM MOORED BUOYS

by WILLIAM S. RICHARDSON
Woods Hole Oceanographic Institution
Woods Hole, Massachusetts

The history of the direct measurement of currents in the deep water of the open ocean is a rather short one. Indirect methods based on the distribution of various chemical and physical properties provide us with a general picture of the deep circulation and calculations based on the distribution of density provide quantitative data which it would be desirable to check by direct measurement.

Many techniques for direct current measurement have been proposed but few have been used to any great extent. Perhaps the most powerful and widely used has been the Swallow float. This technique, developed by Dr. John C. Swallow of the National Institute of Oceanography, utilizes a neutrally buoyant drifter which can be adjusted to drift at any desired depth. The float is tracked acoustically from a ship and may be followed for a period of days or even weeks. This technique in the hands of Swallow, Volkmann, Knauss and others has given us our first glimpse of the details of the movement of the deep water and has contributed greatly to our knowledge of several major current systems. Deep water measurements by this technique in areas well removed from major current systems have shown the currents to be swifter and more variable than had been expected. This points to the necessity for longer time series of current measurements over more extended areas than are easily undertaken with Swallow floats. To provide such measurements, a program of current observations from anchored buoys has been undertaken and as an initial effort a line of stations between Martha's Vineyard and Bermuda has been set. (see Figure 1)

The stations themselves are rather simple. The surface float is a foam filled fiberglass doughnut eight feet in diameter with a three f foot hole. It has about 6000 pounds of buoyancy which is sufficient to part the mooring warp if the mooring strain builds up excessively. The float carries a ten foot high tripod tower on which is mounted a light, a low powered radio beacon for location purposes and a recorder for wind speed and direction. The float is connected to the warp by means of a 3 point, 45° bridle and a 30 foot leader of 1/2 inch galvanized chain. The warp itself is polypropylene rope about 1/2 inch in diameter and having a breaking strength of about 5000 pounds. The rope is somewhat positively buoyant in water and therefore contributes no dead weight strain to the moor. It will stretch about 40% before breaking and this permits the mooring to be set with little or no scope, this being provided by stretch as required. The warp is provided in 500 meter lengths with eyes spliced in each end; instruments are inserted as links between the lengths and must be capable of supporting the full tensile load of the warp. They can therefore be located at any 500 meter multiple in depth or at other depths if special lengths are made up. The bottom end of the deepest length of the warp is connected to a weak link having a strength of about 4000 pounds. This link should part during recovery of the mooring if the anchor is fouled. The ground tackle consists of a cast iron clump weighing 800 pounds followed by 200 feet of 1/2 inch chain (600 pounds) and a 90 pound Danforth anchor.

Because the mooring warp is ordinary rope there is no electrical connection between the various instruments and the surface float. Therefore each instrument must be designed to record internally and the mooring must be pulled in order to retrieve the records. Individual instruments are designed to provide about four months recording so recovery three or four times per year should suffice if the stations last well. The Bermuda line, if fully in place, involves about 150 instruments of various types, current meters, wind recorders, inclinometers, depth recorders and tension recorders. Each of these is capable of storing about 10,000 readings of the variable being measured. This leads to an ultimate data reduction problem with a potential load of 1,500,000 readings, most of which involve more than one measurement, i.e. a current measurement is both speed and direction and the directional measurement is made up of two parts, the orientation of the instrument in the earth's magnetic field (compass) and the relative direction of the current as detected by a vane. Because of this potentially large data reduction problem the recordings in each instrument are made in a digital format on photographic film. The film can then be scanned photoelectrically and the data buffered to a computing machine for processing. Photographic film was selected as the recording medium because many parallel data channels are required and power consumption is less for this type of recording than for magnetic tape or other media.

As an example of the instrumentation we may consider the current meter. This is shown in Figure 4. The instrument is cylindrically

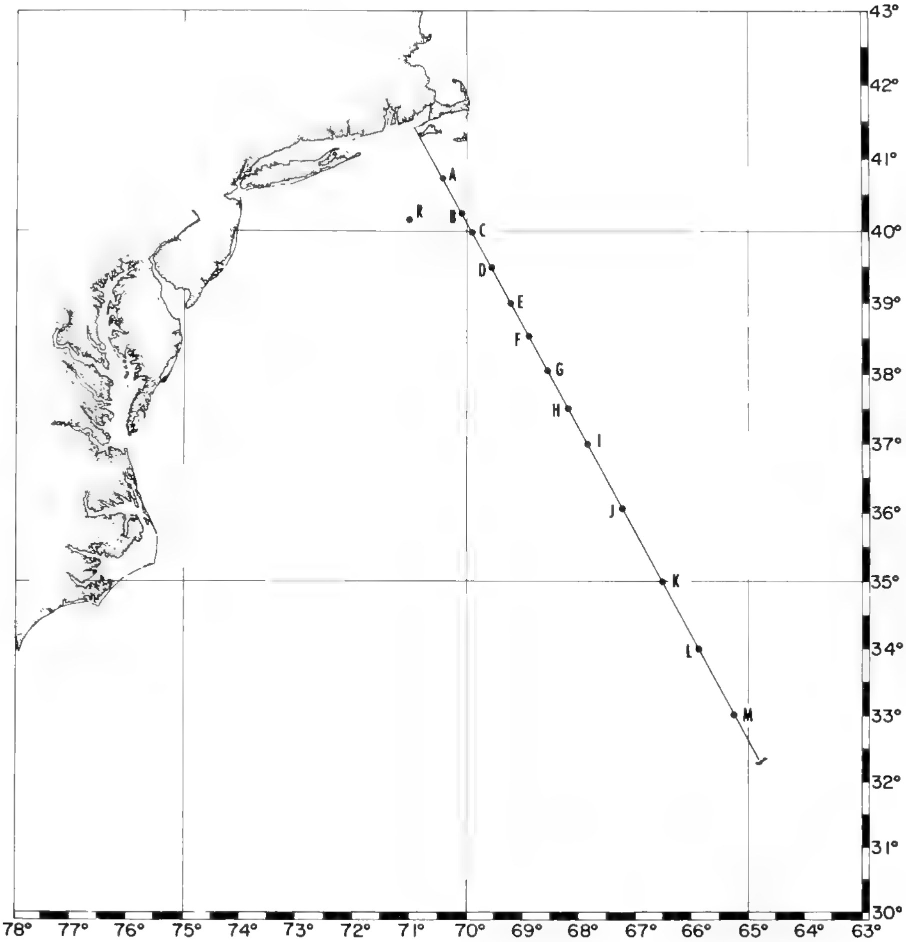

Figure 1 The buoy line.

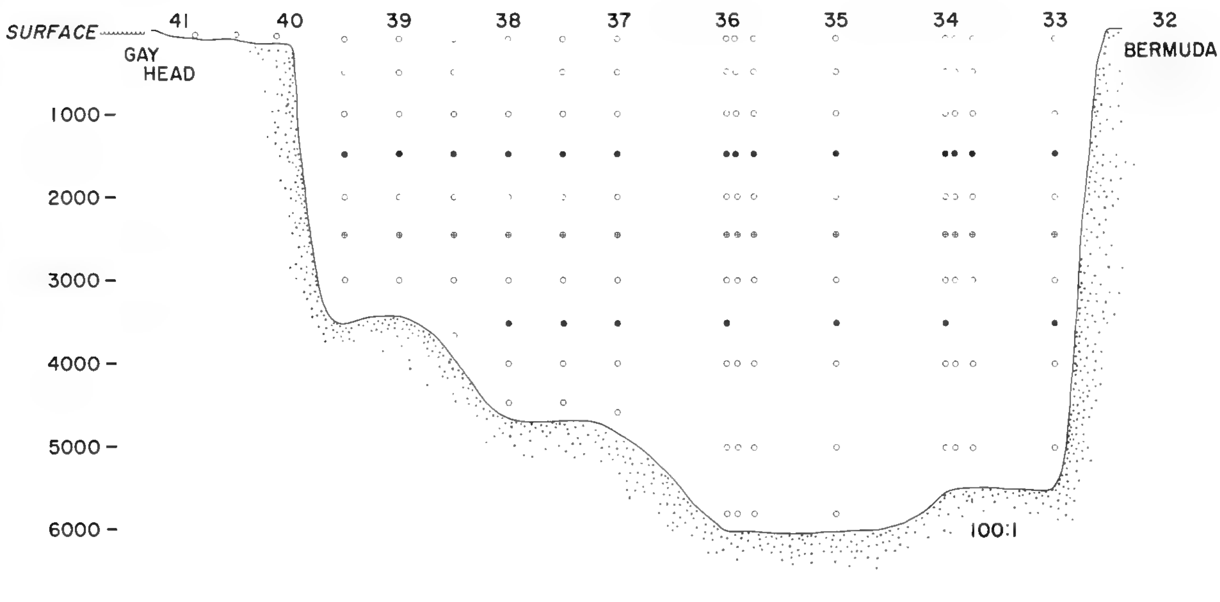

Figure 2 Section of the buoy line.

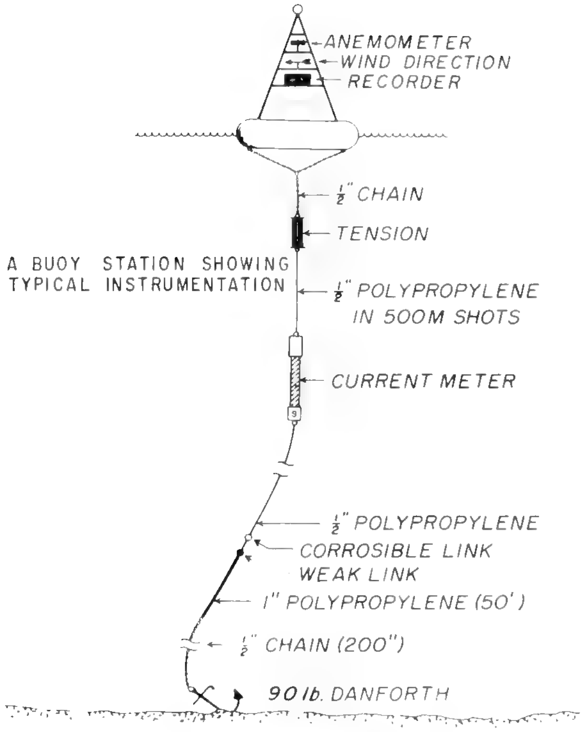

Figure 3 Mooring system

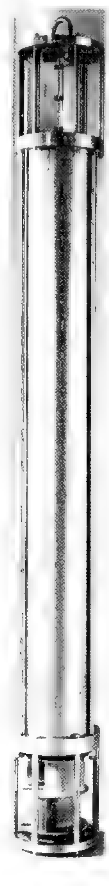

Figure 4 Current meter

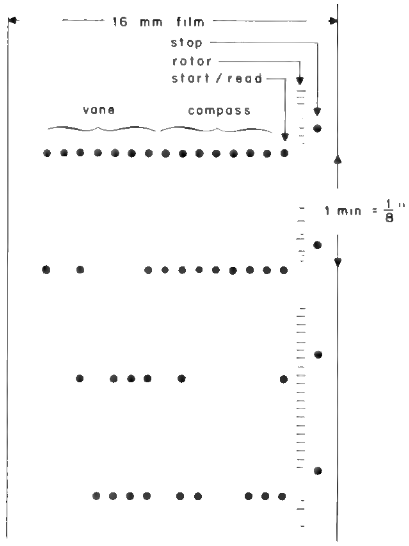

Figure 5 Format of current meter

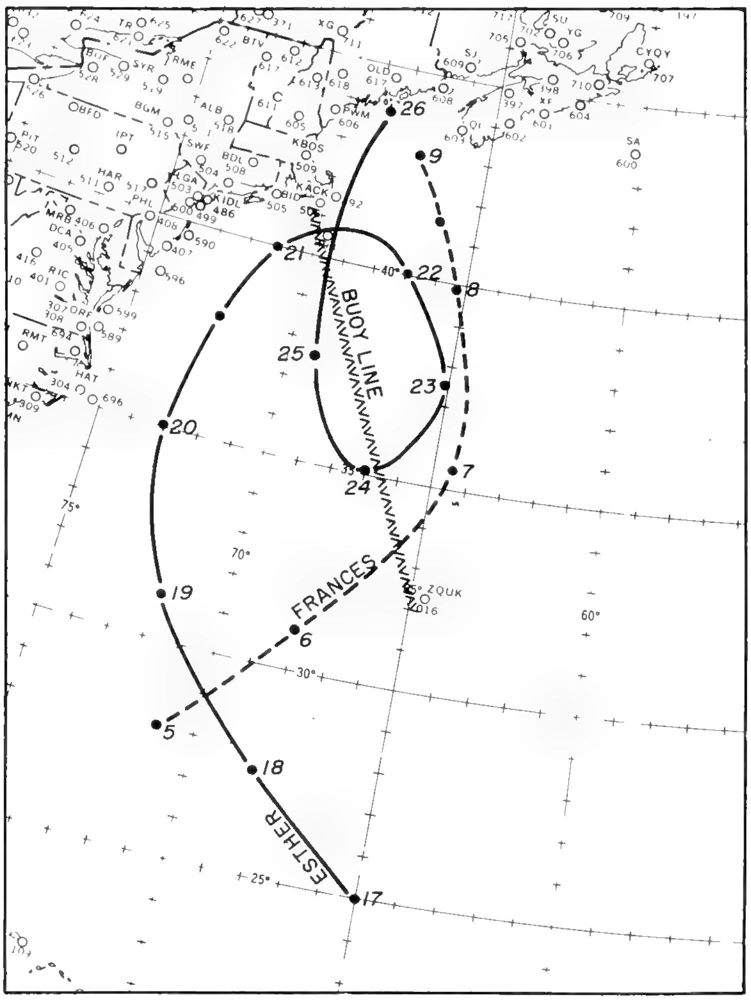

Figure 6 Hurricane tracks.

symmetrical and does not require orientation into the current. Current direction is sensed by a vane in the upper cage which will orient to within 10^o of the current direction at .01 knot. The vane carries a magnet which couples through the end cap of the pressure case to a jewel bearing mounted magnet and seven level gray binary encoding disc. When a light is flashed behind this disc the light passing through the seven channels is "piped" to the field of view of the camera by small plexiglas light guides where it appears as seven spots on the film, either present or not present depending upon the orientation of the vane relative to the pressure case. A similar seven level gray binary number is obtained at the same time from a compass mechanism which also carries an encoding disc. This encodes the magnetic orientation of the instrument as a whole and the difference between the vane and compass readings is the direction of the current. These seven level binary numbers give directions individually accurate to about 2 $1/2^o$ or current direction to 5^o when they are subtracted. The current speed is sensed by a Savonius rotor the bearings of which permit it to start rotating at speeds of less than .01 knot. The rotor is also magnetically coupled through its end cap to a jewel bearing mounted light chopper which provides one pulse of light for each rotation of the rotor. This pulse is "piped" to the field of view of the camera by a fiber optics light guide. The film is advanced at a slow uniform rate by the camera motor (1/8 inch per minute) and the rotor pulses appear as a succession of spots on the film which can be counted photoelectrically. An illustration of the film format is shown in Figure 5.

Tests of the mooring system were made in 1500 fathoms off Bermuda during December and January 1960-61. Tension measurements were made which showed a maximum during this period of about 800 pounds under heavy storm conditions and a typical tension of 100 to 300 pounds. It thus appeared the design was reasonably conservative for a moderate current environment and the instruments required for the line as shown in section in figure 2 were constructed during the spring of 1961. Stations A, R, C and D (Figure 1) were set in early May. Failures of the shallow stations A, R and C occurred after a week or two and this was traced to failure of the bails on the current meters caused by vibration. This fault was corrected and the rest of the line was set in early June. Station H failed and was recovered on a chance encounter of the surface float with R/V ATLANTIS. Failure was attributed to stress corrosion of the tie rods of the upper-most current meter, possibly caused by overstressing during assembly, and the entire moor was lost. Station G failed a few weeks later for the same reason, although evidence for this mode of failure was not available soon enough to allow realization that this was to be a serious problem. Stations I and J (the remaining Gulf Stream stations) were operative for several weeks but were not found when the line was visited for recovery of records in late July. The surface float of station I, together with the upper-most current meter, was recovered by a freighter in October but was set adrift again without retaining the instrument. Thus a good set of Gulf Stream current measurements is still drifting around in the ocean. The surface float from station J has never been reported. Stations A, B, C, D, E, F, K, L and M have been maintained with reasonable success from May or June until late September. The visitations of Hurricanes Esther and Frances, the tracks of which are shown in Figure 6, caused considerable difficulty. The deep stations at D, E, F, K, L, and M which were in place at the time of the storms have survived with only damage to their towers. The shallow stations A, B and C however, are now adrift, although it appears that C was on station some ten days after the passage of Frances.

To summarize, we have been quite successful with deep stations except those in the Gulf Stream where we have had no success at all. The shallow stations (less than 100 fathoms) have been reasonably successful during the summer months but have fallen victim to the fall storms.

At the time of this writing the work of data reduction has just begun. Hopefully we will be able to report on this in the near future.

DEEP CURRENT MEASUREMENTS NEAR BERMUDA

by RAYMOND F. McALLISTER

INTRODUCTION.

IT HAS BEEN CUSTOMARY FOR YEARS TO MEASURE DEEP OCEAN CURRENTS INDIRECTLY, DEDUCING THEM FROM DYNAMIC TOPOGRAPHY. MORE RECENTLY THE JOG-LOG, PARACHUTE DROGUES AND NEUTRAL DENSITY FLOATS, ALONG WITH ANCHORED BUOY RECORDING STATIONS, HAVE BEEN USED.

ALL OF THESE METHODS SUFFER FROM THE SAME DIFFICULTY: THEY FILTER OUT HIGH FREQUENCY FLUCTUATIONS IN CURRENT SPEED AND DIRECTION, EITHER BY THE LONG TIME BETWEEN SUCCESSIVE RECORDINGS, BY MECHANICAL FILTERING DUE TO THE LONG CONNECTING LINE TO THE SURFACE, OR BY THE DIFFICULTY IN OBTAINING ACCURATE GEOGRAPHIC LOCATION. THIS IS NOT TO SAY THAT THESE ARE NOT EXCELLENT METHODS OF MEASURING CURRENTS, BUT RATHER THAT THEY COULD NOT SATISFY THE OBJECTIVES OF THIS STUDY, FOR WHICH A CONTINUOUS RECORDING CURRENT METER WITH A HIGH SPEED OF RESPONSE TO CURRENT CHANGES WAS NEEDED. THIS REPORT DETAILS THE METER DEVELOPED AND SOME OF THE INTERESTING RESULTS ACHIEVED.

THE METER.

IN 1960, THE OFFICE OF NAVAL RESEARCH AGREED TO SUPPORT THE CONSTRUCTION AND INSTALLATION OF A SERIES OF CABLE CONNECTED CURRENT METERS, DESIGNED TO GIVE CURRENT SPEED, AND ULTIMATELY DIRECTION, TO RECORDERS PLACED ON THEIR TEXAS TOWER RESEARCH PLATFORM ON PLANTAGENET BANK, BERMUDA. THIS TOWER, CALLED "ARGUS ISLAND", IS SITUATED ON THE BANK, IN 194 FEET OF WATER, ABOUT 25 MILES FROM BERMUDA. ITS LOCATION IS SHOWN IN FIGURE I, AT THE TIP OF THE ARROW.

THE FIRST METERS INSTALLED WERE SAVONIUS ROTOR SPEED UNITS AT 200 AND 500 FATHOMS, CONNECTED TO ARGUS ISLAND BY A TWO CONDUCTOR PLASTIC INSULATED CABLE WITH SEA RETURN AND A THREE CONDUCTOR DOUBLE ARMORED CABLE RESPECTIVELY. POWER WAS PROVIDED FROM THE SURFACE TO LIGHT A GRAIN OF WHEAT BULB WITH NEAR INFINITE LIFE AT RATED VOLTAGE. THE SPEED SIGNAL WAS GENERATED WHEN THE LIGHT FROM THE BULB, FALLING ON A PHOTOSENSITIVE DEVICE, WAS INTERRUPTED BY A SEGMENTED SKIRT ON THE SAVONIUS ROTOR. THIS IS, IN ESSENCE, THE PHOTO ELECTRIC PICKOFF DEVELOPED IN WM. RICHARDSON'S LAB AT WHOI. A CLEAR "GO-NO-GO" SIGNAL RESULTED, WHICH WAS EXTREMELY DEPENDABLE AND READABLE EVEN THROUGH A HIGH LEVEL OF ELECTRONIC NOISE FROM THE RECORDER OR CABLE.

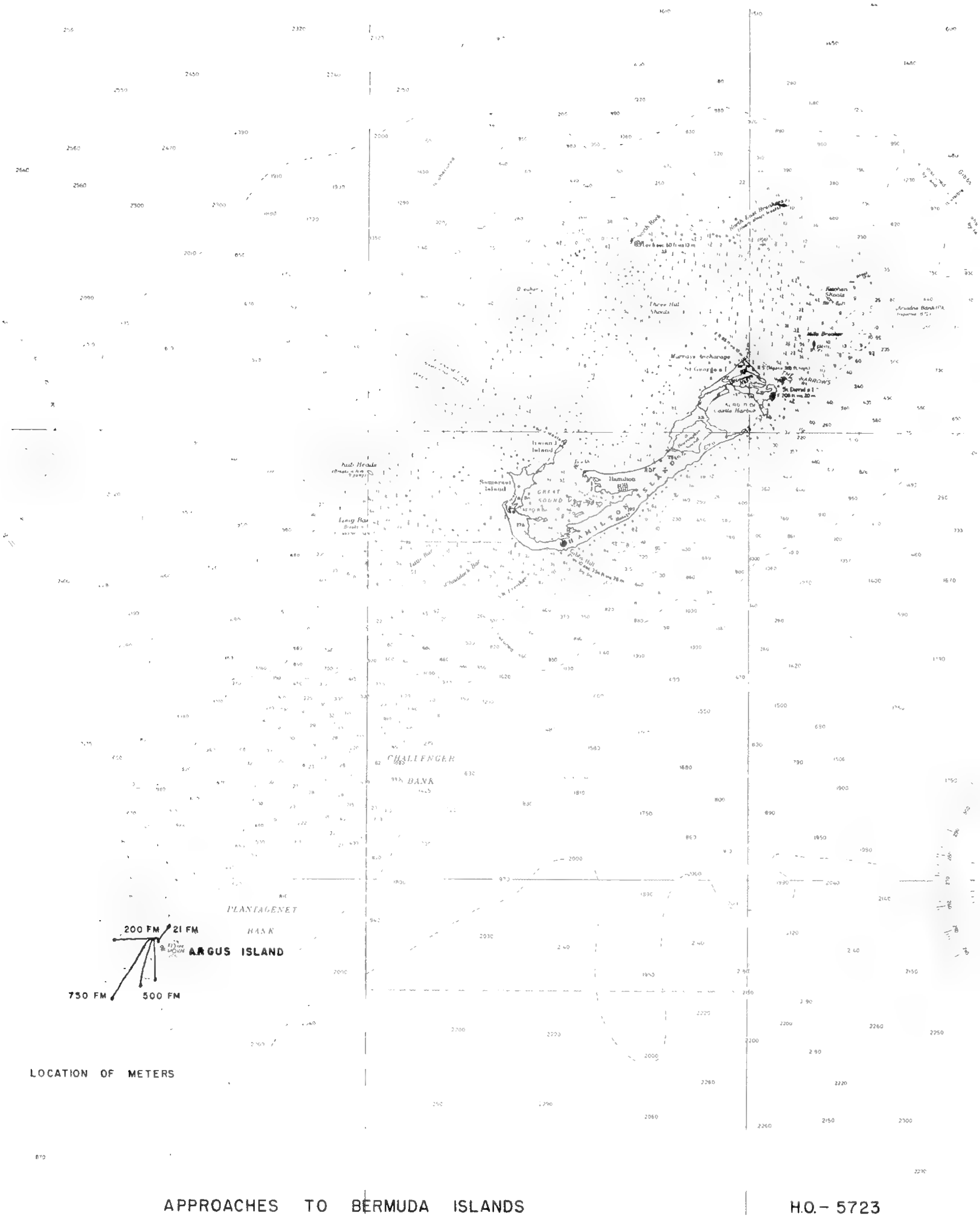

Figure I. BERMUDA, Associated Banks and the Location of Argus Island.

SUBSEQUENTLY, A UNIT WAS PLACED ON TOP OF PLANTAGENET BANK AT A DEPTH OF 21 FATHOMS, AND LATER YET ANOTHER WAS INSTALLED AT 500 FATHOMS, BUT IN A DIFFERENT LOCATION ON THE FLANK OF THE BANK. ALL OF THESE UNITS, AND A LATER ONE WHICH MEASURED RELATIVE DIRECTION, WERE FLOATED 50 FEET OFF BOTTOM TO GET AWAY, IF POSSIBLE, FROM NEAR BOTTOM EFFECTS. FIGURE 2 SHOWS THE LOCATION OF THE VARIOUS UNITS, AND FIGURE 3 THE CURRENT METER INSTALLED ON BOTTOM.

PLANTAGENET BANK SHOWS A LARGE MAGNETIC ANOMALY, AND MAGNETIC DIRECTION SENSING DEVICES WERE ELIMINATED AS POSSIBILITIES FOR DETERMING CURRENT DIRECTION IN THE AREA. A RELATIVE DIRECTION MEASURING DEVICE, CONSISTING OF A CONTINUOUS ROTATING POTENTIOMETER WITH A VERY LONG LIFE EXPECTANCY, WAS BUILT. THE POTENTIOMETER IS CONNECTED TO A VANE WHICH HAS NEAR NEUTRAL BUOYANCY, AND IS RUN UPSIDE DOWN IN LIGHT OIL. A SMALL TIMING MOTOR AT THE INSTRUMENT END OF THE CABLE PROGRAMS THE SPEED AND RELATIVE DIRECTION UNITS, IF DESIRED, AND SENDS A ZERO AND 360^{o} CALIBRATION MARK UP THE CABLE AT REGULAR INTERVALS. FIGURE 4 SHOWS BOTH SPEED AND DIRECTION UNITS BUILT FOR DISPLAY PURPOSES. WHEN THE RELATIVE DIRECTION UNIT IS USED, THE WHOLE PACKAGE IS MOUNTED AT THE TOP OF A 3/8" SOLID STEEL ROD TO PREVENT ROTATION WITH RESPECT TO THE BOTTOM.

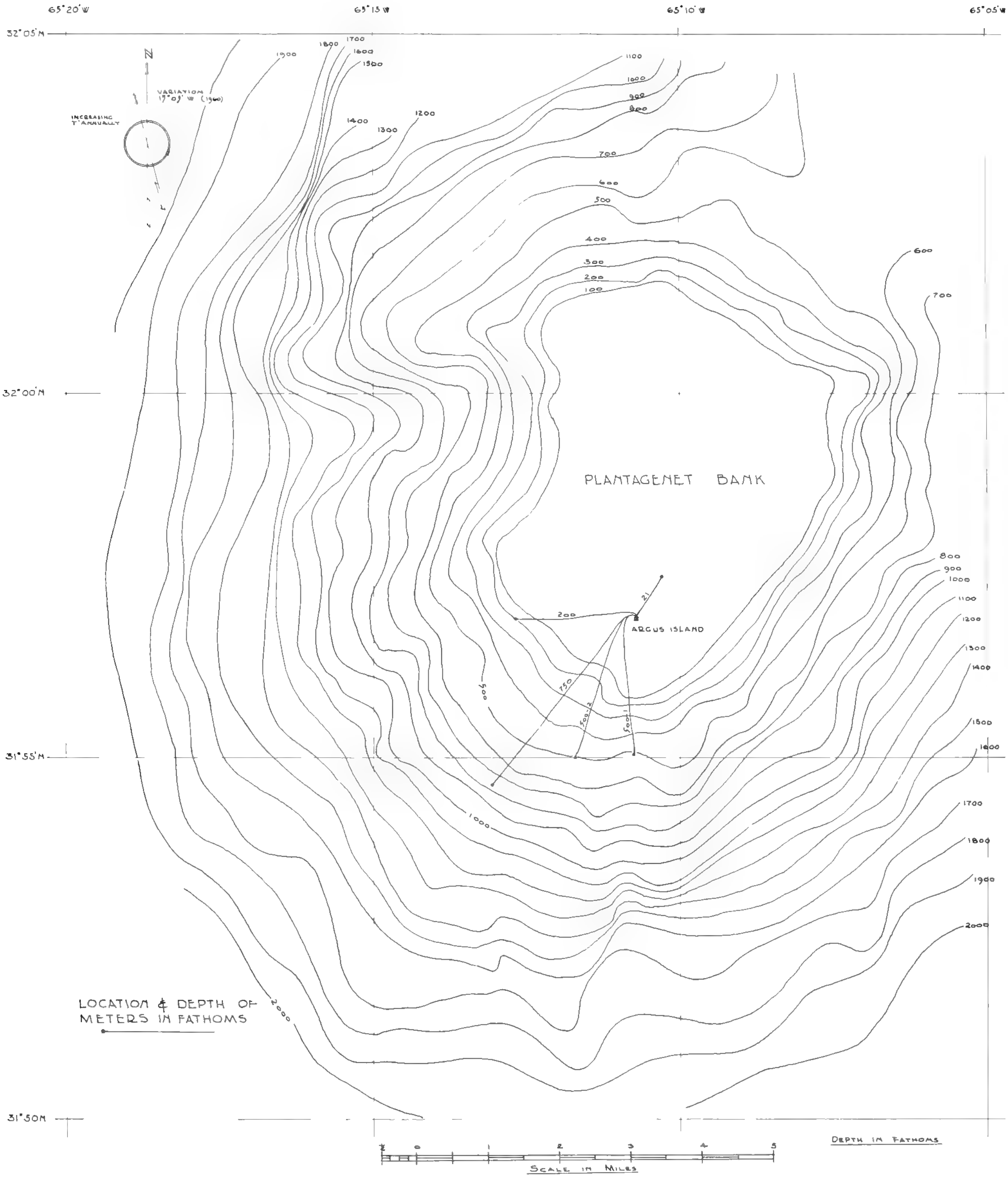

FIGURE 2. LOCATION OF 5 CURRENT METERS ON THE FLANKS OF PLANTAGENET BANK.

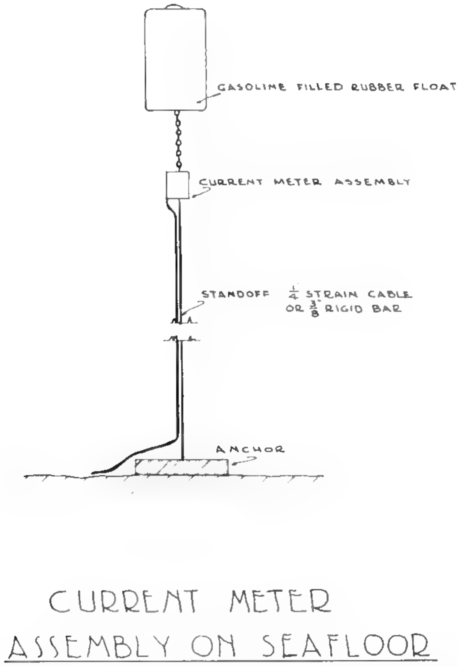

FIGURE 3. THE CURRENT METER ASSEMBLY AS INSTALLED.

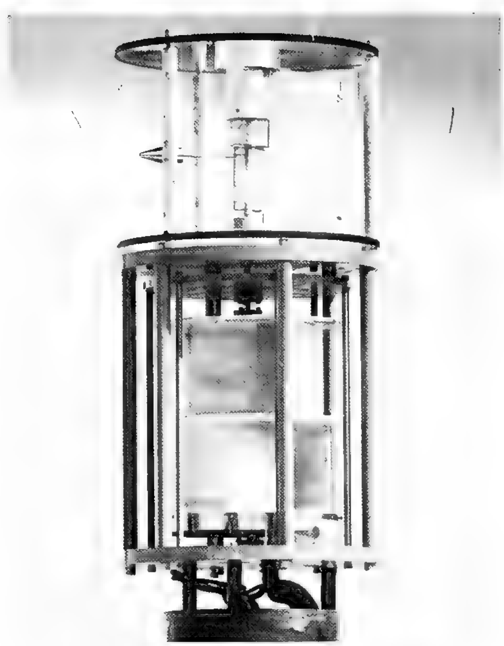

RESULTS.

THUS FAR SIX METERS HAVE BEEN INSTALLED AND HAVE GIVEN RECORDS FOR SOME TIME. ONE FAILED AFTER SEVERAL DAYS, BY DEVELOPMENT OF A SHORT UNDER 2000 FMS OF WATER, AFTER RETURNING A SHORT SEQUENCE OF CURRENT SPEEDS. THE 750 FM UNIT WAS INTENDED TO GIVE SPEED AND DIRECTION, BUT THE SPEED SENSOR FAILED TO OPERATE AND ONLY RELATIVE DIRECTION WAS OBTAINED. THE RECORD CEASED WHEN AN ATTEMPT WAS MADE TO RECOVER THE INSTRUMENT FOR REPAIR. THE REST OF THE UNITS GAVE SPEED SIGNALS FOR PERIODS UP TO TWO MONTHS, AND ALL FAILED BY CABLE BREAKS AT THE ARGUS ISLAND END EXCEPT THE 21 FM UNIT WHICH, PREDICTABLY, FOULED AFTER ABOUT TWO WEEKS OF OPERATION. IT IS INTERESTING TO NOTE THAT ONE OF THE CABLES WAS PROBABLY BROKEN BY A MIGRATING HUMPBACK WHALE AT THE POINT WHERE IT EXTENDED FROM THE TOWER TO THE SEA-FLOOR IN A BIG CATENARY.

ON THIS SAME BANK, ONE INCH STEEL BUOY CHAIN HAS PARTED ON A NUMBER OF OCCASIONS DURING STORMS, AND EXPANDED MESH PLATFORMS HAVE BEEN CURLED UP AND CARRIED AWAY BY STORMS. CABLE TERMINATION HAS THEREFORE PRESENTED A PROBLEM, BUT IN SPITE OF THE RELATIVELY SHORT CABLE LIFE OF THE SEVERAL UNITS, PROPER SHORE TERMINATION OF FUTURE CABLES IS EXPECTED TO INCREASE LIFE BY A FACTOR OF 10 OR MORE.

A typical speed record is shown in Figure 5, at a time when three meters were running simultaneously. Plots of a portion of the three unit record are shown in Figure 6, and of the 750 fm direction signal in Figure 7.

In general, current speeds at depths of 200 and 500 fms are fairly high. A maximum current of 1.16 knots was recorded at 200 fms, with currents in excess of 0.75 knots relatively common. Spurt currents of up to 0.64 knots in one second have been observed at this depth, while currents below the meter threshold occur at other times. Meter threshold is about 0.04 knots. At 500 fms the maximum recorded current speed was 0.58 knots, although this did not occur at the time of year during which drogue measurements indicate the highest speeds at this depth. Reference to Figure 6 will show that no ready correlation exists between the 21, 200 and 500 fm records. Longer records are equally inconclusive in this respect. Currents reported from the short lived 2000 fm meter ranged up to 0.13 knots, with this meter 30 feet off the bottom for easier handling of the unit.

Current directions from the 750 fm unit show a fantastic change in azimuth with time. Figure 7 shows changes of 50^o in 30 sec, 80^o in 60 sec, 130^o in 4 min, 180^o in 8-1/2 min, and 360^o in 77 min. Other portions

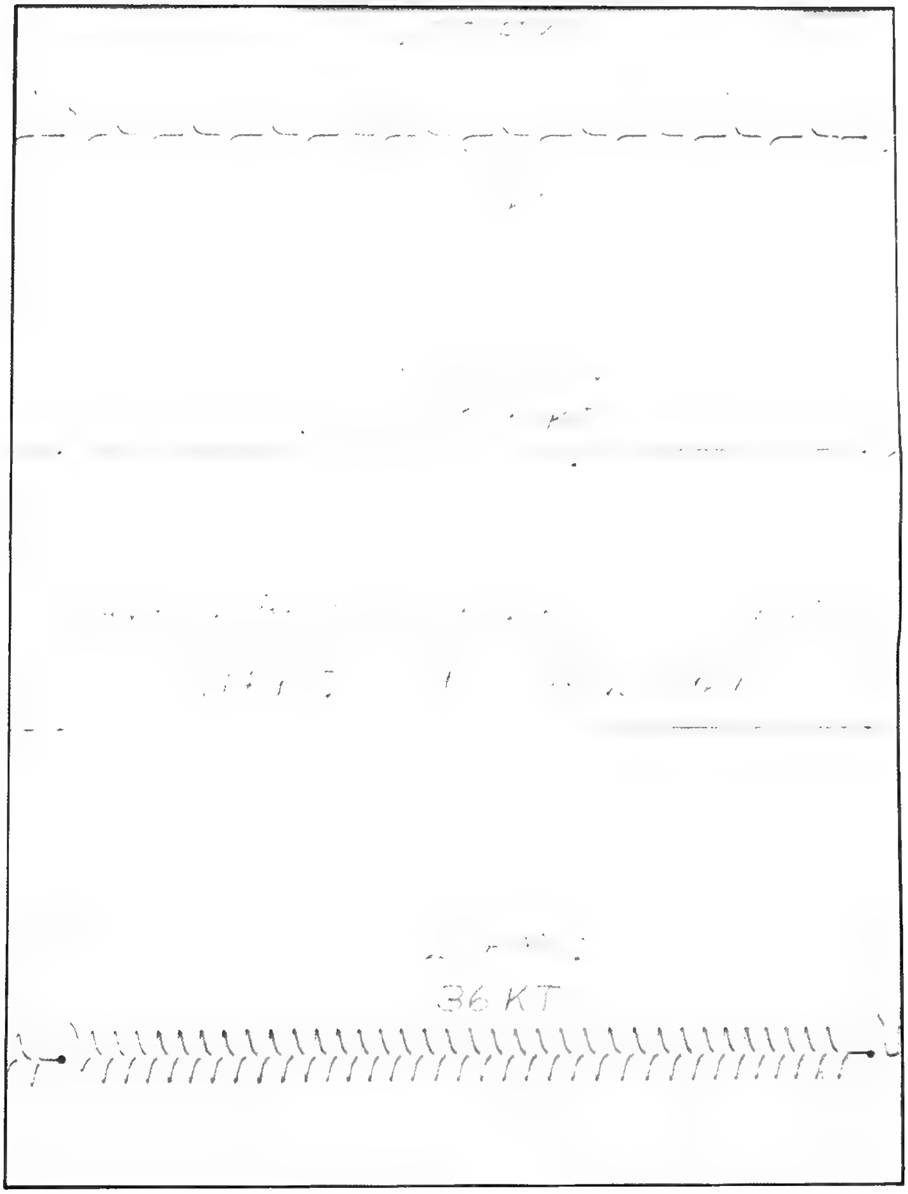

FIGURE 5. HOT PEN PAPER RECORD OF 3 CURRENT SPEED METERS WORKING SIMULTANEOUSLY.

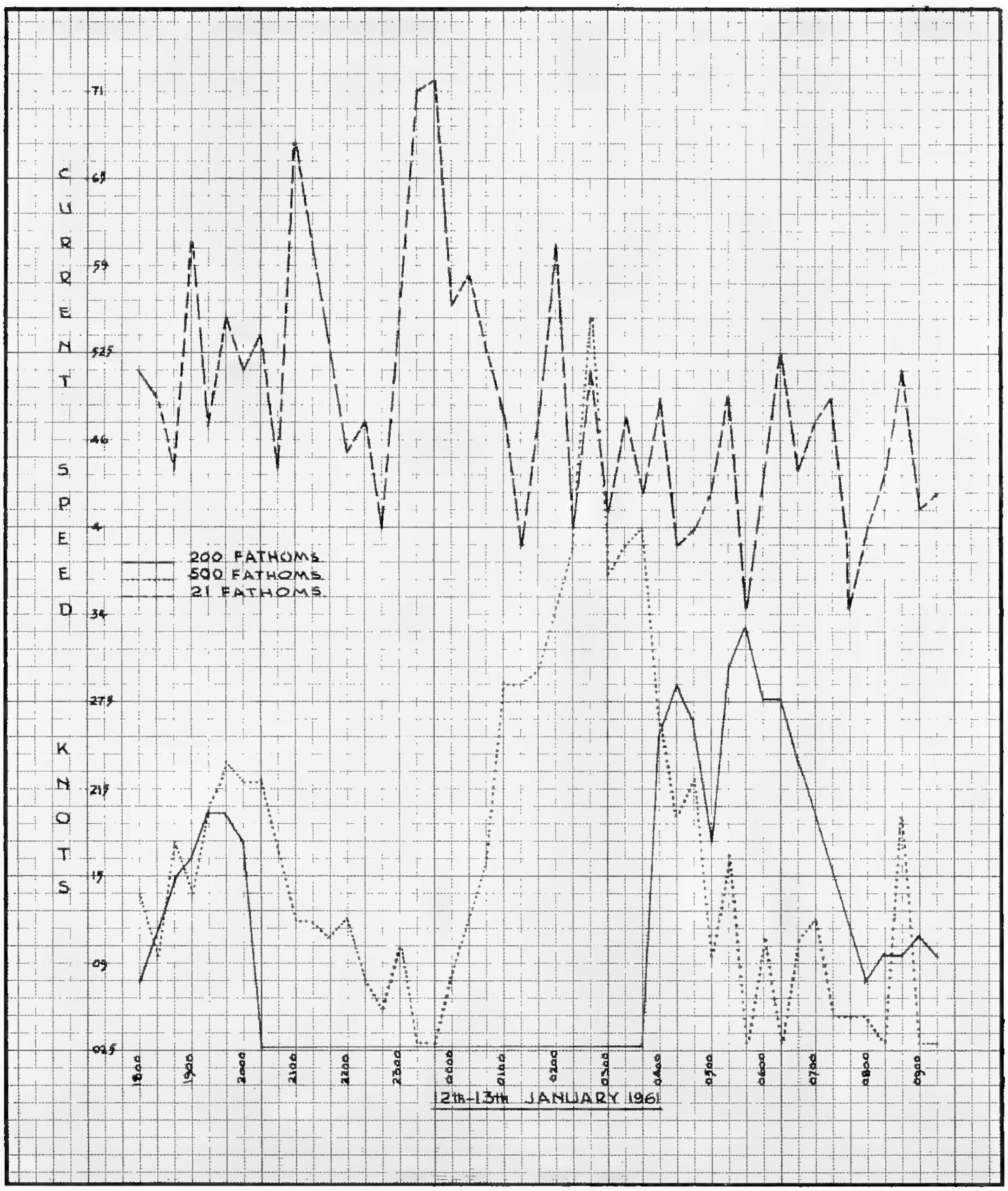

Figure 6. 15 Hour Plot of Current Speeds at Three Depths in Plantagenet Bank Area.

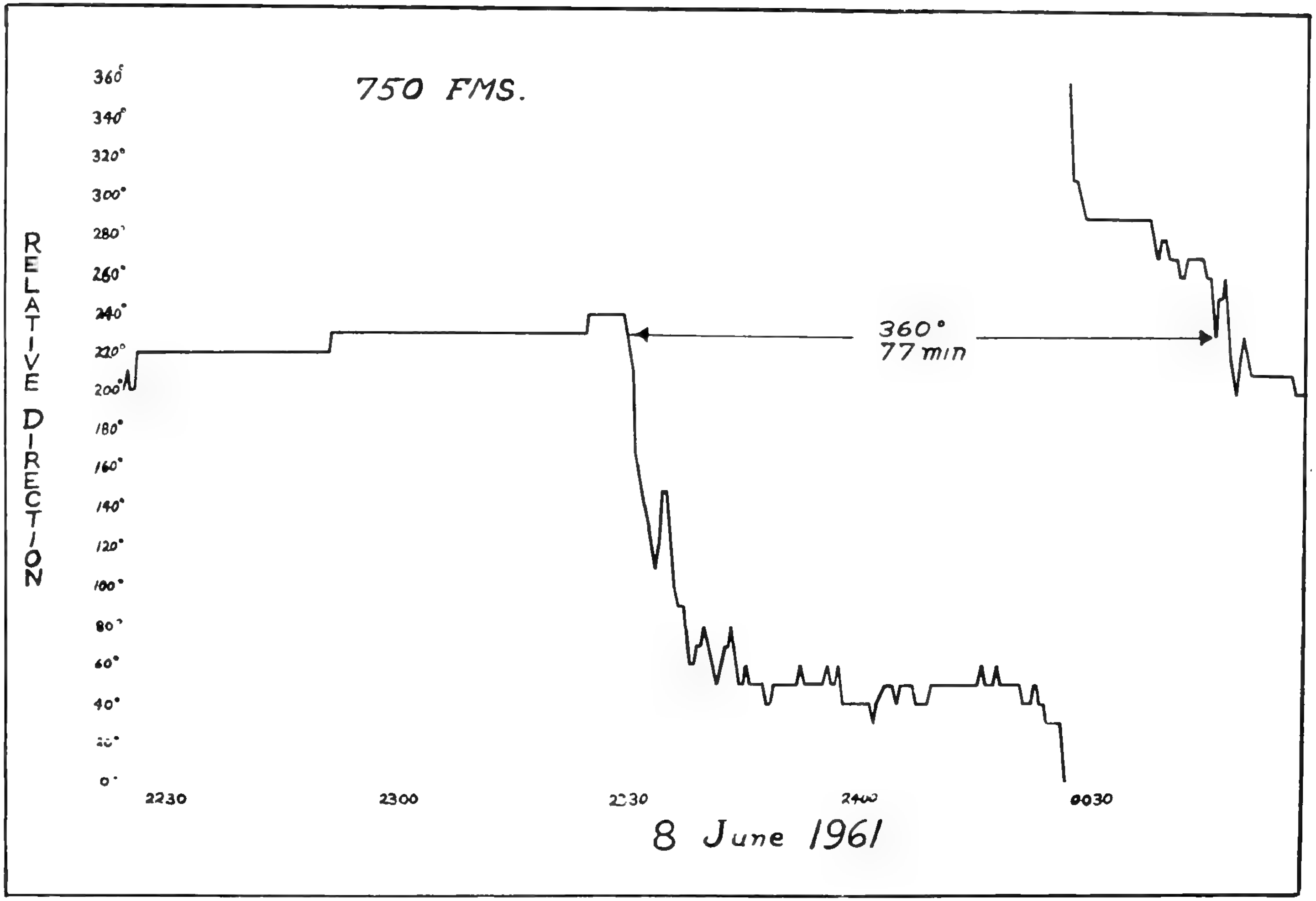

FIGURE 7. TWO AND ONE HALF HOURS OF CURRENT DIRECTIONS AT 750 FM ON THE FLANK OF PLANTAGENET BANK.

OF THE RECORD SHOW 40^0 IN 4 SEC, AND 110^0 IN 30 SEC, 220^0 IN 30 SEC, AND 180^0 IN 4 MIN. THESE RESULTS, COUPLED WITH THE SPURT CURRENT SPEEDS AND WITH SOME RESULTS OBTAINED IN EARLIER YEARS WITH THE PARACHUTE DROGUES, MAKE ONE SUSPECT THE PRESENCE OF EDDIES AND GENERAL TURBULENCE IN THE LEE OF THE BANK, AND PERHAPS ALSO IN THE LEE OF RIDGES AND PROJECTIONS ON THE FLANK OF THE BANK. IT IS PLANNED TO PLACE A GROUP OF THREE METERS AT ACCURATELY KNOWN SPACING, ROUGHLY IN A TRIANGLE, WITH THE OBJECTIVE OF MEASURING SCALE AND DURATION OF THE EDDIES.

MAURICE BLAIK, AT HUDSON LABORATORIES OF COLUMBIA UNIVERSITY, IS STUDYING TURBULENCE IN THE SEA, AND HAS RUN A SPECTRAL DENSITY ANALYSIS OF ONE 72 HOUR RECORD. HE FINDS A SERIES OF PERIODICITIES RANGING FROM $1\frac{1}{2}$ CYCLES PER DAY (CPD), AND A RATHER STRONG 2 CPD, TO A VERY WEAK 26 CPD. WITHOUT CURRENT DIRECTION, SOME OF THE CYCLIC INFORMATION MAY BE UNDECIPHERABLE, SINCE THE METER REACTS TO ALL CURRENTS IN A HORIZONTAL PLANE, BOTH FORWARD AND BACKWARD. HIS FINDINGS, ADMITTEDLY BASED UPON A SHORT SAMPLE AND NECESSARILY TENTATIVE, ARE AS FOLLOWS:

Peak frequencies :-	cycles/day at 200 fm	500 fm
	$1\frac{1}{2}$	2
	$4\frac{1}{2}$	$4\frac{1}{2}$
	$7\frac{1}{2}$	
		9
	12	
	$14\frac{1}{2}$	14
	18	
	20	20
	26	26

No interpretation of this data is attempted.

It is felt that the program of cable connected current meters and other sensors is a promising one and further work will be done to improve it. Serial sampling of several sensors and transmission of the data along a single conductor and sea water ground is possible with the present state of the art, as is simultaneous transmission of several frequency separated sensor outputs. It is expected that this program will continue and be expanded.

SEA STATE — EFFECTS AND PROBLEMS

by LEE M. HUNT, Technical Assistant
Committee on Undersea Warfare
National Academy of Sciences
Washington, D. C.

ABSTRACT

Sea state exerts a greater overall effect on the Navy and merchant marines than any other single environmental factor. This paper, in order to emphasize this point, discusses the effect of wave height on background noise and surface reverberation which imposes limitations on sonar and radar effectiveness, and its effect on ship speed and ship damage. Wave forecasting, wave height observations, and the sea state code are also discussed from the standpoint of present practice and needed improvements.

INTRODUCTION

Since man first went down to the sea in ships, or canoes for that matter, his worst enemy has been heavy seas. What astronomical value figure could we attach to the vessels lost and damaged by this age old enemy -- how many thousands of lives have been lost to its whim? We will never know, but some insight is gained by considering the fact that during the latter phases of World War II this enemy did more damage to our Pacific Fleet than did the Japanese.[1] In one encounter off the Philippines in December 1944, 3 destroyers (HULL, SPENCE, MONAGHAN), 200 aircraft, and 790 men were lost. Twenty-eight ships were damaged, and 9 so badly that they required major overhauls. Admiral Nemitz called this, "The greatest loss that we have taken in the Pacific without compensatory return since the First Battle of Savo."[2]

The "battle of the interface", however, has not been entirely one-sided. Man has made some progress beginning with Maury's sailing charts which, among other things, reduced the average sailing time between London and San Francisco by 47 days. Sverdrup and Munk developed the wave and surf forecasting technique by which countless lives were saved during the amphibious landings of World War II. More recently, Pierson, Neumann, and James formulated the Wave Spectrum Method of wave forecasting used in the Navy's Ship Routing Program through which the average sailing time for Atlantic crossings has been reduced by 1 day and that of the Pacific by 5 days. In addition, it has resulted in a drastic reduction in ship and cargo damage due to heavy seas. Backing up wave forecasting has been the indispensable progress in meteorology which provides the basic imputs to the wave forecasting machinery.

The interface battle, however, is no longer concerned only with the loss of ships and lives in the direct sense. The battle became multifronted with the introduction of the submarine as an efficient and highly effective weapon during World War I. Its performance in sinking nearly 5 percent of the total British shipping during a single month (April 1917), and accounting for 69 percent of the 21,000,000 gross tons of Allied shipping lost to enemy action during World War II[3] has clearly made it a weapon to be countered. But countering must be preceded by detection, and for this we

"Superior numbers refer to similarly numbered references at the end of this paper."

depend primarily upon sound about which it has often been said, "the only thing constant about sound in the sea is its variability."

Since sea water is virtually opaque to electromagnetic waves, we can expect sound to continue to be the cornerstone of our detection systems for some time to come. We do and will continue to depend upon it not only for the detection of submarines by hull mounted, towed, and bottomed systems, but as the sensing element in homing torpedoes, in the location of mines, and to provide the guidance by which future submarines will maneuver through the mountains and valleys of the ocean bottom. We can expect, then, that the evolution in sonar systems will continue towards greater sensitivity and range. One of the greatest stumbling blocks in the path of this evolution is the environment through which sound must propagate, and, not the least of the parameters involved is sea state.

The following discussion is designed to review the most important effects of sea state on naval and merchant marine operations and to point out some of the present and future problems. Some areas of the discussion will, of necessity, be limited either by classification or the lack of adequate data.

THEORY OF OPERATION

EFFECTS

Ambient Noise

The "composite noise from all sources in a given environment excluding the desired signal and noise inherent in the measuring equipment and platform" [4] may be considered ambient noise. Although there are many sources of this noise ranging from the thermal agitation of water molecules to biological and man-made noise, the dominant noise, under open-sea deep-water conditions, orginates at the sea surface and increases with increasing sea state. Its importance to the Navy lies in the fact that as sonar systems and platforms are made quieter it may provide the limiting noise background in which a signal must be detected. Indeed, under proper conditions it serves this purpose now.

During World War II deep-water ambient noise was studied extensively and the results of many wartime measurements have been summarized in the form of the well-known "Knudsen" curves showing the spectrum of deep-water noise and its dependence on sea state. [5] These curves, reproduced in Fig. 1 are still accepted as representative of average ambient noise levels in the frequency range 1 - 25 kc. Over this range the curves indicate a noise level increase of about 25 db as sea state increases from 0 to 6, with a similar increase at a given sea state as the frequency decreases from 25 to 1 kc. More recent investigations have shown that thermal noise poses an absolute limit to the Knudsen curves at about 50 kc [6], and that at frequencies below 500 cps the values deviate somewhat from the extrapolated Knudsen curves.

It is worth emphasizing that the Knudsen curves represent the gross averages of many measurements made at the various sea states. No distinction is made between sea and swell nor do the curves indicate the stage of development or decay of the waves under which the measurements were made. It is possible that the correlation between wave height and ambient noise is such that sea state can be determined by measuring the noise level. Far more detailed measurements with respect to sea conditions will have to be made, however, before this can be demonstrated. Regardless of this application, the unrelenting war on background levels alone requires a better distinction between ambient noise levels and sea conditions.

Although the correlation between ambient noise level and sea state has been well demonstrated, the method by which the noise is produced at the surface is little understood. It has been suggested that such things as breaking waves or white caps, bubbles bursting at the surface after being entrained by breaking

Figure 1. Deep Water Ambient Noise Levels for Sea States 0 Through 6. (Knudsen Curves with 5 db standard deviation.)

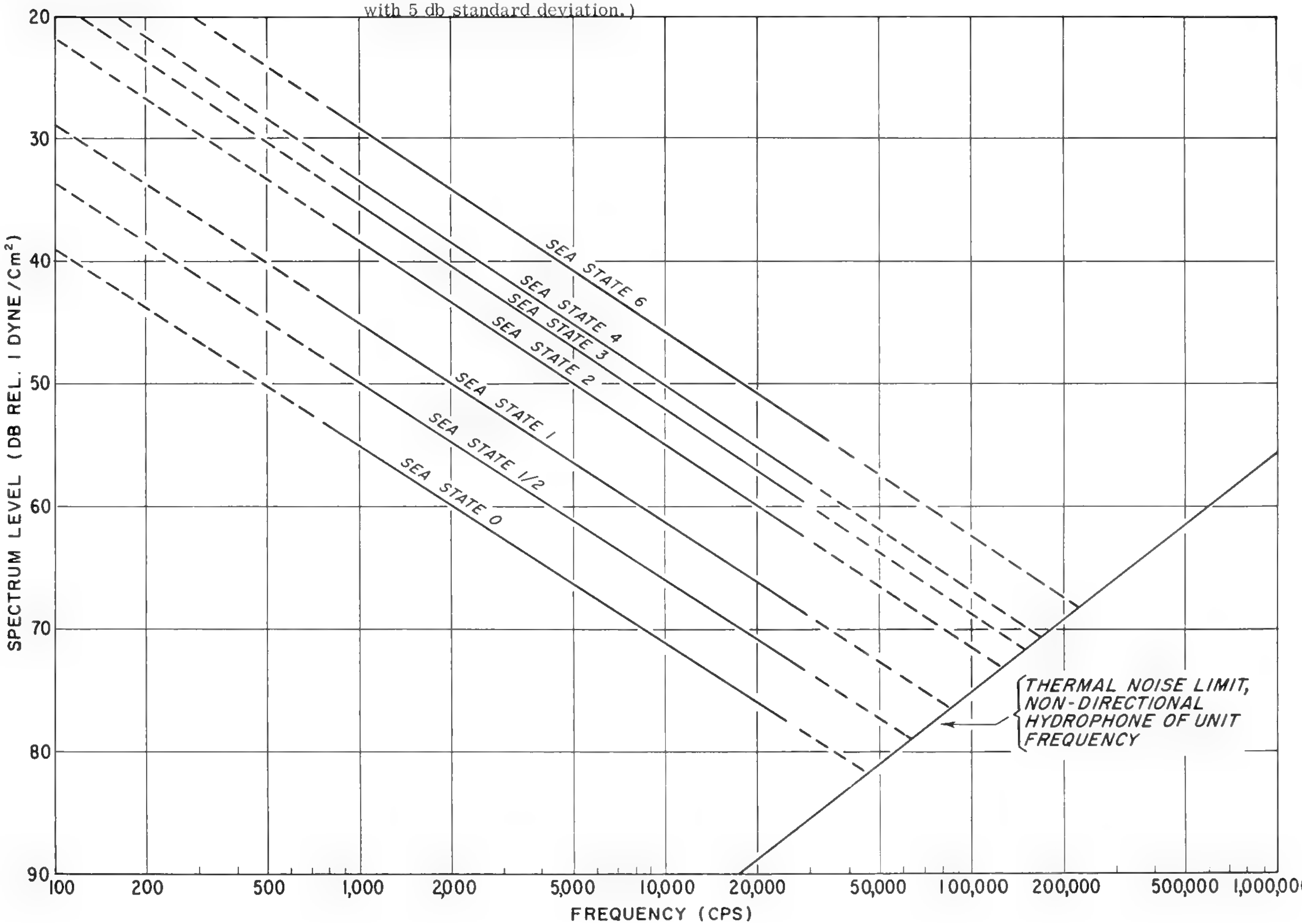

waves, the pressure effect of capillary wave trains, or atmospheric turbulence created by wind over the roughened water surface may be responsible.[7] Certainly, the first two of these produce some noise, but these conditions do not become prevalent until about sea state 3. Fig. 1 shows that of the 25 db increase in spectrum level between sea state 0 and 6, 19 db of this occurs between sea state 0 and 3, and 10 db between sea state 0 and 1 with the maximum significant wave height being 4 feet and 1/3 foot respectively. This indicates that the greatest portion of the noise increase must be explained by factors other than breaking waves and bubbles entrained by such waves.

The declining increment in noise level above sea state 3 itself may be due to the filtering effect of a shallow bubble layer which scatters the sound back to the surface thereby preventing a large portion of it from reaching the hydrophone.

While ambient noise can be produced by fluctuations in hydrostatic pressure, it is doubtful that capillary waves contain enough energy to account for much of the observed noise. Wind, on the other hand, certainly possesses enough energy and may play a significant role in sound production, but more investigation is needed before this can be determined.

As sonar systems become more sophisticated, high ambient noise levels will become increasingly bothersome unless discriminated against or operated around. Too, since the noise is virtually independent of depth, sonar systems designed to escape surface reverberation, adverse thermal conditions, and platform noise will still have to contend with ambient noise. The Knudsen curves coupled with wave forecasts will make it possible to do a passable job of forecasting ambient noise levels under deep-water conditions. Forecast accuracy cannot be improved, however, without a more detailed knowledge of noise level with respect to sea conditions.

Surface Reverberation

Reverberation in underwater sound is the sound scattered back towards the source by various inhomogeneities of the environment. It is customarily designated surface, volume, or bottom reverberation depending upon the source of the scatterers. The irregularities of the surface and bottom are primarily responsible for the reverberation originating at these two surfaces, while biological organisms, particulate matter, and possibly turbulent and thermal microstructures are considered responsible for volume reverberation.

With observed increases in surface backscattering strength of around 28 to 30 db at wind speed as low as 18 knots, providing a level of about -26 db for low grazing angles and considerably greater for high angles (see Fig. 2), the importance of surface reverberation to the Navy is obvious. In deep water it will often provide the limiting noise level, a fact that, as in the case of ambient noise, can only become more serious as the noise from other sources is reduced.

Although there can be little doubt that surface reverberation is caused by surface and near-surface irregularities, and increases with increasing sea state, the data from most investigations have been more easily correlated with wind speed than with sea state. Since the wind can only influence surface reverberation through its effect on the sea surface the reason for this better correlation with wind speed may be due to one or more of the following: (1) the lesser accuracy to which sea state is usually measured as compared to wind speed; (2) the present lack of accurate correlation between bubble density and sea state; (3) very high frequency waves are a more rigid function of wind speed than of sea state; and/or, (4) the mere determination of the significant wave height does not, by itself, give any idea of the stage of development of the wave spectrum.

Figure 2. Surface Back-Scattering Strength vs Grazing Angle at 60 kc for Various Wind Speeds. (Adapted and simplified from Fig. 4, Ref. 8; Fig. 11, Ref. 9 and Ref. 10.)

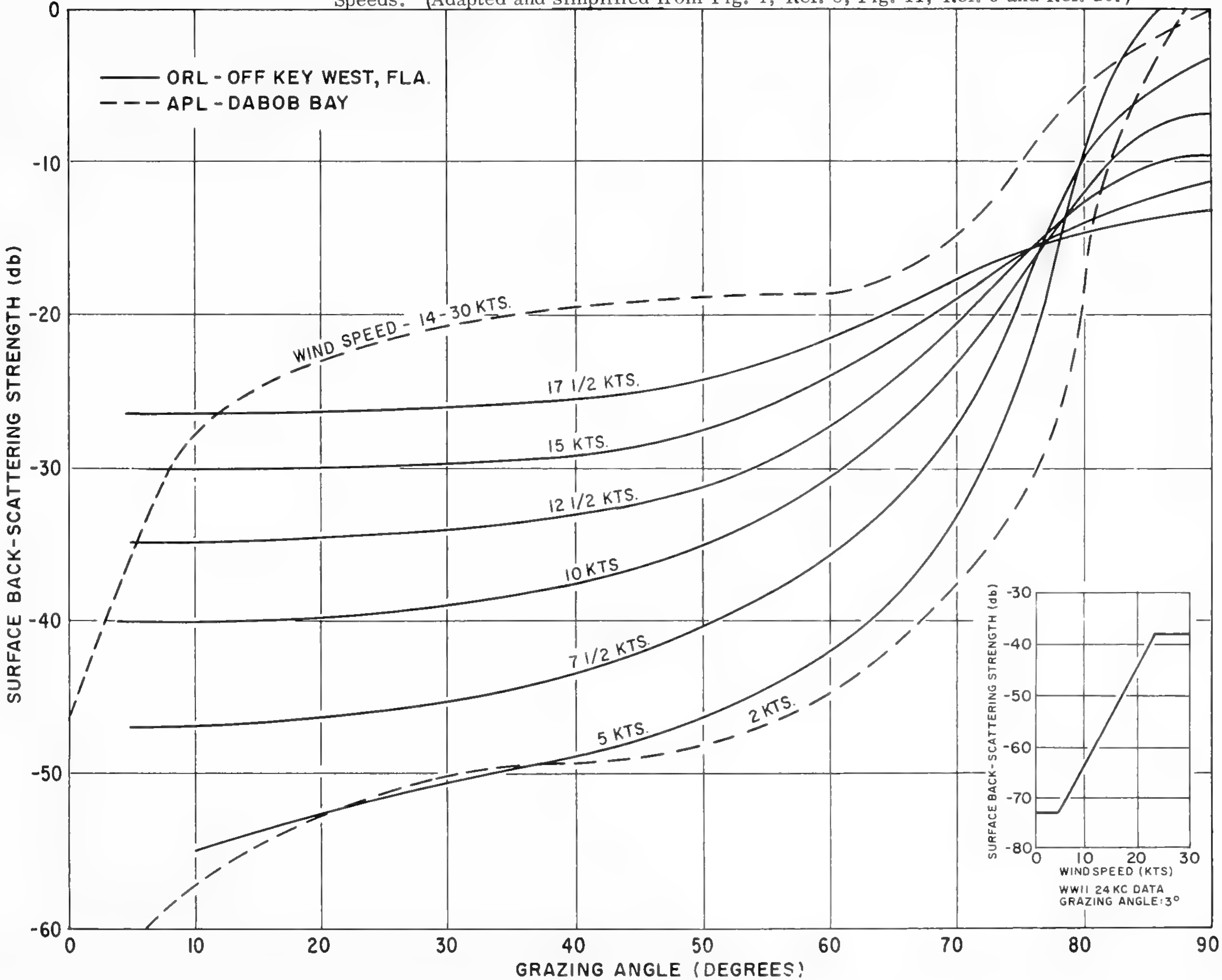

Fig. 2, which results from tests conducted by the Ordnance Research Laboratory (University of Pennsylvania) [8], and the Applied Physics Laboratory (University of Washington)[9] off Key West, Florida, and Dabob Bay near Seattle, shows the effect of wind speed and grazing angle on surface backscattering strength. Surface reverberation is little affected by frequency, but, as shown, it is strongly dependent upon grazing angle and more strongly so at low wind speeds when the grazing angle is high. Although not shown on the curves, volume reverberation probably provides the dominant noise at very low grazing angles which indicates that surface reverberation, for most sound pathes, is troublesome only at relatively short ranges.

Hoover and Urick [8] have offered an explanation for the shape of the curves in Fig. 2. The flatness of the curves at low grazing angles is thought to be due to a near surface scattering layer, possibly bubbles, which was observed during the ORL tests when the wind speed exceeded 10 knots. It might be added here that this scattering layer was not observed during the APL tests in Dabob Bay. The gradual rise at intermediate grazing angles is thought to be due to actual surface roughness such as ripples and wavelets, whereas, at higher angles (greater than 70 degrees) some sort of specular reflector is indicated. This is due, possibly, to small wave facets oriented normal to the sound beam.

An interesting feature of the curves shown in Fig. 2 is that, in the APL tests, a plateau occurs at a wind speed of 14 knots with no further increase in backscattering strength to the 30 knot limit of the test. The ORL curves do not show this plateau even at 17.5 knots, but the increase in backscattering strength over the 2.5 knot increment falls off with increasing wind speed indicating that it may be approaching a plateau. World War II 24 kc data using a grazing angle of 3 degrees shows a plateau at a wind speed of 23 knots (see inset, Fig. 2) which lends support to this idea. [10] The difference in the wind speeds at which the World War II and the APL reverberation levels reach a plateau may be due, at least in part, to the fact that Dabob Bay is almost completely surrounded by mountains limiting the wind to either a 5 or a 25 mile fetch. Six inch waves under a 20 knot wind have been observed in the Bay indicating a considerable departure from open sea conditions.

The reason for this plateau may be due to the fact that the amount of small scale roughness that can be superimposed on a wave form of given dimensions is finite, and in fully developed seas at higher and higher wind speeds the tendency is towards longer period waves. In other words, as seen by a sound beam, the number of surfaces oriented normal to it reaches a point of diminishing return as wind speed or sea state increases beyond a given point. In any event, it is important that the position of this plateau be firmly established under open sea conditions and the reason for its existence determined.

Much of the effect of surface reverberation can be circumvented by divorcing the sonar system or sound path from the surface, but hull mounted systems and active acoustic homing torpedoes must continue to face this background noise problem at short ranges. As in the case of ambient noise, backscattering levels can be forecast through a prior knowledge of wind speeds or sea state, but with considerably less accuracy. An adequate correlation with sea state has not been made, extensive measurements in sea states greater than 3 have not been taken, and the scatterers responsible for the various portions of the curve have not been clearly identified.

Hydrodynamic Noise

The noise produced directly or indirectly by the motion of a ship through the water is classified as hydrodynamic noise. It is produced by cavitation and turbulence about the hull, bubbles striking the sonar dome, wave slap, and quenching. The noise level depends upon hull design, sonar dome design and location, and heading with respect to the sea. Its intensity increases with increasing ship speed and sea state.

Under sea state 0 conditions the noise produced by flow about the dome and hull would be the major source of hydrodynamic noise, but rolling and pitching caused by higher seas bring the other sources into play. Cavitation is produced by violent motion of the bow, while bubbles, either trapped or created by bow motion, cause crashing sounds when they strike the sonar dome. The sound produced by waves striking the side of the ship is obvious even at low speeds, and quenching occurs when the bow and sonar dome clear the water during severe pitching. Each of these sources cause periodic noise, and under proper conditions they may make listening impossible a large percentage of the time.

Little unclassified information on hydrodynamic noise levels as a function of ship speed and sea state exists, nor is it even adequately known. It is sufficient here, however, to say that as ship speed and sea state increase, hydrodynamic noise rapidly becomes the dominant source of undesirable background noise considerably exceeding sea state 6 ambient noise at relatively high frequencies. It can be, and has been to some extent, reduced by streamlining the sonar dome and other protrusions and by hull designs which improve the ship's seakeeping capabilities. In spite of this, however, the operation of hull mounted sonar at high speeds, especially in high seas, can only be accomplished at the expense of detection ranges such that it is of questionable value in the vicinity of sea state 6.

As in the case of the other noise sources discussed, a prior knowledge of wave conditions to be encountered will allow avoidance of unfavorable conditions or time for tactical changes for the best utilization of ships and systems under adverse sea and sound conditions.

Radar

In the detection of snorkeling of surfaced submarines, airborne radar has the advantage of providing precise range and bearing values as well as a high search rate. In a manner similar to that of the surface backscattering of acoustical energy, electromagnetic energy is also backscattered by a rough sea surface. [11] In a phenomena known as "sea clutter" transmitted energy is reflected back to the radar from waves causing a bright spot in the center of the PPI scope, the extent of which increases with antenna altitude and sea state. [12]

Unlike the backscattering of sound from the sea surface, the returned electromagnetic energy is dependent upon the relative bearing and direction of the reflecting waves with reception being better when looking in the direction of wave propagation. If sound experiences this effect the results are obscured by continual fluctuations in intensity. Fig. 3 shows the effect of sea state and look-direction on the blip-scan ratio of an AN/APS-15a radar at an altitude of 500 feet. As indicated, the effectiveness of airborne radar is considerably restricted by state 3 seas, and of dubious value at sea state 4. Some improvement has been made through the introduction of the doppler principle, but sea state is still a major deterrent to the use of airborne radar for surfaced submarine detection, as well as for detecting submarine snorkles or periscopes.

Figure 3. Effect of Sea State and Wind Direction on Blip-Scan Ratio for AN/APS-15A Radar, Altitude 500 feet, Schnorkel Target. (Adopted from Fig. 9, Ref. 12.)

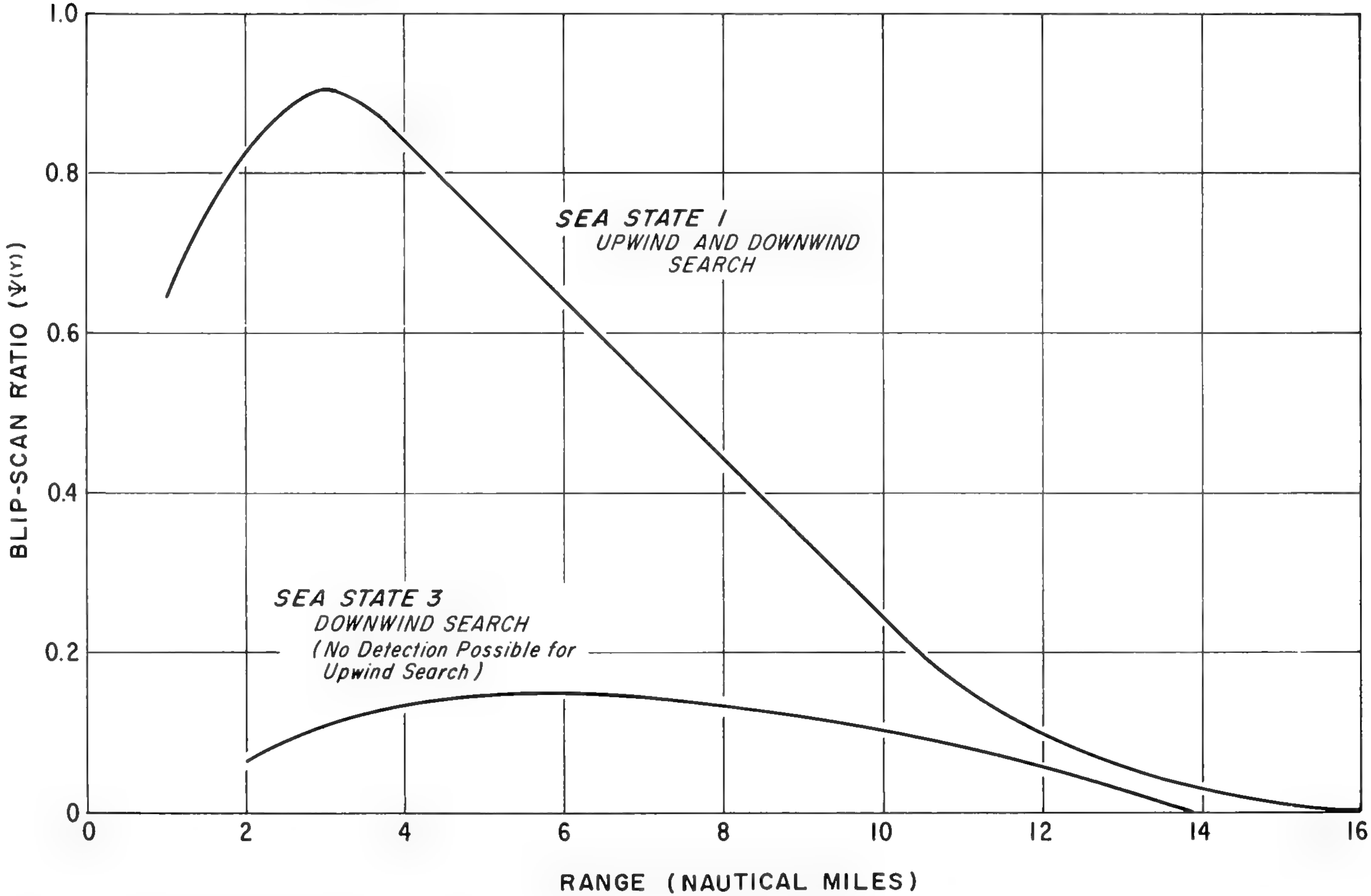

Ship Speed

The fact that surface vessels have not undergone the same degree of evolution in speed as have various other means of transportation does not detract from the considerable economic and military importance of greater speed to the Navy and merchant marines. A part of the reason for this slow evolution is that although the speed of any ship is basically dependant upon its design characteristics, it is further limited by such factors as currents, winds, and most important of all, by sea state which serves to reduce speed through the following effects: (1) added resistance due to wave reflection, especially in short waves; (2) rolling; (3) pitching; (4) indirect effect of added resistance to propulsion; (5) propeller racing; and (6) voluntary reduction in speed to ease severe motion of the ship.

It is difficult to correlate the speed of a given ship with sea state. For one thing, the period of the waves and the frequency of encounter must be considered along with wave height. Too, the degree of voluntary reduction in speed varies with captains and conditions. Voluntary speed reduction, especially in merchant vessels, is an important factor as indicated in Fig. 4 which shows the reduction in speed computed from drag alone, and the average voluntary reduction experienced by a number of merchant ships transiting the North Atlantic.[13] The computed reduction due to drag at the upper limit of sea state 6 was 14 percent, whereas, the actual reduction amounted to 56 percent of the sea state 0 speed.

As a result of many actual measurements, James[13] has been able to construct ship speed versus wave height curves for several merchant ship classes. These curves give average speed reduction values for head, beam, and following seas and are presently being used to construct Least Time Tracks in the Navy's Ship Routing Program. Table 1, taken from these curves, shows the effect of head and following seas of various heights on the speed of several classes of merchant ships. Of interest here is the fact that following seas also cause a consideration reduction in speed.

TABLE 1. THE EFFECT OF WAVE HEIGHT AND HEADING ON SHIP SPEED

Wave Ht. (feet)	SHIP TYPE															
	T5-S-12A		T2-SE-A2		T2-SE-A1		VC2-AP3		VC2-AP2		C1-M - A1/1		P2-S2 - R2		LSD	
	SHIP SPEED (in knots) AND HEADING															
	H*	F*	H	F	H	F	H	F	H	F	H	F	H	F	H	F
0	18.5	18.5	16.0	16.0	14.5	14.5	17.1	17.1	16.0	16.0	10.5	10.5	19.3	19.3	12.3	12.3
10	17.5	18.5	15.1	15.8	13.6	14.5	15.9	17.3	14.2	15.8	9.0	10.4	18.0	19.1	11.2	12.1
20	14.1	17.0	12.7	14.4	10.8	13.4	11.1	15.5	9.0	13.8	5.2	8.1	13.8	12.5	7.8	9.9
30	11.0	15.4	10.8	13.0	8.5	12.0	7.4	13.4	5.9	11.5	3.3	5.7	9.8	15.8	4.9	7.8

* H - Head Seas, F - Following Seas

Figure 4. Effect of Sea State on Ship Speed. Difference in Two Curves Due to Voluntary Reduction in Speed. (Victory Ship, North Atlantic - Adopted from Fig. 7.2, Ref. 13.)

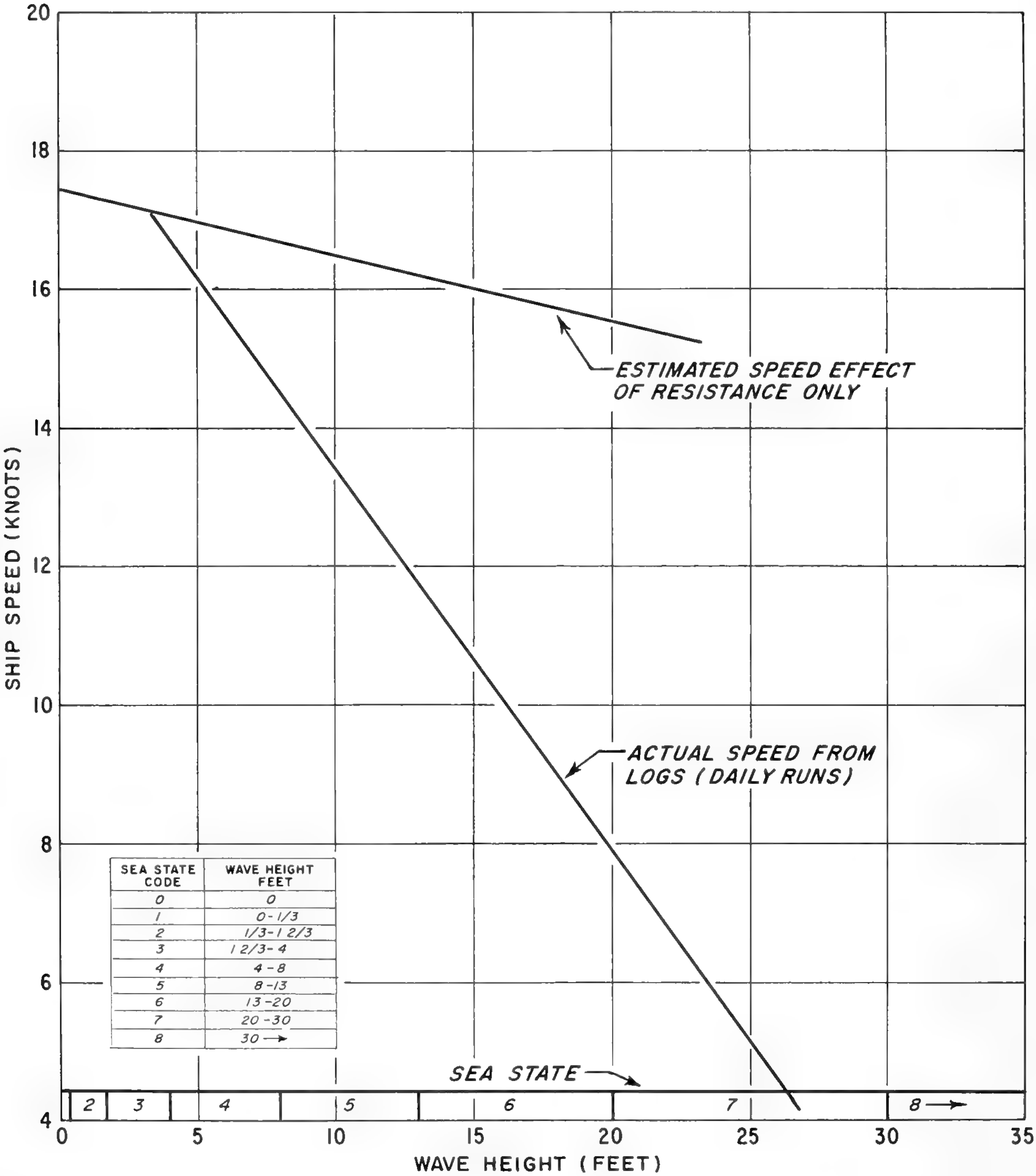

Ship Damage

Extensive cost studies on ship damage due to heavy seas are virtually non-existant. For the most part, the problem has been covered by such statements as, "Throughout the war (WW II) the cost and time lost in the repair of ships damaged by heavy seas were as great as for battle damage."[14] No doubt this estimate is in the right ballpark, and as such it presents the startling fact that we financed two equally expensive naval wars - the "shooting" war and the "interface" war. Even worse is the fact that the latter has never ceased. Of the 32,358 power vessels of over 500 gross tons registered with the various governments of the world at the beginning of 1954, some 1,021 suffered heavy weather damage, 20 foundered and were a complete loss, and another 976 were stranded during the year.[15]

Townsend[16], in a detailed study of forward bottom damage resulting from slamming in heavy seas to 141 American Flag vessels over a 26 month period, found that the total repair cost amounted to $3,084,905 averaging $21,879 per vessel, and requiring a total of 581 days of repair. These figures represent only physical repair and do not reflect the cost of the vessel during repair or loss of earnings. It should also be emphasized that only the damage to shell plating and internal members in the forward bottom of the ship were considered. Any damage which may have been experienced by the rest of the ship, either due to slamming or to green water on the deck, is not included.

Of some interest, in the context of this paper, is the fact that 56 percent of above damage occurred in the North Atlantic, 15 percent in the North Pacific, 10 percent in the Western Atlantic, and 7 percent in the North East Pacific. Only 12 percent of the ships were damaged in the other parts of the world's oceans. Of course, a part of this is due to the position of the main trade routes rather than the geographical incident of heavy seas.

Since sea state cannot be controlled, the cost resulting from ship and cargo damage as well as fuel consumption can only be reduced through better hull designs and ship routing. The Navy, realizing this, is using its Ship Routing Program, which was originally designed to reduce the cost of MSTS vessel operation, to route an increasing number of various fleet units, including submarines. The Program, developed by the Hydrographic Office and operated by the Navy since 1958, has made some 1637 individual routings (not to be confused with the number of ships routed) as of March 1961. As stated in the Introduction, this service has resulted in an appreciable transit time reduction by providing optimum routing through existing sea conditions. Reliable figures for the reduction in ship and cargo damage resulting from this program do not exist, although various estimates indicate a significant reduction. Private shipping lines which, in their present heavily subsidized economic plight, can ill afford unnecessary damage and operating cost, have made only token use of this service although it is offered by several private concerns.

WAVE HEIGHT OBSERVATIONS AND FORECASTING

The Sea State Code

The term sea state, as generally used, may be defined as the average height of the highest one-third of the waves observed in a wave train referred to a numerical code which covers an increasing range of such heights (see Table II). As shown in Table III the code may also be applied to swell conditions, but used alone, as it usually is, it makes no distinction between sea and swell. In addition the code gives no idea of the stage of development or decay of the wave spectrum, nor does it allude to the distribution of periods.

Table II - STATE OF SEA - WIND WAVES
(WMO Code 75)

Code	Description	Height(feet)
0	Calm - glassy	0
1	Calm - ripples	0 - 1/3
2	Smooth - wavelets	1/3 - 1 2/3
3	Slight	1 2/3 - 4
4	Moderate	4 - 8
5	Rough	8 - 13
6	Very rough	13 - 20
7	High	20 - 30
8	Very high	30 - 45
9	Phenomenal	over 45

NOTE: The exact bounding height is to be assigned to the lower code figure, that is, a height of 4 feet is coded as 3.

Table III - SWELL CONDITION CODE

Code	Height in feet	Description	Approximate length in feet
0	0 - no swell		0
1	1 to 6 - low swell	Short or average	0 to 600
2		Long	Above 600
3	6 to 12 - moderate	Short	0 to 300
4		Average	300 to 600
5		Long	Above 600
6	Greater than 12 - high	Short	0 to 300
7		Average	300 to 600
8		Long	Above 600
9	Confused		

There was a time when a general knowledge of the height of the higher waves was sufficient for all practical purposes. This is no longer the case. Acoustical research has indicated that it is desirable to know the significant wave height to within plus or minus 10 percent.[17] Even if the wave height is measured to this accuracy its value is lost if it is coded as, say, sea state 6 which covers a 7 foot range of height. It also is becoming increasingly obvious that the high frequency waves in the spectrum may be as important in the generation and reflection of sound as the lower frequency waves with their greater height. Because of this, some idea of the shape of the frequency spectrum will be needed to forecast background noise levels as soon as these levels have been adequately correlated with detailed sea conditions.

The needs of the naval architect are also beginning to be felt. The seakeeping characteristics of the old as well as the newer more advanced ship designs are dependent upon wave period as well as height so that in order to forecast ship speed and motion both should be known.

The present code evolved to fill a need, but the need has increased such that another evolutionary step is required. The Wave Forecasting Program responding, in part, to this reports significant wave heights. Even this, however, is not sufficient for all needs. For the sake of brevity as well as completeness of information a new code is needed which clearly distinguishes between sea and swell, indicates the period about which the maximum spectral energy is concentrated, and covers a more practical increment of wave heights. The latter is especially needed over the range from 2 to 20 feet.

Wave Height Observations

Wave heights are presently being determined with varying degrees of accuracy by bottomed pressure elements, upward looking fathometers, buoy housed accellerometers, various mechanical and electrical devices, and visual observation. By far the greatest number of day to day observations are made by the latter method. They are made from merchant vessels, naval vessels, weather ships, and oceanographic research vessels from which the observers height above the sea varies from 6 to 60 feet. This factor alone introduces a tendancy for observers close to the sea to exaggerate wave heights, and those higher above the sea to underestimate them.

In addition to this source of error is the fact that the resulting average of the wave heights observed is computed from individual observations ranging in number from 0 to, hopefully, 50. Where the greatest number of reports fall within this range is left to the readers imagination. It has been stated that "at least fifty wave heights (estimates) are needed before any confidence can be place in the computed average wave height."[14] For instance, on the basis of 9 observations from which the significant wave height is computed to be 14.2 feet all that can be said theoretically is that the true value lies somewhere between 11.0 feet and 19.8 feet, or a possible error of 28 percent. Nearly three times greater than the desired error for acoustical purposes. On the basis of 50 observations, however, the true value would theoretically lie between 12.6 feet and 15.9 feet, or a possible error of 10 percent which places it within the desired acoustical error range.

It is obvious that wave height observations must be instrumented if the desired accuracy is to be achieved. The need for wave recorders on mobile platforms such as ships and planes is continually increasing. This need will be partially filled by the shipboard wave recorder now being developed for the Hydrographic Office. Whether it will provide the accuracy needed for acoustical work is yet to be seen.

Wave Forecasting

Twenty-four hour wave forecasts are issued daily by Fleet Weather Central in Suitland, Maryland and Honolulu, Hawaii, as well as the Fleet Weather Facilities in charge of ship routing at Norfolk, Virginia and Alameda, California. The service is also provided by several private concerns on a commerical basis. Wave heights are forecast, as previously stated, by the Wave Spectrum Method developed by Pierson, Neumann, and James in 1955. The meteorological inputs to the method are supplied by synoptic data and the 5 day weather forecast maps of the Northern Hemisphere issued every Monday, Wednesday and Friday by the Extended Forecast Section of the Weather Bureau.

The observational network which supplies the data for the overlapping 5 day forecasts, in addition to continental and island based stations, is made up of 10 weather ships in the North Atlantic (positioned between 35 and 68 degrees north latitude), and 3 in the Pacific. Augmenting the observations made by these stations are those made by naval, coast guard, and merchant vessels. The data from these sources are, of course, variable both in space and time. As a general practice, for instance, aircraft carriers report weather observations every 6 hours, destroyers every 12 hours, and merchant vessels every 24 hours.

On an average day there is an estimated 4000 ships at sea in the Atlantic area. Considering the fact that weather forecasting over the ocean is considered to be simplier than over land this coverage, at first glance, would seem to be more than adequate. Most of this number, however, is made up of merchant vessels, only a small percentage of which make regular weather observations. This, coupled with the fact that ships tend to concentrate along well defined trade routes, considerably reduces the potential number and distribution of mobile weather stations. A further restriction on the number of weather reports fed to the forecast centers is imposed by communication delays. Of the overall total of about 10,000 weather observation stations in the Northern Hemisphere that could report, an average of only 3000 are received.[18] The end result is that weather maps must occasionally be extrapolated over considerable areas having insufficient data. It should also be mentioned that the sea based observational network, inadequate now from the standpoint of optimum distribution, will deteriorate rapidly under war conditions.

Very little data is readily available on the forecast accuracy of the present program. James[13] reported early in the development of the program that a comparison of the forecast and observed wave heights at some 50 grid points across the North Atlantic during winter months showed that 85 percent of the forecast wave heights were within plus or minus 4 feet of the observed heights. Since many of the waves measured were 25 feet and greater in height this was considered an acceptable error at the time. An unpublished average error estimate of plus or minus 21 per cent has been expressed by one of the forecast units. Either of these errors would have to be reduced by approximately 50 percent in order to provide the accuracy desired for the prediction of those sound conditions depending upon the state of the sea. Some researchers believe that a 90 percent accuracy can be achieved[19], but much work will be required before this goal is reached.

A significant increase in the present forecast accuracy will require effort on several fronts. Weather forecasts can, at best, be only as accurate as the data upon which they are based. It goes without saying that, due to the human factor involved and such easily corrected things as the lack of anamometers on many of the reporting merchant vessels, improvements can be made in data acquisition. Even with adequate and accurate data, however, our present level of understanding of the basic meteorological and oceanographic forces involved is not such that perfect forecasts could be made.

The accuracy of the Wave Spectrum Method of forecasting itself is a matter of controversy between its authors and users and those of the several other methods in use here and in other countries. With regard to the differences between these various methods it has been said, "One would almost question whether the different authors were working on the same planet with the same weather conditions".[19] In order to resolve the differences in these forecast methods a rigidly controlled comparison test will have to be conducted in an area such as the North Atlantic where variable sea conditions are available and the weather and wave height observations are reasonably adequate.

The brightest hope for more accurate wave forecasts is NANWEP (Navy Numerical Weather Problems Group), a computer approach to atmospheric and oceanographic forecasting now evolving at the Navy Post Graduate School in Monterey, California. With all its automatic data processing equipment operating this system can, by making 300 million computations, produce a complete pressure pattern forecast in 40 minutes. From this forecast the NANWEP computer can forecast wind direction and velocity and from this the wave heights.

The automation of data processing in weather and wave forecasting is a big step forward, but the full potential of this step will not be realized until data acquisition is equally automated. It seems inevitable that meteorological and oceanographic observations for forecasting purposes will eventually be made by stationary and adequately spaced instrumented buoys. Towards this end a technical and economic feasibility study conducted in the near future would not, in the author's opinion, be premature.

CONCLUSIONS

The following conclusions are drawn from the foregoing discussion:

1. Undesirable noise resulting from the interaction between acoustical energy, electromagnetic energy or the platform with the sea surface is sufficiently correlatable with sea conditions that it is possible to forecast their levels provided the state of the sea is known.

2. The accuracy with which this can be done at present is not sufficient. A better correlation is needed between background noise and surface reverberation, and the state of the sea.

3. The value of routing, both from the standpoint of ship speed and ship damage, has been demonstrated such that non-military vessels are justified in availing themselves of this service to a greater extent.

4. The benefits to be derived from a greater accuracy in wave forecasts are such that an intensified effort to improve them is clearly warranted.

REFERENCES

1. "Geophysics and Warfare", Landsberg, Helmut E., Research and Development Coordination, Committee on General Science, Office of the Assistant Secretary of Defense, Research and Development, March, 1954, p. 30.

2. "United States Destroyer Operations in World War II", Roscoe, Theodore, US Naval Institute, Annapolis, Maryland, 1953, pp. 448-452.

3. "Der Seebrieg", Ruge, Friedrich, Vice Admiral (Navy of the German Federal Republic), US Naval Institute, Annapolis, Maryland, 1957.

4. "Supplementary Definitions for Underwater Acoustical Terminology", Subcommittee on Underwater Noise Standards, BuShips Noise and Shock Panel, BuShips, INST. 3985.1, August 1952.

5. "A Survey Report on Basic Problems of Underwater Acoustics Research", Panel on Underwater Acoustics, Committee on Undersea Warfare, National Research Council, 1950.

6. "The Thermal Noise Limit to the Detection of Acoustical Signals In Water", Mellen, R. H., US Navy Underwater Sound Lab., Tech. Memo. D161d, Ser. No. 946-45, March 12, 1951.

7. "Some Notes on Ambient Noise From Surface Disturbances", Rhian, Elliot, Memo to FF Koczy, Univ. of Miami, July 1, 1960.

8. "The Back Scattering of Sound From The Sea Surface: Its Measurement, Causes, and Application to the Prediction of Reverberation Levels", Urick, R. J., and Hoover, R.M., J. Acoust. Soc. of Amer., Vol. 28, No. 6, Nov. 1956.

9. "Measurement of the Back Scattering of Underwater Sound from the Sea Surface", Garrison, G.R., Murphy, S.R. and Potter, D.S., J. Acoust. Soc. Am., Vol. 32, No. 1, Jan. 1960

10. "Limitation of Echo Ranges by Reverberation (Deep Water)", UCDWR File Report M361, File No. 01.90, Sept. 1945.

11. "Sea Clutter in Radar and Sonar", Hoover, R.M., and Urick, R. J., IRE Convention Record, Vol. 5, Part 9, 1957.

12. "Search and Screening", Operation Evaluation Group, Office of the Chief of Naval Operations, Rpt. No. 56, 1946 pp. 62-74.

13. "Application of Wave Forecasts to Marine Navigation", James, Richard W., US Navy Hydrographic Office, Spec. Pub. No. SP-1, July 1957, pp. 20, 32

14. "Practical Methods for Observing and Forecasting Ocean Waves by Means of Wave Spectra and Statistics", US Navy Hydrographic Office, HO Pub. No. 603, 1955, pp. 223, 152.

15. "Collision at Sea", Sharpley-Schafer, J.M., J. of the Inst. of Navigation, Vol. 8, No. 3, 1955.

16. "Some Observations on the Shape of Ship Forebodies with Relation to Heavy Weather", Townsend, H.S., Paper presented at the April 28, 1960 meeting of the Society of Naval Architects and Marine Engineers.

17. "The Environment and Undersea Warfare", forthcoming report by the Panel on Environment and Undersea Warfare, Committee on Undersea Warfare, National Academy of Sciences.

18. "NANWEP: Weather by the Numbers", Underwater Eng. Vol. 1, No. 3, Nov. 15, 1960.

19. "Known and Unknown Properties of the Frequency Spectrum of a Wind Generated Sea", Pierson, Willard J., Jr., and Neumann, Gerhard, Paper presented at the Conference on Ocean Wave Spectra, Easton, Maryland, May 1961.

THE BATHYPAGE

by DR. A. A. MILLS
Assistant Professor, Institute of Oceanography
Dalhousie University
Halifax, Nova Scotia

ABSTRACT

A design study for an apparatus to obtain living specimens of the bathypelagic fauna.

INTRODUCTION AND PREVIOUS WORK

It has for long been recognised that possession and maintenance of living specimens of the bathypelagic fauna would greatly aid investigation of orientation, sensitivity to light, sound production, bioluminescence, and other characteristics of these little-known inhabitants of the deep sea.

So far, most investigators have followed methods originated on the 'Challenger'[1] 'Blake'[2] and 'Michael Sars'[3] expeditions, using bottom and mid-water trawl nets. Although improvements in the construction and use of this equipment have been made,[4,5,6] examination of the literature discloses few attempts to devise alternative or supplementary methods for collection of pelagic organisms other than the plankton[7,8,9]. The researches of H.S.H. Prince Albert I of Monaco on the new, and sometimes gigantic, squid and cuttlefish found in the stomach of the sperm-whale are well known[10] : less familiar is his use of large, baited traps ("nasse") and submarine electric lamps, to obtain specimens from below 1000 metres.[11,12,13] Quite recently, ISAACS and SCHICK have successfully attached similar traps to deep-sea free instrument vehicles[14].

Cameras[8,15] and television[8] have been used to record underwater life, and marine biologists have themselves descended in bathysphere[16] or bathyscaphe[17,18,19] to observe and photograph the indigenous fauna[20-23]. Attempts to use baited hooks or a wire trap to capture specimens seen from these vehicles were unsuccessful[15,16,24]. Thus, the only <u>living</u> examples of the bathypelagic fauna which have been studied under laboratory conditions are:-

i) Species able to rise naturally to the surface; often at night[25], or during some stage of their life-cycle[26].

ii) Those cast up by natural phenomena[26,27]

iii) Representatives of certain species which have survived trawling from deep water[16,26,28,29,30].

It is generally believed that the abrupt change in temperature, together with abrasion in the net, is of more importance than the decrease in hydrostatic pressure in causing the heavy mortality associated with deep-sea trawling[16,28,31,32]. However, this hypothesis may need qualification in view of N. B. MARSHALL'S recent identification of well-developed swimbladders in many genera of deep-sea fish[26,33]. It appears that the swimbladder is absent in those bathypelagic forms centred below the 1000 m level, but is present in many species above this depth, and re-occurs in numerous benthic species found near the sea-floor far below[34].

There is, therefore, a need for apparatus which will enable living specimens of the bathypelagic fauna to be captured and recovered without injury[35], and with minimum disturbance of their normal environment. This requirement has been recognized for many years[26,36], but little appears to have been achieved.

The Bathypage

This paper reviews some possible methods for the realisation of such apparatus, which would appear to be best met by development of the trap, rather than the net, concept. The name 'bathypage' is proposed for the

"Superior numbers refer to similarly numbered references at the end of this paper".

device, from the Greek βαθυς- deep, and παγη- a snare or trap.

Size

The first point to be considered is size. HARDY[31] warns us against imagining that the rather frightening pictures sometimes reproduced (without accompanying scale!) in the 'popular' press represent creatures of enormous size. In fact, most of the captured specimens average 2-3 inches in length, measurements of 10-12 inches and above being exceptional. On the other hand, BEEBE with his bathysphere[16,29], and later observers in the bathyscaphes, consistently report much larger creatures - 10 feet or more in length [20]. It would seem that the larger fish and invertebrates have sufficient power and agility to evade the relatively cumbrous and slow-moving deep-sea nets.

Direct observations have also tended to refute other long-established conventions concerning life in the deep sea; such as its supposed scarcity[37], decreasing abundance with depth, and inactivity[16,18,20,29,31]. This should be remembered when designing apparatus for use in this region.

It would therefore seem best to build the trap as large as can be conveniently handled by the available research vessel.

Thermal Insulation and Flotation

The need for some form of thermal insulation of the contents of the trap has already been mentioned. Obviously, those substances normally employed for this purpose would rapidly become saturated and inefficient unless enclosed in a pressure-resistant housing. A material which does appear most suitable for this application is gasoline gelled with 'Napalm'[38,39]. Prevention of convection currents reduces the thermal conductivity of this material[40] to approximately 3×10^{-4} cal.sec.$^{-1}$ cm^{-1} per degree - comparable with the conductivities of cork, cloth and firebrick, and about three times that of glass wool[41]. As it is thixotropic and capable of flow[42] the gel may be exposed to the hydrostatic pressure.

Besides being inexpensive, another advantage of this gel is that its low specific gravity (ca-0.7) enables the insulating jacket to act as a float. Other greases and waxes (e.g. petrolatum) may bear a closer resemblance to the blubber of the whale, but are denser (S.G. ca 0.9) and cannot be gelled in situ in the cold. These and various microcrystalline waxes, polythene, etc. may be applicable where the apparent weight is not critical.

Pressure Resistance

So far, then, the apparatus is conceived as a fairly large chamber, constituting the live trap proper, surrounded by gelled gasoline to provide thermal insulation and flotation. To preserve the original hydrostatic pressure necessitates an excessively thick and heavy chamber if alloy steel be employed, but there is some possibility that filament-wound glass fibre-and-plastic vessels might serve above hadal depths. In the exploratory models it is proposed to allow water to escape through a valve to equalise pressures. Provided the rate of ascent is sufficiently slow, those species with well-developed swimbladders might be able to resorb sufficient gas to avoid permanent injury.

Luminous Lures and Bait

If the apparatus is to fulfil its intended purpose within a reasonable period of time, it is presumably advisable to employ some form of lure or bait. The vicious circle resulting from the paucity of our knowledge of the habits and responses of these creatures can only be broken by an empirical choice of technique, based on the fragmentary observations which have been made of those fish surviving for up to thirty-six hours[43]. Luminescence being one of the most obvious characteristics of the deep-sea fauna, it must surely serve some purpose in attraction of mates or prey. BEEBE[43] records that a Pacific myctophid (lantern-fish) reacted to the intermittent exposure of a luminous wrist watch, but was unaffected by the much stronger beam of a flashlight. MARSHALL[26] mentions the use of natural luminous bait by fishermen, and describes the flashes of coloured light emitted by different species of deep-sea angler fish (Ceratioidea). Thus it would seem that a low intensity source of light (perhaps greenish or bluish)[29] is indicated, and that intermittent operation might be beneficial. JERLOV'S[44] demonstration of the transparency of deep oceanic waters means that even a faint light would be visible from a considerable distance.

It is proposed to try both fish muscle inoculated with luminous bacteria (Photobacterium fischeri) and plastic phosphors for this purpose.

Triggering Mechanism

The trap may be designed to close on contact with the bait, by means of a simple mechanical linkage[45] to spring-loaded lucite doors. This tripping mechanism could be made quite delicate if a soluble plug or magnesium link[6, 46] were arranged to act as a 'safety catch' during descent. The lucite doors should have opaque covers to protect the catch against the possible adverse effects of sunlight.

Laying and Recovery

Suspension of the apparatus by means of a wire or nylon[47] cable attached to a vessel (or buoy) at the surface suffers from many obvious disadvantages, although it has some merit for initial trials.

It is preferable that the device should descend freely and rise automatically. For sampling the fauna within, say, 1000 feet of the bottom, it is a simple matter to weigh down the buoyant trap with a sinker attached to an appropriate length of cable. Sampling the mid-water life is more difficult, but it is hoped that the addition of a cluster of sealed aluminum tubes to the bathypage will enable it to become neutrally buoyant at a predetermined depth in the manner of the Swallow float[48].

In either of the above methods, corrosion of a magnesium link[6,46] or the operation of a clockwork mechanism[6], would release the trap after a known time. A radar reflector and flashing light would facilitate recovery.

An alternative method might be considered when the bathypage is to be used off an oceanic island such as Bermuda. Where deep water is available within a few miles of shore, and a fairly continuous watch could be maintained, closing of the trap could be arranged to operate the weight release mechanism.

Conclusions

It is believed that there is a need for alternative apparatus complementing the deep-sea trawl in the investigation of the bathypelagic fauna. This should be free of the disadvantages of the net, and enable the collection of living, undamaged specimens for laboratory study. Such an apparatus appears technically feasible.

REFERENCES

1. Thomson, C. Wyville, "The Voyage of the 'Challenger'. The Atlantic." Harper Brothers, New York, 1878, Vol. 1, pp. 68-70.

2. Agassiz, A., "Three Cruises of the 'Blake'". Sampson Low, London, 1888. Vol. 1, p. 26.

3. Murray, J., and Hjort, J., "The Depths of the Ocean." Macmillan, London, 1912, pp. 36-51.

4. Kemp, S. and Hardy, A. C., 'Discovery' Investigations. Objects, Equipment, and Methods. 'Discovery' Reports, 1929, 1 141.

5. Kullenberg, B., The Technique of Trawling, in Bruun, A. et al., "The Galathea Deep Sea Expedition, 1950-1952". Allen and Unwin, London, 1956, pp. 112-118.

6. Isaacs, J. D., and Kidd, L. W., University of California, Scripps Institution of Oceanography., Oceanographic Equipment Report, 1953, No. 1, S.10.

7. Sverdrup, H. U., Johnson, M. W., and Fleming, R. H. "The Oceans. Their Physics, Chemistry and General Biology". Prentice-Hall, N. J., 1942, pp. 376-385.

8. Barnes, H., "Oceanography and Marine Biology." Allen and Unwin, London, 1959, pp. 15-46.

9. Agassiz, A., "Three Cruises of the 'Blake'". Sampson Low, London, 1888. Vol. 1, p. 36.

10. Herdman, W. A., "Founders of Oceanography and their Work." Arnold, London, 1923, pp. 119-133.

11. Richard, J., "Les Campagnes Scientifiques". Monaco, 1900.

12. Richard, J., Bull. de L'Institut Océanographique (Monaco), 1910, No. 162.

13. Johnstone, J., "Conditions of Life in the Sea." Cambridge Univ. Press, 1908. p. 24.

14. Isaacs, J. D. and Schick, G. B., Deep-Sea Research, 1960, 7, 61.

15. Edgerton, H. E., Nat. Geog. Mag., 1955, 107, 523.

16. Beebe, W., "Half Mile Down". 2nd edition, Duell, Sloan and Pearce, New York, 1951.

17. Piccard, A., "In Balloon and Bathyscaphe." Cassell, London, 1956.

18. Houot, G., and Willm, P., "Two Thousand Fathoms Down." Hamilton and Hart-Davis, London, 1955.

19. Piccard, J. and Dietz, R. S., "Seven Miles Down." Putnam, New York, 1961.

20. Cousteau, J.-Y., Nat. Geog. Mag., 1954, 106, 67.

21. Pérès, J. M. and Piccard, J., Bull. de L'Institut Océanographique (Monaco), 1956, No. 1075.

22. Pérès, J. M., Piccard, J., and Ruivo, M., Bull. de L'Institut Océanographique (Monaco), 1957, No. 1092.

23. Fage, L. et al., Resultats Scientifiques des Campagnes du Bathyscaphe F.N.R.S. III. Annales de L'Institut Océanographique (Paris), 1958, Vol. 35, Part 4.

24. Houot, G. S., Nat. Geog. Mag., 1958, 113, 715.

25. Gibbs, R. H., Deep-Sea Research, 1957, 4, 230.

26. Marshall, N. B., "Aspects of Deep Sea Biology", Hutchinson, London, 1954.

27. Zahl, P. A., Nat. Geog. Mag., 1953, 104, 579.

28. Beebe, W., Nat. Geog. Mag., 1932, 61, 64.

29. Beebe, W., Proc. Nat. Acad. Sci. 1933, 19, 178.

30. Beebe, W., "Unseen Life of New York." Duell, Sloan and Pearce, New York, 1953, Chap. 13.

31. Hardy, A. C., "The Open Sea. Part I, The World of Plankton." Collins, London, 1956.

32. Colman, J. S., "The Sea and its Mysteries." Bell, London, 1958.

33. Marshall, N. B., "Swimbladder Structure of Deep Sea Fishes in Relation to their Systematics and Biology." 'Discovery' Reports, 1960, Vol. 31.

34. Annual Report of the National Oceanographic Council (U.K.) 1959-60, p. 27.

35. Emery, K. O., "The Sea off Southern California". Wiley, New York, 1960, p. 162.

36. Pettersson, H., "The Ocean Floor". Yale Univ. Press, New Haven, 1954, p. 161.

37. Günther, K. and Deckert, K., "Creatures of the Deep Sea." Charles Scribner's Sons, New York, 1956, p. 81.

38. Fieser, L. F., Harris, G. C., Hershberg, E. B., Morgana, M., Novello, F. C., and Putnam, S. T., Ind. Eng. Chem., 1946, 38, 768.

39. Rueggeberg, W. H. C., J. Phys. and Colloid Chem., 1948, 52, 1444.

40. Langstroth, G. O. and Zeiler, F., Can. J. Research, 1948, 26A, 50.

41. Hodgman, C. D. Ed., "Handbook of Chemistry and Physics", 41st ed., Chemical Rubber Pub. Co., Cleveland, 1960, pp. 2436-2443.

42. Agoston, G. A., Harte, W. H., Hottel, H. C., Klemm, W. A., Mysels, K. J., Pomeroy, H. H., and Thompson, J. M., Ind. Eng. Chem., 1954, 46, 1017.

43. Beebe, W. and Vander Pyl, M., Zoologica, 1944, 29 (2), 59.

44. Jerlov, N. G., Optical Studies of Ocean Waters. Rep. of the Swedish Deep-Sea Expedition, Göteborg, 1951, 3, 1.

45. Chitty, D. and Kempson, D. A., Ecology, 1949, 30, 536.

46. Van Dorn, W. G. University of California, Scripps Institution of Oceanography. Oceanographic Equipment Report No. 2, Ref. 53-23.

47. Edgerton, H. E., Cousteau, J.-Y., Brown, J. B., and Hartman, R. H., Deep-Sea Research, 1957, 4, 287.

48. Swallow, J. C., Deep-Sea Research, 1955, 3, 74.

AN EXTERNAL CORE-RETAINER

by DR. A. A. MILLS
Assistant Professor, Institute of Oceanography
Dalhousie University
Halifax, Nova Scotia

INTRODUCTION

For many purposes involving detailed study of the sediment-water interface (e.g. microbiological examination) it is desirable to obtain short cores in which the uppermost layers are completely undisturbed.

The corers most commonly employed with this intention[1,2,3] generally incorporate an internal core-retainer in which fingers of flexible metal or plastic are directed towards the axis of the coring tube. It has been found that such devices frequently agitate the top few centimetres of a loosely-packed or flocculent sediment, and also fail to retain sand or volcanic ash.

APPARATUS

This note describes a device which, by replacing the conventional retainer in the above corers, facilitates the collection of undisturbed samples from a variety of sediments. Two models have been developed for use with deposits of varying consistency - one for stiffer sediments, the other for the more fluid silts or sands.

The construction and mode of operation of this apparatus are shown in Figure 1. The corer is lowered in the open position A. Penetration in excess of a pre-determined length (6 in. has been found satisfactory) forces the collar upwards, allowing the supporting arm to spring free of the catch. Upon withdrawal from the sediment the sliding weight drives the retainer down the coring tube, over the bevelled edge of the cutting head, into the closed position B. When hauled inboard the corer is held vertically, the core-retainer carefully displaced, and a tightly-fitting cork disc pushed through the cutting head into the plastic liner. The latter, with the enclosed core, is then easily removed and sealed.

REFERENCES

1. Emery, K. O. and Dietz, R. S. (1941). Gravity coring instrument and mechanics of sediment coring. Bull. Geol. Soc. Amer. 52, 1685-1714.

2. Hvorslev, M. J. and Stetson, H. C. (1946). Free-fall coring tube: a new type of gravity bottom sampler. Bull. Geol. Soc. Amer. 57, 935-950.

3. Phleger, F. B. (1951). Ecology of foraminifera, northwest Gulf of Mexico. Geol. Soc. Amer. Mem. 46, 1-88.

ACKNOWLEDGMENT

This device was constructed and used aboard Lamont Geological Observatory's research vessel 'Vema', and special thanks are due to Dr. C. L. Drake for helpful suggestions towards its design and practical application.

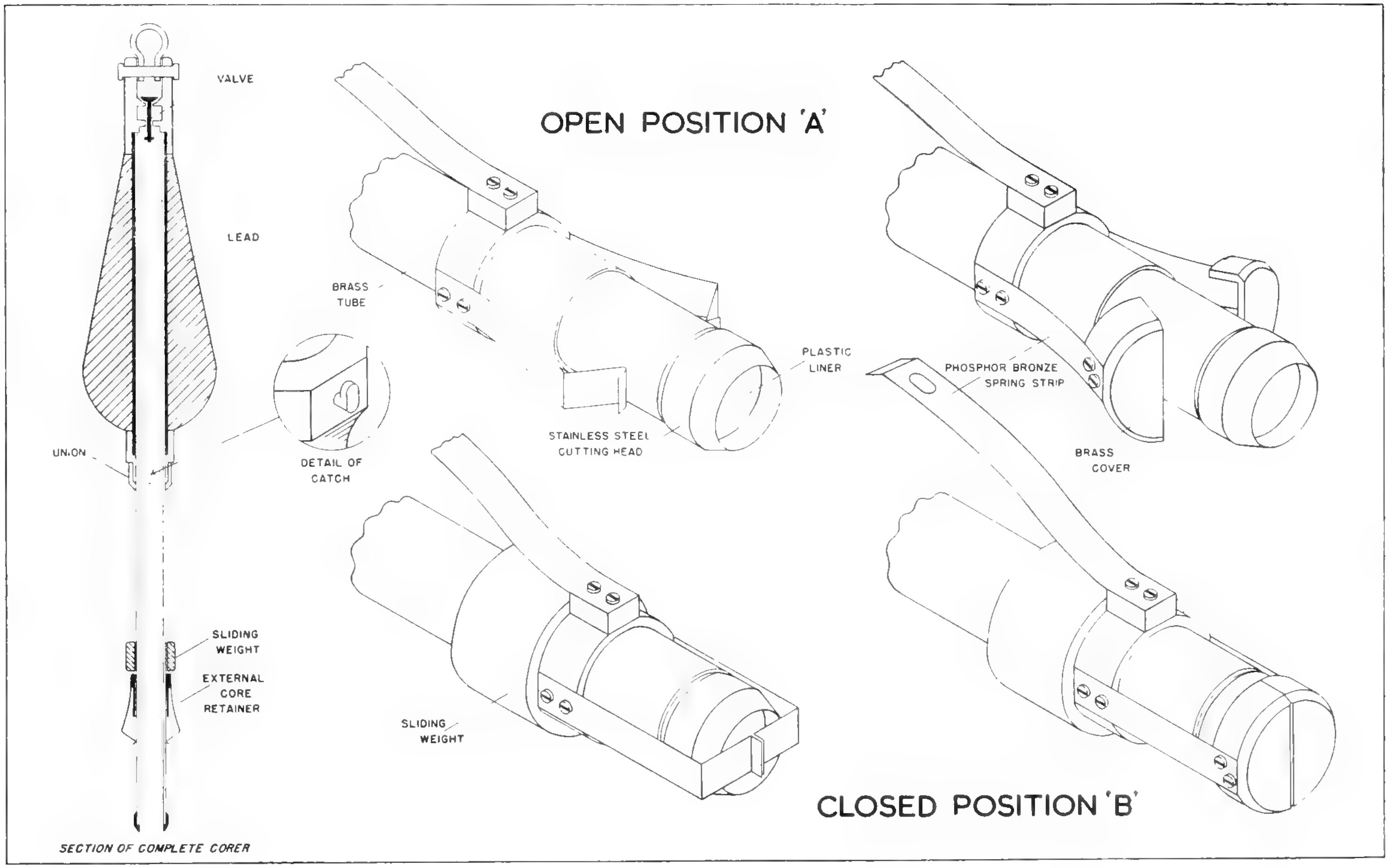
VALVE
LEAD
UNION
SLIDING WEIGHT
EXTERNAL CORE RETAINER
SECTION OF COMPLETE CORER
BRASS TUBE
DETAIL OF CATCH
OPEN POSITION 'A'
STAINLESS STEEL CUTTING HEAD
PLASTIC LINER
PHOSPHOR BRONZE SPRING STRIP
BRASS COVER
SLIDING WEIGHT
CLOSED POSITION 'B'

FIG. 1.

SOME NEW MECHANICAL DEVICES FOR OCEANOGRAPHIC RESEARCH

by SHALE J. NISKIN
Institute of Marine Science
University of Miami
Miami, Florida

ABSTRACT

The areas of principal oceanographic interest to the Institute of Marine Science of the University of Miami are the Straits of Florida, the Bahama Banks, Florida Bay and the Caribbean. The field problems arising in these areas of research, coupled with the specific requirements of the various departments at the Institute, has prompted the development of several new oceanographic tools. Three simple, inexpensive mechanical devices are described in this paper: a stabilized oceanographic reference marker buoy; a sterile biological sampler; and a hydrographic wire slope and azimuth indicator.

OCEANOGRAPHIC MARKER BUOY

INTRODUCTION

Intensive studies are conducted by the Department of Physical Oceanography of current patterns in the Florida Bay area (1. Koczy,F.F. et al., 1959). The movements of current drift drogues are plotted with ship's radar relative to moored reference markers equipped with radar reflectors. As the drogue drifts out of radar range of the reference marker, another such marker is launched and anchored, the original marker being recovered later. Employing these methods, continuous tracking of drogues for extended periods of time has been made possible.

THEORY OF OPERATION

In order to assure maximum range and detection, the marker buoy mast supporting the radar reflector must possess a high degree of vertical stability. Because of the delicate construction of the radar reflector, the mast must be free from sudden and violent movements, regardless of the state of the sea. The markers should be relatively light in weight to facilitate launching and recovery. However, types of marker buoys available in the past have been either too cumbersome or have not offered the desired degree of vertical stability.

"Superior numbers refer to similarly numbered references at the end of this paper."

DESIGN The reference marker buoy subsequently designed to satisfy the requirements discussed in the preceding paragraph consists of a ballasted mast, its metacenter located below the surface of the water and positioned at the center of a buoyant flexible ring by spokes radiating from the mast to the buoyant ring. Wave-induced movements of the buoyant ring are not transferred to the mast, excepting some degree of vertical acceleration, which is considerably dampened by the spokes and the flexible nature of the ring. A mooring line is attached to the buoyant ring and, therefore, has only slight effect on the stability of the mast. Because of its peripheral point of attachment, the mooring line is not likely to foul on the submerged portion of the mast.

In detail, (see Fig. 1) the buoyant ring consists of a length of polyethylene pipe coiled into a ring seven or eight feet in diameter, its ends coupled together and sealed. Nylon spokes radiating from a metal hub which is milled to receive the mast are secured to the buoyant ring. These spoke lashings also hold the ring coils together. One-third of the mast length extends below the central hub. Ballast is secured to the mast heel. The mast is prevented from slipping through the hub by a taped serving, which is applied to the mast. To meet our specific requirements, a radar reflector was secured to the top of the mast.

HYDROGRAPHIC WIRE SLOPE AND AZIMUTH INDICATOR

INTRODUCTION

Hydrographic wire configurations produced by a combination of the Gulf Stream current and vessel drift in the Straits of Florida tend to complicate hydrographic instrument positioning. The usual technique of employing unprotected thermometers for determining instrument location has not proven adequate for the task. A knowledge of wire slope and set can be useful for defining location of instruments attached to the hydro-wire. Furthermore, this information may yield indications of sub-surface currents and their direction.

A detailed discussion concerning the significance of hydrographic wire angle and azimuth information has been provided by Carruthers (2. Carruthers et al., 1954).

In a subsequent paper (3. Carruthers, 1959) he has described an instrument for measuring wire angle and set. Due to various mechanical disadvantages of the Carruthers indicator its performance in the field proved to be somewhat unreliable. A new design approach was pursued, resulting in the development of a more efficient hydrographic wire slope and azimuth indicator.

THEORY OF OPERATION

In this new indicator, (Fig. 2) a vertically orienting and magnetic north-seeking unit of practically neutral buoyancy is housed spherically to allow the inner unit to preserve its northward and vertical orientation, regardless of the disposition of its housing. A float secured to one end of the inner member insures its vertical orientation, while magnetic needles attached to this unit cause it to seek magnetic north. The spherical shape of the inner member permits its being locked accurately, relative to the wire orientation.

DESIGN The plastic hollow inner sphere is provided with a spherical glass float at its upper pole. Two magnetic needles are mounted along the horizontal axis of the inner sphere. Sufficient ballast to cause the inner sphere to approach neutral buoyancy in salt water is attached to its lower pole. A glass bead bearing is fixed to either pole of the inner sphere. The outer housing is composed of two flanged plexiglass hemispheres bolted together through short plastic spacers placed between the flanges. This space is occupied by a pair of caliper clamps, each of which is pinned at one end and free to swing horizontally between the flanges. The unpinned clamp ends are bound together with elastic bands. Upon messenger impact a wedge spreading the clamp ends apart is removed, allowing the clamps to lock securely under elastic tension around the inner sphere. Both inner sphere and outer housing are free-flooding.

The upper hemisphere of the outer housing is inscribed with latitudinal lines representing the degrees of inclination. The inner sphere is marked around its equator with a compass rose; longitudinal lines pass through every 10^{o}. Thus both wire slope and azimuth may be read directly. Due to the convergence of the longitudinal lines at the poles of the inner sphere, precise reading of azimuth becomes increasingly difficult with wire slopes of 7^{o} or less. Because the diameter of the inner sphere is slightly less than that of its spherical housing, slight horizontal displacement is possible. However, the caliper clamps are designed to correctly re-center the inner sphere if this displacement occurs. A framework supports the outer housing longitudinally and may be clamped to the hydro wire with a slotted bolt-and-wing nut arrangement. This framework contains the caliper clamp releasing wedge and plunger rod, as well as the messenger release mechanism, which consists of a short rod butted against the plunger rod and mounted on a compression spring.

STERILE BIOLOGICAL SAMPLER
INTRODUCTION

Investigations by the Department of Microbiology concerning the distribution and biology of salt water yeasts and fungi have given rise to a need for water samples of two liters or more which are free from microbiological contamination from sources other than the point at which the samples are gathered. Available sterile samplers (4. ZoBell, 1946 and 5. Sirokin, 1961) have had inherent depth and capacity limitations.

THEORY OF OPERATION

DESIGN The sampler subsequently designed operates on the principle of a bellows. (Fig. 3). A pliable air evacuated and sterilized container is fitted with a tape-sealed check valve and secured to a hinged framework by means of pockets attached to both sides of the pliable container. This framework consists of two fork-ended plates, hinged together, under-spring torsion. Upon messenger impact, a plunger rod is depressed simultaneously disengaging two levers which hold the plates together, thus permitting the hinged plates to swing apart. The lower lever also serves to remove the tape seal from the valve. The collapsed pliable container is thereby pulled open into its full 3 dimensional configuration, and, in so doing, water is forced into the container. After equilibrium is achieved, no more water may either enter or escape from the container. The messenger release mechanism is activated by the plunger rod upon messenger impact. A small quantity of sterile salt water, initially introduced into the container facilitates valve action.

FIG I

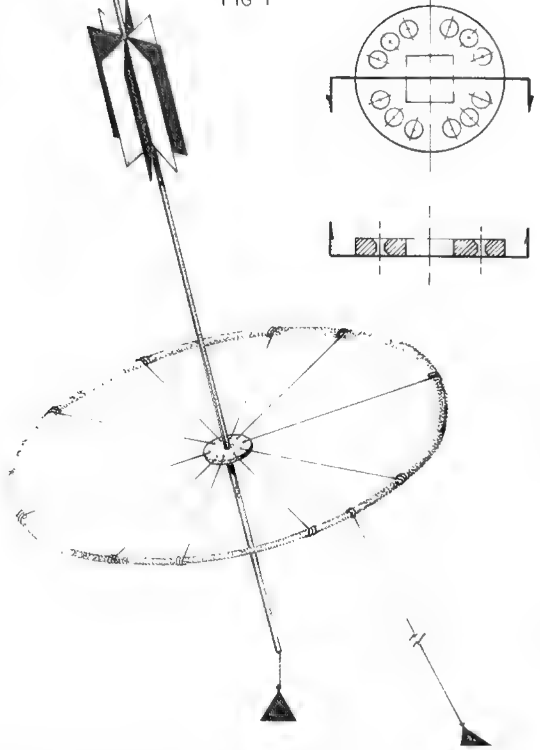

STABILIZED OCEANOGRAPHIC REFERENCE MARKER BOUY

FIG. 2

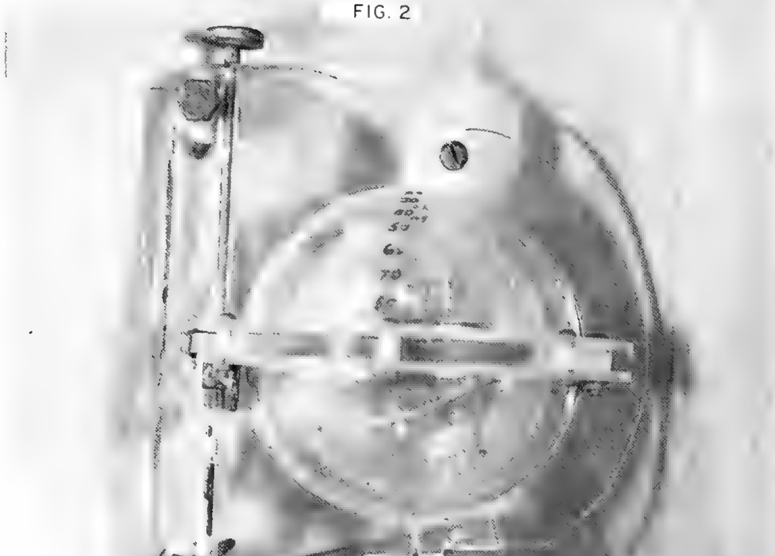

HYDRO WIRE SLOPE AND AZIMITH INDICATOR

FIG. 3

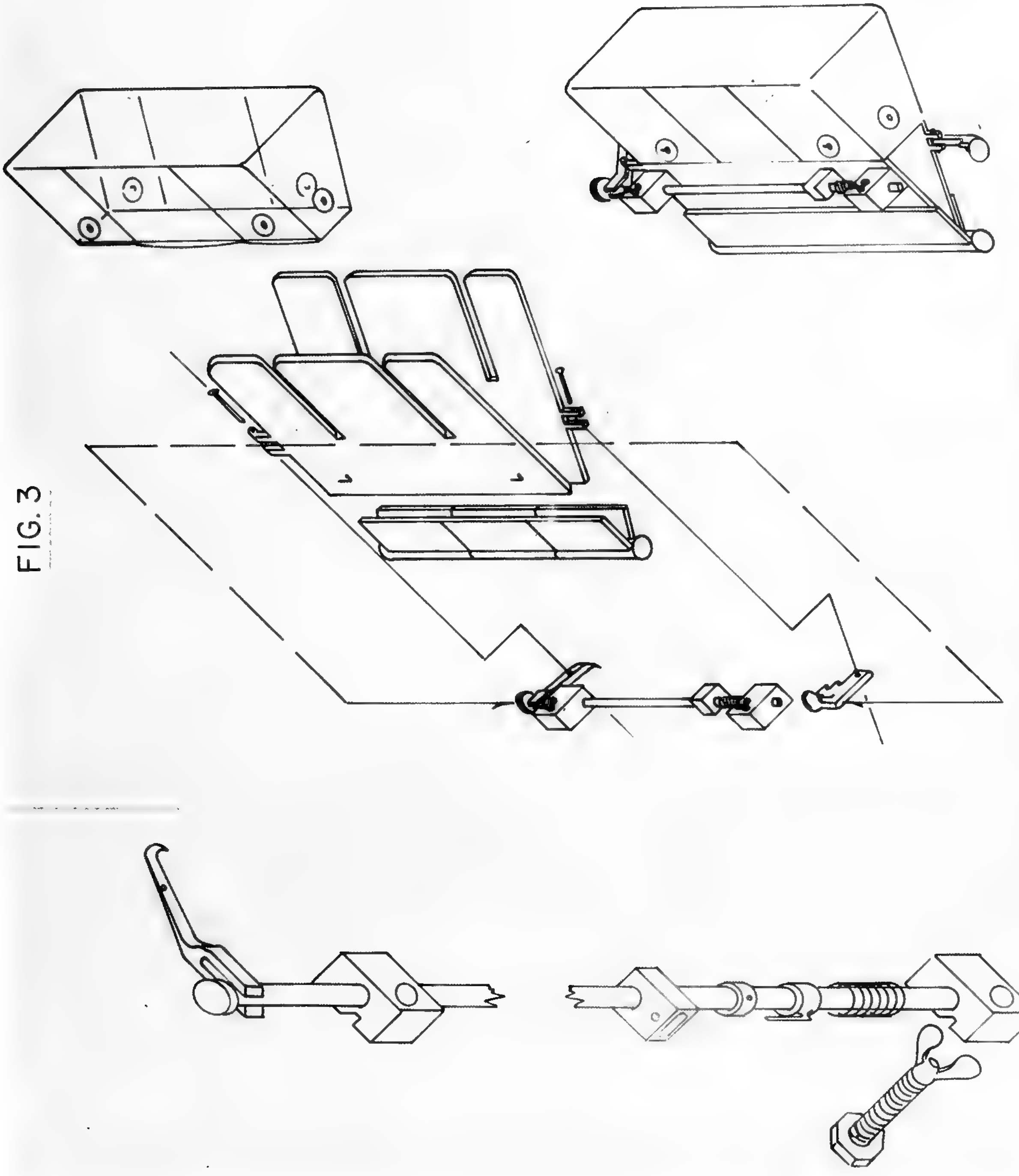

STERILE BIOLOGICAL WATER SAMPLER

The plastic containers are inexpensive enough to be considered disposable. Our microbiological group is currently investigating the possible deleterious effects of various types of plastic material on the microorganisms in water samples.

CONCLUSION

The oceanographic reference marker buoy and wire slope and azimuth indicator are now generally used in our oceanographic survey work. Though it has not been used extensively at sea, the sterile biological sampler has been successfully tested.

REFERENCES

1. "The current patterns on the Tortugas Shrimp grounds". F. F. Koczy, et al., Proceedings of the Gulf and Caribbean Fisheries Institute 12th annual session, November 1959 pages 112-125.
2. "On instrumental measurement of the line shape under water. Concerning the determination of vertical distribution of slope (magnitude and direction) down oceangr. wire, and the measurement of current-caused obliquity of a rope strained between an anchor and a sub-surface buoy." Carruthers, J. N., et. al., Dt. Hydrogr. Z 7 1954, page 22.
3. "On instrumental measurement of hydro wire slope" Carruthers, J. N. Dtsh. Hydrogr. Z 12 1959, 167-171.
4. "Marine microbiology" Zobell, C. E. published by Chronica Botanica Co., Waltham, Mass. 1946.
5. "A sampler for the selection of samples of water for bacteriological analyses." Sorikin, I. Institute of Reservoir Biology Academy of Science, U.S.S.R. bulletin No. 6, 1960, pages 53-54.

ACKNOWLEDGEMENT

The development of these devices was supported in part by the Office of Naval Research, Contract No. 840(01), under the supervision of Dr. F. F. Koczy, Chairman of the Division of Physical Sciences, Institute of Marine Science, University of Miami. The aid and cooperation of the following staff members in the preparation of this paper are gratefully acknowledged: Dr. Koczy for his valuable advice and appraisal; Dr. Gene Rusnak for his corrections and comments; and Mr. M. Rinkel for his cooperation in the field tests of these devices.

USE OF THE PRECISION GRAPHIC RECORDER (PGR) IN OCEANOGRAPHY

by S. T. KNOTT, Research Associate in Engineering
Woods Hole Oceanographic Institution
Woods Hole, Massachusetts

ABSTRACT

This paper briefly describes the Precision Graphic Recorder. How its timing and correlation capabilities are used for collecting acoustically derived data in bathymetry, seismic reflection and refraction profiling, instrument location, navigation and various biological studies is reviewed.

INTRODUCTION

The roots of the name "graphic recorder" are found in early bathymetric work, such as that of Veatch and Smith[1], in the 1930's. The PGR[2], however, might better be described as an event correlation recorder, although its presentation is substantially the same as that of recorders in modern echo-sounders where a recording stylus repeatedly sweeps across a long narrow strip of sensitized paper. It is similar, also, to a delay-triggered "Z" axis modulated oscilloscope, but presents successive samples of time-related data side-by-side for visual correlation. Such a series of samples, each taken at a precise repetition rate on a common, accurate time-base, produces a graphic plot of the data as a succession of offset measurements in time.

Prior to 1954 when Luskin et al[3] discussed the precision measurement of ocean depths, the geophysical research groups at the Woods Hole Oceanographic Institution and the Lamont Geological Observatory had found commercially available echo-sounding recorders to be less precise than was required for their problems. Nor was there an adequate choice of recording resolution available in one instrument. Both laboratories decided to develop instruments, and a healthy scientific competition evolved. Lamont's instrument, the Precision Depth Recorder (PDR), was first in the field. It provides recording resolutions of about 25 and 50 milliseconds per inch for travel time measurement on a time base controlled to better than 1 part in 10^5. Our recorder appeared about six months later. The group at Lamont Observatory conceived a reliable and moderately simple device for the measurement of ocean depths. Our recorder was somewhat more complicated because our objective was a multipurpose tool. Like the PDR, the PGR measures travel-times precisely and with predictable accuracy, but in addition it provides considerably higher resolution for a finer measure of time differences. From its twelve writing rates we obtain recording resolution from 3 milliseconds to 400 milliseconds per inch[4]. Some ten programing arrangements are available to gate the transmission and reception of signals. Its frequency response is flat from less than 100 cycles to over 20 kilocycles per second, and its usefulness extends to beyond 80 kilocycles. Both research groups found facsimile recorders most useful; Lamont uses the Times Facsimile recorder, and we, the Alden.

A tuning fork in the PGR establishes the time base. Its signal controls the synchronous drive of the sweep mechanism and programing switches. The sweep, generated by the intersection of a rotating helix and a straight printing blade is sharply defined and rectilinear, with a timing accuracy of the order of the fork. Signals appear as a darkening on the paper between the helix and blade and must be rectified before recording because the marks are caused by an electrolytic deposition of

Superior numbers refer to similarly numbered references at the end of this paper.

ferric ions from the printing blade. In general, full-wave rectification is used in studies where signal envelopes are to be correlated, and half-wave for effectively correlating wave forms within envelopes. Signal phase may be determined by selecting either the positive or the negative excursions of the signal. Scale or timing lines generated directly from the fork signal serve two purposes, measurement and indication of recorder synchronization.

USES: Bathymetry

The first use of this recorder in bathymetry still remains an important part of its job. During research cruises, the PGR's are routinely put to this task 24 hours a day. Consider what information is to be gained from echo-sounding. Travel time is the most obvious and is now measured with great accuracy. For the most part, resolution of about 30 milliseconds per inch is adequate. This resolution presents a 200-fathom depth interval across eighteen inch paper. In addition to its obvious use in hydrographic charts, this accurate information has been used by physical oceanographers at Woods Hole to guide their Nansen bottle lowerings to within a few feet of the bottom. More recently, however, they have used the acoustic pinger technique described later. Mooring deep-sea buoys also requires this knowledge of depth, for in one method used here, moorings are cut to match the water depth.

The PGR's fastest sweeps ($<$ 10 milliseconds per inch) are useful in the detection of subtle changes in travel time caused by gradual slopes found in the abyssal plains and elsewhere. The PGR can make these measurements because of the constancy of its timing. It is easily seen that cumulative sweep-time errors resulting from inconstant timing would raise havoc on a 50-millisecond sweep when displaying travel times several seconds long.

The high resolution of which the PGR is capable has led to the discovery of small rough features of the bottom and also to areas of sediment ponding[5]. The vertical dimensions of these features seen with sounders are relatively small. The in-the-water length of the pulse cannot be much greater than the dimensions of the features for the pulse alone will cause the detail we seek to be hidden.

There is a part of the Blake Plateau, for instance, where, (see Fig. 1a and b) in spite of many crossings, several canyons and many peculiar bumps having only a few fathoms relief had not been detected with older sounders. These were discovered when we surveyed the area with a PGR, using resolution of less than 30 milliseconds per inch and short pulses of less than one millisecond[6]. Some indications of these features can be found on the old records, but the changes in the travel times defining the features are of the same order or less than the expected errors of the older equipment.

In the sediment ponds, where a long pulse hides, Fig. 2 (from Hersey[5]), the existence of reflecting horizons below the sea-floor, the PGR controls pulse length to in-the-water dimensions which are hopefully less than twice the distance between the reflecting horizons. The structure of the echo-train reveals the presence of the horizons which is most important to display. Much of this work has been done with 0.2 millisecond pulses. The PGR provides the bandwidth, 5000 cycles, necessary to permit these short pulses to pass to the recorder without distortion.

Echoes' structures often change rapidly, Fig. 3, especially at ship's speeds of ten knots or more, yet the validity of these sub-sea-floor reflections depends upon the continuous correlation of particular returns over considerable distances. Strong correlation is obtained because the samples are taken closely enough in space and time so that substantially the same reflection recurs, because changes in transmission path geometry occurring between samples are less than the dimensions of the irregularities in the bottom, and because each of these samples is initiated on a precise time schedule. To achieve the necessary high sampling rate, we cannot wait to receive the echo from one pulse before sending another, but must have as many pulses as possible simultaneously in transit to and from the bottom. The PGR offers such a program. It is designed to have "windows" in the pulse schedule during which echoes may be received uncluttered by the direct reception of the pulse and its reverberation. Programs are based upon a count of integral recorder sweeps. They require the sweep period to be several times less than the travel times in deep water.

The reflecting horizons below the sea-floor are often the boundaries of lenses of differing materials; they may be pinched out at the sea floor and more ancient formations exposed. The PGR gives a permanent display of their echo structures, which may be used for later study or for immediate use in coordinating coring operations. Since 12 kc attenuates rapidly in the sediments these reflections are most often only tens of feet deep, but they are within the reach of deep-sea corers.

It might be asked why an oscilloscope isn't used. A scope is usually a part of the instrumentation, but scope photographs, are not easily compared with one another at a rate of several thousand an hour. Although they give needed amplitude information it is often difficult to obtain representative amplitude differences within the echo structure from only a few samples, because of the fluctuation found in such measurements. A visual integration of the returns on the PGR record is a useful guide in these bottom reflectivity studies.

We also use precision soundings for navigation,[7, 8] and often moor deep sea buoys on a particular bottom contour, a line of position easily followed with the PGR.

Seismic Reflection and Refraction Profiling

We record seismic reflections in a system made up of a broad spectrum sound source actuated by the triggering mechanism of the PGR which in turn records the signals received by a broadband hydrophone suspended from the ship. Adjustable bandwidth filters are used to filter the signal in differing frequency bands for each channel of the PGR. This system is known as the Continuous Seismic Profiler[2, 9, 10] Fig. 4. In its development at Woods Hole the sources most used have been the underwater spark and the E. G. and G. "Thumper". Both have higher peak pressures than most sounders, but in narrow bandwidths at the necessary low frequencies their output is generally below 100 db above a microbar. Yet we obtain good penetration of the sea-floor from these relatively weak sources, and attribute a great part of this success to the correlation capabilities of the PGR. These electrical sources are designed to follow the moderately high repetition rates of the PGR, which are at least an order of magnitude greater than those used in conventional explosive methods. The signal is coherent and generally remains so after sea-surface, sea-floor, and sub-sea-floor reflections, see Fig. 5. The wave length in water at these low frequencies is great enough and the sampling rate fast enough, that changes in geometry or sub-sea-floor structure do not erratically interrupt the correlation of the wave forms in the returning signals. Weak signals are traced through noise with unusual ease, (Fig. 6) for the PGR is in fact an autocorrelation device when it can control the timing of events.

The PGR record from vertical seismic reflections gives us a cross-section profile of the structure below the bottom, but the depth scale must be determined and corrected by propagation velocities obtained from oblique reflection and refraction data taken with the same system. Refraction arrivals, when present, can be immediately identified (Fig. 7) and compressional wave velocities readily computed. In their absence there is an overabundance of reflection data for a more complicated velocity determination [12, 13]. An oscilloscope and tape recorder are necessary accessories to this instrument, however; the scope for instantaneous observations and photography, the tape for storage and future analysis. There are simply not enough PGR channels available at one time, even if "master and slave" techniques are used.

Location of Instruments and other Objects

In addition to high resolution echo sounding studies, the PGR is used for echo location, the finding and identifying of objects suspended in the water. These objects may be animal, as in the case of fish, porpoises, or scattering layer[14]; they may be instruments, buoys which can be tracked and recovered, cameras[15], corers[16], nets and dredges[17], whose lowering, placing and raising can be accurately monitored with this system.

Echo location techniques employ not only the shipboard transducers of sounders or ranging equipment, but also pingers which are attached to cable-suspended and free instruments. The difference between the arrival times of the directly received and bottom reflected signals from this pinger indicates an instrument's height above bottom, (Fig. 8). The signal structure and timing of these arrivals displayed on the PGR disclose such details as when a corer triggers, or the attitude of a dredge e. g. whether or not it is kiting during the lowering. Cameras can be manuevered within their focal lengths above the bottom in water several miles deep. We can tell whether the cameras are over smooth, muddy bottom or rough, rocky bottom. The guesswork in these many operations has for the most part been eliminated. We no longer speculate whether a dredge is on bottom, a camera in focus, cable payed out too fast or a Nansen bottle cast dragged on bottom.

Where depth must be accurately known, for such instruments as the Bureau of Standards Velocimeter, the simple pinger technique is not adequate [18]. However, the additional travel path geometry provided by the inverted echo sounder described by Dow [19] solves this problem.

Navigation techniques involving acoustic pingers and transceivers, and sonobuoys are also used with the PGR. The motion of freely drifting pingers with precisely timed repetition rates can be tracked by measuring the change in time interval between received pings. When sonobuoys and acoustic transceivers are used, a simple travel time measurement is used to compute one's range from them.

Studies of Sea Life

Scattering layer records from the PGR see Fig. 9a and b, often a by-product of bathymetry, show the diurnal migration and distribution of these groups of sound scatterers [19]. Interesting work has been done by lowering a sounding transducer into the layers to learn more of the size, population and movement of individual animals [14, 20]. Echoes are read out on the highest writing speed of the PGR. Earlier this information was used to determine when to trigger an underwater camera; now the camera and its acoustic range finder are in one submersible package.

Fish schools are studied by sounding and echo ranging. A PGR record from such a study illustrates this use of short pulses and high resolution, Fig. 10.

CONCLUSIONS

Some of the salient jobs of the PGR have been mentioned. There is good probability that there will be more. We have not yet used it to measure oceanic tides, for example. Studies of the scattering layer and newly found groups of larger sea life continue. New advances in navigation are most encouraging for those studying bathymetry, for our depth measurement capability is all-too-often better than our navigation. New and more powerful broadband sound sources hold promise of making continuous seismic profiling as routine as echo sounding. Even without the use of new inverted sounders, heat probes, and other equipment there is without a question much future use for the PGR.

ACKNOWLEDGMENTS

The development of the recorder and much of the Continuous Seismic Profiler was carried out by WHOI under U. S. Navy Bureau of Ships' Contracts NObs-43270 and NObsr-72521 as has been previously reported. Other work summarized here have been supported by WHOI under Office of Naval Research contract Nonr-1367(00), and NSF grants.

This is Contribution No. 1223 of the Woods Hole Oceanographic Institution, Woods Hole, Massachusetts.

REFERENCES

1. "Atlantic Submarine Valleys of the United States and the Congo Submarine Valley", Veatch, A. C. and Smith, P. A., Geol. Soc. of Am., Special Papers No. 7, 1939.

2. "High Resolution Echo Sounding Techniques and their Use in Bathymetry, Marine Geophysics and Biology," Knott, S. T. and Hersey, J. B., Deep-Sea Research, Vol. 4, No. 1, 1956, pp 36-44.

3. "Precision Measurement of Ocean Depth", Luskin, B., Heezen, B. C., Ewing, M., and Landisman, M., Deep-Sea Research, Vol. 1, No. 3, 1954, pp 131-140.
4. "Instruction Manual for the Precision Graphic Recorder (PGR)", Knott, S. T. and Witzell, W. E., Woods Hole Oceanographic Institution, Ref. No. 60-38, October 1960, pp 1-42 + Appendix (86 pp).
5. "Evidence for Ponding in Deep Sea Sediments", Hersey, J. B., given at IUGG, Helsinki, Finland, August 1960.
6. "Geophysical Investigation of the Continental Margin between Cape Henry, Virginia and Jacksonville, Florida", Hersey, J. B., Bunce, Elizabeth T., Wyrick, R. F. and Dietz, F. T., Bull. Geol. Soc. Amer., Vol. 70, April, 1959, pp 437-466.
7. "Reconnaissance Survey of Oriente Deep (Caribbean Sea) with a Precision Echo Sounder, Hersey, J. B. and Rutstein, M. S., Bull. Geol. Soc. of Amer., Vol. 69, No. 10, 1958, pp 1297-1304.
8. Bunce, Elizabeth T., 1961, personal communication on a bathymetric survey of the Romanche Trench.
9. "Continuous Reflection Profiling", Hersey, J. B., The Sea, (In press).
10. "Geophysical Investigation of Cape Cod Bay, Massachusetts using the Continuous Seismic Profiler", Hoskins, H. and Knott, S. T., Journal of Geology, Vol. 69, No. 3, 1961, pp 330-340.
11. "Sonar Uses in Oceanography", Hersey, J. B., Edgerton, H. E., Raymond, S. O., and Hayward, G., Instrument Soc. of America - Fall Instrument-Automation Conference and Exhibit, New York City, N. Y., Preprint Number 21-60, September 26-30, 1960.
12. "Analysis of Reflection and Refraction Records taken with the Continuous Seismic Profiler", Hoskins, Hartley, Woods Hole Oceanographic Institution, Reference No. 60-37, 1960.
13. "A Deep-Sea Seismic Reflection Profile", Officer, Charles B., Geophysics, Vol. XX, No. 2, April 1955, pp 270-282.
14. "Suspended Echo-Sounder and Camera Studies of Mid-Water Sound Scatterers", Johnson, Henry R., Backus, Richard H., Hersey, J. B. and Owen, David M., Deep-Sea Research, Vol. 3, 1956, pp 266-272.
15. "Uses of Sonar in Oceanography", Edgerton, H. E., Electronics, June 24, 1960.
16. "Acoustically Monitored Bottom Coring", Hersey, J. B., Deep-Sea Research, Vol. 6, No. 2, 1960, pp 170-172.
17. "Improved Techniques of Deep-Sea Rock Dredging", Nalwalk, Andrew, Hersey, J. B., Reitzel, John and Edgerton, H. E., Deep-Sea Research (In press).
18. "Comparison of Directly Measured Sound Velocities with Values Calculated from Hydrographic Data", Hays, Earl E, The Journal of the Acoustical Society of America, Vol. 33, No. 1, 85-88, January 1961.
19. "Inverted Echo Sounder", Dow, Willard, Stillman, Stephen L., ISA-ASLO, Marine Sciences Conference, September 11-15, 1961, Woods Hole, Massachusetts.
20. "A Scattering Layer Observation", Kanwisher, J., Volkmann, G., (1955), Science 121 (3134), 108-109.

Fig. 1. Echo sounding profiles across (a) a small canyon and (b) small isolated bumps on the relatively flat sea floor of the Blake Plateau. Resolution: 15 milliseconds per inch. Vertical exaggeration: 30 to 1.

Fig. 2. High resolution soundings indicating sediment ponding. In (a) the ship's motion on the ocean waves causes oscillations in the echo sequences from the bottom. In (b) the effect of two pulse lengths, not greatly different, is compared (From Hersey[5])

Fig. 3. High resolution echo soundings of the Nares Abyssal Plain. Indications of sediment ponding are interrupted by a small seamount at the right end of record. Resolution: Approx. 15 milliseconds per inch. Pulse Length: 0.2 millisecond. Vertical exaggeration: 40 to 1.

Fig. 4. A Block diagram of the Continuous Seismic Profiler. The two-channel Precision Graphic Recorder is a part of this system.

Fig. 5. A seismic reflection profile across the southern tip of Stellwagen Bank, Massachusetts Bay. Successive signals maintain their similarity after many reflections. (From Hoskins and Knott[10])

Fig. 6. Seismic reflection records across Georges Bank taken on two, synchronized PGR's. The rippled trace on the left is the sea floor and arrows indicate seismic reflections from deeply buried acoustic and probable geological discontinuities, which are accentuated by this oblique view. Note that these returns correlate and background noise generally does not.

Fig. 7. In an oblique seismic reflection and refraction profile, the travel time of the direct arrivals changes as the source and receiver are separated on the sea surface. Refracted signals having travelled at greater compressional wave velocities than that of water arrive earlier than the directly received water-borne arrivals[10].

Fig. 8. Pinger controlled instrument lowering. The difference in travel time between the direct and bottom reflected pings is measured between the traces displayed on the PGR record.

Fig. 9. (a) Scattering layer migration at sunrise. (b) High resolution echoes from individual scatterers detected by lowering the sounding transducer among the scatterers.

Fig. 10. Echo ranging on fish schools. One of the fish schools in the record to the left is examined with high resolution in the record to the right[2].

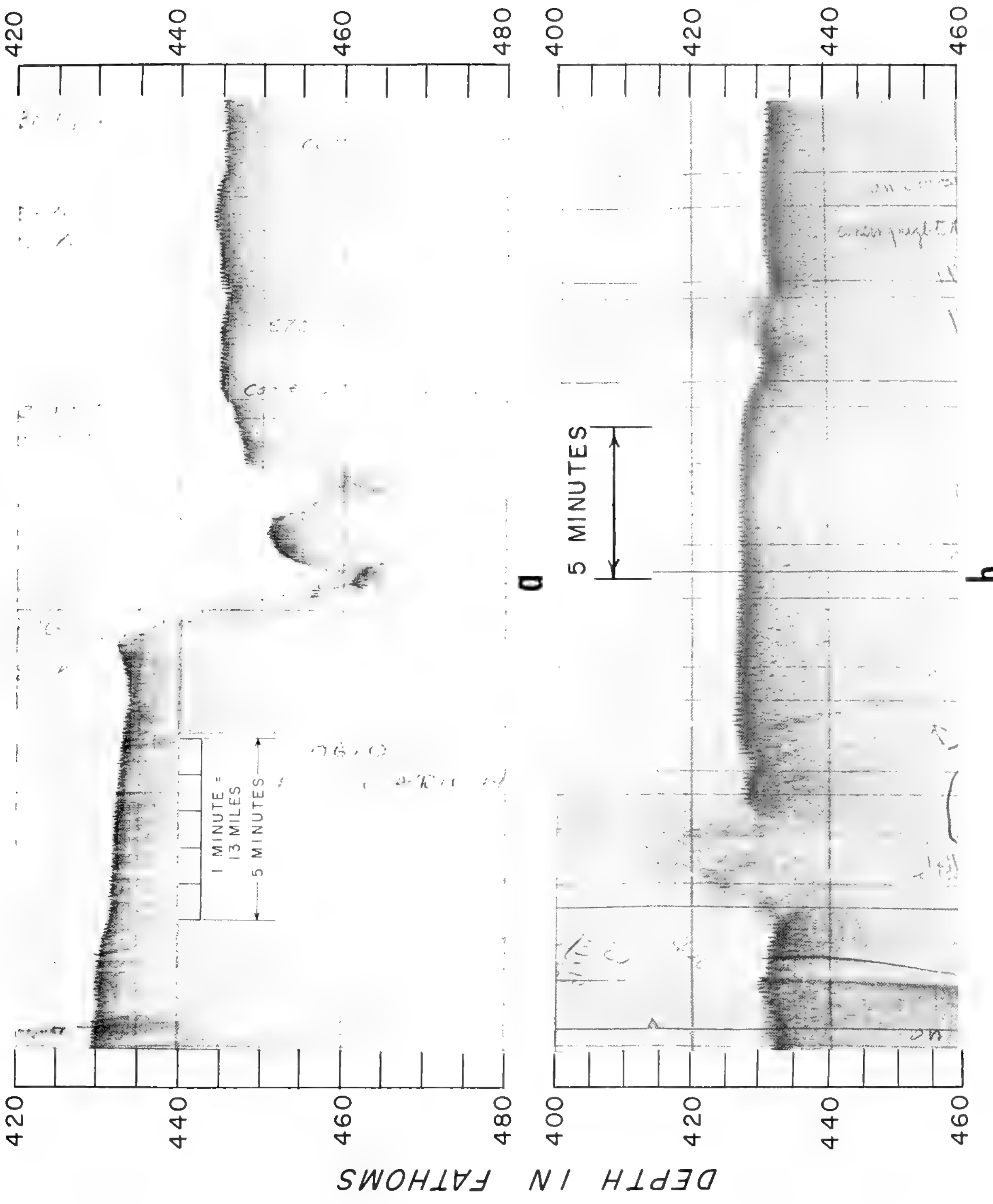
DEPTH IN FATHOMS
420
440
460
480
1 MINUTE = 13 MILES
5 MINUTES
a
400
420
440
460
5 MINUTES
b

Figure 1

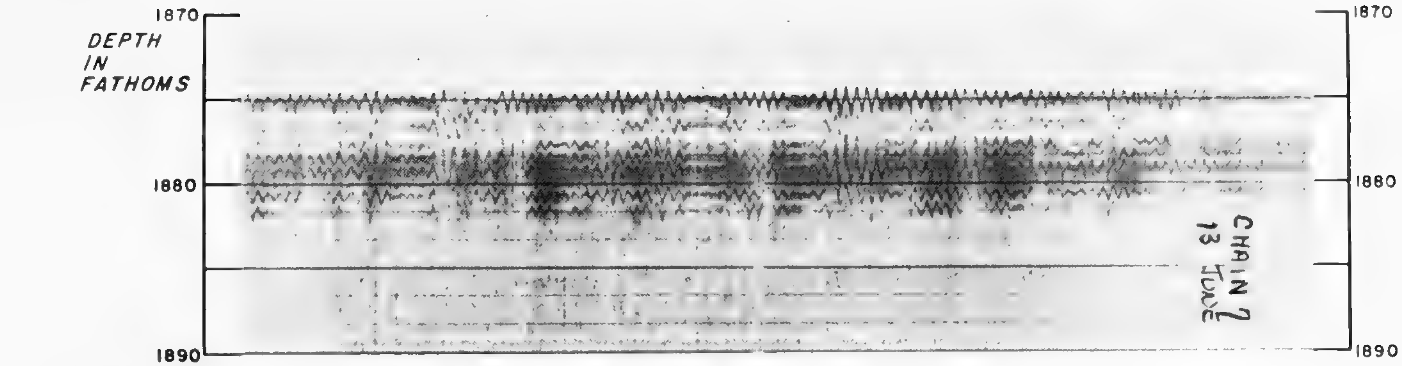

a BOTTOM ECHO SEQUENCE
TYRRHENIAN SEA
PULSE LENGTH CIR 0.4×10^{-3} SEC.

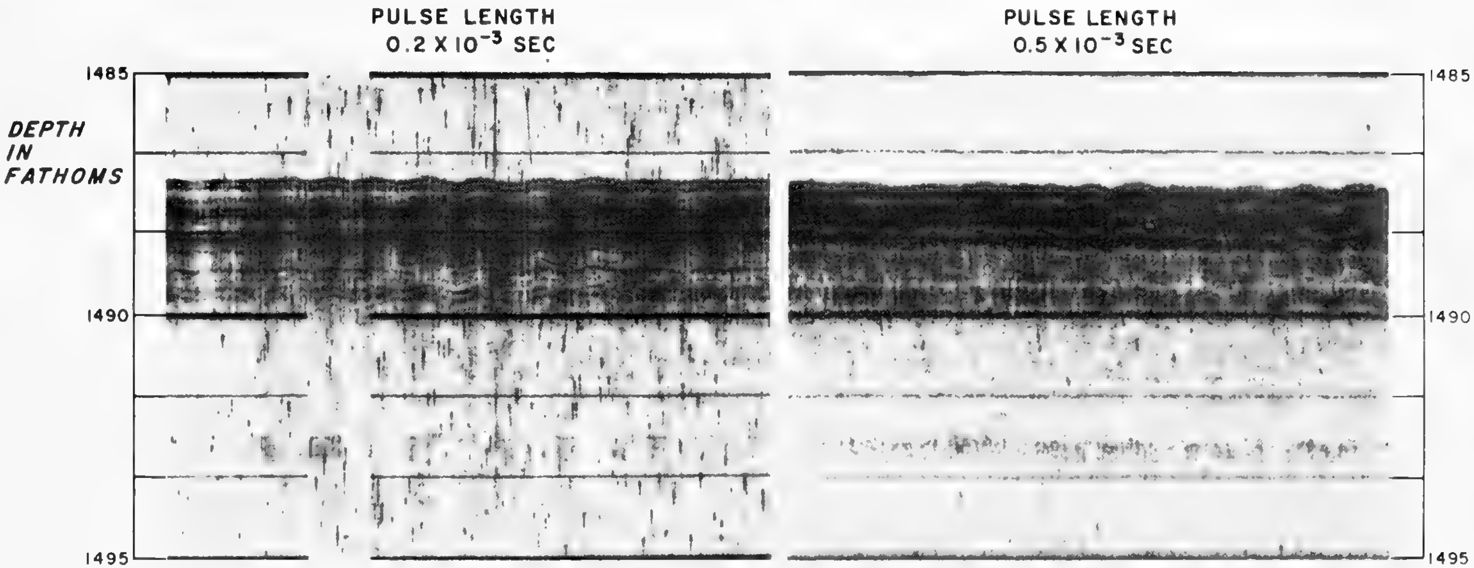

b ALGIERS PROVENCAL BASIN
HIGH RESOLUTION STUDY OF THE BOTTOM ECHO FROM AN ABYSSAL PLAIN

Figure 2

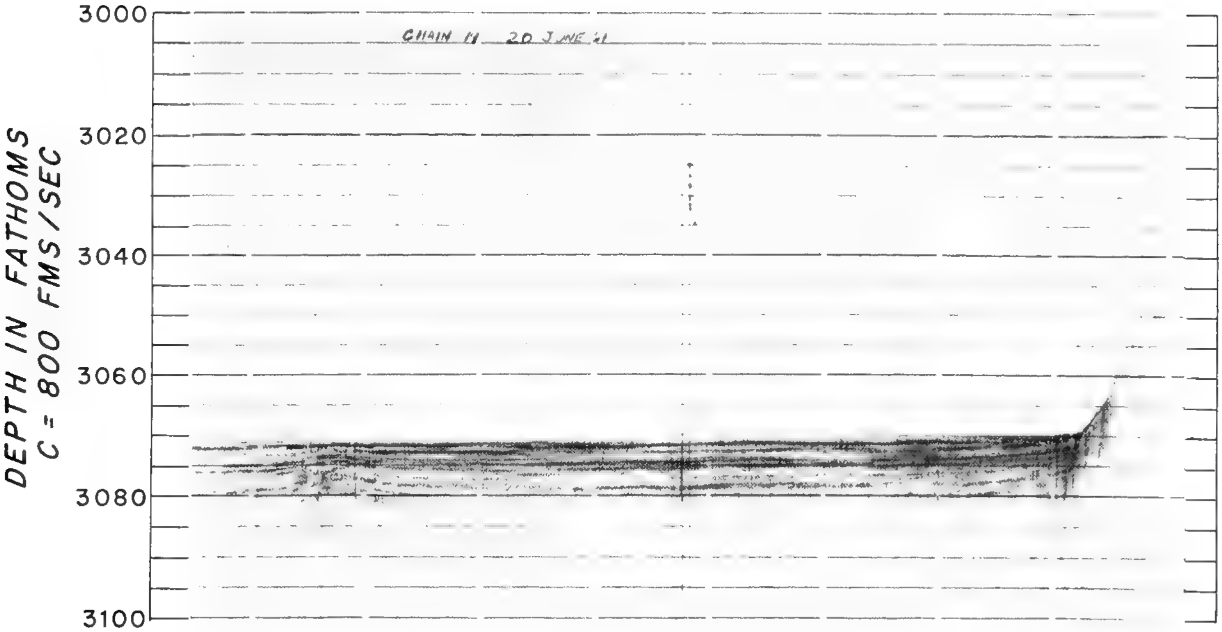

Figure 3

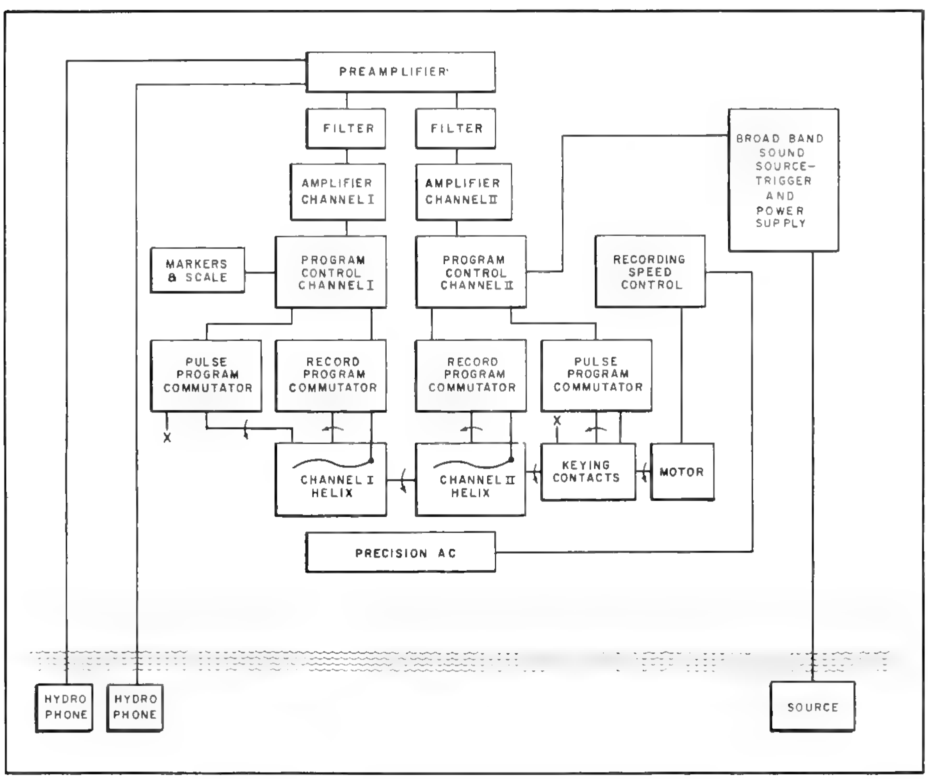

Figure 4

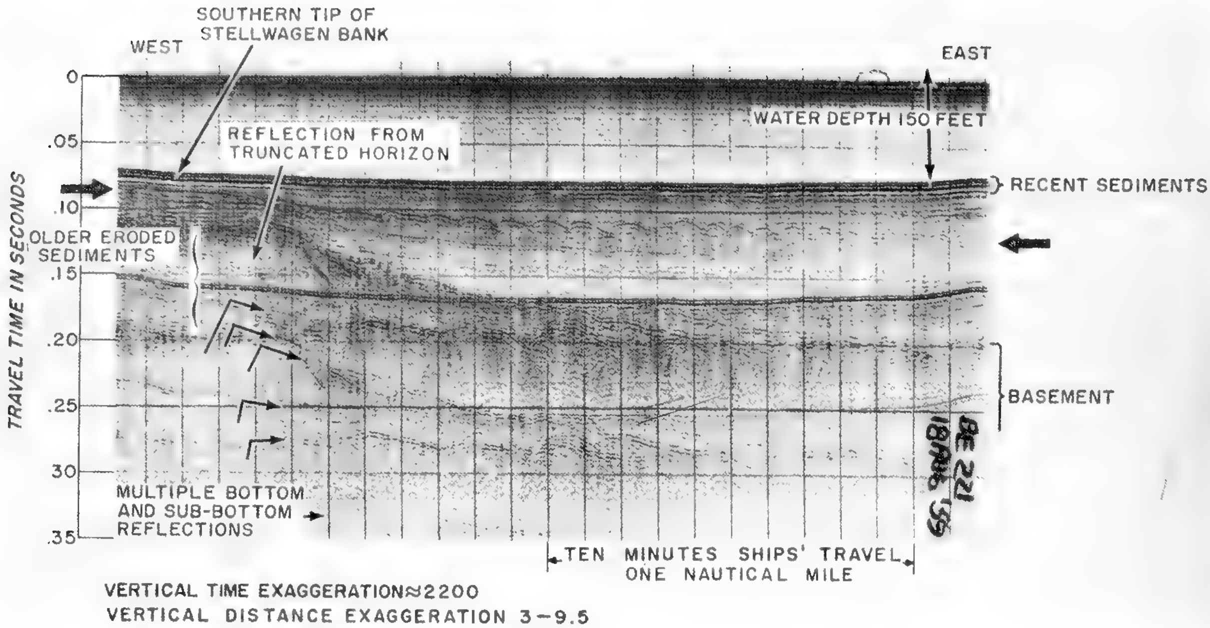

Figure 5

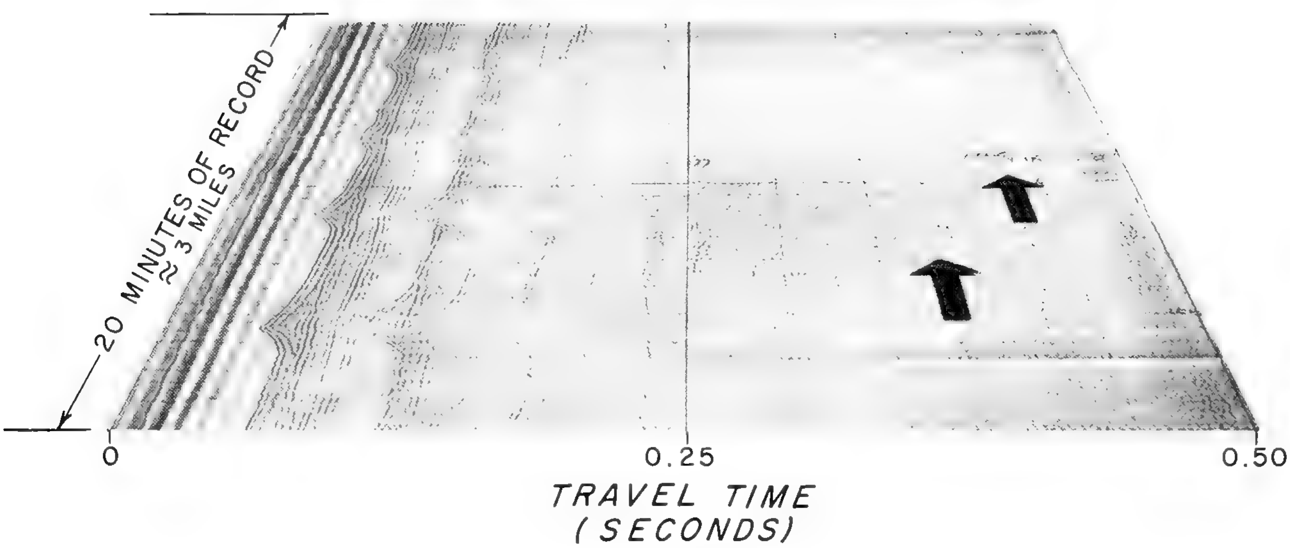

Figure 6

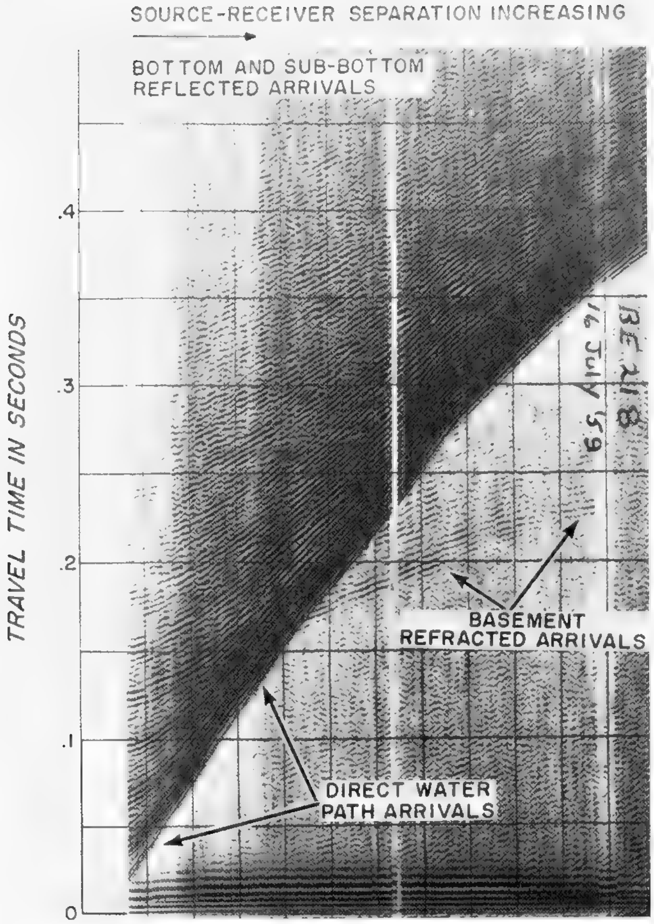

Figure 7

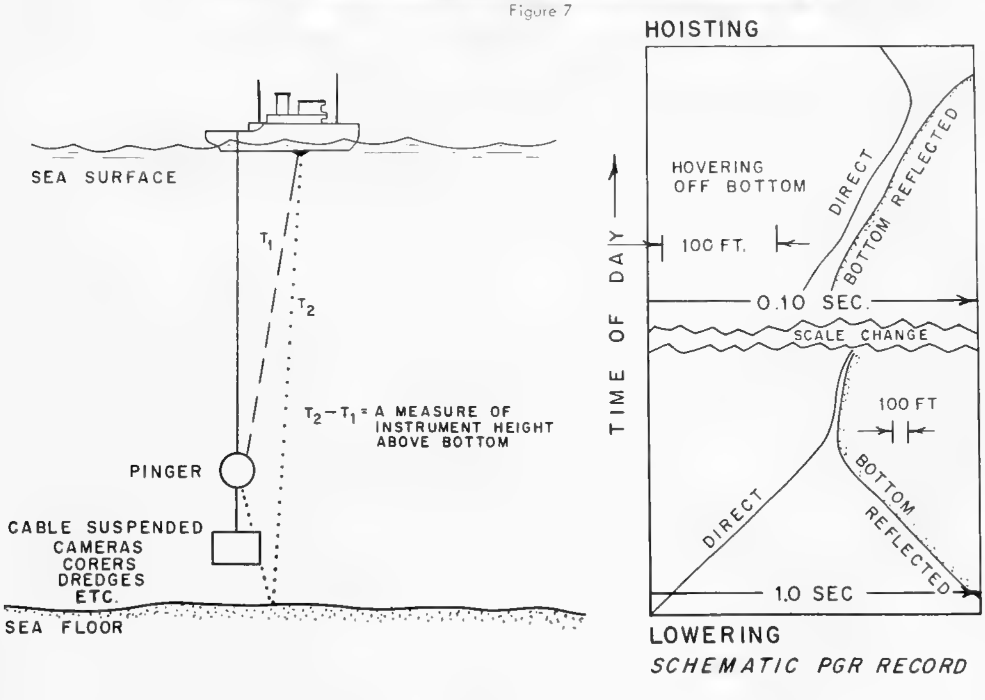

Figure 8

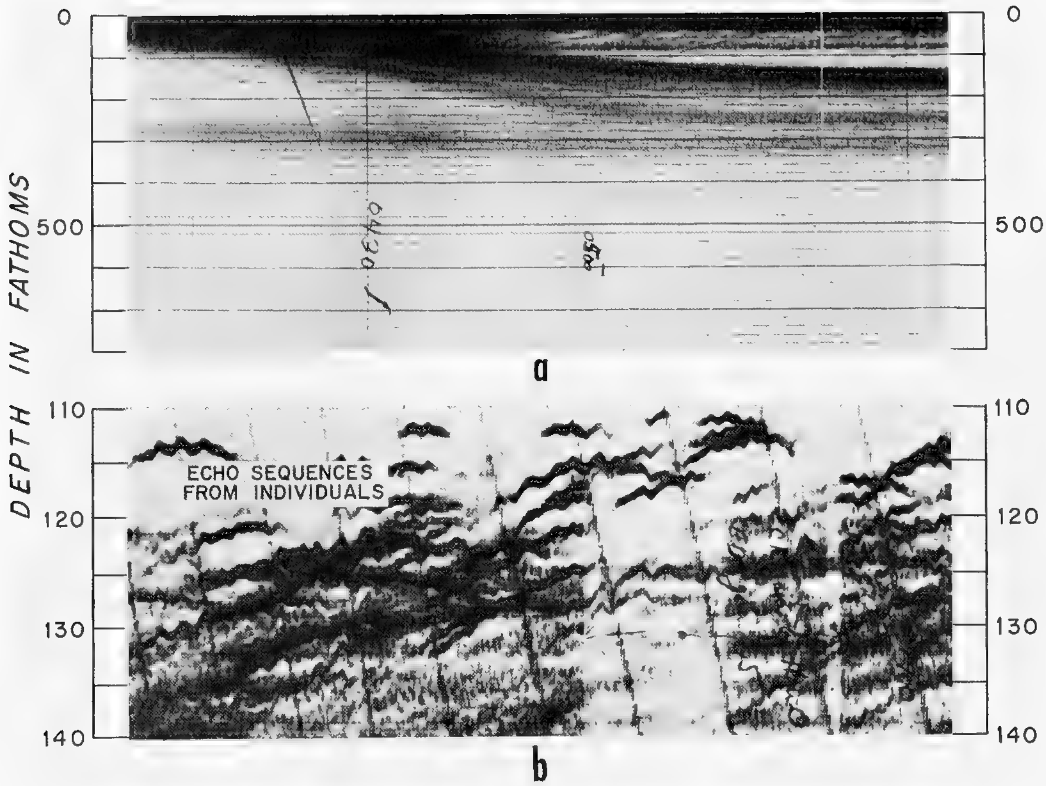

Figure 9

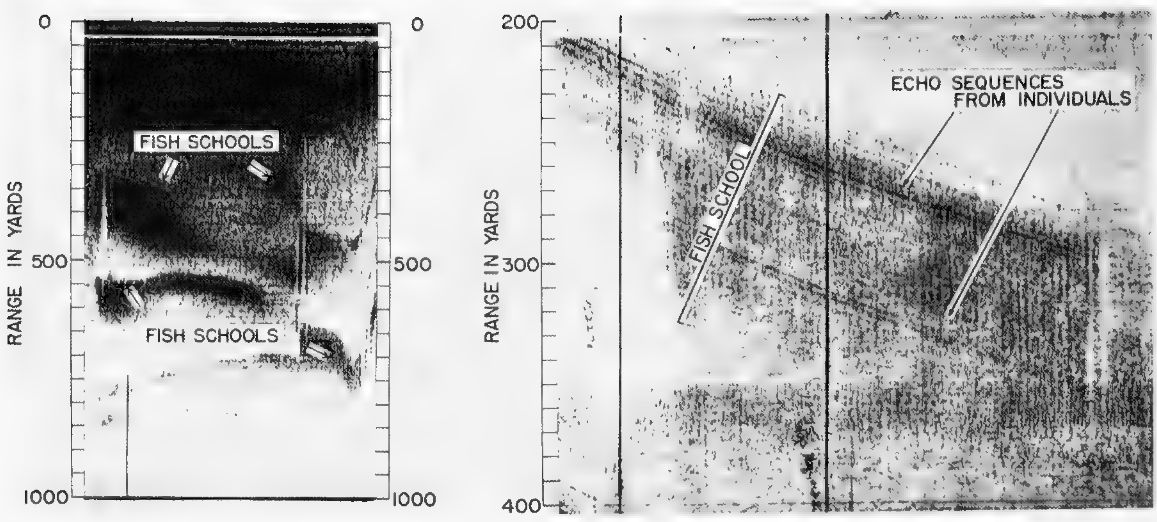

Figure 10

INVERTED ECHO SOUNDER

by WILLARD DOW, Electronics Engineer
and STEPHEN L. STILLMAN, Research Assistant in Engineering
Woods Hole Oceanographic Institution
Woods Hole, Massachusetts

PART 1 - Willard Dow

ABSTRACT

The Inverted Echo Sounder is an instrument primarily designed to provide a continuous and precise measurement of the depth of other instruments, such as the velocimeter being lowered along with it into the sea.

The device has also been used for detailed survey of the ocean bottom in deep water and by simple alteration of its suspension can be used for high powered short pulse echo ranging.

INTRODUCTION

Instruments are now available which are capable of measuring sound velocity, temperature, and salinity to a high degree of precision. However, the value of these measurements is greatly reduced if the depth of the instrument is not also known simultaneously and with comparable precision.

Most devices for such depth measurement incorporate bellows or bourdon tubes which although they can be made sensitive to small pressure changes in shallow water, become of necessity stiff and insensitive to such changes when designed to withstand the high static pressures of the deep ocean.

The Inverted Echo Sounder when coupled to a precision recorder has provided highly precise depth measurements down to at least 16,000 feet, and when perfected should operate considerably deeper.

When towed close to the bottom, the instrument also provides a highly detailed survey of the area showing bottom configuration impossible to resolve with conventional surface echo sounders.

THEORY OF OPERATION

The device consists of a high powered "pinger" as a short pulse transmitting unit mounted along side a sensitive fixed tuned receiver. Both units are connected to a common transducer which is used both as a projector and as a receiving hydrophone. The apparatus is self-contained and battery operated.

When submerged, the transmitter directs short pulses toward the surface at a one second repetition rate (Fig. 1). The surface reflected pulses are detected by the deep receiver, amplified and sent up via a single conductor oil well logging cable to the surface vessel. Here the signal is amplified further and applied to a precision graphic recorder normally used for echo sounding. From this record the depth of the instrument may be read directly.(Fig.1A)

Although the main lobe of the transducer is always directed toward the surface during instrument lowerings, there is also a weaker back lobe directed toward the bottom. Therefore when the gear is lowered to within 600 feet or so of the ocean floor, the bottom also becomes visible on the recorder chart and the winch can be stopped in time to avoid dragging instruments in the mud.

This same back lobe is made use of in bottom survey operations. In this case the sounder is lowered to between 30 and 100 feet of the bottom, and towed slowly across the region of interest. Under these conditions the area covered by the transducer beam at any given moment is comparatively small and details of bottom structure may be observed without the ambiguity produced by side reflections or the losses encountered in sound transmission through thousands of feet of water.

Since the surface is constantly being recorded as well, the depth of bottom features below the surface can also be determined from the recorder chart.

When a velocimeter is used with the gear its output signal passes through a mixer-driver stage in the inverted pinger where it is mixed with the receiver signal for transmission to the surface via the logging cable. At the surface the two signals are again separated by filters, the velocimeter signal being channeled to a counter and printer and the depth pulses to a precision graphic recorder as indicated above.

ELECTRONIC DESIGN

A. The Transmitter

Fig. 2 is a schematic diagram of the transmitter or "pinger" circuit. The transistor power supply consists of two 2N278 transistors in a multivibrator circuit operating at about 800 cycles. The high voltage secondary of the multivibrator transformer drives a voltage doubling rectifier circuit which in turn delivers approximately 1000 volts to the load.

The load consists of the two capacitors C_1 and C_2 in series, which in turn are connected to the plate and grid circuits of the thyratron as shown. When switch SW-1 closes, the high voltage is applied to the grid of the thyratron and the thyratron fires, discharging capacitors C_1 and C_2 through the primary of output transformer T_2. T_2 is a step-up transformer, the secondary of which is tuned to the 12 kc resonant frequency of the crystal transducer. A 14 kv, 400 microsecond ringing pulse is thus developed across this transducer and an acoustic "ping" is produced.

In the first experimental versions of this instrument, switch SW-1 was closed at a one second repetition rate by a motor driven cam. This motor, governor controlled for precision timing, was pre-synchronized to the readout recorder on the ship so as to produce a more legible record. However, this timing system is not entirely satisfactory and an electronic timer of higher accuracy is being developed.

B. Receiver

Fig. 3 is a schematic diagram of the receiver. This unit is fully transistorized and comprises three single ended stages fixed tuned to 12 kc, a push-pull driver and a 10-watt class AB final used as a cable driver. The first two stages are designed for low noise.

The input circuit is somewhat unconventional and therefore should be explained in some detail.

As indicated in Section A, the transmitter develops a 14 kv pulse across the transducer. Since this same transducer is used as a receiving hydrophone during the listening periods, it is essential that the receiver be electrically isolated and protected during the transmission of the 15, 000 volt pulse. It is also important that the receiver input impedance be high compared to that of the 12 kc tank circuit formed by the output transformer and the crystal transducer. Otherwise, loading and detuning effects could easily absorb most of the power in the transmitter pulse.

The solution to the problem is shown in the receiver diagram. A 15, 000 ohm high voltage resistor connects the transducer to a limiter circuit comprising two 10 watt zener diodes back to back. The resistor value is high enough to prevent loading the transmitter and also limits the zener current to a safe value. The zeners clip the receiver input at about 4 volts. As this signal would still overload the receiver, a second clipper follows the zeners consisting of reversed silicon diodes which have a conduction threshhold of about 0. 3 volt, a reasonable input level.

C. The Cable

The oil well logging cable used to support the instruments and conduct the signals to the surface is essentially conventional in design.

It consists of an electrical conductor of No. 19 stranded copper over which is drawn a thin hard layer of extruded nylon. This insulated center conductor is separated from the external sheath by a waterproof soft rubber compound which keeps the cable flexible and provides additional insulation.

The outside sheath consists of two layers of galvanized steel strands in opposed lays to prevent twisting and kinking. The overall diameter of the cable is slightly less than 1/4" and it has a breaking strength of 4, 265 pounds.

This cable was selected because it is strong, small in diameter, relatively cheap (17 cents/foot in 30, 000 foot lengths), and readily available. Although its attenuation is high at the higher frequencies, the transistorized Class B cable driving stages in the receiver and velocimeter amplifiers have more than sufficient power to overcome the losses in a six mile line at the expense of an average battery drain of only a few miliamperes.

D. Accuracy

The accuracy of the depth measurement depends, of course, upon the velocity of sound in the water at the place where the lowering is being made. This velocity in turn depends on the temperature, density, and salinity of the water through which the sound travels. The more accurately these factors are known, the more precise the measurement since the resolving power of the gear is sufficient to indicate vertical changes of a few feet regardless of the depth of the instrument.

When an accurate velocimeter is lowered with the sounder so that the sound velocity is known throughout the transmission path, it is certainly safe to assume that a deep measurement is good to a fathom and perhaps better. Expressed in the usual way, as per cent accuracy of full scale, this would correspond to an accuracy of at least 0. 04%, if full scale were considered to be 15, 000 feet for example.

PART #2 - Stephen L. Stillman

STRUCTURAL DESIGN

A. Orientation

In order to obtain the strongest signal return from the water surface, it is necessary to hold the axis of the main lobe of the transducer perpendicular to the surface. This requirement dictates a self-aligning hydrodynamic design containing components so located as to produce balanced drag effects and to properly locate the center of buoyancy.

B. Vertical Stabilization

Static stabilization of the gear is achieved by pivoting a towing support bail (Fig. 4 at A) at a point just below the center of buoyancy. A strong righting moment is thereby produced about this towing-pivot point thus providing the primary vertical aligning force. When towing, the hydrodynamic drag developed above the towing pivot point must be balanced by the drag below this point. This is accomplished by adding a vane at the top (Fig. 4 at B). It was found necessary to add a second vane to provide a moment of force about the vertical axis. This orients the instrument in the direction of tow allowing the upper vane to position the entire instrument and develop the proper drag for balance. Since the gear will remain vertical regardless of cable angle, towing speeds up to 4 knots even in rough seas are permissable.

C. External Frame

Damage to instruments while handling on deck and over the side has often in the past been disastrous especially when the ship is rolling severely. Mildly rough seas average a good part of ship time at sea, and productive use of this time is obviously advantageous. The instrument described has been developed for use under these conditions.

For example, to avoid damage to the Inverted Sounder and velocimeter a lightweight aluminum tubular frame is constructed around the principal components (Fig. 4 at C) and mounted to the internal structure by neoprene and plastic shock absorbers (Fig. 4 at D and E , for example). The support points of the whole assembly are located on the internal structure itself, not the frame. Therefore, damage to the frame is not apt to affect operation of the instrument.

During bottom survey work a possible cause of loss is snagging the instrument on the bottom. To guard against this, the rubber and plastic shock material present weak links which will part before the supporting steel cable.

An additional way of retrieving snagged gear is provided in a safety cable. One end is fastened at the lower end of the instrument (Fig. 4 at F) the other to the steel support above the clamp (Fig. 4 at G). All external aluminum metal surfaces are coated with an epoxy type paint to resist surface corrosion. Teflon bearing material was used on the bail pivot to reduce noise.

D. Watertight Electronic Chambers

The two watertight compartments containing the transmitter and receiver respectively consist of two 7075-T6 aluminum tubes, (Fig. 5) and end caps of the same material. These compartments will withstand 10, 000 P. S. I. and are sealed with double O-rings mounted on the caps. (Fig. 6 at A and B). One O-ring is located as near as possible to the perimeter of the cap to prevent corrosion from developing between cap and tube surfaces. Such corrosion would cause considerable difficulty in removing the end caps. Each cap is held to its tube by four quick acting stainless steel drawhook latches. Eight standard Joy plugs provide electrical connections through the caps.

The earlier models of the instrument employed a standard model airplane engine spark plug as the high voltage feed-through which conducts the 15, 000 volt pulse through the end cap. These plugs are capable of withstanding the 14, 000 P. S. I. required for deep submergence. Because these plugs are no longer manufactured, a special feed through designed for the purpose is used on the current model.

After considerable investigation it was found that a certain commercial weather-stripping putty had excellent insulating qualities for high voltage even when subjected to high pressure in salt water. This material was therefore used directly to insulate the high voltage terminal described above. The entire high voltage assembly is protected by an external aluminum housing (Fig. 6 at C).

An internal bulkhead incorporating an O-ring seal is placed within the transmitting tube to separate the battery compartment from the high voltage transmitter (Fig. 6 at D). This precaution was taken because silver zinc batteries, when defective or subjected to heavy drain, have been known to emit enough hydrogen to cause an explosion when mixed with air and ignited by a spark such as might accidentally be generated by a defect in the high voltage system.

E. Internal Construction

Stainless steel was used for chassis construction where possible to prevent salt air corrosion. The transmitter and receiver chassis are mounted on the end caps, thus eliminating several connectors. The receiver battery is contained in a plug-in chassis, on which is also mounted the velocimeter mixer-amplifier (Figs. 7 and 8). A fibreglass cover protects the components from salt spray when the battery chassis is removed from the tube on deck. To reduce acoustic noise, the timing motor is suspended by neoprene strips and entirely encased in a sound absorbing plastic foam.

F. Velocimeter

A N. B. S. velocimeter may be attached below the internal assembly, where it is protected by a tubular structure and shock mounts (Fig. 4 at H). This instrument is designed for 20, 000 P. S. I. If it becomes desirable to also operate the sounder under such pressure, this can be accomplished by a slight increase in the wall thickness of the aluminum tubes housing the electronic units

CONCLUSION

This paper has been concerned with a combination precision depth meter and bottom survey instrument, with provision for also transmitting sound velocity information to the surface. Since velocity information is not complete without a precise depth measurement, and since the depth measurement becomes far more accurate when the true velocity is known, these two instruments complement each other rather nicely. However, to complete the velocity picture the factors which affect velocity should also be known. Therefore, we are now preparing to add precise temperature determination and possibly salinity to the velocity and depth determinations.

ACKNOWLEDGMENTS

This gear was developed under Office of Naval Research Contract No. 1367.

The authors of this paper wish to thank J. B. Hersey for promoting and supporting the development of the equipment.

They also greatly appreciate the cooperation and assistance of Earl E. Hays who developed successful techniques for using the gear as a survey instrument for detailed examination of the bottom.

This is Contribution No. 1222 of the Woods Hole Oceanographic Institution of Woods Hole, Massachusetts.

LIST OF FIGURES

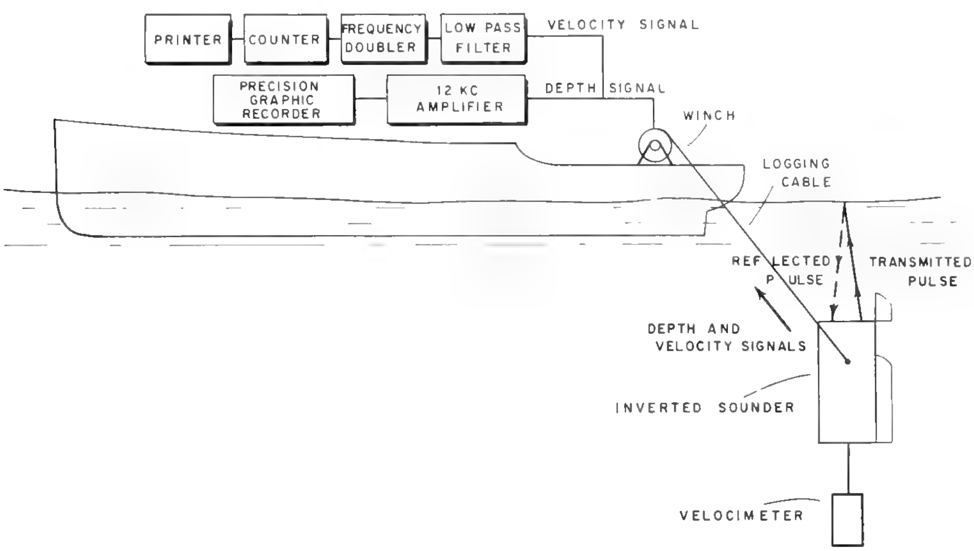

Figure 1

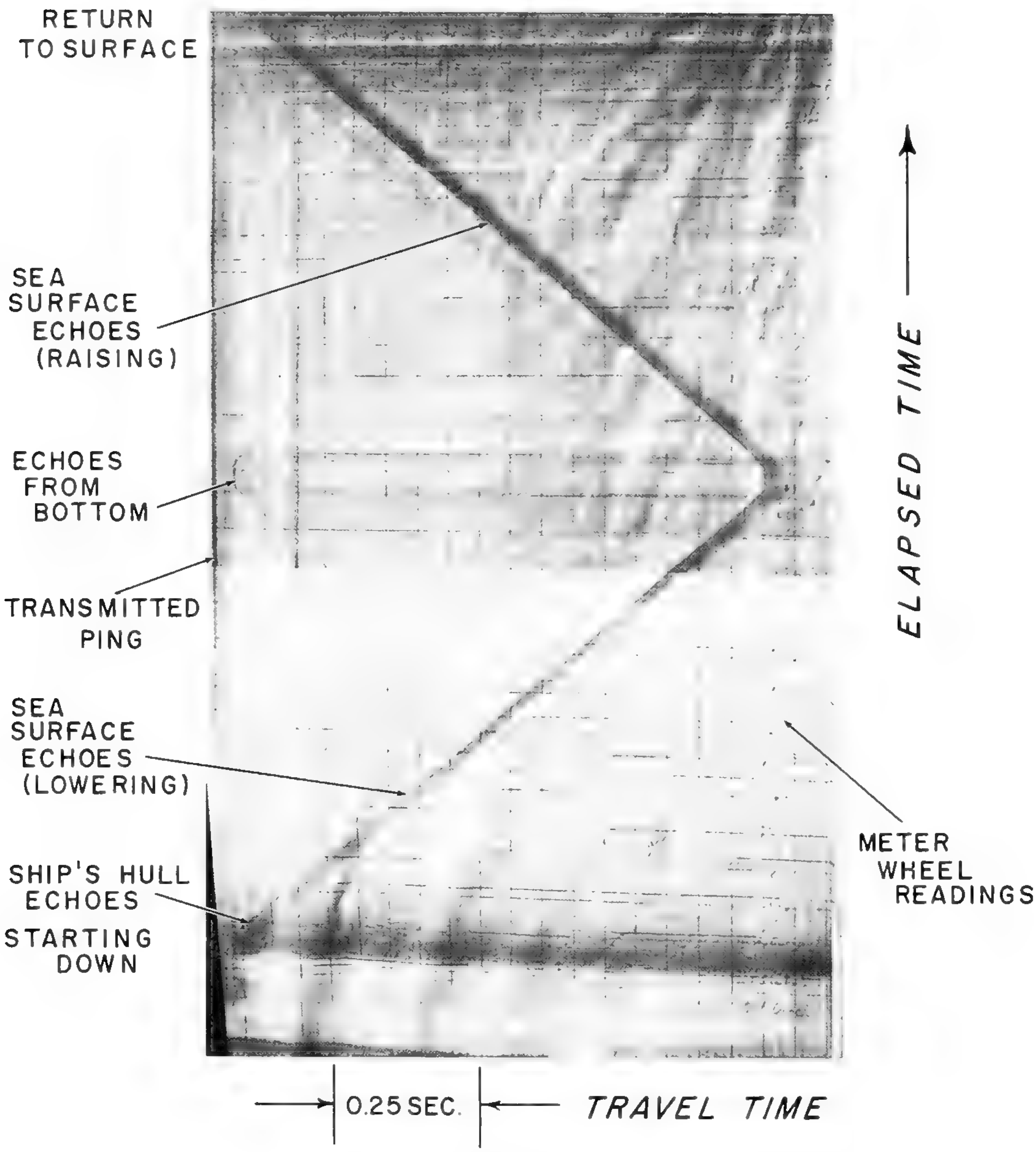
RETURN TO SURFACE
SEA SURFACE ECHOES (RAISING)
ECHOES FROM BOTTOM
TRANSMITTED PING
SEA SURFACE ECHOES (LOWERING)
SHIP'S HULL ECHOES
STARTING DOWN
ELAPSED TIME
METER WHEEL READINGS
0.25 SEC.
TRAVEL TIME

Figure 1A

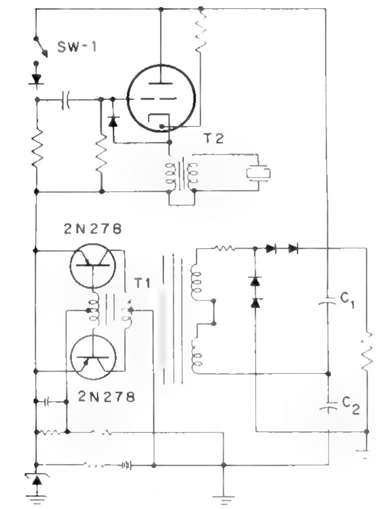

SW-1
T2
2N278
T1
C_1
C_2
2N278

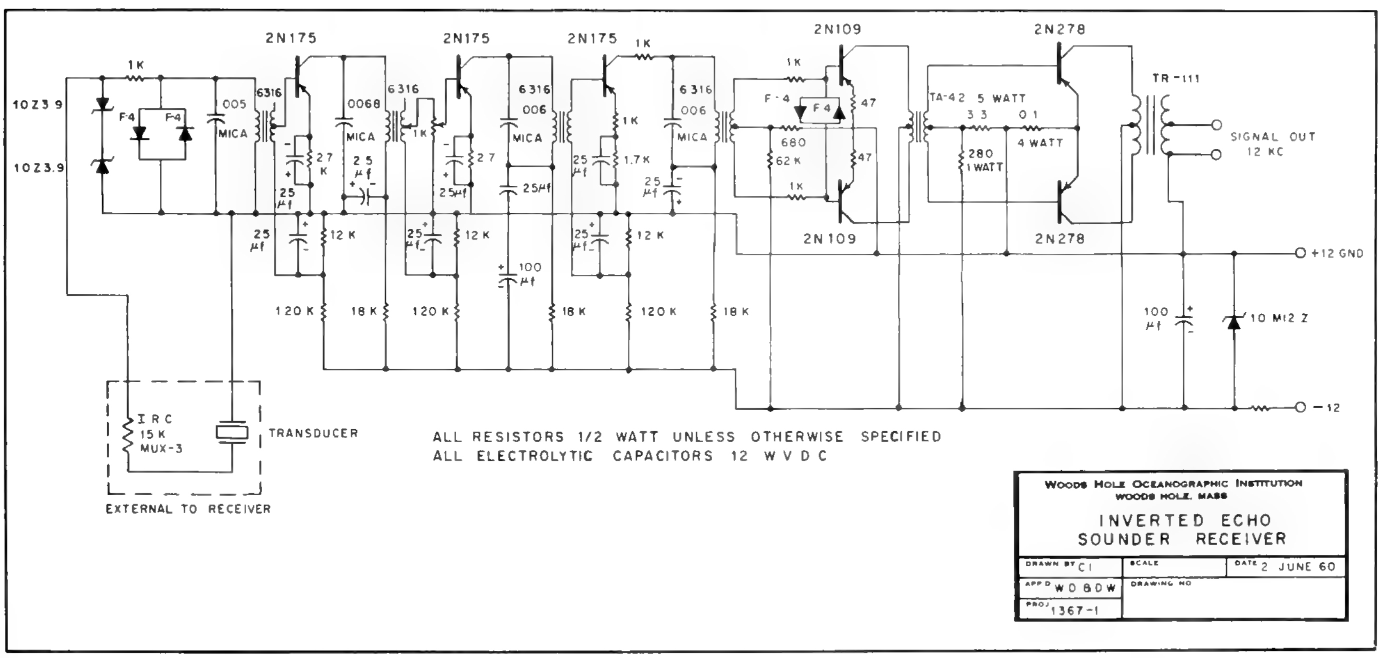

2N175
2N175
2N175
1K
2N109
2N278
1K
10Z3.9
10Z3.9
F4
F-4
.005
MICA
6316
.0068
MICA
6316
1K
6316
.006
MICA
6316
.006
MICA
2.7 K
25 µf
2.5 µf
2.7
25µf
25µf
25 µf
1.7K
25 µf
1K
F-4
F4
47
47
680
62K
1K
TA-42 5 WATT
3.3
0.1
280 1 WATT
4 WATT
TR-111
SIGNAL OUT 12 KC
2N109
2N278
25 µf
12 K
25 µf
12 K
100 µf
25 µf
12 K
+12 GND
120 K
18 K
120 K
18 K
120 K
18 K
100 µf
10 M12 Z
-12
IRC 15 K MUX-3
TRANSDUCER
EXTERNAL TO RECEIVER
ALL RESISTORS 1/2 WATT UNLESS OTHERWISE SPECIFIED
ALL ELECTROLYTIC CAPACITORS 12 WVDC
WOODS HOLE OCEANOGRAPHIC INSTITUTION
WOODS HOLE, MASS
INVERTED ECHO SOUNDER RECEIVER
DRAWN BY CI
SCALE
DATE 2 JUNE 60
APP'D WO BDW
DRAWING NO
PROJ 1367-1

Figure 3

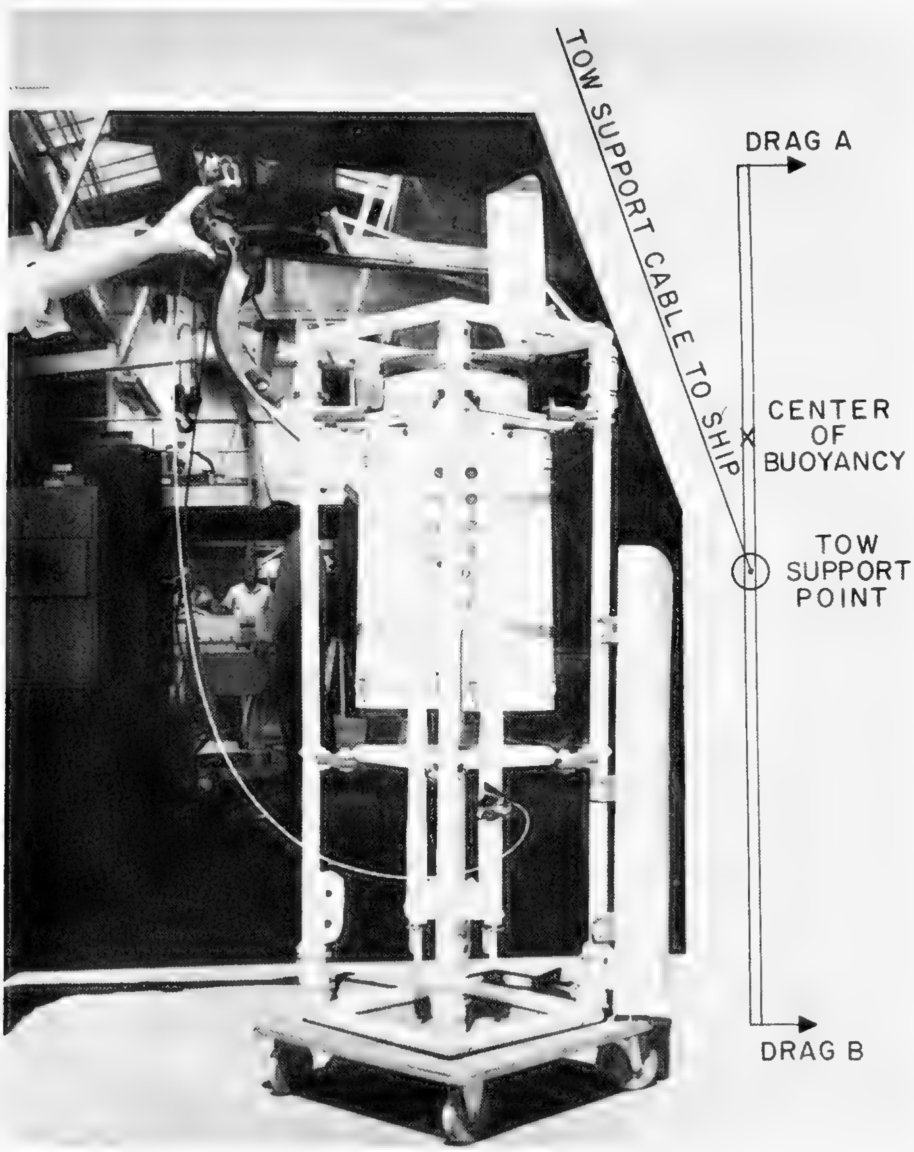
TOW SUPPORT CABLE TO SHIP
DRAG A
CENTER OF BUOYANCY
TOW SUPPORT POINT
DRAG B

Figure 4

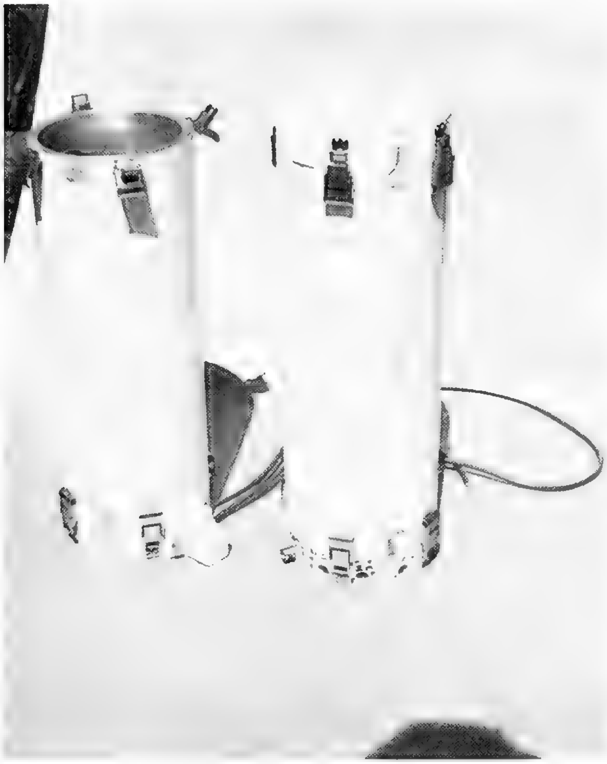

Figure 5

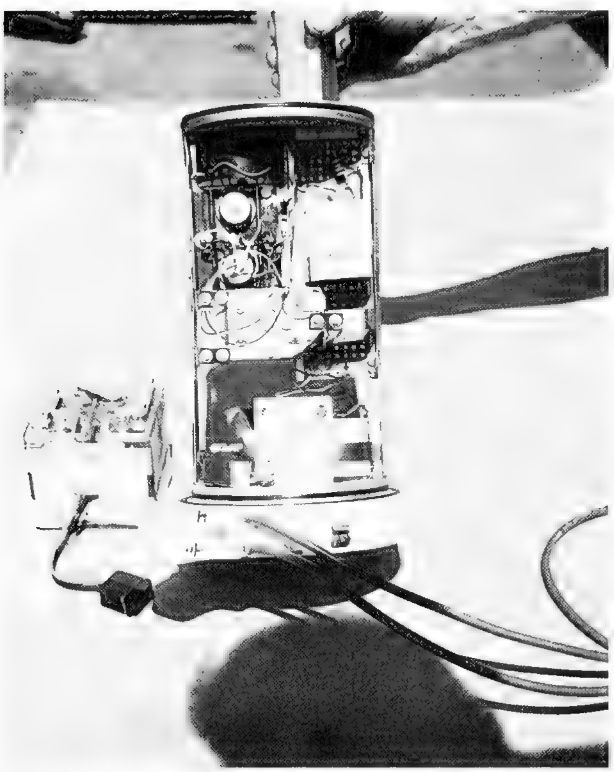

Figure 6

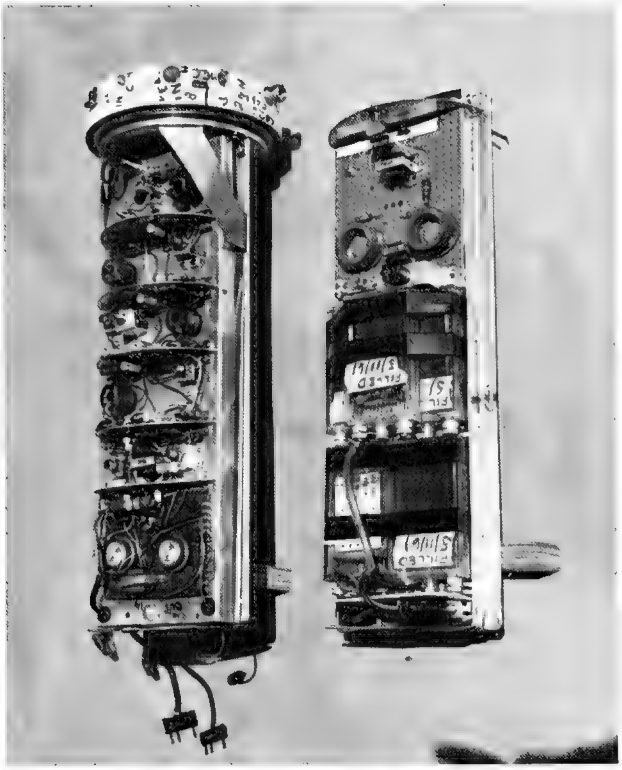

Figure 7

Figure 8

A BOTTOM STRIP MAP CAMERA

by DR. ANGELO J. CAMPANELLA, Senior Physicist
HRB-Singer, Inc.
State College, Pennsylvania

ABSTRACT

A preliminary investigation of photographing a lake bottom using a scanning-type system is reported. An example of the results of tests conducted with a line-scan camera system is presented.

INTRODUCTION

In ocean and lake bottom photography, large area coverage at a suitable illumination level is difficult to obtain. To date, successful bottom photography has consisted of photographs of local coverage on the order of several feet in range in relatively clear water.

The feasibility of a line scan strip map technique for underwater bottom photography is demonstrated herein. This experimental camera system offers the advantage of contrast enhancement, minimum light level requirements, and the ability to trade resolution for sensitivity. This system was installed in a glass bottomed boat and bottom photographs taken of a shallow mountain lake are shown.

CAMERA

Figure 1 illustrates the camera's principle. A line scan motion is produced by rotating a plane mirror on an axis inclined 45° with respect to its surface. This mirror reflects light into an objective aperature which focuses the light onto a photomultiplier cathode. The area of this image impinging onto the cathode is limited by a small variable aperture. The image of the aperture may be considered as being projected onto the ocean bottom. This spot is rapidly swept across the bottom surface in a lateral direction via the rotational motion of the scanner mirror.

The maximum scan rate used was about 60 lines per second. The forward motion of the vehicle carrying the camera unit provides the longitudinal scanning. A contiguous coverage of the bottom will occur for scanning speeds as fast as or faster than that required to lay one scanned strip adjacent to the previous. It is conventional to scan at a slightly greater RPM than that required for contiguity. This minimizes the raster effect in the recorded photograph.

The instantaneous signal amplitude received at the detector, in this case a photomultiplier, is amplified and its dc level carefully controlled so as to have a minimum bottom brightness encountered correspond to the threshold of the recording film. Recording film illumination is accomplished by feeding the signal from the control box into a glow lamp whose light output is a confined spot of brightness proportional to the input current. The recording film is wrapped around a barrel containing a rotating microscope objective, so that the film remains in the focal plane of the objective. The glow lamp output is projected along the axis of the barrel, folded 90° by a mirror, and then enters the objective lens. The spot is projected on the recording film by the microscope objective. A common Plus X type film has been found to have ample sensitivity.

The film is moved past the barrel at a speed proportional to the velocity of the vehicle and inversely proportional to the distance to the bottom. The film speed used for these experiments corresponds to a vehicle velocity of about one foot per second and a bottom distance of seven feet. Gyro-stabilization of the roll axis is provided.

The camera system can accommodate a wide range of illumination levels by the variation of the area of the aperture before the photomultiplier detector. In particular, resolution can be exchanged for sensitivity. (This is impossible in a conventional camera.) The resolution-sensitivity product is proportional to the area of the collecting aperture. Sensitivity greater than that of film can be achieved with some loss of resolution.

Figure 2 is an example of a photograph that a line-scan system has produced. The resolution and dynamic range illustrated here are typical.

DESCRIPTION OF WATER-BORNE EQUIPMENT

The vehicle used to carry the camera equipment was a 12-foot, all-aluminum pram modified as shown in Figure 3.

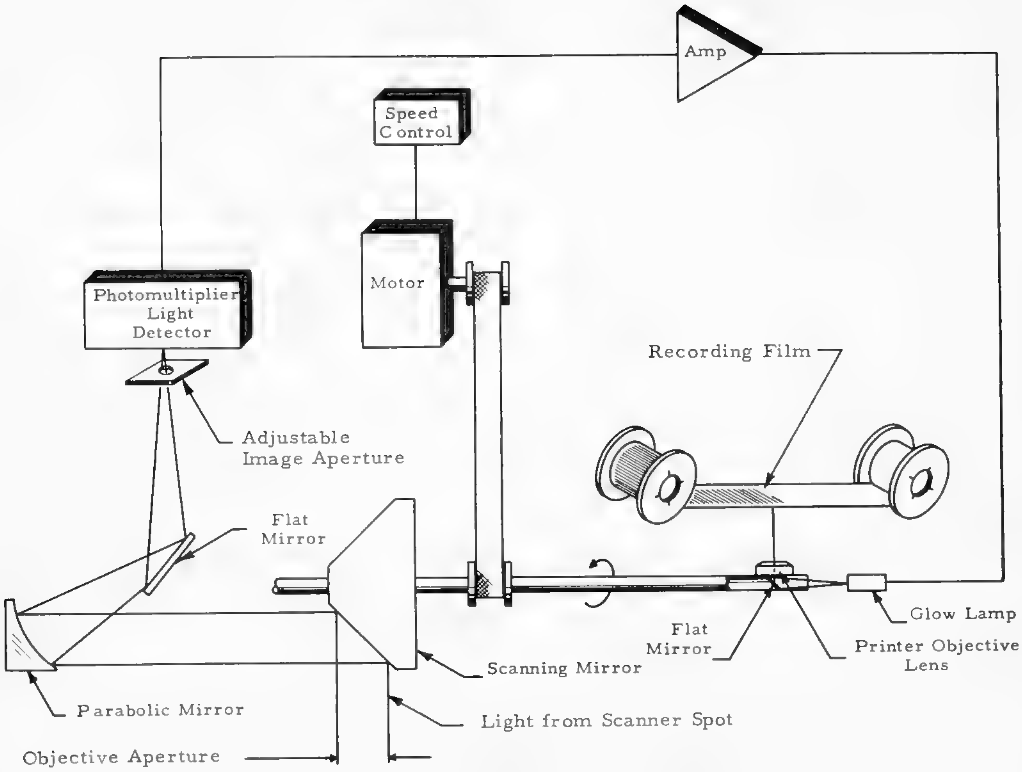

Fig. 1 - **Basic Camera Scheme**

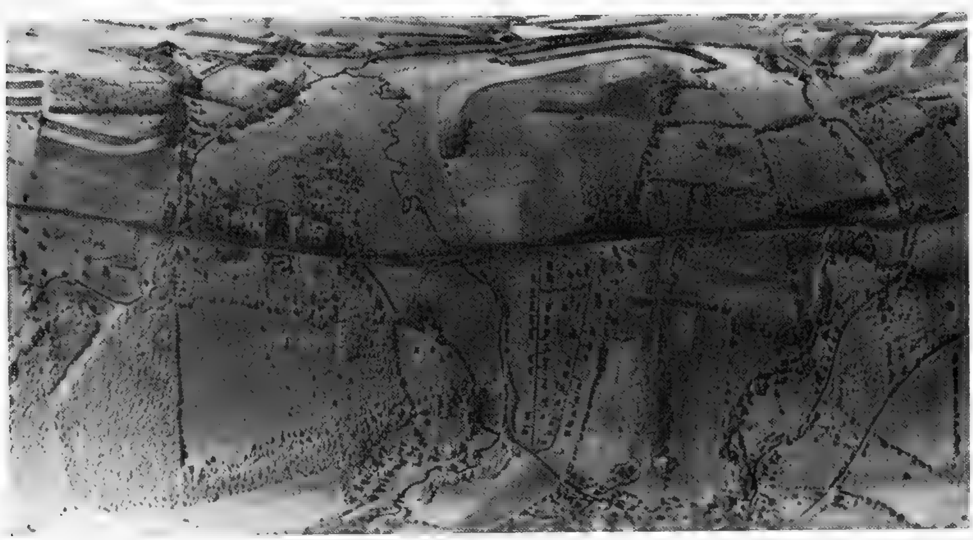

Fig. 2 - A Line Scan Strip Map

The center seat of the boat was removed, a 6-inch by 34-inch hole was cut athwartships in the bottom, and a like-size section of auto safety-glass window was installed. The area adjacent to the window was painted dull black to minimize stray reflections. An electric trolling motor, powered by two 6-volt auto batteries, propelled the boat. Two crewmen were used to maneuver the craft and operate the system.

High voltage for the photomultiplier was obtained from the control box cathode ray tube power supply. The control box and battery (two 12-volt auto batteries in series) were installed in the bow along with a 400-cycle inverter.

The window, which extended the full width of the boat bottom, was wide enough to accommodate the 3-inch wide scanning aperture and to provide an approximately 80° lateral field of view after refraction at the air-water interface.

EXPERIMENTS

Roosevelt Lake, a small artificial lake near State College, Pennsylvania, was chosen as the site at which photography with the water-borne equipment would be tried. The bottom of this lake slopes gently from the beach to a maximum depth of about 12 feet.

Two targets were prepared for the tests. The first was a one-foot square sheet of aluminum painted to produce a black and white checker-board comprising four 6-inch squares; the second target was a pair of 6-inch by 18-inch aluminum strips set in the form of a cross. One strip was painted black, the other white. These targets were placed near each other on the lake bottom and their position marked by a buoy.

Both natural light and artificial light photographs were planned, but time limitations prevented the latter. The water was relatively clean, enabling the bottom to be seen through the glass window. A coating of moss and silt significantly reduced the r eflectivity and contrast of the bottom, resulting in very low contrast objects. This bottom situation, probably representative of the worst conditions to be encountered, points up the need for contrast-increasing devices including side lighting. Under conditions of little or no silt, considerably better results are naturally expected.

It was possibly to vary the speed of the pram in six steps from less than 1/2 knot to about 3 knots. A maximum of about 2 knots was used during the photographic runs because higher speeds caused lapping under the bow, producing an accumulation of air bubbles under the blass window. Since the recording film speed must be matched to the boat's velocity in relation to depth, the maximum available film speed of one foot per minute dictated a boat speed of one foot per second when the depth was seven feet, the depth at which the targets were planted. Future models of a system could accommodate considerably greater velocities.

Figure 4 shows a photograph which was taken with this gear. The angular size of the scanning spot was three milliradians. The left-hand side of the upper photo shows some tree branches or, perhaps a tree stump. The boat-shaped object in the center appears to be a sunken canoe. The checkered target appears at the center-right, and the cross in the upper right corner. It is noted that the whites of the targets are extremely bright while the blacks are not immediately evident. This is a consequence of the poor reflectivity and the presence of some scattering particles in the water respectively. The uniform lateral striations are spontaneous variations of the electronic level at very low frequencies. More recent developments have minimized these lines. The day on which this run was made was very cloudy with intermittant drizzle. The second photo was made on a sunny day. The shadow of the boat is evident as a black stripe down the photo. Bottom objects, such as tree stumps and a silt-covered plank are evident with better contrast. Surface wave patterns caused occasional light patterns. In the left portion, the checkered target is evident despite the boat's shadow.

CONCLUSIONS

Acceptably identifiable photographs of targets on a shallow lake bottom have been obtained using a scanning-type system. These results are encouraging, and further work is required to illustrate the ultimate worth of the system for oceanographic research.

In order to simulate the lighting conditions which are found at the ocean floor, a series of photos should be taken at night using artificial illumination. Figure 5 shows one possible mounting configuration of these lights, which would be encased in a watertight container and immersed in the water.

A high intensity beam spot which would scan along with the camera so as to coincide with the look spot of this equipment is another possibility. This configuration permits either an increase in brightness or a decrease in power requirements or both over the system utilizing fixed lights.

The scanning beam source would be as much displaced from the scanner aperture as physically feasible.

Although intense scattering from the beam would find its way into the instantaneous field of view of the scanner aperture, the contrast-enhancing capabilities of the electronic processing system permit the large steady component of the signal due to backscattering to be cancelled. Moreover, the volume of water directly illuminated by the light beam would be relatively small since it is necessary to provide light flux for only a small picture element at any given instant. This reduces the amount of cross-scattered light

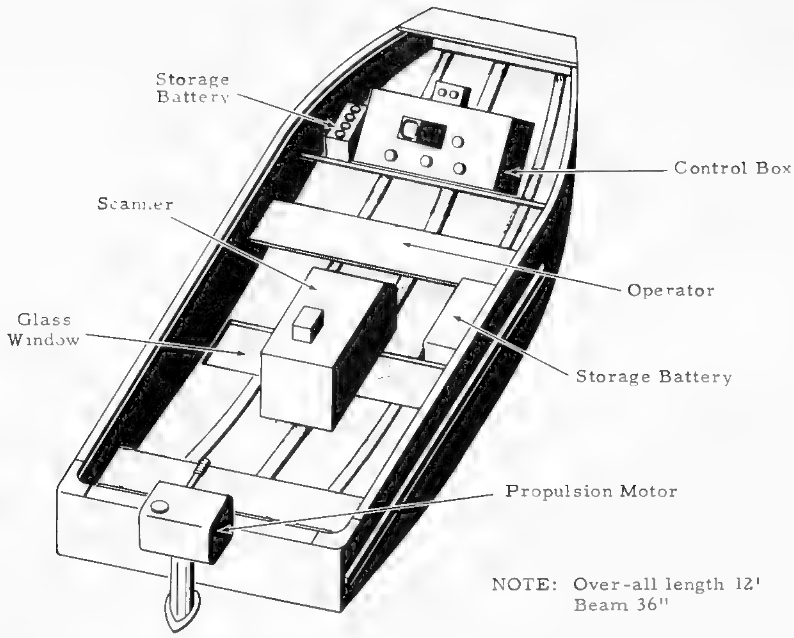

Fig. 3 - Experimental Boat

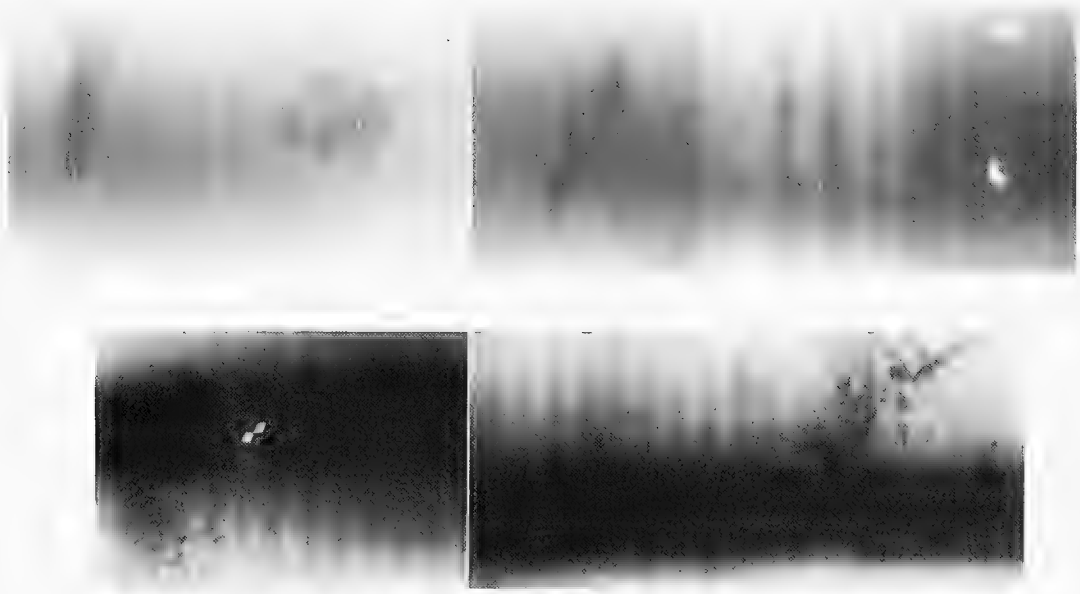

Fig. 4 - Photograph of Lake Bottom

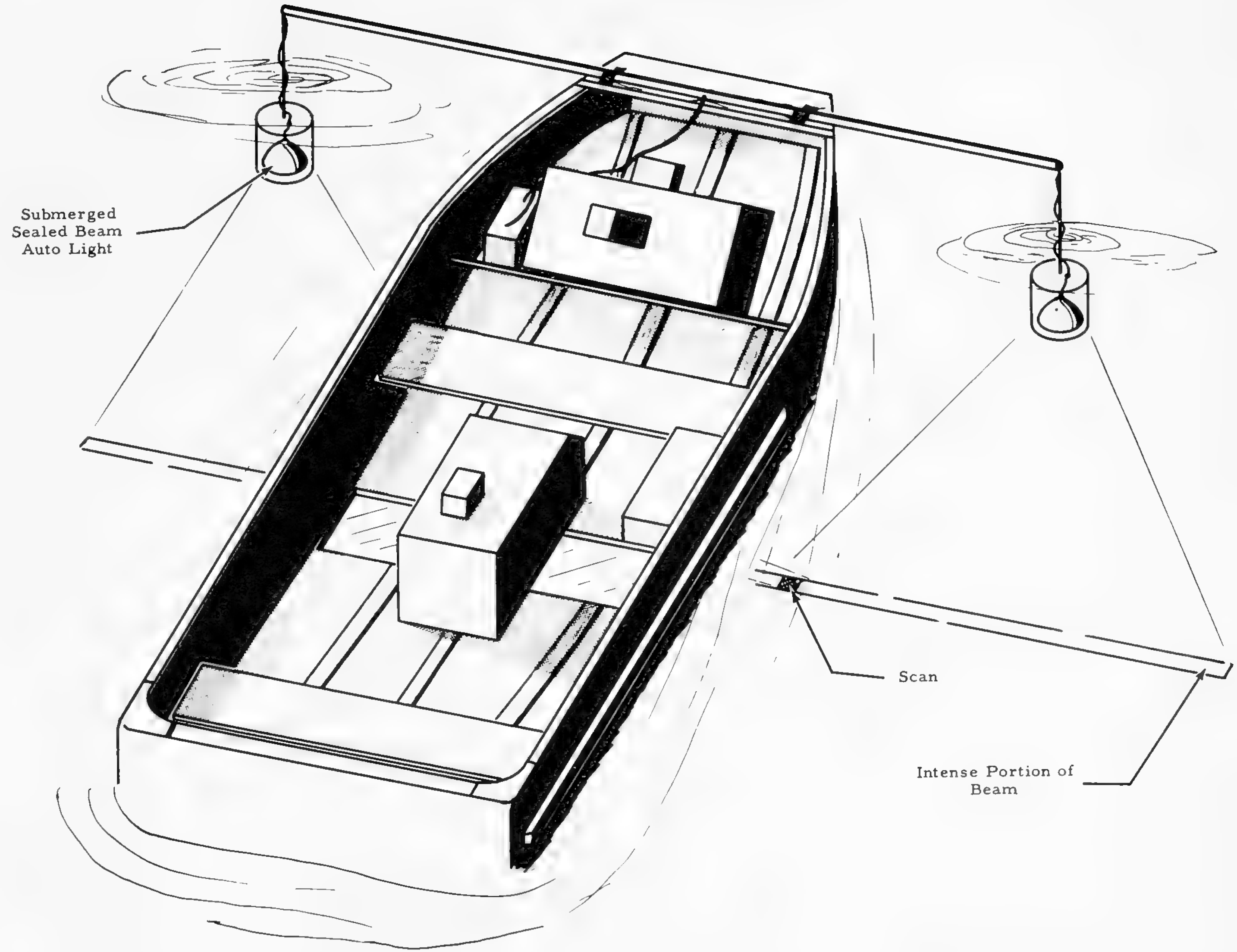

Fig. 5 - Suggested Night Configuration

that travels from the illuminated column to the viewed volume.

It is noted that the brightness required at the target and, hence, the flux density in the illuminating beam are no greater than that required for normal camera photography, assuming that the line scan system is adjusted to have the same sensitivity as the film. Conversely, with some sacrifice of resolution, photographs can be taken under light conditions insufficient for normal camera photography.

It is realized that the system set forth has the shortcoming for deep oceanographic photography, of requiring a large slot-shaped window. This can be overcome by utilizing conical scan instead of linear scan. This requires a small circular-shaped window, whose inner diameter may be smaller than its outer diameter. This then allows the use of conventional conical deep-vehicle windows. Power requirements for the camera unit exclusive of illumination would be modest. One or two automotive type storage batteries would be sufficient for a few hours of continuous operation. The system can be slowed down for slower line rates in the event that telemetering to the surface over low bandwidth cabling is desired.

SOME RECENT ADVANCES IN UNDERWATER CAMERA EQUIPMENT

by HAROLD E. EDGERTON, Professor of Electrical Engineering
Massachusetts Institute of Technology
Cambridge, Massachusetts
and SAMUEL O. RAYMOND, Senior Engineer
Edgerton, Germeshausen & Grier, Inc.
Boston, Massachusetts

ABSTRACT

There is a continuing need in the field of deep sea ocean floor photography to take pictures at greater distances above the ocean floor so that more area of the bottom can be covered with each picture. With this technique, a means for photographically "mapping" the ocean floor might approach the means of mapping land areas as used in aerial photography, but on a much smaller scale. Recent advances using faster lenses, more light, and better light placement are discussed.

INTRODUCTION

Aerial photography is a technique that has been of tremendous value in mapping the surface of the earth. A pair of stereo photographs taken from an altitude of 30,000 feet can map in detail an area of over 20 square miles. It might take a land surveyor years to map this area in equal detail. Aerial photography has moved up to 80,000 feet and beyond into the field of earth satellites and rockets which travel hundreds of miles above the earth, covering correspondingly greater areas of the earth's surface with each picture.

If deep sea ocean floor photography could be advanced to equal even 5% of what has been possible with aerial photography of land, the benefits to oceanographers, hydrographers, and marine geologists would be tremendous. Therefore, the trend in deep sea ocean floor photography is toward taking pictures farther and farther off the ocean floor covering more and more area. Until several months ago, most deep ocean photography was being done at a distance of about 10 feet above the ocean floor covering an area of about 50 square feet. The camera used was the type shown in Figure 1. The electronic light source was essentially the same distance above the ocean floor as the camera. The light was rated at 100 watt-seconds. The lens used was the F-11 underwater lens designed by Professor Robert Hopkins of the University of Rochester for underwater use behind a flat glass window. (If a normal camera lens which is designed for use in air is used underwater behind a flat glass window, "pillow" distortion occurs as shown in Figure 2. Professor Hopkins' lens is calculated to overcome this distortion. A photograph taken with it is shown in Figure 3. Of course, if the Hopkins lens is used in air, the pictures will have "barrel" distortion.)

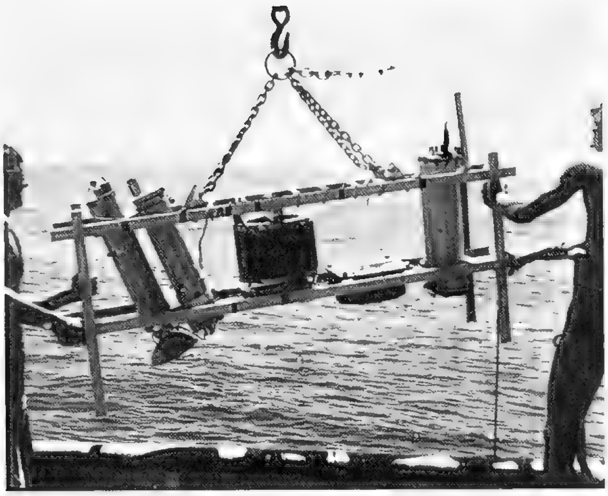

Figure 1. Deep sea camera employing one 100 watt-second electronic flash light source and two 35mm cameras with Hopkins F-11 lenses for stero use. The object on the center of the framework is an experimental "sonar pinger", a sound device for positioning the camera the proper distance above the ocean floor.

Figure 2. A photograph of the tile on the side of the M.I.T. swimming pool showing distortion obtained when an ordinary camera lens is used behind a flat glass window underwater.

The success of the lens was very important because of the high quality of the photos, but the need for a faster lens was felt so that pictures could be taken farther off the ocean floor. Under sponsorship of Woods Hole Oceanographic Institution, Professor Hopkins next designed an F-4.5 lens for underwater use. The design was completed in August, 1960, and these lenses with an optional shutter are standard on all EG&G underwater cameras. The new lens will not fit old model EG&G cameras without a longer pressure case, but the longer cases are available.

Figure 3. A photograph taken using the new Hopkins F-4.5 underwater lens. Compare the parallelism of the tile lines with those in Figure 2. The "data chamber" on the right is an internal part of the camera and records, date, time, and depth of each picture. The "data chamber" in the camera has been found to be invaluable in preventing the accidental switching of films. A small photo is taken with each photograph of pressure (depth), time on a 24-hour basis, and written in longitude and latitude information as well as the ship, date, etc.

In April, 1961 plans were being made for the June, 1961 cruise of Woods Hole's Research Vessel Chain to the Puerto Rican Trench. Chief Scientist J. B. Hersey needed a camera that would take pictures showing a fairly wide continuous strip of ocean floor at depths of 20,000 feet. This was to be the first use of the new F-4.5 lens.

In order to get the cameras farther off the ocean floor, a special camera rack was used which placed the light closer to the bottom than the cameras. The new rack is shown in Figure 4. This new rack reduces the light source-to-bottom distance, thus increasing the illumination of the subject. The camera was wired such that it took pictures at 6-second intervals with a light source output ratings of 50 watt-seconds. Two of these camera assemblies were used, and hundreds of photographs were obtained. A sample photograph is shown in Figure 5.

The results of the Puerto Rican Trench expedition indicated that still more light should be used. Consequently, a new lighting system was designed and two assemblies were built. The new system consists of the same framework as is shown in Figure 5. In place of the one, six volt, 50 watt-second light source are two, 24 volt, 200 watt-second light sources giving a total rating of 400 watt-seconds. This increase by 8 fold in the light permits the use of wider angle reflectors to produce more even lighting. (The 24 volt light sources were originally designed for the bathyscaphs FNRSII Trieste and Archemede. No batteries or automatic cycling controls are used since the lights are normally powered and controlled manually from inside the bathyscaph.) The automatic control

Figure 4. Special deep sea camera used by Woods Hole Oceanographic Institution from the Research Vessel Chain for photographing the Puerto Rican Trench at a depth of 20,000 feet. The camera features F-4.5 lens stereo cameras mounted side by side at the top of the framework, two electronic light sources mounted at the bottom of the framework and a sonar pinger for positioning the camera. The framework originally was designed in 1960 by Edgerton, Germeshausen & Grier, Inc. for the U.S. Navy Hydrographic Office.

and batteries for the lights on the new assembly are inside a separate pressure-proof housing which is mounted adjacent to the lights.

Two of these new F-4.5 lens, 400 watt-second, sloping rack, stereo cameras are presently on board the Chain en route to the Mediterranean. With them it is hoped that pictures will be obtained 30 feet off the ocean floor covering an area of over 500 square feet.

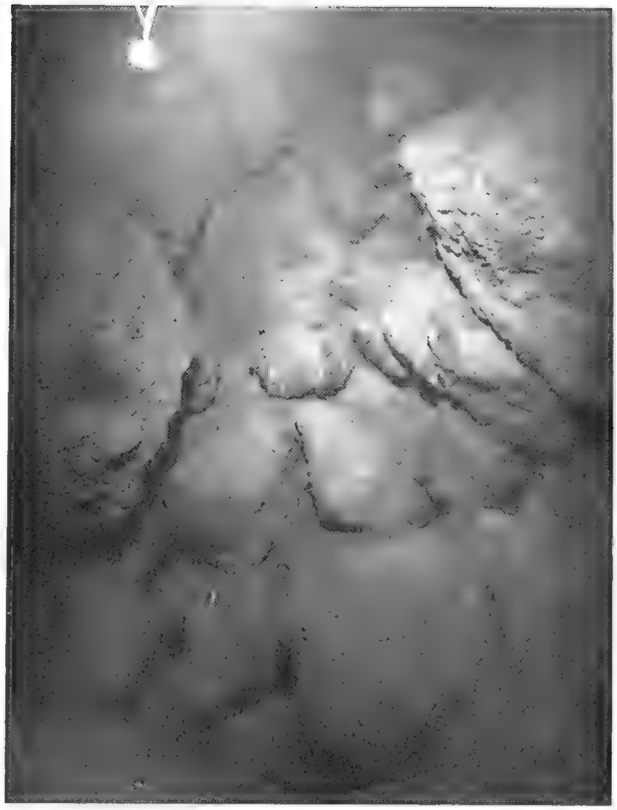

Figure 5. A photograph taken in June, 1961, in the Puerto Rican Trench at a depth of about 20,000 feet from the Chain using the camera described in the text with 50 watt-seconds at F-4.5 on plus x film. The white object is a compass and flow indicator. Special printing is required to show the compass needle.

BIBLIOGRAPHY

Photography of The Ocean Bottom, M. Ewing, A. Vine, J. L. Worzel. Journal Optical Society of America, vol. 36, 1946, pp. 307-321.

Cameras and Lights for Underwater Use, H.E. Edgerton, L. D. Hoadley. SMPTE Journal, July 1955, pp.345-350.

Deep-Sea Photography, E. N. Harvey, E. R. Baylor. Journal of Marine Research (Sears Foundation), vol. VII, No. 1, April 1948, pp. 10-16.

Submarine Photography with the Benthograph, K. O. Emery. Scientific Monthly, vol. 55, No. 1, July 1952, p. 1.

A Wide-Angle, Underwater Camera Lens, E.M. Thorndike. Journal Optical Society of America, vol. 40, 1950, p. 823.

The High Speed Photography of Underwater Explosions, P. M. Fye. SMPTE Journal, October, 1950.

Underwater Photography, H. Schenck, H. Kendall. Cornell Maritime Press, 1954.

Photographing The Sea's Dark Underworld, H. E. Edgerton. National Geographic Magazine, April, 1955, p. 523.

Deep-Sea Cameras of The Lamont Observatory, E. M. Thorndike. Deep-Sea Research, vol. 5, 1958.

Suspended Echo-Sounder and Camera Studies of Mid-Water Sound Scatterers, H. R. Johnson, R. H. Bakus, R. H. Hersey, D. M. Owen. Deep-Sea Research, vol. 3, 1956, p. 266.

The Luminescence Camera, H. E. Edgerton, L. R. Breslau. Journal of the Biological Photographic Association, May 1958. Woods Hole Oceanographic Institute Report 58-14.

Report No. 768, NEL Type III Deep-Sea Camera, C. J. Shipek. U.S. Navy Electronics Laboratory, San Diego, California, March 13, 1957.

A New Deep-Sea Camera, A. S. Laughton. Deep-Sea Research, Pergamon Press, Ltd., vol. 4, 1957, pp. 120-125.

J. B. Hersey, H. E. Edgerton, S. O. Raymond, and G. Hayward, Sonar Uses in Oceanography, Instrument Society of America Conference, Preprint #21-NY-60, September 1960.

A COMPLETE SONAR THUMPER SEISMIC SYSTEM

by EARL D. VAN REENAN, Senior Geophysicist
Edgerton, Germeshausen & Grier, Inc.
Boston, Massachusetts

ABSTRACT

A complete continuous seismic profiling system consists of the Sonar Thumper unit, Sonar Recorder, transducer fish, receiving hydrophone, preamplifier if necessary and variable filter. Sonar Thumper units are available from 1,000 watt-sec models up to 13,000 watt-sec experimental models. Thumpers have been extensively used for marine geological studies and dredging surveys. The safety and economy of the large thumper units make them ideal for reconnaissance offshore oil prospecting.

I. INTRODUCTION

Major oil companies and off-shore seismic contractors often conduct extensive seismic surveys which expend as much as 5 tons of explosives daily. High explosives generally give great reflection penetrations, but they are costly and hazardous to use. Several contінous sub-bottom profiling devices have been developed such as the Sparker, Gas Popper, and Marine Sonoprobe. These devices have found considerable application to limited depth penetration problems.

This report describes a complete and effective seismic profiling system consisting of the Sonar Thumper and Sonar Recorder along with all necessary auxiliary equipment. The Sonar Thumper is available in the standard 1,000 watt-sec unit on up to an experimental 13,000 watt-sec unit. The complete thumper seismic system fulfills a need by research organizations, educational institutions, and government of a safe, simple, effective, and inexpensive system for marine geological studies. The high power, low frequency pulse generated by large thumper units give them a great po-

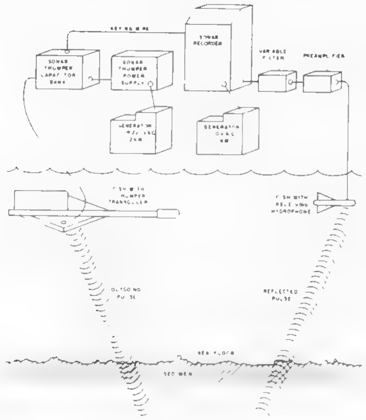

Figure 1. Sonar Thumper seismic system with all necessary auxiliary equipment.

tential as an inexpensive offshore oil prospecting tool.

II. SONAR THUMPER

A. General Description

The standard thumper unit consists of a power supply cabinet, capacitor bank cabinet, and transducer. The power supply converts ship's power or electrical generator power (110 or 220 volts A.C.) to high voltage D.C. which is fed to the capacitor bank cabinet. When the trigger circuit is activated by a recorder contact, the capacitors discharge into the transducer. The epoxy encapsulated flat coil has an aluminum plate which is spring loaded against the face of the coil. The aluminum plate is violently repelled from the coil when the strong pulse of current flows through the coil.

A precisely repeatable positive pressure pulse is produced by the repulsion of the plate in the water. The standard 1,000 watt second thumper gives a pulse duration of 0.5 milliseconds and a peak pressure of approximately 1×10^6 dynes/cm^2 at one yard. The 5,000 watt-second unit gives a pulse duration of 2 milliseconds and somewhat higher peak pressure.

B. Large Thumper Units

The unique design of the thumper transducer makes it inherently a non-saturable type of device. Therefore very high power thumpers can be built using the basic transducer design. The first 5,000 watt-second transducer was a scaled up version of the standard model. Several double coil transducers were then designed to eliminate the bulkiness of the scaled up version and produce a greater concentration of energy. However, the energy concentration of the double coil transducers was so great, the back pressure of the coils caused the epoxy encapsulation to shatter. To eliminate this difficulty, a symmetrical transducer was designed with two coils arranged back to back and an aluminum plate mounted against each coil. Thus the backward pressure of one coil counterbalances the pressure of the opposing coil. Initial tests of this transducer design at powers up to 14,000 watt-seconds have been very encouraging.

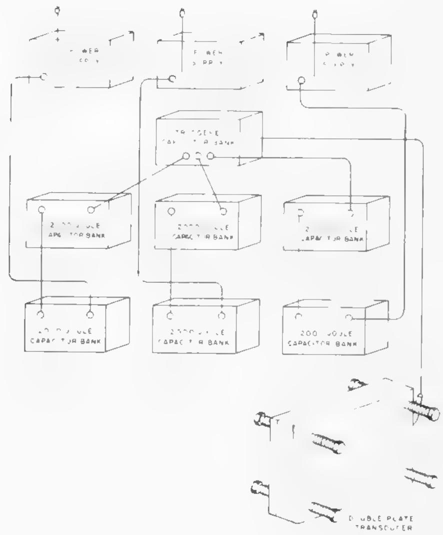

Figure 3. 13,000 watt-second Sonar Thumper system.

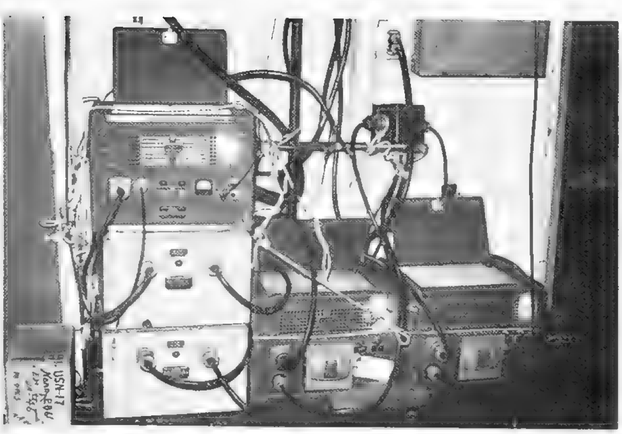

Figure 2. 5,000 watt-second Sonar Thumper installation on board the R.V. Chain during the June, 1961 cruise to the Puerto Rico Trench

The larger thumper units are completely modular in design to give great flexibility. The standard thumper components can be used along with more capacitor bank cabinets for greater power storage. The firing rate can be stepped up by simply adding more power supply cabinets. Figure 2 shows a photo of a 5,000 watt-second unit consisting of two 2,000 joule capacitor banks, the standard triggered capacitor bank, and two power supply cabinets. This particular system was used on a June, 1961 cruise by Woods Hole Oceanographic Institution on the ship R.V. Chain to the Puerto Rico Trench area. Figure 3 illustrates a schematic diagram of the 13,000 watt-second Sonar Thumper unit.

C. Installation and Operation of the Thumper

The installation and preliminary check of the Sonar Thumper components can be done in a short time. The components are designed to be portable by two men. The power supply and capacitor bank cabinets are ordinarily placed in a cabin or sheltered area to avoid salt water exposure.

The power supply should be situated in a well ventilated area near the generator or other source of 110 or 220 line voltage. If the power supply must be placed at some distance from the generator, the thumper should be operated on 220 volts to reduce peak currents. To change over from 110 to 220 volt operation requires a simple change of transformer jumpers.

The capacitor bank should be placed relatively close to the point where the output cable to the transducer leaves the ship in order to keep the high current cable as short as possible. High voltage D.C. from the power supply is brought into the capacitor bank and charges the 160 microfarad bank to approximately 4 kv. A 110-115 volt a-c line is also plugged into the capacitor bank to power heater lamps, safety interlocks, the trigger circuit, and indicator lights.

After installation, the unit can be checked by firing into a dummy transducer consisting of a 2-ohm, 200 watt resistor or a standard transducer with aluminum plate removed. The standard transducer should never be fired in the air without a damping water load. When fired, the force is so great the transducer plate of the standard thumper will leap 30 to 40 feet vertically if it is fired in air without its retaining bolt. Testing at the dock can be carried out by lowering the transducer into the water alongside the ship. Proper grounding of all units should be checked before firing.

For operation underway, a towing vehicle is necessary for the transducer. A number of vehicles have been used. The Naval Electronics Lab initially mounted the transducer on the hull of the ship and now uses an aluminum towing vane. The U.S. Coast and Geodetic Survey has used the transducer mounted in an internal water filled hull well to transmit pulses through the hull. Woods Hole Oceanographic Institute has a sled with heavy nose weight which they call the "flounder". The National Institute of Oceanography of England uses a fiberglass dinghy with a reaction mass above the transducer of 200 lbs. of concrete. Two towing vehicles are now commercially available. One is a fiberglass "V"-fin (1) designed with negative lift and the other is an arrow-like unit with a counterweight in front and the transducer mounted in the tail (2).

The size of the boat used has varied widely from 30 ft or 40 ft fishing boats to large naval survey vessels. The only requirement is sufficient enclosed cabin space for the thumper and recorder components. Towing booms are easily rigged for support of the transducer fish. For small vessels, a 4" x 4" timber across the stern or a boat davit can be used. The transducer fish is towed by means of a rope or cable which should withstand at least 1,000 pounds for an adequate safety factor. Cable tension depends on towing speed and is considerably less than 1,000 pounds unless fast speeds of over 8 knots are required. Ordinarily, water, and ship noises become excessive above 5 knots; therefore towing usually will be below this speed.

The larger thumper units simply require a little more space for electronic components than the standard model. The symmetrical transducer can be mounted horizontally or vertically because the frequency of the pulse is so low that it creates an essentially spherical wave front with equal signal intensity in all directions.

III. Receiving System

A. Noise Problem

Before reviewing possible hydrophone setups for a receiving system to use with the thumper, a consideration of noise problems is in order. The sources of troublesome noise which may partially or completely mask the seismic signal are: 1) Ship screw noises from propeller cavitation and drive shaft vibration, 2) Engine vibration transmitted through the ship's hull, 3) Cavitation or burble produced by the hydrophone and towing element moving through the water.

Each vessel has its own characteristic noise level at various speeds. The optimum operating speed is the maximum speed possible at which useable records can be obtained. Ship noises can be partially eliminated by towing either at a considerable distance behind the ship or on large vessels a long boom off the bow is sometimes effective. Distance between the receiver and the sound source can be varied considerably. Separations of several hundred feet can be tolerated in relatively deep water. For shallow water reflection work, the receiver should be relatively close to the thumper if an accurate representation of shallow reflection layers is desired.

B. Hydrophones

A number of hydrophones are commercially available which are adaptable to the thumper system. The pressure type hydrophone with wide response is preferable. Preamplification of the signal may be necessary if a considerable length of cable is used. The preamplifier can be sealed in with the hydrophone unit or it can be used on board the vessel before the signal is fed to the recorder amplifiers.

One approach for increasing signal to noise ratio is the use of a multiple crystal arrangement of detectors hooked in parallel with a null along the axis to partially cancel noise.

(1) Braincon Corporation Type 108 V-Fin
(2) EG&G Model 261 Transducer Fish

The National Institute of Oceanography of England reports good results at ship speeds up to 7 knots using a multiple crystal arrangement in a plastic oil filled hose. EG&G markets an effective hydrophone with towing fish, the rocket hydrophone (see Figure 4). Braincon Corporation also markets a special "V"-Fin lollipop hydrophone which is suitable for use with the thumper system.

Figure 4. E.G.&G. Rocket Hydrophones.

IV. SONAR RECORDER

The thumper has been successfully recorded with a number of systems. Excellent results have been obtained by using the Alden Precision Graphic recorder and the EG&G Model 250 Sonar Recorder, both of which use Alden Alfax paper. These recorders work on the same principle of a resilient negative helix electrode and a positive moving loop electrode, which provides high accuracy and resolution.

The EG&G Sonar Recorder was designed specifically for use with the Sonar Thumper and EG&G's Sonar Pinger. Figure 5 shows the Sonar Recorder in operation on a contract job for the U. S. Corps of Engineers. The recording unit is compact and versatile and emphasizes simplicity and ease of operation. Three recording speeds are provided to give basic full-scale sweeps of 50 fathoms, 200 fathoms and 800 fathoms. A record gating system allows presentation of the first, second, third, or fourth sweep after keying; thus the 0-50, 50-100..., 0-200, 200-400..., 0-800, 800-1600... fathom intervals can be recorded, depending on water depth and scale desired. A middle keying feature is also provided to give greater scale flexibility.

Sweep accuracy is .005% derived from an internal tuning-fork oscillator. Recording can be either full wave, positive half wave, or negative half wave. Connections are provided for independent headphone monitoring and oscilloscope display of the signal being recorded. The paper feed speed is controlled by a separate shunt wound motor with continuously variable speed control. An event marker line can be recorded either with a panel-mounted button or remotely.

Amplifier response can be selected to give either a broad band for thumper recording or 12-kilocycle peaked response for pinger recording. A built-in RC filter can be cut in for reducing high- or low-frequency noise on the broad-band response. A separate variable filter can also be used to provide fine control of frequency response.

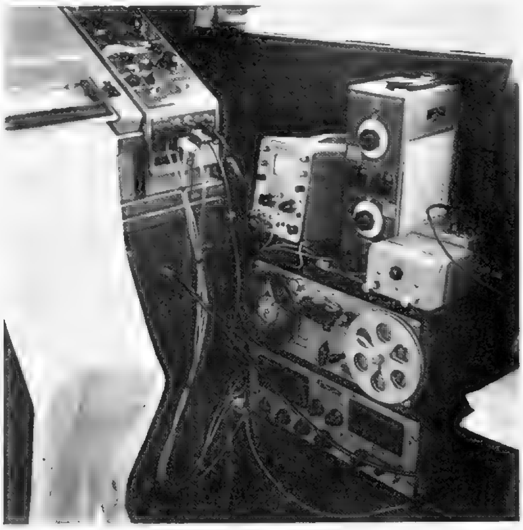

Figure 5. Sonar Recorder at left. The seismic returns were also recorded on the tape recorder at the right for experimental replay.

V. ELECTRICAL POWER REQUIREMENTS

The power requirements for the thumper seismic system can be supplied by a ship's generator or auxiliary generator. A voltage fluctuation may be noticeable when the thumper is fired because of the high peak currents. Therefore it is recommended to run the thumper on a separate generator, if possible, to avoid voltage fluctuations to the recorder.

Many generators are available for sale or rental which are suitable for powering the thumper. A portable unit with a minimum of 2 kilowatts, 110 volts or 220 volts, 60-cycle a.c. is perfectly adequate for the standard thumper. The larger thumper units require somewhat larger generators. For example, a 5000-watt-second unit with a firing rate of 2.5 secs requires a 4-kilowatt generator or larger.

VI. FIELD SURVEY PROCEDURES

Assuming that a specific program with desired coverage has been outlined, an experimental program should be carried out initially to optimize filter settings and field procedure. The initial program may require several days, particularly if the survey area is extensive.

An experimental program should be carried out in a geologically known area if possible. If cores or probe information is available in an area, initial thumping should be done over these areas. Filter settings should be optimized in a known area to best delineate the features of greatest interest, such as bedrock depth. If any known structural features near the prospect area, such as faults, can be initially delineated, it will be of great help in recognizing similar features in the unknown area.

Optimum boat speed can be determined during initial work. The filter settings, gain, paper speed, positive, negative, or full-wave recording, and the most efficient procedures can also be optimized.

If radio positioning techniques are used, calibration and position-checking can be done during the initial program. Whenever a position fix is made, a remotely controlled marker can mark the record. For rough reconnaissance work, celestial navigation and dead reckoning may be sufficiently accurate. If the survey is carried out near shore, it may be possible to obtain accurate fixes from charted shore landmarks.

It is desirable to keep one man stationed at the recorder to record station numbers continuously and monitor recording results as the survey progresses. Any features of particular interest can be immediately marked on a map for future reference. The surveyor, navigator, or radio positioning operator can automatically mark the thumper record with the remote event marker when a position fix is made. The Sonar Recorder operator marks the corresponding time or station number directly on the record to correspond to the event mark.

VII. APPLICATIONS AND RESULTS

A. Providence River Channel Survey for the U. S. Corps of Engineers

The Providence River Channel thumper survey was done to delineate portions of the channel where bedrock or boulder removal will be necessary for a dredging grade level of 45 feet below mean low water. The field survey was commenced 8 May 1961 and completed 19 May 1961. The first day was spent in setting up equipment and the second day was used for experimental work.

The vessel used for the survey was a modern 40-foot fishing boat with flying bridge. The boat was equipped with two-way radio and a fathometer.

Boat positioning was done by sextant angle to charted landmarks on the shore. Sextant angle charts covering most of the Providence River Channel area enabled the surveyors to plot station positions continuously as the survey proceeded.

Equipment used consisted of the standard Sonar Thumper unit, the Sonar Recorder, a BC50 Atlantic Research hydrophone, and a Minneapolis-Honeywell lollipop hydrophone, and "V"-Fin towing fishes for the transducer and the receiver hydrophone. Two electrical generators were used, one supplying 2 kilowatts for the Sonar Thumper and a small auxiliary generator to supply the recorder power.

Three main longitudinal lines were run along the channel, one down the middle, and the other two toward the sides of the channel. In areas where shallow bedrock or boulders were suspected, additional cross lines were run for added detail. Preliminary thumping was done near the area of previous core information. However, the only cores to bedrock in this area were in shallow water which was not navigable for the vessel. Good core information was available south of the channel area west of Patience Island. A thumper traverse was run in this area to correlate to the core information. A portion of this thumper record is illustrated in Fig. 6. The Sonar Thumper was fired at a half-second repetition rate and half power. This faster rate gives greater resolution and is recommended for seismic studies which do not involve great depths.

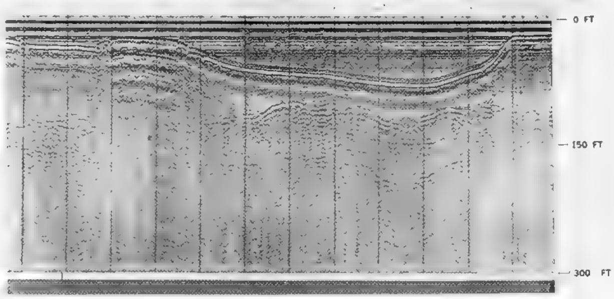

Figure 6. Thumper record of a traverse west of Patience Island, Narragansett Bay. The 50 fathom sweep of the Sonar Recorder was used. The channel surface is shown underlain by an irregular reflection surface at 100 to 120 ft. Core information in this area shows bedrock at a depth of 111 ft corresponding to the irregular reflection surface.

The optimum filter setting for this survey appeared to be 300 cps on the low end and 1200 cps on the high end. Recording was done on the positive half-wave form. Paper speed was normally 2.2 inches per minute. The gain attenuation setting normally used on this survey was 0 db, which represents full gain without a preamplifier. The recorder has a wide range of attenuation settings, from 0 db to 80 db.

Tide gage readings were recorded continuously throughout the day at a shore station, and these readings were radioed to the ship and then recorded directly on the thumper seismic profiles. Fathometer readings were taken at one-minute intervals corresponding to sextant position fixes on major lines and 1/2-minute fixes used for detail work. Corrected mean-low-water depths were recorded for each station. A lead sounding line was used to calibrate the fathometer and a 2-1/2-foot correction was added to each fathometer depth. These fathometer readings were not absolutely necessary. However, they simplified the correction factor for the depth of the thumper transducer, depth of the hydrophone receiver, and distance between the transducer and receiver. A constant correction factor was readily determinable by comparison of the fathometer depth to the seismic profile recorded depth. This was approximately 5-1/2 feet for the major portion of the survey. The transducer and hydrophone were towed at depths of approximately 3 feet each. The sediment velocity was estimated to be approximately that of sea water in the upper section of interest. This assumption is based on previous velocity studies in the general Narragansett Bay area by Woods Hole Oceanographic Institution.

Figure 7. Thumper record from Hydrographer's Canyon Area. The 200 fathom recording sweep was used. The depth scale is on the basis of 4800 ft/sec water velocity.

A number of areas were located in the channel where bedrock removal or boulder removal appears to be necessary if deepening is to be to 45 feet below mean low water. The best quality records were obtained in the southern portion of the channel where the probable bedrock surface can be delineated at depths of over 150 feet below mean low water. Some portions of the channel are characterized by very strong initial reflections and subsequent multiples. This highly reflective channel floor condition often results in a serious loss of subsequent sub-bottom reflections at these locations. The high reflectivity of this initial layer may be caused by above-average consolidation of the bottom sediments.

The bedrock surface in this area generally appears to be extremely irregular, and it is often difficult to determine whether an irregular reflecting surface represents bedrock or large and irregular boulders. A number of boulder areas are suspected in the channel area on the basis of point-source parabolic patterns on the record.

Because of the lack of usable core or probe information in this area, a probing study is recommended to corroborate the existence of boulders or bedrock in questionable areas. During the probing survey to be conducted, a close check on seismic records and correlations to probing will give considerably more information than was extracted from the preliminary study.

B. Thumper Field Test by the U. S. Coast and Geodetic Survey

A short familiarization and test run was made of the Sonar Thumper on board the U. S. Coast and Geodetic Survey vessel, the "Explorer", July 20 through July 24, 1961. Comparisons were made between the transducer mounted inside the ship in a well situated below the water line and on an externally towed transducer. The pulses from the internal well mounted transducer suffered considerable transmission losses through the hull of the ship. However, usable results can be obtained with an internal well mounted transducer, although depth of penetration is reduced.

A number of thumper profiles were obtained across Hydrographer's Canyon. One of these is shown in Figure 7. The depth of penetration on these tests varied somewhat but was usually on the order of 400 to 600 feet and in some cases weak, but continuous events were detected at depths exceeding 1,000 feet. Water depth generally varied from 50 to 300 fathoms. The standard thumper was used for these tests and the EGG Sonar Recorder was used for recording. The external transducer was mounted on a V-fin fish. A V-fin hydrophone and the EG&G Rocket Hydrophone were used alternatively as receivers.

VIII. CONCLUSION

Many off-shore areas of the world have never been explored for possible oil structures because of the tremendous expense of maintaining conventional seismic crews and the expense and difficulty of obtaining explosives. Some localities also forbid the use of explosives in off-shore seismic work because of possible damage to fish and navigational hazards to shipping in harbors. Large thumper units of 5000 watt-seconds on up can often give sufficient penetration to be of great value as a reconnaissance tool in off-shore oil prospecting. The Sonar Thumper is simple, reliable and rugged, and requires nothing more than 110 or 220 volts a.c. for power. The effectiveness of the Sonar Thumper and high powers available, along with continuing improvements in receiving and recording equipment, are all factors which point toward the increasing future use of the thumper as an off-shore oil prospecting tool.

THERMOELECTRIC POWER FOR OCEANOGRAPHIC RESEARCH

by MELVIN BARMAT, Manager, Thermoelectric Division
General Instrument Corporation
Newark, New Jersey

The utility of thermoelectric generators in oceanographic research is outlined. The history and basic technology of thermoelectricity are briefly reviewed and generators currently being developed for oceanographic service are mentioned.

Much of modern oceanographic research is conducted by the collection and transmission of data over long periods of time from unmanned stations. Furthermore, it appears that this trend is increasing in use. There are many potential missions in this category, but to mention a few---

1. anchored buoys with weather and oceanographic instrumentation
2. bottom mounted instruments for current measurement and recording
3. freely moving buoys for following currents

One of the most critical components of these systems is the source of power. A power supply for these missions must have:

a. long life
b. high reliability
c. low volume
d. freedom from environment
e. low cost

Thermoelectric generators now being developed for various government agencies give great promise towards fulfilling these requirements. Before describing these new developments I would like to briefly provide some background in thermoelectricity.

In 1823, Johann Seebeck reported to the Prussian Academy of Sciences his discovery of a magnetic field when a temperature difference was applied to the junctions of dissimilar metals. This magnetic field was, of course, due to the current developed by the generated voltage. Eleven years later, in 1834, Peltier announced his discovery that heat was developed or removed at a similar junction when a direct current electrical potential was applied. These have been classified as "thermoelectric" effects (See figures 1 and 2) For over fifty years these phenomena remained only laboratory curiosities, the physicist had too many other, more promising phenomena to explore. However, in this first half of the present century the thermoelectric phenomena was widely applied for temperature measurement, in fact it remains today the most important method for scientific and industrial temperature measurement.

It had been recognized for many years that these thermoelectric effects could be used for electrical power generation if a temperature difference were maintained between the junctions, or as a heat pump if electrical energy was applied to the system. However, it was not until the pioneering work of Maria Telkes in the U.S.A. and A.F. Ioffe in the U.S.S.R. that intermetalic semiconductor materials were utilized, resulting in the potentiality of achieving useful efficiency levels. It has been the growth of knowledge of semiconductors that has given the impetus to an even more widespread scientific and industrial interest in thermoelectricity. In this country there is considerable government supported research in the field of material and device development, due to potential applications as diverse as submarines and satellites.

Why has this later work been so fruitful as compared to the earlier 130 years? It is the result of a happy coincidence; the previously mentioned development of solid state physics and semiconductor technology coupled with a genuine industrial, commercial and military need for the kind of devices thermoelectricity makes possible. Understanding of the reasons for the greatly advanced thermoelectric utility of semiconductors will enable us to obtain insight into thermoelectric material requirements.

The properties of a thermoelectric material that govern its performance are:

α Seebeck Coefficient - expressed as volts per unit temperature difference, usually microvolts/°C.

ρ Electrical resistivity, usually ohm-cm

K Thermal conductivity, usually watts/cm°C.

A thermoelectric generator, schematically shown in Figure 3 consists of a heat source, a cold dump, and a thermocouple (in normal practice, a number of thermocouples in series). This device, to be efficient, requires a high output voltage, therefore

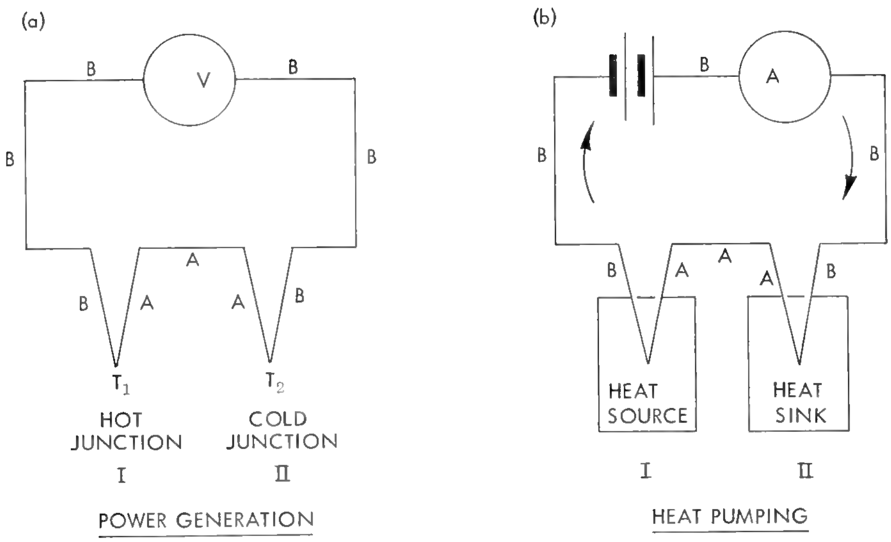

SCHEMATIC REPRESENTATION OF THERMOELECTRIC CIRCUITS WHERE A&B ARE TWO DISSIMILAR MATERIALS

FIGURE 1

THERMOCOUPLE CONSTRUCTION

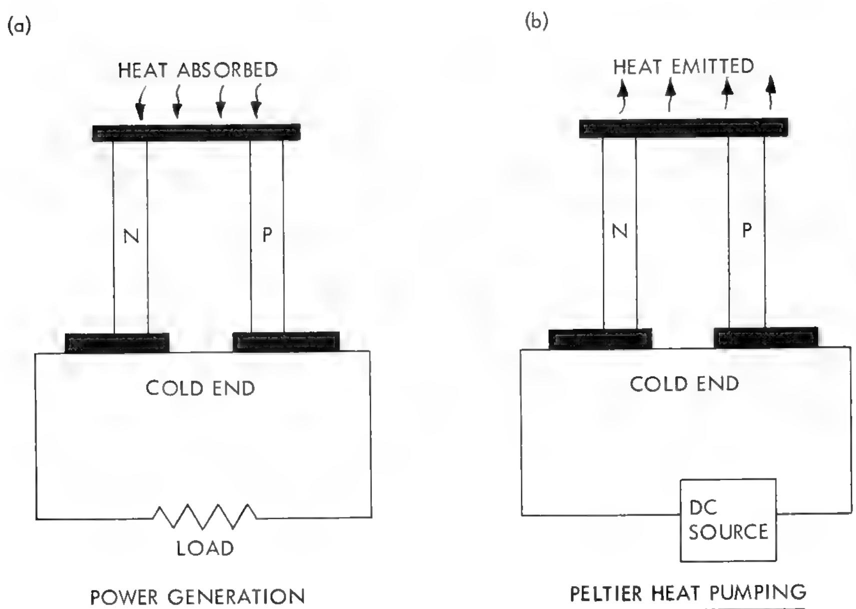

FIGURE 2

α should be as large as possible and the temperature difference, hot to cold, should be as large as possible. If the thermal conductivity, K, is small then a smaller amount of heat will be required to maintain a given temperature difference. To minimize the amount of power consumed internally by the generator, the electrical resistivity, ρ, should be small. A figure of merit Z is defined where

$$Z = \frac{\alpha^2}{\rho K}$$

is an index of material efficiency. The higher the value of Z the better the thermoelectric material.

Now, with metals it is possible to obtain reasonable values of α and ρ, but it is not possible to get low values of K. Thus, the Z of metals is too low for useful power generating or cooling devices. With semiconductors, however, even higher values of α are obtainable and by the proper addition of impurities (doping) the relationship between ρ and K can be adjusted to give useful values of Z.

Some of the intermetallic semi-conductor materials currently used are lead telluride, bismuth telluride, zinc antimonide, silver antimony telluride, all with various and complex dopings. Extensive work is currently being done to improve these materials and to find new ones with higher figures of merit (Z) over wider temperature ranges.

In addition to the problems of semiconductor material one of the most serious problems facing the designer of a thermoelectric device falls into the realm of heat transfer. The heat input must be sufficient to maintain the hot junction at the desired temperature and the cold dump mechanism must be sized to maintain the proper cold junction temperature. The power level of some generator design concepts is directly limited by the cold side heat transfer. In the case of generators for oceanographic research, however, the sea can usually be used as a large and efficient heat sink.

A thermoelectric device is used to convert heat into electricity, or vice versa. No discussion of these devices is complete without examining the heat sources that can be used. All thermal energy sources can be classified as: fossil fuels, solar, chemical, geophysical and nuclear. All these energy sources can, and most are, being applied to thermoelectric converters. Missions in space vehicles are primarily considering solar and nuclear and chemical heat sources while terrestrial or air-breathing applications are relying heavily upon fossil fuels. It is in these latter categories that generators for oceanographic research can be found.

Since both the initial and operating cost of a thermoelectric device will depend on the power and voltage level required, some attention to this requirement is essential In some applications a continuous constant power level is required and the generator will be directly coupled, with suitable voltage transformation and regulation, to the utilization equipment. There will, however, be many applications where the power requirement will be intermittent and an average power analysis is required. Such applications may be periodic data transmission systems, alarm devices, flashing lights, etc. In these cases a low average power output may be stored in chemical batteries or capacitor systems, for use as required. Average power can be defined as

$$\text{Avg. Pwr.} = \frac{\text{Power consumption X time of consumption}}{\text{Time of Cycle}}$$

for example a data transmission system required 300 watts for 20 minutes every four hours

$$\text{avg. pwr.} = \frac{300 \text{ X } 20}{240 \text{ mins.}} = 25 \text{ watts average}$$

A twenty-five watt power supply has considerable operating and capital cost economy compared to a 300 watt system.

A second important consideration is selection of a heat source for a maximum economy, reliability, and availability. While nuclear and chemical heat sources have a most important role to play in undersea applications, fossil fuels, such as propane, are preferred in air breathing applications for economy reasons. In cases where volume is important in long life missions, a nuclear heat source can be used, if cost and hazard considerations are also in consonance.

It would be interesting to consider the overall efficiency values that might realistically be expected from presently available fossil fueled devices and those that might reasonably be expected in the future.

EFFICIENCY COMPONENT	Present	Near Future
Thermoelectric converter	5%	8%
Combustion	70%	75%
Voltage conversion	90%	90%
Energy Storage	80%	80%
Overall	2.5%	4.3%

Since cost will always be a significant parameter in power sources, selection of a cost analysis for a typical application

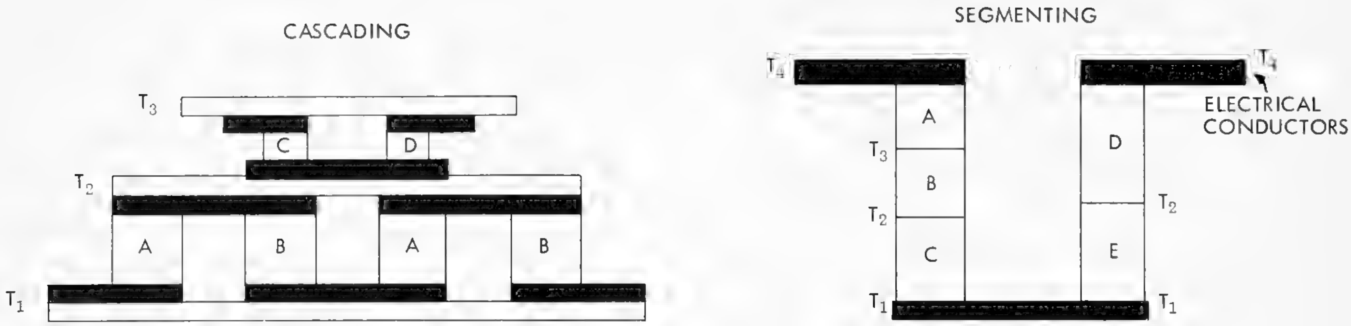

CASCADING OR SEGMENTING OF T/E SEMICONDUCTORS TO OBTAIN OPTIMUM Z OVER SPECIFIC TEMPERATURE INTERVALS & THEREFORE OPTIMIZE DEVICE EFFICIENCY

FIGURE 3

FIGURE 4

will be made.

Given:

Power Required: 25 watt (average)

Fuel: Propane at $20 gallons

	Present	Near Future
Fuel Cost per KW-hour (approximate)	$.30	.17

The situation in regard to capital cost of thermoelectric generators is extremely uncertain at the present time and in the near future. Most generators now being sold are individually built for evaluation purposes and are priced at hundreds of dollars per output watt. Furthermore the useful life of these devices is not really known at this time. Thus, the annual costs attributable to the initial price of an operational unit must be based on at least pilot plant production and a projected, reasonable life time. Industry estimates of generator cost for small quantities in the twenty five watt region are in the ten to fifty dollars per watt range. If a conservative value of forty dollars be used, and a five year life is expected, the kilowatt-hour cost is approximately 80 cents. Comparing this to the estimated fuel cost, it can be seen that the capital depreciation can be the determining factor in overall cost. It should be noted however, that these conservative cost estimates compare very favorably to all types of batteries as well as silicon solar cells.

Figure 4 depicts a ten (10) watt thermoelectric power supply recently developed by the General Instrument Corporation for evaluation by the U.S. Coast Guard. It is designed for use with shore based lights as well as large buoys and obviously is directly applicable to oceanographic research installations. This device utilizes catalytic combustion of propane fuel as a heat source. The use of a catalyst to promote the reaction of propane and oxygen gives high combustion efficiency due to the low reaction temperature and it is virtually impossible to extinguish the reaction except by interrupting the fuel supply. It is designed to operate in near hurricane winds (70 mph) and in any position of roll. The system has an automatic restart provision in the event of excessive winds or swamping. The system tries to restart once an hour. In this way we avoid the possibility of trying to restart under impossible conditions and thus depleting the energy storage system.

Utilizing some similar design principles and techniques the General Instrument Corporation is developing a thirty (30) watt thermoelectric generator for the Bureau of Standards and the Navy's Bureau of Weapons. It is to be evaluated for use aboard their Gulf of Mexico based weather boat buoy-NOMAD. In comparison to the Coast Guard generator mentioned above, we will take advantage of the sea water sink by directly coupling the cold junction to the hull below the water line.

Fossil fueled thermoelectric generators are available from other industrial sources but, in general, these are not specifically designed for, nor take advantage of, the ocean environment.

The U.S. Atomic Energy Commission, through its office of Isotope Development as well as its SNAP (System for Nuclear Auxiliary Power) office of the Division of Reactor Development, is developing a series of radioisotope fueled thermoelectric generators for oceanographic missions and environments. These are briefly discussed below.

A five watt demonstration device is being developed for a Lamont Geophysical Laboratory mission using Cesium - 137 as the fuel. It is specifically aimed at the underwater environment since little shielding is provided for the very penetrating radiations (Cs-137 is often used as a teletherapy source).

Strontium-90 is being employed as the heat source for another series of developmental thermoelectric generators in the five to thirty watt range. These units contain a considerable amount of shielding and can be used on land. The first of these has been built and is planned for early Weather Bureau service in the Arctic in conjunction with an automatic weather station.

The obstacles to the widespread use of the above mentioned radioisotope fueled generators are; potential hazards and the high cost of separated radionuclides. In an effort to reduce the cost of radioisotope heat sources for the oceanographic environment, the General Instrument Corporation, under USAEC sponsorship, is developing techniques for the utilization of Mixed Fission Products in thermoelectric generators. The goal of our current effort is a demonstration device for unshielded, underwater use. There is a very large, existing AEC program, including an existing pilot plant, for the solidification and concentration of nuclear waste materials, that directly assists these efforts.

APPLICATION OF MODERN REMOTE HANDLING TECHNIQUES TO OCEANOGRAPHY

by JOHN W. CLARK
Nucleonics Laboratory
Hughes Aircraft Company

INTRODUCTION

Oceanography is an eclectic science covering a wide gamut of the older scientific disciplines. In accomplishing the objectives of oceanography one must, among many other things, obtain physical measurements of the ocean floor and the ocean itself. One must also obtain samples of the flora and fauna of the ocean, as well as geological or physiographic specimens from the ocean bottom. In the following discussion I would like to concentrate attention upon this data and sample gathering aspect of oceanography, since it is to this aspect that the new art of remote handling can make a genuine contribution.

Modern remote handling technology, which is beginning to be recognized as a new subdivision of engineering, might perhaps be better described as the technology of accomplishing physical operations in hostile environments. This new technology is being created by a combination of electronic control engineering, human engineering, and remote handling techniques as developed by and for the nuclear industry.

As a typical example of a modern system for operating within a hostile environment, let us consider Figure 1, which shows the Hughes Mark II Mobot system. This system, which was developed for use in nuclear laboratories, is mobile, being mounted upon a three-wheel chassis. It is controlled by means of a three-wire cable which may be as long as a few thousand feet. The "hands" and "eyes" of the machine are electronically commanded by its operator; practical experience has demonstrated that this system can accomplish such complex functions as pouring, stacking, operating power drills or wrenches and the like, employing only electronic communication means between operator and vehicle. The experience gained with this and similar machines forms an effective starting point from which underwater handling systems can be developed to accomplish specific oceanographic tasks.

REMOTE HANDLING VOCABULARY

The new technology of remote handling and operation in hazardous areas is sufficiently unfamiliar as to justify a preliminary discussion and a few basic definitions before exploring in more detail the applications of this technology to underwater programs.

In most general terms, consider Figure 2, which shows a hazardous area in which one desires to perform some operation. This area may be hazardous

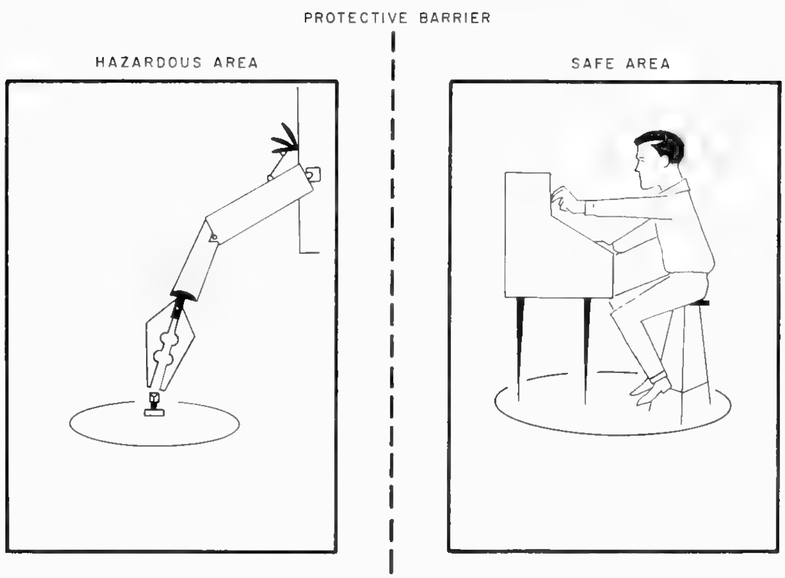

GENERALIZED REMOTE HANDLING SITUATION

Figure 2

due to lack of air, the presence of nuclear radiation, to high temperature, or to any other hostile environment which makes it impossible for a man to enter. The operations required may be equally broadly considered. Typically, it is necessary to translate objects from one position to another, to operate tools, such as screw drivers or wrenches, or to operate measuring equipment of many kinds. Usually, fixed obstacles are contained within the hazardous area, limiting the freedom of motion of any equipment contained therein.

A typical problem to be handled by a general-purpose underwater remote handling system is that of engaging a power-operated wrench with a nut or screw. This engagement and the operation of the wrench itself must, of course, be done in a manner which is independent of the separation between the operator who controls the operations and the equipment, and it must be done even in the presence of numerous fixed obstacles.

In the past, problems of this type have sometimes been attacked by the use of long tongs or forceps. Some of these have become extremely complex and have employed hydraulic or electromechanical actuators to supplement the physical strength of the operator. All such devices may be considered extensions of the man's arms, and the man himself is just outside the hazardous area and protected from it by a suitable barrier or shield.

Let us approach this problem in a more generalized way, and let us assume that the separation between the hazardous area and the safe area is so great that tong-like tools cannot be used. This requires us squarely to face the problem of operating in areas which are inaccessible. This is sometimes done by providing the operator with protective clothing suitable to the environment. Movable personnel shields may be used in nuclear environments, and the space suit of science-fiction is often proposed for the space environment.

In all such cases we find that we have actually not solved the problem. We have, on the contrary, merely changed the geometry. The safe area is now contained within the hazardous area, but the operator is still separated from his work by his protective system and must use tongs rather than his own hands for manipulation.

From the viewpoint of solving the fundamental problem of operating within an inaccessible as well as hazardous area, let us analyze a man as a handling system. For this purpose we may ignore many of his more interesting attributes and note that just four interrelated systems are involved. These may be identified briefly as his brain, his eyes, his hands, and his feet. More seriously, the eyes and the sensory nervous system provide information concerning his surroundings. The hands, as controlled by the motor nervous system, are able physically to move objects as desired. The feet and legs, controlled by their separate motor nervous system, enable the entire organism to move about; and finally, the brain assembles and organizes all these data and directs the motor systems as required.

The three functions symbolized by eyes, hands, and feet may readily be extended by modern electronic means over any desired distance. In this way, a man's senses and his ability to accomplish useful work may be extended to any distance, while his brain, which can be duplicated by no existing computer, remains in safety and comfort at any desired location.

This simple concept is the basis of the new technology of hostile environment operations. Remote handling systems ("Mobots") are not to be looked upon as competitive with a man in a diving suit or diving bell; rather, the effective utilization of such systems will increase the ability of the man to accomplish functions in the depths of the ocean. This paper is concerned primarily with a preliminary outline of ways in which the modern concept of remote handling systems can be applied to several realistic underwater situations.

ANALYSIS OF GENERALIZED REMOTE HANDLING SYSTEMS

In order to analyze in a systematic manner any hostile environment problem, it is highly desirable to consider the basic subsystems which make up any remote handling system. Figure 3 presents a generalized block diagram of any remote handling system. Consideration of this block diagram leads to an understanding of the fundamental elements which make up any remote handling system so that the design of such systems may be approached in an orderly and systematic manner.

As noted above, remote handling systems are artificial extensions of man's senses and muscles over considerable distances. In order to accomplish this, in addition to the systems which duplicate the senses and muscles, a link must be provided actually to bridge the physical gap between the man and the remote machine, and a control console must be provided with which the man communicates with the remote machine.

Figure 3 shows the interrelationship among the six subsystems which make up any remote handling systems. These subsystems, as discussed in somewhat more detail below, may be identified as follows:

- the manipulating subsystems ("hands" and "arms")
- the sensory subsystems
- the locomotion subsystems
- the command and data link
- the power subsystems, and
- the control console.

As a further addition to the vocabulary of this topic, the term "Mobot* Vehicle" has been coined to refer to the mobile remote portion of the system. Mobot vehicles are mechanical units and are the most conspicuous portion of remote handling systems in action. One basic psychological observation can be made, namely, the ease with which a Mobot operator learns to identify himself with the Mobot vehicle and to forget the existence of the interconnecting systems. This psychological identification appears to be a basic necessity for successful operation of fully-remote handling systems.

Let us consider briefly the requirements upon the several basic subsystems.

---

*Trademark of Hughes Aircraft Company

The Manipulating Subsystems. It seems impossible to avoid the anthropomorphic terms, hands and arms, to refer to the manipulating devices. In general, however, these do not much resemble human hands or arms, but are designed specifically to perform tasks as required. It is extremely difficult to rival the versatility of the human hand. However, special-purpose handlers can usually out-perform the human hand in either dexterity, strength, small size, or other specific attributes. In addition to having sufficient strength to handle the assigned tasks, Mobot manipulating systems must be able to work in the presence of obstacles and to perform complex and intricate motions.

The Senses. While all the human senses can rather readily be transmitted via electronic means, vision is the most important by far, and the only one which will be discussed in this brief analysis.

Spatial orientation is normally accomplished by a variety of methods. Parallax, scale, relative motion, and the like, are probably most important of these. Binocular vision is surprisingly unimportant, as demonstrated by the fact that one-eyed men are but little handicapped in perceiving spatial orientations in their vicinity. Based on this analysis, excellent success has been obtained with a simple vision system utilizing two TV cameras, as shown in Figure 4. These two cameras show the operator two mutually perpendicular projections of the area viewed, from which he can learn to deduce the spatial orientation of all objects within his visual field. Learning time of a few hours has proven quite adequate for this system.

Certain special problems are often encountered in underwater viewing due to the fact that in many cases the ocean water is turbid or murky and presents a rather inadequate optical medium. A variety of methods are available to aid the operator's vision. For example, the skillful placement of artificial light sources may reduce the scattering of light by suspended particles in the water and improve operator visibility. The use of intense pulsed light sources synchronized with the frame-rate of the TV cameras may also be helpful. For long distance vision, sonar systems may be preferable to optical systems. While sonar systems are limited in their ability to resolve extremely fine details, they may furnish to the operator completely adequate information for navigation of his remote handling system until it comes within the rather limited range of the optical systems.

As a general principle of Mobot system design, the engineer makes fullest use of all sensory inputs available to him. These may include, in addition to sonar and optical vision, touch, hydrostatic pressure, system attitude and heading, apparent speed and direction of water flow past the Mobot vehicle, and a variety of others.

Locomotion. In order for the Mobot to move freely about in the underwater environment, several different means of locomotion are available. The remote handling engineer will select the one best suited to the particular problem presented to him; in many cases a combination of Mobots employing different means of mobility is the most economical solution.

The distinction between handling and locomotion is an important one which is basic to effective handling system design. The term "manipulation" is reserved for complex and delicate motions, as described in the section preceding. The term "locomotion" refers to the process of bringing the

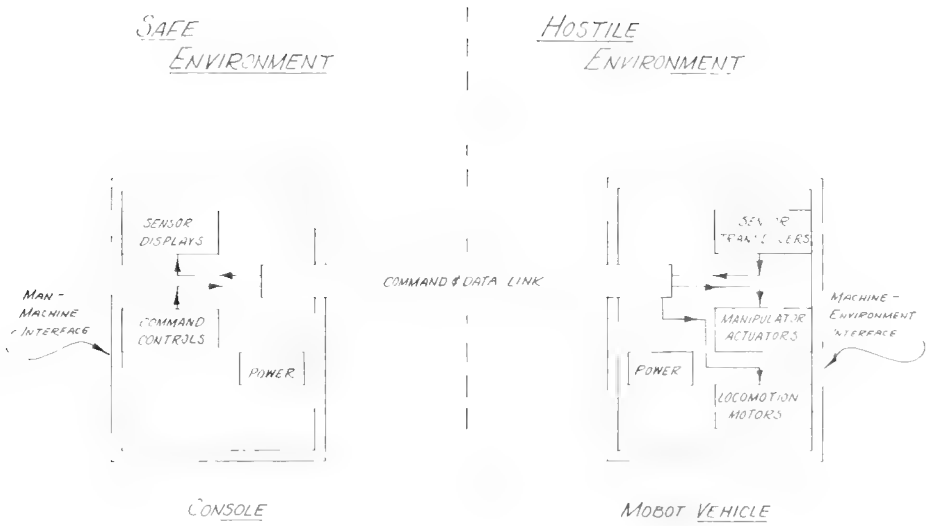

Figure 3

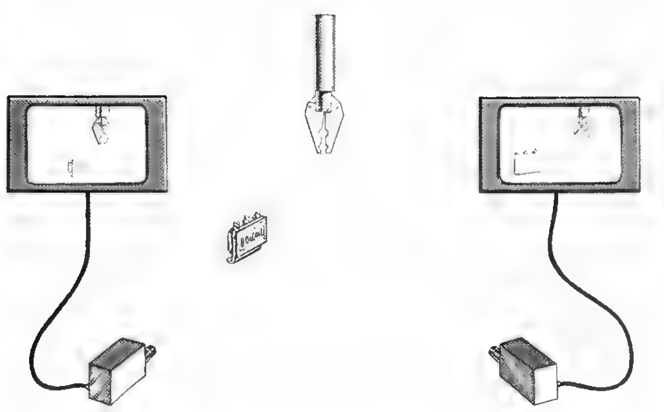

Figure 4

manipulating devices within reach of the object to be manipulated. In many cases, in addition to methods for moving the entire vehicle about, auxiliary locomotion subsystems taking such configurations as telescoping lifts, jack-knife booms, or the like, may be employed to enable the operator to position his handling arms without requiring him to move the entire vehicle.

For general-purpose operations, a versatile Mobot may be suspended by a cable from a barge or other surface vessel. Gross motions of the Mobot are accomplished by maneuvering the surface vessel; fine control may be accomplished by small propellers on the Mobot with which it can locate itself precisely.

A freely-moving Mobot is sometimes preferable. This can be accomplished by providing sufficient power to drive propellers which will propel the Mobot in any desired direction. Depending upon the situation, one may wish to furnish Mobots which travel mainly horizontally (like unmanned submarines) or, in contrast, Mobots which travel mainly vertically (like an underwater version of a helicopter).

For maneuvering heavy objects or for detailed exploration of the sea bottom or similar applications, bottom-crawling vehicles are desirable. These may be adaptations of caterpillar tractors or tanks or, alternatively, may use large soft rubber tires; in any case, the familiar techniques which may have been developed for off-road vehicles on land can be employed underwater as well.

Command and Data Link. This link is the communication medium between the operator and the Mobot. It transmits from the operator to the Mobot the command information which directs the Mobot's motions; and it transmits from the Mobot to the operator sensory data which inform the operator of the situation at the Mobot. Most important of the sensory data is the television information which (unless special systems are employed) requires an extremely wide band-width. In addition, sonar information and other data such as temperature, radioactivity level, pH of the water, and the like, may be transmitted. This link must obviously be capable of providing command information at a sufficiently rapid rate to control the Mobot, and of transmitting sensory data from Mobot to operator, again at an adequate rate. Since a cable must be provided to enable the operator to communicate with the Mobot (this is necessary since radio energy does not propagate in sea water), this same cable can be used to transmit electrical power to the Mobot. Modern multiplexing technique makes it quite feasible to combine the two functions of communications and power in a very small number of electrical conductors.

For very long distances the mechanical problems involved in handling the cable and the electrical problems involved in transmitting energy through it become quite formidable. It may therefore be necessary in such cases to employ repeaters within the cable to facilitate the transmission of command and TV information. This obviously implies the necessity for furnishing power by other means. In some cases it may be desirable to construct permanent underwater conduit installations, thus eliminating the necessity for carrying the entire length of cable on the Mobot itself.

Power Subsystems. Power subsystems for remote handling systems are based upon standard power technology. In most cases prime power for underwater mobile vehicles is best transmitted through the cable which serves as the command and data link. In order to economize on copper, power is transmitted at high voltage and a local distribution system is included within the mobile vehicle. Hydraulic power is highly advantageous for underwater actuators, for handling arms, as well as wrenches, jacks, and other auxiliary power tools. Accordingly, one often includes a hydraulic power subsystem within the Mobot vehicle.

Large and heavy vehicles, or vehicles required to operate at very great distances from the operator, may more economically generate prime power within the vehicle itself rather than transmitting it via cable. Any power system capable of operating within the ocean can of course be used for such vehicle. The control of the power subsystem is accomplished through the Mobot command system which, without difficulty, can accommodate the necessary additional command channels.

Control Console. The control console, or control subsystem, is the man-machine link, the only point in which the human operator interacts with the Mobot system. Human factors engineering methods are fully applicable to control console design. Uppermost in importance is minimizing of operator fatigue so that a man can spend long periods at the console without undue deterioration of his performance.

As noted above, an experienced operator becomes completely unaware of the mechanics of the console itself and subjectively identifies himself with the Mobot vehicle. A most subtle point in console design is facilitation of this subjective identification.

SCIENTIFIC APPLICATIONS OF REMOTE HANDLING TECHNIQUES TO OCEANOGRAPHY

In the light of the foregoing general discussion of remote handling techniques and methods for operating in hostile environments, it may be of interest to describe a few applications of these techniques to oceanography. These illustrative examples are not intended to exhaust the subject; on the contrary, it is hoped that they will stimulate the thinking of the oceanographer and that as a result it will be possible to propose new advanced handling systems which will facilitate the obtaining of scientific information concerning the oceans and their contents.

Vehicles for obtaining scientific information in the ocean may be required to operate at or near the ocean bottom, or in some cases to obtain information concerning the ocean itself. This indicates a need for free-swimming vehicles as well as for vehicles which can operate on the ocean floor.

The scientific observer is of course the most vital element in the data-gathering process. He may desire to be reasonably close to the site of the information to be gathered, in a diving bell, submarine, or Bathyscaphe. In some cases, on the contrary, he may prefer to remain in a surface vessel or shore station from which he can control the motions of a Mobot vehicle and can see, hear, and feel the local situation with as much or more facility as if he were physically present. This rather subjective data-gathering process is of course added to the more physical capability of gathering specimens. It is to be noted that the specimen-gathering process, as accomplished by remote control, is in some respects decidedly advantageous as compared to the "blind" obtaining of specimens by various pieces of equipment dropped over the side on lines or cables. In the former case one not only obtains the specimen, but also considerable information concerning its nature and surroundings.

General-Purpose Underwater Handling System. Figure 5 illustrates a general-purpose remotely-controlled underwater handling system which might be called a "remote-controlled deep sea diver". This freely-swimming system can maneuver either vertically or horizontally and can rest on the bottom if desired. It is equipped with general-purpose handling arms with which it can gather specimens either biological or geological. Its activities are directed by means of TV and sonar; the additional senses, such as touch, temperature, pressure, etc., can be added if desired. The cable, which contains only three electrical conductors, transmits electric power to the vehicle as well as serving as a data and command link. One can readily visualize a great variety of uses for a machine of this type in exploration of the ocean bottom, in locating and perhaps even reading scientific instruments on the ocean bottom itself, as well as in the basic process of gathering scientific specimens.

Accessory System for Bathyscaphe. Bathyscaphes and other vessels intended for exploration of the very deep ocean offer the important ability to bring the man in the near vicinity of the area to be explored. The Bathyscaphe, as such, seriously limits the activity of its occupant to visual observation of his surroundings and to taking readings on permanently installed scientific instruments.

The attachment to the exterior of a Bathyscaphe of even a simple remote handling system would greatly increase the effectiveness of the scientific observer, since it would enable him physically to handle and work with the items in his surroundings, as well as merely to look at them. Such handling systems might range from a simple arm mounted upon the exterior of the vessel to a complete auxiliary Mobot system, including both handling arms and supplementary TV vision which could operate up to some little distance away from the Bathyscaphe. This latter combination would eliminate the necessity of maneuvering the Bathyscaphe itself, which is a rather difficult and power-consuming operation. Systems intermediate in complexity between these two can of course be readily engineered to meet the requirements of particular programs.

It is important to realize that even in the case of manned submersibles one is still confronted with the hostile environment operating problem. The man is not "really there". He is separated from his surroundings by the pressure hull of the Bathyscaphe, and his senses and his manipulations must of necessity be accomplished by remote control equipment of some sort.

Bottom-crawling Systems. It is sometimes desirable to employ remote handling systems which move about on the ocean floor as opposed to the free-swimming systems discussed in the preceding paragraphs. Figure 6 shows a typical system of this type. Like all Mobot systems, it is remotely controlled by means of a cable. The man who directs its motions may be located either on a shore station or on a surface vessel, depending upon the surroundings. The principal utility of a bottom-crawling vehicle lies in its ability to handle heavy objects. It may also be equipped with earth-moving

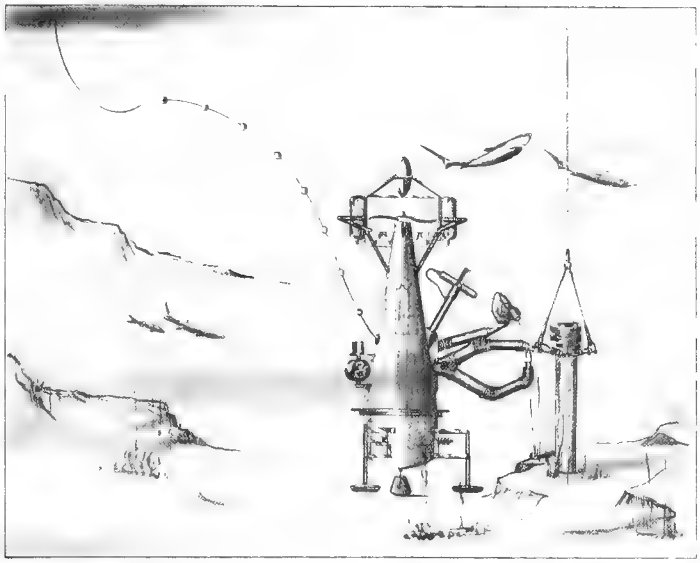

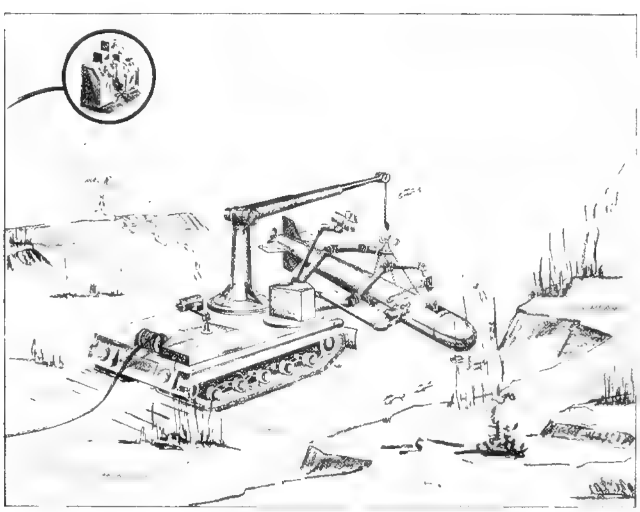

Figure 6

equipment, such as a bulldozer blade or a power shovel so that extensive excavations or structural work can be accomplished. It is realized that this type of effort is not of direct application to scientific oceanography; one may however find it necessary in connection with oceanographic investigations to excavate the ocean floor or to install rather complex permanent structures thereon.

A bottom-crawling vehicle may be equipped with an "underwater helicopter". This accessory will enable the operator to lift the vehicle off the bottom in order to avoid underwater cliffs, crevasses, or other obstacles.

CONCLUSION

The foregoing sections have outlined some of the major principles of hostile environment operating technology and the applications of these to oceanography. It is to be hoped that this discussion will stimulate new ideas in this general field. Experience to date in both nuclear laboratories and underwater operations has clearly demonstrated that equipment of the type discussed is completely practical, and in many cases is also economic as compared to alternate methods of accomplishing the same function. A great deal of activity is now in progress in this branch of engineering; it is to be expected that in the very near future numerous systems of the type discussed will become a reality and will become a creative part of the total complex of equipment available to the oceanographer.

PORPOISE — OCEANOGRAPHIC RESEARCH VEHICLE

by W. L. CANNON, Project Engineer
Chance Vought Corporation
Dallas, Texas

ABSTRACT

A description of an oceanographic research vehicle called Porpoise is presented. The vehicle, under development by Chance Vought Corporation under contract with the Office of Naval Research, is essentially an underwater glider that utilizes buoyancy control as a means of propulsion. The vehicle described is 12 feet in length with a maximum range of about 26 nautical miles and a depth capability of 1,000 feet. Performance increases are predicted for various sizes of vehicles using several types of gas generators.

INTRODUCTION

Porpoise is an underwater glider that utilizes buoyancy control as the motivating force to obtain forward velocity. The vehicle is being developed as an oceanographic research vehicle by Chance Vought Corporation, under a license agreement with Oceanic Systems Corporation. At the present time Chance Vought has a contract with the Office of Naval Research to design and fabricate one vehicle for demonstration of the feasibility of the concept for oceanography.

CONCEPT AND OPERATION

Fig. 1 shows a sketch of the Porpoise vehicle and a portion of a typical mission profile. The mission would begin with launch of the Porpoise vehicle from an oceanographic vessel. The launch operation would consist of simply lowering the vehicle into the water from the deck of the ship and releasing the vehicle on the desired heading. The vehicle will take on water through the flood valve while the entrapped air escapes through the vent valves located along the upper surface of the vehicle. Since the flooding begins forward of the center of gravity, the Porpoise vehicle will pitch over and, as it becomes negatively buoyant, begin its descent. At a preset depth below the ocean surface, perhaps 60 feet, a hydrostatic pressure sensing control mechanism will close the flood valve and the vent valves. At this point, the vehicle will be full of water and will descend at an angle of approximately 14 degrees with a velocity of about 10.5 knots. Then, at a preset depth, the compressed gas control valve will be opened, allowing the air or nitrogen from the storage tank to enter the ballast compartment. The water is then expelled from the ballast compartment through the ballast outlet valve which is a spring loaded valve. Since the water is expelled from the forward portion of the vehicle first, a moment is obtained which causes the vehicle to begin a pitch-up maneuver. When the water is completely expelled from the vehicle, and the gas flow terminates, the pressure across the hull equalizes and the spring loaded ballast outlet valve closes. The vehicle now is positively buoyant and is rising at an angle of about 14 degrees and a velocity of approximately 10.5 knots. As the vehicle approaches the surface, the depth sensing mechanism opens the flood valve and the vent valves to again flood the vehicle. Then, of course, the vehicle becomes negatively buoyant, pitches over, and begins another cycle.

The wing configuration is designed to provide high roll stability, and the wings have equal angular travel (11°) both up and down since the wings will be up when the vehicle is gliding downward and down when the vehicle is gliding upward.

The instrumentation payload is located in the nose of the vehicle. The payload case will be separated from the ballast compartment by a double watertight bulkhead to facilitate instrumentation payload installation and removal. This allows all instrumentation checkout, calibration, and maintenance to be done in the laboratory, then installation of the payload case on the vehicle just before the vehicle is launched. By providing a number of payload cases with different instrumentation configurations, a good flexibility of mission types would be available with a minimum of change to the vehicle or any payload case.

The flotation and marker system will be actuated on the final cycle of the mission as the vehicle reaches the surface. The flotation bag is inflated to a diameter of about

PORPOISE

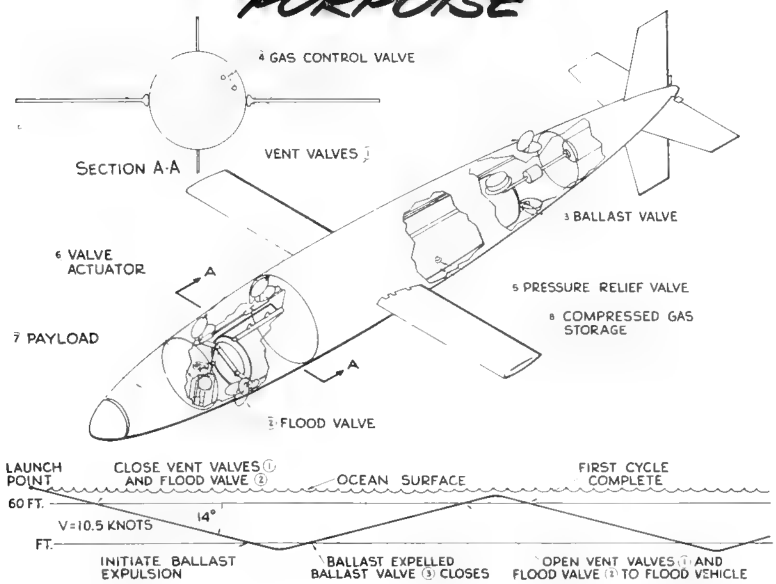

Fig. 1

DESIGN CHARACTERISTICS

- **CONFIGURATION**

LENGTH	12 FT.
MAXIMUM DIAMETER	20.58 IN.
WING SPAN	76 IN.
SEMI-MONOCOQUE STRUCTURE	
HULL MATERIAL	0.100 6061 ALUMINUM
WING MATERIAL	0.58 6061 ALUMINUM
TAIL MATERIAL	0.125 6061 ALUMINUM
WEIGHT IN AIR	620 LB.
DISPLACEMENT	1080 LB.
PROPULSION SYSTEM	NITROGEN 3000 PSI
RECOVERY SYSTEM	INFLATABLE SPHERE

- **PERFORMANCE**

DIVE AND ASCENT ANGLE	14 DEG.
VELOCITY	10.5 KT.
DEPTH	500 FT.
RANGE	2.7 NM
PAYLOAD CAPACITY	1 CU. FT., 100 LB.
OPERATING CYCLES	4

RANGE LIMITATIONS

LIQUID PROPELLANT
14° 10.5 KNOTS

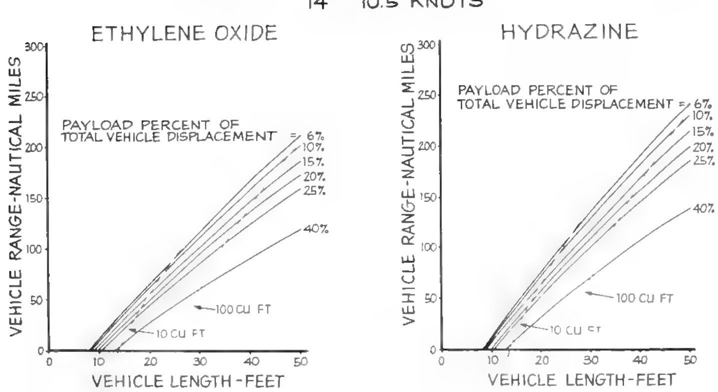

F...

3 feet to insure that the vehicle will remain afloat even if any of the various flood and vent valves leak. Also, the flotation bag will be painted a highly visible color and perhaps have a radar reflective surface.

Fig. 2 shows in tabular form the physical and performance characteristics of the first Porpoise vehicle. It is emphasized that the performance data is for a vehicle equipped with a 3,000 psi gas storage cylinder. With a solid or liquid fueled hot gas generator, which is proposed as the system for the operational vehicle, the performance will be greatly increased. For example, with a hydrazine or ethylene oxide gas generator system, this 12 foot long vehicle would have a range of about 26 nautical miles and a depth capability of at least 1,000 feet. Also, use of a hot gas generator in a 12 foot vehicle will allow increasing the instrumentation payload to about 2.5 cubic feet.

PROGRAM PLAN

Under the present contract with the Office of Naval Research, Chance Vought will design and fabricate one twelve foot long vehicle configured with a compressed gas system. The vehicle will be delivered to the Navy in early 1962. Proposals for follow on work including additional vehicles, a hot gas generator development program, and a field test program are currently being evaluated by the Office of Naval Research. The test program proposed consists primarily of feasibility demonstrations in the Dabob Bay test facility of the U. S. Naval Torpedo Station, Keyport, Washington. The instrumented test range of the Dabob Bay facility is considered to be ideal for the initial demonstration since tracking accuracy of about ± 1 foot is obtainable. Water depth is about 600 feet and total available range at the facility is several miles. Therefore, for demonstration of the full capabilities of the hot gas generator configured Porpoise, it will be necessary to move to the open ocean.

FUTURE CAPABILITIES

Fig. 3 shows the range performance which is expected from Porpoise vehicles of various sizes with two types of liquid monopropellant fueled gas generator systems. Vehicle length is plotted against range since range remains practically constant for a given amount of fuel regardless of the maximum depth of operation. For example, a 20 foot vehicle configured with an ethylene oxide gas generator system would have a range of about 56 nautical miles with a 10 cubic foot payload. Operating this vehicle at a maximum depth of 1,000 feet, the distance traveled per cycle is about 1.33 nautical miles, requiring about 42 cycles for the mission. If the maximum depth is changed from 1,000 feet to 2,000 feet, then the distance traveled per cycle is about 2.67 nautical miles requiring only 21 cycles for a 56 nautical mile range. However, since the pressure against which the gas generator must expel the ballast is doubled, then the fuel requirement is approximately doubled for each cycle. Therefore, total range will not change. Depth of operation is limited by the amount of fuel required for one cycle to that depth and by the pressure at which the decomposition of the ethylene oxide or hydrazine can be made to take place.

The curves for various payload volumes as a percentage of total vehicle displacement simply indicate the effect of reducing fuel volume and increasing instrumentation payload volume.

The use of hydrazine fuel in the vehicle will result in a 10% or 15% greater performance than that obtainable with the ethylene oxide fuel. However, hydrazine costs about $3.00 per pound whereas ethylene oxide costs only about $0.25 per pound. The difference in cost may well justify selection of the ethylene oxide for most applications.

Similar performance curves are shown in Fig. 4 for a solid propellant fueled gas generator and a water reactant fueled gas generator. An obvious disadvantage of the solid propellant system is that a separate propellant cartridge or charge must be provided for each cycle desired,and each cartridge must be sized to expel the water ballast at a specific maximum operational depth. If it is desired to go to a greater depth, two or more charges must be fired simultaneously. Therefore, maximum range can be obtained only at the cartridge design depth and even multiples of that depth.

The water reactant curve shown indicates that lithium hydride as a fuel could provide more than twice the performance of the solid or liquid fuels. However, lithium hydride as a fuel for Porpoise may be further in the future than the other fuels because of availability, cost, and the difficulties that may be encountered in controlling the lithium hydride gas generation reaction.

Fig. 5 illustrates some profile variations attainable with future Porpoise vehicles. Since the vehicle is a glider, the limits on flight path angle and velocity are relatively small. By simply providing a wing incidence adjustment, it will be possible to obtain a velocity of about 15 knots at a 20° glide angle. This, of course, reduces the horizontal distance traveled per cycle for the same

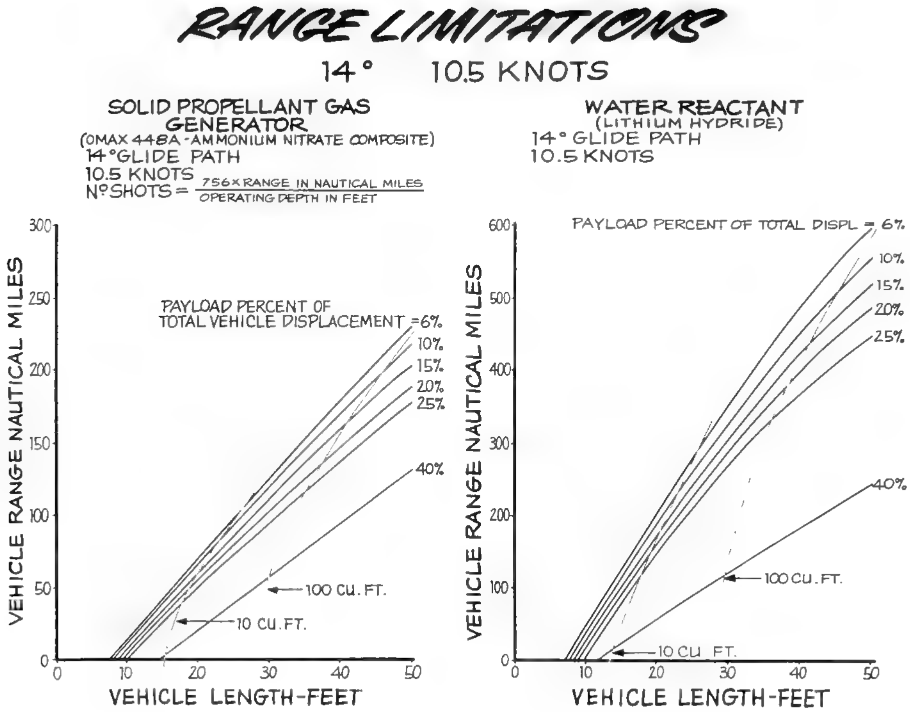
RANGE LIMITATIONS
14° 10.5 KNOTS
SOLID PROPELLANT GAS GENERATOR
(OMAX 448A - AMMONIUM NITRATE COMPOSITE)
14° GLIDE PATH
10.5 KNOTS
N° SHOTS = 756 X RANGE IN NAUTICAL MILES / OPERATING DEPTH IN FEET
WATER REACTANT
(LITHIUM HYDRIDE)
14° GLIDE PATH
10.5 KNOTS
VEHICLE RANGE NAUTICAL MILES
PAYLOAD PERCENT OF TOTAL VEHICLE DISPLACEMENT = 6%
10%
15%
20%
25%
40%
100 CU. FT.
10 CU. FT.
VEHICLE LENGTH-FEET
PAYLOAD PERCENT OF TOTAL DISPL = 6%

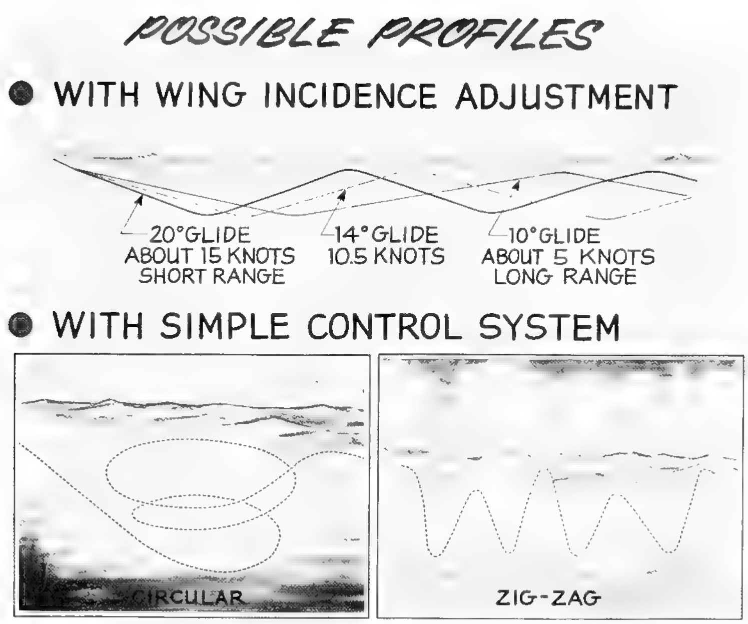
POSSIBLE PROFILES
WITH WING INCIDENCE ADJUSTMENT
20° GLIDE
ABOUT 15 KNOTS
SHORT RANGE
14° GLIDE
10.5 KNOTS
10° GLIDE
ABOUT 5 KNOTS
LONG RANGE
WITH SIMPLE CONTROL SYSTEM
CIRCULAR
ZIG-ZAG

maximum depth. Conversely, range and endurance can be increased by changing to a glide angle of about 10 degrees which will result in a velocity of about 5 knots.

Variations in mission profile could be obtained in future vehicles by addition of a simple heading control system. Before launch, the desired mission profile could be programmed into the heading control system, allowing the vehicle to perform circular, zigzag, or other maneuvers while gathering oceanographic data.

CONCLUSIONS

It is believed that the Porpoise concept offers a unique and effective method of obtaining oceanographic data. The vehicle size for most instrumentation payloads is small enough to be operated from existing oceanographic vessels. A vessel operating several Porpoise vehicles while also taking oceanographic data using the shipboard equipment would be able to collect data from large areas of the ocean simultaneously. In addition, utilizing a fuel such as ethylene oxide should make operating costs reasonable, and the simplicity of the vehicle inherently should provide high reliability and long life.

SCUBA AS A TOOL FOR SCIENTISTS

by EUGENE K. PARKER
General Engineering Laboratory
General Electric Company
Schenectady, New York

ABSTRACT

Scientists opportunity to observe underwater environment "in situ" by use of scuba (self contained underwater breathing apparatus). The "Scuba Zone" encompasses: Air-water barrier through hyperbenthal, mesobenthal, hypobenthal to parahypobenthal stratas to a depth of 150 feet. Description of scuba. Comparison with some other underwater observation and sampling devices. The Use of scuba by scientists.

THE PAPER

From the shoreline out to a depth of 50 meters lies an area called the scuba zone. This is the zone accessible to the scuba (self-contained underwater breathing apparatus) diver.

(Fig. 1 The Scuba Zone)

For centuries man has waded the tidal pools and shallows. He has sailed the surface. He has probed into the water; raking, scratching, netting, and dredging up samples of underwater life and bottom. More recently he has invaded this domain in diving bells, suit and helmet rigs and underwater vehicles. None of these have permitted man to comfortably study the underwater ecology with an appreciable degree of ease or continuity.

The advent of workable scuba has changed this picture. Instead of trudging on the bottom, or hanging suspended, man has almost attained the freedom of a fish. As yet his free diving range is limited to relatively shallow waters. Recent experiments with special scuba indicate that this range may someday extend to a thousand feet deep. (Hans Keller experiments)

In this discussion we are concerned principally with diving at depths of twenty to fifty feet, occasionally to one hundred feet, and rarely to one hundred and fifty.

Although skindiving has become as socially acceptable as golf, its acceptance by some scientists as a legitimate scientific medium has not grown proportionately. Many men of science have been deprived of the opportunity to make "in situ" examination and study of subjects within the "scuba zone". Sometimes this deprivation is because of real or assumed physical or psychological inability to use scuba. Occasionally it is because they feel scuba has little to offer. The purpose of this paper is to demonstrate the usefulness of this medium for underwater scientific study.

That the scuba zone is still a fertile area for scientific exploration is becoming more apparent.

Willis Pequegnat, in his article "New World for Marine Biologists" (April 1961 Natural History) states: "During each descent into these shallow waters, we encountered more and more unfamiliar species, especially among the rock inhabiting faunas. It soon became clear that we were investigating an almost untouched domain of the sea: untouched, not from lack of interest, but simply because of its previous inaccessibility."

In underwater ecological problems many aspects of lymnology and similarly, of oceanography meet. The biology, geology, physics and chemistry are interrelated. Scuba permits otherwise land- and deck-bound scientists to study this interrelation. Studies of the interrelation of currents, salinity, temperatures, subsurface topography, sedimentary deposits, fossils, and animal life are enhanced by personal underwater study. It may not be too far fetched to suggest that by actually insinuating oneself into this environment a better sympathy with these factors can be achieved. This could be likened to the entymologist observing insects in their natural habitat.

At this juncture a capsule sketch of scuba diving equipment is helpful.

There are two basic classifications of scuba: closed circuit and open circuit. The diver wearing closed circuit literally rebreathes a major part of his own exhalations. Exhaled breath is reconstituted by a chemical filter, a small amount of oxygen is added and the revitalized mixture is rebreathed. A very small amount of excess exhausted air is dissipated into the water. Very little bubble trace can be discerned on the surface. This is one reason why underwater demolition teams use closed circuit scuba. The other reason is that several hours of

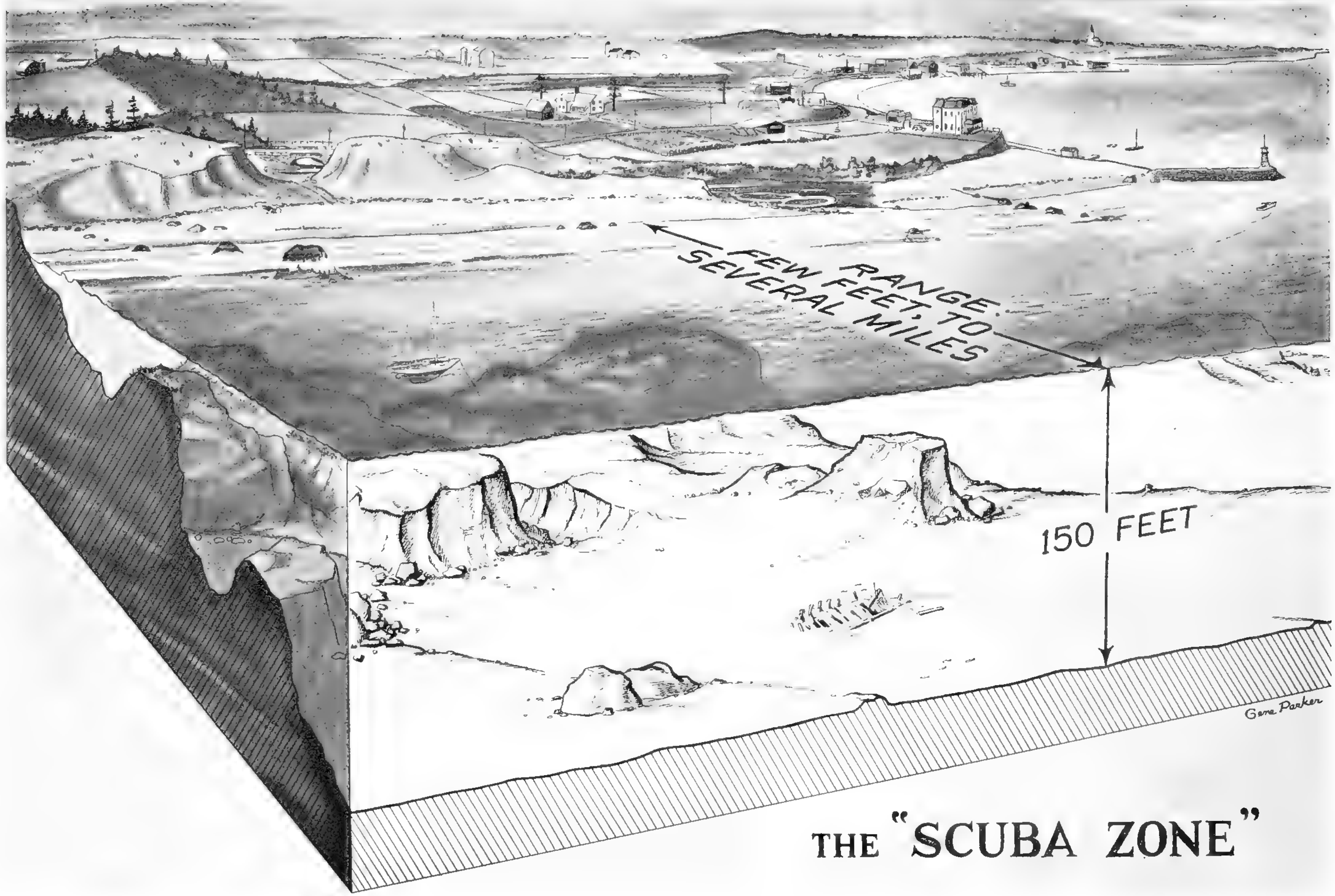
RANGE
FEW FEET, TO
SEVERAL MILES
150 FEET
Gene Parker
THE "SCUBA ZONE"

Figure 1.

immersion may be achieved on one unit.

Amateur use of closed circuit scuba can be dangerous. The diver may be poisoned by faulty chemical filtering. He may suffer from anoxia or from oxygen poisoning.

Use of closed circuit scuba in scientific diving is unnecessary since there is no need to extend submerged time or to conceal bubbles.

Open circuit is recommended for scientific diving. The diver wears a high pressure air cylinder on his back. An automatic demand regulator mounted on the valve of the tank provides air through a hose to the mouthpiece or to the mask. The diver breathes air at ambient pressure. The exhaled air bubbles out into the water, hence the name open circuit.

About an hour of submerged time is achieved with the most common size of scuba tank. This varies with depth and with the individual's respiratory rate.

(Fig. 2 The Scuba Diver)

Basic skindiving (breath holding diving) equipment is the mask, snorkel and fins.

In addition to the basic equipment the scuba diver will need his breathing apparatus. He may also need a suit to protect him from cold, a weight belt, knife, compass, depth gauge, watch, and an inflatable flotation device. In some cases he might tow a surface float in which samples or tools can be carried.

Many new pieces of accessory equipment are now available:

Metal detectors, underwater prospecting and mining equipment, underwater lights, self-powered sleds and towing devices, small salvage equipment, underwater cameras, communication devices, diver sonar, and a host of others.

(Fig.3 Accessory Equipment)

Scuba diving has to be experienced to be believed. The diver can hover almost effortlessly over most scuba zone underwater locations while making continuous observations. He can rapidly change vantage points, pursue specimens, and handle objects. It is even possible to make notes or sketches, using special materials, underwater.

Scuba is unparalleled for efficient shallow water search of an area. In fresh waters two divers on towed planes can cover a swath fifteen feet wide and mile long in less than a half hour. They will expend little energy compared to free divers. Using diving planes in depths to 40 feet, it is possible to double the air duration time of scuba.

(Fig. 4 Use of Diving Planes)

Unfortunately, most salt water areas do not lend themselves to the diving plane type of scuba search. The towed diver feels entirely too much like a trolled bait when in shark waters.

Compare the diving ease of scuba with the difficulties of the traditional "hard hat" diver as he trudges slowly over the ocean floor in heavy gear, stirring up the mud. He is tethered to the surface by lines. A large boat or barge, a line tender, and usually a crew is necessary. His gear is expensive. He requires a great deal of training.

(Fig. 5 "Hard Hat" Diver)

These factors preclude the use of "hard hat" rigs by most scientists. He traditionally had an advantage over scuba divers. This was constant telephone communication with the surface which increased work efficiency and safety. Now the scuba diver can obtain underwater wire or wireless communications.

The same inflexible rules regarding the physics and physiology of hard hat diving apply to the scuba diver. Proper training and adherence to the rules will minimize the danger of decompression sickness (bends), diving induced embolism, nitrogen narcosis, and other diving diseases.

Before delving into the individual's physical and psychological ability to use scuba, let us compare scuba observation with other contemporary observation or sampling media. We must, of course, bear in mind that we are discussing only depths readily accessible to scuba divers.

One type of observation medium is the reproduction of an underwater environment such as an aquarium.

Let us begin by admitting that there is no completely satisfactory artificial environment in which to reproduce actual underwater conditions. Indeed, to make an authentic artificial reef of (for instance) underwater biological life would require that we reproduce conditions of current, depth, animal interdependence, and many other factors.

A sampling medium such as trawling or dredging may bring up some undamaged marine specimens. This method gives scant information regarding the specimen's relationship to its environment.

Figure 2. The Scuba Diver.

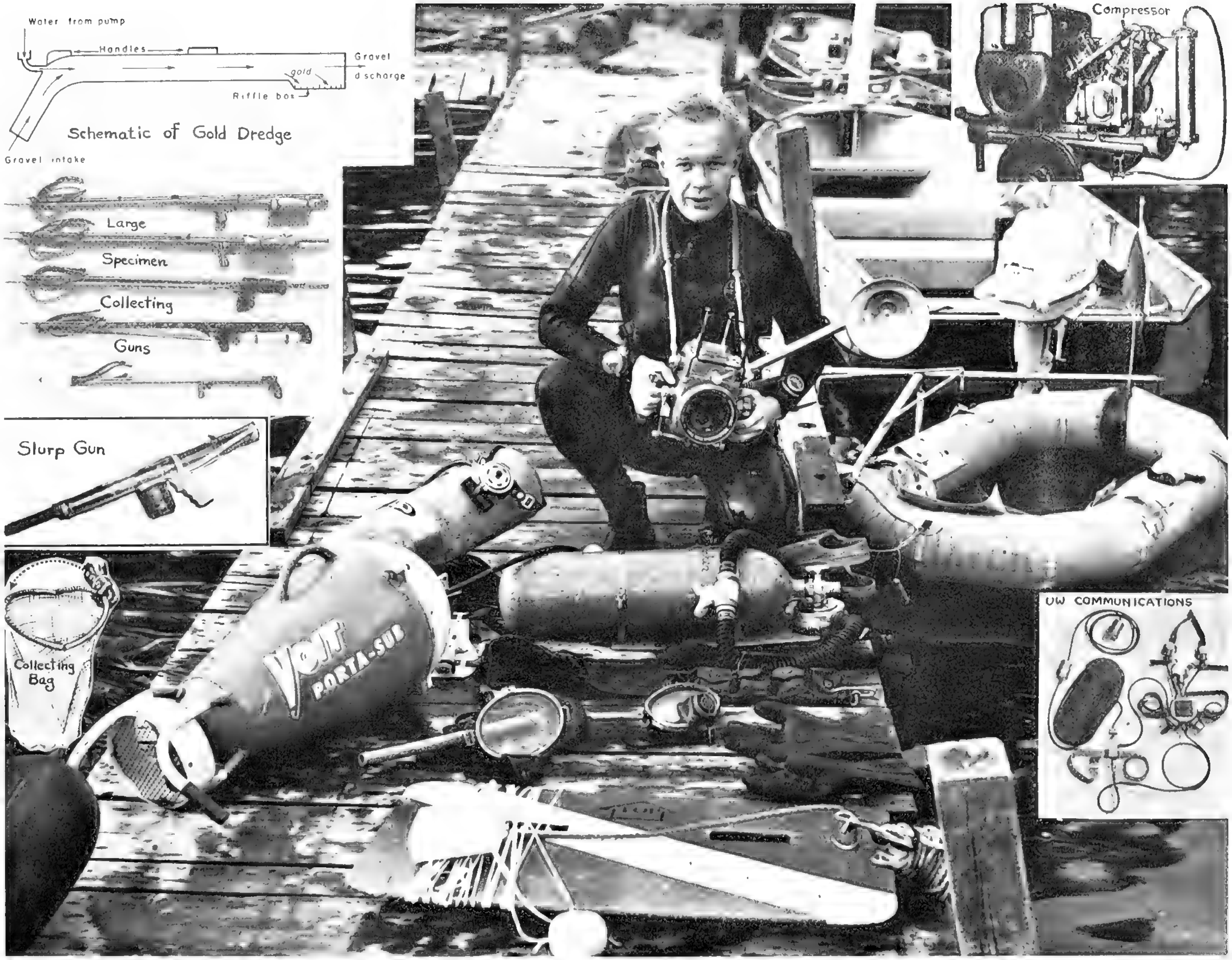

Figure 3. Accessory Equipment.

Figure 4. Use of Diving Planes.
1. Diver releases plane from towline.
2. Fastens a line to plane which ascends as marker buoy.

Figure 5. "Hard Hat" Diver.
(Comparison with scuba diver).

Attempting to dredge or grab specimens from rocky regions is obviously even more unsatisfactory. This is compounded by the fact that marine environments vary according to reef, shoal, or bottom type. It is difficult to correlate marine fauna or flora with geological structures when blindly groping the bottom.

(Fig. 7 Trawls and Grabs)

Naturally, it is not valid to state that scuba is a substitute for plankton nets, underway samplers, or some electronic devices. However, a surprising number of conventional oceanographic equipments can be used by a scuba diver. Among these are small sampling equipments like slurp guns, water bottles, traps, some samplers, some corers, small electronic gear, and of course still, movie and TV cameras.

(Fig. 6 Cameras Used by Scuba Diver)

Lymnology also contains fertile fields for the scuba diver. Most fish are surprisingly unafraid of divers. Possibly this is because their limited mental capacities have geared them to fear only instinctively recognized predators. A scuba diver sitting on the bottom of a pond becomes the focal point for curious fish. It is even possible to catch some species in one's bare hands.

In lake or ocean the relationship of the biomass and geology ranging from the hyperbenthal down through mesobenthal,hypobenthal to the parahypobenthal zones can be conveniently studied by the scuba diver. He can chip materials and organisms from rock or reef. He can sit on a reef to make pelagic fish counts. He can even spear or catch selected fish.

The naturalist finds skin and scuba diving excellent for observation of shallow water life of denizens of the air-water barrier.

(Fig. 7 Underwater Archeology)

Other very gratifying pursuits can be underwater archeology and underwater photography. There is almost no limit of uses which an active mind can find for scuba diving.

Let us turn now to the physiological aspects of scuba diving. Scuba diving is not the peculiar province of the young, healthy athlete. This statement needs qualification. True, if the diver is participating in a spearfishing contest, is attempting to combat strong adverse currents, or is flirting with decompression sickness, then robust, good health is a great asset. However, we are discussing the scientist that drops overside into relatively calm waters, swims down to a reef, and stays in the immediate vicinity of the boat and another qualified diver.

A major portion of the exertion expended in most skin and scuba diving is actually encountered above the water. It is no easy chore to lug from fifty to over a hundred pounds of cumbersome equipment to the diving location.... Especially when this may involve unloading a vehicle, climbing down slippery cliffs, clamboring into a wave-tossed small boat, fighting the boat through breakers, struggling into the snug fitting suit and equipment straps, and finally plunging overside. It is then actually a relief to be underwater and neutrally buoyant. This feeling of relief may be somewhat marred by the thought that after diving he must go through the above water ordeal again, in reverse order. No wonder physical fitness is stressed!

In most cases the underwater scientist will be able to obviate much of the above water exertion by diving directly from a larger vessel.

Youth itself is not a criterion of diving. There are many divers over 60 years of age, some over seventy and even a few diving octogenarians. Conversely, there are also a lot of healthy younger persons for whom diving is contraindicated. A sound respiratory and circulatory system is required.

The underwater depths which can be tolerated vary with the individual. This is not to say that the basic laws of underwater physics and physiology do not apply to all of us. Some people become distinctly unhappy in the gloom of deeper water. Others find themselves quite at ease in scuba at greater depths. This is a very cogent factor in diving, and because of its abstruse nature is seldom mentioned in books on diving. It is perhaps related to the most common sentiment expressed by non-divers: "You wouldn't catch me diving around down there!" Many of these people discover, to their delight, that their fears evaporate as soon as they gain confidence in their scuba. These same persons may never venture more than thirty feet deep. This is perfectly acceptable. A lot of research can be done in less than thirty feet of water.

A good instruction course in skin and scuba diving is essential. The neophyte diver can then decide whether diving is for him. A physical examination is required before taking a diving course. Most courses are from 12 to 30 hours duration. This includes classroom and pool work. One of the first, and still one of the best, books on scuba diving was written by David Owen of Woods Hole Oceanographic Institution. There are several other books on diving available. None of these books are a substitute for a good instruction course.

Figure 6. Camera Used by Scuba Diver.

Ribs showing above mud bottom.

UW excavation begun.

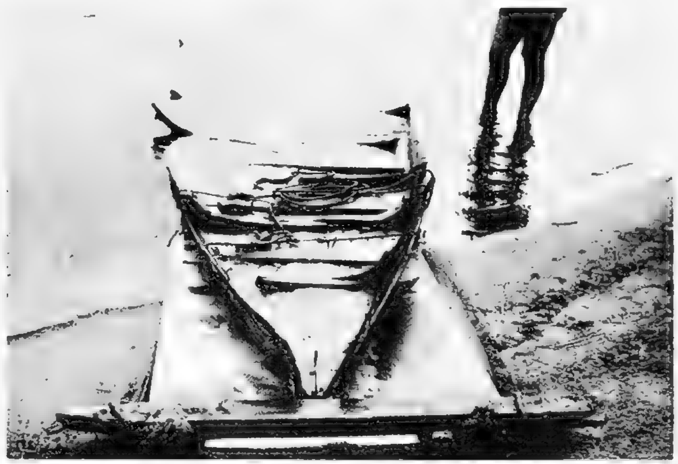

After 200 years underwater.

Measuring.

French and Indian War Bateaux Discovered in Lake George, N. Y.
Figure 7. Underwater Archeology.

A fully outfitted scuba diver may wear from a hundred dollars to three or four hundred dollars worth of gear. This compares very favorably with the price of "hard hat" rigs which may cost in the thousands of dollars.

Scuba diving as a sport is safer than skiing, or even driving a car. But, like these other avocations can be as dangerous as you make it.

As an adjunct to your vocation it can be considered even safer since the best of equipment and safeguards should be available.

It might be well worthwhile to use it as a tool in your profession.

REFERENCE: Natural History Magazine
April 1961

EQUIPMENT FOR OBSERVATION OF THE NATURAL ELECTROMAGNETIC BACKGROUND IN THE FREQUENCY RANGE 0.01-30 CYCLES PER SECOND

by W. N. ENGLISH, D. J. EVANS, J. E. LOKKEN, J. A. SHAND, and C. S. WRIGHT
Pacific Naval Laboratory
Defense Research Board of Canada
Esquimalt, British Columbia

ABSTRACT

The instruments designed and constructed for measuring the geomagnetic background between 0.01 and 30 cps, which has a great dynamic range in frequency and time, are described. Large effective area detector loops combined with high gain, very low noise amplifiers form an effective receiving system. Methods of absolute calibration are discussed.

INTRODUCTION

Because sea water is an electrical conductor, electromagnetic radiation is attenuated appreciably as it penetrates the water. The attenuation is a function of frequency and is about 55 db per wavelength. Figure 1 shows the wavelength as a function of frequency in sea water. At 100 cps the wavelength is 150 meters, and the skin depth about 25 meters. At 1 cps the wavelength is 1500 meters and the skin depth 250 meters, a very useful penetration. Since PNL is primarily interested in frequencies which penetrate sea water to an appreciable extent, we have chosen 100 cps as the upper limit of our region of interest and have so far made measurements up to 30 cps. Our lower limit is set by convenience and probable application at about 0.01 cps. The magnetic disturbances at lower frequencies have been extensively studied by magnetic observatories and many of their properties are known. The upper end of our region of interest overlaps the lower end of the ELF range.

Antenna and noise problems at very low frequencies make the magnetic component of an electromagnetic wave much more accessible to measurement than the electric component, hence we have restricted our observations to the former. Furthermore, possible applications tend to use the magnetic rather than the electric field. The naturally occurring geomagnetic fluctuations are often referred to as background noise, but their character is very different from that usually associated with "noise"; for example, the distribution of energy with frequency is not random over any convenient time interval. The prominent

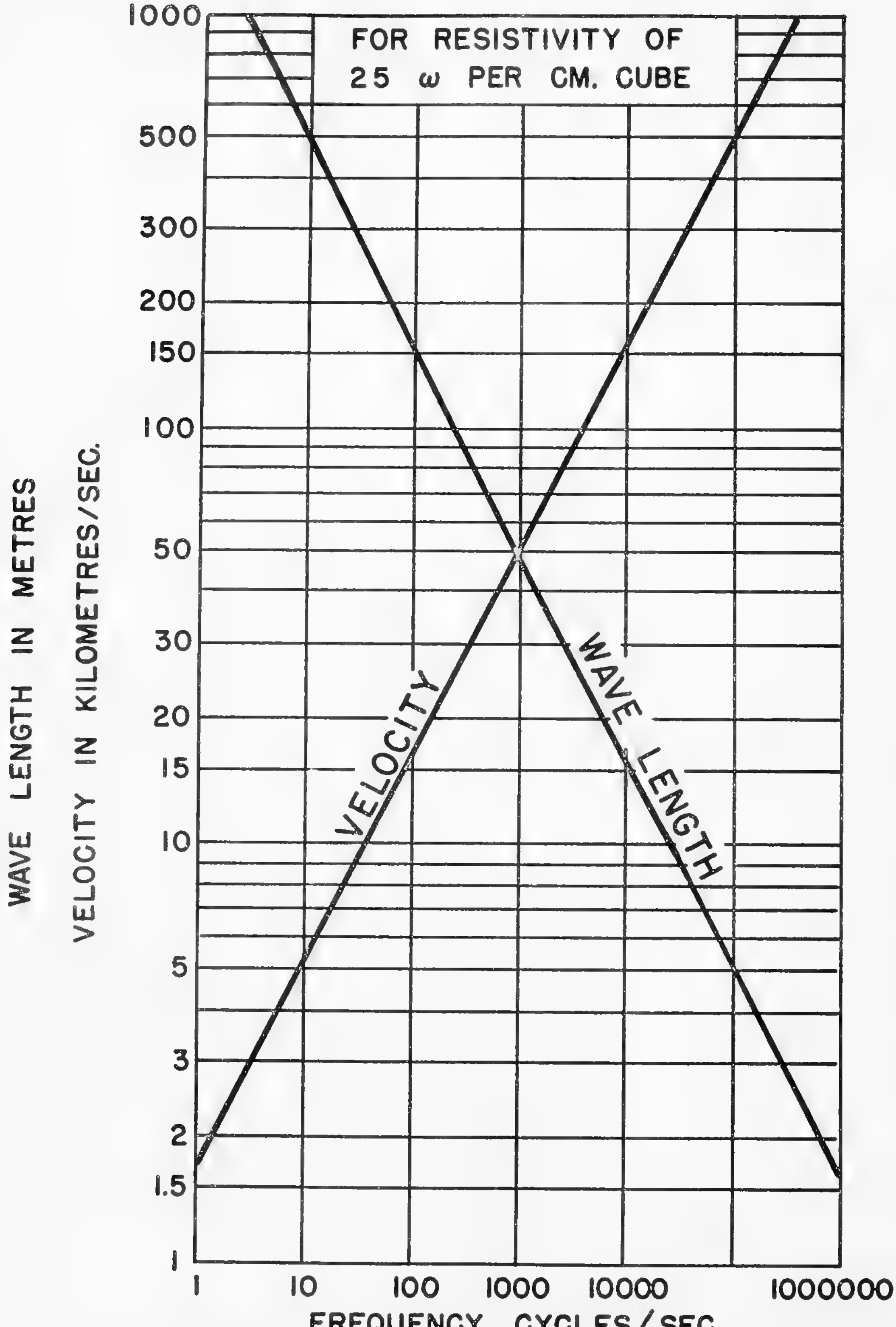

1. THE FREQUENCY DEPENDENCE OF WAVELENGTH AND VELOCITY OF AN ELECTROMAGNETIC WAVE IN SEA WATER.

signals displayed by Figure 2(b) and (c) having periods of the order of 15 to 30 seconds are characteristic of a recognized type whose occurrence and frequency distribution are decidedly not random.

PROBLEMS IN MEASUREMENT

1. The small percentage fluctuation: A large disturbance at 100 seconds period is only about 10^{-3} of the earth's main field while small signals at a few cycles per second may be as low as 10^{-10}. The amplitudes of some typical micropulsations are shown by Figure 2. Signal levels such as those recorded in part (a) dictate the use of sensitive detecting systems.

2. The amplitude-frequency relation: As a general rule the mean amplitude level increases with increasing signal period. Figure 2 also illustrates this point. Part (a) shows a typical signal of about 1 cps while parts (b) and (c) show that much greater amplitudes characterize the lower frequencies. Further, the longest period signals of part (c), technically outside the scope of this discussion, are of even greater amplitude because they have been attenuated by 20 to 30 db below the indicated scale. Until recently little has been known about the continuous background between 0.1 and 3 cps because of the low signal levels and the inadequate receiving equipment in this frequency range. Even with the detector systems which are sensitive to rate of change of flux it is normally necessary to filter out the low frequencies sharply in order to receive these elusive signals.

3. Wide dynamic range: The received signal levels may change abruptly by orders of magnitude. Thus, as Figure 2 shows, the amplifiers and recording system must have a wide dynamic range.

4. Man-made interference: The receiving site must be chosen to minimize power line, radio and especially teletype interference. Surprisingly low frequencies can occur in such interference and in populated areas these signals can be larger than the geomagnetic activity even when care is taken to choose a site as far removed from power lines, radio transmitters, roads, etc. as possible. Filters must be used to reduce the level of this interference. Moving vehicles within several hundred feet are of course intolerable.

5. Effects of the site: The noise observed is greatly influenced by the conductivity and permeability structure near the site and it will be different at sea and on land. Structural discontinuities can determine the total signal strength and its partition among field components. It will also materially affect the region of coherence of the signals. The site must be removed from trees or other objects likely to cause wind interference.

DETECTORS

It has been established that although the flux density of micropulsation activity is low compared to the earth's main field it is coherent over a large area, especially over regions of uniform sub-surface conductivity. Thus antennas which gather signal energy over a large area can do so without an appreciable loss of resolution, and therefore possess an inherent advantage over devices which utilize only a small area or volume for their activation. This paper is restricted to discuss equipment which utilizes large effective area fixed loop antennas. Within limits set by other considerations the most economical method of increasing sensitivity is to increase the effective area of the antenna. It can be shown that for a circular air-core coil of constant available power the inductance-to-resistance ratio is approximately inversely proportional to the cube of the diameter of the coil, and the mass of the copper conductor to the inverse square. Hence large diameter coils such as those to be described are desirable.

On a two-station operation near Ralston, Alberta, low impedance air-cored coils were used to detect the vertical component, which in that region is considerably smaller than the horizontal components. The two coils were wound 30 miles apart, on level ground, electrostatically shielded and buried. Each was 400 feet in diameter and contained 40 turns of PVC-insulated No. 12 wire giving a resistance of 80 ohms and an inductance of 1.1 henries. Another air-cored antenna which has been successfully used consists of two-conductor No. 16 shielded cable arrayed in a circle 4000 feet in circumference. One advantage in such a configuration is apparent in that for 32 ohms resistance, with the conductors in series, the inductive reactance at 40 cps is only 2.8 ohms. On the other hand detectors which depend on a much smaller proportion of the available flux for their activation possess great advantages in portability and convenience. Thus coils with high permeability cores have been used in lieu of large rigid air-core coils for detecting the horizontal components.

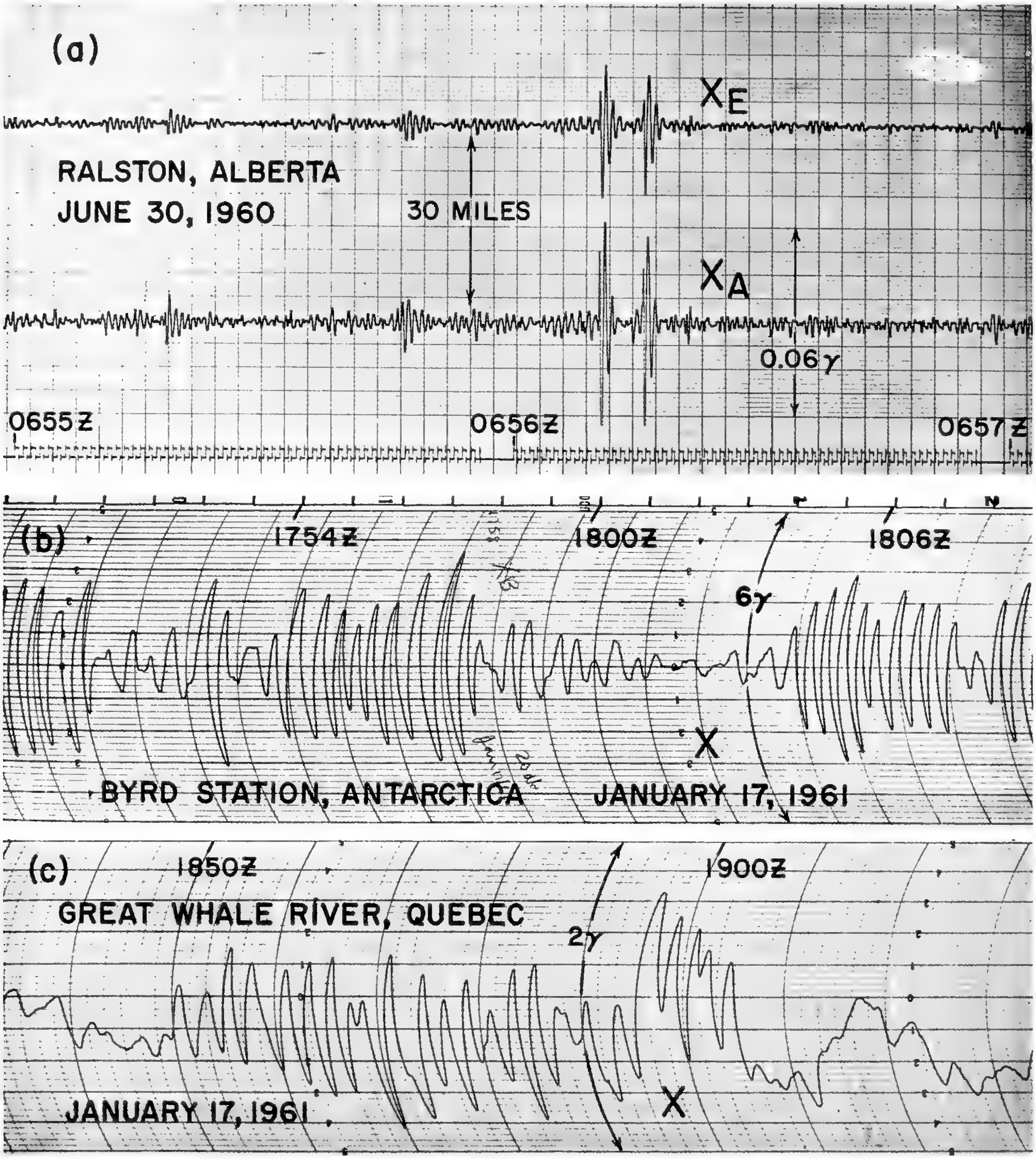

2. TYPICAL MICROPULSATION RECORDS. THE FULL-SCALE NOTATIONS OF PEAK TO PEAK FLUX LEVELS ARE APPROXIMATE ONLY FOR THE MORE PROMINENT SIGNALS. All are X (NORTH-SOUTH) COMPONENTS.

The most recent type consists of 20,732 turns of No. 18 HF-insulated wire taper wound on a core consisting of 35 Telcon 79 strips, each 0.015" x 0.75" x 72", about one-half square inch in cross-section. All wire splices are welded. A copper shield with an insulated lap encloses the winding while this in turn is enclosed in a section of plastic pipe with watertight end fittings and cable connectors. The resulting resistance is 47 ohms and the inductance about 210 henries. In service these coils and their connecting cables are buried.

AMPLIFIER SYSTEMS

Two types of amplifier designed and built at PNL have been successfully used; a DC amplifier for frequencies below 3 cps and an AC amplifier for frequencies above 2 cps. Each type together with its auxiliary equipment is described.

1. DC System[1,2]

(i) Input filter - The input filter contains two bridged-T, 60 cycle rejection sections having a total DC resistance of 18 ohms inserted between the antenna and amplifier. In some locations an RF filter is also required. Since the frequencies below 1 cps have much larger amplitudes than higher frequencies, and a chopper amplifier is used, a low pass section is not required. The input filter includes the capacitors for series tuning the detectors and a set of resistors which, if required, could reduce the "Q" of the detector circuit. A line-balance potentiometer is incorporated. The filter chassis also incorporates a 1 ohm precision copper resistor in series with the detector circuit for calibration when an air-cored antenna is used. Low thermal solder is used in the filter and DC amplifier input stage.

(ii) DC amplifier - The low frequency system uses a chopper type DC amplifier operating at 60 cps. An electrostatically shielded, specially built input transformer is used to match the chopper to the first stage of the amplifier. The chopper noise has been materially reduced by lowering the chopper-drive voltage and using a "bucking coil", fed by current which can be adjusted in phase and amplitude, to cancel out pick-up in the contacts introduced by the drive coil. Each chopper is carefully adjusted in the laboratory for minimum noise. With a source impedance of 40 ohms the maximum DC voltage gain is about 10^7. An attenuator allows the gain to be reduced in 10 db steps to -80 db. A properly adjusted instrument has a noise level of about 0.005 microvolts rms in the frequency band 0.02 to 3 cps with a 40 ohm source resistance.

Figure 3 depicts the amplifier chassis, Figure 4 the block diagram of a three component-two station installation, and Figure 5 shows a family of frequency response curves.

A monitor point for the amplified 60 cycle signal is provided in the circuit before demodulation. The signal at this point can be displayed on an oscilloscope to determine if unwanted 60 cycle pick-up is entering the amplifier through the detector circuit or if a steady DC bias such as would be produced by a thermal EMF is present. The latter may be counteracted by an adjustable bias in the amplifier whereas the former cannot be balanced out in the amplifier.

Experience has shown that the amplifier is exceedingly sensitive to certain environmental conditions and surprisingly tolerant toward others. A few of the precautions which seem to be well worth observing are detailed as follows:

(a) Installation - Heaters of the tubes must be supplied from a DC source. The amplifier should be kept as far as possible from electrical apparatus that might produce 60 cps magnetic fields (minimum distance 5 ft). The amplifiers in a multiple installation should be spaced at least 2 ft apart.

(b) The Grounding System - It is desirable to obtain a grounding system such that there is no appreciable pick-up of unwanted signals. The line balance potentiometer in the input filter will have no effect if the pick-up is negligible. Experience has shown that the interference pick-up is very much reduced if a high resistance, at least 20 megohms, is maintained between coil and shield, and between shield and ground. The ground connection should be made only at the amplifier with the detector connected as a balanced input.

(c) Thermal EMF's - An inspection of the signal at the AC monitor point may show a constant carrier signal (60 cps) which cannot be eliminated with the line balance potentiometer. This may be due to thermal EMF's in the input circuit, and can be

Superior numbers refer to similarly numbered references at the end of this paper.

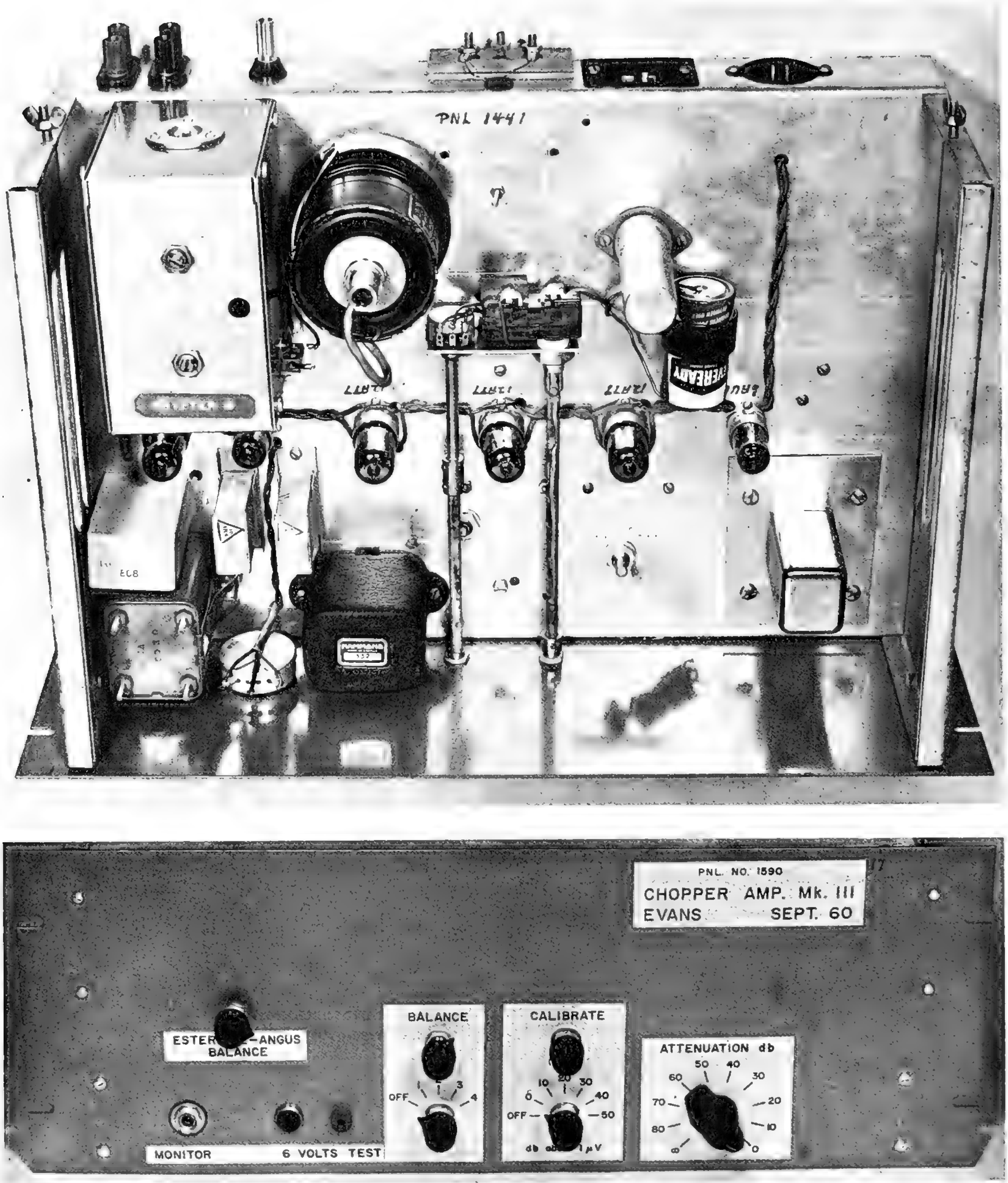

3. THE DC AMPLIFIER CHASSIS, TOP AND FRONT VIEWS.

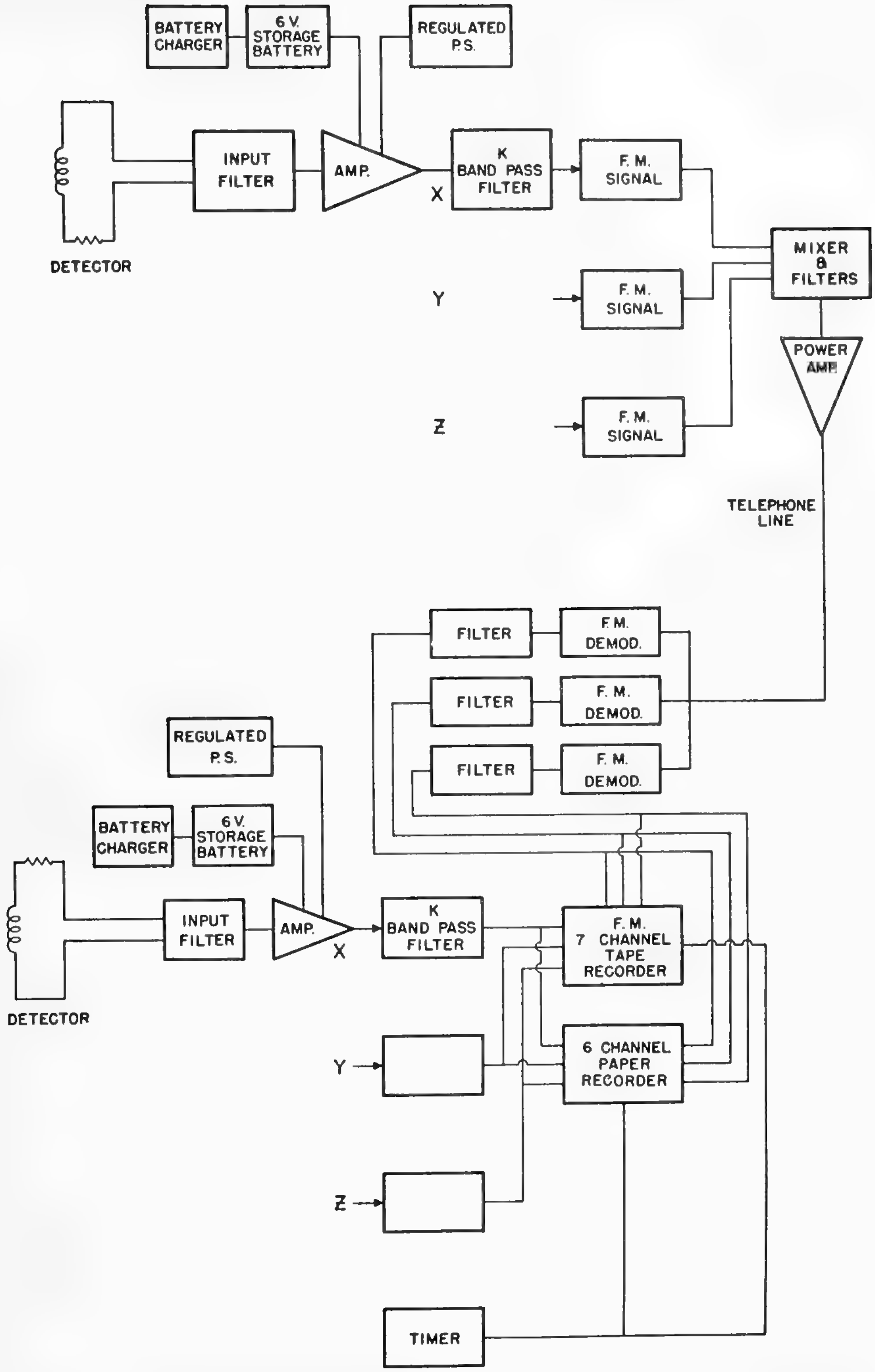

4. THE ARRANGEMENT OF UNITS IN A TWO-STATION, THREE-COMPONENT DC DETECTOR, AMPLIFIER AND RECORDER SYSTEM. THE THREE COMPONENTS X, Y, Z, SPECIFY THE CONVENTIONAL ORTHOGONAL COMPONENTS ARRAYED ON GEOGRAPHIC AXES. X_A AND X_E WERE SEPARATED IN DISTANCE BY 30 MILES.

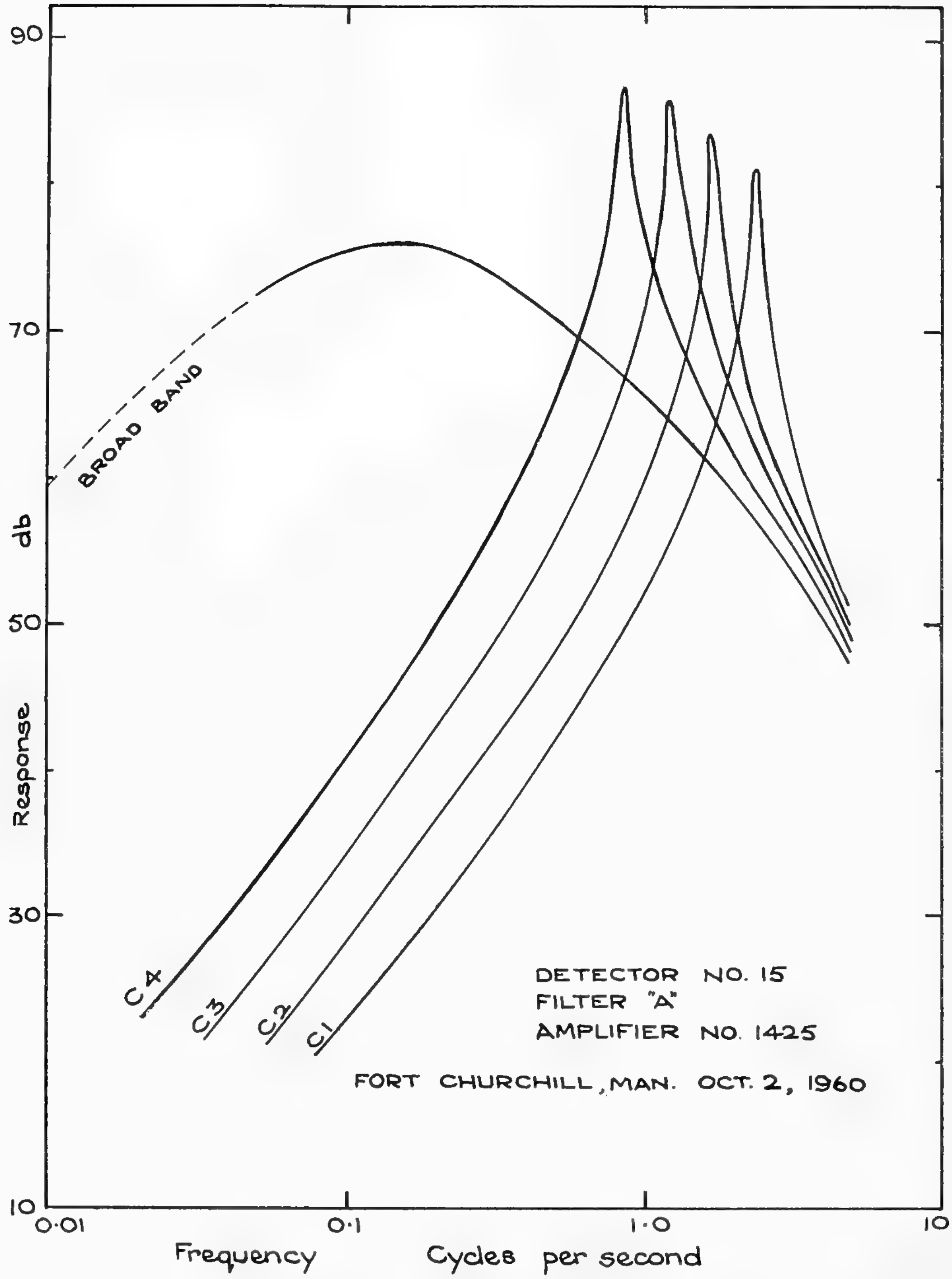

5. TYPICAL RESPONSE CURVES FOR THE DC SYSTEM. THE NOTATIONS C1 to C4 REFER TO VARIOUS SERIES CAPACITORS USED IN THE DETECTOR SYSTEM. THE CURVE MARKED "BROAD BAND" SHOWS THE RESPONSE WITHOUT TUNING CAPACITORS.

eliminated with the balance control on the front panel of the chopper amplifier which inserts a small DC signal in series with the input circuit. When the line balance potentiometer and the thermal EMF balance control are properly adjusted, there should be no steady AC signal at the AC monitor point but only a fluctuating signal. These adjustments must be made at the lowest detector signal level to prevent overloading of the amplifier at high gain settings

(iii) Outputs - Two outputs are provided on the amplifier, a low impedence balanced output for directly driving the milliammeter movement of a strip chart recorder, and a high impedance single-ended output for driving another amplifier or an active bandpass filter.

2. AC System[2,3]

The AC amplifier system, capable of accepting signals in the 2 to 40 cps range, was designed to operate on the 4000 foot circumference air-cored detector coil which has been described. Such a detector should yield 14.8 millivolts per gamma RMS at 10 cps. Because the signal level at this frequency is likely to approximate 10^{-4} gamma, or less, a sensitive amplifier is required.

(i) Input filter - The input filter is designed to pass frequencies from DC to 40 cps and to reject all higher frequencies. In addition to a 60 cps rejection section and line balance potentiometer similar to that used in the DC system, a low-pass section is required to reduce power line harmonics and RF interference which is usually of comparable amplitude to the geomagnetic activity between 2 and 40 cps. The line balance potentiometer is used to check for a satisfactory ground in the same way as with the DC system. The filter also incorporates a one ohm precision resistor for injection of a calibrating voltage.

A separate 30 cps rejection filter has been found necessary in the vicinity of Victoria but has not been required at remote sites.

(ii) Preamplifier - The preamplifier has two stages of amplification separated by a 60 cps rejection filter. The input stage is a vacuum tube amplifier, and a special low-level high step-up ratio input transformer matches the detector to the grid of the first tube of the input stage. The second stage is a transistor amplifier. The B+ and transistor stages are supplied from self-contained batteries. A 6-volt storage battery is used to supply the heater voltage. Both stages are plug-in units.

With an input transformer primary impedance of 40 ohms and a generator of internal impedance of 40 ohms, the amplifier gain from generator to output is 270,000 times. If the input signal should be large enough to overload the second amplifier stage this can be removed and replaced by a unit having no amplification.

The preamplifier noise depends to a large extent on the characteristics of the input tube, which operates under special low-noise conditions. It has been found on test to be as low as 0.004 microvolt for an input impedance of 40 ohms and a bandwidth of 2 to 30 cps, which is approximately the thermal noise level. A noisy tube can easily raise this value by a factor of ten to 0.04 microvolt which is still acceptable although regular checks should be made to avoid a further increase in noise. This is accomplished by removing the detector from the input filter and plugging in instead a dummy source which contains the resistive input impedance plus a calibration attenuator. The system noise is then compared with a small known signal.

(iii) Postamplifier - The transistor postamplifier provides the extra gain necessary to amplify small signals to the level required by the recorders. The maximum gain is about 35 db and can be reduced to zero db in 5 db steps. The maximum overall gain from a 40 ohm source to the postamplifier output is now about 1.6×10^7, times or 144 db. The postamplifier power supply is run from the 115V, 60 cps supply.

(iv) Output - The postamplifier is followed by a commercial active bandpass filter which serves to attenuate the frequencies persisting above 40 cps, primarily 60 cps, and its harmonics. The bandpass filter output can be monitored on an oscilloscope or recorded on a high-speed paper recorder or tape recorder.

In order to record the average level of activity in this frequency range continuously a rectified and integrated signal can be fed to a slow-speed paper recorder. A rectifier-integrator whose time constant can be varied from zero to 25 seconds in five steps has been used.

Figure 6 shows the block diagram of an AC amplifier installation and Figure 7 shows a typical system frequency response curve.

CALIBRATION

Two methods of system calibration are in current use. In one the calibration signal is induced into the detector circuit from an auxiliary winding of a few turns. In the other a small measured voltage is injected into the detector circuit by means of a series precision resistor and dividing network. The former is conveniently applied to compact metal-cored coils and the latter to large air-cored coils of known area-turns. Obviously the two methods behave differently because a constant current in the calibrating coil introduces a corresponding constant change of flux yielding a frequency-dependent detector voltage output, while a constant injected sinusoidal voltage is independent of frequency.

When the induction system is used the effectiveness of the calibrating current must be determined by comparison with a known flux density. This is accomplished by placing the detector under test concentric and coaxial with a multi-turn coil 200 feet in diameter which, in turn, is fed with a measured sinusoidal current over the range of frequencies desired. A single, large diameter coil was selected because it was simple to construct, is capable of accommodating detectors having a considerable range of size and configuration, and is not critical with respect to positioning the coil under test. Both axial and radial deviations from the (axial) flux density within 20 feet of the coil centre are small (less than 2%) and known. Vozoff[4] has shown theoretically that the error due to the underlying earth is less than 1% if normal conductivities, frequencies below 100 cps and a coil radius of less than 100 meters are assumed. This has been experimentally verified by noting that the effectiveness of the calibration current in the auxiliary winding is essentially independent of frequency and detector orientation. Thus neither the effect of proximity to the ground nor possible core saturation materially invalidate the calibrations.

It has been standard practice to measure the calibration voltage (or current) on the DC scale of a calibrated dual-beam oscilloscope. Hence it is practical to compare the amplifier output with the input voltage and phase over the desired frequency range.

In order to avoid the simultaneous effect of natural signals it is desirable to attenuate the amplifiers by 30 db or more during calibration. Their effect is further reduced by choosing, for routine checks, a calibration frequency where the natural signals are usually small.

The calibration signal is applied to all of the components at once thus affording a convenient check on detector polarities. In spite of care, inadvertent transpositions occasionally occur. Detailed calibrations are made every few days at a time when the background is uninteresting, but single frequency gain checks are made every few hours.

The following precautions have been found effective in reducing interference introduced through the calibration circuitry:

(i) When a voltage is injected for calibration it may be necessary to power the signal generator through an isolation transformer or to use a battery operated model. It may help to isolate the oscilloscope too.
(ii) An induction calibration circuit must use its own shielded leads, separated from the signal cables.
(iii) An RF filter has been required on some calibration circuits.
(iv) When not actually in use the calibration circuit is completely disconnected from the signal generator, oscilloscope and other components.

TIMING

A rated chronometer with electrical contacts is used to actuate timing pens on the paper charts and to provide minute and/or seconds pips on the magnetic tape. Crystal chronometers have been obtained and will be used in the future. The absolute accuracy required depends upon the signal frequencies and the resolution of the chart or magnetic tape. Radio time signals are often applied directly to one of the tape channels. All records are kept in Greenwich or Universal time.

A primary problem in timing is one of determining when an event commences.

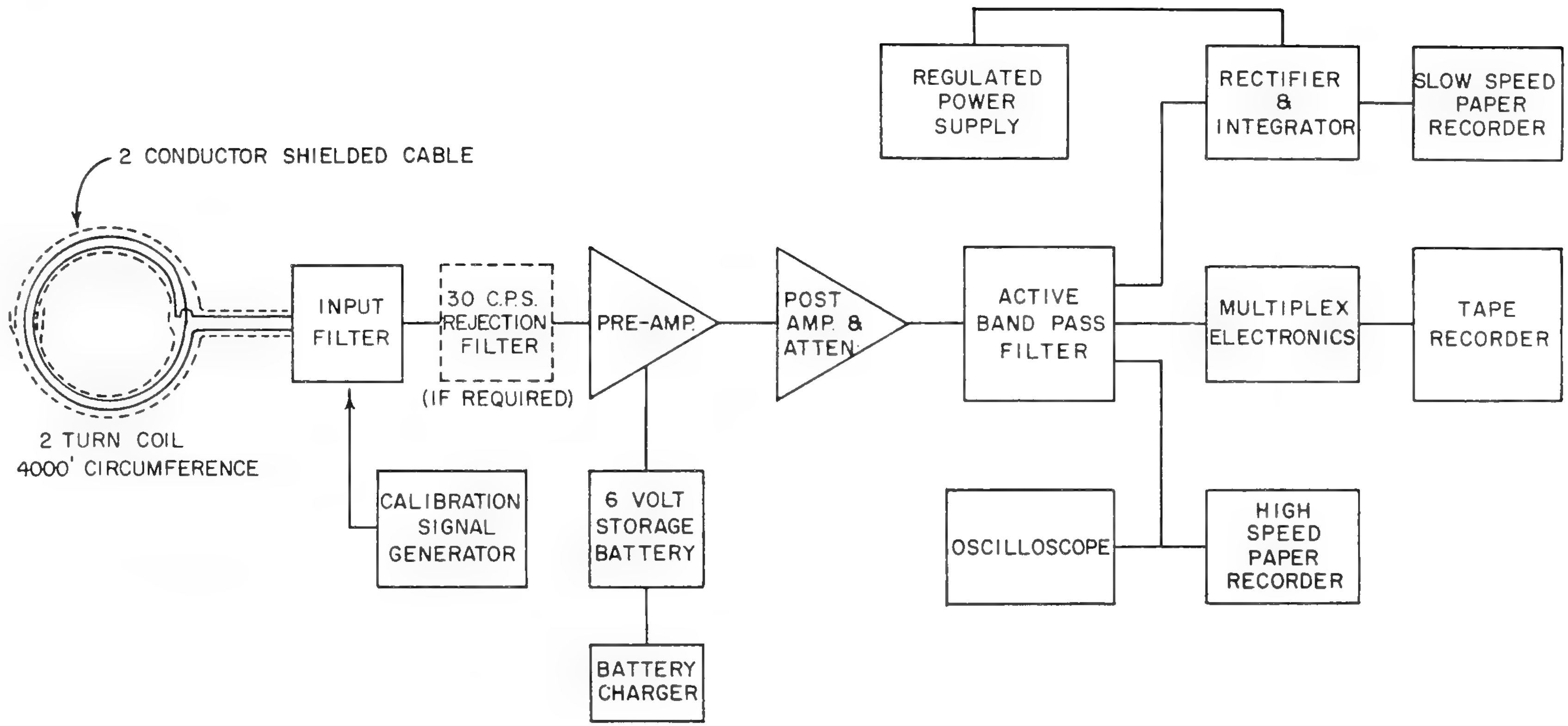

6. THE ARRANGEMENT OF UNITS IN AN AC RECEIVING SYSTEM.

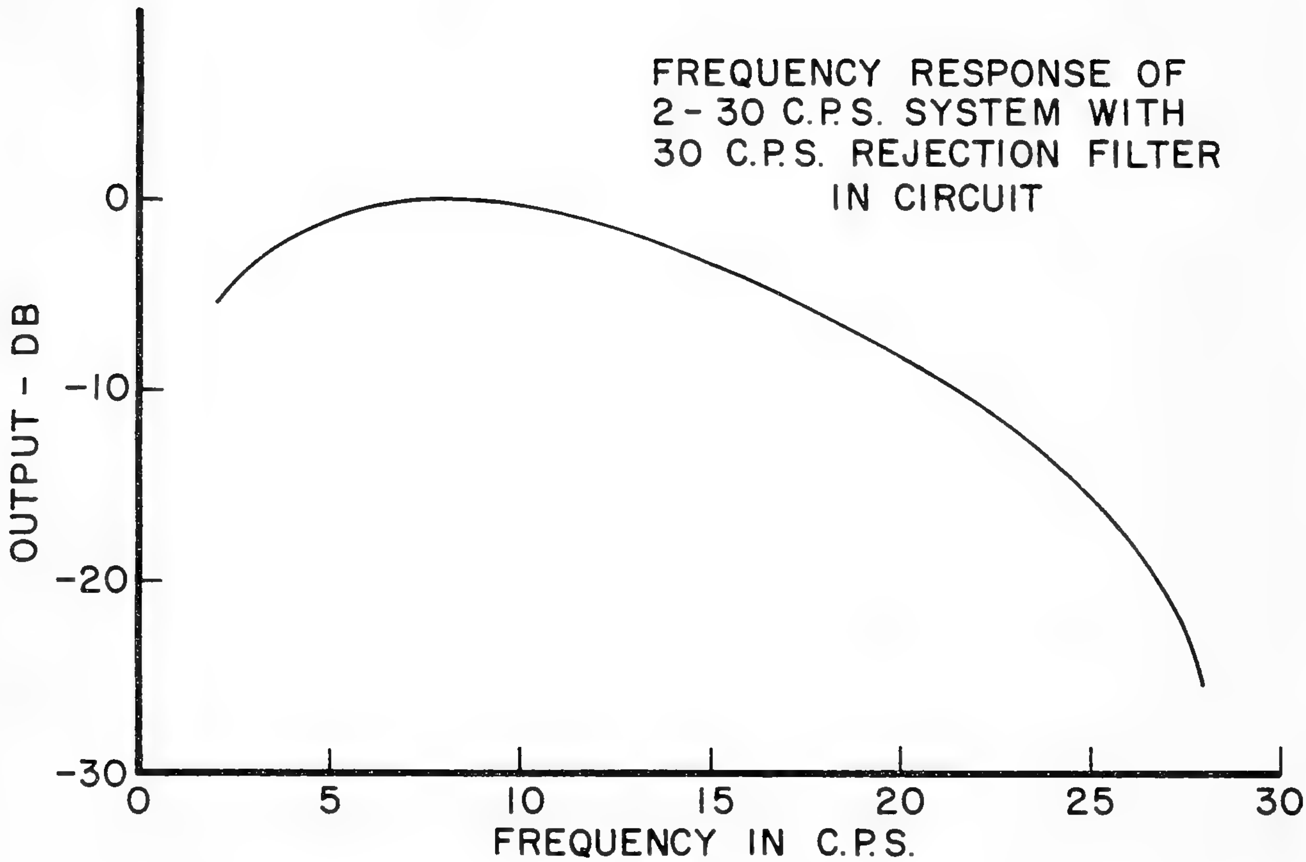

7. A FREQUENCY RESPONSE CURVE FOR THE AC SYSTEM. THE INCLUSION OF A 30 CPS REJECTION FILTER IS NOTED.

For example, a given excursion or event will appear to arrive at different times at each of the components on one station. On another station the time displacements will usually be distributed quite differently among components. These displacements are often a significant proportion of the signal period. Hence it is difficult to determine the absolute time of the commencement or peak of an event. Correlation techniques on the total "pulsating magnetic field" may be used in some cases to minimize the uncertainty.

REFERENCES

1. "The Low Frequency Electromagnetic Detector-Amplifier System Used During PNL Field Operation at S.E.S., June, 1960", by D.J. Evans, PNL Laboratory Note 60-11, July 1960.

2. "The Pacific Naval Laboratory - Stanford University Conjugate Point Experiment", by D.J. Evans, S. Horner, J.E. Lokken, J.A. Shand and C.S. Wright, PNL Laboratory Note 60-41, December 1960.

3. "Measurement of the Vertical Component of Magnetic Micropulsations in the 2 to 40 cps Band", by D.J. Evans, PNL Laboratory Note 60-34, November 1960.

4. Private communication from K. Vozoff, University of Alberta.

OXYGEN AND CARBON DIOXIDE INSTRUMENTATION

by JOHN W. KANWISHER, Research Associate
Woods Hole Oceanographic Institution
Woods Hole, Massachusetts

The sum of the biological processes going on in the oceans is frequently considered in terms of the opposing processes of photosynthesis and respiration. In most cases we can consider these phenomena as reciprocally exchanging equivalent amounts of oxygen and carbon dioxide (O_2 and CO_2), with the environment. For every CO_2 molecule removed from solution in sea water during the ph tosynthetic production of carbohydrate an O_2 molecule is released. An opposite exchange occurs when this carbohydrate is later oxidized in the respiration of some plant or animal. We can represent this schematically as:

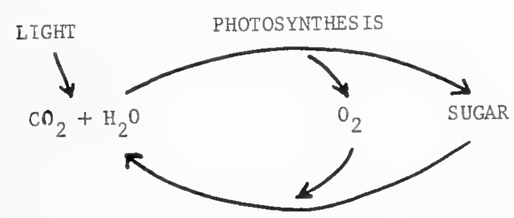

A quantitative knowledge of this gas exchange in a water mass is basic to any estimation of the overall biology taking place. The resulting variation of these gases in the water is also frequently of hydrographic interest because of the way biological activity types a water mass. In fact, O_2 content probably follows temperature and salinity as the most measured hydrographic variable.

One would of course like to have as complete a picture as possible of the distribution of any variable being studied. With O_2 we must currently be satisfied with a relatively few points in the vastness of the oceans. Most of these points have been determined only once or twice, so our knowledge of time variations is equally hazy. In addition, the only method currently in use involves a chemical titration and is surrounded by considerable uncertainty. Direct measurements of CO_2 are nearly nonexistent. Some new techniques which allow continuous recording of the O_2 and CO_2 dissolved in sea or fresh water will be described. O_2 has been determined polarographically and CO_2 has been monitored by infrared absorption of a gas phase which has been equilibrated with the water. The methods are applicable to both laboratory and field studies. Some of both will be covered.

I. OXYGEN ELECTRODE RECORDING

Recent references describe a polarographic electrode suitable for recording dissolved O_2 [1,2]. It consists of a platinum electrode separated from the medium being measured by a layer of polyethylene or teflon, both of which are markedly permeable to molecular O_2. As this gas diffuses through the surface, it reacts immediately at the platinum surface to form OH^- ions. The OH^- ions diffuse through the film of electrolyte behind the membrane and react at the Ag surface to form Ag_2O, which appear as a dark coating. Thus the eventual fate of the dissolved oxygen is to appear as Ag_2O. Although the Ag is actually being consumed, in practice it will last semi-indefinitely. The current passing through the electrode is proportional to the rate of diffusion, and this in turn depends on the external tension (partial pressure). We thus have in essense a device for measuring the quantity of dissolved O_2 since it varies directly with the tension (Henri's law).

The electrode assembly is shown in Figure 1A. A Ag-Ag_2O electrode is concentric around the center platinum electrode. A plastic film is stretched over this and traps a small amount of alkali behind it. The platinum is kept at -.7 volts. When there is no O_2 the electrode current is very close to zero. It increases linearly with increasing O_2 tension in the external medium. A more complete treatment of the electrode occurs in the original references cited.

It should be kept in mind that the electrode is a tension-measuring device. It will read the same in fresh or salt water if they are equilibrated with the same gas mixture, although the 3-1/2 per cent salt content reduces the gas solubility by 25 per cent. Thus its reading must be referred to the solubility of the liquid being measured. The extremes of salinity in the open sea, however, cause less than a 2 per cent error. It is worth noting that the electrode will work in any liquid which does not attack the plastic membrane, even gasoline.

Such an electrode has been operated for as long as 6 weeks with less than 25% change in current. Since no abrupt changes occur, it is sufficient to calibrate only once per day to provide values good to a few per cent. If there is any doubt about the condition of the electrode it can be quickly remade with new plastic and KOH. Operation for a long

Superior numbers refer to similarly numbered references at the end of this paper.

period of time is aided by placing a disc of filter paper over the end of the electrode under the plastic. However, this increased the time constant, at least several-fold.

It has been found empirically that the reference electrode must "see" the solution directly through the plastic film and so should not be covered by the retaining ring. This observation is inconsistent with the view that the OH^- ions diffuse only through the layer of electrolyte, and it is not yet understood.

Such electrodes are easy to make. The silver and platinum parts are cast in some plastic such as an epoxy. Electrical connections are made to the back of the electrodes. Care must be taken that only silver and platinum are exposed on the outside. Any polyethylene can be used. Thicknesses of .001 to .002 inches give convenient diffusion rates and response times.

This polarographic technique is a valuable tool in experimental physiology. I have used electrodes to follow oxygen changes in a 1 ml. chamber containing a bit of seaweed or a single copepod. It has also been just as readily applied in a 55 gallon oil drum, following the respiration of a 30 kg. shark. In one instance it was used to measure the oxygen in the expired breath of a whale. These indicate to some degree the versatility of such electrodes. Here, however, I will only describe their use for in situ recording in the ocean.

This is probably the most difficult and also the most desired oceanographic task to which they might be applied. To accomplish it one must overcome several inherent shortcomings in the electrode. These will be discussed in turn.

A. Stirring

The electrode current represents an actual consumption of molecular O_2 from the solution being measured. This depletes the thin layer of liquid immediately in front of the plastic membrane. Stirring the solution renews this depleted surface layer. If the solution is not stirred this layer will progressively lose more of its O_2 and a gradient will be set up in the liquid. In such a situation the flux of O_2 reaching the platinum will be limited by a combination of the diffusion resistance through the solution as well as through the plastic. Since anything that changes this resistance will alter the electrode current it is necessary to maintain constant diffusion conditions. The most direct way of realizing this is to mix the solution so strongly that it contributes a negligible fraction to the overall O_2 diffusion resistance. This can be accomplished in over-the-side work by running the winch fast or accentuating the current past the electrode by funnel arrangements or small stirring motors.

In laboratory applications the stirring may be below saturation as long as it is constant. A synchronous motor rotating a large magnet (from a magnetron) can be used to induce rotation in a small teflon corrected magnet over a considerable distance. I have used such a method to stir small containers deep inside a water bath. The constant speed of the motor insures a steady record.

Figure 1B shows an electrode holder for line monitoring. The stream is directed against the plastic film directly over the Pt electrode. This creates a maximum of effective stirring with a minimum of flow. If the incoming tube is brought very close to the electrode a flow of 10 ml/min. may give a saturation (maximum) electrode current.

Thinner and more diffusible membranes (i.e. teflon as compared to polyethylene) present less diffusion resistance. This produces a larger electrode current as well as making its response faster. But it accentuates stirring difficulties since the diffusion resistance in the liquid must be likewise reduced. Thus a compromise must be struck between sensitivity, speed, and stirring difficulties.

B. Speed of response

An electrode with a .001" thick polyethylene layer will show a 90 per cent response in about 15 seconds. If the silver area is large (more than 10 times) compared to the platinum, the response to a step function will be very closely exponential. With much less silver area, there is a long slow component in the current. This presumably represents some polarization phenomena at the silver surface.

One would like a faster electrode for vertical recording in the sea since with a fast winch the electrode can cover more than 100 meters in the 90 per cent response time.

From diffusion theory it can be shown that the time to reach diffusion equilibrium across a barrier of thickness t is proportional to $\frac{t^2}{\text{diffusibility}}$. This suggests the dual approach of thinner and more diffusible films to lessen the time. Teflon is better than polyethylene by this criterion since O_2 diffuses through it about 3 times faster. It is also tougher in thin films. I have recently used electrodes in the laboratory with .00025" teflon which showed a 90 per cent response in 3 seconds. As already indicated, however, the stirring problem then is more severe.

C. Pressure response

When the electrode is exposed to a constant O_2 tension, its current decreases with increasing hydrostatic pressure. This dependence is shown in Figure 2 for pressures up to 15000 lb/in^2. (which equals about 30,000 ft. in depth). Over the first 5000 pounds the curve is approximately linear. For each 1000 feet increase in depth (500 pounds in hydrostatic pressure) the current decreases about 3 per cent. Beyond 5000 pounds the rate decreases. At 15000 pounds only 30 per cent of the initial electrode response is left.

The decreasing electrode current represents a decrease in the permeability of the plastic film to the diffusion of O_2. The shape of the curve indicates that diffusion through the plastic is more of a pore-type phenomenon than one of the gas being in solid solution. The first part of the curve is the same for teflon and polyethylene so there seems little chance of decreasing this undesirable pressure dependence by using a different plastic. The only approach at this time seems to be to compute it out of the raw signal. Fortunately much of the most interesting O_2 variations are close to the surface where the pressure dependence can either be neglected or assumed linear.

D. <u>In situ recording</u>

The electrode has been tested twice for recording vertical profiles in the ocean. The first measurements were done by Dr. Richardson with his ingenious free-falling instruments. The electrode current was recorded in the instrument along with temperature. Depth was determined by time and the rate of fall. The current was then corrected for temperature and pressure to obtain O_2 concentration. The location off Bermuda is one where frequent chemical determinations of O_2 are made. The two curves in Figure 3 show essential agreement. The electrode showed interesting detail below the O_2 minimum. These would ordinarily not be seen from the usual spot measurements made from Nansen bottle samples.

I later lowered an electrode along with a pressure transducer on the end of a 3-mile length of well-logging cable. No amplification was needed. This allowed direct x-y recording of O_2 <u>vs</u> depth during the lowering. The curve in Figure 4 shows a well mixed surface layer with a sharp drop in O_2 at 125 meters. This drop did not come at a thermocline. The temperature actually increased .7° C. In such a case O_2, more clearly than temperature or salinity, shows two water types. A regular hydrographic station was made at this time. The Nansen bottles were placed at the standard depths and the chemical determinations from these are included on the plot. One can easily see the difficulty of accurately determining the shape of the curve from such spot values. If the electrode does not replace the chemical method it can at least be used to determine the best depths at which to place the Nansen bottles.

I have also lowered the electrode from rowboats for continuous O_2 profiles in lakes. Initially an uncorrected electrode was used and temperature was simultaneously recorded. The advent of solid state choppers has allowed me to record the corrected O_2 value directly, using thermistor temperature correction, with light battery-operated apparatus.

II <u>CO_2 MEASUREMENT</u>

The measurement of CO_2 requires a different approach from that used for O_2. It occurs in only 1/600 the concentration in air (.03 as compared with 21 per cent). But its chemical and physical properties result in its being nearly 10 times as concentrated in sea water (45 ml/l <u>vs</u> 5 ml/l O_2). We can summarize this chemistry by the following equations:

AIR CO_2

$$CO_2 + H_2O \rightleftharpoons H_2CO_3 \rightleftharpoons HCO_3^- \rightleftharpoons CO_3^=$$

SEA WATER

$\uparrow\downarrow$ COMPLEXES

Any change in the amount of CO_2 in this system will, through these reversible equilibria, alter the values of pCO_2 and pH. I have been able to use the former as a convenient and sensitive index of such changes [3].

The measurement of CO_2 is accomplished by equilibrating sea water with a gas phase and then measuring the CO_2 concentration in the gas. The partial pressure in the gas is then equal to that in the water, if equilibration is gentle and complete. It is an attractive approach since CO_2 in gas mixtures can be determined to better than 1 part per million by means of a modern infrared analyzer.

We can expect surface sea water to be more or less equilibrated with the atmosphere above the surface. Since air contains 300 ppm CO_2, the values of pCO_2 in the water will center about this value. With the infrared analyzer technique outlined it is possible to determine pCO_2 in this range to 1 per cent (± 3 ppm).

The chemistry of CO_2 outlined in the above equations results in pCO_2 being non-linearly related to the total amount of the gas in sea water. This makes it necessary to calibrate the apparatus by introducing known changes in total CO_2 and measuring the resulting partial pressure. Figure 5 shows the result of such a procedure. It can be seen that there are very large changes in the partial pressure for the variations in total CO_2 we know to exist in the deep ocean waters. When such water is anaerobic, or nearly so, its pCO_2 may be 10 times that of equilibrated surface water. I have tested this in Eel Pond, a small bay here in Woods Hole. It has a sill at its entrance which prevents free exchange of the bottom water. Sewage from the surrounding houses creates a large biological O_2 demand (CO_2 production). The bottom

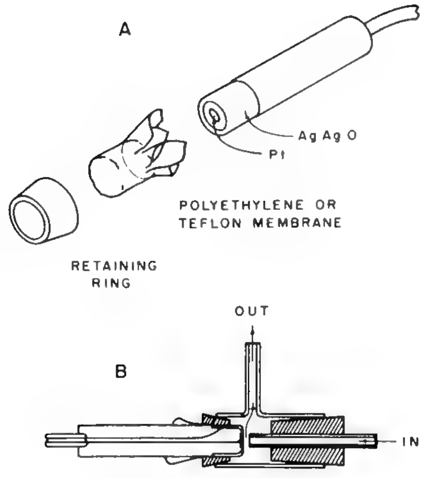

Figure 1

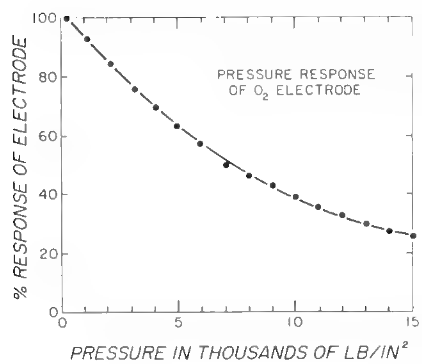

Figure 2

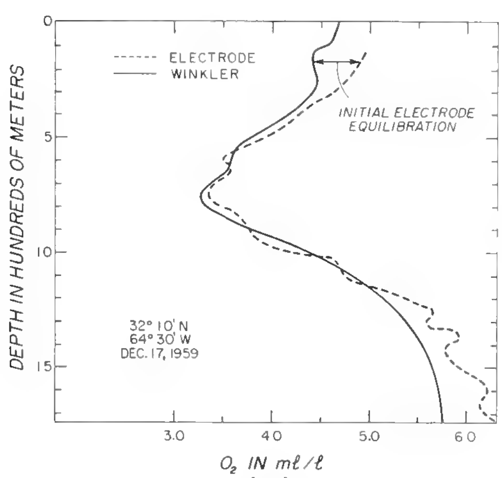

Figure 3

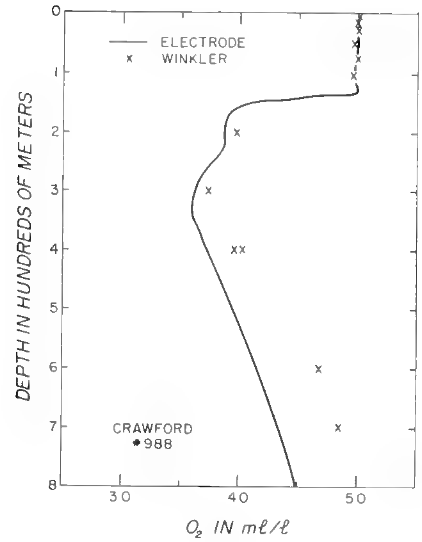

Figure 4

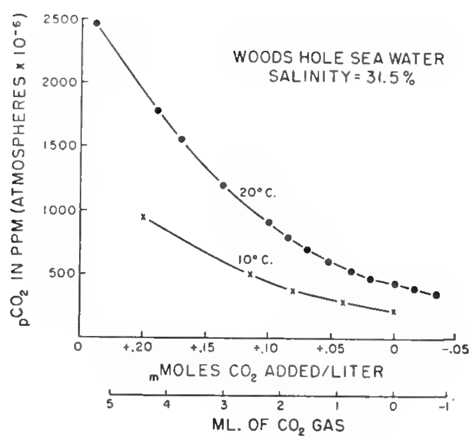

Figure 5

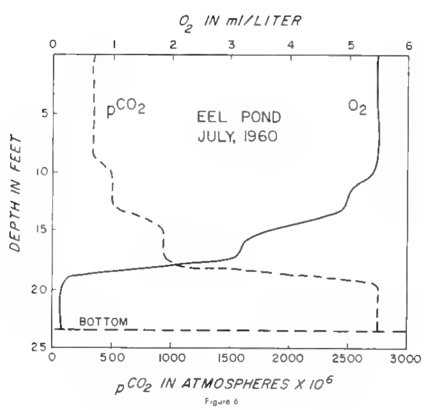

Figure 6

layers go anaerobic in mid-summer. I have measured the profiles of pO_2 and pCO_2 (Figure 6). The surface waters support a large algal population due to the supply of nutrients from the sewage. This results in a diurnal variation in both gases due to photosynthesis during the day and respiration at night. The variation is manyfold greater than in the unfertilized ocean immediately outside.

Continuous-track measurements of surface water pCO_2 have recently been made between Woods Hole and the equator. This showed interesting latitude variations in the tropics. The changes occur at points where we have some evidence that there are major east-west currents. I feel that such pCO_2 variations are due to different amounts of upwelling of the high CO_2 intermediate water.

In local waters along this coast there are variations in pCO_2 during the year. The spring plankton bloom is a time of rapid photosynthesis. This removal of CO_2 may drop the pCO_2 to below 200 ppm. In the middle of the summer much of the spring growth is decaying and the partial pressure may then be as high as 550 ppm.

CO_2 is better than O_2 as an index of recent biological change because it exchanges with the atmosphere some 15 times slower. In the spring and summer, weather conditions tend to be gentle and the gas exchange across the sea surface is slow. pCO_2 can then be used to tell the time-integrated amount of photosynthesis and respiration. Storms during the winter tend to more quickly bring the oceans and the atmosphere back into equilibrium whenever biological events change the amount of CO_2 in the water.

SUMMARY

These techniques of O_2 and CO_2 recording represent my answers to problems that arose in my own research. It has been necessary for me to develop them because there has been no one else to fill the need. There may be more suitable means when real engineering skill is applied. However, I feel that most useful new instruments result from a current research need.

REFERENCES

1. Bolin, B., and Eriksson, E., 1959. Rossby Memorial Volume (Rockefeller Institute Press, New York), pp. 130-142.

2. Carritt, Dayton E. and Kanwisher, John W. 1959. Analytical Chem. 31: 5-9.

3. Kanwisher, John, 1960. Tellus XII(2): 209-215.

WHOI Contribution No. 1229

AN ANALYSIS OF A CLASS OF PATTERN RECOGNITION NETWORKS

by LAVEEN KANAL
General Dynamics/Electronics
Rochester, New York

ABSTRACT

Recent articles show that considerable research is currently being devoted to the realization of Pattern recognition by a class of adaptive networks. This paper presents a few results of studies aimed at finding the relationships between work in this area and various classification procedures, and seeing how efforts in machine recognition of patterns can be reconciled with some formal principles in decision making.

INTRODUCTION

Research in classification procedures has been largely concerned with two situations. One, where an individual (pattern, sound) is to be assigned to one of k groups, with the numerical value of k known but information on the probability distributions of observables ranging from complete ignorance of the functional form of the distribution to the case where the functional form and all parameters are known. The other situation is similar except that the value of k is unknown. The first case is typical of many simple pattern and limited vocabulary speech recognition situations. Thus for example, it may be desired to recognize a sound as being one of k known sounds. The second situation may be encountered for example, in the identification of targets from underwater return patterns when only limited information is available. Only the first situation is considered here.

Let a pattern be specified by the results of a number of measurements or tests, x_i, $i=1,2,...N$. In any given instance, the results of the tests or measurements may be represented by $x= (x_1, x_2,...x_N)$. The case where the x_i are either 0 or 1 is considered here. This situation would obtain for instance when a pattern is placed on an "artificial retina" with the outputs of the retina elements being quantized in this manner. The cases where the x_i, $i=1, 2,..N$ can take on a number of discrete values and where the x_i are continuous are considered elsewhere[1].

Let $p (x_1, x_2.....x_N)$ denote the joint probability distribution of the x_i in a given group. In section 1 a parametric representation for this distribution is presented. In this context the classification cabablities of some proposed pattern recognition networks are

"Superior numbers refer to similarly numbered references at the end of this paper."

examined in section 2. Comments on a few iterative techniques and some experimental work conclude the paper.

1. A representation of the joint distribution. Let X denote the set of all points $x=(x_1, x_2, \ldots x_N)$ with each $x_i=0$ or 1. Since there are 2^N points in X any parametric description of arbitrary probability distribution will, in general, require (2^N-1) independent parameters. The particular parametric representation considered here is due to Bahadur[2].

Using E_p to denote the expected value when the underlying distribution is $p(x)$, define for each $i=1, 2\ldots N$,

$$m_i = p\{x_i = 1\} = E_p(x_i), \quad o < m_i < 1;$$

$$z_i = (x_i-m_i)/\sqrt{m_i(1-m_i)} \;;$$

$$r_{ij} = E_p(z_i z_j), \quad i<j \;;$$

$$r_{ijk} = E_p(z_i z_j z_k), \quad i<j<k \;:$$

$$r_{12..N} = E_p(z_1 z_2 \ldots z_N).$$

Further define

$$p_{1}(x_1,x_2,\ldots x_N) = \prod_{i=1}^{N} m_i^{x_i}(1-m_i)^{1-x_i},$$

so that $p(x_1,x_2,\ldots x_N)$ denotes the joint probability distribution of the x_i when (1) the x_is are independently distributed and (2) they have the same marginal distributions as under the distribution $p(x)$. It is shown by Bahadur that for every $x=(x_1,x_2,\ldots x_N)$ in X,

$$p(x) = p_{[1]}.f(x)$$

where

$$f(x)=1+\sum_{i<j} r_{ij}z_i z_j + \sum_{i<j<k} r_{ijk}z_i z_j z_k + \ldots + r_{12\cdots N}z_1 z_2 \ldots z_N.$$

The 2^N-N-1 correlations and the N marginal frequencies m_i are the parameters which determine the probability distribution $p(x)$. In order that an arbitrary set of 2^N-N-1 real numbers r serve as the correlation parameters of a probability distribution $p(x)$ for any set of numbers m_i with $o<m_i<1$, it is necessary and sufficient that $f(x)$ be non-negative for each x.

The distribution $p(x)$ can now be approximated by distributions of lower order. Thus $p_1(x)$ is a first order approximation to $p(x)$,

$$p_2(x) = p_1(x).\left[1+\sum_{i<j} r_{ij}z_i z_j\right]$$

is a second order approximation to $p(x)$, and so on. For $1 \leqslant m < N$, the approximation $p_{[m]}(x)$ has the interesting and useful property that it is the only distribution of order not exceeding m, under which any set $\{x_{j1}, x_{j2}, \ldots x_{jm}\}$ of m variables has the same joint distribution as under the given $p(x)$. Of course, approximations to $p(x)$ may also be obtained by retaining various selected terms in the expansion for $f(x)$ and dropping the remaining terms. Because any approximation to $p(x)$ is obtained by dropping terms of $f(x)$ a classification procedure based on it will not do as well as the same procedure when $p(x)$ is used.

2. Application to the analysis of some pattern recognition networks. The representation for the joint distribution $p(x)$ can now be used to examine the capabilities of various pattern recognition networks which have been proposed. Typically[3] these are linear summation networks with thresholds (see Fig.1), which operate on the weighted outputs of selected groups of "retina" elements, the selection being usually random. Variations on this scheme are reported by Hawkins[4] from whose article Fig. 2 is taken.

Consider Fig. 1 first. Of the total $x=(x_1, x_2, \ldots x_N)$ each summation unit gets some subset, with the x_i's multiplied by variable weights. Let a_{ij} denote the weights between the retina elements and the summation units, where a_{ij} can take on the value o, and let T_k be the thresholds for the response units. Then for a given response unit, say No. 1 the operation for producing an output is described in general by

$$(a_{11}x_1 + a_{21}x_2 + \ldots + a_{N1}x_N)$$
$$+ (a_{12}x_1 + a_{22}x_2 + \ldots + a_{N2}x_N)$$
$$+ \ldots\ldots\ldots\ldots > T_1$$
$$\text{or} \quad \sum_{i=1}^{N} a_i x_i > T.$$

Consequently a weighted sum of input variables is used to perform classification for the type of network described. Rather than obtain the coefficients $(a_1, a_2, \ldots a_N)$ from assumption concerning the functional forms of the probability distributions or from a program of estimation, interest has centered on starting from an arbitrary initial state $(a_1', a_2', \ldots a_N')$ and using iteration based on experience, i.e., some learning procedure, to go from the initial state to a desired final state.

The evaluation of the classification capabilities of the network in its final state is considered here. The problem of using experience to go from an initial state to a final desired state is commented on in the next section.

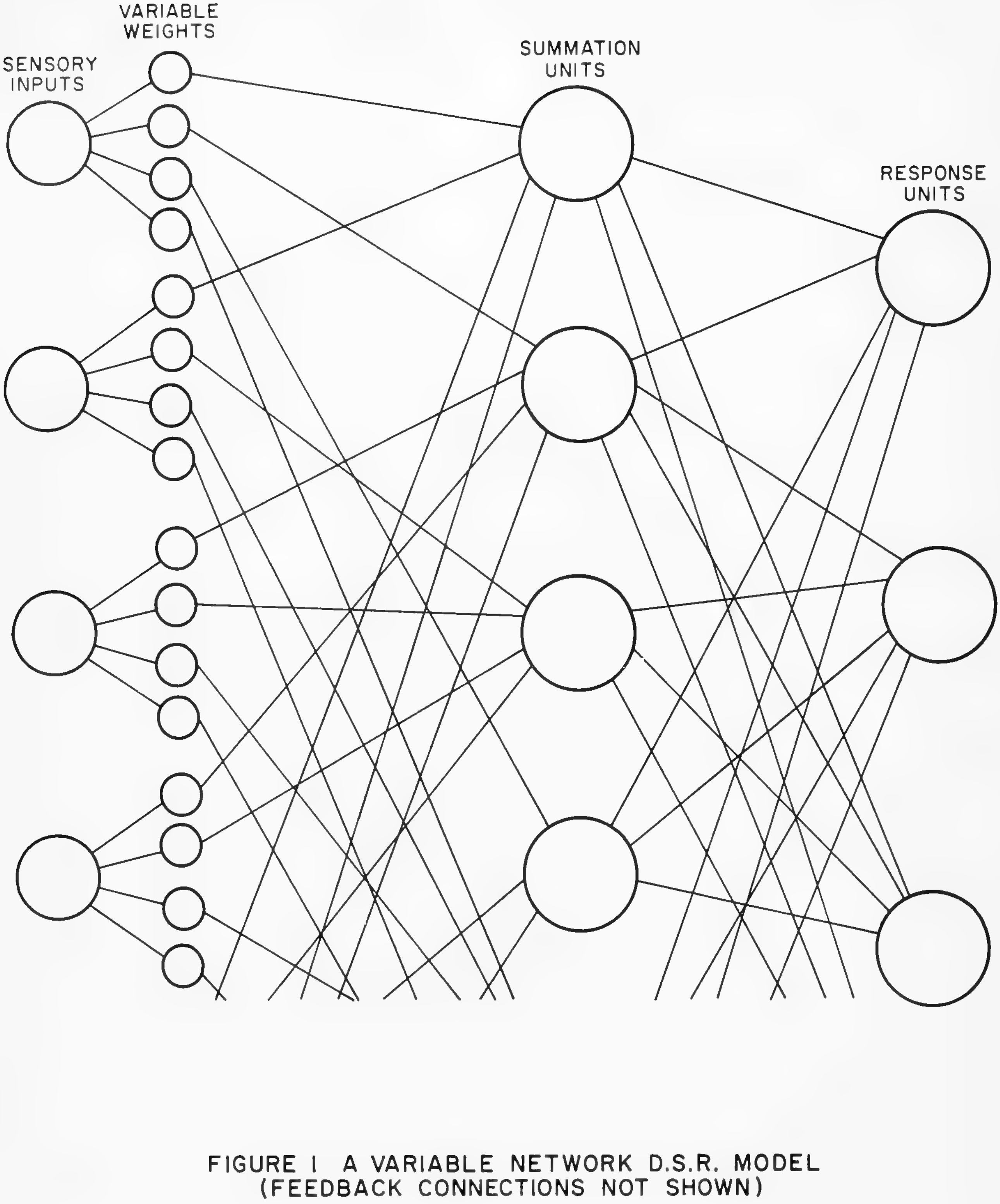

FIGURE I A VARIABLE NETWORK D.S.R. MODEL
(FEEDBACK CONNECTIONS NOT SHOWN)

The classification criterion used by the pattern recognition network is evaluated by comparing the resulting error curve with those obtained from likelihood ratio classification functions resulting when different approximations to the joint distribution are used. It is also compared with some well known intuitive classification procedures based on linear functions of the variables x_i. To simplify the exposition only the case of two groups is treated here.

Let $p(x/i)$, i=1,2., denote respectively the probability distribution for x under group 1 and group 2. Then the likelihood ratio regions for classification are defined by:

$$R_1: L(x) = \frac{p(x/1)}{p(x/2)} > t;$$

$$R_2: L(x) \leqslant t.$$

Thus if $L(x) > t$, the pattern is classified as belonging to group 1, otherwise the pattern is classified into group 2. The error curve can be obtained by computing the probabilities of misclassification for different choices of the threshold t. For a given threshold, the probability of incorrectly classifying a pattern from group 1 into group 2 is given by

$$u_t = \sum_{x:L(x) \leqslant t} p(x/1)$$

and the probability of incorrectly classifying a pattern from group 2 into group 1 is $v_t = \sum_{x:L(x) > t} p(x/2)$. The classification functions and corresponding networks which result when various approximations to $p(x)$ are used in a likelihood ratio procedure can now be derived.

If a first order approximation is used, $p(x)$ is replaced by $p_{[1]}(x)$. This implies an assumption of independence of x_i. Letting

$m_i = E_{p(x/1)}(x_i)$ and $n_i = E_{p(x/2)}(x_i)$, the likelihood ratio

$$L(x) = \frac{\prod_{i=1}^{N} m_i^{x_i}(1-m_i)^{1-x_i}}{\prod_{i=1}^{N} n_i^{x_i}(1-n_i)^{1-x_i}}$$

taking the logarithn gives $\sum_{i=1}^{N} (a_i x_i + c_i)$

where $a_i = \log \frac{mi}{n_i} \frac{(1-n_i)}{(1-m_i)}$, and $c_i = \log \frac{(1-m_i)}{(1-n_i)}$.

The summation over c_i can be absorbed in the threshold and a particular weighted sum is obtained for the classification function. If a priori probabilities are included, one gets the cognitive nets suggested by Minsky [5],

The second order approximation $p_{[2]}(x)$ neglects all correlations except those of the second order, thus implying that the joint distribution for the x_i is a multivariate normal distribution. If the further assumption is made that the groups have equal covariance matrices (no assumption of statistical independence of the x_i is made) then it can be shown[6,7] that the likelihood ratio, which is now the ratio of two multivariate normal density functions which differ only in their means, leads to a linear function of the x_i, called the discriminant function, given by

$$\sum_{i=1}^{N} a_i x_i, \text{ where } a_i = (q_{1i}d_1 + q_{2i}d_2 + \ldots + q_{Ni}d_N),$$

where q_{ji} are elements of Q the inverse of the common covariance matrix, and $d_j = m_j - n_j$ $(j=1,2,\ldots N)$. This function, which according to the likelihood ratio is optimum for the case of continuous variables with multivariate **normal** distributions and equal covariance matrices in the group is, for the case of arbitrary distributions the linear function introduced by Fisher[8]. The sense in which maximum discrimination between the two groups is provided by Fisher's discriminant function is to choose the coefficients a_i; such as to maximizes the ratio

$$\frac{(\sum a_i d_i)^2}{\sum_{i=1}^{N} \sum_{j=1}^{N} a_i a_j q^{ij}}$$

where q^{ij} are elements of the covariance matrix Q^{-1}. It is the linear function which maximizes the variance between samples relative to the variance within samples[6,7].

Without the assumption of equal covariance matrices in the groups, even the second order approximation would result in a network involving multipliers. So would higher order approximations of the form $p_{m]}(x)$ or other approximations which neglect all terms in the expansion of $f(x)$ except for the first term and a particular higher order correlation.

If the total distributions $p(x/i)$ are used along with a priori probabilities and costs, the networks which result are those derived by Chow[9]. The best error curve is of course obtained when the complete joint distributions are used.

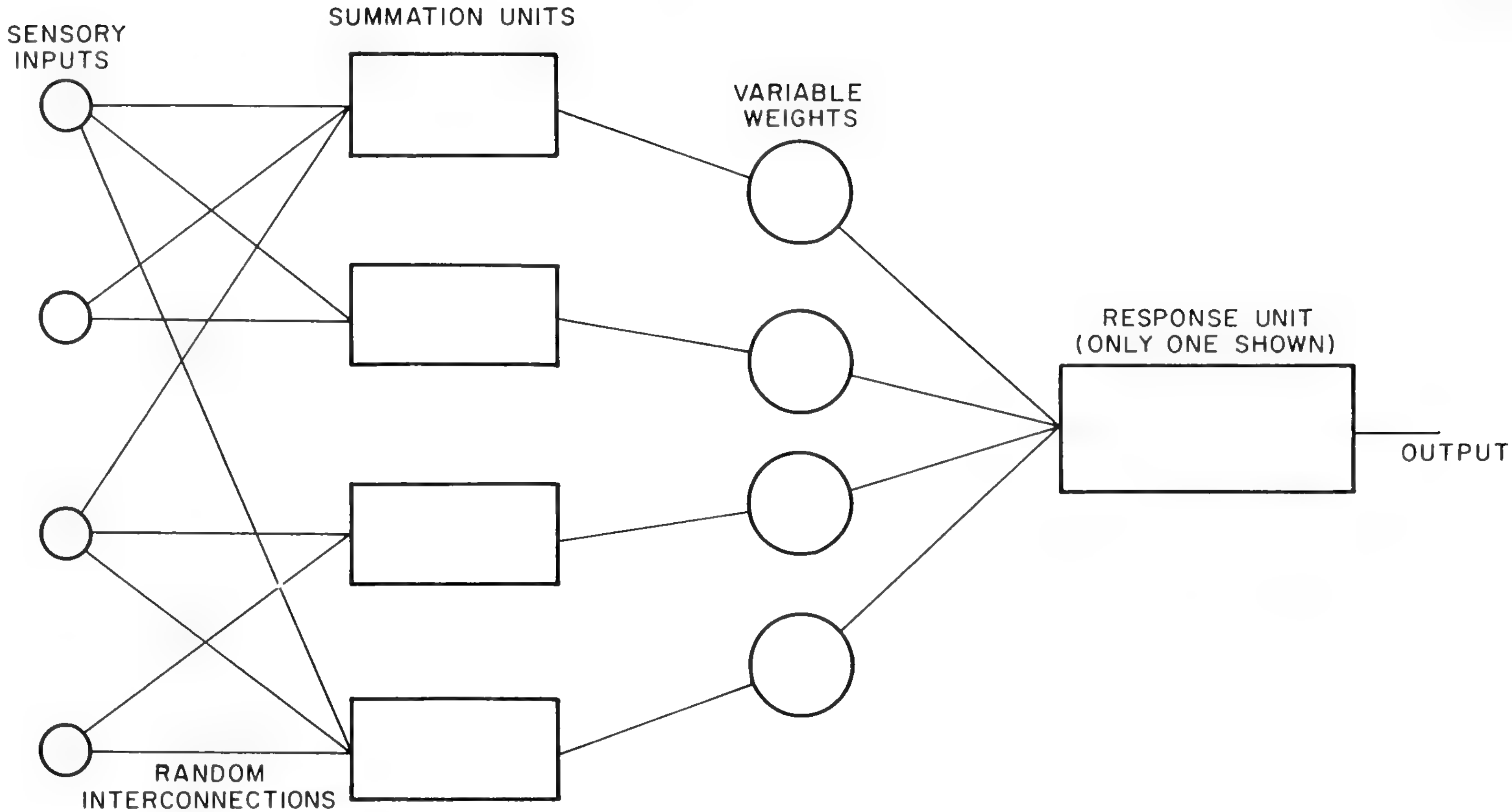

FIGURE 2 PERCEPTRON TYPE LINEAR SUMMATION NETWORK FOR PATTERN RECOGNITION (AFTER HAWKINS)

For some given classes of patterns the classification provided by functions based on approximations to $p(x)$ may be quite acceptable. In view of their simple implementation, a weighted sum of the x_i, or even a unweighted sum or score of the x_i are attractive candidates for classification functions. However, their worth as classification functions in a given context can only be evaluated to the extent that the deterioration in the error curve or risk curve with respect to the optimum is assessed.

It is known that when using procedures which are not optimum, a classification procedure based on a subset of the x_i may do better than a procedure based on all the x_i: this has been found, for example in a slightly different context, in the application of discriminant functions to speech patterns. It is also known that for some situations, when using approximate procedures, dividing the x_i into a number of (mutually exclusive) subsets s_j, deriving classification functions f_j based separately on the s_j and using f_j to obtain a final classification function F can be better than a similar function based directly on all the x_i. This is accomplished to some degree by learning networks such as those of Fig. 1 and Fig. 2, in which subsets of the x_i are selectively connected to summation units. However, the x_i have usually been selected by a random method. Tailoring the grouping of the x_i's to given classes of patterns will generally give better results.

In the network of Fig. 2, subsets of the x_i, selected in a random manner, are connected through fixed weights to summation units with with thresholds, the outputs of a number of these summation units being then multiplied by weighting coefficients, summed and compared against a threshold in the response unit. Let b_{ij} be the fixed weights between the retina elements and the summation units, where b_{ij} can be 0. Let T_j be the thresholds for the summation units, W_{jk} the variable weights between summation units and response units, and T_k the thresholds for the response units. Also, let y_j be the outputs from the summation units with y_j being 0 when the threshold T_j is not exceeded, and a constant otherwise. Then the classification functions used by the network are

$$\sum_{i=1}^{N} b_{ij}x_i > T_j : \quad j = 1,2,\ldots$$

$$\sum_{j} y_j w_{jk} > T_k : \quad k = 1,2,\ldots$$

Unlike applications of classification theory in many fields, in many pattern recognition situations it is possible for the experimenter to check how well a particular procedure performs since independently he knows to which group a given pattern belongs. The easy availability of additional samples from each group makes it possible to introduce an iterative or "adaptive" procedure to improve the performance of the classification function.

An evaluation of the worth of the classification function resulting when iteration based on experience is used to modify the state of a learning network, is provided by comparing its error curve with error curves obtained from a likelihood ratio procedure using $p(x)$ and various approximations to it, with the error curve resulting when the a_i are obtained according to Fisher's discriminant function, and with the curve obtained when an unweighted score of the x_i is used[10].

3. Iterative procedures for learning. The problem of using experience to go from some arbitrary initial state $(a_1', a_2', \ldots a_N')$ to a final state $(a_1, a_2, \ldots a_N)$ which will produce a desired result can be approached in many ways. Typical of a number of efforts is the approach used by Gabor[11] of minimizing a mean square error criterion. The problem may be also stated as one of applying a set of transformations T to the state vector. In this form, varying degrees of complexity can be introduced into the formulation of the problem, as is illustrated by the work in Dynamic Programming. Useful iteration procedures can be derived from the simple point of view provided by the techniques used in stochastic models for learning[12,13,14,15], and from the point of view provided by Stochastic approximation methods[16].

4. Discussion. The operation of some proposed networks for pattern recognition has been examined in the context of classification theory, and related to a class of classification procedures. It is clear that the classification properties of the networks are acceptable for many pattern recognition situations of interest.

Experimental work on pattern recognition and iterative procedures is being carried out by the author and his associates C. F. Fey, N. J. Molgaard, D. F. Smith and D. F. Parkhill. When using various iteration procedures, a number of learning nets have produced-learning curves similar to those shown in Fig. 3 and 4. Fig. 5 shows a device, suggested by D. F. Parkhill and designed by D. F. Smith to facilitate experimentation on pattern recognition networks using simple iterative techniques.

REFERENCES

1. Kanal, L., "Pattern Recognition Studies".
   I. Use of discriminant functions, distance functions and clustering transformations in pattern recognition.

1. II. Evaluation of a class of pattern recognition networks.

III. Iterative procedures for learning: stochastic approximation and random search.
NOTES: General Dynamics/Electronccs 1961.

2. Bahadur, R. R., " A Representation of the Joint Distribution of Responses to n Dichotomous Items". USAF SAM series in statistics, Report No. 59-42. Randolf AFB, Texas, 1959.

3. Parkhill. D. F., "Distributed State Response Pattern Recognition Systems", Proc. Rochester Conference on Data Acquisition and Processing in Biology and Medicine. July 1961.

4. Hawkins, J. K., "Self-organizing Systems- A Review and Commentary". Prod. IRE Jan. 1961, p. 31-48.

5. Minsky, M., "Steps Toward Artificial Intelligence", Proc. IRE. Jan. 1961, p. 8-30.

6. Rao, C.R., "Advanced Statistical Method in Biometric Research". New York, John Wiley, 1952.

7. Anderson, T.W., "An Introduction to Multivariate Statistical Analysis". New York, John Wiley, 1958.

8. Fisher, R. A , "The Use of Multiple Measurements in Taxonomic Problems". In Contributions to Mathematical Statistics. New York, John Wiley.

9. Chow, C.K., "An Optimum Character Recognition System Using Decision Functions". IRE Trans. on Electronics Computers, Vol. EC-6 p. 247-254. Dec. 1957.

10. Solomon, H., "Classification Procedures Based On Dichotomous Response Vectors". Contributions to probability and Statistics, Olkin: Stanford University Press, 1960.

11. Gabor, D., Wilby, W., Woodcock, R., "A Universal Nonlinear Filter, Predictor and Simulator which Optimizes Itself by a Learning Process." Proc. Inst. of Electrical Engrs. Vol. 108, Part B. 1961.

12 Bush, R. R. and Mosteller, F., "Stochastic Models for Learning". New York, John Wiley, 1955.

13. Luce, R. D., "Individual Choice Behaviour," New York, 1959.

14. Kanal, L., "Analysis of Some Stochastic Processes Arising From A Learning Model". Ph.D. Thesis, University of Penn. June, 1960.

15. Kanal,L., "On a Random Walk Related to a Nonlinear Learning Model", IRE, March 1961, National Convention Record.

16. Dvoretzky, A., "On Stochastic Approximation" Third Berkely Symposium on Mathematical Statistics and Probability, University of California, Press, 1956.

ACKNOWLEDGEMENTS

I am indebted to C. F. Fey, N. J. Molgaard D. F. Parkhill, and especially D. F. Smith for helpful discussions and comments.

I am also grateful to K K. Maitra, J. Dietz and A. Wolf for their comments and encouragement.

AN ADAPTIVE CORRELATOR FOR UNDERWATER MEASUREMENTS

by DR. ALFRED A. WOLF, Director of Research
and J. H. DIETZ, Fellow Engineer
Emertron, Inc.
Silver Spring, Maryland

ABSTRACT

The measurement and display of the correlation functions of quasi-stationary random processes containing energy in the frequency range 0.01-100,000 cps have become increasing important in oceanography and underwater acoustics. Correlation techniques yield useful statistical descriptions of sea state, ocean background noise, and the acoustical properties of bodies of water. In addition, since the correlation functions of periodic processes are also periodic, correlation may be used to separate weak signals from noise.

INTRODUCTION

At present correlation functions are usually determined by means of a digital computer,[1] which employs sampled records of the processes to compute approximating sums for the time integrals that define the correlation functions. Disadvantages of this method are (1) the need for the computer itself, (2) the fact that the required number of samples must be determined experimentally, (3) the bandwidth limitation imposed by sampling, and (4) the discrete display of the correlation functions.

The defining time integral may also be approximated by analogue techniques. The required time delays are introduced by means of tapped delay lines; analogue multipliers are used to obtain the products of the delayed and undelayed signals; and averaging is accomplished in a low-pass filter. Like the digital method, this scheme gives discrete values of the correlation functions. The bandwidths of the signals to be correlated are restricted by the pass band of the signal multiplier. The principal disadvantage of this method is the need for low-distortion delay lines capable of producing delays of order of seconds and in some cases minutes.

In this paper an analogue method requiring no delay lines and yielding a continuous approximation of the correlation function is considered. An outgrowth of the work of Wolf and Dietz[2] in system identification, the method consists in expanding the correlation function in a series of orthonormal functions the coefficients of which are determined by analogue techniques. A similar but less general method was independently developed by Lampard.[3] Since in practice the series must always contain a finite number of terms, the problem of an optimum approximation to the correlation function is treated. The filters that generate the orthonormal functions automatically adjust their transmission characteristics to give an optimum approximation in the minimum-integral-square-error sense.

ORTHONORMAL EXPANSION OF A CORRELATION FUNCTION

In Fig. 1 a stationary random process $g_1(t)$ is applied to the inputs of a set of time-invariant linear filters the impulse responses of which form a set of orthonormal functions $\{h_n(t)\}$ over the interval $(0,\infty)$, i.e.,

$$\int_0^\infty h_n(t)\, h_m(t)\, dt = \begin{cases} 1, & n = m \\ 0, & n \neq m \end{cases} \qquad (1)$$

The response of the nth filter to $g_1(t)$ applied at $t = 0$ is the random process $v_n(t)$, given by

$$v_n(t) = \int_0^\infty g_1(t-\tau)\, h_n(\tau)\, d\tau \qquad (2)$$

Multiplying the response $v_n(t)$ by a second stationary random process $g_2(t)$ and time-averaging the product leads to

$$A_n = \overline{g_2(t)\, v_n(t)} = \int_0^\infty \overline{g_2(t)\, g_1(t-\tau)}\, h_n(\tau)\, d\tau \qquad (3)$$

Since

$$\overline{g_2(t)\, g_1(t-\tau)} = \phi_{21}(-\tau) = \phi_{12}(\tau) \qquad (4)$$

the cross-correlation function of $g_1(t)$ and $g_2(t)$, (3) may be written:

$$A_n = \int_0^\infty \phi_{12}(\tau)\, h_n(\tau)\, d\tau \qquad (5)$$

an integral equation of the first kind, a solution of which is

$$\phi_{12}(\tau) = \sum_{n=1}^{\infty} A_n\, h_n(\tau) \qquad (6)$$

That (6) is a solution can be verified by substituting (6) in (5), interchanging the order of summation and integration, and invoking (1). Hence averaging the products of $g_2(t)$ and the responses of the filters to $g_1(t)$ leads to the coefficients, A_n, of the orthonormal expansion of the correlation function for $\tau \geq 0$.

A second set of identical filters are excited by a unit step, to give the indicial responses $a_n(t)$:

$$a_n(t) = \int_0^t h_n(\tau)\, d\tau \qquad (7)$$

Each $a_n(t)$ is then multiplied by the corresponding coefficient A_n, all such products are summed, and the resulting sum is differentiated, yielding

$$\frac{d}{dt} \sum_{n=1}^{\infty} A_n \int_0^t h_n(\tau)\, d\tau = \sum_{n=1}^{\infty} A_n\, h_n(t) \qquad (8)$$

which is the correlation function displayed in real time.

A CLASS OF ORTHONORMAL FUNCTIONS AND FILTERS

A class of orthonormal functions suitable for the expansion of correlation functions are defined by the following theorem:

<u>Theorem</u>. The set of square-integrable time functions $\{h_n(t)\}$ form an orthonormal set over the interval $(0,\infty)$ if each member possesses a Laplace transform $H_n(s)$ with

$$H_1(s) = K_1 \frac{B_1(s)}{C_1(s)} \qquad (9)$$

and

$$H_n(s) = \frac{K_n}{K_{n-1}} \frac{C_{n-1}(-s)}{C_n(s)} H_{n-1}(s) \quad n \geq 2 \qquad (10)$$

in which $B_1(s)$ and the terms $C_n(s)$ are polynominals in s, and if the constants K_n are such that

$$\frac{1}{2\pi j} \int_{Br} H_n(-s)\, H_n(s)\, ds = 1 \qquad n = 1, 2, \ldots \qquad (11)$$

in which Br denotes an appropriate Bromwich contour in the s-plane enclosing the poles of $H_n(s)$.

(A proof of this theorem appears in the Appendix.)

Examples of members of this class of orthonormal functions are the Laguerre[1] functions, for which

$$H_n(s) = \sqrt{2s_1}\, \frac{(s_1 - s)^{n-1}}{(s_1 + s)^n} \quad n = 1, 2, \ldots \qquad (12)$$

with multiple poles at $s = -s_1$ and multiple zeroes at $s = s_1$; and the Kautz[4] functions for which

$$H_1(s) = \frac{\sqrt{2s_1}}{s + s_1} \qquad (13)$$

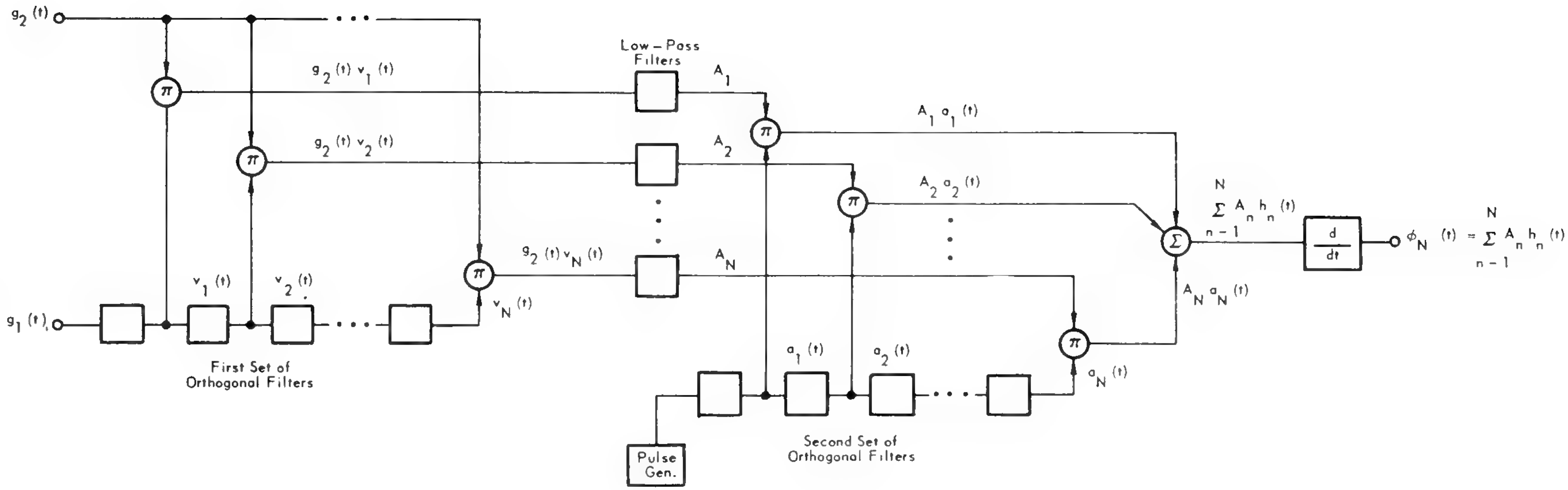

Fig. 1 Analogue Correlator

and

$$H_n(s) = \sqrt{\frac{s_n}{s_{n-1}}} \frac{s-s_{n-1}}{s+s_n} H_{n-1}(s) \quad n \geq 2 \quad (14)$$

The physical realization of a set of filters with impulse responses $h_1(t)$, $h_2(t)$,... is readily accomplished by analogue-computer techniques. Denoting the input to the first filter by $g(t)$ and the output by $x_1(t)$, one sees from (9) that these quantities are related by the linear differential equation

$$C_1(D)\ x(t) = K_1\ B_1(D)\ g(t) \quad (15)$$

in which $D = \frac{d}{dt}$. Similarly, from (10) it is seen that the outputs of the succeeding filters are recursively related by the linear differential equations

$$K_{n-1}\ C_n(D)\ x_n(t) = K_n\ C_{n-1}(-D)\ x_{n-1}(t) \quad n \geq 2 \quad (16)$$

Operational amplifiers connected to solve (15) and (16) are the physical realization of the orthonormal filters.

OPTIMUM ORTHONORMAL EXPANSION

In practice it is desirable to truncate the series expansion of the correlation function after as few terms as possible. Denoting the exact correlation function by

$$\phi(\tau) = \sum_{n=1}^{\infty} A_n\ h_n(\tau) \quad (17)$$

and the N-term approximation by

$$\phi_N(\tau) = \sum_{n=1}^{N} A_n\ h_n(\tau) \quad (18)$$

one may write the integral-square error of the approximation:

$$\epsilon_N^2 = \int_0^{\infty} \left[\phi(\tau) - \phi_N(\tau)\right]^2 d\tau \quad (19)$$

Squaring the integrand of (19), substituting (17) and (18) therein, interchanging the orders of integration and summation, and invoking (1) in evaluating the resulting integrals leads to

$$\epsilon_N^2 = \int_0^{\infty} \phi^2(\tau)\ d\tau - S_N^2 \quad (20)$$

in which

$$S_N^2 = \sum_{n=1}^{N} A_n^2 \quad (21)$$

The orthonormal time functions $h_n(t)$ are also functions of a set of real parameters $\{\alpha_i\}$, e.g., the poles and zeros of the Laplace transforms of the Laguerre and Kautz functions. Hence from (6), (20), and (21) so, too, are A_n, S_N^2, and ϵ_N^2. The optimum expansion of $\phi(\tau)$ for a given N and a particular set of orthonormal functions is defined as the expansion obtained when the α_i are selected to minimize ϵ_N^2. Since the right member of (20) is always nonnegative, the optimum expansion occurs when the α_i are selected to give

$$\max_{\{\alpha_i\}} S_N^2 = \max_{\{\alpha_i\}} \sum_{n=1}^{N} A_n^2 \quad (22)$$

Hence the determination of the optimum orthonormal expansion is the multivariate maximization of the sum of the squares of the coefficients of the orthonormal series over a set of parameters $\{\alpha_i\}$.

If the orthonormal functions employed to expand the correlation function yield S_N^2 that are well-behaved functions of parameters $\{\alpha_i\}$, the gradient method[5] may be used to reduce the multivariate maximization to a convergent iterative procedure involving a single variable θ. This is accomplished by transforming the initial set of parameters $\{\alpha_i^0\}$ to a new set $\{\alpha_i^1\}$ by setting

$$\alpha_i^1 = \alpha_i^0 + \left(\frac{\partial S_N^2}{\partial \alpha_i}\right)_0 \theta \qquad i = 1, 2, \ldots \quad \theta \geq 0 \quad (23)$$

in which the subscript 0 on the partial derivative indicates that it is evaluated at $\alpha_1 = \alpha_1^0$, $\alpha_2 = \alpha_2^0$, . . . Thus (23) represents the equations of a straight line in a hyperplane tangent to S_N^2 at the point $(\alpha_1^0, \alpha_2^0, \ldots)$. Since in the neighborhood of this point one may approximate the function S_N^2 by the straight line, in this region

$$S_N^2(\alpha_1, \alpha_2, \ldots) \approx S_N^2(\theta) \quad (24)$$

Maximizing the right member of (24) yields

$$(S_N^2)_1 = \max_{\theta \geq 0} S_N^2(\theta) \quad (25)$$

The value of θ that satisfies (25) is substituted in (23) to give the new set of parameter values $\{\alpha_i^1\}$. Repeating the procedure by letting

$$\alpha_i^2 = \alpha_i^1 + \left(\frac{\partial S_N^2}{\partial \alpha_i}\right)_1 \theta \qquad i = 1, 2, \ldots \quad \theta \geq 0 \quad (26)$$

leads to $(S_N^2)_2 \geq (S_N^2)_1$ and to a set of parameters $\{\alpha_i^2\}$. Continuing the process yields the monotone nondecreasing sequence

$$(S_N^2)_1 \leq (S_N^2)_2 \leq \ldots \leq (S_N^2)_j \leq \ldots \qquad (27)$$

which converges to $\underset{\{\alpha_i\}}{\text{Max}}\, S_N^2$. The values of the parameters that yield this maximum form an optimum set of parameter values.

IMPLEMENTATION OF THE ADAPTIVE CORRELATOR

The block diagram implementation of the correlation principle discussed above is shown in Fig. 1. Random process $g_1(t)$ is applied to the input of the first set of orthogonal filters. The resulting outputs -- $v_1(t)$, $v_2(t)$,..., $v_N(t)$ --are multiplied by the second random process, $g_2(t)$, by means of analogue multipliers; and the respective products are passed through low-pass filters, to give the averages A_1, A_2,..., A_N. At the same time a second set of identical orthogonal filters receives a repetitive square-wave input, producing outputs $a_1(t)$,..., $a_N(t)$. Each of these responses is multiplied by the corresponding average, and the products are summed. Finally, the sum is differentiated to obtain $\phi_N(t)$, the approximate expansion of the correlation function.

Fig. 2 shows the block diagram of the mechanization of a correlator capable of self-adjustment to achieve an optimum orthogonal expansion in the minimum-integral-square-error sense. The quantity S_N^2, obtained by squaring each of the averages A_1,..., A_N and summing the squares, is applied as an input to an optimization computer and parameter controller, which iteratively determines the optimum settings of the parameters of the orthogonal filters by the routine of Fig. 3. After storing the set of initial parameter values, $\{\alpha_i^0\}$, and the initial value of the sum of the squares of the averages, $(S_N^2)_0$, the computer determines the set of approximate initial parameter sensitivities, $\left\{\frac{\Delta S_N^2}{\Delta \alpha_i}\right\}_0$. It then normalizes these sensitivities by dividing each by the absolute value of the largest, P_0. Each parameter is then varied over its range in steps proportional to its normalized sensitivity. The set of parameter values $\{\alpha_i^1\}$, yielding the largest value of S_N^2 is compared to the initial set $\{\alpha_i^0\}$. If all corresponding members of the two sets differ by less than preassigned amounts, the process is terminated; if not, the initial parameter values are replaced by the values giving the greatest S_N^2, and the process is repeated. Each parameter is thereby iteratively adjusted to its optimum value. The optimization computer and parameter controller is amenable to mechanization by hybrid-computer and step-servo techniques.

CONCLUSIONS

In this paper we have considered certain theoretical and practical aspects of a correlator that approximates correlation functions by series of orthogonal time functions and iteratively adjusts itself to minimize the approximation error. Since operational-amplifier methods are employed to synthesize the orthogonal filters and analogue multipliers are used to obtain the required signal products, the device is restricted to the correlation of signals containing no significant energy at frequencies greater than 100 kc. With amplifiers and multipliers capable of operating at higher frequencies, however, the range could be increased.

A method for synthesizing a class of linear orthogonal filters has been presented. Typical members of this class are the well-known Laguerre and Kautz filters. Other members are filters with transfer functions

$$H_1(S) = \frac{2\sqrt{\zeta_1\omega_1}\, S}{S^2+2\zeta_1\omega_1 S+\omega_1^2} \qquad (28)$$

and

$$H_n(S) = \sqrt{\frac{\zeta_n\omega_n}{\zeta_{n-1}\omega_{n-1}}} \cdot \frac{S^2-2\zeta_{n-1}\omega_{n-1}S+\omega_{n-1}^2}{S^2+2\zeta_n\omega_n S+\omega_n^2}\, H_{n-1}(S) \qquad (29)$$

The impulse responses of such filters contain exponentially damped cosinusoids and are therefore applicable to the expansion of correlation functions with periodic components.

REFERENCES

1. Y. W. Lee, Statistical Theory of Communication, John Wiley & Sons, Inc., New York, 1960.

2. A. A. Wolf and J. H. Dietz, "A Device for Measuring Correlation Functions and Spectral Density Functions," Technical Report No. 1, and "A Study of White-Noise Fault Diagnosis in Linear Passive Systems," Technical Report No. 2, Stromberg-Carlson Company (now General Dynamics/Electronics) Applied Mathematical Studies Department, Rochester, N.Y., Nov., 1960.

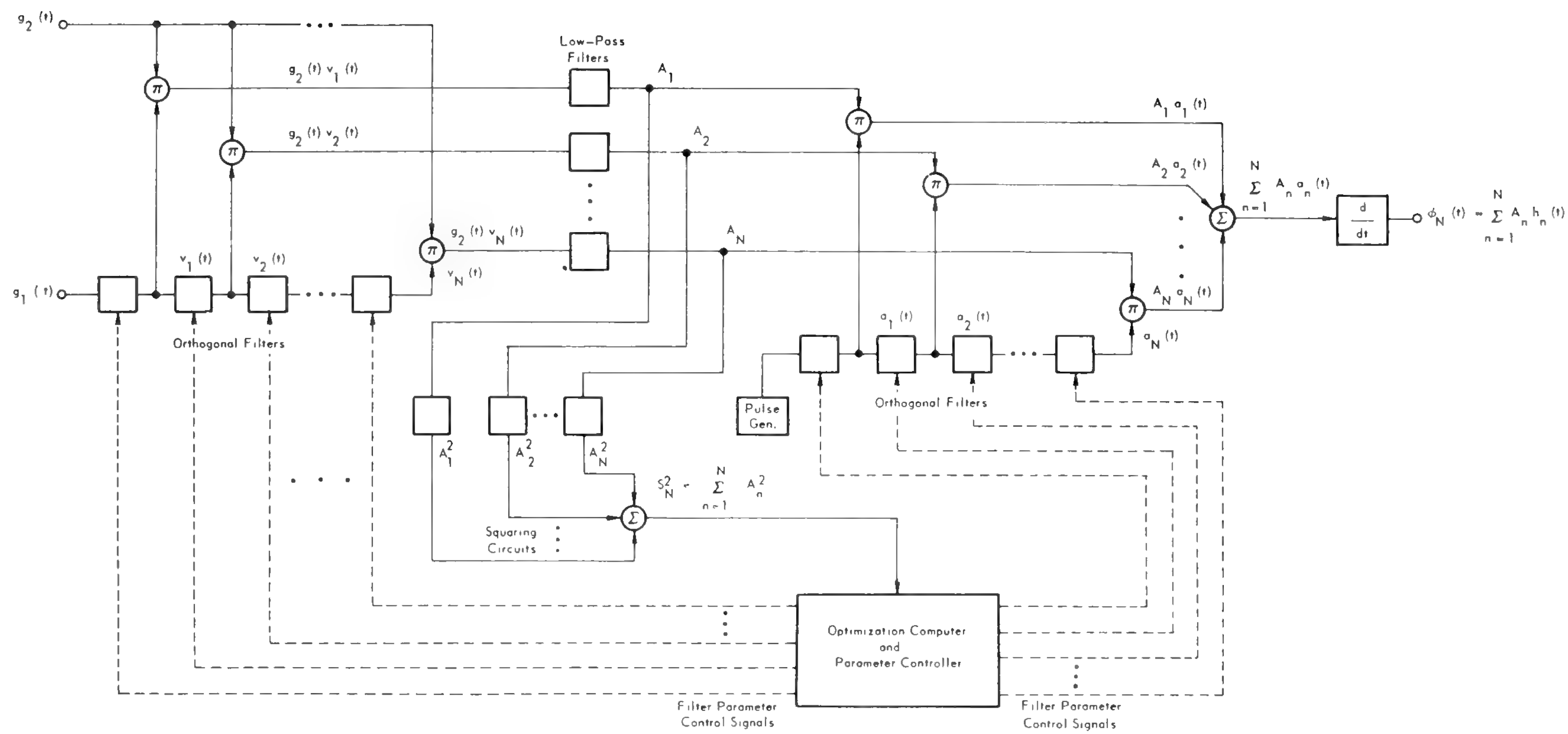

Fig. 2 Adaptive Correlator

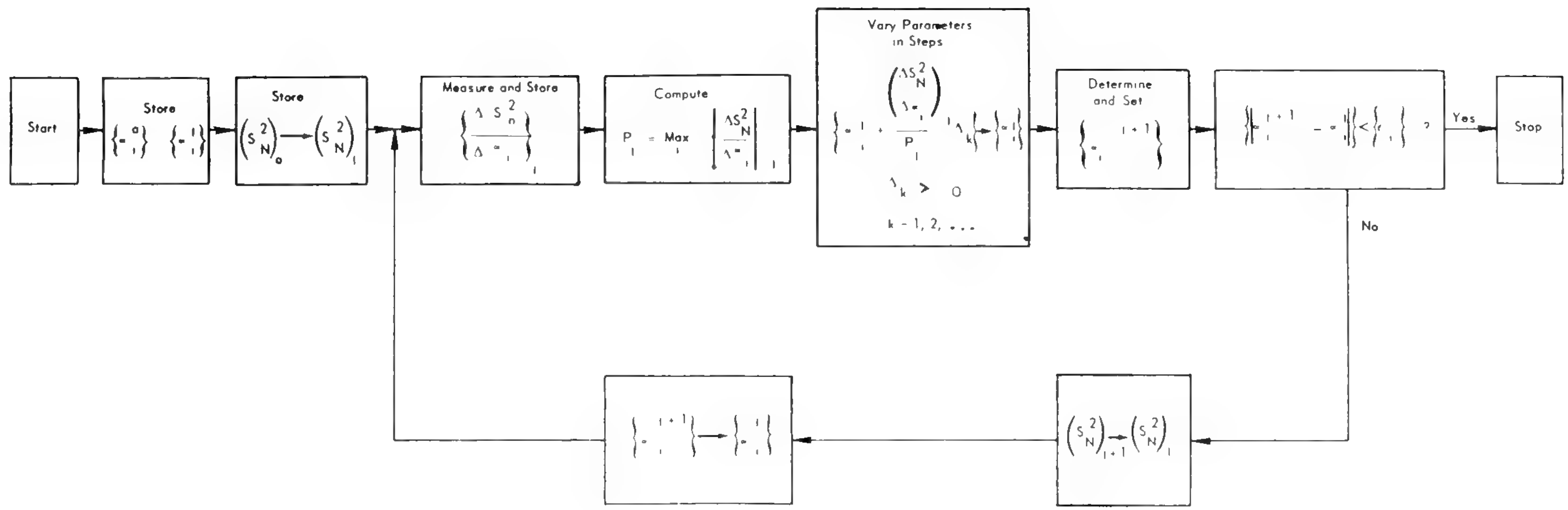

Fig. 3 Simplified Flow Chart of Optimization Computer

3. D. G. Lampard, "A New Method of Determining Correlation Functions of Stationary Time Series," J. Inst. Elec. Eng., part III, No. 73, pp. 343 f., Sept., 1954.

4. W. H. Kautz, "Transient Synthesis in the Time Domain," Trans. IRE PGCT, vol. CT-1, No. 3, pp. 29-39, 1954.

5. T. L. Saaty, Mathematical Methods of Operations Research, McGraw-Hill Book Co., Inc., New York, 1959

APPENDIX

Proof of Theorem

Since each $h_n(t)$ is square-integrable, it follows that

$$\int_0^\infty h_n(t)\, h_m(t)\, dt < \infty \qquad (30)$$

for all n,m 1. Since in the Laplace transforms $H_n(s)$ the terms $C_n(s)$ are polynomials in s, the transforms contain only poles in the left half-plane. One may therefore write:

$$\int_0^\infty h_m(t)\, h_n(t)\, dt = \frac{1}{2\pi j}\int_{Br} H_m(-s)\, H_n(s)\, ds$$

$$= \frac{1}{2\pi j}\int_{Br'} H_n(-s)\, H_m(s)\, ds \qquad (31)$$

in which Br and Br' denote Bromwich contours in the s-plane enclosing the poles of $H_n(s)$ and $H_m(s)$, respectively.

Noting that the repeated application of (10) leads to

$$H_n(s) = K_n\, B_1(s) \frac{\prod_{k=1}^{n-1} C_k(-s)}{\prod_{k=1}^{n} C_k(s)}, \quad n \geq 2 \qquad (32)$$

we consider the following three cases in which $n \neq m$:

(1) n = 1, m ≥ 2

Substituting (9) and (32) in (31) gives

$$\frac{1}{2\pi j}\int_{Br} K_m K_1\, B_1(s)\, B_1(-s) \frac{\prod_{k=1}^{m-1} C_k(s)}{\prod_{k=1}^{m} C_k(-s)} \times \frac{1}{C_1(s)}\, ds = 0 \qquad (33)$$

because the denominator term $C_1(s)$ is cancelled by $C_1(s)$ in the numerator, leaving no terms in the denominator with zeros in the left half-plane.

(2) n ≥ 2, m < n

$$\frac{1}{2\pi j}\int_{Br'} K_n K_m\, B_1(-s)\, B_1(s) \frac{\prod_{k=1}^{n-1} C_k(s)}{\prod_{k=1}^{n} C_k(-s)} \times \frac{\prod_{k=1}^{m-1} C_k(-s)}{\prod_{k=1}^{m} C_k(s)}\, ds = 0 \qquad (34)$$

because the denominator terms $C_1(s)\, C_2(s) \ldots C_m(s)$ are cancelled, again leaving no terms in the denominator with zeros in the LHP.

(3) m ≥ 2, n < m

$$\frac{1}{2\pi j}\int_{Br} K_m K_n\, B_1(-s) \frac{\prod_{k=1}^{m-1} C_k(s)}{\prod_{k=1}^{m} C_k(-s)} \times \frac{\prod_{k=1}^{n-1} C_k(-3)}{\prod_{k=1}^{n} C_k(s)}\, ds = 0 \qquad (35)$$

because the denominator terms $C_1(s)\, C_2(s) \ldots C_n(s)$, having zeros in the LHP, are cancelled.

For n = m, (11) applies. Hence

$$\int_0^\infty h_n(t)\, h_m(t)\, dt = \begin{cases} 1, & n = m \\ 0, & n \neq m \end{cases} \qquad (36)$$

and the theorem is proved.